UNIVERSITY OF ADELAIDE LIBRARY 3-4-95

THE CRETACEOUS STRATIGRAPHY AND PALAEOGEOGRAPHY OF THE WESTERN AND SOUTHWESTERN MARGINS OF THE GULF OF CARPENTARIA, NORTHERN TERRITORY

ANDREW A. KRASSAY

Thesis submitted for the degree of
Doctor of Philosophy
in
The University of Adelaide
(Faculty of Science)

September 1994

Awarded 1995

CONTENTS

Abstract XIII

Statement XV

Acknowledgements XVI

1. Introduction

1.1 General Introduction 1

1.2 High-frequency Changes in Relative Sea Level in Shallow-marine Settings 2

1.3 Thesis Setting, Aims and Approach 4

1.4 Thesis Outline 6

2. Regional Geology

2.1 Introduction 8

2.2 Basin Setting 8

2.3 Previous Work 10

2.4 Previous Stratigraphic Nomenclature 14

2.4.1 The Coastal Belt 16

2.4.2 The Inland Belt 16

2.5 New Stratigraphic Names (Walker River Formation and Yirrkala Formation) 17

2.6 The Carpentaria Basin: Central Basin Strata and their Western Onshore Equivalents, the Mullaman Beds 18

2.6.1 Stratigraphy 19

2.6.2 Structure 23

2.7 Chapter Summary 25

3. Cretaceous Shelf Facies of the Western Carpentaria Basin

3.1 Introduction 27

3.2 Sedimentary Facies 27

3.2.1 Facies 1 - chert-cobble conglomerate and coarse sandstone 29

3.2.2 Facies 2 - chert-pebble conglomerate and pebbly sandstone 31

3.2.3 Facies 3 - lag 32

3.2.4 Facies 4 - bioturbated pebbly sandstone 33
3.2.5 Facies 5 - cross-stratified and planar bedded pebbly sandstone 34
3.2.6 Facies 6 - plant-bearing pebbly sandstone 35
3.2.7 Facies 7 - trough cross-stratified coarse sandstone 37
3.2.8 Facies 8 - trough and swaley cross-stratified fossiliferous sandstone 38
3.2.9 Facies 9 - ferruginous lithic sandstone 39
3.2.10 Facies 10 - bioturbated clayey sandstone 40
3.2.11 Facies 11 - cross-stratified plant-bearing sandstone 40
3.2.12 Facies 12 - fossiliferous bioturbated clayey sandstone 41
3.2.13 Facies 13 - bioturbated silty sandstone 42
3.2.14 Facies 14 - hummocky cross-stratified sandstone 44
3.2.15 Facies 15 - thinly interbedded sandstone and siltstone 46
3.2.16 Facies 16 - thinly-bedded graded sandstone and siltstone 48
3.2.17 Facies 17 - pebbly siltstone 49
3.2.18 Facies 18 - laminated clayey siltstone and sandy siltstone 50
3.2.19 Facies 19 - weakly bioturbated laminated siltstone 51
3.2.20 Facies 20 - laminated clayey siltstone 52
3.2.21 Facies 21 - intensely bioturbated siltstone 53
3.2.22 Facies 22 - silty claystone 54
3.2.23 Ferricrete 1 55
3.2.24 Ferricrete 2 56
3.3 Chapter Summary 57

4. Facies Successions: Stacking Patterns of Carpentaria Basin Shelf Facies

4.1 Introduction 58
4.2 Definitions and Concepts 58
4.3 Facies Successions 59
4.4 Coarsening-upward (or Sandier-upward) Successions 61
4.4.1 Facies succession 1 - storm-influenced lower-offshore marine 61
4.4.2 Facies succession 2 - storm- (and wave-) dominated shoreface (progradational) 64
4.4.3 Facies succession 3 - fluvial interdistributary/channel fill 67
4.5 Fining-upward Successions 69
4.5.1 Facies succession 4 - storm-influenced lower shoreface to offshore marine 69
4.5.2 Facies succession 5 - storm- (and wave-) dominated shoreface (retrogradational) 72

4.5.3 Facies succession 6 - paralic (estuarine and deltaic-marine) systems....74
4.5.4 Facies succession 7 - fluvial channel fill....76
4.6 Irregular Successions....78
4.6.1 Facies succession 8 - sheltered/restricted marine (bay/lagoon)....78
4.7 Chapter Summary....80

5. Depositional Environments and Lithostratigraphic Correlation in the Northern Region: The Coastal Plain to Inner Shelf

5.1 Introduction....81
5.2 Database and Methods....81
5.3 Detailed Stratigraphic Correlation Diagrams....83
5.4 Northeastern Arnhem Land Zone (ALZ)....85
5.4.1 Correlation diagram A - A' (Fig. 5.4)....85
5.4.2 Correlation diagram B - B' (Fig. 5.5)....88
5.4.3 Biostratigraphic control....90
5.4.4 Summary of facies successions in the ALZ....91
5.5 Bath and Parsons Ranges Zone (BPRZ)....93
5.5.1 Correlation diagram C - C' (Fig. 5.7)....93
5.5.2 Correlation diagram D - D' (Fig. 5.7)....95
5.5.3 Correlation diagram E - E' (Fig. 5.8)....99
5.5.4 Correlation diagram F - F' (Fig. 5.9)....102
5.5.5 Correlation diagram G - G' (Fig. 5.10)....105
5.5.6 Biostratigraphic control....107
5.5.7 Summary of facies successions in the BPRZ....108
5.6 Chapter Summary....111

6. Depositional Environments and Lithostratigraphic Correlation in the Central Region: The Shoreline to Middle Shelf.

6.1 Introduction....112
6.2 Database for Detailed Stratigraphic Correlation Diagrams....112
6.3 Detailed Stratigraphic Correlation Diagrams....115
6.3.1 Correlation diagram H - H' (Fig. 6.3)....115
6.3.2 Correlation diagram I - I' (Fig. 6.4)....118
6.3.3 Correlation diagram J - J' (Fig. 6.5)....122

6.3.4 Correlation diagram K - K' (Fig. 6.6) 126
6.3.5 Correlation diagram L - L' (Fig. 6.7) 130
6.4 Biostratigraphic Control 133
6.5 Summary of Facies Successions in the Central Region 134
6.6 Chapter Summary 137

7. Depositional Environments and Lithostratigraphic Correlation in the Southern Region: The Shoreline to Outer Shelf

7.1 Introduction 138
7.2 Database for Detailed Stratigraphic Correlation Diagrams 140
7.3 Detailed Stratigraphic Correlation Diagrams 140
7.3.1 Correlation diagram M - M' to N - N' (Figs. 7.3 and 7.4) 140
7.3.2 Correlation diagram O - O' (Fig. 7.5) 147
7.3.3 Correlation diagram P - P' (Fig. 7.6) 150
7.4 Biostratigraphic Control 155
7.5 Summary of Facies Successions in the Southern Region (Correlation diagram Q - Q', Fig. 7.7) .. 156
7.6 Problems of Correlation in the Southern Region 159
7.7 Chapter Summary 161

8. Regional Lithostratigraphy and Biostratigraphy: A Stratigraphic Framework for the Western Carpentaria Basin

8.1 Introduction 162
8.2 Regional Biostratigraphy 162
8.2.1 Biostratigraphic dating on the mainland 163
8.2.2 Biostratigraphic dating on Groote Eylandt 165
8.2.3 Biostratigraphic dating in the present study 166
8.2.4 Summary of biostratigraphic dating and age control for the western shelf of the Carpentaria Basin 169
8.3 Regional Correlation of Composite Outcrop Sections 170
8.3.1 The basal (pre-Albian) part of the shelf sequence 172
8.3.2 The middle (Albian) part of the shelf sequence 172
8.3.3 The upper (post-Albian) part of the shelf sequence 173
8.4 Comparison of Stratigraphic Nomenclatures 175
8.4.1 Stratigraphic nomenclature in the northern region 175

8.4.2 Stratigraphic nomenclature in the central region 175
8.4.3 Stratigraphic nomenclature in the southern region 177
8.4.4 Discussion 177
8.5 Stratigraphic Data from the Subsurface 178
8.5.1 Drillholes near Nhulunbuy 178
8.5.2 Correlation of Nhulunbuy drillholes with outcrops in the ALZ 179
8.5.3 Drillholes and quarries on Groote Eylandt 180
8.5.4 Correlation of Groote Eylandt drillholes with mainland outcrops 182
8.5.5 Drillholes near Numbulwar (Rose River) 185
8.5.6 Correlation of Numbulwar drillholes with mainland outcrops 188
8.6 Integration of the Stratigraphic Data: A Stratigraphic Framework for the Shelf 189
8.6.1 Regional stratigraphic correlation of facies successions 189
8.6.2 Age of facies successions of the Mullaman Beds 191
8.7 Shelf-to-Basin Regional Correlation: Stratigraphic Ties to the Great Artesian Basin 193
8.7.1 Carpentaria Basin shelf-to-basin regional correlation 194
8.7.2 Correlation between deep stratigraphic drillholes 194
8.7.3 Correlation between deep drillholes and Mullaman Bed outcrops 196
8.8 Chapter Summary 199

9. Sequence Stratigraphy of the Western Carpentaria Basin

9.1 Introduction 200
9.2 Concepts, Definitions, and Rationale for this Chapter 200
9.3 Methods 203
9.4 Sequence Boundary Unconformities 205
9.4.1 Walker River sequence boundary 207
9.4.2 China Wall sequence boundary 208
9.4.3 Carpentaria sequence boundary 209
9.4.4 Stoney Ridge sequence boundary 210
9.4.5 Arnhem Land sequence boundary 210
9.4.6 Lawn Hill sequence boundary 211
9.5 Sequences and Systems Tracts 211
9.5.1 Sequence *IA* 213
9.5.2 Sequence *IB* 215
9.5.3 Sequence *II* 217

9.5.4 Sequence *III* 220
9.5.5 Sequence *IV* 225
9.5.6 Sequence *V* 227
9.5.7 Sequence *VI* 232
9.5.8 Summary of sequences on the Carpentaria Basin shelf 236
9.6 Sequence Stratigraphic Discussion 237
9.6.1 Do fining- and deepening-upwards marine parasequences exist? 237
9.6.2 Fluvial successions: deposition during the LST or TST/HST? 238
9.6.3 Origin of lags and breccias in the Mullaman Beds 240
9.7 A Sea Level Curve for the Western Carpentaria Basin, and Comparison with Great Artesian Basin Sea Level Curves 243
9.7.1 Pre-Aptian marine flooding of the western Carpentaria Basin shelf 245
9.7.2 Aptian transgression 248
9.7.3 Early Albian (?) transgression 248
9.7.4 Major marine flooding from the late early Albian to the late Albian: Maximum flooding of the southern shelf 250
9.7.5 Major marine flooding from the late Albian to the latest Albian-early Cenomanian: Maximum flooding of the northern shelf 251
9.7.6 Early to middle (?) Cenomanian transgressions, terminal Cenomanian regression, and complete emergence in the Turonian 252
9.8 Comparison with Global and Northern Hemisphere Sea Level Curves 253
9.8.1 Eustatic sea level curves 253
9.8.2 Problems of precision for the sea level curves 256
9.8.3 North American sea level curves 257
9.8.4 European sea level curves 258
9.8.5 Russian (CIS) sea level curves 259
9.9 Sequence Development: Mechanistic Models and Speculation 260
9.9.1 Hierarchy of sequences and parasequences 260
9.9.2 Allocyclic versus autocyclic processes 262
9.9.3 Northern Australian tectonism 263
9.9.4 Glacio-eustasy 265
9.10 Chapter Summary 267

10. Palaeoclimate, Palaeogeography, Shelf Dynamics, and a Depositional Model for the Western Shelf of the Carpentaria Basin

10.1 Introduction 268

10.2 Cretaceous Palaeoclimates of Northern Australia 268

10.2.1 Introduction 268

10.2.2 Palaeontological evidence for Cretaceous climates 269

10.2.3 Isotopic evidence for Cretaceous climates 270

10.2.4 Discussion of Cretaceous climate of northern Australia 270

10.3 Ice-rafting or Storm-transport? 272

10.3.1 Introduction 272

10.3.2 Evidence for ice-rafting in the Mullaman Beds 272

10.3.3 Discussion 275

10.4 Carpentaria Basin Palaeogeography 276

10.4.1 Introduction 276

10.4.2 Palaeogeography of the northern region (Arnhem Land Zone) 277

10.4.3 Palaeogeography of the northern region (Bath and Parsons Ranges Zone) 283

10.4.4 Palaeogeography of the central region 288

10.4.5 Palaeogeography of the southern region 294

10.5 Palaeogeographical Significance of the Clay Mineralogy of the Mullaman Beds 301

10.5.1 Trends of clay mineral distribution in the marine Mullaman Beds 301

10.5.2 Models to account for the observed clay mineral trends 302

10.5.3 Discussion 304

10.6 Shelf Dynamics 305

10.6.1 Introduction 305

10.6.2 Storm generation potential 306

10.6.3 Palaeobathymetry 308

10.6.4 Sediment supply and shelf profile 311

10.6.5 Palaeocurrents 313

10.6.6 Regional palaeoflow and shelf circulation 318

10.6.7 Cretaceous Oceanic Anoxic Events: Links to Carpentaria Basin stagnation and anoxia during the Albian (stage 3)? 320

10.7 Shallow-marine Depositional Systems 322

10.8 Depositional Model 325

10.8.1 Introduction 325

10.8.2 Ideal vertical and lateral trends for coarsening- and shoaling-upwards facies successions 326
10.8.3 Ideal vertical and lateral trends for fining- and deepening-upwards facies successions 328
10.8.4 Development of coarsening- and shoaling-upwards facies successions: shoreface drowning and rapid nondepositional transgression, followed by aggradation and limited progradation 330
10.8.5 Development of fining- and deepening-upwards facies successions: gradual shoreface incision and retrogradation 333
10.8.6 Deviations from the model: The real Mullaman Beds 338
10.9 Comparisons of the Depositional Model with Other Studies 341
10.9.1 Analogues 343
10.10 Chapter Summary 345

References 347

Appendices

1. Field Techniques & Details of the Study Area 1-3
2. New Stratigraphic Names & Definitions 1-5
3. Field Site Table & Expanded Base Maps 1-9
4. Petrographic Descriptions 1-28
5. Geochemical Methods 1-4
6. XRD Results 1-3
7. XRF & Atomic Absorption & ICP Results 1-6

Figures

2.1 Late Albian Palaeogeography 9
2.2 Carpentaria Basin Setting 11
2.3 Mullaman Bed Outcrop Belt 13
2.4 Skwarko's Stratigraphic Scheme 15
2.5 Schematic diagram of Shelf-to-basin Stratigraphic Relationships 20
2.6 Central Carpentaria Basin Stratigraphy 20
3.1 The Three Regions 28
4.1 Map of numbered Field Sites 62
5.1 Location Map for the Northern Region 82
5.2 Legend for stratigraphic sections 84
5.3 Base Map for the ALZ 86

5.4 Correlation Diagram A-A' 87

5.5 Correlation Diagram B-B' 89

5.6 Base Map for the BPRZ 94

5.7 Correlation Diagrams C-C' and D-D' 96

5.8 Correlation Diagram E-E' 100

5.9 Correlation Diagram F-F' 103

5.10 Correlation Diagram G-G' 106

5.11 Composite Sections and Correlation in the Northern Region 109

6.1 The Central Region of the Study Area 113

6.2 Location Map for the Central Region 114

6.3 Correlation Diagram H-H' 116

6.4 Correlation Diagram I-I' 119

6.5 Correlation Diagram J-J' 123

6.6 Correlation Diagram K-K' 127

6.7 Correlation Diagram L-L' 131

7.1 The Southern Region of the Study Area 139

7.2 Location Map for the Southern Region 141

7.3 Correlation Diagram M-M' 142

7.4 Correlation Diagram N-N' 143

7.5 Correlation Diagram O-O' 148

7.6 Correlation Diagram P-P' 151

7.7 Correlation Diagram Q-Q' 157

8.1 Drillhole Location Map 168

8.2 Regional Correlation of Composite Sections 171

8.3 Comparison of Composite Sections and Stratigraphic Nomenclature 176

8.4 Stratigraphic Correlation on Groote Eylandt 181

8.5 Location Map for Groote Eylandt 183

8.6 Stratigraphic Correlation of the Numbulwar Drillhole Sequence 186

8.7 Shelf-wide Stratigraphic Framework 190

8.8 Shelf-to-basin Regional Correlation 195

9.1 Regional Sequence Stratigraphic Correlation on the Shelf 204

9.2 Sequences, Systems Tracts, and Age of Sequences 206

9.3 Sequence Stratigraphic Evolution of the Mullaman Bed Succession 214, 218, 221, 228, 234

9.4 Cretaceous Relative Sea Level Curve for the Western Shelf of the Carpentaria Basin 244

9.5 Comparison of Northern Australian Sea Level Curves 247

9.6 Comparison of Carpentaria Basin, Northern Hemisphere, and Global Sea Level Curves....254
10.1 Location of Basement Terrains....278
10.2 Late Jurassic to Early Cretaceous Palaeogeography of Australia....280
10.3 Stage 1 Shorelines: Aptian....282
10.4 Stage 1 Palaeogeographic Sketch Map....284
10.5 Stage 2 Shorelines: ?Early Albian....286
10.6 Stage 2 Palaeogeographic Sketch Map....287
10.7 Stage 3 Shorelines: Late Early Albian to Middle Albian....289
10.8 Stage 3 Palaeogeographic Sketch Map....290
10.9 Stage 4 Shorelines: Late Albian to Latest Albian....292
10.10 Stage 4 Palaeogeographic Sketch Map....293
10.11 Stage 5 Shorelines: ?Early Cenomanian....295
10.12 Stage 5 Palaeogeographic Sketch Map....296
10.13 Stage 6 Shorelines: ?Middle Cenomanian....298
10.14 Stage 6 Palaeogeographic Sketch Map....299
10.15 Late Cretaceous Regional Shorelines....300
10.16 Biofacies Model for Aptian-Albian Northern Australian Basins....310
10.17 Typical Shallow-marine Profile....310
10.18 Palaeocurrent Plots for Stage 3....314
10.19 Palaeocurrent Plots for Stages 1, 4, and 5....316
10.20 Schematic Shelf Profile of the Western Carpentaria Basin....324
10.21 Idealised Coarsening- and Shoaling-upwards Depositional System....327
10.22 Idealised Fining- and Deepening-upwards Depositional System....329
10.23 Model for the Evolution of Coarsening- and Shoaling-upwards Depositional Systems....331
10.24 Model for the Evolution of Fining- and Deepening-upwards Depositional Systems....334

Tables

3.1 Cretaceous Facies of the Western Carpentaria Basin....30
4.1 Cretaceous Facies Successions of the Western Carpentaria Basin....60
8.1 Previous Workers' Biostratigraphic Data from Mainland Macrofossils....164
8.2 Previous Workers' Biostratigraphic Data from Mainland Microfossils....165
8.3 Biostratigraphic Data from Groote Eylandt Microfossils and Macrofossils....166
8.4 Biostratigraphic Data from Mainland Microfossils in this Study....167
9.1 Nature and Amount of Erosional Relief along Sequence Boundaries....207

9.2 Age and Thickness Variation of Sequences by Area 212

9.3 Summary of Depositional Sequences and their Internal Composition and Age 245

10.1 Major Mainland Basement Blocks which affected Cretaceous Palaeogeography 279

10.2 Clay-mineral Trends in Marine Facies Successions of the Mullaman Beds 301

10.3 Shallow-marine Depositional Systems on the Shelf 323

10.4 Rock Type and Processes within Shallow-marine Depositional Systems on the Shelf 325

Plates

1. Outcrop Exposures of the Mullaman Beds ..... between 18 & 19

2. Sedimentary Facies (1-8) ..... between 29 & 30

3. Sedimentary Facies (9-16) ..... between 39 & 40

4. Sedimentary Facies (18-22, and ferricretes) ..... between 50 & 51

5. Facies Successions (1-3) ..... between 62 & 63

6. Facies Successions (4-8) ..... between 70 & 71

7. Plant Fossils and Trace Fossils ..... between 163 & 164

8. Shelly Fossils ..... between 164 & 165

9. Stratal Discontinuities-Flooding Surfaces ..... between 203 & 204

10. Stratal Discontinuities-Sequence Boundaries ..... between 207 & 208

11. Parasequences/Facies Successions ..... between 224 & 225

12. Sedimentary Features Suggestive of Ice-rafting ..... between 273 & 274

13. Sedimentary Features of Storm-dominated Sedimentation ..... between 306 & 307

14. Photomicrographs ..... between 312 & 313

15. Photomicrographs ..... between 312 & 313

ABSTRACT

Cretaceous rocks are exposed intermittently as mesas and plateaus along the western and southwestern margins of the Gulf of Carpentaria in the Carpentaria Basin of northern Australia. The rocks form an undeformed clastic succession which accumulated on a broad, gently sloping shallow-marine shelf. This western shelf occupied part of an extensive Cretaceous intracratonic seaway, the Great Artesian Basin, which covered much of central and northern Australia.

This thesis is a stratigraphically-based study of the nature of the shelf succession and its relationship to surrounding successions of the central Carpentaria Basin and the Great Artesian Basin as a whole. The study provides an integrated stratigraphic framework for the Carpentaria Basin. Regional correlations that underpin the stratigraphic framework have significant implications for targeting zones of sedimentary mineral enrichment, and for providing stratigraphic ties in an area where such data are highly limited.

The rocks are divided into a series of lithofacies, which in turn are grouped into vertical facies successions. Most of the lithofacies occur in distinct coarsening- or fining-upward cycles. It is argued that the formation of such cycles was primarily controlled by changes in relative sea level. The shelf had a very low gradient, and did not experience any significant tectonic uplift or deformation during its depositional history. The Cretaceous sea transgressed across the low-lying exhumed topography formed by eroded Proterozoic rocks of the McArthur Basin. Local palaeogeography controlled the extent and shape of the Cretaceous sea during periods of high relative sea level. There was local rapid accumulation of coarse-grained facies in proximity to topographically-high basement terrains at times, but much of the shelf was characterised by low rates of sediment supply. Stratal geometries, petrography, ichnofacies, and sedimentary structures indicate that high-energy storm-dominated depositional environments occurred on many parts of the shelf. This combination of factors led to intense reworking of early deposited rocks and semi-lithified sediment, resulting in the formation of numerous erosional discontinuities and complex lateral facies changes within the succession.

The facies successions exhibit characteristic stacking patterns, thickness trends, and stratal geometries with respect to bounding discontinuities (unconformities, disconformities, and marine flooding surfaces). In most places facies successions correspond to parasequences, and there are at least 25 stacked, regional parasequences in the shelf succession. The parasequences have recognisable stacking patterns and form systems tracts, which in turn are grouped into six major depositional sequences (third-order cycles) bounded by six regional sequence boundaries. The exact timing and duration of many of these sequences are poorly resolved due to a general lack of biostratigraphic control, but the duration of the parasequences is estimated as being considerably less than 1 million years. As such, these cycles represent a fourth-order or higher cyclicity (for thinner sub-cycles), and their origin must be related to some high-frequency mechanism that occurred over the 20 million year depositional history of the shelf.

Documentation of regional stratigraphic correlations enables construction of a relative sea level curve for the western shelf of the Carpentaria Basin. This curve is related to variations in grain size, thickness, and sedimentary structures of parasequences, and shifts in their stacking patterns. This curve, encompassing the Aptian-Cenomanian interval, has close correspondence with other Cretaceous regional sea level curves for the Great Artesian Basin. An advantage of this study over previous studies is that the shelf was very sensitive to even small changes in relative sea level due to its extremely low gradient. Thus, a detailed knowledge of the lithostratigraphy in this study has resulted in the most detailed documentation of the sea level history of the region. There is good correspondence in part between sea level curves for the Carpentaria Basin and the northern hemisphere (and global cycle charts), but this correspondence diminishes towards the end of the mid-Cretaceous. Judging by the matches and mismatches of the various sea level curves, Aptian and Albian relative sea level variations in the Carpentaria Basin record a eustatic signal, whereas late Albian and younger relative sea level variations are dominated by a tectonic overprint for northern Australia.

The nature of the controlling mechanism(s) for high-frequency relative sea level changes on the western shelf of the Carpentaria Basin is intriguing. The regional extent of the cycles across the shelf and their independence with respect to stratigraphic level and local depositional trends infers that the cycles are allocyclic in origin. The short durations of the cycles, their regional extent and distribution, and their repetition throughout the stratigraphy precludes most known tectonic mechanisms, and a rapid-response glacio-eustatic mechanism is an attractive alternative. The general consensus would be that this is highly unlikely, because the climate during the Cretaceous Period is commonly regarded as having been warm and equable, with little or no ice in existence (hence no potential for glacioeustasy). However, sedimentological and palaeontological evidence in this study combined with known isotopic data indicate that the waters of the Carpentaria Basin were cool to cold, and that winter freezing occurred. Furthermore, the discovery of ice-rafted debris in fine-grained marine rocks on the shelf during this study is significant for understanding the palaeoclimate. Most likely, seasonal icefloes were responsible for rafting coarse clastic debris into the deeper basin.

Change in the amount of this type of ice is unlikely to have had much affect upon sea levels within the Carpentaria Basin on its own. More likely, the relative sea level changes apparent in the Carpentaria Basin are due to a combination of factors. Such a combination may have been short-term, high-frequency changes in groundwater storage and ice volume, superimposed upon a longer-term tectono-eustatic signal. Whatever mechanism is invoked, it must be able to account for the numerous, significant relative sea level changes that had such a marked effect upon sedimentation on the western shelf of the Carpentaria Basin. It is argued that the rate of transgression, and storm-dominated sedimentary processes are important in controlling the thickness and style of high-frequency cycles and shallow-marine depositional systems on the shelf. This has broad implications for discerning sea level histories from preserved stratigraphic architecture in many other shallow-marine settings.

STATEMENT

This work contains no material which has been accepted for the award of any other degree or diploma in any university or other tertiary institution and, to the best of my knowledge and belief, contains no material previously published or written by another person, except where due reference has been made in the text.

I give consent to this copy of my thesis, when deposited in the University Library, being available for loan and photocopying.

Andrew Krassay, September 1994

ACKNOWLEDGEMENTS

In undertaking work towards this thesis I have benefited greatly from assistance, advice and technical support given by a large number of individuals and organisations.

I thank Prof. Larry Frakes for his supervision of the project, for his friendly advice and continual encouragement, for his tireless reviews of drafts of the manuscript, for numerous lively discussions about the project and the science in general, and for his stimulating company and support during parts of the fieldwork.

I thank Dr. Brian McGowran, Dr. Neville Alley, and Barrie Bolton for their valuable input into the thesis review process. I acknowledge the support and advice from Dr. Yvonne Bone and Dr. Victor Gostin regarding general thesis matters and for helping the progression of my studies during my time at the Department of Geology and Geophysics, University of Adelaide.

I thank staff members of the Department of Geology and Geophysics at the University of Adelaide for their technical support throughout the study, in particular: Rick Barrett for photography and computing, Sherry Proferes for drafting, John Stanley, Chris Badcock, and Phil McDuie for geochemistry, Geoff Trevelyan and Wayne Mussared for preparation of rock samples, and Sophie Craddock for her friendly secretarial assistance over the years.

I thank reviewers for critically reading drafts of the manuscript and associated papers, in particular: Prof. Robert Dott, Jr., Dr. Jane Francis, Dr. Brian McGowran, Dr. Albert Brakel, Ian Sweet, Colin Pain, and other anonymous reviewers.

In the course of this study much time was spent in the field. For this aspect of the study I am grateful to Harald Barents and other staff of B.H.P. Minerals Ltd. Co. for their financial and logistical support of the fieldwork. I thank Barry Pietsch, Tania Madigan, Dave Rawlings, Dr. Peter Haines (NTGS) and Ian Sweet, Ken Plumb, and Peter Pieters (AGSO) for good company and valuable discussions of the geology at the field camps. Special thanks are due to our helicopter pilot Adrian Wagg who ferried us across the study area over some treacherous terrain with great skill. I also thank the traditional landowners of the Arnhem Land Aboriginal Reserve for permission to access their land, and for allowing us to camp at various outstations.

To my friends in the Geology Department I give special thanks for their company and shared thesis (and other) joys and woes over the years of university life, especially Bunge, Martin, Kathy, Bernd, Richard, Graham, Gary, Chris, and my housemates of the legendary 1st Ave.

Lastly, and most importantly, I am very grateful to my parents who supported and encouraged my university career at all times, and to Jules who has provided great moral support, has shared (coped with) all my moods during the study, has helped me with typing, collating, and artwork, and has always been able to keep me sane and happy.

UNIVERSITY OF ADELAIDE LIBRARY

1. INTRODUCTION

1.1 GENERAL INTRODUCTION

Sedimentary rocks found in shallow epicratonic seas near passive margins probably provide the best record of the evolution of marine shelves and ramps over time in response to changes in the major variables (sea level, sediment supply, subsidence). The depositional architecture of such shelf or ramp successions is strongly controlled by the superimposed effects of these variables, which may change in relative importance during the evolution of any shallow-marine setting. The critical question is whether one can distinguish the signal and effects of each separate variable from the total sedimentary response.

Changes and variations in most sedimentary features within such shallow-marine successions can be related in some fashion to the interplay of these variables, and the extent to which these variables affect the depositional environment is commonly a function of other complex processes such as climate change, regional tectonics, and eustasy. With the advent of sequence stratigraphy and allied methods and techniques in recent years, much progress has been made in understanding the relationships and feedbacks between these variables in sedimentary environments, particularly in siliciclastic shallow-marine settings. However, the inter-relationship of these variables in the evolution of most sedimentary successions is very complex and varies both on short- and long-time scales.

A potentially useful approach (one which has been adopted in many of the latest research projects, *e.g.* Brown, 1993) is to select the study area so as to minimise the number of variables which must be considered, or at least so that one or more of the variables is of subordinate importance. Broad shallow-marine seas which formed in tectonically quiescent areas (such as the western Carpentaria Basin) during recognised global intervals of high sea level, such as during the Cretaceous Period, provide such an opportunity. An attempt is made to utilise this approach in the present study, but the potential power and applicability of the approach was not immediately recognised in this case because the nature of the shelf succession was virtually unknown, and there was no prior knowledge about which sedimentary process(es) had actually controlled the development of the sedimentary succession of the western Carpentaria Basin.

1.2 HIGH-FREQUENCY CHANGES IN RELATIVE SEA LEVEL IN SHALLOW-MARINE SETTINGS

It is generally accepted that long-term changes (10-300 m.y.) of sea level (first- and second-order cycles) are due to tectono-eustasy (Hallam, 1984; Pitman, 1978). The driving mechanism for tectono-eustasy involves variations in the volume of ocean ridges resulting from changes in spreading rates, varying lengths of spreading axes, and evolution of new ridges or subduction of old ridges, which in turn cause variations in the volume of ocean basins and hence fluctuations in eustatic sea level.

The origin of 1-10 m.y. cycles is more problematic, but it is commonly assumed that tectonic processes vary only on long time scales (>10 m.y.), and that high-frequency oscillations of relative sea level are of glacio-eustatic origin (*e.g.* Haq *et al.*, 1988). However, Cloetingh (1988), Cloetingh *et al.* (1985; 1989), and Karner (1986) have proposed that variations in horizontal stresses within the lithosphere can induce vertical motions of tens of metres (resulting in third-order cycles) over a million years or so. In a slightly different model, Cathles and Hallam (1991) suggested that intra-plate horizontal stress changes could cause massive changes in lithospheric density, which might be responsible for eustatic sea level changes and third-order cycles. However, the inherent problem of why the stress field should change repeatedly with a frequency of less than one million years is unresolved.

Epeirogenic movements of continents or parts of continents may also provide a mechanism for short-term variations of relative sea level. However, very little is known about the ultimate cause of such broad-scale uplifts of continental areas, although various models have been proposed (*e.g.* Giunchi *et al.*, 1993; Gurnis, 1993). Many authors propose that epeirogeny is caused by mass transfers or chemical processes in the mantle (*e.g.* Kominz and Bond, 1991; Sahagian, 1987). Recently, it has been suggested that large mantle plumes involving lateral temperature variations may cause lithospheric stretching and rifting and resultant vertical movements of continental lithosphere of up to one kilometre (Caldeira and Rampino, 1991; Davies, 1988; Gurnis, 1990; Larson, 1991a, 1991b). These vertical movements would presumably cause significant changes in sea level, and exert some influence on the deposition of sedimentary cycles in basins surrounding the mantle 'perturbations' (or possibly affecting all basins, *i.e.* truly eustatic).

Other tectonic mechanisms such as geoidal eustasy (Devoy, 1987) and polar wander (Sabadini *et al.*, 1990) have been invoked to explain third-order cycles, but these processes operate on

regional scales and are probably ultimately related to changes in the mantle (similar to other models above). Although third-order cycles are influenced to some extent by processes such as subsidence, thrust-belt tectonics, or basement-involved uplift, in a large number of cases it appears that higher-order fluctuations in relative sea level are ultimately controlled by eustasy (*e.g.* Devlin *et al.*, 1993), and cannot be accounted for by the above tectonic mechanisms. For such higher-order fluctuations in relative sea level, glacio-eustasy (the waxing and waning of continental ice masses) takes over as the most plausible explanation.

A conceptual problem arises for times in earth history when the amount of continental ice is considered to have been negligible, such as during the Cretaceous Period. Rapid relative sea level changes still occurred in these times (*e.g.* Plint, 1991), but true glacio-eustasy seems unlikely to have been the single controlling mechanism. A great deal of current research is aimed at attempting to solve the problem of the nature and origin of high-frequency sea level changes (*e.g.* Brown, 1993) during non-glacial intervals, and their effects (if any) on depositional architecture in shallow-marine settings.

The present study is timely in that it presents a detailed analysis of relative sea level changes and their affects on a Cretaceous shallow-marine succession, in a broad shelf setting which is interpreted to have been unaffected by major tectonic events (at least in northern Australia) for most or all of its history (see discussion in chapters 9 and 10). Whilst it is not possible to completely rule out the potential subtle affects upon relative sea level of Cloetingh-type intra-plate stresses due to irregular subduction of the Australian plate or related tectonic processes, there is no evidence for significant tectonic activity recorded in the Cretaceous rocks or in the evolutionary history of the Carpentaria Basin.

Recently, Gurnis (1994) has shown that the Australian continent was apparently stable for a period of about 50 Ma encompassing the mid-Cretaceous, and was not affected by major epeirogenic movements. Moreover, Gurnis (1994, p. 5) states that "it is clearly not a valid scenario to explain the flooding in the eastern interior seaway (*i.e.* the Great Artesian Basin (GAB)) by a simple vertical translation of the entire continent"; eustasy must have played some role in continental flooding of northern Australia during the Cretaceous. The basin also appears to have had unusually stable rates and types of sediment supply over time, due in part to the lack of tectonic activity and little (if any) Cretaceous uplift in the hinterland, but also to low stream gradients and subdued topography of the coastal regions. The depositional architecture was apparently controlled largely by changes in relative sea level.

Even if the exact timing and duration of relative sea level changes in such a setting cannot be tied down due to inadequate biostratigraphic control, the documentation of stratigraphically-complex shallow-marine successions in tectonically quiescent areas itself provides valuable clues to the nature, timing, and origin of sea level changes and their associated effects upon sedimentary architecture. There is a great need for such physically-based studies, particularly with the current trend toward more common computer modelling of basin and shelf settings, so that the parameters used in the models may be constrained by and checked against real-life examples.

1.3 THESIS SETTING, AIMS AND APPROACH

This thesis is based on the study of a stratigraphically-complex shelf succession which accumulated in a large intracratonic epeiric sea (Great Artesian Basin seaway) in northern Australia in Cretaceous time, in a setting analogous to parts of the Cretaceous Western Interior Seaway of North America. The western margin of the Carpentaria Basin in the northwestern part of the Great Artesian Basin seaway was one of a number of broad, low-gradient shallow-marine depositional environments which were created by large-scale transgression and inundation of continental landmasses during the time of global high sea level in the Cretaceous.

After retreat of the sea in Late Cretaceous time (Dettmann *et al.*, 1992), the area was emergent and Cretaceous rocks were subjected to a lengthy period of erosion and weathering. The result of these processes is that the Cretaceous shelf succession is preserved as erosional remnants, in the form of mesas and plateaux, over an area of approximately 150,000 km^2 along the western and southwestern margins of the Gulf of Carpentaria. Due to the nature of the outcrop, the distance between investigated localities varies between several hundred metres and tens of kilometres, and is in most cases several kilometres.

Shallow-marine depositional processes that operated in large, epeiric seaways such as the Great Artesian Basin seaway and the Western Interior Seaway of North America, showed considerable variability. Local palaeogeography, tectonic movements, and palaeoclimate controlled the wind and current parameters (Ericksen and Slingerland, 1990). These in turn determined whether the seaway was storm-, wave-, or tide-dominated, or a combination of the three. Superimposed on changes in relative sea level, this combination of parameters controlled the depositional architecture of the sediments. Examination of preserved lithologies and sedimentary structures within such seaways is imperative for determining the controls on deposition of any ancient shelf succession.

The large extent of the Great Artesian Basin, a scarcity of adequate subsurface information, and the limited exposure of many rocks has resulted in a poor understanding of all aspects of this the ancient seaway. To improve this, the thesis has the following broad aims:

1) to make a detailed description and analysis of the shelf succession in terms of physical properties, sedimentary structures, petrology, geochemistry, biological components, and source characteristics of sedimentary particles;
2) to identify the nature of controls on sediment transport, deposition, and accumulation (particularly for the marine realm, which once occupied the bulk of the study area);
3) to develop a comprehensive palaeogeographic reconstruction for the study area;
4) to define the evolutionary history of the shelf over time;
5) to identify or constrain the origin of high-frequency relative sea level changes which effected the area (and surrounding GAB) using palaeoclimatic, sedimentologic, and palaeogeographic analyses and hypotheses developed as part of the study;
6) to make detailed comparisons of the western shelf of the Carpentaria Basin and its evolutionary history with other shallow-marine siliciclastic successions of broad epeiric seas, and to attempt to advance the state of knowledge of the sedimentary processes in such settings.

The nature of depositional processes in this setting have not been previously documented, and other related settings within the Great Artesian Basin seaway are also poorly understood. The lack of previous detailed stratigraphic work in the region, and the enormous area of exposed Cretaceous rocks, necessitates that this study is regional in scope. Most aspects of the description and related discussion of rocks in this thesis reflect the regional scope of the study, and it is only pertinent to focus on particular problems or areas in great detail where they are of fundamental importance to the study as a whole.

The overall thesis approach is to break the study area into three regions, the northern, central, and southern regions. Each of the three regions characterises a particular palaeogeographic zone on the ancient shelf, a fact which was previously unrecognised, but became increasingly apparent as the present study progressed. Rocks were described, and facies informally defined, within each of these regions. Local correlation of measured sections and tracking of lateral facies changes enabled the main facies stacking patterns (facies successions) to be defined and correlated in stratigraphic correlation diagrams.

All available petrological, geochemical, and biostratigraphic data were integrated with sedimentological and stratigraphical data to enable correlation between the regions and erection

of a stratigraphic framework for the western Carpentaria Basin. The whole stratigraphic framework was reassessed and is then discussed in terms of stratal geometry and sedimentary processes in order to document the sequence stratigraphic evolution of the shelf succession. Local and regional palaeogeographic reconstructions of the shelf were then developed and were related to the lithostratigraphic framework, sequence stratigraphic framework, and the preserved depositional architecture and sedimentology of the shelf succession.

1.4 THESIS OUTLINE

This thesis is based on extensive fieldwork, measurement of sedimentary sections, and associated laboratory-based geochemical and petrological work. The outcrops investigated cover an enormous area of the eastern Northern Territory and northwestern Queensland, and form isolated erosional remnants commonly separated by large distances. For this reason field maps were not made, but most detailed observations of the rocks are recorded on measured sections, of which over two hundred were measured in this study, along with numerous other field observations. All hand specimens, thin sections, polished sections, rock powders, and clay-mineral XRD mounts are stored in the University of Adelaide, Department of Geology and Geophysics under the accession number 899-. The scientific methods and techniques used in this study, numerical results of geochemical analyses, and detailed tables of sample locations and field sites are all presented in appendices at the end of the thesis.

Chapter 2 provides the regional setting of the study area, and details of field techniques, physiography, and cultural features of the study area are presented in Appendix 1. An early and fundamental part of the study was to fully describe the rocks of the western Carpentaria Basin, and a large amount of time was spent devising an informal subdivision for these rocks that was truly representative of the entire shelf. Chapter 3 provides the detailed description of the entire Carpentaria Basin shelf sequence, with division of the sedimentary sequence into a number of facies. Interpretation of the depositional environments and salient features of each facies are also presented there.

Chapter 4 groups these facies into facies successions, which are recognisable on a regional scale and reflect important facies changes brought about by changes (both lateral and temporal) in the depositional environments. Local correlations of facies successions and individual facies provide an understanding of the depositional environments and palaeogeography on a local to semi-regional scale. This in turn enables construction of a number of composite

lithostratigraphic sections for subareas of the western and south-western shelf of the Carpentaria Basin.

In Chapters 5, 6, and 7 (which each focus on a different area and palaeogeographic zone on the ancient shelf) detailed stratigraphic correlation diagrams (similar to cross-sections) are constructed with the aid of biostratigraphy, drill-hole data, and extrapolation of seismic data to enable regional correlation and the construction of the shelf-wide lithostratigraphic framework, encompassing the entire outcrop belt (>500 km long) of the exposed shelf succession. Chapter 8 takes the broader view of the regional stratigraphy of the Carpentaria Basin shelf succession, and documents regional stratigraphic correlations and ties to sedimentary successions throughout the Great Artesian Basin seaway, along with correlations to related or connected basins to the north and east.

Chapter 9 discusses and analyses the Carpentaria Basin shelf sequence in terms of sequence stratigraphy to form a sequence stratigraphic framework for the entire shelf sequence, and to document the evolutionary history of the shelf sequence-by-sequence. Here, a relative sea level curve is developed for the western shelf of the Carpentaria Basin, and this sea level history is tied to and compared to northern Australian curves, northern hemisphere curves, and global sea level curves. This exercise attempts to place the sedimentary evolution of the Carpentaria Basin into a regional, Australia-wide, and global context.

Chapter 10 concludes by combining the interpretations of chapters 3 through 9 into a regional synthesis of the dynamics of the depositional environments, and provides a depositional model for shallow-marine depositional systems of the western Carpentaria Basin, and attempts to provide unifying criteria for processes on broad shallow-marine shelves characterised by high-frequency changes in relative sea level. The importance and relevance of storm-dominated sedimentation and storm processes in these settings is established. The model and associated ideas developed here are then compared and discussed in relation to the scientific literature, particularly that concerning sedimentary architecture and depositional processes within other epeiric shallow-marine settings.

~~~~~~
~~~~~~

UNIVERSITY OF ADELAIDE LIBRARY

2. REGIONAL GEOLOGY

2.1 INTRODUCTION

This chapter takes a broad view of the regional geology of the study area, in order to establish the stratigraphic context of the thin erosional remnants of Cretaceous rocks (Mullaman Beds) exposed along the western and southwestern margins of the Gulf of Carpentaria. The stratigraphy of the central Carpentaria Basin succession and the tectonic history of the basin are described and discussed with respect to the onshore rocks of the Mullaman Beds, and the history of the study of these rocks is presented along with important new stratigraphic definitions and correlations developed in the present study.

2.2 BASIN SETTING

The Jurassic to Cretaceous Carpentaria Basin is a classic example of a cratonic-interior basin, and exhibits distinctive features of such settings including basin configuration as a broad depression overlying older sags between basement blocks, and slow overall rates of flexural subsidence (Klein and Hsui, 1987). The basin is located within northern Queensland and the Northern Territory, and is essentially a north-south trending depression, the northernmost of three main interconnected Jurassic-Cretaceous downwarps which formed the Great Artesian Basin (Fig. 2.1). Marine connection was not maintained at all times, because the Euroka Arch (Fig. 2.2) occasionally barred full circulation between the Carpentaria and Eromanga Basins (Smart *et al.*, 1980). In general the Carpentaria Basin, closest to the northern marine connection with the open ocean, was affected greatly by marine circulation, fair-weather waves and tides, and storm processes, whereas generally quieter marine sedimentation characterised much of the southern portion of the Great Artesian Basin seaway south of the Euroka Arch.

The Carpentaria Basin has dimensions of about 1000 km north-south and 650 km east-west, covering an area of approximately 600,000 km^2 (Burgess, 1984). The margins of the basin closely follow the coastline of the present day Gulf of Carpentaria (Fig. 2.2). The western margin of the Carpentaria Basin was a hingeline during Early Cretaceous subsidence (Smart *et al.*, 1980), and sediments eastward of this fault bounded margin were relatively structurally undisturbed (Passmore, 1979). The eastern margin of the basin is bounded by Precambrian

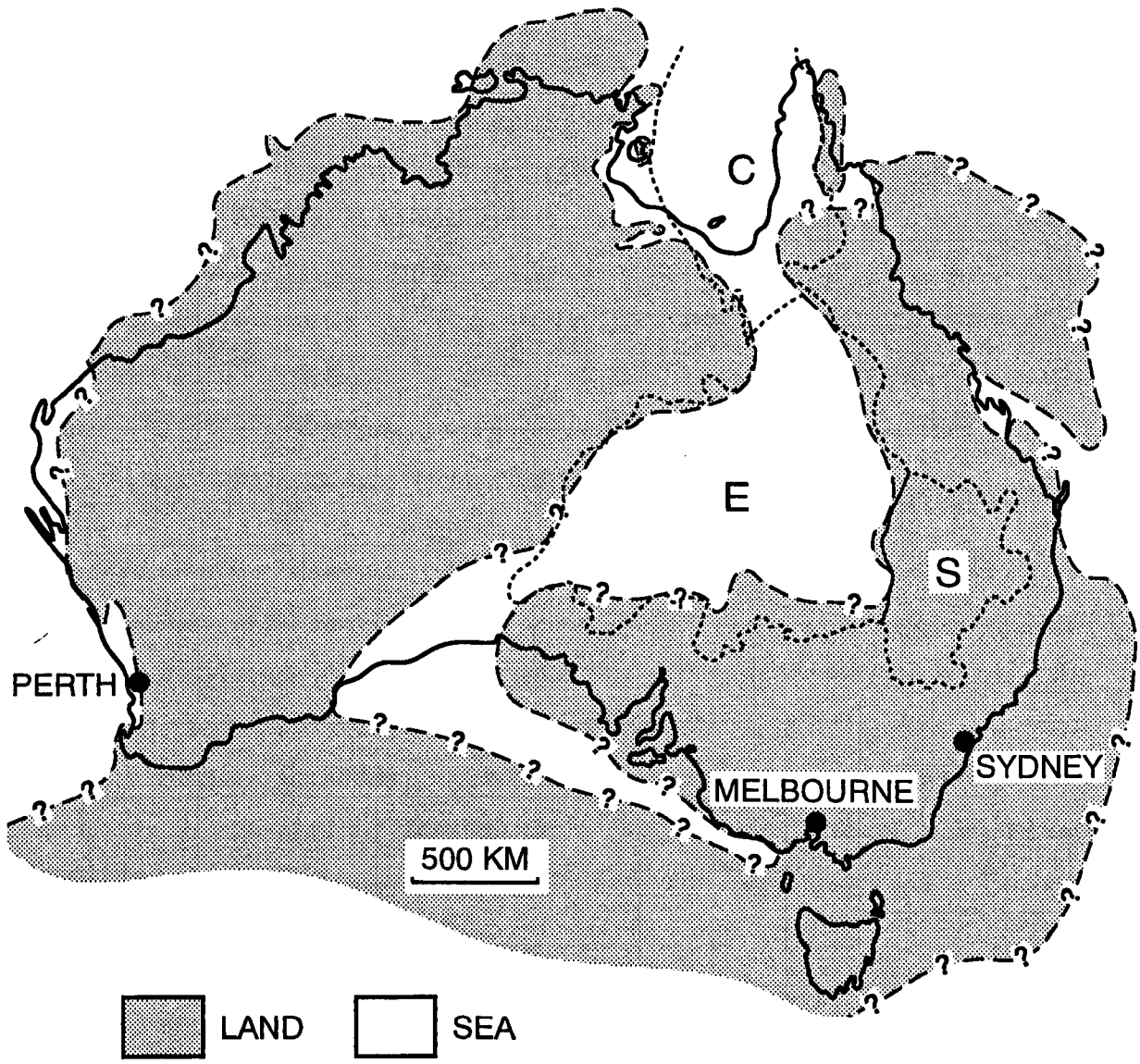

FIGURE 2.1. Late Albian palaeogeography of Australia. Outlines of Carpentaria (C), Eromanga (E), and Surat (S) Basins, which together form the Great Artesian Basin, are shown by thin dashed lines. Late Albian regional shorelines are shown by bolder dashed lines. Dashed lines with question marks represent regions where shoreline position is uncertain. Modified from Frakes *et al.* (1987).

igneous rocks of the Coen, Yambo, and Georgetown Inliers, together with Carboniferous igneous rocks of the Cape York-Oriomo Ridge (Fig. 2.2).

To the north, the Carpentaria Basin is in probable lithologic continuity with the Morehead Basin (Fig. 2.2). A probable tie to the Laura Basin occurs in this region to the north of the Coen Inlier. To the south, over the Euroka Arch, the sediments are continuous into the Eromanga Basin. According to Smart *et al.* (1980) deposition was generally continuous over the Euroka Arch, with subsidence away from the basement structure on either side. For detailed correlations of units between the Carpentaria and Eromanga Basins on the basis of lithology and biostratigraphy the reader is referred to Senior *et al.* (1978) and Morgan (1980), respectively. Furthermore, comprehensive summaries of geological aspects of the Eromanga Basin, the sister basin to the Carpentaria Basin, are presented in a symposium volume (Gravestock *et al.*, 1986).

There is little, if any, relationship between sedimentation in the Carpentaria Basin and the Money Shoal Basin to the west because the two sedimentary regimes were separated by an extensive structural barrier. The eastern margin of this barrier, the Wessel Rise, was an active high from Late Cambrian to at least Tertiary times (Smart *et al.*, 1980). Onshore, in the west, the Carpentaria Basin is flanked by Precambrian rocks of the Arnhem and Mount Isa Blocks, and Proterozoic sediments of the McArthur Basin, which the shelf succession overlies with angular unconformity. The Mullaman Beds in the study area are partly covered by Cainozoic rocks of the Karumba Basin sequence.

The main structural elements of the Carpentaria Basin were formed during pre-Jurassic movements before major sediment accumulation (Passmore *et al.*, 1992). There is no evidence of structural movement in the basin in Jurassic time, and only minor structural movement occurred in Early Cretaceous time (Passmore *et al.*, 1992; 1993; Smart *et al.*, 1980). Such syn-depositional movements appear to have been limited in extent and influence and had only minor effects on deposition (Passmore, 1979). Structural activity increased in Late Cretaceous-Tertiary time, but still produced only mild deformation within the Carpentaria Basin succession.

2.3 PREVIOUS WORK

The stratigraphy and palaeontology of Cretaceous rocks of northern and central Australia has been the focus of numerous local and regional studies. In many of these studies the Carpentaria, Eromanga, and Surat Basins have been collectively studied as one large basin, the "Great Artesian Basin" of Whitehouse (1954) and Day (1969). There have been far fewer

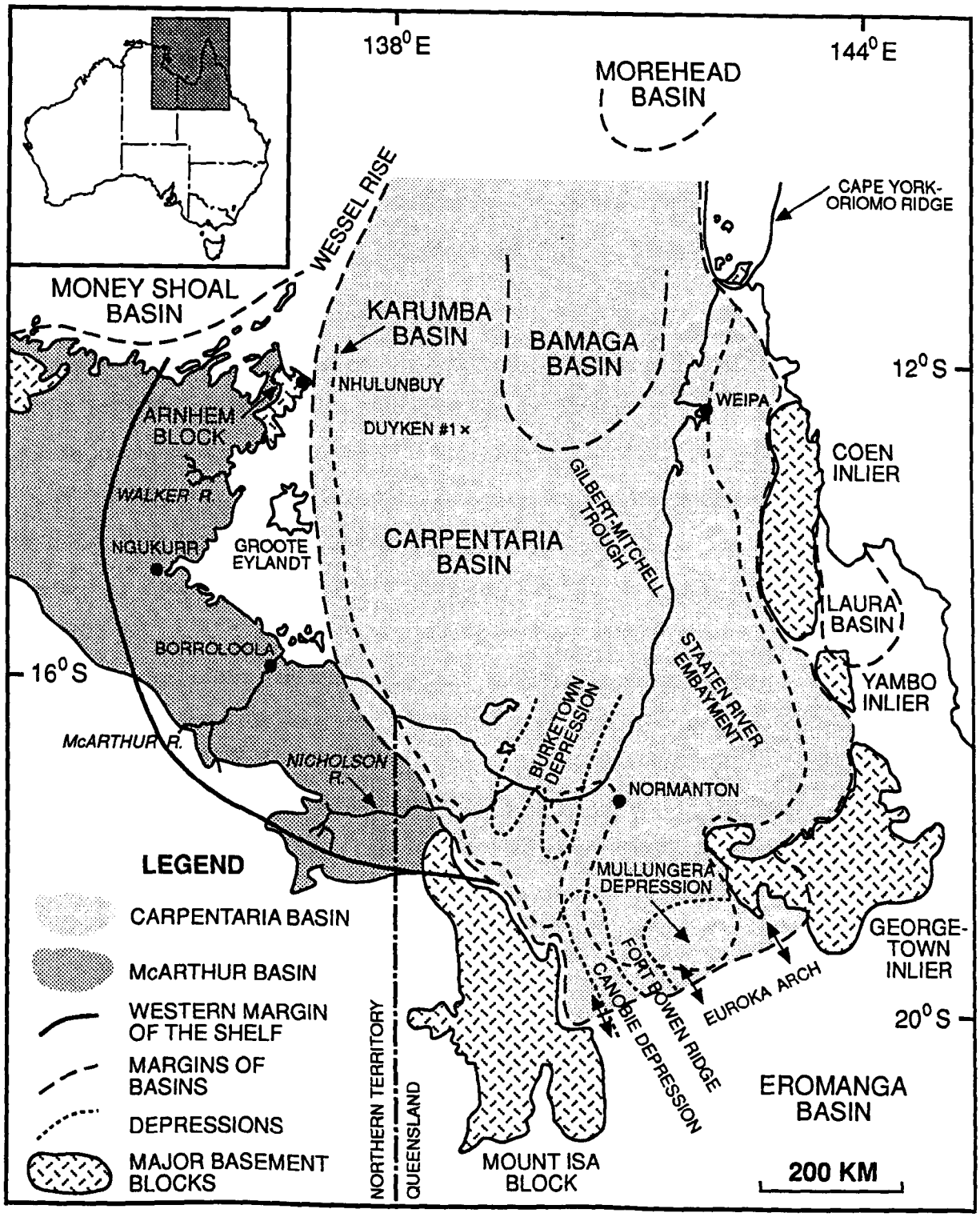

FIGURE 2.2. Geological setting of the Carpentaria Basin. The region of the Carpentaria Basin as recognised by previous workers (*e.g.* Smart *et al.*, 1980), is shown by the dashed line and lightly shaded area. The thick solid line shows the approximate westerly transgressive limit of the Cretaceous sea, near the western edge of the study area. Marine shelf sediments of the Mullaman Beds accumulated to the east of the thick line, and are correlative with central Carpentaria Basin rocks which were deposited in deeper water in the eastern part of the basin. Modified after Thomas *et al.* (1992) and Passmore *et al.* (1992).

studies concentrating on the Carpentaria Basin, and only one study has provided any detail on the stratigraphy and palaeontology of onshore shallow-marine Cretaceous rocks of the western and southwestern margins of the Gulf of Carpentaria, *i.e.* Skwarko (1966).

H.Y.L. Brown was the first geologist to map and describe in detail the Mesozoic strata of the inland Northern Territory, and undertook fieldwork between 1895 and 1908. He also correlated units around Pine Creek and Katherine with those in Darwin. In 1914, H. Jensen mapped the Pine Creek district and separated the Cretaceous units at Darwin from all the inland Mesozoic strata, which he thought possibly ranged in age from the Permo-Carboniferous to the early Mesozoic.

Noakes (1949) proposed that all Cretaceous sediments from Darwin and other coastal areas in the Northern Territory be placed in his Mullaman Group. This group was composed of two units, with all inland Mesozoic strata placed in the lower unnamed unit. Geologists from the Bureau of Mineral Resources (BMR) later down-graded this term to Mullaman Beds in line with the Australian code of stratigraphic nomenclature (Skwarko, 1966). In the course of this work, a large number of separate Cretaceous rock types, and some Jurassic rocks, were mapped as Mullaman Beds (Fig. 2.3). This ill-defined grouping of all so-called Cretaceous rocks has led to a poor understanding of the field appearance, age, and stratigraphic relationships of onshore Cretaceous rocks throughout the Northern Territory and much of northwestern Queensland.

Skwarko (1966) examined the palaeontology, and to a lesser extent the stratigraphy, of the Mullaman Beds as the basis for his Ph.D thesis. His study is the only detailed one concerning the Mullaman Beds, except for local studies by geologists from mineral exploration companies. A summary of Skwarko's stratigraphic divisions for the Mullaman Beds is presented in Sect. 2.4.

The central Carpentaria Basin succession has been documented by Doutch (1976), Passmore (1979), Smart (1976), and Smart *et al.* (1980), but none of these studies contains any detail regarding the onshore Cretaceous rocks of the western and southwestern parts of the basin, *i.e.* the Mullaman Beds. Similarly, numerous biostratigraphic studies have focused on the Great Artesian Basin or the eastern Carpentaria Basin (*e.g.* Morgan, 1980), but none have attempted detailed correlation of the Mullaman Beds with the Great Artesian Basin succession. However, these prior regional stratigraphic studies established the biostratigraphic framework for the Great Artesian Basin, and this preliminary work assisted important biostratigraphic correlation between isolated onshore localities during the present study.

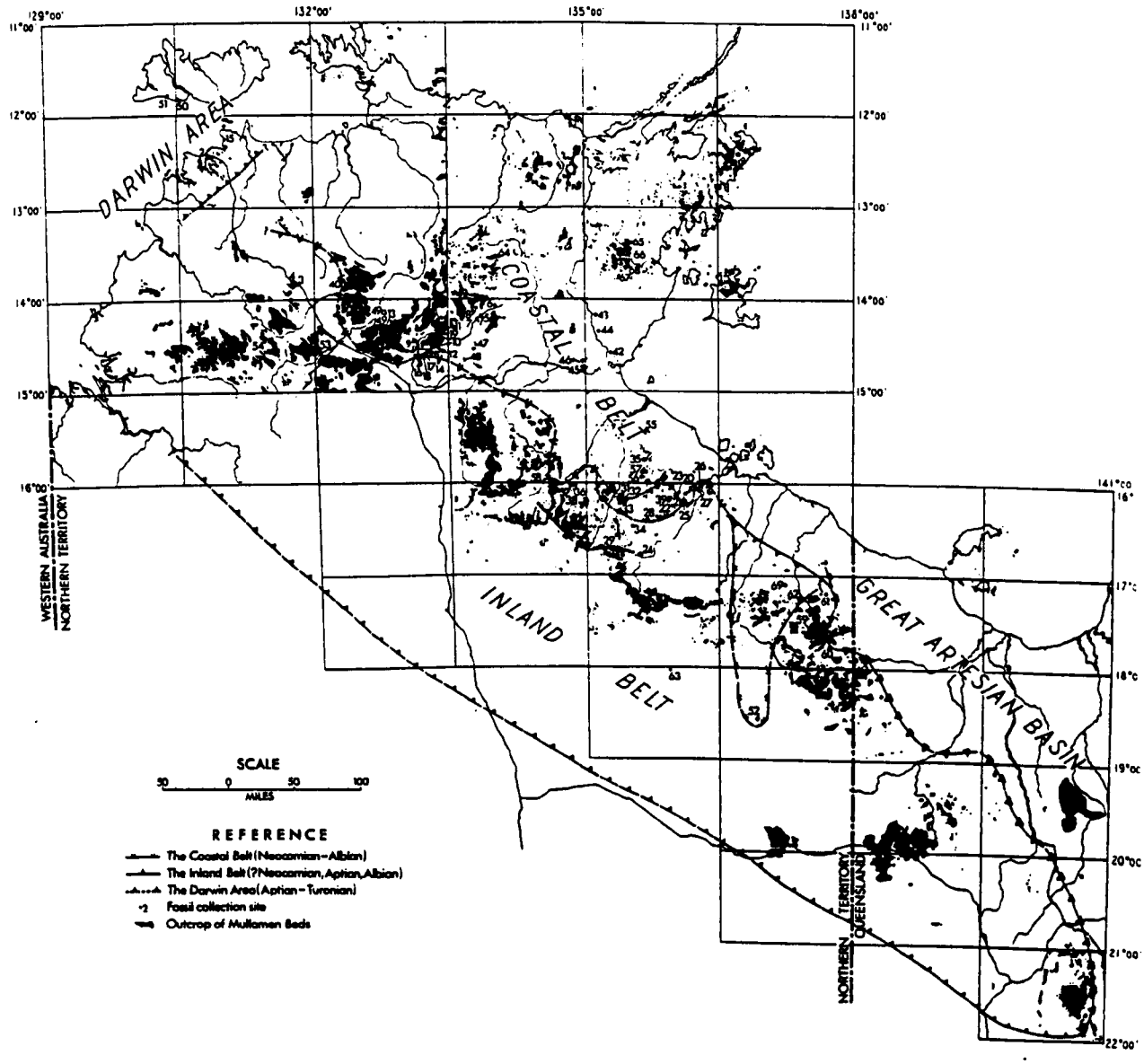

FIGURE 2.3. Outcrop distribution map of the Mullaman Beds along the western and southwestern margins of the Gulf of Carpentaria, Northern Territory and Queensland. Outcrops are shown in black. The superimposed grid of 1:250,000 geological map sheet areas is also illustrated. Skwarko (1966) divided Mullaman Bed outcrops into two broad belts, the "Coastal Belt" and "Inland Belt". Modified from Skwarko (1966).

The biostratigraphic framework for the Great Artesian Basin relies on early studies of molluscan fossils, especially ammonites, which were used in attempts to subdivide the mudstone sequences of the Great Artesian Basin (*e.g.* Whitehouse, 1926), including the Carpentaria Basin, into two units; the Roma and overlying Tambo Series. This division was developed further by Ludbrook (1966) and Day (1969) in establishing biostratigraphic frameworks related to the rock nomenclature of the time.

Both Ludbrook (1966) and Day (1969), and to a lesser extent others like Crespin (1963), realised that the accuracy in applying European stage names (*e.g.* Aptian, Albian) was limited by the endemic nature of the molluscan faunas; even pelagic belemnites and some of the ammonites were restricted to Australasia (Paltech, 1980a). In subsequent studies most attention focused on microfossils, which have proved to be more useful for biostratigraphic zonation in the Great Artesian Basin. These studies include detailed studies of foraminiferal faunas (Haig, 1979a, b; Haig and Lynch, 1993; Scheibnerova, 1976) and dinoflagellates and microfloras (Burger, 1973; 1982; 1986; Dettmann and Playford, 1969; Evans, 1966; Helby *et al.*, 1987; Morgan, 1980). The biostratigraphic framework for the Carpentaria Basin is discussed in more detail in chapter 8.

2.4 PREVIOUS STRATIGRAPHIC NOMENCLATURE

Skwarko (1966) was the first worker to attempt a regional study of Cretaceous sediments along the western and southwestern margins of the Gulf of Carpentaria. His study was based primarily on invertebrate palaeontology and resulted in a division of the rocks into two groups; the generally marine "Coastal Belt" and the generally non-marine "Inland Belt" (Figs. 2.3 and 2.4). Although this two-fold division is simplistic, the rocks studied during this project are roughly equivalent in position to rocks in his Coastal Belt. Many of Skwarko's field descriptions and detailed records of fossil collections are valuable. However, his interpretive age assignments for fossils and enclosing facies of the Mullaman Beds are in conflict with more accurate, reliable biostratigraphic data of this study which is supported by the modern, established biostratigraphic framework for the Great Artesian Basin. In spite of the fundamental problems with biostratigraphic zonations proposed by Skwarko (1966) (see Sect. 8.2.4), his study provides the only real background data for the present study.

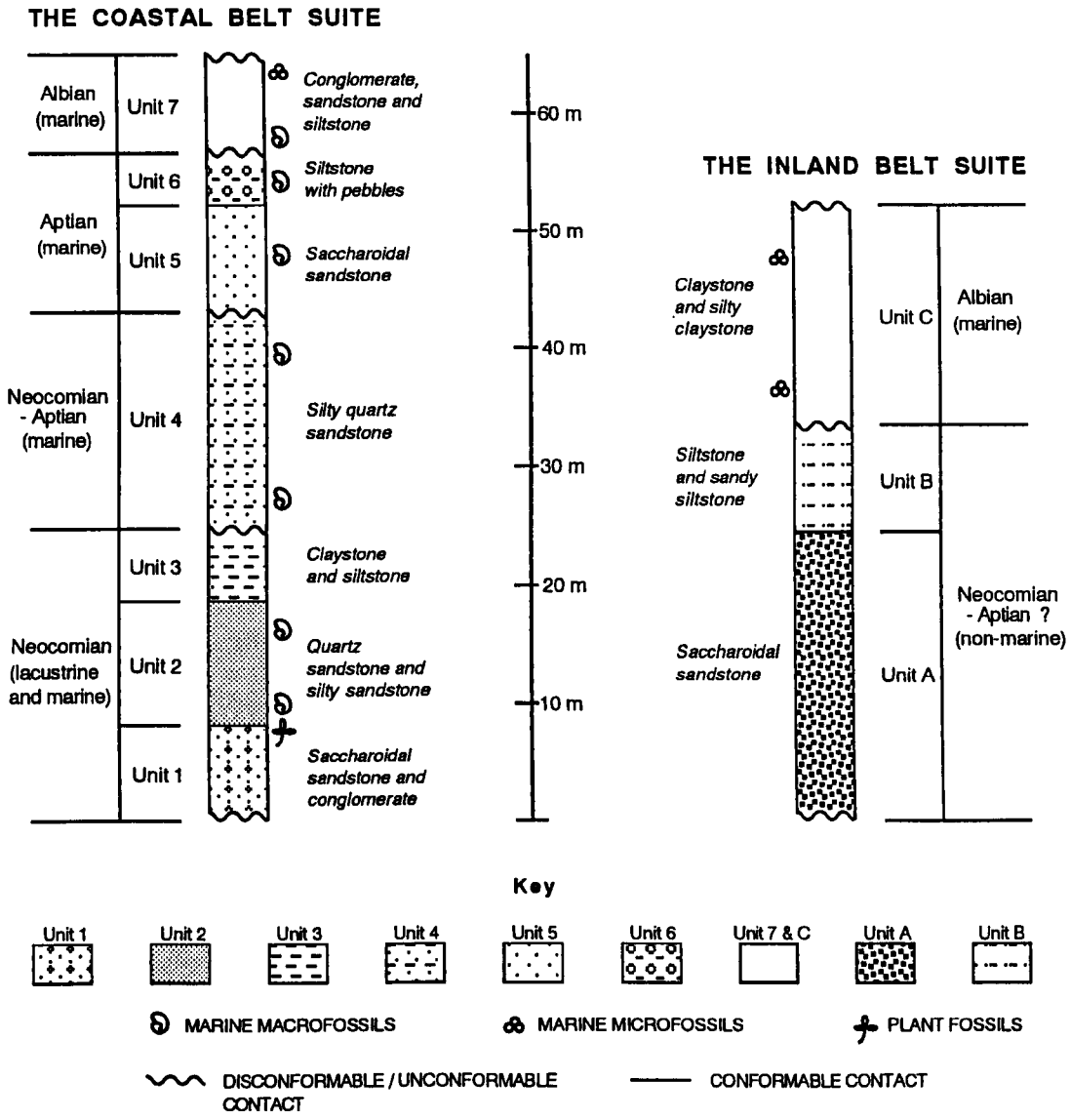

FIGURE 2.4. Skwarko's stratigraphic scheme for the Mullaman Beds. Modified from Skwarko (1966).

2.4.1 The Coastal Belt

Skwarko (1966) recognised seven lithological units within his Coastal Belt Suite (Fig. 2.4). Unit 1 is a middle to early late Neocomian lacustrine sandstone and conglomerate up to 8 m thick which contains indeterminate plant fossils. Unit 2 conformably overlies unit 1 and is a marine quartz sandstone and silty sandstone which grades upward to siltstone or claystone and has a maximum thickness of about 10 m. Unit 2 is richly fossiliferous and contains marine molluscs, brachiopods, corals, bryozoans, echinoids and plant remains. Skwarko's interpretation of the fauna led him to propose a late Neocomian age for unit 2. Unit 3 conformably overlies unit 2 and is a marine siltstone and claystone which is less than 7 m in thickness. Unit 3 is sparsely fossiliferous and contains strongly distorted and compacted indeterminate fossils to which Skwarko (1966) tentatively assigned a late Neocomian age.

The contact between unit 3 and unit 4 is not exposed but the top of unit 3 is invariably an erosional surface, indicating that the observed thickness of 7 m is most likely a minimum estimate. Unit 4 is about 18 m thick and consists of marine silty quartz sandstone with a molluscan fauna, which Skwarko (1966) believed was transitional in age between the Neocomian and the Aptian. The 9 m thick saccharoidal sandstone of Unit 5 occurs as a few scattered exposures with indeterminate plant fossils and a distinct molluscan macro-fauna, which Skwarko regarded as being Aptian in age. Skwarko (1966) did not describe the contact between units 4 and 5. Unit 6 is a 5 m thick Aptian marine siltstone with pebbles and contains a marine molluscan macro-fauna, and wood fragments. The base of this unit is not in contact with unit 5, although Skwarko proposed that they were conformable. The top of unit 6 is an erosional surface, which Skwarko believed to be a regional unconformity. Unit 7 is 8 m thick and is composed of Albian marine conglomerate, sandstone, siltstone, and shale containing numerous marine molluscan macro-fossils and rare plant fossils.

2.4.2 The Inland Belt

Skwarko's Inland Belt Suite is composed of three units, one of which (unit C) is marine and not limited to the Inland Belt (Fig. 2.4). The basal unit A, sometimes known as the Lees Sandstone, is a non-marine sandstone approximately 25 m in thickness. This unit yields a large, long-ranging fossil flora which gives a poorly constrained age of Late Mesozoic. Skwarko (1966) suggested that this unit was probably Neocomian to Aptian in age. Unit B conformably overlies unit A, and is a non-marine siltstone less than 10 m thick containing indeterminate plant fossils. Skwarko proposed an Aptian age for unit B on the basis of

stratigraphical evidence. In some parts of the Inland Belt unit C, also known as the Polland Shale, disconformably overlies units A and B. Unit C is approximately 18 m thick and contains marine microfossils (arenaceous foraminifera) of Albian age. Unit C includes claystone, shale and silty claystone and is equivalent to the upper part of unit 7 of the Coastal Belt (Skwarko, 1966).

2.5 NEW STRATIGRAPHIC NAMES (Walker River Formation and Yirrkala Formation)

Hughes (1978) discouraged the use of the name Mullaman Beds due to the recognised stratigraphic inadequacy of the term in its original form, where it was used to describe most Mesozoic rocks, not just those of proven Cretaceous age, throughout the northeastern Northern Territory. To clarify this confusion, two new names are proposed here to replace the term Mullaman Beds for Cretaceous rocks distributed onshore along the western and southwestern margins of the Gulf of Carpentaria.

The *Walker River Formation* is proposed as the formal name for moderately to well sorted, crossbedded, fossiliferous (containing marine shelly fossils), fine- to coarse-grained quartz sandstone interbedded (typically thinly) with laminated clayey siltstone and chert granule to pebble conglomerate. Most of these rocks represent shallow-marine, transitional marine, and paralic depositional environments.

The *Yirrkala Formation* is proposed as the formal name for poorly sorted, large-scale trough crossbedded, very coarse- to fine-grained matrix-poor quartz sandstone and pebbly sandstone with rare segmented plant fossils. These rocks represent nonmarine depositional environments. It is possible to distinguish between the two units on the basis of fossil content, lithological homogeneity, grain size, sorting, colour, weathering characteristics, matrix proportion and other textural and compositional attributes. Detailed definitions of these two new stratigraphic units are presented in Appendix 2, and are based on a large amount of new stratigraphic data (lithostratigraphic and biostratigraphic correlations) developed in the thesis, and related work (Krassay, 1994a, b).

The new stratigraphic names are introduced in this thesis, but their application and acceptance by the broader geological community awaits approval from the Stratigraphic Names Subcommittee of the Geological Society of Australia, and subsequent presentation in forthcoming publications. This official process is currently underway, but in the interim

period, and for the purposes of this thesis, the rocks will be referred to by the old name of the Mullaman Beds.

2.6 THE CARPENTARIA BASIN: CENTRAL BASIN STRATA AND THEIR WESTERN ONSHORE EQUIVALENTS, THE MULLAMAN BEDS

The maximum thickness of the Carpentaria Basin sequence is 1760 m, of which 1200 m is Jurassic-Cretaceous rocks, and occurs offshore, west of Weipa. However, the thickness of Mesozoic rocks exposed onshore is much reduced; the stratigraphic relationships of the western shelf to the central Carpentaria Basin are schematically illustrated in Fig. 2.5. Detailed ties between the Mullaman Bed succession and the central Carpentaria Basin are developed in this thesis, and are presented in chapter 8.

Cretaceous and Upper Jurassic rocks onshore are restricted in distribution to two main areas. Firstly, sediments of the Gilbert River Formation and the Rolling Downs Group occur at the surface within the Burketown Depression (Fig. 2.2), and along the eastern margin of the Gulf of Carpentaria. These are basinal sediments and generally represent relatively deep-water environments (except for the Gilbert River Formation) with deposition some distance from the palaeoshoreline.

Secondly, sediments of the Mullaman Beds occur as erosional remnants (Plate 1a-h) along the western and southwestern margins of the Gulf of Carpentaria (Fig. 2.3). These sediments are genetically related to basinal sediments but are distinctly different in terms of thickness, sedimentary structures, distribution, and depositional environment. These sediments were probably once continuous with those of the central Carpentaria Basin to the east; Grimes (1974) suggested that the Mullaman Beds were equivalent in time to the Gilbert River Formation and the overlying Wallumbilla Formation, Toolebuc Formation, and Allaru Mudstone. Hughes (1978) suggested ties to the Petrel Formation and the Darwin Member of the Bathurst Island Formation, but this correlation has not yet been substantiated.

The Mullaman Beds accumulated on a broad, low gradient, shallow-water marine shelf which did not always have a fully open-marine connection with the basin centre. Description of sediments deposited within this setting, and documentation of the western and southwestern shelfal depositional environments of the Carpentaria Basin are major objectives of this thesis.

PLATE 1

a Typical outcrop in the northeastern Arnhem Land Zone, showing densely vegetated ridge of laterised Cretaceous sandstone about 10 m-thick. Near site 196, northern region.

b Common type of exposure of Cretaceous rocks in the Bath and Parsons Ranges Zone. Illustrates several coarsening-upward cycles of interbedded sandstone and siltstone of facies succession 2 forming tiers on hillside. Covered intervals represent recessively weathered siltstone. Site 174, northern region.

c Mesa of Cretaceous rocks showing the isolated of nature of the Mullaman Beds compared to Proterozoic basement and patchy Quaternary cover of the surrounding plains. Marine silty sandstones capping the mesa are about 10 m-thick. Near site 81 in the central region.

d 12 m-thick cliff exposure of sandstones of facies succession 6. Dark colouration is due to superficial staining by manganese-oxides due to surface runoff. Site 69, central region.

e Poorly exposed low-lying Cretaceous ridges (typically less than 10 m in height) along the far western edge of the study region. The change in lithology from Cretaceous rocks to unconsolidated Cenozoic sediments is illustrated by the marked change in vegetation from a dense dark-green tree cover to a sparse lighter-coloured scrub cover. Near site 82, central region.

f Wedge of dark-coloured Cretaceous valley-fill conglomerate and overlying marine sandstones resting unconformably (see arrow) against a large dip-slope exposure of Proterozoic sandstones. Such weathered outcrops are common in elevated parts of Proterozoic basement terrains. Site 93, central region.

g Relatively thick Cretaceous sequence exposed as mesas and plateaus scoured by modern drainage channels. The sequence represents the transition from lower nonmarine conglomeratic facies, through transitional sandstones, to a series of marine siltstones and sandstones. The total thickness of the Cretaceous sequence in this area is about 40 m. Helicopter (arrowed) for scale. Site 106, southern region.

h Large mesas and ridges of flat-lying Jurassic and Cretaceous rocks rising above the valley-floor of Proterozoic units in the extreme southeastern part of the study area. Mesa heights are about 30-35 m. Near site 124. southern region.

a

e

b

f

c

g

d

h

2.6.1 Stratigraphy

The broad stratigraphy of the Carpentaria Basin is known from eight onshore petroleum wells, several water bores and one offshore petroleum well, Duyken #1 (Fig. 2.2), but the current geological interpretation of the offshore area is based on extrapolation of geological knowledge from onshore, interpretation of marine seismic data, and integration of factual well-completion data from Duyken #1. Reliable extrapolation from the onshore to the offshore is possible because the lack of structural disturbance within the basin allows confident correlation of reflectors (Burgess, 1984). Extension of the established Eromanga Basin stratigraphy into the Carpentaria Basin is based largely on lithological similarity, although some micropalaeontological control is available along the eastern margin (Burger, 1986; Morgan, 1980).

The main period of deposition within the Carpentaria Basin commenced in the Jurassic with the deposition of fluvial sands. The Jurassic sequence is restricted to a series of basement depressions. As a result of gentle sagging and high relative sea levels, deposition became more widespread during the Cretaceous, and a thick sequence of non-marine grading to marine clastics accumulated over the entire basin. Most of the basin fill is interpreted to have been derived directly from adjacent Precambrian and Palaeozoic highstanding terrains (Doutch, 1976; Smart *et al.*, 1980). A summary of the stratigraphy of the Carpentaria Basin is presented below and in Fig. 2.6, and readers are referred to Doutch (1976), Passmore (1979), and Smart *et al.* (1980) for more detail.

Basement

Basement intersected in the onshore petroleum wells and water bores includes a variety of Archean igneous intrusives and metasediments (Fig. 2.6). Dolomite intersected in Burketown 1 within the Burketown Depression also forms part of the basement sequence to the Jurassic-Cretaceous succession. According to Burgess (1984) the Burketown Dolomite is possibly equivalent to Proterozoic carbonates of the McArthur Group, or may be analogous to similar rocks of Palaeozoic age in the Georgina Basin. Overlying the dolomite in Burketown 1 is a thick unit of probable glacial origin regarded as a tillite (Fig. 2.6), and tentatively dated as Permian based on the glacial nature of the sediment. Finally, some Permian and possible basal Mesozoic rocks have been intersected in scattered onshore shallow drillholes, although the offshore distribution of these sediments is unknown. All petroleum wells in the basin terminated in igneous or metamorphic basement units (Smart *et al.*, 1975).

FIGURE 2.5. Schematic diagram showing thicknesses and stratigraphic relationships of the Mullaman Beds and the Carpentaria Basin depocentre sequence. Modified from Krassay (1994a).

FIGURE 2.6. Stratigraphic column for the central Carpentaria Basin with thicknesses of maior formations shown in metres. Modified from Burgess (1984)

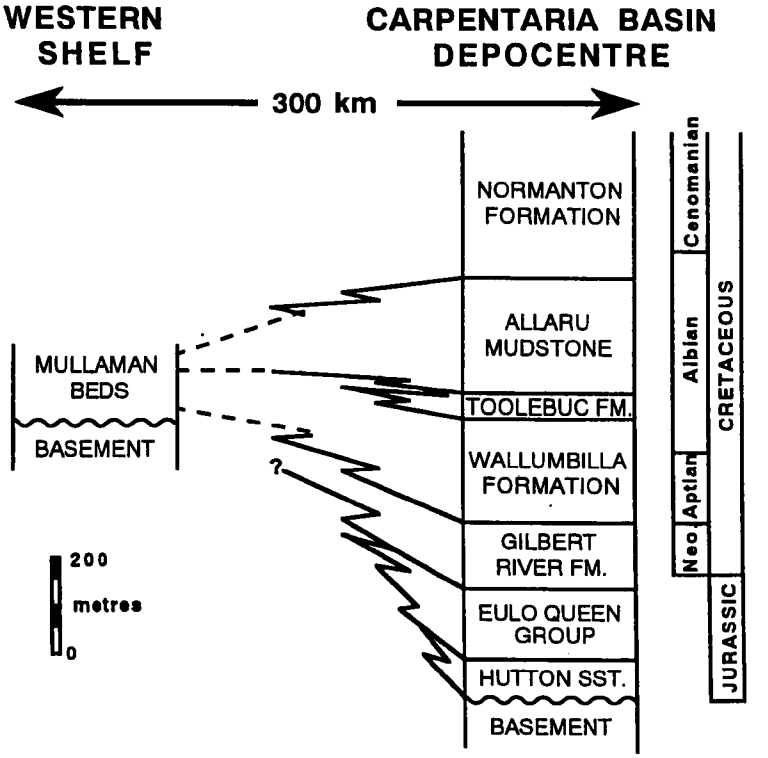

CARPENTARIA BASIN STRATIGRAPHY

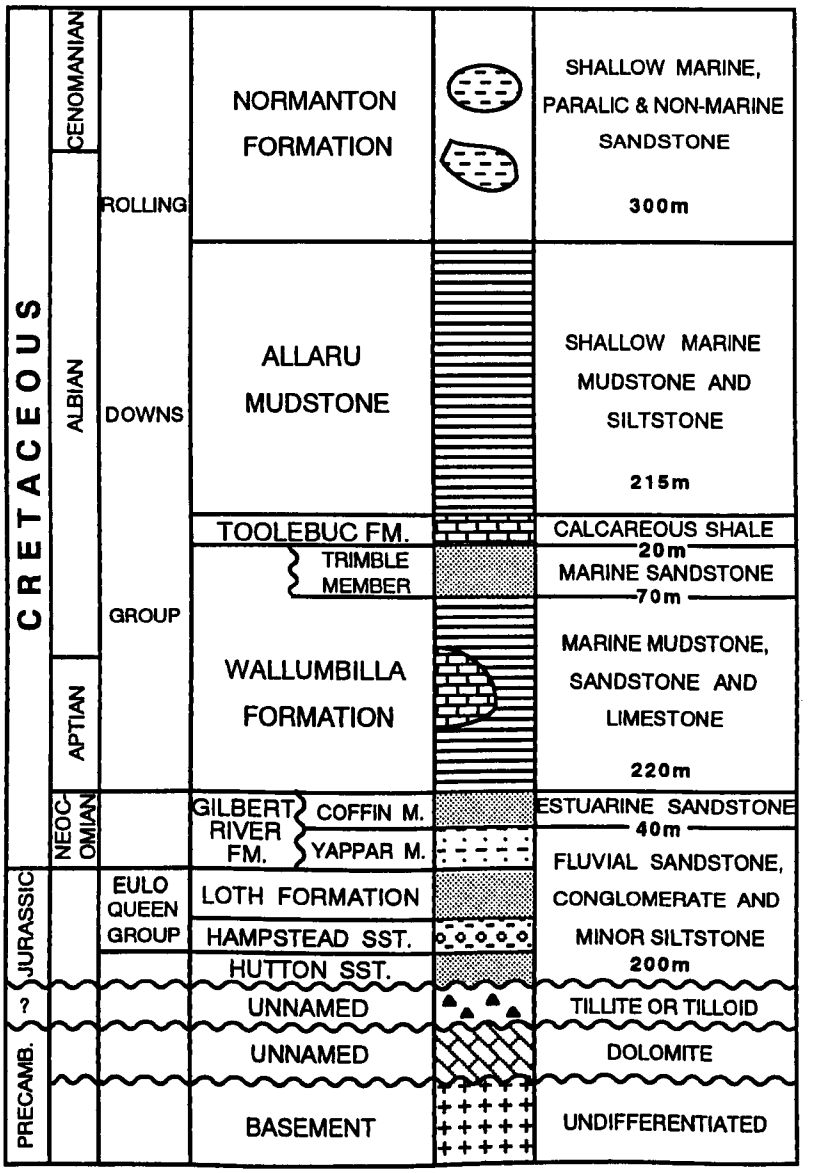

In most parts of the study area the Mullaman Beds are underlain by the thick Middle Proterozoic McArthur Basin succession, which is composed of relatively undeformed sedimentary rocks and minor volcanics. For more detail on the nature of these basement rocks and their structural setting the reader is referred to the comprehensive regional study of Jackson *et al.* (1987), and local studies of Pietsch *et al.* (1991).

Jurassic

The basal unit of the Jurassic-Cretaceous succession in the central Carpentaria Basin is the fluvial Hutton Sandstone (Fig. 2.6), which appears to be continuous into the Eromanga Basin. The Hutton Sandstone was deposited in topographic lows in the western part of the basin where the base Mesozoic unconformity is very rugged and irregular, probably due to karstic topography associated with the Proterozoic-Palaeozoic dolomite. Overlying the Hutton Sandstone is the Middle to Late Jurassic Eulo Queen Group and its equivalents, the Garraway and Helby Beds. The Eulo Queen Group is about 100 m thick and is confined to structurally controlled erosional depressions in the southern part of the basin. It has been divided into two units, the Hampstead Sandstone and the Loth Formation, which are composed of fluvial quartzose sandstone and subordinate siltstone and conglomerate. The Eulo Queen Group is a lateral equivalent of the Injune Creek Group in the Eromanga Basin (Burgess, 1984).

Cretaceous

The Gilbert River Formation is a transitional facies representing the change from non-marine Jurassic sedimentation to marine Cretaceous deposition; it conformably overlies the Eulo Queen Group (Fig. 2.6), or unconformably overlies basement. The formation is divided into two members, the lower 70 m-thick non-marine Yappar Member, and the upper 37 m-thick marine Coffin Hill Member (Smart *et al.*, 1980).

In some areas the Gilbert River Formation is regarded as wholly Cretaceous because the only definite fossil age was obtained from marine (Cretaceous) macrofossils in the Coffin Hill Member (Smart *et al.*, 1980). However, plant fossils in the Yappar Member indicate that the basal part of the Gilbert River Formation may be Jurassic (Smart *et al.*, 1980). The Gilbert River Formation is present as far north as the Weipa area where it passes laterally into the upper part of the Helby Beds, and is equivalent in the south to the Hooray Sandstone in the Eromanga Basin. In the southwest the Gilbert River Formation is overlain by the Wallumbilla Formation (Smart *et al.*, 1980).

The Yappar Member was deposited in a sand-dominated fluvial environment and the lower section consists of clayey, pebbly quartzose sandstone and conglomerate bands, whereas the upper part contains finer-grained sandstone and minor siltstone in thin irregular beds (Burgess and Reford, 1982). The Coffin Hill Member consists of coarse- to fine-grained clayey, quartzose sandstone and siltstone and conformably overlies the Yappar Member. In places the Coffin Hill Member is glauconitic and represents the first transgression of the Cretaceous sea in the region. Some of the earlier fluvial sands and gravels may have been reworked by transgressive erosion during this initial marine inundation of the area. Thin non-economic coal seams have been intersected within the Gilbert River Formation in the eastern onshore Carpentaria Basin (Burgess, 1984), and are taken to indicate intermittent subaerial exposure and peat formation. The great lateral extent and uniform thickness of the Gilbert River Formation is evidence of low relief over much of the Carpentaria Basin during the Early Cretaceous, a situation analogous to that in the Eromanga Basin. Such subdued topography was apparently characteristic of much of the Carpentaria Basin, and allowed rapid transgression with the onset of high relative sea level in the Cretaceous, particularly in the Aptian and Albian.

The bulk of the Carpentaria Basin Cretaceous marine sequence is named the Rolling Downs Group, which includes the Wallumbilla Formation, Toolebuc Formation, Allaru Mudstone and Normanton Formation (Fig. 2.6). The Wallumbilla Formation, conformably overlying the Gilbert River Formation, is a thick sequence (up to 220 m) of Aptian and Albian mudstone deposited in a restricted marine environment. It consists of mudstone and siltstone with grey concretionary limestone, minor lenticular sandstone, and intraformational conglomerate. The formation is micaceous and commonly glauconitic and is equivalent to the formation of the same name in the Eromanga Basin. Smart *et al.* (1972) defined the Trimble Member as an upper member within the Wallumbilla Formation consisting of massive fine-grained sandstone with interbeds of mudstone and minor limestone; it may represent a slight regression within the basin. The Trimble Member is probably equivalent to the Coreena Member of the same formation to the south in the Eromanga Basin (Smart *et al.*, 1980).

The Toolebuc Formation, previously considered as middle to late Albian in age (Deighton, 1985; Ingram, 1985) and now recognised as being late middle Albian to early late Albian in age on the basis of foraminiferal evidence (Haig and Lynch, 1993), is a calcareous unit up to 20 m-thick. The Toolebuc Formation varies lithologically, but typically is calcareous shale containing abundant *Inoceramus* fragments, calcareous nodules, and rare fish fragments (Burgess, 1984). The Toolebuc Formation accumulated in the central part of the epeiric seaway, and represents a

condensed section deposited under anoxic conditions (Haig and Lynch, 1993). Similar to many other condensed sections (Loutit *et al.*, 1988) the Toolebuc Formation is radioactive, and can be traced into the Eromanga Basin on the strength of a prominent gamma-ray anomaly.

The Albian to Cenomanian Allaru Mudstone comprises marine argillaceous sediments, dominantly shale and mudstone and is very similar in lithology and depositional environment to the Wallumbilla Formation. The Allaru Mudstone is sometimes glauconitic, contains *Inoceramus* prisms, and probably thickens towards the centre of the basin and is continuous into the Eromanga Basin. The greatest onshore thickness of 215 m occurs in the southern part of the basin (Smart *et al.*, 1980).

The Normanton Formation, of probable early Cenomanian age (Morgan, 1980), is a generally non-marine unit that marks the conclusion of Cretaceous deposition and the top of the Carpentaria Basin succession. The Normanton Formation consists of fine-grained sandstone and minor siltstone and cone-in-cone limestone. Rare marine fossils are found in places within the limestone, although the formation is dominantly non-marine in origin. The Normanton Formation is equivalent to the Mackunda Formation in the Eromanga Basin and has its greatest onshore thickness of 300 m south of Weipa (Smart *et al.*, 1980).

Post-Cretaceous rocks in the study area typically belong to the cover succession of the Cainozoic Karumba Basin (Fig. 2.2), which is an epicratonic basin superimposed on the Mesozoic Carpentaria Basin (Smart *et al.*, 1980). The Karumba Basin has its greatest onshore extent in northern Queensland but it also covers the far northeastern part of the Northern Territory and the southern part of Papua New Guinea. The maximum thickness of Cainozoic Karumba Basin sediments is 300m, and occurs in the central part of the Gulf of Carpentaria; onshore the maximum thickness is 230m.

2.6.2 Structure

The present coastline of the Gulf of Carpentaria appears as three dominant lineaments; an approximate north-northeast trend along Cape York Peninsula, a northwest trend on the southern coastline between Queensland and the Northern Territory, and a north-northeast trend to the east of the McArthur Basin. Most structural analyses of the region suggest that these roughly parallel coastlines are fault controlled, and that away from these fault bounded margins the basin sediments are relatively undisturbed (Passmore *et al.*, 1992, p. 85), except for gentle downwarping and minor movement along pre-existing faults (Passmore, 1979; Pietsch *et al.*,

1991). The present western margin was probably a hingeline during gentle Early Cretaceous basin sagging (Smart *et al.*, 1980), but undisturbed, very gentle depositional dips preserved within the Cretaceous succession provide evidence of the mild nature of deformation associated with movement along this hingeline. However, tectonic activity increased into the Tertiary, especially along the eastern margin of the basin which was established by regional Pliocene uplift (Smart *et al.*, 1980).

The base Mesozoic unconformity marking the base of the Carpentaria Basin succession shelves to the west near Groote Eylandt, where the Gilbert River Formation onlaps a rising ancient landscape in the western Carpentaria Basin. Offshore, east of longitude 139^0 30' E, the pre-Mesozoic surface is flat and featureless with the exception of a few minor normal faults. West of this longitude the unconformity becomes very rugged, probably due to a karstic topography (Burgess, 1984), and produces some positive features which disrupt the layer-cake Jurassic-Cretaceous stratal geometry.

Offshore the eastern limits of the Carpentaria Basin are shown by structural contours derived wholly from geophysical information. Onshore the basin can be divided into three structural areas, namely the region south of the Gulf of Carpentaria, and the central and northern parts of Cape York Peninsula (Smart *et al.*, 1980).

In the region south of the Gulf of Carpentaria the Euroka Arch is the structural boundary between the Carpentaria and Eromanga Basins (Fig. 2.2). This structure appears to have been topographically high for most of the Cretaceous, with both basins sagging away from it (Smart *et al.*, 1980). Paltech (1980a) believed that the Euroka Arch first acted as a barrier between the Carpentaria and Eromanga Basins during initial accumulation of the Gilbert River Formation in the Late Jurassic. The north-plunging Boomarra and Kamileroi Horsts occur to the west of the Euroka Arch, and according to Smart *et al.* (1980) these horsts were upthrown or left upstanding in Albian or later times. Passmore (1979) noted the absence of basin sediments across part of the Boomarra Horst and postulated that the faults bounding this basement high were reactivated and the horst uplifted at least once during the basin's history. Passmore (1979) also believed that the Euroka Arch developed syn-depositionally in the Cretaceous.

The Boomarra and Kamileroi Horsts are associated with the Burketown Depression to the north, and the Canobie Depression to the east (Fig. 2.2). These depressions are Jurassic or older erosional features, and faults bounding the horsts might be inherited from basement. The Canobie Depression is a northwestern lobe of the depositional Eromanga Basin of Jurassic

times. It is separated from the similar Mullungera Depression to the east by the Fort Bowen Ridge, which trends northwest, perpendicular to the Euroka Arch. Movements along these structures probably only involved gradual displacements with the creation of relatively minor topographic relief (Paltech, 1980a). The northwest trend of the Fort Bowen Ridge roughly parallels the present eastern and western structural boundaries of the Carpentaria Basin.

The central Cape York Peninsula structural area is dominated by the northwest plunging Mesozoic Staaten River Embayment and its Cainozoic modification, the Gilbert-Mitchell Trough (Fig. 2.2). The southeast boundary of the embayment is a complex of shallow folds and minor low horsts and grabens plunging northwest into the embayment, but the character of the embayment under the Gulf of Carpentaria is unknown. All faults are normal and have little displacement, and do not appear to affect the complete Cretaceous succession (Burgess, 1984).

In the northern Cape York Peninsula structural area, deposition of Jurassic-Cretaceous strata and subsequent tilting and faulting of the basin were related not only to sagging to the west, but also to episodes in the structural history of the north-trending Cape York-Oriomo Ridge. However, Carpentaria Basin rocks in this northern area are not greatly disturbed (Smart *et al.*, 1980). Recently, a new depocentre, named as the Bamaga Basin (Passmore *et al.*, 1993), has been identified offshore to the west of Weipa (Fig. 2.2), beneath the thickest Cretaceous sedimentary section in the Carpentaria Basin. The northern boundary of this Palaeozoic(?) depocentre is unknown, but the sediments thin markedly through erosion in all other directions, and the new basin has a relatively limited extent.

2.7 CHAPTER SUMMARY

This study involves detailed stratigraphic analyses of onshore Cretaceous rocks along the western and southwestern margins of the Gulf of Carpentaria, over an area of about 150,000 km^2. In this region Cretaceous rocks consist of an undeformed, flat-lying shelf succession in the order of 150 m maximum thickness. These rocks have long been known as the Mullaman Beds, but new stratigraphic names (Walker River Formation and Yirrkala Formation) are proposed here on the basis of new stratigraphic data documented in this thesis. However, as official sanction of these names has not yet been obtained, Cretaceous rocks are referred to as the Mullaman Beds in this thesis.

The Mullaman Beds are exposed as isolated erosional remnants overlying Proterozoic rocks of the McArthur Basin, and are considered as coarse-grained, shelfal equivalents of finer-grained rocks of the central Carpentaria Basin to the east and southeast. The Mullaman Beds are overlain by a Cainozoic cover succession of the Karumba Basin.

The Mullaman Beds have been relatively poorly studied, and their exact age and internal stratigraphic relationships were not firmly established prior to this study. Similarly, the detailed stratigraphic relationship of the Mullaman Beds to the Great Artesian Basin succession was not clear from previous studies, most of which were concerned with regional stratigraphic problems elsewhere within the Great Artesian Basin. The stratigraphic and palaeontological study by Skwarko (1966) presents the only detailed data regarding the Mullaman Beds, although some correlations and most biostratigraphic interpretations of Skwarko's study have been superseded by more comprehensive analyses of the Cretaceous stratigraphy as part of this thesis.

In this chapter I have outlined the nature of onshore Cretaceous rocks along the western and southwestern margins of the Gulf of Carpentaria, and summarised the known data regarding their stratigraphic and structural relationship with the better-studied succession in the central Carpentaria Basin, which in turn is related to the Mesozoic stratigraphy for the Great Artesian Basin as a whole. In the following two chapters the Mullaman Beds are systematically divided into facies and facies successions, which are recognisable across the entire study area at different stratigraphic levels.

~~~~~~
~~~~~~

3. CRETACEOUS SHELF FACIES OF THE WESTERN CARPENTARIA BASIN

3.1 INTRODUCTION

This chapter provides detailed descriptions of all facies in the onshore western and southwestern parts of the Carpentaria Basin. Facies can be separated into several broad interconnected groups on the basis of their position relative to the regional palaeoshoreline. Facies from the northern and central regions (Fig. 3.1) *generally* represent inner to middle shelf positions. Facies from the southern region generally represent outer to inner shelf positions where more basinal marine deposition, or early nonmarine deposition, was occurring. The northern region is divided into two zones of good rock exposure, the Arnhem Land Zone (ALZ) and the Bath and Parsons Ranges Zone (BPRZ).

The scale of facies subdivision used in this study is designed to make correlations possible at a variety of different scales without being hampered by unnecessary detail. The study is regional in scope and the facies relationships are very complex, therefore the number of distinct facies is high compared to similar studies concerning smaller areas or a less complex sedimentary sequence. The facies descriptions presented here are purely descriptions of the total field aspect of the rocks. The brief interpretation following each facies description is intended to be a concise summary of the major conclusions reached from examination of each facies in the field. These interpretations are expanded in later chapters to give regional scope to the study. Vertical and lateral facies relationships and their stacking patterns (facies successions) are presented in chapter 4. Local correlations are presented in chapters 5, 6, and 7, and regional correlations used to erect a lithostratigraphic framework for the shelf are presented in chapter 8.

3.2 SEDIMENTARY FACIES

A facies is defined as "a body of rock characterised by a particular combination of lithology, physical and biological structures that bestow an aspect ("facies") different from the bodies of rock above, below and laterally adjacent" (Walker, 1992, p. 2).

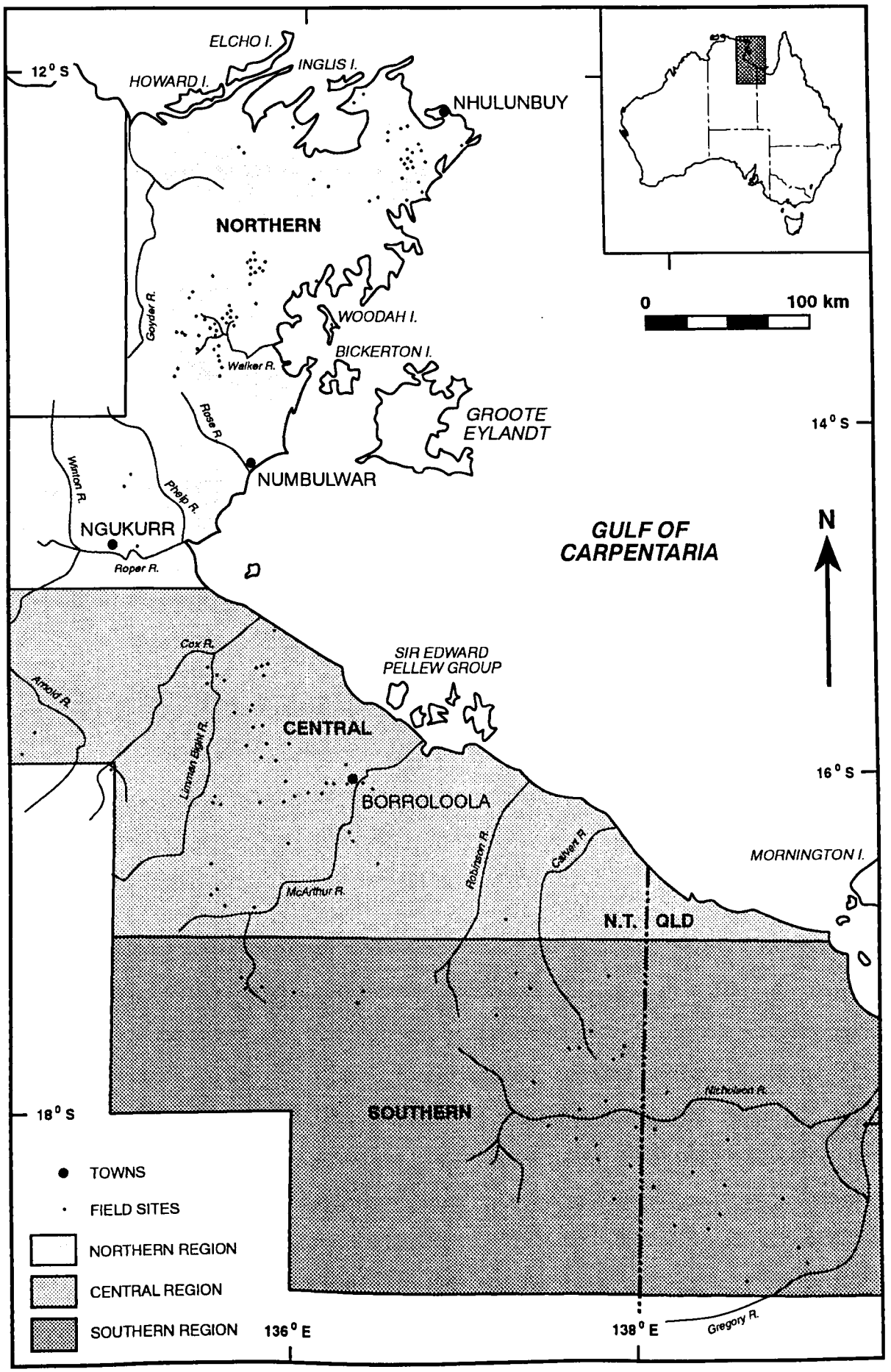

FIGURE 3.1. Location map showing the subdivision of the study area into three related regions, the position of field sites, and the geography of the regions.

Twenty two sedimentary facies and two main weathering horizons have been recognised in the Mullaman Beds. These were defined by features readily recognisable in the field, such as grain size, primary sedimentary structures, degree of bioturbation, colour, and the nature of bounding surfaces. Features of subordinate importance in facies division include petrography, geochemistry, and weathering or diagenetic characteristics.

The facies descriptions below are arranged as closely as possible according to grain size, coarsest first, except for weathering horizons (ferricretes) which are described last. The terminology for basic sedimentological parameters, *e.g.* grain size, sorting, roundness, and bedding, is based on the schemes presented in Pettijohn *et al.* (1987) and Tucker (1991). A summary of all facies descriptions and interpretations is presented in Table 1.

3.2.1 Facies 1 - chert-cobble conglomerate and coarse sandstone

This facies occurs in the BPRZ, south-southwest of Nhulunbuy. In many measured sections this facies forms the oldest Mesozoic unit in the region and overlies Proterozoic McArthur Basin units with an angular unconformity. The maximum thickness of the facies is 12.5 m, with an average thickness of 3 m.

The conglomerate is normally graded, although this vertical trend is subtle. In several sections the grading is more complex with at least two normally graded intervals separated by an inversely graded interval. Other sedimentary structures are absent, except for very rare intervals with planar or trough cross-stratification in the upper part of the facies.

The conglomerate is clast-supported with a moderate to poor degree of sorting. Clasts typically range from small pebbles to large cobbles, with rare boulders. Nearly all of the clasts comprise chert, silicified sandstone, and other lithologies typical of McArthur Basin basement rocks exposed in the BPRZ (Plate 2a). Clasts are subrounded to rounded, with the clast shape being spherical to moderately elliptical. The matrix for the conglomerate is poorly sorted, subrounded to subangular, medium to coarse quartz sandstone. The basal part of this facies contains only a small amount of matrix and the amount of matrix increases upward with decreasing clast size. Commonly the facies is heavily stained by red iron oxides or cemented by amorphous silica. Both body fossils and trace fossils are rare, although the matrix-rich upper part of the facies contains some poorly preserved moulds of molluscan fossils and *Thalassinoides* burrows.

PLATE 2

a Silica-cemented chert cobble to pebble conglomerate of facies 1 above a sequence boundary at the base of a large incised valley. Most clasts are composed of rounded pale-coloured chert and silicified siltstone. Near site 174, northern region.

b Pale grey outcrop (about 15 m-thick) of chert-pebble conglomerate and pebbly sandstone of facies 2. This facies (arrowed) occurs towards the base of the Cretaceous sequence, but is poorly exposed due to its friable nature and large matrix component. 250 m east of site 106, southern region.

c Typical moderately to well sorted conglomeratic lag of facies 3 within the Mullaman Beds. The conglomerate has a sandy matrix, and is sharply overlain by an intensely bioturbated sandstone layer which contains well preserved *Diplocraterion* burrows. Site 179, northern region. Hammer is 32.5 cm long.

d Poorly sorted conglomeratic lag of facies 3 at the base of a thick fluvial facies succession. Note the poor sorting and the wide range in clast size, shape and composition. Site 78, central region. Hammer is 32.5 cm long.

e Weathered outcrop of pebbly sandstone of facies 5. Note the poor sorting and random orientation of the various cherty clasts surrounded by dark-coloured iron-oxide stained sandstone. Site 102, southern region. Hammer is 32.5 cm long.

f Herringbone cross-stratification within medium-grained sandstone of facies 6. This interval is relatively well-sorted and occurs towards the top of a cycle of facies succession 6. Near site 68, central region. Hammer is 32.5 cm long.

g Trough cross-stratified coarse-grained slightly pebbly sandstone of facies 7 at the base of a fining-upward fluvial cycle. The partially eroded layer (arrowed) is a poorly sorted conglomeratic lag at the base of the fluvial cycle. Site 210, northern region. Hammer is 32.5 cm long.

h Small- to medium-scale trough cross-stratification and swaley cross-stratification (best seen at right) in medium-grained clayey quartz sandstone of facies 8 at the base of a fining-upward marine cycle. Site 7, northern region. Hammer is 30 cm long.

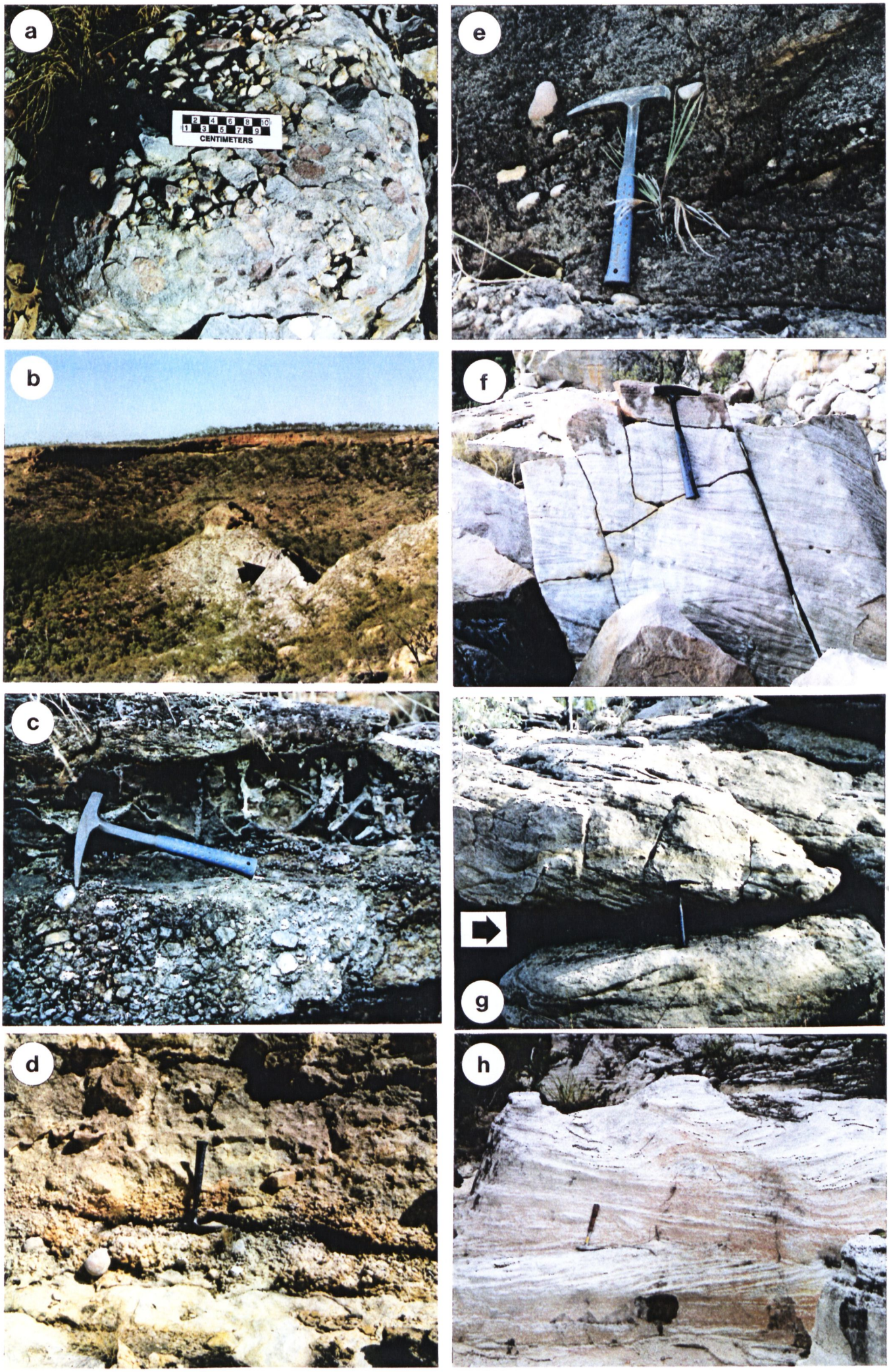
a
CENTIMETERS
b
c
d
e
f
g
h

TABLE 3.1. Cretaceous facies of the western Carpentaria Basin.

	FACIES DESCRIPTIONS	INTERPRETATION OF DEPOSITIONAL ENVIRONMENTS
1	**Chert-cobble conglomerate and coarse sandstone**	**High-energy fluvial (valley fill)**
2	**Chert-pebble conglomerate and pebbly sandstone**	**Various (high-energy fluvial to marginal marine)**
3	**Lag**	**Various (mostly marine deposits)**
4	**Bioturbated pebbly sandstone**	**high-energy fluvial (*e.g.* crevasse splay, channel) to marginal marine**
5	**Cross-stratified and planar bedded pebbly sandstone**	**High- to moderate-energy fluvial**
6	**Plant-bearing pebbly sandstone**	**Fluvio-deltaic to estuarine**
7	**Trough cross-stratified coarse sandstone**	**Fluvial (meandering stream system)**
8	**Trough and swaley cross-stratified fossiliferous sandstone**	**Middle to upper marine shoreface (rarely foreshore)**
9	**Ferruginous lithic sandstone**	**Fluvial (*e.g.* scour/channel fill) or marginal marine**
10	**Bioturbated clayey sandstone**	**Shallow-marine (close to fair-weather wave base)**
11	**Cross-stratified plant-bearing sandstone**	**Brackish-marine (*e.g.* foreshore to terrestrial-strandplain)**
12	**Fossiliferous bioturbated clayey sandstone**	**Restricted/sheltered marine (*e.g.* bays) to offshore marine**
13	**Bioturbated silty sandstone**	**Lower shoreface to upper offshore marine**
14	**Hummocky cross-stratified sandstone**	**Shallow-marine (between fair-weather and storm wave base)**
15	**Thinly interbedded sandstone and siltstone**	**Lower shoreface to upper offshore marine**
16	**Thinly-bedded graded sandstone and siltstone**	**Upper offshore marine (close to storm wave base)**
17	**Pebbly siltstone**	**Offshore shallow-marine to brackish-marine (*e.g.* lagoon)**
18	**Laminated clayey siltstone and sandy siltstone**	**Offshore shallow-marine (beneath average storm wave base)**
19	**Weakly bioturbated laminated siltstone**	**Offshore shallow-marine to sheltered/restricted marine**
20	**Laminated clayey siltstone**	**Fluvial overbank to lacustrine**
21	**Intensely bioturbated siltstone**	**Offshore shallow-marine**
22	**Silty claystone**	**Offshore shallow-marine**

Interpretation

This facies was produced after a long period of erosion and non-deposition associated with lowstand or falling sea level. The exact age of the facies is not directly known, but it commonly unconformably overlies Proterozoic basement and the upper part of the facies contains Cretaceous macrofossils.

Clasts in the basal part of the facies show features typical of fluvial deposition in their sorting, shape and roundness. The lack of fossils and imbrication in the lower and middle parts of the facies indicates deposition under nonmarine (high-energy fluvial) conditions. The typical normally graded aspect of the facies indicates a gradual reduction in flow-strength, probably due to initial transgression and the beginning of marine deposition. In terms of Miall's (1985; 1992a) architectural element classification of fluvial deposits, this facies corresponds best to element GB (gravel bars and bedforms) and associated minor SB (sandy bedforms) elements.

The conglomeratic basal and middle parts of this facies are very similar to deposits termed basin-margin conglomerates (formerly fanglomerates) by Miall (1992a). He proposed that such sheet or tongue like bodies, bounded at the base by regional disconformities, represent valley-fill deposits formed at times of low base level (see Sects. 9.5.1 and 9.7.2). The upper part of the facies shows rare marine fossils which indicate that this facies represents the oldest observed transition from non-marine to marine Cretaceous deposition in the northern and central parts of the Carpentaria Basin shelf.

3.2.2 Facies 2 - chert-pebble conglomerate and pebbly sandstone

This facies was observed in the northern region and in the central part of the southern region. It has a thickness of 14 m (Plate 2b), unconformably overlies Proterozoic basement, and is among the oldest Mesozoic units in the region. The basal 6 m is normally graded and clast-supported. Clasts range from granule to large pebble size and are usually subrounded and moderately sorted. Clasts are composed of chert, silicified siltstone, and cherty sandstone similar to clasts of facies 1. The matrix is uncemented, friable, pale grey to purple, poorly sorted, clayey, fine sand and silt. XRD analysis shows that the matrix is composed of quartz, kaolinite, and minor amounts of hematite and muscovite/illite. The upper 5 m of the facies is bioturbated and the degree of bioturbation increases upward. The upper part of the facies contains two, thin, coarser, partially cemented, highly bioturbated layers, which probably represent hardgrounds. Fossils were not observed in this facies.

Interpretation

The depositional environment of this facies is not readily interpreted. The normal grading, sorting, and roundness tend to suggest a transgressive marine environment. However, the large amount of fine-grained matrix, and the fine grain size of the upper part of the facies are puzzling considering the size and number of clasts in the lower part of the facies. The basal part of the facies apparently is a nonmarine conglomerate which was partially reworked upon initial marine transgression. The upper 5 m of the facies is bioturbated, contains marine hardgrounds and grades into rocks with recognisable marine influence. The fact that this facies was only observed at a few localities is probably due to its unconsolidated and friable nature, which would have facilitated rapid erosion.

3.2.3 Facies 3 - lag

Seaward of the lower shoreface, individual facies and facies successions commonly have basal lags, intraformational lags, and may have upper discontinuous lags. Lags at the base of individual facies and facies successions are typically 0.2 to 0.75 m thick, with a maximum thickness of 2 m. Basal lags contain numerous components, may be weakly normally graded, and display subtle erosive reactivation surfaces defined by laterally continuous variations in clast size. Most basal lags are polymict clast-supported conglomerates, with a medium to fine sand matrix (Plate 2c-d). Maximum observed clast size is 26 cm, though nearly all clasts fall within the pebble size range. Pebbles are mostly well-sorted, well-rounded and composed of quartzite, chert and other lithologies typical of McArthur Basin basement rocks exposed along the western and southern margins of the Carpentaria Basin.

Rarely, basal lags are composed of shelly fossils, which are highly fragmented and chemically altered; only a diagenetic 'ghost' fabric is present. These factors limit precise taxonomic assignments, although most shelly lags are composed of low-diversity molluscan faunas. Shelly lags at the base of facies or event beds are thin (0.25 to 5 cm thick), may be graded, and tend to be laterally discontinuous over tens of metres. They are composed of well-sorted, densely packed layers of granular shell debris (fragments < 0.5 cm) in a matrix of quartz silt and sand, and may form amalgamated beds up to 10 cm thick.

Intraformational conglomeratic lags are common within the Mullaman Beds, particularly in facies 15-19. Here, the lags are thin (0.5 to 3 cm), laterally continuous and crudely graded. The basal surface is erosional and the upper surface is commonly sharp and irregular. Clasts

are matrix-supported and range from granule to mid-pebble size (maximum is 4 cm), with many clasts being small pebbles. Clasts are moderately-sorted, well-rounded and composed of the same rock types as basal lags. Very rarely these intraformational conglomerates contain a few molluscan shell fragments.

Lags also form discontinuous lenses or pods, which are commonly associated with HCS beds and coarser-grained cross-stratified sandstone (facies 8 and 14). These lags have a smooth, undulating or locally-erosional contact on hummocky cross-stratified sandstone, and are confined to asymmetrical lenses up to 60 cm thick and 2 m long. Lags are clast-supported conglomerates, with well-sorted and well-rounded clasts composed of chert and quartzite. The maximum clast size is 6 cm and most clasts are middle-sized pebbles. Lags are crudely graded and may grade upward into coarse sandstone over a vertical distance of a few centimetres.

Concentrations of shelly fossils form similar lags, but they are thin (< 2 cm thick), laterally discontinuous (< 1 m long), and less common. In some places they overlie large scale hummocky cross-stratified beds with an undulating contact, and only occur in large swales in the top surface of the underlying bed. These lags may be densely or loosely packed, and generally include well-sorted shell material, consisting of both whole valves and large fragments of broken valves. Occasionally they form shell pavements where disarticulated bivalves, both convex-up and convex-down, are stacked to form thin (< 5 cm) beds. Fossils within these swales do not show preferred orientation. Bioturbation is rare or absent in all lags, and only occurs in the finer-grained top of some graded lags, where *Arenicolites*, *Skolithos*, and rare *Thalassinoides* burrows have penetrated the matrix-rich part of the lag from above.

Interpretation

Most lags within the Mullaman Beds were formed in relation to changes in relative sea level during various stages of sequence development. Therefore, discussion and interpretation of the formation of all types of lags is presented within a sequence stratigraphic framework in Sect. 9.6.3.

3.2.4 Facies 4 - bioturbated pebbly sandstone

This facies occurs in the central and southern parts of the southern region and commonly overlies facies 20 with a gradational contact. South of the Nicholson River this facies has a

sharp contact with underlying facies (4, 5, or 10). The maximum thickness is 13 m; typically less than 5 m is exposed.

Facies 4 is composed of fine to very coarse, friable, mottled, clayey sandstone (Fig. 5), and typically grains are fine to fine-medium sand. Grains are subangular to subrounded and moderately sorted, and the matrix is iron-oxide stained fine clay. In some exposures this facies contains zones with dispersed 'lonestone' clasts up to mid cobble size. Lonestone clasts are rounded to subrounded, poorly sorted and comprise numerous sedimentary lithologies. The facies is massive and slightly bioturbated with a marginal upward increase in the degree of bioturbation. The base of the facies has *Planolites* and *Arenicolites* trace fossils.

Interpretation

The depositional environment of this facies is similar to that of facies 7 and parts of facies 5. The bulk of the facies was deposited in a high-energy fluvial setting, as indicated by the poor sorting, coarse grain size, overall lack of bioturbation, lack of marine fossils, and the scale of trough cross-stratification. The bulk of the facies can be classified as the Sh and St facies, and SB architectural element of Miall (1985; 1992a), and possibly reflects deposition as crevasse splays. The presence of 'lonestone' clasts is problematic, but Frakes and Krassay (1992) proposed that these rocks were formed by rafting of coarse clastic debris by seasonal ice floes along marine shorelines and rivers during cold winters (see discussion in Sect. 10.3). The upper part of this facies shows indications of increasing marine influence, including an increase in the degree of bioturbation and the presence of possible marine trace fossils. The lack of wave-generated stratification and marine body fossils suggests only a minor marine (probably brackish) influence.

3.2.5 Facies 5 - cross-stratified and planar bedded pebbly sandstone

This facies occurs in parts of the BPRZ and the northwestern part of the southern region, especially in the Calvert Hills 1:250,000 sheet area. It unconformably overlies Proterozoic basement with an erosional lag in most exposures, and has a maximum thickness of 38 m.

The facies is composed of moderately to well sorted, subrounded, medium quartz sandstone and dispersed clasts (Plate 2e). Clasts are poorly sorted, up to 10 cm in diameter, and are composed of chert and silicified sedimentary lithologies. The number of clasts decreases upward with a corresponding increase in the degree of sorting. The base of the facies is

typically conglomeratic and contains little matrix. Clasts at the base of the facies have the same composition as clasts dispersed throughout the facies, but are up to small cobble size. Trough cross-stratification with sets up to 1.2 m thick occur in coarse-grained parts of the facies. Finer-grained parts of the facies are planar bedded and contain high-angle planar cross-stratification with set thicknesses between 40 and 60 cm. In places the facies contains abundant segmented plant fossils and appears to be slightly bioturbated.

Interpretation

This facies represents a fluvial depositional environment. Indicators of fluvial deposition include the relatively coarse grain size, its presence within fining-upward facies successions, the poor degree of sorting, irregular conglomeratic intervals, the lack of marine fossils, and the lack of pervasive bioturbation. The large-scale and style of cross-stratification and the isolated, lenticular geometry of the outcrops also point to a fluvial origin. This facies corresponds well to facies Gm, Gt, Gp, St, Sp, and Sh of Miall (1985; 1992a), which are grouped under gravel bar (GB) and channel (CH) architectural elements.

Coarser-grained parts of the facies represent a high-energy fluvial regime, possibly reflecting deposition in braided streams. Finer-grained intervals exhibit planar cross-stratification, and may reflect a decrease in energy in the fluvial system to meandering streams. The lack of any fine-grained (overbank or swamp) sediments may indicate that fine-grained material was held in suspension, and bypassed this region as it was transported out on to the marine shelf or to the basin centre. Alternatively, the lack of fine-grained facies may be due to their poor preservation potential because fine-grained facies were eroded during lateral accretion and fluvial reworking (see Sect. 9.6.2), or simply due to minimal fluvial aggradation because of a lack of accommodation space.

3.2.6 Facies 6 - plant-bearing pebbly sandstone

This facies is restricted to the region surrounding, and enclosed by, the Bath, Parsons and Mitchell Ranges in the southern part of the northern region. It is particularly well exposed on the eastern side of the Parsons Range, where the facies is unconformably overlies Lower Proterozoic McArthur Basin sediments.

Facies 6 is composed of thickly planar bedded, moderately to poorly sorted, rounded, clean, friable, iron-oxide cemented or stained coarse to medium quartz sandstone. The facies

commonly occurs in fining-upward facies successions and contains little matrix. The base of this facies is typically a lag up to 0.5 m thick, which comprises a monomict, matrix-supported, poorly sorted, rounded to subrounded, quartzite pebble conglomerate. Some exposures display granule to large pebble sized, subrounded to rounded chert clasts. Rarely these clasts are confined to poorly defined zones or form the foresets of high-angle cross-stratification, which have set thicknesses up to 1.3 m. Trough cross-stratification commonly occurs in the coarse-grained part of the facies, and finer-grained parts may display asymmetrical current ripples (wavelength 8 to 10 cm; height 1 to 1.5 cm) and rarer intervals with bipolar (herringbone) cross-stratification (Plate 2f).

The facies is typically not bioturbated but contains numerous segmented plant fossils on some bedding surfaces, and very rare unidentified trace fossils. The largest of these plant fossils are manganese-stained external moulds of logs up to 48 cm long and 9 cm wide. Other fossils include seed pods, twigs, stems, and rare leaves.

Interpretation

The depositional environment of this facies is problematic. Most likely this facies was deposited in a fluvio-deltaic to estuarine setting, although it is difficult to distinguish between the products of these depositional settings given the nature of the outcrops.

The bulk of the facies reflects deposition adjacent to topographically-high Proterozoic ridges. Local mapping shows that most sand and clasts were derived directly from erosion of Proterozoic sedimentary basement lithologies. Many of the Proterozoic lithologies in the hinterland have mature to supermature textures. Therefore, erosion and redeposition of this material has resulted in Cretaceous units with normal fluvial-estuarine characteristics including poor sorting and coarse grain size, but an anomalous degree of roundness in places inherited from the basement. Even though the grains in this facies are rounded, they have probably only been transported a short distance during Cretaceous deposition.

This facies contains the fluvial Se, Sl, Sp and St facies of Miall (1985; 1992a) and probably LA and SB architectural elements, which typify deposition in sandy meandering, stream systems. Here, palaeocurrent analysis of individual fining-upward sandbodies show dominantly uni-directional flow, although there is marked variation between units. The lack of bioturbation, the large-scale cross-stratification with coarse foresets, and the presence of rare plant fossils also supports a fluvial depositional environment. In more distal locations, parts of this facies are

finer-grained and contain some bi-directional current indicators; these may reflect a change to fluvio-deltaic or estuarine deposition in a tidal inlet or delta setting.

3.2.7 Facies 7 - trough cross-stratified coarse sandstone

This facies occurs in the ALZ and has a maximum thickness of 15 m. The facies is also exposed in the southern region, where it is slightly bioturbated and occurs in association with pebbly sandstone (facies 4). Typically facies 7 is unconformable on underlying marine units (*e.g.* facies 22), and is possibly a facies equivalent to facies 6 in the BPRZ.

The facies consists of massive clayey, rounded, moderately sorted, very coarse- to fine-grained quartz sandstone, and forms fining-upward facies successions. Sedimentary structures include trough cross-stratification with set thicknesses up to 2 m, and high-angle planar cross-stratification (Plate 2g). The base of this facies is commonly erosional and features erosional cut out of underlying lithologies, rip-up clasts and rare erosional lags. The sandstone is friable and contains a large amount of pale orange to white clay matrix, and is highly stained or partially cemented by iron oxide in places. In the southern region the facies is slightly bioturbated. Body and trace fossils were not observed. The degree of weathering is typically high and in several exposures incipient lateritisation is apparent.

Interpretation

Facies 7 has a lenticular or channel-like geometry and displays lateral accretion surfaces, which clearly indicate deposition in a sandy fluvial system, probably in meandering rivers. In some places the erosional base to this facies can be seen to cut out up to 10 m of underlying marine facies over a lateral distance of 90 m. The nature of the erosional surface is highly irregular and suggests channel formation (with point bars) in a meandering pattern.

The poor sorting, coarse grain size, and the large scale trough cross-stratification suggest deposition in bedload or mixed-load streams. The lack of significant bioturbation and fossils also points to a nonmarine origin for this facies. The bulk of the facies corresponds to Miall's (1985; 1992a) St and Sp facies, which reflect lower flow regime fluvial deposition in the form of dunes, bars or sand waves. These stacked facies form LA (lateral accretion macroform), SB (sandy bedform), and CH (channel) architectural elements (Miall, 1992a).

3.2.8 Facies 8 - trough and swaley cross-stratified fossiliferous sandstone

This facies is well exposed in the ALZ, in the central region surrounding Borroloola, and at a few localities in the southern region. This facies is commonly associated with coarse-grained facies (1 or 13) and grades into finer-grained facies (14, 15, 21, or 22). In places it is overlain by fluvial to marginal marine facies.

Facies 8 occurs in proximal localities and consists of pale clayey, massive or thickly planar bedded quartz sandstone. Grains are typically well sorted, well rounded, and have a very coarse to medium sand size. The base of the facies is very coarse and displays large-scale trough cross-stratification and rarer mid- to small-scale trough cross-stratification; as grain size decreases internal stratification changes progressively to high-angle planar cross-stratification, and further to small-scale trough and swaley cross-stratification (SCS; Plate 2h). Finer-grained parts of the facies show flat lamination and asymmetrical ripples, and rare coarse foresets of granule to very small pebble sized clasts. XRD analysis of this facies in proximal locations shows a mature composition of quartz with a kaolinite matrix containing minor muscovite/illite.

In the central region this facies is stained by iron oxides and displays liesegang banding. Body fossils include trigonids, ammonites and bivalves. Bioturbation is apparently pervasive, but the lack of lithological contrast makes identification of specific forms difficult, although *Skolithos* was recognised.

Interpretation

Swaley cross-stratified sandstones have been interpreted as having formed in middle to upper shoreface environments, typically in about 5 to 10 m of water (Leckie and Walker, 1982; Plint and Walker, 1987; Plint and Norris, 1991). Also typical of this depositional setting is small-scale trough cross-stratification associated with SCS, and HCS farther offshore (Nottvedt and Kreisa, 1987). In this setting, reworking by both storm and fair-weather waves is thought to prevent the accumulation of mud, resulting in a very unstable environment inhabited by only a few well adapted infaunal organisms of the *Skolithos* ichnofacies. In some exposures of facies 8 flat lamination (formed by swash and backswash) is present and an even shallower (foreshore) depositional setting is inferred. Large-scale trough and high-angle cross-stratification in similar rocks is considered to be characteristic of a high-energy upper shoreface position (Ainsworth and Crowley, 1994). Further, the high energy conditions of the middle

shoreface to foreshore depositional environments are apparent from the low abundance and low diversity of trace fossils, which reflect the instability of the habitat.

The amount of matrix is high in proximal localities in the ALZ. Here the amount of matrix decreases down-section, and the matrix is interpreted to have formed by lateritisation and soil-forming processes rather than by primary deposition. In the central region this facies occurs in more distal settings where SCS is rare, the amount of fine-grained sediment is larger, and the degree of bioturbation is greater.

3.2.9 Facies 9 - ferruginous lithic sandstone

This facies occurs in a few localities in the ALZ and in the central part of the southern region, on the flanks of topographically-high Proterozoic ridges. The facies is up to 8.8 m thick, and overlies facies 3 or 12 in the southern region. Facies 9 is composed of massive, orange, friable ferruginous quartz sandstone (Plate 3a). Grains are rounded, medium to coarse sand with moderate to poor sorting. Most grains are quartz but the lithic component (<10%) is higher than that of other coarse-grained facies. Dispersed pebble-sized ferruginous, lithic clasts sometimes occur near the base of this facies, and the matrix is pale clay with a small amount of ferruginous or manganiferous cement. Sedimentary structures are absent except for traces of planar cross-stratification in coarser-grained intervals of the facies, and the amount of bioturbation is insignificant.

In the southern region the facies is conglomeratic and is normally graded in places. Clasts are subrounded and poorly sorted, and are composed of granules and small cobbles of quartz sandstone and chert. The facies is stained or cemented by iron oxides (Plate 3a). The upper 3 m of the facies displays a high degree of bioturbation and contains *Planolites* burrows.

Interpretation

The depositional environment of this facies is not readily interpreted. Indicators of a nonmarine (probably fluvial) depositional environment in the northern region include the lack of bioturbation, coarse grain size, unfossiliferous nature, poor sorting, and high lithic content. It is difficult to assess this facies in terms of classical fluvial facies analysis. Generally, the features described above are similar to facies Se and Ss (scour fill facies) of Miall (1985; 1992a), but may represent a number of separate fluvial architectural elements.

PLATE 3

a Ferruginous medium-grained quartz sandstone of facies 9. Note the high degree of weathering at this site and the formation of iron-oxide-rich bands (liesegang bands), probably derived in part from weathering of relatively abundant lithic grains within the facies. Site 3, northern region. Hammer is 32.5 cm long.

b Intensely bioturbated clayey sandstone of facies 10. Note *Skolithos* and *Rhizocorallium* burrows filled by white clay and surrounded by orange iron-oxide stained quartz sandstone. Individual burrows tend to be at least partly overprinted by successive trace fossil generations. Site 132, northern region. Hammer is 32.5 cm long.

c Numerous crude external moulds of segmented plant fossils (twigs, small stems, and rarer seed pods) within clean, fine-grained quartz sandstone of facies 11. Site 33, northern region. Pencap is 6 cm long.

d Low-angle planar crossbedding within fine/medium-grained quartz sandstone of facies 12. Site 31, northern region. Hammer is 32.5 cm long.

e Yellow bioturbated slightly sandy siltstone of facies 13. Note the concretionary aspect of the upper bedding surface at the level of the hammer head. Site 65, central region. Hammer is 32.5 cm long.

f Large-scale hummocky cross-stratified fine quartz sandstone and siltstone of facies 14. Note the long wavelength of the HCS. Site 148, northern region. White scale bar (12 cm wide in total) is located in the centre of a large swale.

g Thinly interbedded orange, ferruginous quartz sandstone and paler clayey siltstone of facies 15. Most intervals are ripple-laminated or wavy/flaser bedded and are interbedded on a centimetre- to millimetre-scale. Note the small pebble sized clasts (largest is near bottom right-hand corner of scale bar) of a thin intraformational conglomeratic lag. Site 154, northern region.

h Thinly-bedded graded sandstone beds (red to purple) and siltstone beds (white) of facies 16. The thin sandstone beds show good normal grading up close, and their bases commonly have small-scale erosional pits and scours. Beds in the upper part of the photo have been disturbed by bioturbation. Site 118, southern region. Lens cap is 5.75 cm in diameter.

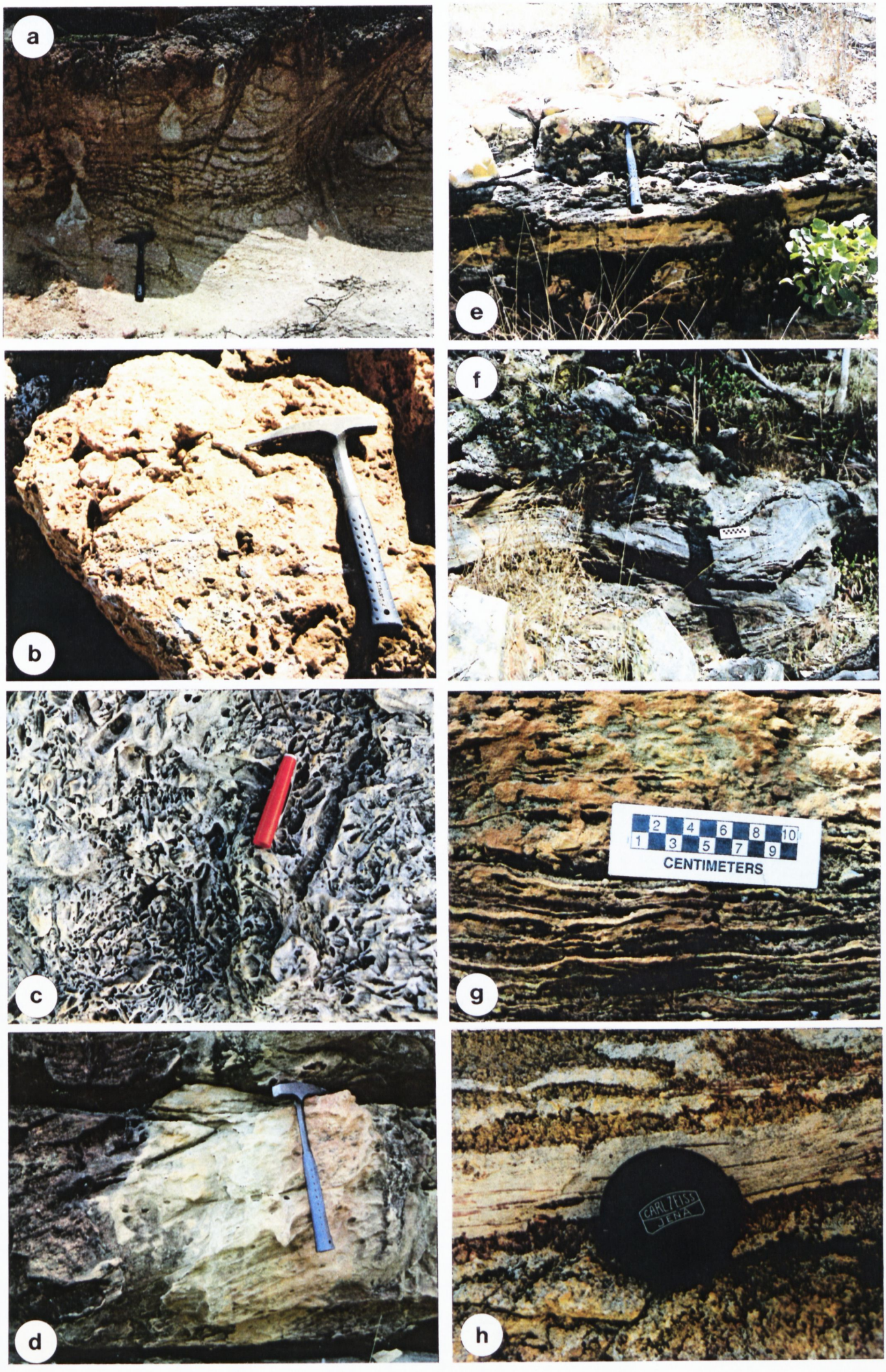
a
e
b
f
c
g
2 4 6 8 10
1 3 5 7 9
CENTIMETERS
d
h
CARL ZEISS
JENA

In the southern region the upper part of the facies contains rare marine trace fossils and is highly bioturbated. This suggests a shallow marine depositional environment for southern exposures of this facies. Thus it is likely that this facies is dominantly fluvial in origin, especially in the northern region, although the upper part of the facies in the southern region represents a transition from fluvial to shallow marine deposition.

3.2.10 Facies 10 - bioturbated clayey sandstone

This facies occurs in the ALZ and the central part of the southern region, where it has a maximum thickness of 8.5 m and overlies facies 5 with a locally erosional contact. This facies consists of ferruginous, orange, friable, clayey, fine-medium to coarse sandstone (Plate 3b). The facies is well sorted and moderately to intensely bioturbated, with bioturbation increasing upward. In most facies successions this facies has a gently coarsening-upward grain size and contains planar cross-stratification. Trace fossils include *Thalassinoides*, *Rhizocorallium*, small *Skolithos*, and several types of unidentified horizontal burrows. XRD analysis indicates a composition of quartz, kaolinite, hematite, and minor muscovite/illite (Appendix 6).

Interpretation

The coarse grain size, pervasive bioturbation, typically coarsening-upward character, and presence of marine trace fossils clearly indicate that this facies was deposited in a shallow-marine environment. The rarity of wave-generated features suggests that deposition occurred close to, or possibly beneath fair-weather wave base in a low to moderate energy environment. The presence of *Skolithos* burrows indicates that the environment was aerobic to dysaerobic and probably involved an unstable, sandy substrate which was only suitable for a low diversity, opportunistic ichnofacies (Pemberton *et al.*, 1992).

3.2.11 Facies 11 - cross-stratified plant-bearing sandstone

This facies occurs in nearshore zones in the northern and central regions, especially within the BPRZ, and is commonly associated with facies 8 and 15. The maximum thickness is 9 m and the average thickness is 3 m. Facies 11 is composed of massive to very thickly planar bedded medium to fine quartz sandstone. Grains are subrounded to rounded, moderately to well sorted, and the sandstone is texturally and compositionally mature. Commonly the weathered sandstone is cemented by silica, but fresh samples are quite friable. In several localities the facies contains dispersed subrounded, granule sized clasts of cherty siltstone or quartz.

This facies displays planar cross-stratification with set thicknesses of 25 to 40 cm and is moderately bioturbated in most intervals. The foresets of some cross-strata are defined by granule sized clasts. Rarely, poorly preserved asymmetrical current ripples and molluscan macrofossil impressions and trace fossils are evident in fine-grained parts of the facies. The most distinctive feature of the facies is the high abundance of plant fossils, including small segmented wood stems, 'fern-like' structures and seed pods (Plate 3c). The plant fossils typically occur in the upper part of the facies and are rather poorly preserved as external moulds on silica-cemented bedding surfaces.

Interpretation

This facies is very similar to facies 8 except that it is coarser, has a lower degree of bioturbation, has far fewer marine macrofossils, and has an abundance of segmented plant fossils in finer-grained parts of the facies. This facies may also be a facies equivalent to the upper part of facies 6. Facies 11 probably reflects brackish marine to fluvial deposition in the terrestrial-strandplain to foreshore, and is particularly well exposed close to topographically-high Proterozoic ridges. It is interpreted that much of the coarse material and plant debris was derived from fluvial input and erosion in close proximity to Proterozoic basement terrain.

3.2.12 Facies 12 - fossiliferous bioturbated clayey sandstone

This facies is widely exposed in the BPRZ, in the central area surrounding Borroloola, and also throughout the southern area. It has a maximum thickness of 14 m and commonly overlies facies 8 or 22. The facies consists of clayey, moderately sorted, subrounded, massive or crossbedded (Plate 3d) fine to fine-medium quartz sandstone with a silty clay matrix.

In proximal locations the facies is slightly conglomeratic, containing dispersed clasts of chert and silicified fine-grained sandstone up to 1.5 cm in diameter. The facies exhibits a range of sedimentary structures including wave-ripple lamination, flasers, rare flat lamination, escape burrows, dewatering structures, and very rare HCS near the base of the facies. The contact with facies 8 or 22 is locally erosional. Facies 12 is mottled, slightly friable, generally uncemented, and is invariably intensely bioturbated and highly fossiliferous. In some places the abundance and diversity of fossils is enormous, much greater than in other facies. Macrofossils include ammonites, trigonids, bivalves, unidentified vertebrate bone fragments, and a large range of segmented plant fossils. Trace fossils include *Rhizocorallium*, *Planolites*, *Arenicolites*, *Teredolites*, *Skolithos*, and possibly *Ophiomorpha*.

In the central region the facies typically has a conformable, coarser-grained upper unit with a thickness of less than 3 m. This unit consists of massive, mottled pale red to orange, highly ferruginous, friable, fine- to medium-grained sandstone, in which the grains are subangular and moderately to poorly sorted. The unit is intensely bioturbated and has *Skolithos* burrows, but no observable macrofossils. XRD analysis indicates that all samples of this facies are composed of quartz, kaolinite, and minor muscovite/illite and hematite. Petrological analysis shows that much of the clay in this facies was derived from the weathering of microcline(?) feldspar (Appendix 4).

Interpretation

The scarcity of large-scale crossbedding in this facies, the fining-upward grain size trend in many exposures, and the well preserved nature of many of the marine macrofossils suggest that this facies was deposited in a relatively quiet marine environment. Facies 12 probably reflects deposition in sheltered shallow-marine regions such as large bays. The trace fossils belong to the *Cruziana* ichnofacies, which is considered to be characteristic of an offshore shelf environment between storm and fair-weather wave base, or a shallower restricted marine setting (Pemberton and Frey, 1984; Pemberton *et al.*, 1992).

In places intense bioturbation has destroyed the primary sedimentary fabric, and sedimentary structures are not preserved. This suggests that the seafloor was well oxygenated and able to sustain an abundant and diverse biota. In several places the abundance and diversity of preserved marine macrofossils is great, and finer-grained parts of the facies display delicate bivalve fossils, which are preserved with the two valves still joined. The delicate preservation of these fossils argues against significant transport, whilst the fossil abundance suggests local dense communities of living organisms.

3.2.13 Facies 13 - bioturbated silty sandstone

This facies occurs on the eastern side of a palaeoembayment along the western margin of the Bath Range in Arnhem Land, and in the central region. In Arnhem Land the facies has a maximum thickness of 5.5 m and only occurs where the basal Mesozoic chert conglomerate (facies 1) is missing. In the central region this facies is associated with facies 8 or 11 and has a typical thickness of 6 to 10 m.

The facies can be divided into several slightly different units, depending on position relative to the palaeoshoreline, but has an overall fining upward character in most facies successions. Lithologically it consists of slightly friable white to pale yellow, well to moderately sorted, subrounded to subangular, silica cemented, fine sandstone to coarse siltstone (Plate 3e). The matrix is pale, fine-grained clay with minor staining by iron oxides. The base of the facies has thick planar bedding, which changes upward to medium scale planar cross-stratification, to herring-bone cross-stratification, and finally to flat lamination, slump structures, and ripple lamination. Weathered exposures contain dark coloured limonite concretions up to 12 cm in diameter. Elsewhere, pale coloured, early sedimentary concretions are occasionally present in the upper part of the facies (Plate 3e).

In the central region small pods and stringers (discontinuous layers) of outsized clasts set in a muddy matrix are dispersed randomly throughout the facies, which otherwise has a uniformly fine-sand grain size. The clasts range from granule to small pebble size, show a wide range in composition, and display a highly variable degree of rounding. The pods extend no more than about 30 cm, usually 5 - 8 cm, in any direction and are often irregularly elliptical or lens shaped. The stringers comprise sand and clasts of granule size in discontinuous layers up to 20 cm in length.

The facies is moderately to intensely bioturbated throughout and contains numerous macrofossils including bivalves, trigonids, and scaphopods. Rare exposures display segmented plant fossils. In several cases the upper bioturbated bedding surface is highly cemented and was probably a firmground or a hardground. Trace fossils include *Planolites*, *Skolithos*, *Rhizocorallium*, *Palaeophycus, Thalassinoides,* and rare *Diplocraterion.*

Interpretation

This facies represents marine deposition under a regime of increasing water depth in the lower shoreface to upper offshore region, as shown by an upward decrease in grain size and change in stratification. The coarser-grained base of the facies shows evidence of wave activity in the form of planar cross-stratification. The finer-grained top of the facies, with its trace fossil assemblage and fine lamination, indicates quieter marine deposition below fair-weather wave base. The facies is thoroughly bioturbated and contains abundant marine macrofossils and trace fossils of a mixed *Cruziana* and *Skolithos* assemblage. In the northern region the facies is interpreted as a distal facies equivalent of facies 9.

Concretions in the upper part of the facies suggest slow deposition in an intermediate to distal marine setting, possibly related to condensed sedimentation during a highstand of relative sea level (*e.g.* Van Wagoner *et al.*, 1990). The high degree of bioturbation suggests that the water column was oxygenated and conducive to biological activity.

The presence of dispersed clasts and pods or stringers of coarse grains is rather problematic. The dispersed clasts show a wide range in composition, and display a highly variable degree of rounding, suggestive of multiple provenance. These features may be the result of intense biological reworking and concentration of storm-deposited lags. However, the presence of undisturbed sedimentary structures such as crossbedding, delicate lamination and rare slump structures in close proximity to the pods and stringers makes the idea of intense, but highly selective bioturbation unlikely. Frakes and Krassay (1992) propose that such coarse material was rafted out into the basin by seasonal ice, which formed along marine shorelines and rivers, during the Cretaceous. Facies 4, 17, and 22 also show these probable ice-rafting features, and are discussed further in Sect. 10.3.

3.2.14 Facies 14 - hummocky cross-stratified sandstone

Hummocky sandy beds occur on the shelf in localities close to the interpreted palaeoshoreline, and are commonly associated with facies 3, 8, and 15. The facies is composed of fine sandstone to coarse siltstone exhibiting well preserved, small- to large-scale hummocky cross-stratification (HCS; Plate 3f). Commonly HCS beds are 20 to 80 cm thick with individual sets 5 to 30 cm thick, but may form thicker amalgamated beds. Set wavelengths range from 0.75 to 6 m, with most HCS having a wavelength of 1 to 2 m. HCS beds contain parallel laminae which dip at angles of 5^0 to 12^0 in random directions. Reactivation surfaces between individual fine sandstone (HCS) beds are common and are highlighted by truncation of internal lamination. Laminae thickness increases towards the hummock crest in a characteristic hummock and swale pattern in three-dimensional view (see Plate 13a).

Flat lamination and low-angle lamination are commonly associated with HCS beds. The inclined low-angle (typically less than 5^0) cross-bedding surfaces have wavy or irregular bases, and in some outcrops it appears that cross-bedding grades laterally over tens of metres into small scale HCS. The tops of thick HCS beds or low-angle cross-bedded layers may have symmetrical ripples with a wavelength of 5 to 10 cm and an amplitude of 0.5 to 2 cm. The finer-grained tops of HCS beds occasionally display interference wave-ripples of a similar scale, and in some outcrops the interference ripples grade into symmetrical ripples along a

single bed. Rarely, coarser-grained parts of the facies contain megaripples (*sensu* Leckie, 1988) with a maximum wavelength of 1.2 m and a maximum amplitude of 10 cm. Megaripples are typically slightly asymmetric and occur on the top surface of thick HCS beds or in medium- to coarse-grained sandstone overlying HCS beds.

Event beds (up to 25 cm thick) with a thin granule or shelly base, normal grading, and a fine-grained rippled top are occasionally recognisable amidst amalgamated hummocky beds. Event beds are sometimes separated from HCS beds and other tempestites by a millimetre- to centimetre-thick bioturbated siltstone layer. The base of these graded beds display thin lags, small gutters and gutter casts, and complex erosional scours. Larger sand-filled gutters (up to 40 cm wide and 0.8 m long) tend not to be attached to any laterally continuous sandy bed, but are enclosed within siltstone. Commonly individual centimetre- to decimetre-thick sandy beds and event beds have abrupt lateral pinch-outs, or rapid lateral decreases in thickness. Rare sedimentary structures in this facies include dewatering structures and small-scale trough-cross-stratification in medium- to coarse-grained parts of the facies. Trace fossils include *Skolithos*, *Diplocraterion*, and rare *Thalassinoides*.

Interpretation

Facies 14 shows the most compelling evidence for storm-influenced sedimentation on the Carpentaria Basin shelf. Storm features include HCS, event beds, megaripples, intraformational lags, lateral pinch-out of beds, and wave-ripples on the tops of graded beds.

HCS has been reported from a large number of localities in a variety of shallow-marine environments, from the tidal flat to the inner shelf (Dott and Bourgeois, 1982), and is generally considered to have formed from oscillatory-dominant combined flow during the waning stages of storms (Duke *et al.*, 1991; Nottvedt and Kreisa, 1987; Yagishita *et al.*, 1992), although recent experimental work (Southard *et al.*, 1990) has shown that some HCS may be generated by purely oscillatory flows. It has also been postulated that some variation of HCS may form in fluvially-dominated environments (Cotter and Graham, 1991). In storm-dominated facies successions of the Mullaman Beds the close spatial association of hummocky cross-stratified sandstone with marine shelly and conglomerate lags (facies 3) and offshore siltstone (facies 21 and 22), suggests a purely marine origin for HCS beds of facies 14. HCS beds occur to the northwest (shoreward) of offshore siltstone and to the southeast (seaward) of swaley cross-stratified shoreface sandstone (facies 8). This suggests that HCS beds were deposited below

fair-weather wave base in the transitional zone between the middle to lower shoreface and storm wave base.

Associated with the HCS facies of the Mullaman Beds are individual beds with abrupt lateral pinch-out, hummocky sandy event beds with a thin laminated or rippled silt-sized drape, sand-filled erosional gutters and megaripples; all of these features are typical of storm-dominated environments (Brenchley, 1985; Jennette and Pryor, 1993; Kreisa, 1980; Leckie, 1988; Monaco, 1992). Lenticular micro-hummocky sandy beds occur where preservation of HCS bedforms is not complete, or where the amount of available sand was low. The intense nature of the bioturbation within the fine-grained tops of beds in facies 14 suggests low sedimentation rates and high rates of biological turnover between storms (*e.g.* Wheatcroft, 1990), and such stratigraphically-restricted intense bioturbation is a general characteristic of storm deposits (Dott and Bourgeois, 1982). Occasionally burrows can be seen to completely penetrate thin storm beds from above; this is typical of colonisation after episodic storms (Frey and Goldring, 1992).

3.2.15 Facies 15 - thinly interbedded sandstone and siltstone

This facies is well exposed in the BPRZ, in the ALZ, and in the southern region. The maximum thickness is 13 m and the facies is commonly associated with facies 3, 14, 16, 18, 19, 21, and 22. Facies 15 is composed of centimetre- to millimetre-thick ripple laminated interbeds (Plate 3g) of clayey siltstone and coarser-grained rocks, including sandstone, intraformational conglomerate, and fossiliferous sandstone.

In northern localities the sand content is great and interbeds tend to be 1.5 to 5 cm thick, but rare decimetre-scale interbeds are present. Sandstone- and siltstone-dominated intervals have a typical thickness of 0.5 to 2 m. Within each of these intervals the two units are thinly interbedded. The sandstone is composed of moderately sorted, rounded quartz grains with a pale coloured, very fine-grained clay matrix. Lithic grains are rare but granule to small pebble sized siliceous clasts sometimes occur near the base of the facies. The bases of thicker interbeds display load casts, scour and tool marks and thin lags, whilst the tops of beds have low-amplitude, straight-crested or interference wave ripples in places (wavelength 5 to 8 cm; amplitude 2 to 3 cm). Internal stratification comprises ripple cross-lamination with 1 to 2 cm-thick sets and erosional bases. Other prominent features are discrete lags with erosional bases and sharp tops, and rare gutter casts up to 20 cm wide, 25 cm thick and 50 cm long. Planar

cross-stratification and small-scale trough cross-stratification with set thicknesses of 8 to 15 cm occur locally where sandstone is medium-grained.

In southern localities, closer to the basin centre, the sand content is lower and clayey siltstone interbeds (typically < 2 cm thick) dominate facies 15. Here, a greater range of sedimentary structures is recognisable due to the large contrast in grain size between individual laminae and beds in the facies. Each 0.2 to 2 cm thick clayey siltstone layer has flat to wavy lamination or ripple cross-lamination. Not all lamination is perfectly horizontal; many sets of laminae undulate regularly to form wavy lamination, or irregularly to form highly convoluted lamination.

The tops of some siltstone interbeds contain symmetrical or asymmetrical current ripples with wavelengths of 8 to 10 cm and amplitudes of 0.5 to 1 cm, and spherical concretions up to 6 cm in diameter and 4 cm in height. XRD analysis of the siltstone identified quartz, kaolinite, hematite, and minor muscovite/illite as the components. Similar to other facies, feldspar is rare or absent. Lenticular sandy ripples (up to 17 cm long and 3 cm in height) with internal ripple cross-lamination are present in the middle part of the facies, and typically form semi-continuous layers where sets of ripples are partly separated by fine-grained drapes. Smaller sandy ripples or micro-hummocky bedforms are completely enclosed by clayey siltstone in finer-grained parts of the facies. Body fossils are rare within this facies, and are limited to fragmented, unidentified molluscan shells. The amount of bioturbation increases upward and well preserved trace fossils, including *Thalassinoides*, *Diplocraterion*, and rarer *Rhizocorallium* and *Planolites* occur at the contacts between interbeds.

Interpretation

This heterolithic facies represents marine deposition in water depths between storm and fair-weather wave base in the lower shoreface to upper offshore zone. The facies shows a range of storm-generated wave and current features, which indicate that normal, quieter sedimentation was overprinted by episodic storm deposition.

Vertical changes in sedimentary structures and grain size within this facies indicate changes in wave and current energy. Relatively low energy sedimentation is indicated by lenticular ripples isolated in clayey siltstone (linsen); sets of ripple-laminated very fine-grained sandstone separated by clayey siltstone drapes (flasers), and amalgamated units of ripple- laminated sandstone with finer-grained drapes were deposited in higher-energy settings. Load casts

overlying reactivation surfaces at the base of interbeds indicate that deposition of beds was rapid, whilst thin lags suggest at least minor erosion of underlying facies.

Lenticular micro-hummocky cross-stratified beds and planar cross-stratified intervals with coarse-grained foresets attest to occasional vigorous storm currents, which were able to scour the sediment surface in deeper water. These structures are smaller and less continuous than those of facies 14. The trace fossil assemblage belongs to the *Cruziana* ichnofacies and is very similar to ichnofacies described in similar rocks of the Cretaceous Interior Seaway of North America (Pemberton and Frey, 1984; Pemberton *et al.*, 1992). Although burrows are common in facies 15, physical reworking of the sediment was the dominant process. The lack of pervasive bioturbation and the preservation of delicately laminated beds indicates that the infauna were unable to completely homogenise the sediment between storms.

3.2.16 Facies 16 - thinly-bedded graded sandstone and siltstone

This facies is best preserved in the western region of an east-west trending palaeoembayment which occupied the northern part of the Wallhallow 1:250,000 sheet. It is also exposed in the central part of the southern region, and more rarely in the northern region. The facies is up to 25.5 m thick and overlies facies 19 or 21 with a sharp, apparently conformable contact.

Facies 16 is composed of centimetre- to millimetre-thick alternating laminae or thin beds of pale claystone and iron-stained, coarser-grained rocks (Plate 3h). Coarser-grained interbeds are composed of coarse siltstone to medium-grained sandstone with rare, coarser clasts. Bed thickness varies laterally over 5 to 10 cm in an undulating manner (wavy bedding). XRD analysis identified quartz, kaolinite, and muscovite/illite as the major components.

Coarse siltstone and sandstone beds are commonly graded, have even tops and irregular bases with small scale erosional scours, and may show internal low-angle cross-lamination, although most lack prominent cross-stratification. Rarely, coarse-grained interbeds have a morphology similar to HCS beds in facies 14 and 15, but with a wavelength of a few to tens of centimetres. These beds display top surfaces with a hummocky aspect, and internal laminae thicken towards hummock crests. Claystone interbeds are massive or planar laminated, do not show grading, and exhibit a higher degree of sorting than coarser-grained interbeds. This facies exhibits two distinct ichnofabrics. Coarse-grained graded beds are not bioturbated and contain only a few unidentified burrows. However, silty claystone beds are intensely bioturbated and contain

small trace fossils, including *Planolites*, *Rhizocorallium*, *Chondrites*, and probably *Teichichnus*.

Interpretation

This facies accumulated in deeper-water zones in the southern and south-eastern parts of the shelf, distal from the palaeoshoreline. In this region relatively great water depths meant that the seafloor was only affected by major storms. The rhythmic interstratification of relatively coarse and fine layers is most probably the product of episodic storm sedimentation. Trace fossils and internal stratification lead to the inference that deposition occurred mostly in the upper offshore to offshore transition zone (Pemberton *et al.*, 1992).

Beds contain erosional rills, pinch and swell couplets, and rare very small-scale low-angle cross-lamination; all of which are common features of distal storm beds (Aigner, 1985; Schieber, 1990). Many of these beds appear to have been formed under less vigorous flow conditions than most HCS beds (such as those of facies 14 and 15). These features, and the localised nature of the bioturbation, indicate that deposition of the graded coarser beds is likely to have occurred by settling of mostly suspended material after episodic storms, whereas finer-grained beds were formed by continuous background sedimentation (Davis and Byers, 1989). Facies 16 closely resembles the "graded rhythmite" lithology of Reineck and Singh (1972), and the sedimentary features are similar to those observed in other distal storm-generated units (*e.g.* Brenchley, 1985; Schieber, 1990).

3.2.17 Facies 17 - pebbly siltstone

This facies occurs throughout the southern region and has a maximum thickness of 4.5 m; it is commonly associated with facies 4. The facies consists of white to light brown, massive, partially silicified, clayey very fine sandstone to coarse-medium siltstone. The facies is moderately sorted and has a clayey matrix, which is stained or cemented by brown to purple iron oxides. This sandstone-siltstone contains a great variety and abundance of lonestones of various sizes, shapes, and compositions. The facies also contains discontinuous stringers and pods of poorly sorted coarse sand to granule sized grains. XRD analysis shows that this facies is composed of quartz, kaolinite, hematite, goethite, and a minor amount of muscovite/illite.

Flat- and ripple-lamination are the only sedimentary structures. Parts of the facies are slightly to moderately bioturbated and contain very rare segmented plant fossils. The upper part of this facies displays *Skolithos* burrows filled in by sand from the overlying facies.

Interpretation

The depositional environment of this facies is not readily interpreted. The basal and middle parts of the facies contain flat lamination and ripple lamination, indicating deposition in relatively quiet water. The lack of intense bioturbation or marine fossils in most parts of the facies suggests a poorly oxygenated offshore marine environment, or possibly a back-barrier lagoon depositional environment, although no associated barrier facies were observed. In most exposures marine trace fossils near the top of the facies document a upward increasing marine influence. Facies 17 is lithologically similar to, and may be equivalent to, facies 22 in the northern and central regions. The presence of dispersed clasts (lonestones) and pods and stringers of coarse grains is very similar to facies 22. The interpretation for these features is the same as that proposed for similar features in facies 4, 13 and 22; that is, coarse-grained debris was probably rafted offshore by ice into regions characterised by fine-grained substrates.

3.2.18 Facies 18 - laminated clayey siltstone and sandy siltstone

This facies is widely distributed throughout the southern region and has a thickness of 2 to 6.4 m. The facies typically overlies facies 4 with a sharp, conformable contact. The facies is composed of well sorted, clayey, fine siltstone to very fine sandstone. The facies is thickly to thinly laminated, with distinct laminae being cemented by dark brown to purple iron oxide (Plate 4a). Some thicker laminae or thin beds contain coarse sand grains and are normally graded. In places the lamination is wavy and irregular, and the bases of coarser-grained interbeds exhibit small scale erosional scours. XRD analysis shows that the facies consists of quartz, kaolinite, hematite and minor amounts of muscovite/illite. The facies contains rare ripple lamination and is slightly bioturbated in places. The middle part of the facies displays rare *Planolites* burrows. Fine-grained parts of the facies have liesegang banding, limonite concretions and small *Skolithos* and *Arenicolites* burrows.

Interpretation

Bioturbation and the presence of marine trace fossils suggest a marine depositional environment. The facies is similar to facies 16, but was deposited in a lower-energy, deeper

PLATE 4

a Laminated siltstone with very thin sandstone interbeds (facies 18). Most lamination is flat and even, but some of the thicker sandstone beds are graded and show evidence for minor erosion along their bases. Site 103, southern region. Hammer is 32.5 cm long.

b Siltstone of facies 19; grey portions are relatively fresh, whereas paler sections are weathered and have a thin coating of iron-oxide. This facies is thinly laminated and exhibits pseudomorphs after pyrite. Site 96, southern region. Lens cap is 5.75 cm in diameter.

c Mottled intensely bioturbated siltstone of facies 21. Most primary sedimentary structures have been obliterated by bioturbation. Site 65, central region. Hammer is 32.5 cm long.

d Pale yellow clayey siltstone and claystone of facies 22 overlying ferruginous quartz sandstone with a sharp contact (arrowed and dashed). The contact represents a marine flooding surface. Note the crude bedding of the upper siltstone; blocks are breaking along the bedding planes. This facies is intensely bioturbated and other internal sedimentary structures are rare. Near site 143, northern region. Upper siltstone interval is 2 m-thick.

e Contact (dashed line) of the two main weathering horizons recognised in the study area. Ferricrete 1 (base) consists of lithic and ferruginous clasts set in a sandy clayey matrix. Ferricrete 2 (top) is more highly cemented, commonly massive or pisolitic, and is typically darker in colour. Site 8, northern region. Hammer is 32.5 cm long.

f Thick massive outcrop of ferricrete 2 showing the strongly iron-oxide cemented nature of this unit. In the northern region this unit commonly exhibits secondary weathering features such as vertical solution pipes (seen as greenish-brown tone on the photo) lined with goethite or packed with soil pisoliths. Site 188, northern region. Hammer and scale bar for reference.

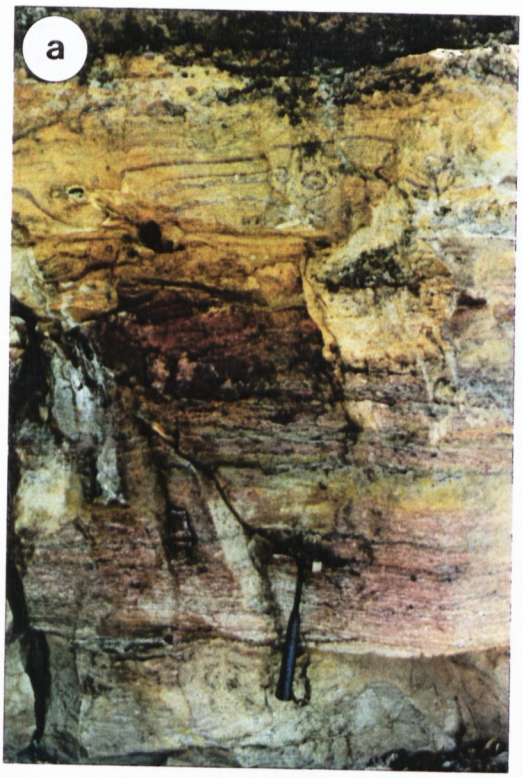
a

d

b

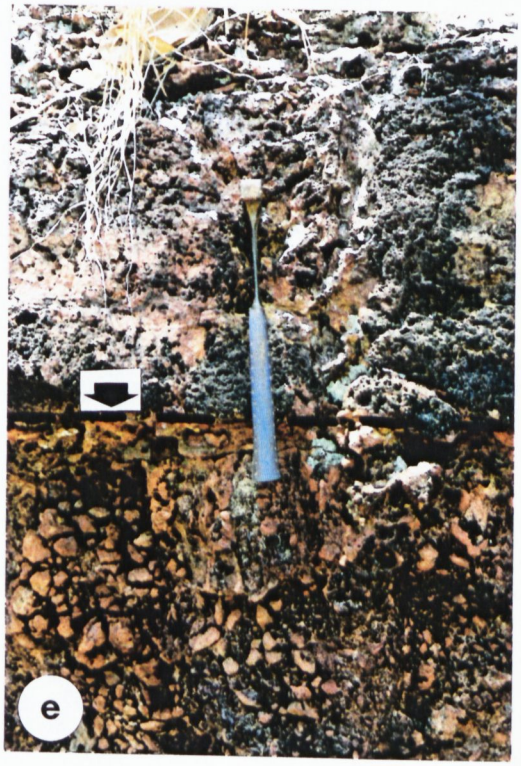
e

c

f

water setting. The fine lamination and lack of wave-generated structures suggest a setting in the offshore zone beneath fair-weather wave base and beyond the influence of most storms. However, the presence of graded coarser-grained beds indicates that fair-weather sedimentation was intermittently interrupted by coarser-grained sedimentation during and immediately after major storms. Concretions in finer-grained parts of the facies suggest slow, condensed sedimentation in the intervals between major storms.

The generally weak nature of the bioturbation and the lack of marine body fossils suggests that benthic infauna were inhibited, probably due to dysaerobic to anaerobic bottom waters combined with episodic burial due to high sedimentation rates during storms. The presence of a large amount of reduced iron species supports the interpretation of a poorly oxygenated depositional environment.

3.2.19 Facies 19 - weakly bioturbated laminated siltstone

This facies accumulated in two main areas. First, an east-west zone of outcrop in the northern half of the Wallhallow 1:250,000 sheet in the southern region. Second, to the north of Numbulwar in the northern part of the central area where the facies is intersected in a number of shallow drillholes. Facies 19 commonly grades into facies 18 and has a thickness of at least 10 m; contacts with underlying rocks were not observed.

The facies comprises dark to light grey, well sorted, silty claystone to clayey siltstone (Plate 4b). The rocks are fractured in places and the fractures are stained by brown iron oxide and gypsum (derived from the weathering of pyrite). The base of the facies is slightly bioturbated and some intervals are thickly laminated. Cone-in-cone structure in visible in the basal part of the facies. XRD analysis of samples from both areas shows that the facies has a distinctive matrix composed of iron-enriched smectitic clay and kaolinite. In places the base of this facies contains marine microfossils and palynomorphs. Preservation of trace fossils is not distinct due to the lack of lithological contrast, although *Planolites*, *Chondrites*, and *Palaeophycus* were recognised along with poorly preserved *Thalassinoides* and *Zoophycos*.

Interpretation

This facies was deposited in an offshore marine setting beneath storm wave base. The weak nature of the bioturbation, the dark colour, the high organic content (Alley, 1991), and the presence of gypsum (and rare pyrite) are distinctive features of this facies.

Weak bioturbation suggests that the basal and middle parts of the facies were deposited under dysaerobic conditions (which are restrictive to many benthic invertebrates). The *Cruziana* trace fossil assemblage and the nature of the stratification indicate that deposition probably occurred in the lower offshore region (MacEachern and Pemberton, 1992), or in shallower, restricted marine settings. The combination of reduced oxygen levels in the water and abundant organic matter resulted in strongly reducing conditions, which favoured the reduction of sulphate to yield hydrogen sulphide. In a situation similar to that described by Curtis (1977) and Berner (1981), the hydrogen sulphide probably reacted with ferrous iron to produce pyrite as an end product. In this case most of the pyrite was subsequently altered by weathering to form gypsum. Cone-in-cone structure near the base of the facies indicates that calcareous cement may have formed, but this is not preserved.

3.2.20 Facies 20 - laminated clayey siltstone

This facies occurs in the central part of the southern region and has a maximum thickness of 13 m. The facies is composed of white, silicified, well sorted, clayey siltstone (see Plate 5f). The only sedimentary structures are delicate, thin planar lamination and rare ripple lamination. The facies is slightly to moderately bioturbated in the upper 5 m. The basal half of the facies contains rare plant fossils in the form of several segmented wood fragments. The upper parts display *Planolites* and *Palaeophycus* burrows. XRD analysis shows that this facies is composed of quartz, kaolinite, muscovite/illite, and a small amount of feldspar.

Interpretation

Facies 20 may reflect quiet nonmarine deposition in a lacustrine or overbank fluvial setting. However, given the interpreted nonmarine depositional environment it is problematic that root casts or other evidence for subaerial exposure were not observed in this facies. The lack of bioturbation and the presence of fine lamination indicate that much of the material settled out of suspension in quiet water, which was not suitable for a burrowing infauna. The rare plant fossils were possibly transported to the depositional site by streams. This facies may correspond to the Fl or Fsc (overbank to backswamp) facies, and OF (overbank fines) architectural element of Miall (1985; 1992a). The facies is associated with a coarse-grained fluvial facies (4), and may have been deposited in the same fluvial system. The restricted areal distribution of this facies in a shelf setting is interesting but not unique (*cf.* Shanley and McCabe, 1991), and may be due to significant erosion and reworking of fluvial deposits during lateral accretion (see also discussion in Sect. 9.6.2).

3.2.21 Facies 21 - intensely bioturbated siltstone

This facies occurs throughout the field area, but is particularly well exposed in the BPRZ. Facies 21 commonly has a thickness of only a few metres and is typically associated with facies 15 or 16.

Facies 21 consists of extremely bioturbated siltstone with few preserved sedimentary structures. In places the facies is similar to facies 19, however facies 21 has a lower organic content, a much higher degree of bioturbation, and is paler in colour (Plate 4c). Where bioturbation is less intense, flat lamination is the most common internal stratification; rare silty graded beds (< 1 cm thick), and convolute lamination are present. The top of the facies in proximal exposures contains very rare starved sandy ripples and micro-hummocky lenticular beds, but these are much smaller and less common than similar structures in facies 15 and 16. The degree of bioturbation is so intense locally that identification of individual trace fossils is difficult. However, rare *Planolites*, *Zoophycos*, and *Arenicolites* burrows are present, whilst the dominant trace fossil is small (1 to 2 mm diameter), silt-filled *Chondrites* burrows. Body fossils were not observed.

Interpretation

This marine facies was deposited in distal regions that were generally beyond the influence of storm waves. The overall lack of wave-formed sedimentary structures suggests deposition beneath storm wave base, in deeper water than most marine facies (*e.g.* facies 8, 12, 13, 14, 15, 16).

Rocks of facies 21 are interpreted as largely the product of suspension settling of fine-grained clastic material in an offshore or transitional zone during periods of fair-weather. Fine-grained hemipelagic sedimentation was intermittently overprinted by coarser-grained sedimentation during large storms. The action of storms during accumulation of this facies was weaker than that affecting other facies, due to greater water depth and distance from the palaeoshoreline. The presence of very rare starved sandy ripples and micro-hummocky lenticular beds indicates disturbance of the seafloor by occasional vigorous storm currents, or deposition of thin tempestites in a distal setting. Convolute lamination within siltstone in slightly coarser-grained parts of the facies suggests rapid deposition by settling of suspended material after episodic storms, similar to parts of facies 16.

The intense nature of the bioturbation (*Cruziana* ichnofacies) is a distinctive feature of this facies, and the presence of such abundant infauna suggests deposition under mostly aerobic to slightly dysaerobic conditions in the lower offshore zone (MacEachern and Pemberton, 1992). However, the dark colour of fresh samples suggests at least intermittent deposition in dysaerobic to anaerobic bottom waters, but still under better oxygenated conditions than facies 19. The relative abundance of *Chondrites* burrows in most exposures also supports the interpretation of intermittently dysaerobic to anaerobic bottom waters, because the *Chondrites* ichnogenera has a relatively high tolerance to depressed oxygen levels (Ekdale and Mason, 1988). These apparent changes in bottom water oxygenation may have been enhanced or caused by vigorous circulation during and after large storms.

3.2.22 Facies 22 - silty claystone

This is an important facies for regional correlation and occurs in the northern, central and southern regions. Facies 22 is typically 1.5 to 2 m thick with a maximum thickness of 4 m, and is commonly associated with facies 15, 16, 18, 19, and 21.

In proximal localities facies 22 consists of clayey fine siltstone (Plate 4d), and in intermediate to distal localities the facies consists of silty claystone. The facies is commonly massive, and internal stratification such as flat lamination is poorly preserved due to intense bioturbation. Many exposures of this facies display irregular, discontinuous streaks or small lenses, usually less than 5 cm in diameter, where fine sand to fine granule sized grains are concentrated without a large amount of clay matrix. These streaks or lenses are sometimes stained or cemented by iron oxide and have a distinctive purple to dark red colour. Coarser-grained parts of the facies contain small-scale HCS and wave-ripple lamination. XRD analysis shows the facies consists of quartz, kaolinite, and minor muscovite/illite. Facies 22 has not yielded macro- or micro-fossils, and the degree of bioturbation is typically so intense that most trace fossils have been obliterated. However, the basal part of the facies contains *Rhizocorallium* and *Planolites* burrows and the upper bedding surface forms a *Skolithos* burrowed hardground in some localities.

Interpretation

Pervasive homogenisation by a burrowing infauna has destroyed most evidence of primary sedimentary structures in this facies. However, the rare HCS and wave-ripple lamination suggest that sedimentation was partly controlled by episodic storms. It seems likely from the

fine grain size, trace fossils, and the high degree of bioturbation that this facies was deposited in an open-marine setting in well oxygenated bottom waters. The general lack of wave-formed sedimentary structures suggests that deposition occurred in the offshore zone beneath fair-weather wave base.

The light colour of the facies and the high degree of silicification indicate that this facies has undergone intense weathering and chemical diagenesis. The presence of pods and stringers of sand to small granule sized clasts is the same as in facies 13, and the same interpretations are suggested here; that is, either rafting of coarse material by seasonal ice, or selective bioturbation and concentration of coarse-grained storm-transported debris by abundant infauna.

3.2.23 Ferricrete 1

Ferruginised or lateritic plateaux and tablelands are well exposed throughout northeastern Arnhem Land. Ferricretes are the most common component of these landforms, but in places true laterites are present and show a distinctive vertically-zoned deep weathering profile. Ferruginisation of sandstone at Cape Arnhem (about 10 km east from the nearest outcrop of ferricrete 1, and 5 to 10 km southeast of the nearest known bauxite deposit) has been tentatively dated as Late Cretaceous (M. Idnurm, written comm., 1994). Moreover, other lateritic profiles or ferricretes are considered to be Cretaceous in age by correlation (Bardossy and Aleva, 1990) because they are directly related to Cretaceous rocks (their parent lithologies). However, many of these ferricretes and other weathered zones probably formed in Tertiary time. The development of ferricrete partly depends on the nature of the underlying parent material, and in this sense the presence of ferricrete or other resistant duricrusts as a cap overlying particular Cretaceous facies can be useful for correlation on a local scale.

This unit is the more common of the two ferricretes (Plate 4e) and consists of lithic and ferruginised clasts set in a matrix of ferruginous clay, silt and sand. It has a maximum thickness of 5 m. The clasts are granule to mid-cobble size, poorly sorted and rounded to subrounded. Clasts are composed of ferruginised sandstone and other unidentifiable, highly weathered lithic fragments. The matrix is very poorly sorted and highly variable in composition; the main matrix type is subrounded, poorly sorted, argillaceous, ferruginous, coarse to fine quartz sand. In places the unit is cemented or intensely stained by iron oxides and manganese oxides with a porous, mottled texture, which resembles a fine boxwork. Primary sedimentary structures are absent.

Interpretation

Ferricrete 1 represents a ferricrete or ferruginous hardpan, and it appears that parts of the horizon have been brecciated by mechanical surface weathering and short-distance (in the order of metres) lateral transport before the fragments were again cemented by iron oxides.

The ages of initial ferruginisation and subsequent reworking and cementation associated with this unit are difficult to assess from this regional study. Indeed, it is likely that this ferricrete is not associated with any particular geomorphic surface or event, but rather occurs where conditions were suitable for iron accumulation and hardening (*e.g.* Pain and Ollier, 1992). In places the base of the unit exhibits a brown/purple mottled 'boxwork' texture which is characteristic of deep weathering and ferruginisation in humid climates (Bardossy and Aleva, 1990). This weathering profile shows varying degrees of mechanical reworking and chemical reconstitution. It appears to occur in lower lying regions than the overlying weathered horizon (ferricrete 2), and in many places ferricrete 1 is found in gradational contact with underlying Cretaceous fluvial sandstones.

3.2.24 Ferricrete 2

This unit also occurs in the northern part of the ALZ, but is not as widely exposed as ferricrete 1. It has a maximum thickness of 5 m and consists of massive or pisolitic, strongly cemented ferruginous sandstone or lithic debris. Where cementation is less intense, concentrically zoned pisoliths with a poor to moderate degree of sorting are preserved. The matrix is commonly iron-oxide stained, clayey, lithic, quartz sand of variable grain size. The unit varies in colour from brick red to a blackish-red, depending mainly on the type and amount of cement. In rare exposures the facies has a ferromanganese or manganese oxide cement. Sedimentary structures are absent, but weathering features (solution pipes and soil pisoliths) are present (Plate 4f).

Interpretation

This unit is considered to be a residual weathering profile and forms a duricrust in most exposures. In most areas it can be classified as a ferricrete, although to the north superficially similar landforms form true bauxites, and are currently being mined in the vicinity of Nhulunbuy in the northeastern corner of Arnhem Land. However, there is little, if any, obvious relationship between either of the ferricretes described in this study and the bauxites near Nhulunbuy. In general, the ferricretes associated with Cretaceous facies are less

commonly pisolitic, have much poorer sorting, contain higher percentages of contaminants (weathered lithic clasts), and have a high proportion of silty kaolinitic clay and quartz sand as matrix compared to the bauxites at Nhulunbuy. Whether these textural and compositional differences are due to a different degree of weathering, unusual fluid migration and remobilisation of iron species, or different parent material is unclear. For a full discussion of the bauxites at Nhulunbuy and their possible origins the reader is referred to the comprehensive text on lateritic bauxites by Bardossy and Aleva (1990, p. 438-445).

3.3 CHAPTER SUMMARY

The mid-Cretaceous shelf sequence of the western and southern margins of the Carpentaria Basin has been subdivided into twenty two sedimentary facies, largely on the basis of grain size, primary sedimentary structures, fossil content, and degree of bioturbation. A large proportion of the facies represent shallow marine depositional environments, and fluvial to coastal-plain depositional environments are also important.

Most of the marine facies exhibit features indicative of storm- or wave-dominated deposition. Tidal processes do not appear to have been important during accumulation of the Mullaman Beds. Trace fossils within marine facies belong to the *Skolithos* and *Cruziana* ichnofacies, and suggest shallow-marine deposition under aerobic to slightly dysaerobic conditions in high to moderate energy depositional environments. The facies subdivision outlined in this chapter is used throughout the thesis, and forms the basic descriptive part of the study. This facies subdivision is fundamental to the description and recognition of facies successions, and also for stratigraphic correlations in following chapters.

~~~~~~
~~~~~~

4. FACIES SUCCESSIONS: STACKING PATTERNS OF CARPENTARIA BASIN SHELF FACIES

4.1 INTRODUCTION

The logistical problems associated with simple stratigraphic correlation in this project are unusual when compared to many more orthodox stratigraphic studies. By the very nature of the preservation of the sediments, the lateral facies changes are difficult to recognise without exhaustive and detailed comparison of numerous individual measured sections. For this reason a large part of the project involved description and recognition of important vertical changes in the rocks to enable local correlation. The vertical changes in the rocks are generally described as grain size trends defined by the stacking of facies to form facies successions.

Chapter 4 is designed to incorporate the detailed facies descriptions of the previous chapter with lateral facies relationships and vertical facies stacking patterns to describe facies successions that occur over the entire study area. Correlation of these facies successions in chapters 5, 6, and 7 forms the basis for interpretation of local and semi-regional depositional environments. Information concerning the distribution and nature of facies successions is then combined with correlations using specific marker horizons, biostratigraphy, and drill-hole data to erect a regional lithostratigraphic framework in chapter 8.

4.2 DEFINITIONS AND CONCEPTS

Before beginning a detailed description and interpretation of facies successions it is useful to look at the scale of subdivision of facies used in this study, and the methodology used in grouping separate distinct facies in a logical way to enable accurate correlation.

Most workers dealing with the stratigraphic and sedimentological analysis of siliciclastic strata by outcrop, divide a sedimentary package into a number of lithofacies, which are largely descriptive and have only a brief environmental interpretation assigned to them. One then looks for repeated vertical and lateral patterns of organisation in these facies, and defines these patterns using facies assemblages or facies successions. The problems are; how finely is it

necessary to divide the sedimentary package into lithofacies?; and how is it possible to group lithofacies logically together to enable interpretation of depositional environments?

A facies succession is defined as "a vertical succession of facies characterised by a progressive change in one or more parameters..." (Walker, 1992, p. 2). The concept of a facies succession implies that certain facies properties change in a specific direction (vertically and/or laterally); these properties might include the proportion of sand, the amount of bioturbation, or the grain size of the sand. It is implied that the facies are genetically related inasmuch as particular sedimentological characteristics are progressively changing throughout the succession; for example, grain size might be gradually increasing, and there might be a change upward from dominantly biologically formed structures to physically formed ones.

In this study, Cretaceous sediments exposed along the western and southwestern margins of the Gulf of Carpentaria are subdivided into twenty two distinct lithofacies (Chapter 3). Commonly, these facies can be grouped into larger cycles which show important vertical changes in the rocks at an outcrop-scale. In this way the facies have been grouped to define eight common facies successions which are recognisable in the rocks, and which document important environmental changes on the shelf over time.

4.3 FACIES SUCCESSIONS

The vertical facies successions described below are based on observations of repeated and systematic facies relationships in outcrop and core. Facies successions described below represent distinct two-dimensional lithofacies assemblages. Mapping and correlation of facies successions (chapter 5-8) adds the third dimension and defines the depositional systems, and indicates that some facies successions tend to occur together while others are mutually exclusive.

Most facies successions on the Carpentaria Basin shelf are less than 10 m thick and are commonly bounded by discontinuities, such as marine flooding surfaces, transgressive surfaces of erosion, and sharp based channels (regressive surfaces of erosion). The contacts between facies within a succession are typically gradational, although local erosion and minor surfaces of reactivation are common. Repeated vertical stacking of thin discontinuity-bounded successions on the Carpentaria Basin shelf has resulted in a stratigraphically and sedimentologically complex sequence which exhibits multiple facies changes.

Eight distinct facies successions have been recognised in the Mullaman Beds, and they follow three basic patterns: 1) coarsening-upward or (sandier-upward) successions; 2) fining-upward successions; and 3) irregular successions, which commonly contain nonmarine and marine indicators (Table 4.1). The interpretive titles of the successions are discussed in the individual descriptions below. These interpretations are further substantiated by lateral correlation, thickness trends, and sand body geometries in later chapters.

TABLE 4.1. Cretaceous facies successions of the western Carpentaria Basin.

	FACIES SUCCESSION	FACIES STACKING (from base to top)
1	**Storm-influenced lower offshore marine**	**coarsening-upward (19-18-16)**
2	**Storm- (and wave-) dominated shoreface (typically progradational)**	**coarsening-upward (22/21-13-12/15-14-8/3)**
3	**Fluvial interdistributary / channel fill**	**coarsening-upward (20-7-4)**
4	**Storm-influenced lower shoreface to offshore shallow-marine**	**fining-upward (10/13-16-18/21/22)**
5	**Storm- (and wave-) dominated shoreface (typically retrogradational)**	**fining-upward (3-8-12/15-14/13-21/22)**
6	**Paralic systems (estuarine and deltaic-marine)**	**fining-upward (variable)**
7	**Fluvial channel fill**	**fining-upward (1/2-5-7/11-6)**
8	**Sheltered / restricted marine (bays and lagoons)**	**irregular (10/12-13)**

Measured sections showing typical outcrop examples of each facies succession and their important variations are illustrated in stratigraphic correlation diagrams in chapters 5-7. Examples of each type of facies succession are presented in chapters 5-7 in the form of measured sections in stratigraphic correlation diagrams. The overall grain size trends characterising each succession are shown by fining- or coarsening-upward symbols. The boundaries of the northern, central, and southern regions and the locations of field sites are shown in Fig. 4.1, and on more detailed base maps in Appendix 3.

4.4 COARSENING-UPWARD (OR SANDIER-UPWARD) SUCCESSIONS

4.4.1 Facies Succession 1 - storm-influenced lower-offshore marine

This facies succession has a slightly coarsening-upward character and occurs in the western part of the southern region, and in drillholes immediately north of Numbulwar in the northern part of the central region. Stacked cycles of this facies succession are at least 30 m thick (contact with basement was only observed in at a few sites). In the central region the succession is overlain by sandstones (facies 12 and 8) of the middle to upper shoreface. In the southern region the succession is overlain by fining-upward lower shoreface to offshore marine facies of succession 4.

The basal part of the succession consists of dark to light grey, well sorted, silty claystone and clayey siltstone (facies 19), with a thickness greater than 10 m (Plate 5a). This finely laminated rock coarsens gently upward and passes into 5 to 8 m of laminated clayey siltstone and silty sandstone (facies 18; Plate 5b). The degree of sorting decreases upward as the grain size increases. As the grain size continues to increase upward, fine lamination gives way to irregular lamination and normally graded fine- to medium-grained sandstone beds (<1 cm thick) interbedded with siltstone. The number and thickness of graded sandy beds is greatest in the upper 2 m of the succession. The contact at the top of the succession between interbedded sandstone and siltstone (facies 16) and underlying laminated siltstone is gradational.

The base of the succession is only slightly bioturbated and has small *Planolites*, *Chondrites*, and *Palaeophycus* burrows. In the central and southern regions the less weathered base of the facies yields arenaceous foraminifera and palynomorphs. The degree of bioturbation increases toward the top of the succession where finer-grained interbeds are intensely bioturbated and contain *Rhizocorallium*, *Palaeophycus*, *Teichichnus*, *Planolites*, and *Thalassinoides* trace fossils. Lateritisation has affected the upper part of the succession in the southern region.

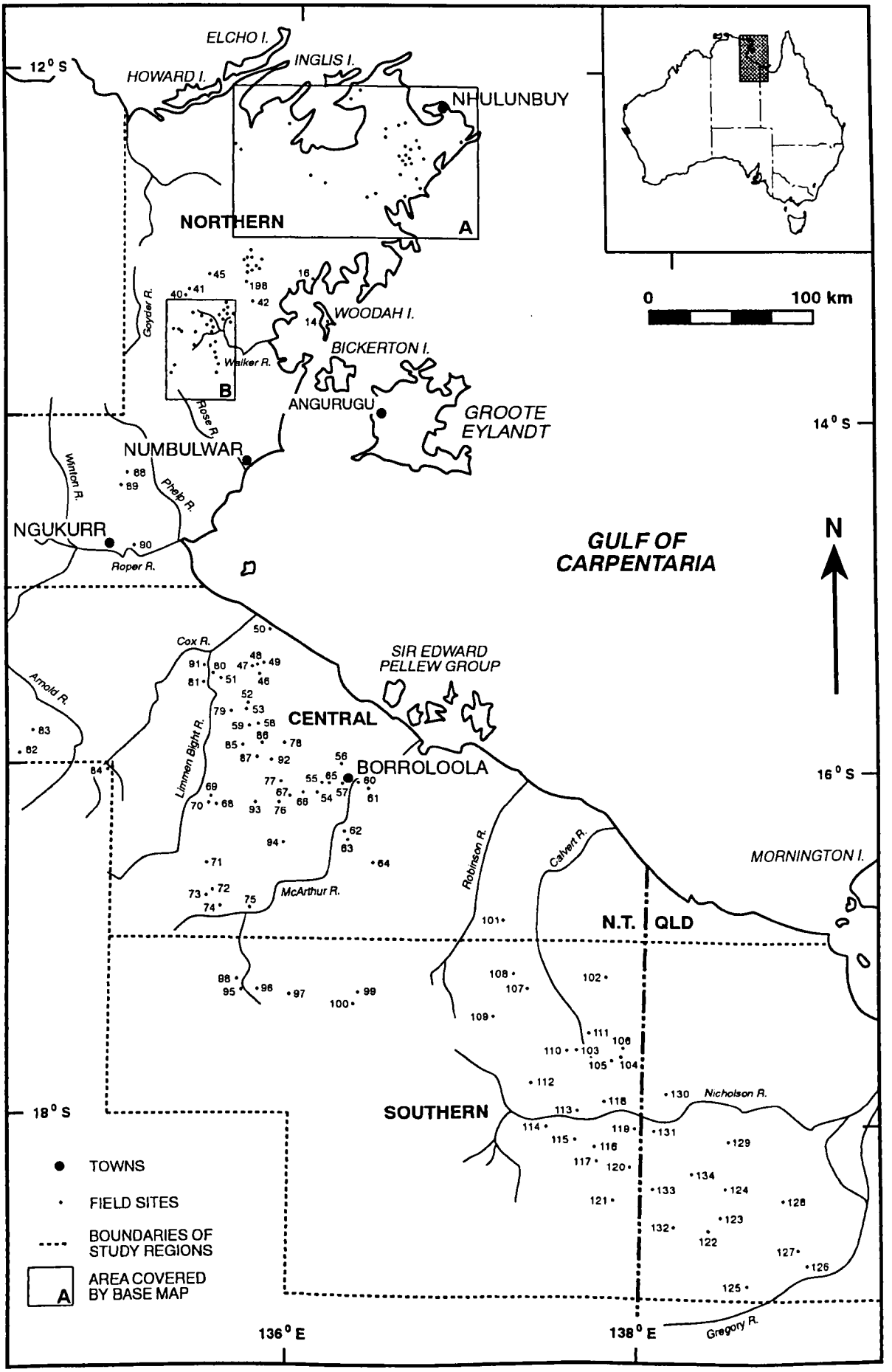

FIGURE 4.1. Location map showing numbered field sites over the entire study area. Due to crowding, the numbers for field sites in the northern region are shown on base maps in Appendix 3

PLATE 5

a Typical low-relief exposure of dark-coloured, organic-rich fine-grained facies at the base of coarsening-upward facies succession 1. For a close-up of these basal fine-grained rocks see plate 4b. Site 96, southern region. Note people for scale.

b Similar rocks to those in plates 5a and 4b, except here the siltstones are becoming sandier, they are paler in colour, the lamination is thicker, and they occur stratigraphically higher within cycles of facies succession 1. Site 96, southern region. Pen is 13.5 cm long.

c General outcrop view of interbedded siltstone and sandstone forming coarsening- and thickening-upwards cycles of facies succession 2. Rock ledge in foreground corresponds to the bulk of a single cycle of facies succession 2, and is about 5 m thick. Site 174, northern region.

d Close-up of thinly bedded basal fine-grained rocks which coarsen-upward to crossbedded shoreface sandstones at the top of facies succession 2. Top of cycle occurs about 2m above top of photo. Site 143, northern region. Hammer is 32.5 cm long.

e Basal half of a coarsening- and thickening-upwards cycle of facies succession 2 overlying a basal conglomeratic pebble lag. Note the relatively dark colour and weak lamination of the basal siltstone, which passes up into thinly interbedded clayey siltstone and sandstone of the middle part of the cycle. Site 180, northern region. Hammer is 32.5 cm long.

f Rare exposure of facies succession 3. The basal part consists of pale grey to white thinly laminated claystone and siltstone which passes rapidly up into grey, poorly sorted, very coarse- to medium-grained quartz sandstone. The contact is marked by a white dashed line and black arrow. Site 116, southern region. The section in the photo is about 10 m thick.

a

b

c

d

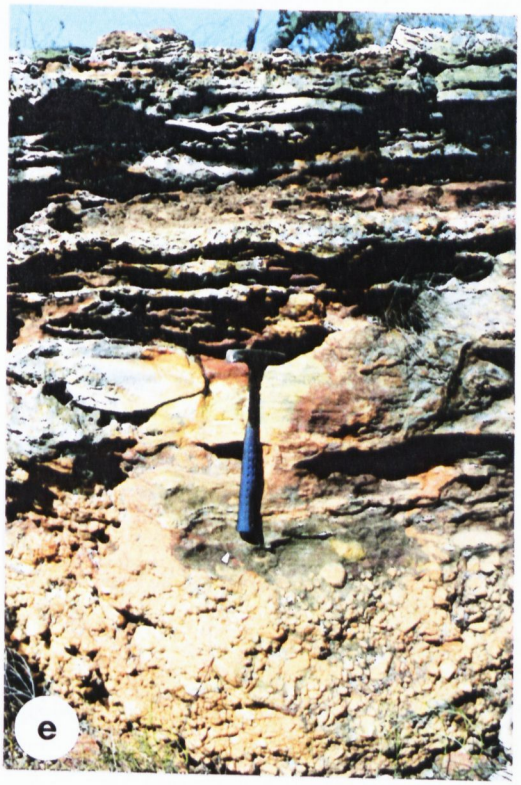
e

f

Interpretation

Facies succession 1 is interpreted as the deposit of an offshore marine setting under the influence of episodic storms. The coarsening-upward grain size and change from flat lamination to coarser-grained graded beds suggests deposition under decreasing water depth in a quiet, offshore marine environment. The rhythmic interstratification of relatively coarse and fine layers near the top of the succession is the product of episodic storm sedimentation, which deposited sandy graded beds with erosional bases.

The slight degree of bioturbation and the finely laminated nature of the basal part of the succession suggests deposition beneath storm wave base under dysaerobic conditions (which are restrictive to many benthic invertebrates). The *Cruziana* trace fossil assemblage indicates that deposition probably occurred in the lower offshore region (MacEachern and Pemberton, 1992), or in shallower, restricted marine settings. Reduced oxygen levels in the water may have also favoured the preservation of organic matter (Davis *et al.*, 1989), and resulted in the formation of pyrite (subsequently altered to gypsum) near the base of the facies.

Siltstone in the intermediate part of the succession was also deposited in an offshore marine setting, but in even shallower (and possibly more oxygenated) water. This is shown by a higher content of oxidised iron, the thicker and less-even style of lamination, the coarser grain size, and the presence of thin sandy beds near the top of the facies. The oxygenation of bottom waters may have been episodic in response to increased circulation during and after storms.

Beds in the upper part of the succession commonly have irregular bases and even tops and show clear evidence of distal storm sedimentation including erosional rills, pinch and swell couplets, and rare internal, very small scale, low-angle cross-lamination (Aigner, 1985; Schieber, 1990). Sedimentary structures here indicate that deposition of graded coarser beds occurred by settling of suspended material after episodic storms, whereas the finer-grained layers were formed by continuous background sedimentation. Details of important vertical and lateral variations within succession 1 are presented in the discussion of Carpentaria Basin shallow-marine depositional systems in Sects. 10.7 and 10.8.

4.4.2 Facies Succession 2 - storm- (and wave-) dominated shoreface (typically progradational)

The northern and central parts of the shelf are sand-dominated, and measured sections in these areas commonly consist of numerous smoothly coarsening-upward or irregularly coarsening-upward successions (Plate 5c). In the northern region the thickness of each succession is 3 to 6 m, with an average thickness of 4 to 5 m. In the central and southern regions vertical grain size trends are more subtle, and some exposures are possibly composed of a number of stacked, poorly defined coarsening-upward successions, which are only apparent as a single crude coarsening-upward trend.

In the northern region the base of succession 2 consists of fine-grained silty claystone (facies 22) or siltstone (facies 21), which commonly overlies coarse-grained marine sandstone of an underlying facies succession with an erosional or disconformable contact. The grain size increases upward as the basal facies grades smoothly upward into coarser siltstone of facies 13. The grain size continues to increase toward the top of the succession and silty sediments are gradationally overlain by fine-grained sandstone (facies 12), or interbedded sandstone and clayey siltstone (facies 15). These two facies form the bulk of succession 2.

The heterolithic facies (15) is commonly overlain by hummocky cross-stratified fine sandstone and coarse siltstone (facies 14), which is typically less than 2 m thick. The contact between facies 14 (if present) and facies 15 is sharp and commonly erosional on a small scale. The grain size increases rapidly upward from this part of the succession to crossbedded medium-coarse sand (facies 8; Plate 5d). The contact between facies 8 and facies 14 or 15 is locally erosional and the base of facies 8 sometimes displays a thin pebble to granule sized lag. The top of the succession is marked by a discontinuous conglomeratic lag or coquina (facies 3). The basal and intermediate parts of succession 2 are smoothly coarsening-upward, and the upper part displays increasing grain size with one or two rapid 'jumps' across sharp contacts between facies.

The upward change in physical sedimentary structures is readily apparent in succession 2. The basal claystone and siltstone facies (22 and 21) are intensely bioturbated, but contain some preserved structures where biological reworking has been less intense; these include flat lamination, small scale wave-ripple lamination, and starved sandy ripples.

The middle part of succession 2 consists of facies 15 and sedimentary structures change upward from lenticular ripples isolated in clayey siltstone (linsen), through sets of ripple laminated, very

fine-grained sandstone separated by clayey siltstone drapes (flasers), to amalgamated units of ripple laminated sandstone with rare finer-grained drapes and sand-filled gutters in the upper part of facies 15. In places intermediate parts of the succession consist of facies 13 and 12, and flat lamination and wave-ripple lamination change upward into very rare small-scale HCS, thin discontinuous pebble beds, and rare flaser bedding. Fine sandstone and coarse siltstone (facies 14) overlying the intermediate part of the succession contains thick, amalgamated beds with hummocky cross-stratification. The top of the succession may contain coarser-grained intervals with megaripples and planar-, swaley-, and trough- cross-stratification. The fine-grained drapes of some of these coarse-grained beds contain current ripples and micro-hummocky cross-stratification. Lags at the top of succession 2 are unstratified and occur as discontinuous pods and lenses, which appear to have random shapes and orientation.

The degree of bioturbation is moderate to intense throughout the succession, with the most intense bioturbation at the base. The basal facies (21 and 22) do not contain any preserved macrofossils, but trace fossils such as *Thalassinoides*, *Diplocraterion*, *Rhizocorallium*, *Planolites* and *Arenicolites* are recognisable. In coarser-grained sections the intermediate part of the succession (facies 12 and 13) contains some macrofossils including bivalves, trigonids and rare scaphopods. Trace fossils here include *Planolites*, *Skolithos*, *Ophiomorpha*, *Rhizocorallium*, *Palaeophycus*, *Thalassinoides*, and rare *Diplocraterion* and *Teichichnus*.

In finer-grained sections the amount of bioturbation increases upward in the interbedded part of the succession (facies 15), and well preserved trace fossils occur near the contacts of silty and sandy beds. The clayey siltstone beds invariably exhibit a higher degree of bioturbation than the sandy beds and contain the same trace fossils as the basal part of the succession. Hummocky cross-stratified beds are generally not bioturbated, except where their drapes consist of intensely bioturbated siltstone and claystone. The upper part of the succession (medium to coarse sandstone) contains rare body fossils including bivalves, trigonids and ammonites, and rare segmented plant fossils; bioturbation here is apparently pervasive, but the lack of lithological contrast makes identification of specific forms difficult. Lags at the top of succession 2 may contain rare molluscan macrofossils, but are not bioturbated.

Interpretation

Facies succession 2 is interpreted as the deposit of a typically prograding storm- and wave-dominated shoreface. The succession represents marine deposition under a regime of decreasing water depth, in the offshore to foreshore zone. Most examples of this succession

contain both storm- and wave-generated structures. Whether a single example of this succession is storm- or wave-dominated depends largely on location relative to the palaeoshoreline and on the type of exposure. Fining-upward storm-, wave-, and combined storm- and wave-dominated successions have been grouped together here.

In coarser-grained examples of this succession individual beds are relatively thick and contacts between facies are distinct. This type of succession occurs in nearshore localities, where wave reworking of the sediment was a continual process. Under these conditions the succession is dominated by structures formed under fair-weather conditions, because most storm-generated features were subsequently obliterated by 'normal' wave reworking. Storm-generated features are present, but they are normally restricted to the lower (deeper water) parts of the succession. Finer-grained examples of this succession were deposited in slightly deeper water, commonly between fair-weather and storm wave base. Characteristic features here include interbedding of fine and coarse layers (Plate 5e), large-scale wave and current bedding (HCS) and scours (gutters), and normally graded beds. Storm-generated features dominate this type of the succession and are preserved due to the offshore shallow-marine location.

Facies 21 and 22 at the base of the succession show a high degree of bioturbation with numerous trace fossils of the *Cruziana* ichnofacies, and represent a marine environment with dysaerobic to aerobic bottom conditions. Bioturbation has obliterated any sedimentary structures, but the fine grain size of the facies suggests deposition in a relatively quiet marine setting in the offshore to lower shoreface zone. The interbedded facies (15) shows a range of features which indicate that normal, quieter sedimentation was overprinted by episodic storm deposition. Lenticular micro-hummocky beds, cross-stratified beds, ripple laminated beds, and gutters were sporadically formed in facies 15 by storms. The vertical changes in sedimentary structures and grain size within this facies indicate an upward increase in wave and current energy.

Sedimentary structures indicate that after deposition of the basal part of the succession, areas of offshore marine mudstone were first invaded episodically by HCS sandstones deposited during storms. As the shoreface aggraded and prograded the sediment surface built gradually upward, until it was affected by stronger wave energies, storm waves being the most energetic. With continued shallowing more and more storm events affected the beds, and more deposits were preserved, culminating in amalgamated HCS sandstones of the upper offshore to middle shoreface. Crossbedding is preserved in coarser sandstone of the upper shoreface. Discontinuous lags and coquinas are common near the top of the succession and testify to

reworking of the upper part of the succession by large storm waves and currents. In proximal localities the upper half of the succession is dominated by cross-stratified medium to coarse sandstones, and HCS and other storm generated structures (*e.g.* gutters, graded beds, interference ripples) were not formed or preserved here.

With continued shallowing, the sea floor was affected by higher and higher energy processes and thick, amalgamated sandstone beds with hummocky cross-stratification were formed. The hummocky bedforms have a long wavelength and low amplitude and attest to the presence of large waves (Dott and Bourgeois, 1982; Duke *et al.*, 1991). Discontinuous lags at the top of the succession rarely contain any fine-grained sediment due to winnowing and reworking under maximum energy conditions during storms. At proximal localities more and more crossbedded deposits were preserved as grain size increased upward, culminating in swaley cross-stratified (SCS) sandstones of the lower shoreface. However, well-preserved SCS is rare within the Mullaman Beds. At some localities cross-stratification is overlain by flat lamination (produced by swash and backswash) characteristic of a beach setting.

Nonmarine facies with root traces or coal were not observed in succession 2. This suggests that the succession was not subaerially exposed, or that subsequent erosion of the nonmarine facies was common. The successions were probably only rarely emergent, because erosion is unlikely to have removed all traces of nonmarine facies at the top of succession 2 at all localities. Beach lamination is relatively rare and this indicates that the succession typically accumulated in water depths no shallower than the middle shoreface.

Most variations on the ideal succession above involve changes in thickness and grain size of selected facies in relation to distance from the palaeoshoreline. Details of important vertical and lateral variations within succession 2 are presented in the discussion of shallow-marine depositional systems in Sects. 10.7 and 10.8.

4.4.3 Facies Succession 3 - fluvial interdistributary/channel fill

This facies succession has a two-stage coarsening-upward character and occurs in the western part of the southern region. It is the least common of the facies successions (by far) and has a maximum thickness of 27 m, and an average thickness of 9 m.

The base of the succession consists of pale grey laminated siltstone (facies 20) up to 13 m thick. The contact of this facies with underlying rocks was not directly observed; however, at section

117 a cross-stratified sandstone (interpreted to be of fluvial origin) is exposed 4 m stratigraphically below this facies. The laminated siltstone is a highly uniform rock, and no vertical grain size change was detected for the bulk of the facies. The top metre of the facies either grades rapidly up into medium- to very coarse-grained sandstone (Plate 5f), or has a sharp planar contact with the coarsest sandstone. This sandstone is up to 10 m thick, and as the grain size of the sandstone increases dispersed pebbles become more common; eventually the rock grades into trough cross-stratified coarse to very coarse sandstone (facies 7) with a higher content of dispersed pebbles. The top of the succession consists of pebbly medium to very coarse sandstone (facies 4). The unit is matrix supported and the small pebble to very rare cobble sized clasts are dispersed randomly throughout the facies. The contact between the two coarse-grained upper facies (7 and 4) is gradational over about 0.5 to 1 m, and these facies are crudely interbedded in some exposures.

The upward change in sedimentary structures is obvious due to the large contrast in grain size from the base to the top of succession 3. The basal siltstone displays very regular and even flat lamination, and rare small scale ripple lamination. Sedimentary structures are absent in the basal part of facies 7, but the coarser-grained upper part contains trough cross-stratification with set thicknesses of 40 to 60 cm. The pebbly sandstone at the top of the succession is massive, with no imbrication or discernible bedding.

Generally the succession is only slightly bioturbated and contains few fossils; however the basal siltstone contains rare plant fossils in the form of partly silicified logs and poorly preserved trace fossils (possibly *Planolites* and *Palaeophycus*). The degree of bioturbation increases marginally from the middle to upper part of the succession, though no body or trace fossils are preserved in these parts of succession 3.

Interpretation

Succession 3 is interpreted as a fluvial interdistributary to channel-fill deposit. The very fine lamination of the siltstone at the base of the succession suggests deposition in quiet water. The presence of rare plant fossils and a sparse trace fossil assemblage combined with the lack of marine indicators, suggest a nonmarine origin for the siltstone; possibly as overbank deposits in small lagoons or lakes between high energy fluvial channels. In places this succession may reflect a slightly brackish depositional environment, but still with much less of a marine influence than facies successions 6 and 8.

The transition to much coarser rocks in the upper half of the succession is very rapid, and indicates an upward change to much higher energy conditions. The grain size continues to increase upward within the sandstone-rich part of the succession and more and more dispersed pebbles are present toward the top. The degree of bioturbation of the succession is slight, but does increase very gradually toward the top. This lack of pervasive bioturbation, the complete lack of marine body fossils, the poor sorting, and the nature of the sedimentary structures in the sandstone (massive or trough cross-stratified), suggest a high-energy fluvial environment (fluvial channel or crevasse splay deposit) for the coarse sandstone and pebbly sandstone. At some localities the top of the succession is better sorted, more strongly bioturbated and contains some preserved trace fossils of possible marine origin. Here, the upper part of the succession may reflect a slight marine influence, or moderate marine reworking of the upper part of the fluvial sandstone during transgression.

The main variation of the ideal succession 3 above, excluding examples caused by erosion, occurs where the thickness of the upper pebbly sandstone is expanded and the underlying trough cross-stratified sandstone (facies 7) is missing. This variation of succession 3 occurs in areas which were proximal to the source of coarse-grained material (presumably topographically-high basement terrain), or in the upper part of fluvial systems where the stream gradient was higher and the transported bedload was coarser.

4.5 FINING-UPWARD SUCCESSIONS

4.5.1 Facies Succession 4 - storm-influenced lower shoreface to offshore marine

Facies Succession 4 typically has a smoothly fining-upward character, or more rarely an irregularly fining-upward character. This succession occurs in two main areas: First, in the western part of the southern region near topographically-high basement terrain on the Wallhallow map sheet, where the maximum thickness of the succession is 25.5 m, and the average thickness is 4.5 to 8 m. Second, the succession commonly occurs in offshore zones throughout the central region and the northern part of the southern region; here the upward decrease in grain size is less obvious, the maximum thickness is 22.5 m, and the average thickness is 5 to 8 m.

The base of the succession in the western part of the southern region consists of clayey medium to coarse sandstone with a variable lithic content (facies 10), or silty sandstone (facies 13). The

basal facies is only 1-2 m thick in this succession, and grades upward into thinly-bedded graded sandstone and siltstone (facies 16). Many of the beds in facies 16 are less than 1 cm thick, and the thickness and frequency of sandstone beds decreases upward. As the grain size continues to decrease upward, laminated siltstone and sandy siltstone (facies 18) is developed, or more rarely siltstone (facies 21) and/or silty claystone (facies 22). The top of the laminated siltstone is highly weathered in most localities, and the contact with overlying units was not observed.

In the central region and the northern part of the southern region the base of succession 4 is composed of clayey bioturbated sandstone (facies 10) up to 4 m thick, which contains some medium-scale planar cross-stratification and rare dispersed clasts, and overlies a thin conglomeratic lag in places. Grain size gradually fines upward and the bulk of the succession comprises pale grey to white, silicified, moderately sorted and subrounded silty sandstone and siltstone (facies 13; Plate 6a-b). This facies is up to 16 m thick and is moderately to intensely bioturbated throughout. The grain size continues to fine upward and the top of the succession consists of clayey siltstone (facies 18 or 21), or more rarely silty claystone (facies 22). The fine-grained top of succession 4 is moderately bioturbated and contains siliceous concretions, although other preserved sedimentary structures are rare.

There is an obvious change in sedimentary structures from the base to top of this succession. The basal sandstone contains planar cross-stratification and some randomly dispersed small-pebble sized lithic clasts. The overlying silty sandstone contains rare wave-ripple lamination and flat lamination, small concretions (5-10 cm diameter), and rare discontinuous coarse sand layers near the top of the facies. Facies 16 displays a range of sedimentary structures, including very small-scale low-angle cross-lamination, small-scale erosional features at the base of the coarser beds (rills, pinch and swell couplets), and flat lamination. The upper siltstone or silty claystone shows even, flat lamination in places. In the central region this succession contains relatively few preserved sedimentary structures due to the moderate to intense degree of bioturbation, which tends to increase upwards. Where bioturbation is less intense, sedimentary structures include rare small-scale HCS, starved sandy ripples, cross-lamination, and small discontinuous stringers of sand grains.

Numerous molluscan body fossils occur in the basal and intermediate parts of the succession in the central region, but fossils are rare in the southern region and at the top of succession 4. Intermediate parts of succession 4 contain *Rhizocorallium*, *Planolites*, *Teichichnus*, *Palaeophycus*, *Thalassinoides*, and rare *Diplocraterion* and *Skolithos* trace fossils. Fine-grained interbeds contain the greatest abundance of trace fossils and are intensely bioturbated.

PLATE 6

a Basal conglomeratic lag and overlying thickly planar bedded quartz sandstones of facies succession 5, which in turn are overlain by thinly bedded silty sandstones of facies succession 4. The contact between the two successions occurs at the base of the overhanging sandstone bed (creating the shadow). At such intermediate palaeogeographical localities, rocks of facies succession 5 are finer-grained and do not show the pervasive crossbedding of the same succession in proximal localities. Site 67, central region. Hammer is 32.5 cm long.

b Silicified pale grey siltstone, fine sandstone, and silty sandstone of facies succession 4. Note the slight fining-upward character of the outcrop. The coarser, thicker-bedded, basal part of the succession (in shadow) contains coquinas and rarer thin graded beds. Site 54, central region. Person (seated) for scale.

c The upper half of a fining-upward cycle of facies succession 5 partly covered in scree. The top of the cycle consists of a recessively-weathered condensed bed of soft marine claystone (in shadow between the two white lines; the same level at the same site is shown just beneath the dashed line in plate 6e). This facies (22) passes downwards into siltstone, then progressively down into coarser and coarser sandstones (see plate 2h). Site 7, northern region. Condensed bed is 1.5 m thick.

d Thickly planar bedded and massive quartz sandstones of facies succession 6. Such relatively thick sandbodies occur in localities close to the palaeoshoreline. Site 68, central region. Note person for scale.

e Fining-upward fluvial channel deposit of facies succession 7. Scoured base of channel is shown by the dashed line and overlying arrow. Here, the erosional scour is regional in extent, and is recognised as a major sequence boundary. Rocks beneath the dashed line are fine-grained marine rocks of the upper part of facies succession 5 (see plate 6c). Site 7, northern region. Helicopter for scale.

f Thickly interbedded siltstone and muddy sandstone of facies succession 8. Note the intense degree of bioturbation of the silty sandstone, and the numerous (silica-cemented) *Diplocraterion* burrows with positive relief. Site 12, northern region. Pen (arrowed) is 13.5 cm long.

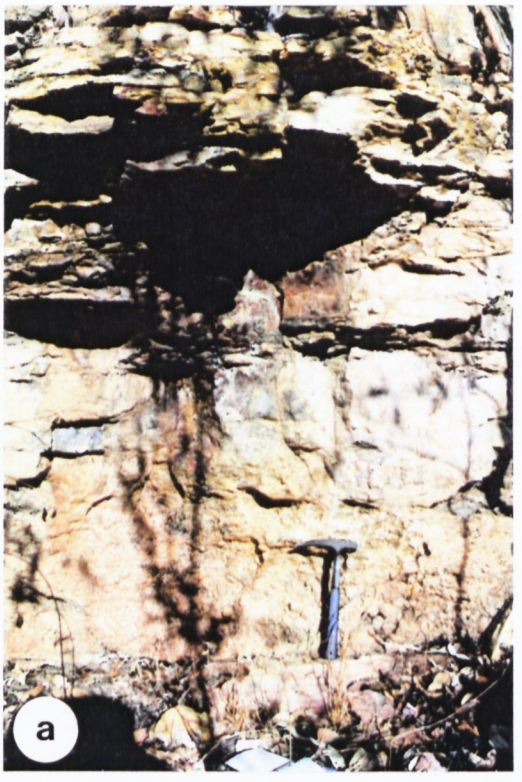
a

b

c

d

e

f

In all regions the upper part of the succession is at least moderately bioturbated and contains *Planolites* and *Chondrites* burrows. Measured sections of succession 4 in the central region contain a higher abundance and diversity of body and trace fossils than exposures of succession 4 elsewhere, and the overall degree of bioturbation is also greater.

Interpretation

Facies Succession 4 is interpreted as the deposit of an offshore marine setting under the influence of episodic storms. Succession 4 contains elements of facies successions 1 and 2, but was deposited in marine regions where transgression or retrogradation of the shoreline caused a marked increase in water depth.

The succession has a smoothly fining-upward character in intermediate to distal localities, and a less regular fining-upward character in more proximal localities. The succession accumulated under increasing water depth, as shown by the decrease in grain size, the change in sedimentary structures, and the change in trace fossils and degree of bioturbation. The rhythmic interstratification of relatively coarse and fine layers in facies 16 in the southern region is the product of episodic storm sedimentation. The presence of HCS and stringers of sand grains in facies 13 in the central region also suggests storm sedimentation in an offshore marine setting.

During storms, oscillatory waves and shelf (geostrophic) currents combined to scour the seabed during peak storm conditions, after which silty claystone beds were deposited from suspension as turbulence waned (Aigner, 1982; Davis and Byers, 1989). Beds commonly have irregular bases and even tops and show characteristic features of distal storm beds, such as erosional rills, pinch and swell couplets, and rare, internal, very small-scale, low-angle cross-lamination (Aigner, 1985; Schieber, 1990). These sedimentary structures indicate that deposition of the graded, coarser-grained beds occurred by settling of suspended material after episodic storms, whereas finer-grained layers were formed by continuous background sedimentation (*cf.* Davis and Byers, 1989; Reineck and Singh, 1972).

The upper fine-grained rocks of succession 4 (facies 18, 21, and 22) were deposited in deep water beyond the influence of storm waves. These facies contain sedimentary structures and trace fossils which indicate deposition under quiet conditions in an offshore marine setting. The *Cruziana* ichnofacies and the stratification infer that deposition occurred mostly in the upper offshore to offshore transition zone (MacEachern and Pemberton, 1992). However, some proximal exposures, where rocks have a coarser grain size and display rare suspension feeding

structures (*Skolithos* and *Diplocraterion*), reflect deposition in the lower shoreface. Details of important lateral and vertical variations within succession 4 are presented in the discussion of Carpentaria Basin shallow-marine depositional systems in Sects. 10.7 and 10.8.

4.5.2 Facies Succession 5 - storm- (and wave-) dominated shoreface (typically retrogradational)

Facies succession 5 occurs throughout the study area and exhibits a smooth, continuously fining-upward grain size trend. It has a maximum thickness of 7.5 m and an average thickness of 4 to 5 m. This succession contains many of the same facies as succession 2 and displays similar lateral trends. The main difference between succession 5 and succession 2 is the upward change in grain size; succession 5 is fining-upward and succession 2 is coarsening-upward. Most other differences between these two successions can be related to vertical differences in grain size.

Facies succession 5 commonly begins with a thin conglomeratic lag or more rarely a sedimentary breccia (facies 3). The conglomeratic lag consists of poorly sorted, rounded lithic clasts up to mid-pebble size (Plate 6a). Occasionally this lag has a ferruginous and/or manganiferous cement. This facies passes gradationally upward into very coarse-grained sandstone of facies 8 (Plate 2h). As the grain size decreases upward over several meters, trough cross-stratification gives way to swaley cross-stratification and small-scale planar cross-stratification in fine-medium sandstone (facies 12), and hummocky cross-stratification in coarse siltstone and fine sandstone (facies 14).

In finer-grained sections interbedded sandstone and siltstone (facies 15) occur above the coarse sandstone, and facies 12 is thin or missing. In sections where the intermediate part of the succession is coarser than fine sandstone, facies 12 predominates over facies 14 and grades upward into silty sandstone (facies 13). Elsewhere, the intermediate part of the succession (facies 15) is thick and passes gradationally upward into hummocky cross-stratified fine sandstone (facies 14). At the top of succession 5, facies 13 or 14 grades upward into a thick siltstone (facies 21) and/or bioturbated claystone (facies 22; Plate 6c).

The change in sedimentary structures is the same as in succession 2, but occurs in the reverse order in a vertical sense. The type of sedimentary bedding structure is dependent on grain size and ranges from trough-, swaley-, and planar- cross-stratification in coarser sandstone at the base of the succession, to wave-ripple lamination, planar cross-stratification, graded beds, and

rare planar bedding in the intermediate medium to fine sandstone part of the succession. Above hummocky cross-stratified fine sandstone and coarse siltstone and small-scale cross-stratified sandstone, the upper part of the succession is intensely bioturbated and preserved sedimentary structures within facies 13, 21 and 22 are rare. Where they have not been completely destroyed by bioturbation these structures change upward from small scale ripple cross-stratification to wave-ripple lamination, to flat lamination.

The degree of bioturbation and fossil content of individual facies of this succession are very similar to succession 2. However, the amount of bioturbation increases upward in this succession whereas bioturbation decreases upward in succession 2. Body fossils are very rare in this succession and are usually limited to poorly preserved molluscan macrofossils. Trace fossils are indistinct and comprise poorly preserved burrows of the *Skolithos* ichnofacies.

Interpretation

Facies succession 5 is interpreted as the deposit of a fining- and deepening-upwards (typically retrograding) storm- (and wave-) dominated shoreface. In proximal localities the basal and intermediate parts of the succession are dominated by coarse to medium sandstone of facies 8 and 12 overlain by finer sandstone and siltstone of facies 13. In places measured sections record two or more stacked examples of succession 5. In more distal localities the basal and intermediate parts of the succession are composed of interbedded sandstone and siltstone of facies 15, and fine sandstone and coarse siltstone of facies 14. In all regions the siltstone and claystone of facies 21 and 22 capping the succession represent the end result of retrogradation (or drowning) of the shoreface, and the transition from a lower shoreface to offshore depositional environment. Here the seafloor was beneath the average storm wave base and would have only been affected by occasional large storms.

Flat lamination in the coarse sandstone interval in proximal localities was probably produced by swash / backswash on the beach. This sandstone passes upward into coarse sandstone (facies 8) of the upper shoreface or beach, which in turn gives way to SCS sandstone of the middle to lower shoreface. In more distal localities crossbedded sandstones of the upper shoreface give way to HCS beds and thinly interbedded facies with wave-ripple lamination, which were deposited as water depth increased. Here storm-generated structures (*e.g.* HCS and sand-filled gutters) are preserved, because the seafloor was beyond the influence of fair-weather processes. With increasing water depth the grain size continued to decrease and laminated to massive silts and clays were deposited under maximum water depth.

The upward change from dominantly vertical burrows (*Skolithos* ichnofacies), to a mixed trace fossil assemblage, to dominantly horizontal burrows (*Cruziana* ichnofacies) records the increase in water depth from the base to the top of the succession. Essentially, the temporal changes in the depositional environment are in the reverse sense to that of succession 2, which was deposited in a similar setting during shoaling events. Details of important lateral and vertical variations within succession 5 are presented in the discussion of Carpentaria Basin shallow-marine depositional systems in Sects. 10.7 and 10.8.

4.5.3 Facies Succession 6 - paralic (estuarine and deltaic-marine) systems

This succession is the most variable in the study area and occurs in proximal localities in all three regions of the shelf, especially in the northern half. In most places it has a fining-upward character, although some deposits are massive.

In the eastern part of the BPRZ facies succession 6 typically occurs as thin sandbodies enclosed within marine sandstones of succession 2. Here the base of succession 6 consists of thickly planar bedded and large-scale planar cross-stratified coarse-medium to medium/fine-grained sandstone. In proximal localities the sandstone (facies 6) is coarse and relatively poorly sorted and fines upward above a basal lag. In more distal localities the basal sandstone (facies 11) is finer-grained, better sorted and contains abundant plant fossils. The plant-bearing sandstone grades into bioturbated, fossiliferous, clayey finer-grained sandstone (facies 12). Commonly, the contact between these two lower facies of the succession is sharp, but is apparently conformable. The grain size may continue to decrease upward until interbedded sandstone and siltstone (facies 15) or silty sandstone (facies 13) is present.

As grain size decreases upward set thickness and foresets of the cross-stratification decrease and the degree of bioturbation increases. Above this zone rare bipolar (herringbone) cross-stratification and current ripples are present. The number and diversity of plant fossils increases from the top of facies 6, through facies 11 and finally decreases near the contact of facies 11 with overlying facies 12. In most parts of the succession the fossil assemblage contains a mix of plant fragments and molluscan shells as well as *Rhizocorallium*, *Skolithos*, and *Arenicolites* trace fossils.

In the western part of the BPRZ there is one similar deposit of facies succession 6 (*e.g.*section 37). Here fining-upward cross-stratified and ripple-marked sandstones with rare marine fossils

overlie thick fluvial channel deposits of facies succession 7. All deposits of facies succession 6 within the BPRZ are very similar.

The same types of marginal marine or paralic sandbodies of facies succession 6 occur in the southern region, but only in a few localities. At section 128 the upper sandbody belongs to facies succession 6 and is composed of fining-upward fossiliferous sandstone and barren sandstone overlying a thin basal conglomeratic lag. The sandstones become slightly finer-grained and have better sorting towards the top of the deposit, and the top 2 metres contains abundant segmented plant fossils mixed with marine bivalves.

In section 106 a similar deposit of facies succession 6 is exposed. Here fining-upward sandstones of facies succession 6 conformably overlie thick normally-graded fluvial conglomerate and sandstone. As the grain size decreases toward the top of the succession the degree of sorting increases along with the degree of bioturbation. The top of the succession is marked by several closely-spaced thin hardgrounds, which mark the boundary with overlying shallow-marine sandstones.

Deposits of facies succession 6 within the central region are different to other areas. They are thicker (up to 14 m), mostly coarser-grained, and contain rare fossils. The bulk of the succession consists of thick massive sandstone (facies 8 and 12; Plate 6d). These sandstones contain rare marine molluscan fossils and a few *Skolithos* and *Diplocraterion* burrows. The sandstones exhibit large-scale trough- and planar- cross-stratification and rare ripple marks.

Overlying this thick sandbody, with an apparently conformable contact, is plant-bearing finer-grained sandstone (facies 11). Facies 11 sandstone is thickly planar bedded and contains large-scale high-angle planar cross-stratification with gravelly foresets. The facies contains an abundance of segmented plant fossils and rare marine bivalve fossils. The number of plant fossils increases upward whilst the degree of bioturbation decreases slightly.

Interpretation

Facies succession 6 shows considerable variation across the shelf, but all deposits of this succession represent paralic or marginal marine depositional environments. In most places deposits of facies succession 6 record an upward increase in marine influence; indicated by increasing bioturbation, decreasing grain size, better sorting, and the presence of marine fossils and hardgrounds in the upper part of the succession.

Most deposits of facies succession 6 can be broadly considered as being deltaic of brackish-marine in nature. For example, in the eastern part of the BPRZ a thin 'brackish' sandbody can be seen to wedge out offshore and is enclosed by thick marine sandstones. The 'brackish' sandstones contain a mixed fossil assemblage of plant fossils and marine macrofossils. Most probably these sandstones represent small, thin prograding marine deltas, but it is difficult to unequivocally assign a deltaic origin to these deposits because a fluvial source and delta morphology are not recognisable. This same interpretation holds for thicker 'deltaic to brackish-marine' deposits of facies succession 6 in the southern region (*e.g.* sections 106 and 128).

In the central region deposits of facies succession 6 seem to indicate deltaic to shallow-marine deposition under the influence of waves. Elements of facies succession 2 are present in the middle to upper parts of succession 6 here. However, there are two main differences between successions 2 and 6; Firstly, the base of succession 6 did not accumulate in a fully marine setting, as indicated by the coarser grain size, lower degree of bioturbation, and rarity of marine fossils compared to facies succession 2. Secondly, succession 6 is commonly capped by a thin interval of coastal plain sandstones, indicating a fluvial influence at the top of the succession after a brief period of subaerial exposure (evidenced by abundant carbonaceous debris).

Evidence of strong wave reworking in succession 6 is preserved in the well-sorted and well-rounded character of facies 8 and 12, which are extensively cross-stratified and contain marine body and trace fossils. At the top of central region exposures of facies succession 6 there is an upward transition from paralic to fully-marine deposition, followed by a sharply-defined change to nonmarine deposition. This succession has features which are similar to those displayed by prograding wave-influenced deltas (*e.g.* Bhattacharya and Walker, 1991), or possibly related to retrograding estuarine systems (*e.g.* Dalrymple *et al.*, 1992). Support for the interpretation of prograding wave-influenced deltas is given by stratigraphic correlation (Sect. 6.3.4), which shows the lateral facies equivalence of facies succession 6 'deltaic' sandbodies as they prograde and wedge out amongst marine sandstones of facies succession 2.

4.5.4 Facies Succession 7 - fluvial channel fill

Facies Succession 7 is common along the western edge of the study area. Generally it has a fining-upward grain size trend, but in places succession 7 is massive or has an irregular vertical grain size trend. The maximum thickness of stacked channel sandstones is 50 m and the average thickness is 8 m.

The basal part of succession 7 consists of normally graded chert conglomerate and coarse sandstone (facies 1 or facies 2, depending on clast size and abundance). This facies is commonly 2 to 5 m thick and grades upward into cross-stratified pebbly sandstone, with or without planar bedding (facies 5). Overlying this facies with a gradational contact is trough cross-stratified, coarse-grained, moderately to poorly sorted sandstone (facies 7). This facies is typically several metres thick and comprises the coarsest sand sized part of the succession, where dispersed clasts are relatively rare. This facies is overlain by finer-grained sandstone (facies 6), still with relatively poor sorting, which contains plant fossils and rare clasts. The contacts between facies are gradational throughout the succession, or at least within each of the fining-upward sub-cycles, which are stacked to make the succession. These small fining-upward sub-cycles typically have erosional-bases produced by local scour, which are defined by erosional truncation of crossbedding and thin conglomeratic lags overlying scours.

Where exposure is good, a distinct upward change in sedimentary structures in succession 7 is distinguishable. The basal conglomeratic facies is normally graded but contains no other structures. The overlying facies (5 and 7) display trough cross-stratification with sets up to 1.2 m thick near the base, high-angle planar cross-stratification (set thicknesses of 40 to 60 cm), and medium to thin planar bedding. The upper facies has planar cross-stratification on a smaller scale, asymmetrical and symmetrical current ripples, and rare trough cross-stratification.

Facies 1, 2 , 5, and 7 are not bioturbated and contain no body or trace fossils. However, facies 6 at the top of the succession is slightly to moderately bioturbated and the degree of bioturbation increases upward. Near the top of succession 7 rare *Skolithos* burrows and several other poorly preserved, unidentified trace fossils are present. The top metre or two of the succession contains segmented plant fossils, mostly logs and stems.

Interpretation

Facies succession 7 represents channel fill or point bar deposits. This is suggested by the overall fining-upward of the succession, and the fining-upward of individual sub-cycles with erosional bases (Plate 6c). The linear or shoestring geometry of the sand bodies in plan view also supports the interpretation of channel deposits. Topographically-high basement ridges, which typically outcrop close to succession 7, are interpreted as the source of much of the pebbles and coarse sand in succession 7. The lack of marine facies indicates that the channels are fluvial-dominated, and the presence of sub-cycles in succession 7 suggests channel filling by a series of waning flows, perhaps associated with flood stages of rivers. Similar sub-cycles

have been previously recognised in river- and wave-dominated Cretaceous depositional systems in the Western Interior Seaway of North America (Bhattacharya and Walker, 1991).

Succession 7 shows significant variation between areas and does not always exhibit a continuously fining-upward character. For example, in places the bulk of the succession is composed of facies 7 and 11 and the succession is massive or fining-upward. Elsewhere, the upper cross-stratified sandstone (facies 11) and basal lag are thicker and the intermediate facies are missing or greatly reduced in thickness. These variations were most likely due to changes in the energy of flow within channels, with thicker and coarser sediments deposited in upstream locations. The *Skolithos* burrows at the top of the succession in places were possibly produced by organisms burrowing down from an overlying marine unit which has since been eroded.

4.6 IRREGULAR SUCCESSIONS

4.6.1 Facies Succession 8 - sheltered/restricted marine (bay/lagoon)

This succession has a fining-upward or irregular grain size trend and is well-exposed in the BPRZ and the central region, and also occurs in a few localities in the southern region. The succession has a maximum thickness of 14.5 m, and an average thickness of 7 to 10 m.

The base of the succession sometimes consists of a thin conglomeratic lag. The lag is less than 1 m thick, and contains moderately sorted granule to large pebble sized clasts of quartzite, silicified siltstone, and various other fine-grained lithic clasts. This basal lag erosionally overlies facies of succession 2 or 5. Where a lag is missing, the base of the succession is clayey medium- to fine-grained sandstone (facies 10 or 12). Here, the sandstone typically overlies a marine flooding surface (marking the top of succession 5 or 6) with a sharp planar contact.

Grain size trends within succession 8 are somewhat irregular, but fining-upward cycles tend to occur in older or basal parts of the succession whilst coarsening-upward tend to occur in the upper part of succession 8. In any cycle or interval, the dominant rock type is silty fine- to medium-grained sandstone (facies 12 and 13; Plate 6f). In places the grain size decreases to fine silt size, but these intervals are thin and poorly defined. The most characteristic feature of the succession is the lack of wave-generated sedimentary structures, even in the coarsest parts of the succession. The dominant bedding style is medium to thick planar bedding, with rarer

flat and ripple lamination in the finer-grained parts. Other rare structures include herringbone cross-stratification and stringers of coarse sand and granule sized grains.

Rocks of succession 8 are moderately to intensely bioturbated and the amount of bioturbation increases upward. The succession is highly fossiliferous, and contains a high diversity and abundance of both body and trace fossils. Body fossils include ammonites, bivalves, trigonids, scaphopods, possible belemnites, unidentified bone fragments, and a large range of segmented plant fossils. Plant fossils are restricted to several intervals near the top of the succession. Trace fossils include *Rhizocorallium*, *Planolites*, *Arenicolites*, *Teredolites*, *Skolithos*, *Ophiomorpha*, *Teichichnus*, and *Thallasinoides*.

Interpretation

Facies succession 8 is interpreted as the deposit of a sheltered or restricted marine environment, such as a bay or lagoon. The presence of abundant marine body and trace fossils throughout the succession indicates that the bay or lagoon had a full marine connection at most times. Plant fossils suggest a brackish marine influence toward the top of succession 8.

The lack of pervasive wave-generated sedimentary structures suggests that this succession was deposited in a relatively quiet marine environment, where wave energy was significantly reduced compared to high-energy marine environments typical of other facies successions. In several places the upper, finer-grained part of the succession displays delicately-preserved bivalve fossils, which are still articulated; this adds support for an interpretation of a quiet, restricted marine environment.

The trace fossils belong to the *Skolithos* and *Cruziana* ichnofacies. Normally the *Cruziana* ichnofacies is considered to be characteristic of a shallow offshore shelf environment between storm and fair-weather wave base (Pemberton and Frey, 1984; Pemberton *et al.*, 1992). However, it is also widely recognised that the same ichnofacies can occur in shallower, restricted or quieter marine regions. The high degree of bioturbation suggests that the seafloor was well oxygenated and able to sustain abundant and diverse biota.

In several places the abundance of preserved marine macrofossils is enormous, and it appears that the fossils may have been concentrated in banks or shoals. The fact that many of these body fossils are preserved with shells still joined argues against significant transport. The presence of rare bipolar (herringbone) cross-stratification in these areas may indicate bi-

directional palaeocurrents, but convincing evidence for tidal processes is lacking. The concentration of plant fossils near the top of the succession may be related to an influx of fluvial debris, and a possible change to brackish marine conditions in the upper 1 or 2 metres of the succession.

There is no common variation of succession 8 above due to the gradational nature of facies contacts within the succession, and the irregular stacking of facies. The major lateral trend involves a slight increase in the thickness of the basal lag coupled with a more obvious fining-upward character in proximal locations.

4.7 CHAPTER SUMMARY

Facies of the Mullaman Beds exhibit repeated vertical stacking patterns in outcrop and core. These patterns can be defined by eight separate facies successions, which represent distinct depositional environments. Shallow marine siliciclastic facies successions are recognisable along the entire epeiric shelf of the western Carpentaria Basin and are repeated at different stratigraphic levels, indicating that shallow marine deposition occurred on the shelf for much of the mid-Cretaceous. Six of the facies successions represent shallow marine to brackish marine depositional environments, and successions with a strong marine influence are most important in terms of both areal distribution and overall thickness.

Along the western and southwestern margins of the Carpentaria Basin, storms imposed the dominant physical processes on the epeiric shelf. Deposition in the intervals between episodic storms was wave-dominated, and is highlighted in proximal (lower shoreface to foreshore) locations by sediments with trough-, planar-, and swaley- cross-stratification. The eight facies successions documented in this chapter are referred to throughout the thesis and form the basis for construction of stratigraphic correlation diagrams (chapters 5-7) and the regional lithostratigraphic framework (chapter 8).

~~~
~~~

5. DEPOSITIONAL ENVIRONMENTS AND LITHOSTRATIGRAPHIC CORRELATION IN THE NORTHERN REGION: THE COASTAL PLAIN TO INNER SHELF

5.1 INTRODUCTION

Cretaceous shallow-marine strata of the Carpentaria Basin shelf are exposed in three regions of similar area along the western and southwestern margins of the Gulf of Carpentaria. In between the three regions or along their outer edges, Cretaceous rocks are highly weathered or not exposed. Significantly, the morphology and facies distribution of Cretaceous rocks indicates that each region corresponds in a broad sense to a particular palaeogeographical zone on the ancient shelf: the northern region represents the inner shelf and coastal plain; the central region represents the shoreline to inner shelf; and the southern region represents the shoreline to outer shelf. Thus the study area is naturally subdivided into three regions in terms of both modern-day geography and Cretaceous palaeogeography.

In all three regions of the study area Cretaceous rocks occur as isolated "spot" outcrops, which may be weathered or poorly exposed. Consequently, lateral correlation of strata and surfaces on the Carpentaria Basin shelf is not at all obvious. However, local correlation is possible after careful documentation of facies, recognition of facies successions and the bounding surfaces between successions, and detailed comparison of numerous measured sections, well logs and cores. Local lithostratigraphic correlation of "spot" outcrops in the northern region (inner shelf and coastal plain) is documented in this chapter, and is supported by biostratigraphic data where available. Such local correlation forms the basis for regional correlation in chapter 8, which in turn enables construction of a lithostratigraphic framework for the entire shelf.

5.2 DATABASE AND METHODS

This chapter is based on the measurement of 84 outcrop sections and observations from numerous other field stations ranging from Nhulunbuy in the north to Roper River in the south (Fig. 5.1). The relationship of subsurface data (3 deep stratigraphic boreholes) to outcrops in the area around Nhulunbuy is discussed in Sects 8.5.1 and 8.5.2.

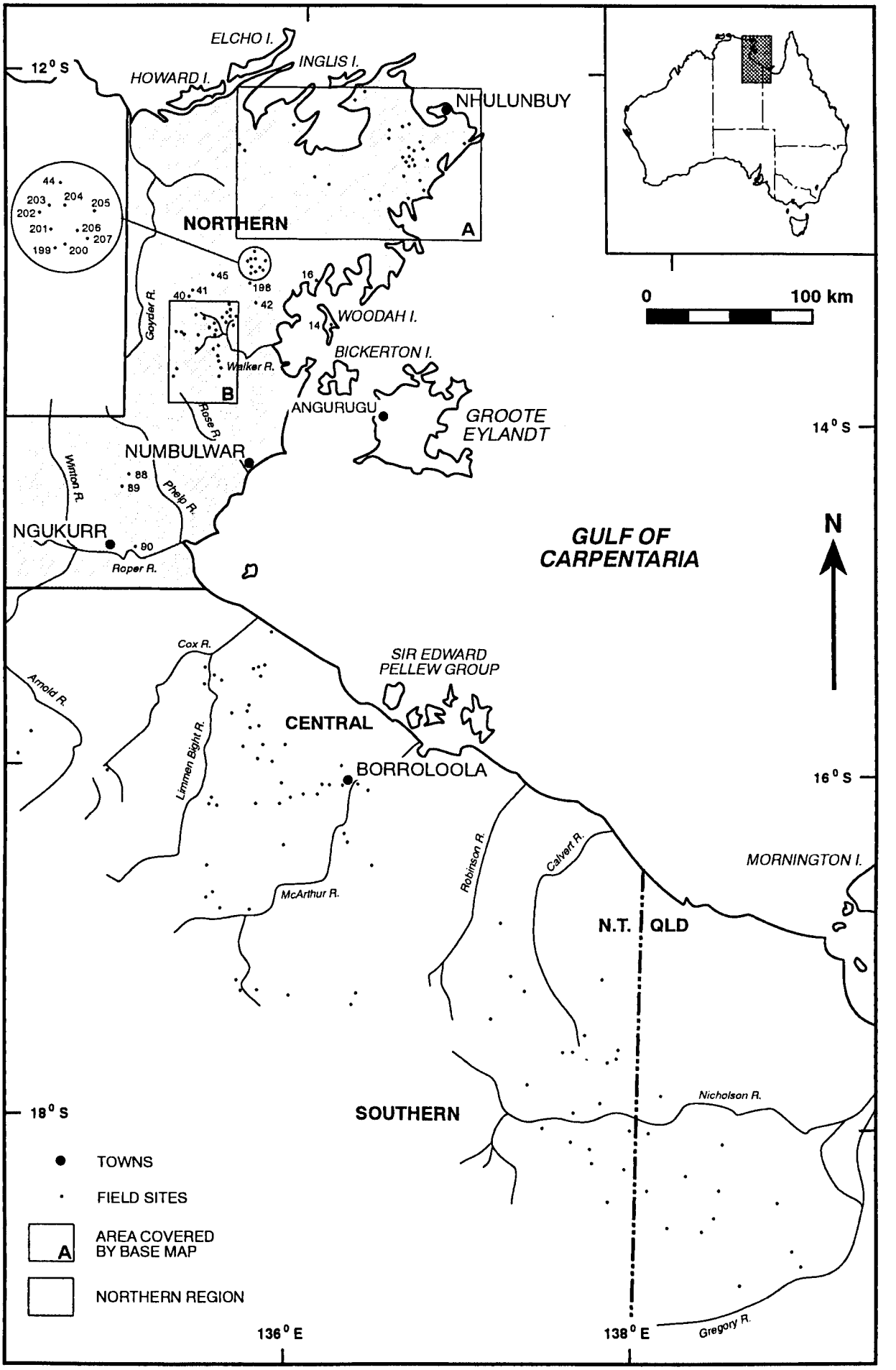

FIGURE 5.1. Location map for the northern region showing field sites referred to in chapter 5. See base maps for more detail.

Before attempting to correlate between outcrops over large distances, or to correlate outcrop with subsurface sections, a series of 34 intersecting stratigraphic correlation diagrams was constructed. Although a through-going marker horizon is lacking in many sections, more subtle marker beds, individual coarsening-upward and fining-upward cycles, and regionally extensive facies successions enabled 'first-pass' correlation over distances of a kilometre to tens of kilometres.

Only after this local correlation was tested and refined and the extent of various facies had been distinguished were detailed stratigraphic correlation diagrams constructed. Cretaceous rocks are best exposed in two main zones in the northern region, and are covered by alluvium between these two zones. The northern zone encompasses northeastern Arnhem Land, and the southern zone covers the area between the Bath and Parsons Ranges. Detailed stratigraphic correlation diagrams from both of these zones are presented in this chapter. Numbered field sites are shown on Fig. 5.1 and on base maps in Appendix 3. Symbols for the measured sections are illustrated on Fig. 5.2.

5.3 DETAILED STRATIGRAPHIC CORRELATION DIAGRAMS

The factual data for this chapter is summarised in seven local to semi-regional correlation diagrams. For economy of space and clarity of correlation, these have been "condensed" from longer correlation diagrams, and only those measured sections and well logs that illustrate important elements of the stratigraphy have been included. Correlation diagrams for the northeastern Arnhem Land Zone (ALZ) are located on a base map (Fig. 5.3) and are illustrated in Figs. 5.4 and 5.5. Correlation diagrams for the Bath and Parsons Ranges Zone (BPRZ) are located on another base map (Fig. 5.6) and are illustrated in Fig. 5.7 through Fig. 5.10.

All the measured sections are drawn to the same scale, and most are hung on the same datum, a prominent marker labelled C 2 (claystone 2), in the upper part of a transgressive marine cycle. The C 2 marker was chosen as a datum for several reasons:

1) it is the most extensive marker horizon in the entire study area;
2) it is lithologically homogeneous and has a similar thickness in all three regions, regardless of position on the shelf;
3) it is one of the rare very fine-grained rocks on the shelf and is easily recognisable amidst enclosing coarser-grained rocks; and
4) it is flat-lying and typically conformable on underlying rocks, and the base of the C 2 marker is strongly inferred to represent a time-line across the shelf.

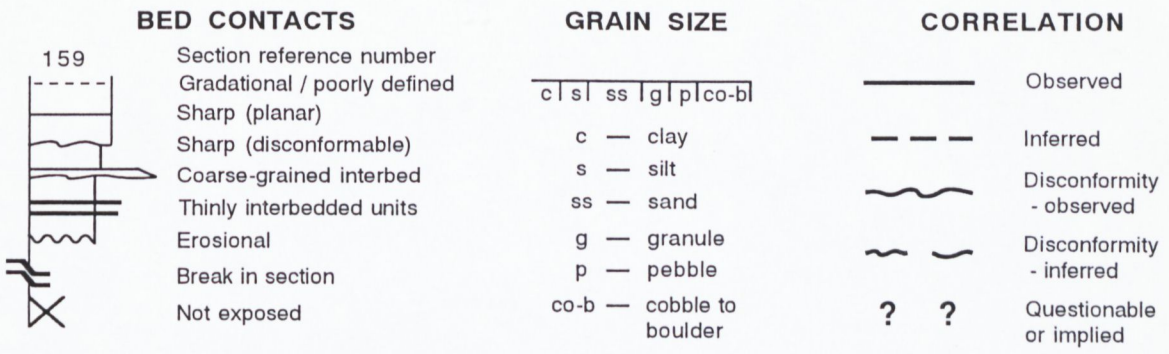

SEDIMENTARY STRUCTURES, FOSSILS AND GEOCHEMICAL FEATURES

FACIES SUCCESSIONS

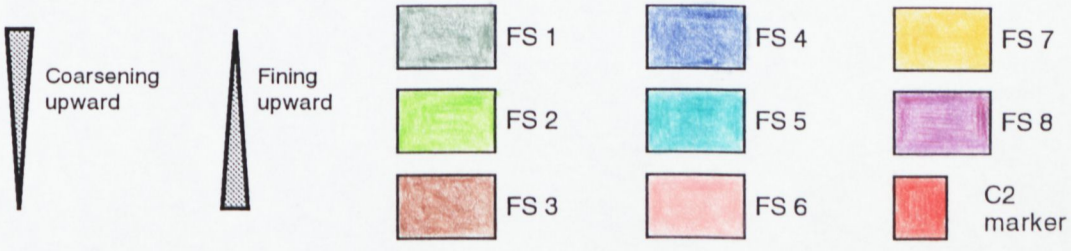

FIGURE 5.2. Symbols used in measured sections and composite sections which appear throughout the thesis.

5.4 NORTHEASTERN ARNHEM LAND ZONE (ALZ)

5.4.1 Correlation diagram A - A' (Fig. 5.4)

This correlation diagram starts with section 18 in the extreme north of the study area at the Cato River and extends 92.3 km (Fig. 5.3). From the Cato River to section 189 in the southeast, the bulk of the exposed Cretaceous sequence consists of fluvial facies. The fluvial facies are composed of coarse-grained, poorly sorted sandstones with large-scale trough- and planar cross-stratification. Body fossils are absent, and trace fossils are very rare within these fluvial facies. In all sections the fluvial facies are interpreted as channel-fill deposits and have the general morphology of facies succession 7.

The thickness of fluvial facies in the west of A-A' is at least 15 m, and may be significantly greater since most measured sections in this region are incomplete and the contact of fluvial facies with underlying rocks was not observed (except in section 1). There are numerous small, highly weathered outcrops of fluvial sandstone not included in this correlation diagram, and the stratigraphic position of these outcrops and all fluvial facies illustrated in Fig. 5.4 is inferred to be identical, although their exact age equivalence is problematic due to the lack of fossils and marker beds. This interpretation is supported by good correlation of ferricretes overlying the fluvial deposits, and the close similarity in the size and style of sedimentary structures in fluvial sandstones across northeastern Arnhem Land.

In section 1 thick fluvial sandstone disconformably overlies a series of marine sandstones. These marine facies also occur in the southern part of the ALZ, towards the base of sections 4 and 9. There the thickness of preserved marine facies is greater than that of fluvial facies. The basal marine facies consist of massive and coarsening-upward rocks of facies succession 2, and these are the oldest Cretaceous rocks exposed in the ALZ. Further correlation of these basal marine facies with other marine facies is illustrated in Fig. 5.5. In section 1 fluvial deposits of facies succession 7 have a disconformable contact with underlying marine sandstones of facies succession 2 . In the southern and eastern parts of the correlation diagram (sections 4, 7, and 10) transgressive marine facies succession 5 occurs stratigraphically above facies of succession 2, and beneath fluvial deposits of succession 7 which characterise the northern and western parts of A-A'. The transgressive marine deposits are composed of coarse- to fine-grained sandstones which fine upward into siltstone and silty claystone. The upward change in sedimentary structures indicates increasing water depth up section and the transition to a lower-energy, offshore shallow-marine depositional environment.

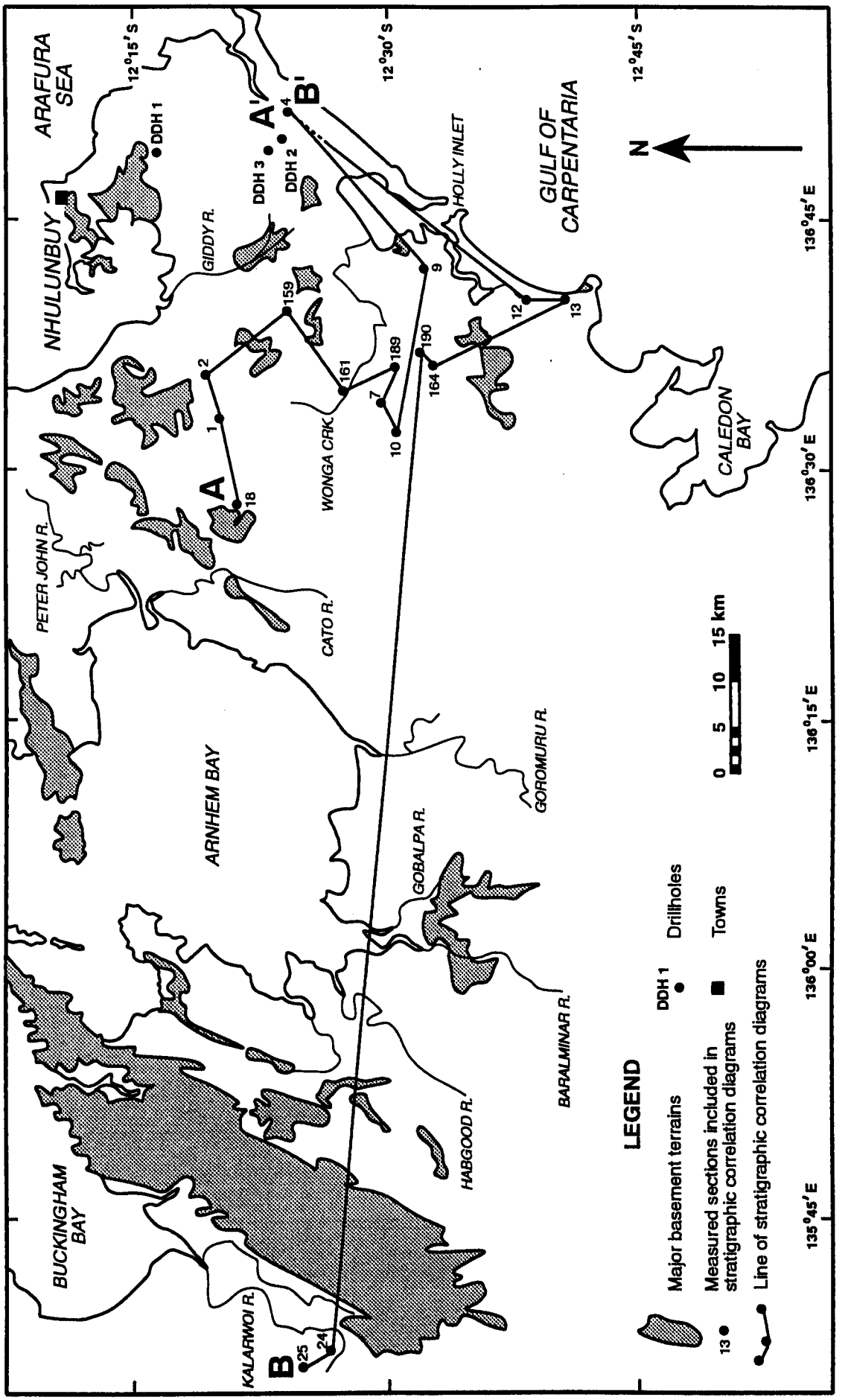

FIGURE 5.3. Base map (A) for the Arnhem Land Zone (ALZ). See Fig. 5.1 for the position of the base map relative to the northern region.

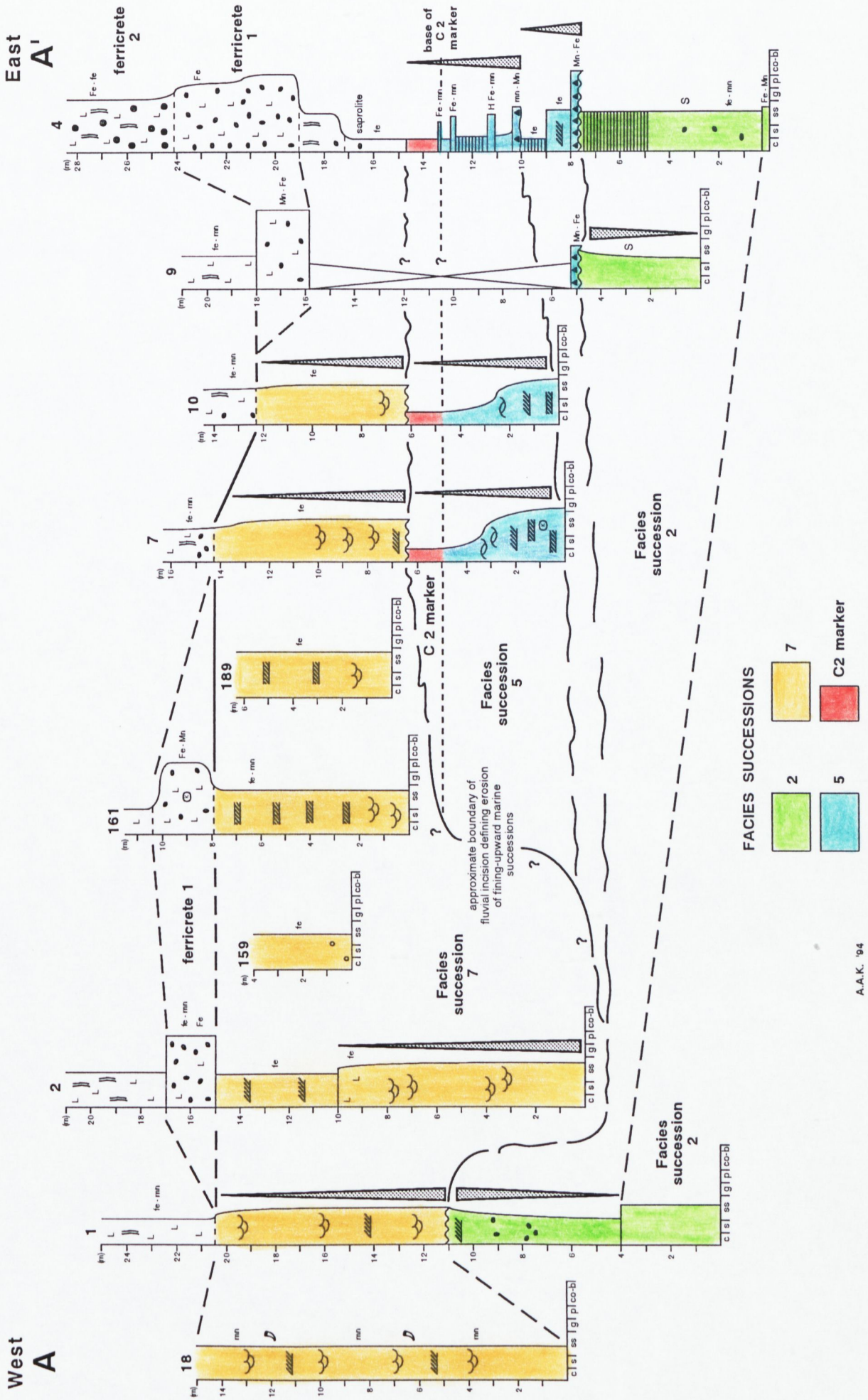

FIGURE 5.4. Stratigraphic correlation diagram for the Arnhem Land Zone. Refer to Fig. 5.3 for location of sections along A-A'.

In general there is an increasing marine influence along A-A' towards the south and east, and a corresponding decrease in the thickness of fluvial facies. Fluvial incision and deposition has progressively truncated marine facies northward along A-A', and only in the southern part of the correlation diagram is the complete record of marine facies preserved. Evidence for fluvial incision occurs at sections 1, 7, and 10, where an erosional disconformity separates marine facies and younger fluvial facies. In the vicinity of sections 7 and 10, fluvial deposits of succession 7 are incised up to 10 m into transgressive marine deposits of succession 5 (see Plate 6e). The irregular nature and extent of fluvial incision is probably due to localised channel scouring in a broad regime of lateral accretion. In regions near the present coastline (presumably close to the palaeoshoreline at sea level lowstand), fluvial deposits are thin or missing (*e.g.* section 4). Overall the extent of fluvial incision increases markedly to the north and northwest, inland from the present coastline. The approximate extent of fluvial incision into older transgressive marine successions is illustrated in Fig. 5.4.

Overlying marine facies succession 2 in section 4 are stacked fining-upward rocks of facies succession 5. On the basis of the stratigraphic position of the C 2 marker, fining-upward marine rocks of facies succession 5 can be confidently correlated between sections 4, 7, and 10. In this correlation diagram these three sections contain the only true marker bed (C 2), and the inferred stratigraphic position of all other sections is relative to this marker bed, which occurs just beneath fluvial sandstones in sections 7 and 10. Much of section 9 is covered by alluvium and scree, and the transgressive marine successions expected to occur here are not exposed. However, there is good correlation of coarse-grained marine sandstones between the basal parts of sections 4 and 9.

5.4.2 Correlation diagram B - B' (Fig. 5.5)

This correlation diagram extends along a 167.9 km line and illustrates dominantly marine deposits from Kalarwoi River in the west to an area 30 km south of Nhulunbuy in the east of the ALZ (Fig. 5.3). In the western part of Arnhem Land marine and/or restricted marine facies of facies succession 8 occur in numerous measured sections. Here the rocks consist of stacked interbedded sandstone and siltstone displaying marine body and trace fossils. Sedimentary structures, texture, and grain size indicate alternating low-energy (siltstone) and moderate-energy (sandstone) depositional environments, and abundant delicate lamination indicates a sheltered shallow-marine environment. In places this restricted marine sequence is relatively thick (*e.g.* section 24) and is composed of stacked alternating siltstone- and sandstone-dominated intervals.

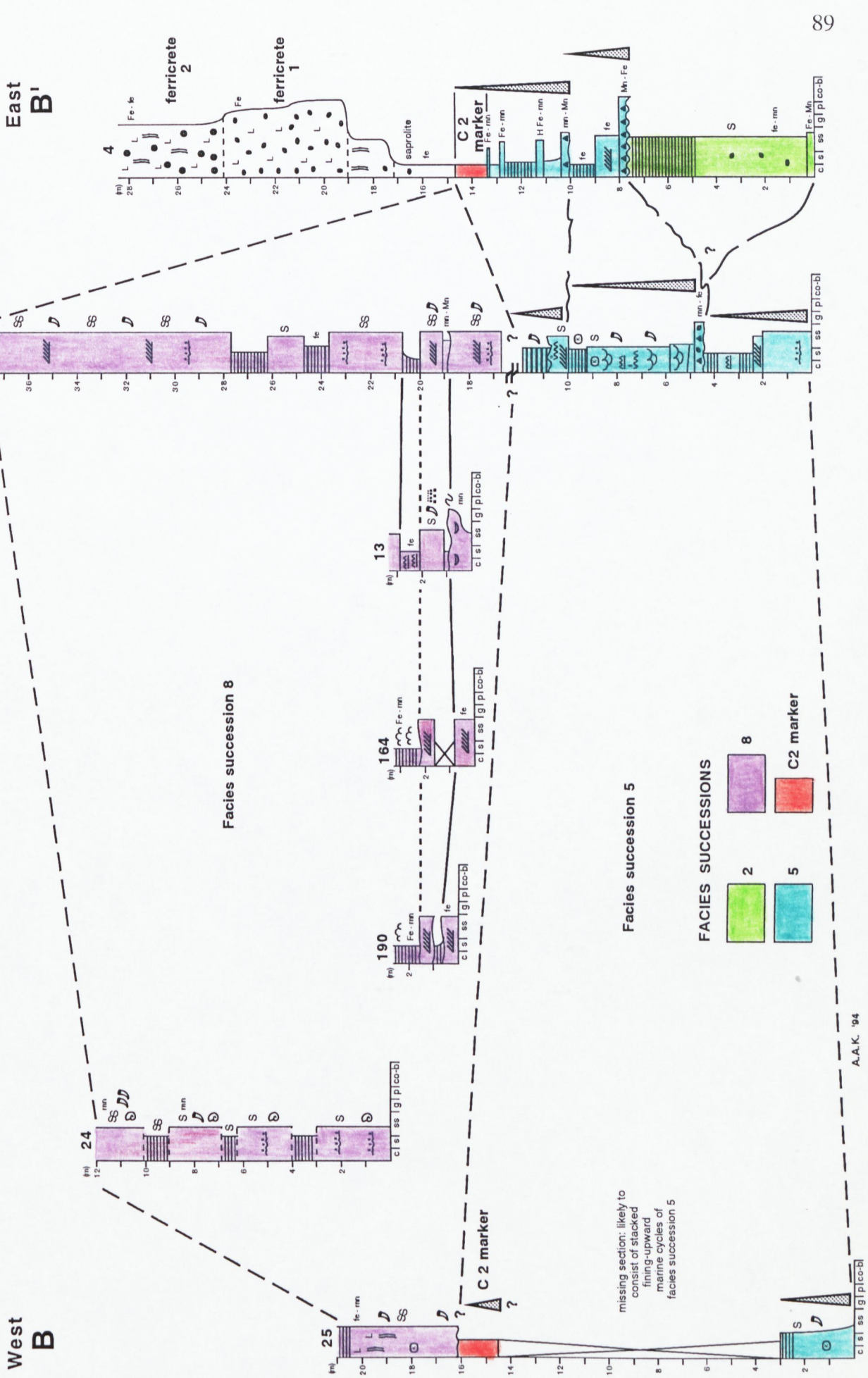

FIGURE 5.5. Stratigraphic correlation diagram for the Arnhem Land Zone. Refer to Fig. 5.3 for location of sections along B-B'.

A similar sequence occurs in section 12 near Holly Inlet over 110 km to the east of section 25. Interbedded sandstone and siltstone in both these regions are considered to be correlative and are assigned to facies succession 8. In the area surrounding Holly Inlet and up to 15 km to the northeast (including sections 164 and 190), there are numerous small outcrops of the interbedded sequence, which can be confidently correlated with the more complete sequence at section 12. Such restricted shallow-marine deposits do not occur at section 4 farther to the east, where a series of stacked transgressive marine rocks is overlain by a younger weathering profile.

In the Kalarwoi River region (*e.g.* section 25) the restricted marine sequence disconformably overlies fine-grained transgressive marine rocks, including the C 2 marker in section 25 and in several other incomplete sections. If, as seems likely, sections in the Kalarwoi River area are correctly correlated with those over 110 km to the east at Holly Inlet and Stoney Ridge (sections 12 and 4 respectively), it is apparent that a thick series of fining-upward transgressive marine deposits of facies succession 5 occur over a large part of the ALZ.

Correlation of individual fining-upward transgressive marine successions in the eastern part of this correlation diagram is relatively simple, due largely to the presence of several distinctive brecciated and mineralised beds (see Plate 9c) overlying disconformities in the thicker sections (*e.g.* at 7.5 m and 10 m in section 4; at 4.5 m in section 12). The upper transgressive facies succession in section 4 contains the C 2 marker, which can be correlated with section 25 to the west. However, the C 2 marker is not exposed in section 12, and the stratigraphic level where it should occur is covered. Unequivocal correlation of individual transgressive successions between sections 12 and 25 is difficult due to the incomplete nature of section 25, although they clearly represent closely related depositional environments.

On the eastern edge of the ALZ at section 4, thick transgressive marine deposits of succession 5 disconformably overlie coarse-grained marine facies assigned to facies succession 2. Outcrops of coarse-grained marine rocks of facies succession 2 are restricted to an area close to the present coastline, and were not recorded farther inland. The marine rocks of succession 2 in sections 1 and 4 represent the oldest Cretaceous rocks observed in outcrop in the ALZ.

5.4.3 Biostratigraphic control

Most facies successions in the ALZ are unfossiliferous and biostratigraphic data are highly limited. Body fossils, if present, occur as poorly preserved, low diversity molluscan

macrofaunas of indeterminate age (*cf.* Paltech, 1980a). In a previous regional palaeontological study of the Mullaman Beds, Skwarko (1966) did not record any fossil occurrences in northeastern Arnhem Land. However, during this study a few fossil localities were recorded; for example, at section 25 several ammonites were observed, but their poor preservation precluded positive taxonomic identification and biostratigraphic zoning. Faunas appear to be similar to molluscan macrofossils which occur in Cretaceous facies farther to the south in the BPRZ (see Tables 8.1, 8.2, 8.3, and 8.4).

Microfossils were not recovered from any outcrops in the ALZ, and this thus limits biostratigraphic control in the northern region. However, microfossils from fluvial successions in stratigraphic drillholes in northeastern Arnhem Land yielded a late Albian age (Table 8.2). The fluvial successions occurring in the stratigraphic drillholes are considered to be correlative with outcrops of fluvial rocks of facies succession 7 in the ALZ (Sect. 8.5.2).

In summary, biostratigraphic control from outcrop data in the ALZ is poor. Body fossils are rare and cannot be placed in biostratigraphic zones and accurately dated due to their poor preservation, their endemic nature (Paltech, 1980a), and their poor correlation with other Cretaceous molluscan faunas in Australia and the southern hemisphere (Ludbrook, 1966; Day, 1969). Trace fossils are often well preserved in facies in the northern region, and assist in initial correlation of successions in areas where other fossils are absent and the environments of deposition are not readily apparent from sedimentological criteria alone. However, there is no apparent biostratigraphic zonation based on trace fossils, and similar trace fossils occur within particular facies independent of age, at least for mid-Cretaceous times.

5.4.4 Summary of facies successions in the ALZ

The oldest Cretaceous rocks observed in *outcrop* in northeastern Arnhem Land are marine sandstones occurring at the base of sections 1 and 4. Their contact with pre-Mesozoic basement was not observed, but the position of Cretaceous rocks near to Proterozoic granite outcrops suggests that basement occurs close to the base of these Cretaceous marine sandstones. The oldest Cretaceous facies have been assigned to facies succession 2, although the succession is thin and the exposures are relatively poor.

A marine depositional environment has been assigned to these rocks, largely on textural and compositional criteria, since body fossils are lacking and trace fossils are rare. Although the marine nature of these rocks is not unequivocal, their environment likely was offshore marine to

shoreface marine with progressively shallower water depth up-section. This idea is supported by the disconformable contact of this succession with overlying marine facies of facies succession 5. The contact is represented in most places by a brecciated and/or mineralised bed (*e.g.* sections 4, 9, and 12) which represents a major regional surface of submarine erosion, and is the result of shoaling towards the top of succession 2.

Stacked fining-upward marine successions occur directly above the basal erosional surface defined by mineralised breccias, and are also bounded above by an erosional surface in the form of a sharp disconformable contact between the fine-grained top of a fining-upward succession 5, incorporating the C 2 marker, and the overlying coarse-grained fluvial sandstones. Both of these erosional surfaces have an irregular topography, with the overall thickness of stacked fining-upward cycles of succession 5 controlled by the amount of localised erosion. There are two or three stacked fining-upward cycles of facies succession 5 overlying the basal disconformity (*e.g.* section 12), with the number of cycles exposed in outcrop dependent on the amount of erosion. Each of these fining-upward successions represents a change in relative sea level across the northern region involving transition from shoreface to offshore shallow-marine deposition, followed by a further change in relative sea level which led to accumulation of coarse-grained marine sandstones of the shoreface at the base of the next fining-upward succession (refer to chapter 9).

After accumulation of the final fining-upward marine succession, a major fall in relative sea level resulted in erosion and fluvial incision into underlying marine deposits in the central parts of the ALZ. The fluvial facies deposited in this region correspond largely to coarse-grained channel-fill facies of succession 7 (see northern half of A-A'). Similar facies also occur in three stratigraphic drillholes in the same area (Dodson, 1967), and show a large thickness of stacked fluvial channel and interfluvial deposits with the characteristics of facies successions 7 and 3 respectively.

The other main Cretaceous deposits in the ALZ are thick restricted-marine to shallow-marine sandstones and siltstones which occur close to the present coastline of Arnhem Land (*e.g.* sections 12, 13, 24, 25, 164, and 190). It is likely that these facies accumulated in large bays or along sheltered coastlines to the northwest and southeast of the inland fluvial-dominated area. These restricted marine deposits of facies succession 8 form a thick sequence (*e.g.* upper half of section 12, and section 24), for which there is no direct age control. However, their stratigraphic position overlying stacked transgressive marine facies of succession 5 is identical to fluvial deposits farther inland (*e.g.* sections 7 and 10). This suggests that restricted marine

deposition of facies succession 8 occurred along sheltered parts of the palaeoshoreline, with concurrent fluvial incision and deposition of facies succession 7 farther inland. If this is interpretation is correct, both fluvial deposition and restricted marine deposition occurred during the late Albian to early Cenomanian in different parts of the ALZ.

5.5 BATH AND PARSONS RANGES ZONE (BPRZ)

5.5.1 Correlation diagram C - C' (Fig. 5.7)

This correlation diagram includes measured sections on a line 132.6 km long in the area between zones of good outcrop in the ALZ and BPRZ (for the position of sections along C-C' see circular inset map on Fig. 5.1). In this area the Cretaceous successions are thin and poorly exposed, but their documentation is important for regional correlation and for assessment of the extent of marine incursion.

Most Cretaceous successions along C-C' are composed of fining-upward coarse-grained fluvial sandstone with thin conglomeratic pebble lags, and they commonly overlie Proterozoic basement with an angular unconformity (Fig. 5.7). The sandstone exhibits plant fossils in places, and marine body and trace fossils are absent. The most common sedimentary structures are medium- to large-scale trough cross-stratification and high-angle cross-stratification. The fluvial deposits have a maximum thickness of 4.5 m, and correspond to channel-fill facies of succession 7. Whilst the stratigraphic equivalence of these numerous small fluvial outcrops cannot be directly proved using biostratigraphic data or marker beds, they occur at a similar topographic height, overlie the same basement unit with an erosional unconformity, and are all very similar in grain size, texture, and composition. Their assignment as Cretaceous age is based on similarity of their morphology and stratigraphic position in comparison with Cretaceous fluvial successions to the north and south. All the fluvial deposits along C-C' occur as thin caps on isolated basement inliers, and probably originally formed a much more extensive and thicker fluvial depositional system before post-Cretaceous erosion dissected the fluvial deposits.

There are also two marine successions or facies within correlation diagram C-C'. The northernmost of these successions consists of coarse- to medium-grained quartz sandstone which fines upward into fine-grained siltstone and silty claystone. This succession is considered to be correlative with fining-upward marine facies of succession 5 to the north and south. The maior differences here are that the succession is thinner and does not contain

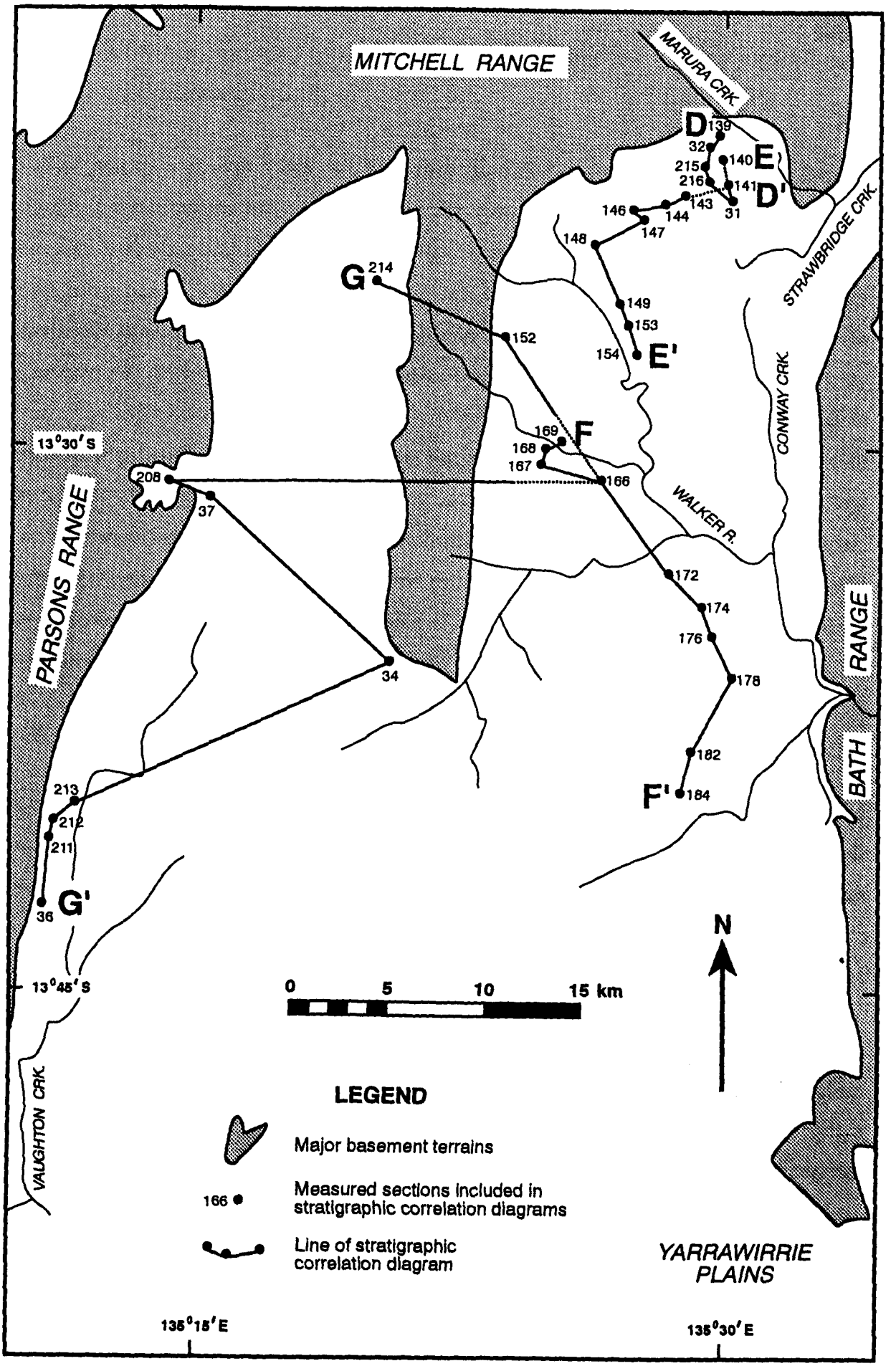

FIGURE 5.6. Base map (B) for the Bath and Parsons Ranges Zone (BPRZ). See Fig. 5.1 for the position of the base map relative to the northern region.

obvious marine fossils (the highly weathered nature of the outcrop indicates that marine fossils are unlikely to be preserved).

The other marine succession has not been identified elsewhere on the mainland, and its stratigraphic relationships are obscure. This succession unconformably overlies the same Proterozoic basement unit as Cretaceous fluvial deposits in this area. This unusual marine facies is composed of fine- to medium-grained quartz sandstone with poorly defined hummocky cross-stratification, and is cemented and stained by ferruginous and ferromanganese oxides (*e.g.* section 42) The upper part of the deposit contains ferromanganese pisoliths in a sandy matrix. The inferred marine depositional environment for this succession is questionable because marine fossils were not recorded, but the presence of pisoliths and HCS supports an interpretation of a high-energy shallow-marine environment. The sandstone is thin, although the scree-covered area around the section indicates a greater true thickness for this facies. Whether this unusual pisolitic and mineralised sandstone is contemporaneous with the fluvial deposits farther to the north along C-C' is unclear, but it occurs at a similar stratigraphic level and overlies an identical basement unit. However, this facies may be post-Cretaceous in age.

5.5.2 Correlation diagram D - D' (Fig. 5.7)

This correlation diagram illustrates the foreshore to shoreface transition in an area where the palaeoshoreline was highly irregular in close proximity to the Bath, Parsons, and Mitchell Ranges (Fig. 5.6). This correlation diagram highlights the inter-stratified nature of rocks deposited in fully marine and paralic environments close to the palaeoshoreline. The correlation diagram covers a distance of 4 km near Marura Creek and enables the sensitive changes at the marine/terrestrial interface to be documented.

The oldest Cretaceous unit here is a thick, massive to normally graded cobble to pebble chert conglomerate (Plate 2a). The contact with basement was not observed in the area of this correlation diagram, but slightly farther to the south this same facies unconformably overlies Proterozoic siltstone. The conglomerate is up to 4 m in thickness in the area covered by correlation diagram D-D', but has a thickness of at least 20 m farther to the south. The presence of conglomerate is interpreted to represent a long period of erosion and accumulation of very coarse-grained clastics during lowstand of sea level when the entire area was subaerially exposed or was sited close to the palaeoshoreline. As such, the normally graded conglomerate represents a fluvial valley-fill. The basal part of the conglomerate grades and fines upward into fossiliferous, conglomeratic Cretaceous marine sandstones (Fig. 5.7), and the upper part of the

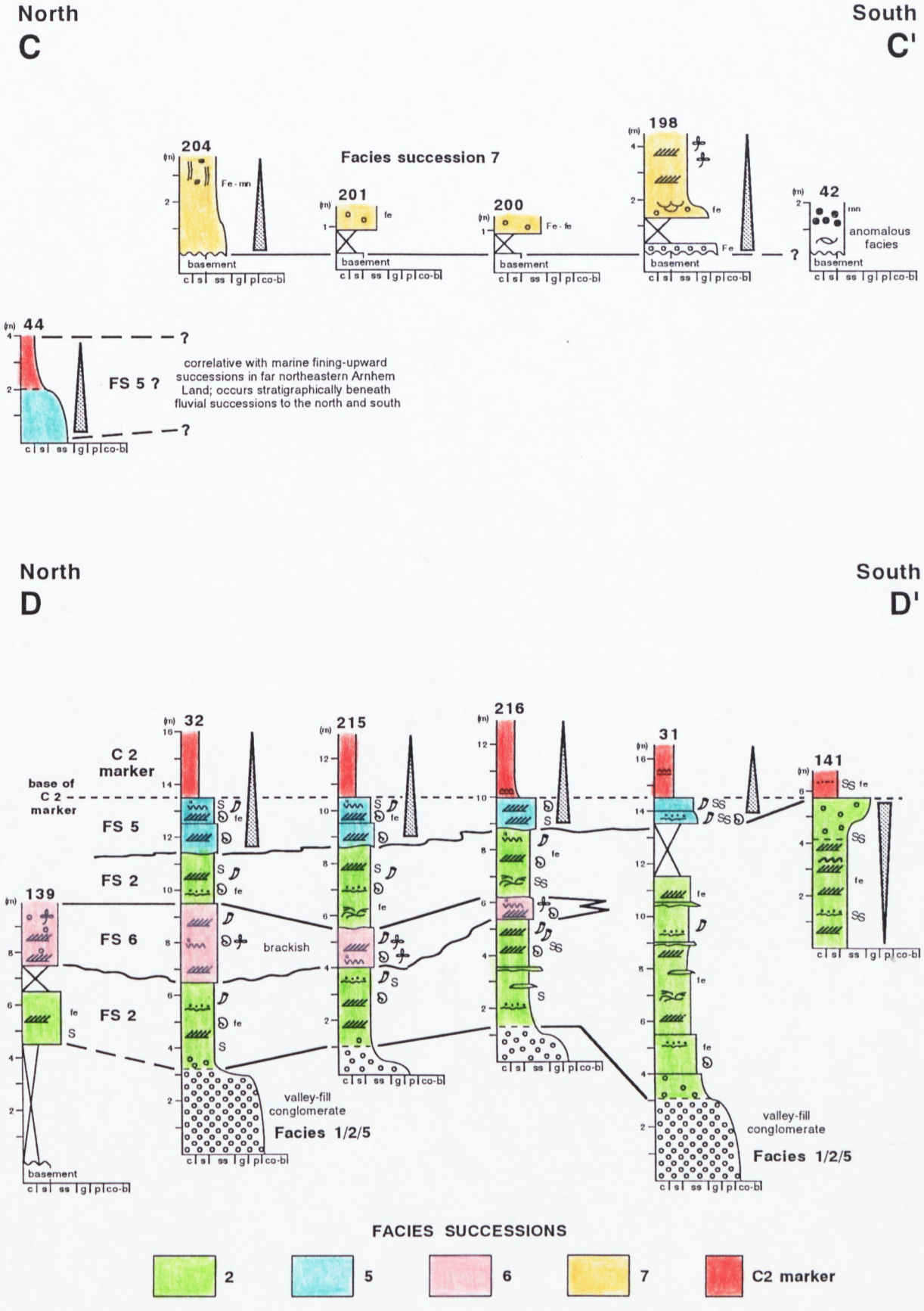

FIGURE 5.7. Stratigraphic correlation diagrams of the alluvial/coastal plain (C-C'), and the nearshore marine zone (D-D') in the BPRZ. See Fig. 5.2 for legend, inset map on Fig. 5.1 for location of sections along C-C', and Fig. 5.6 for sections along D-D'.

conglomerate shows evidence of marine reworking. This whole succession represents the initially nonmarine fill of an incised valley, which became progressively more marine as the area was drowned (see Sect. 9.5.1).

The overlying marine sandstones are up to 11 m thick and contain numerous marine body and trace fossils, abundant cross-stratification and ripple marks, and are significantly bioturbated. In places sandstone forms coarsening-upward successions (*e.g.* section 141), but more commonly sandstone intervals are massive. Sandstones here are interpreted to have been deposited in the foreshore to upper shoreface, and are examples of facies succession 2. In this area, at or near the palaeoshoreline, marine sandstones of facies succession 2 are thickly interbedded with sandstones containing a mixed marine/nonmarine fossil assemblage. These are brackish or paralic sandstones of facies succession 6, which are similar to surrounding marine sandstones in most respects, except for their coarser grain size and abundant plant fossils.

There is one main tongue of brackish sandstone, which can be seen to thin markedly to the south (offshore) until the brackish sandstone interval wedges out (*e.g.* between sections 216 and 31) and is replaced further offshore by fully marine fossiliferous sandstones of facies succession 2 (*e.g.* section 31). Both the upper and lower contacts of the brackish sandstone are sharp, and in several places the basal contact is defined by erosional incision and a thin lag. Brackish sandstone intervals form massive or fining-upward successions in this region.

The interpretation of the depositional environment for sandstones of facies succession 6 is problematic (see also Sect. 4.5.3) because they are thin, do not occur in many sections, and their three-dimensional geometry is not well defined from the available outcrops. Most likely they represent thin prograding deltaic deposits or estuarine sandbodies. It is difficult to assign a deltaic origin to these deposits with complete confidence because the fluvial source and delta morphology are not recognisable. Similarly these brackish sandstones do not contain any diagnostic features or facies stacking patterns of estuarine deposits. For these reasons they have been assigned as a more general paralic depositional environment where marine and nonmarine processes were mixed, and have not been given a more specific environmental interpretation.

The top of the Cretaceous sequence along D-D' is defined by transgressive fining-upward facies of succession 5, representing deposition in the shoreface to upper offshore zone. Fining-upward cycles of succession 5 can be confidently correlated between sections in this area, and

have a disconformable contact with underlying coarsening-upward and massive sandstones. Fining-upward succession 5 shows a change in grain size from coarse-medium sandstone to silty claystone. Abundant cross-bedding at the base of the succession reflects deposition in a high-energy upper shoreface environment, whilst current and wave ripples, and wavy lamination in the upper part of the succession reflect deposition in a lower-energy, deeper water environment. The succession contains numerous marine molluscan body fossils, abundant but low-diversity trace fossils, and is extensively bioturbated in the fine-grained upper part.

The fining-upward succession illustrated in the upper part of correlation diagram D-D' is identical to those seen in the ALZ and elsewhere within the BPRZ, and contains the regional C 2 marker. On that basis, this cycle of fining-upward succession 5 is considered correlative throughout the entire northern region. In some places where the marine sediments are very coarse-grained and represent a very high-energy shoreface to foreshore environment, fining-upward succession 5 is not complete (*e.g.* above the shoreface conglomerate in section 141). Here the fining-upward nature of succession 5 is not obvious, and fine-grained facies in the upper part of the succession directly overlie facies of the underlying coarsening-upward or massive shoreface succession. This type of succession occurs in close proximity to the palaeoshoreline, at sites of intense reworking and sediment bypass in the shoreface to foreshore zone.

In a previous study, Skwarko (1966, fig. 4) divided the Cretaceous rocks in the area of site TT 65 (between sections 31 and 141) into 3 simplified, conformable units. The basal "unit 1" was interpreted as a lacustrine sandstone, the intermediate "unit 2" as a marine sandstone, and the upper "unit 3" as marine siltstone and claystone. In this study "unit 3" corresponds to marine facies succession 5, including the C 2 marker bed; "unit 2" corresponds to coarsening-upward rocks of facies succession 2; and "unit 1" corresponds to fining-upward transitional marine conglomerate and sandstone at the base of facies succession 2. Detailed correlation during this study shows that the contact between the "units" are typically disconformable, and does not support a lacustrine origin for the basal rocks. Despite these differences, Skwarko's (1966) detailed palaeontological analysis is useful for comparison of fossil assemblages between measured sections in the BPRZ, and provides palaeontological detail which is otherwise beyond the scope of this study. At site TT 65 Skwarko (1966) recorded 7 species of bivalves in sandstones of facies succession 2 (his "unit 2"), but did not record any fossils in the overlying rocks of facies succession 5 (his "unit 3") which includes the C 2 marker bed. The inferred

marine origin and wide distribution of facies succession 5 as illustrated in Fig. 5.7 is confirmed by Skwarko (1966, p. 26).

5.5.3 Correlation diagram E - E' (Fig. 5.8)

This correlation diagram is a continuation of correlation diagram D-D' from Marura Creek to the northern arm of the Walker River (Fig. 5.6), and illustrates facies variations along a 15.6 km line across the shoreface to offshore transition zone on the inner shelf. As in correlation diagram D-D', most sections are hung on the base of the C 2 marker which marks the upper part of the regionally extensive transgressive marine facies succession.

In the northern part of the correlation diagram rocks are relatively coarse-grained and were deposited largely above fair-weather wave base, where constant reworking obliterated much of the detail of individual beds (Fig. 5.8). In these areas coarse-grained marine sandstones and shoreface conglomerate dominate the stratigraphy (*e.g.* sections 140, 141, 143, and 144) and finer-grained rocks are poorly preserved. Farther offshore towards the south there is a general trend towards finer-grained rocks, and sedimentary structures and successions are better preserved. Here the stacking patterns of marine cycles are easily recognisable, and this allows confident correlation between individual coarsening- and fining-upward facies successions.

The base of the sequence in this inner shelf setting is a normally graded chert cobble to pebble conglomerate as described previously for D-D'. Along E-E' this facies is up to 12.5 m thick and overlies Proterozoic basement with an angular unconformity. The conglomerate fines upward into Cretaceous fossiliferous marine sandstone and siltstone of facies succession 5, which occurs at the base of sections 143, 144, 146, 147, and 148 and represents the initial marine incursion in the region. This fining-upward transgressive succession is not preserved to the north in correlation diagram D-D', presumably due to reworking and erosion during subsequent relative sea level fall. The transgressive marine succession is disconformably overlain by a series of stacked coarsening-upward cycles of facies succession 2. The disconformable contact is marked by a pebble conglomerate or shelly lag up to 2 m thick (typically 0.5 to 0.75 m thick), which contains clasts or fossil fragments up to cobble size (*e.g.* section 148 at 4 to 4.5 m level).

There are at least 3 stacked cycles of succession 2 (Plate 1b), although the exact number and thickness of all cycles is not always clear due to erosion between cycles. The contacts between coarsening-upward successions are also erosional and are commonly mantled by thinner

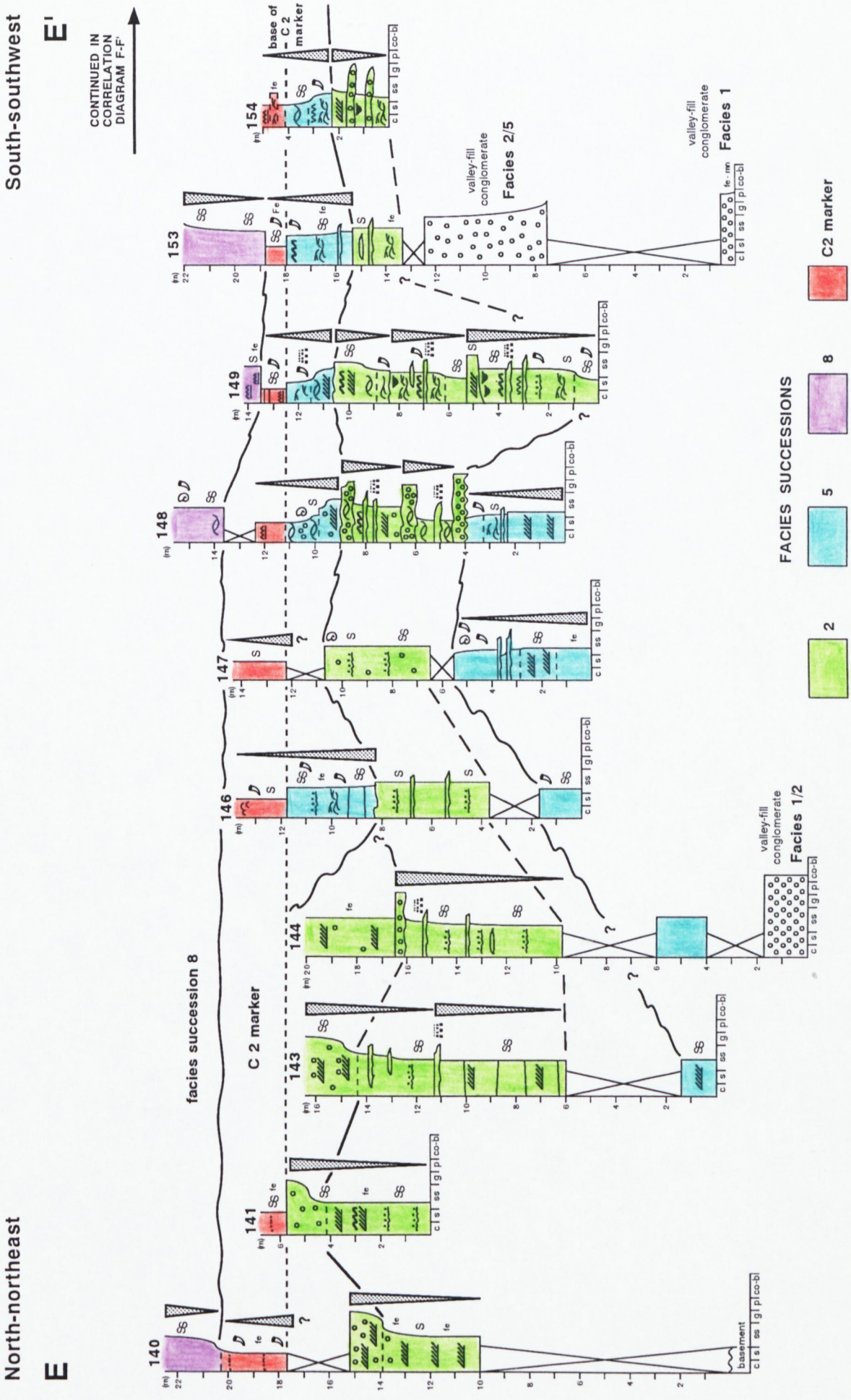

FIGURE 5.8. Stratigraphic correlation diagram for the nearshore marine area in the Bath and Parsons Ranges Zone. Refer to Fig. 5.6 for location of sections along E-E'.

conglomeratic and shelly lags, or very coarse-grained sandy beds. In the foreshore to upper shoreface zone at the same stratigraphic level in sections 140 through 144, the boundaries of individual coarsening-upward successions are not readily apparent due to the coarse grain size and lack of preserved sedimentary structures relative to areas farther offshore.

A regionally extensive transgressive fining-upward marine cycle disconformably overlies the stacked coarsening-upward successions in the area covered by correlation diagram E-E'. The same fining-upward cycle of facies succession 5 is also illustrated in correlation diagrams A-A', B-B', C-C', and D-D' and represents a major marine flooding event across the shelf. The contact of this succession with underlying successions is sharp and involves minor transgressive erosion in places, but not to the same degree as erosion which occurred between accumulation of each of the underlying coarsening-upward successions. This sharp contact is occasionally defined by a thin conglomeratic or rip-up lag, but the erosional nature of the contact becomes less obvious farther offshore along F-F' (Fig. 5.9).

The preserved thickness of the transgressive facies succession ranges from 2.5 to 5 m, with the upper part composed of fine-grained pelagic facies including the C 2 marker. The thickness of this transgressive succession decreases slightly in an offshore direction along with a general decrease in grain size; this reflects limited sedimentation during a time of active landward shoreface movement (retrogradation), and a progressive change to a quieter, more distal depositional environment.

The succession at the top of the Cretaceous sequence in this region in composed of clayey fine-grained sandstone and siltstone. These facies contain numerous body and trace fossils and prominent sedimentary structures including HCS, delicate flat and wavy lamination, and thinly interbedded facies. These facies are stacked in an irregular pattern with no regionally consistent vertical grain size trend, and have been grouped as succession 8, which is significantly different from marine facies of successions 2 and 5. Facies of succession 8 reflect deposition in marine to restricted marine settings, and changes in the energy of the depositional environment are apparent from one outcrop to another. The generally fine grain size, high clay content, fine lamination, and delicate preservation of articulated fossils implies that much of this succession was deposited in low to moderate energy marine settings, such as large bays. However, the presence of HCS and conglomeratic facies in this succession (particularly farther to the south) indicates that quieter sedimentation was episodically overprinted by high-energy storm reworking and rapid sedimentation.

The contact of succession 8 with underlying transgressive marine facies of succession 5 is sharp and typically disconformable, and the C 2 marker was eroded in places prior to accumulation of the overlying rocks of facies succession 8.

5.5.4 Correlation diagram F - F' (Fig. 5.9)

This correlation diagram is a continuation of correlation diagram E-E' and illustrates the same Cretaceous successions as in correlation diagrams D-D' and E-E'. This correlation diagram forms a 23.5 km line close to the Walker River (Fig. 5.6).. The main differences between the Cretaceous sequence present in correlation diagram F-F' *vs.* E-E' are:

1) the stacked coarsening-upward cycles of facies succession 2 are thicker and better preserved;
2) the basal fining-upward succession overlying the valley-fill conglomerate along E-E' is missing here;
3) the transgressive fining-upward succession disconformably overlying the stacked coarsening-upward successions is missing or greatly reduced in thickness in most places;
4) the preserved thickness of restricted marine deposits of succession 8 at the top of the sequence is much greater;
5) fluvial incision and subsequent accumulation of fluvial sandstones occurred in this area in close proximity to topographically high-standing basement ridges (*e.g.* section 166), and;
6) in general the evidence for erosion at the contacts between successions is less obvious, although many of these contacts are still disconformable on this part of the inner shelf.

Marine body and trace fossils, and rare plant fossils occur in rocks of facies succession 2 in the region of correlation diagram F-F', particularly in the south. At sites TT 66 and TT 67 (close to sections 174 and 184 respectively), Skwarko (1963; 1966) described 9 species of bivalves and indeterminate plant fossils within rocks of facies succession 2. This fossil assemblage is common for the succession, and can be used to aid local correlation. Unfortunately, the exact age of the fossil assemblage is unknown; the fossils have poor biostratigraphic resolution (see Sect. 5.5.6).

Good exposure of individual coarsening-upward marine cycles of facies succession 2 in this area allows accurate correlation between successions, and highlights subtle lateral changes in grain size and sedimentary structures within particular coarsening-upward cycles. The contacts between these successions are obviously erosional and feature discrete conglomeratic lags in places, but at the identical stratigraphic level in other outcrops the same erosion surface may be

FIGURE 5.9. Stratigraphic correlation diagram for the Bath and Parsons Ranges Zone. Refer to Fig. 5.6 for location of sections along F-F'.

defined by a shelly lag, or just a sharp contact with overlying fine-grained siltstone of the overlying succession. Local correlation indicates that individual coarsening-upward successions have a similar thickness in different outcrops, but that grain size (and hence many sedimentary structures) vary laterally within these cycles, particularly in the upper coarse-grained parts of the cycles.

Another lateral trend involves the decrease in thickness and eventual wedging-out of the upper transgressive fining-upward facies succession 5 towards the south. This succession contains the C 2 marker bed and can be traced southwards along correlation diagrams D-D' and E-E' to the vicinity of section 168 in F-F'. South of section 168 the transgressive succession has been eroded by overlying restricted marine to marine facies of succession 8. However, there is a noticeable thinning of the fining-upward succession 5 north of section 168, probably due to condensed sedimentation in more distal regions to the south.

On the inner part of the shelf in the BPRZ there are several areas where Cretaceous facies have an onlapping stratal relationship with high-standing basement terrain. These topographically-high basement regions are not capped by Cretaceous marine facies, and formed islands or barriers on the Cretaceous shelf. However, these basement highs are commonly partly covered by fluvial units (*e.g.* section 166). Fluvial facies here contain unidentified plant fossils of uncertain age, but regional correlation and similarity in lithology and stratigraphic position with northern fluvial outcrops places these fluvial successions as Albian to Cenomanian in age. Marine deposition on the inner shelf was seemingly concurrent with Cretaceous fluvial deposition on basement highs.

In the southern part of F-F', coarsening-upward marine cycles of facies succession 2 are immediately overlain by restricted marine to marine facies of succession 8. The contact of succession 8 with underlying coarsening-upward marine succession 2 is sharp and disconformable in most places, but involved only minor erosion farther offshore to the south. In correlation diagram F-F' and areas to the south, the thickness of succession 8 is relatively great, and a gradual increase in thickness of this succession is apparent along E-E' to F-F'. Succession 8 becomes thicker and more conglomeratic towards the south, where sedimentary structures indicate an increasing storm influence. This trend is more apparent in the southern part of G-G'.

5.5.5 Correlation diagram G - G' (Fig. 5.10)

Measured sections in this correlation diagram occur along a line 75.4 km stretching from west of the Walker River to Vaughton Creek (Fig. 5.6), and illustrate Cretaceous nonmarine, paralic, and shallow-marine depositional environments. In the northern part of correlation diagram G-G' a relatively thin interval of fluvial rocks are incised into a thick marine sequence composed of stacked coarsening-upward marine successions. Farther to the west and south near the flanks of topographically-high basement ridges, Cretaceous fluvial deposits are much thicker and marine facies were not deposited (*e.g.* sections 37 and 208-210).

Section 208-210 is a composite section of a thick Cretaceous fluvial succession which overlies Proterozoic basement with an angular unconformity along parts of the eastern edge of the Parsons Range in the southwest of the BPRZ. The upper part of this thick fluvial succession contains rare plant fossils, and is considered correlative with fluvial successions to the north and east, including those at sections 166 and 214. Presuming this correlation is correct, part of the thick fluvial succession at section 208-210 is equivalent in age to coarsening-upward marine facies of successions 2 and 8 offshore to the east and south. Slightly to the east of section 208-210 and close to the palaeoshoreline, there is a transition from the Cretaceous fluvial succession into a paralic (deltaic or estuarine) succession (*e.g.* upper 3 m of section 37).

The paralic rocks of facies succession 6 fine upward and contain rare marine molluscan fossils, shallow-water ripple marks and cross-stratification, indicating an increasing marine influence. The paralic succession is not overlain by marine successions and there is no obvious correlation with marine successions just to the east and south. This paralic succession probably reflects partial drowning of the alluvial zone which existed along the eastern edge of the north-south striking Parsons Range, and is possibly a facies equivalent of fining-upward facies succession 5 marking maximum transgression on the inner shelf.

Offshore to the south and east of section 37, the Cretaceous sequence is composed entirely of marine facies of successions 2 and 8. The lower part of the sequence is composed of stacked coarsening-upward and massive cycles of succession 2, similar to those documented to the northeast along D-D', E-E', and F-F' (*e.g.* sections 34, 36, and 213). Similar to the southern half of F-F', the upper transgressive fining-upward succession 5 is missing and storm-influenced restricted marine deposits of succession 8 directly overlie coarsening-upward marine deposits of succession 2 (*e.g.* sections 36 and 213). Facies of succession 8 along G-G' are coarser-grained than similar deposits to the north and show abundant indicators of storms

FIGURE 5.10. Stratigraphic correlation diagram for the Bath and Parsons Ranges Zone. Refer to Fig. 5.6 for location of sections along G-G'.

including coquinas, event beds, and dispersed granule to pebble-sized clasts. Comparison of Figs. 5.9 and 5.10 highlights the increasing storm-influence and general coarsening of succession 8 to the south. This trend probably indicates a less sheltered depositional environment to the south, and a sheltered/restricted marine environment to the north; sheltered by the topographically-high Bath Range to the east which acted as a barrier for most depositional episodes. In the less-sheltered region to the south, succession 8 has a number of similarities with underlying rocks of succession 2; farther to the northeast differences between the two successions are more readily apparent and they are often separated by transgressive fining-upward deposits of succession 5.

5.5.6 Biostratigraphic control

Biostratigraphic control for Cretaceous outcrops in the BPRZ is similar to the ALZ. That is, there is no accurate biostratigraphic zonation directly available because the only fossils recovered from outcrops are poorly preserved, low diversity molluscan macrofaunas of indeterminate age (*cf.* Paltech, 1980a) and trace fossils of no use in detailed biostratigraphic zonation. Ammonites were recorded at several field stations, but their poor preservation precluded positive taxonomic identification and age dating. Laboratory analysis of samples from the BPRZ for microfossils proved fruitless, probably due to the high degree of weathering at most sites.

The molluscan faunas in the BPRZ appear similar in all respects to molluscan macrofossils which occur in Cretaceous marine facies farther to the north in the ALZ, and in the central and southern regions to the south. Plant fossils observed in fluvial successions in the BPRZ appear to have similar sizes, affinities, and styles of preservation in all outcrops. However, the plant fossils are not diagnostic of any particular age, and may only be regarded as being Lower Cretaceous in age (Skwarko, 1963, p. 9; 1966, p. 62).

The details of marine macrofossil assemblages in these rocks (equivalent to part of the "Coastal Belt") were presented in a previous palaeontologically-based study (Skwarko, 1966). Skwarko divided the sedimentary sequence into 7 units on the basis of fossil content, and then attempted to correlate these fossil assemblages with other northern Australian and European faunas to give definitive biostratigraphic ages for the fossils (and hence units) of the northern region, including those in the BPRZ.

According to this scheme (Skwarko, 1966) most Cretaceous marine units of the Mullaman Beds were deposited during the Neocomian and Aptian, with minor marine deposition in the Albian. However, during this study of the Mullaman Beds in the BPRZ regional correlation with Groote Eylandt and Numbulwar to the southeast (Sects. 8.5.4 and 8.5.6), indicates that all Cretaceous facies successions illustrated in correlation diagrams C-C', D-D', E-E', F-F', and G-G' are younger than middle Albian. Skwarko's age assignments for marine macrofossils and facies of the area are consistently older than those of more-accurate recent palaeontological analyses of Cretaceous rocks of the Carpentaria Basin (*e.g.* Alley, 1991; Haig, 1991; Morgan 1980; Paltech, 1980e, 1981b).

Skwarko's stratigraphic interpretations are based on recognition and correlation of fossil assemblages from widely spaced outcrops of unknown age. Although Skwarko's (1966) palaeontological age determinations appear to be superseded, his study documents fossil systematics and the fine taxonomic details of fossil assemblages which are beyond the scope of the present study. Using these data, fossil assemblages can be compared between widely spaced outcrops in the onshore western Carpentaria Basin, and can be used to test or refine lithostratigraphic correlations made during the present study. Age estimates for various Cretaceous facies of the northern region are presented in chapter 8 on the basis of regional correlation, which links facies in all three regions of the shelf. For a systematic and detailed discussion of biostratigraphic control on an outcrop-scale see Sect. 8.2.

5.5.7 Summary of facies successions in the BPRZ

Regional correlation of facies successions in the northern region is summarised in Fig. 5.11, and is related to the BPRZ in the discussion below. The oldest Cretaceous rocks observed in *outcrop* in the BPRZ are cobble to pebble chert conglomerate and coarse-grained sandstone which have an angular unconformity with underlying Proterozoic units. The conglomerate is normally graded and grades into conglomeratic sandstone near the top of the facies. The base of the conglomerate represents a fluvial valley-fill conglomerate which becomes reworked upwards and grades into a shoreface marine conglomeratic sandstone. The upper conglomeratic sandstone contains molluscan macrofossils which are inferred to be middle to late Albian in age by regional correlation. The age of the basal cobble conglomerate is problematic because it contains no fossils and directly overlies Proterozoic basement; it could be older than Cretaceous, but most likely is early Aptian in age.

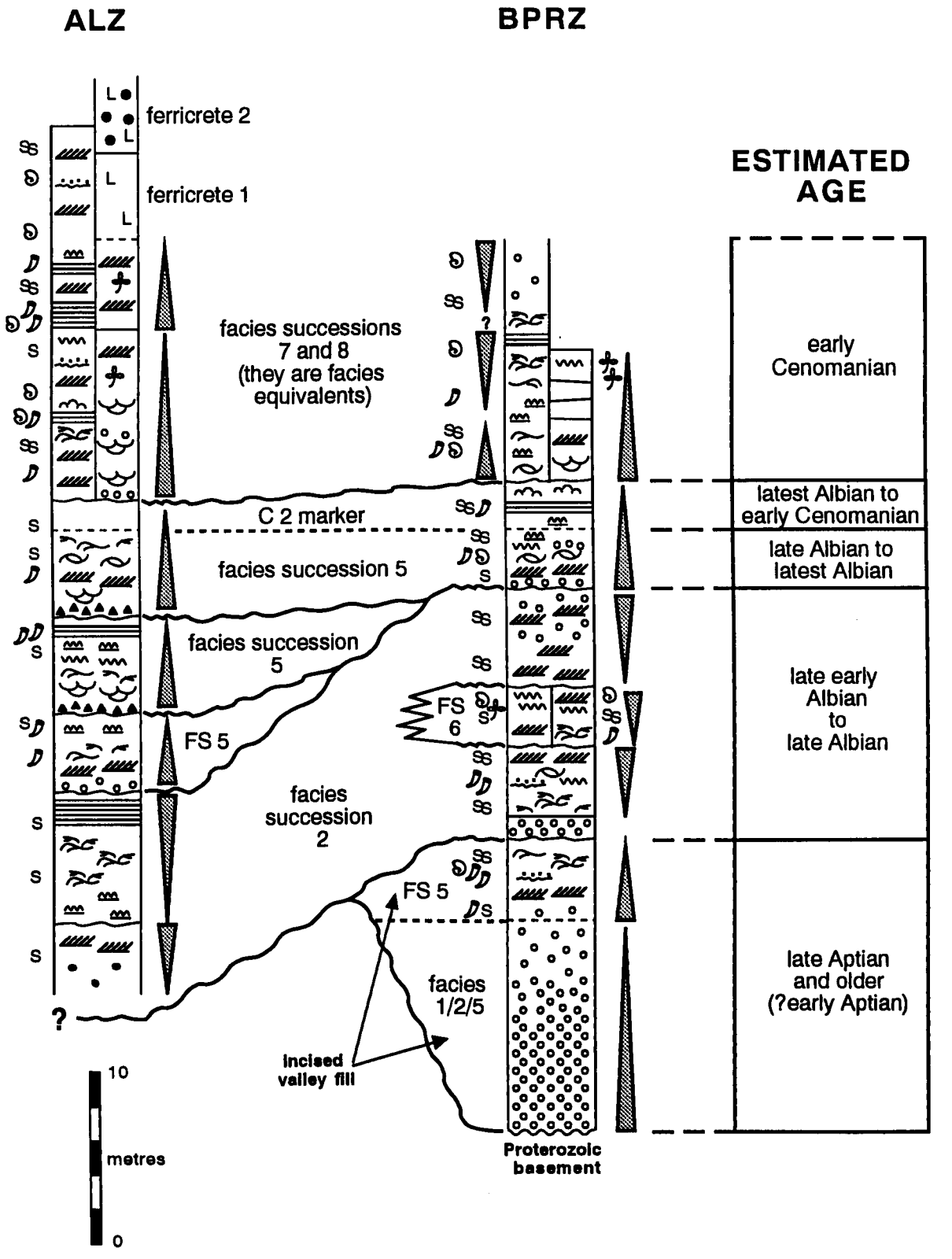

FIGURE 5.11. Regional facies successions, lithostratigraphic correlations, and estimated ages of Cretaceous rocks in the northern region. Age estimates are based on regional correlations and biostratigraphic analyses (see chapter 8). FS = facies succession.

Along E-E' the conglomerate and conglomeratic sandstone are apparently overlain by fining-upward marine shoreface rocks (facies succession 5), although the contact between these units was not directly observed. This fining-upward succession represents the first major transgression of the Cretaceous sea in the BPRZ, and drowning of older fluvial or fluvio-deltaic deposits. The fining-upward transgressive succession (or the conglomeratic sandstone where the transgressive succession is missing) is disconformably overlain by stacked coarsening-upward and massive cycles representing shallowing-upward marine shoreface successions. These cycles are well exposed throughout the region, and compose the entire Cretaceous sequence in places. In nearshore zones (*e.g.* Fig. 5.7, D-D'), the shallowing-upward shoreface successions are massive, coarser-grained, and are interbedded with sandstone containing mixed nonmarine/marine fossils. These sandbodies only occur close to the palaeoshoreline, thin rapidly in an offshore direction, and represent localised paralic or deltaic depositional environments.

In most parts of the BPRZ stacked coarsening- and shallowing-upward shoreface successions are disconformably overlain by an upper fining-upward transgressive shoreface succession. This succession marks the time of maximum transgression on the shelf and can be correlated over the entire study area using the C 2 marker, which occurs toward the top of the fining-upward succession. Where the Cretaceous sequence is complete, restricted marine facies of succession 8 overlie the fining-upward transgressive succession with a disconformable contact. Where the transgressive succession is missing, restricted marine facies directly overlie stacked coarsening- and shallowing-upward shoreface cycles of facies succession 2.

In many areas the restricted marine sandstones and siltstones of facies succession 8 represent the top of the preserved Cretaceous sequence. However, Cretaceous fluvial facies are present in close proximity to high-standing basement ridges, and have incised into underlying marine successions. These fluvial successions are facies equivalents of marine successions in other parts of the BPRZ. Their greatest thickness occurs on the edges of large basement ridges. Rare paralic sandbodies in the upper part of the fluvial succession (*e.g.* top of section 37) represent the transition from a fluvial to a marine depositional environment at the palaeoshoreline. These fluvial and paralic facies successions represent the youngest preserved Cretaceous deposits in the BPRZ.

5.6 CHAPTER SUMMARY

The Cretaceous sequence exposed in the northern region is composed of coarse-grained fluvial sandstones and a range of shallow-marine facies, many of which are also coarse-grained. Nearly all of the marine facies contain sedimentary structures which indicate that the energy of most local depositional environments was high, and that the seafloor was within the influence of fair-weather waves and storm waves. Storm-generated sedimentation, transport, and erosion appear to have been important processes in this region. The general morphology, sedimentary structures, and fossil content of facies in the northern region are characteristic of deposition on a shallow inner shelf to coastal plain, with rare facies reflecting localised deposition in paralic environments along the palaeoshoreline.

Series of stacked coarsening- and fining-upward marine facies successions occur in more complete outcrops over the entire region. These successions or 'cycles' reflect important changes in relative sea level which occurred across the shelf, and resulted in changes in base level on the coastal plain and migration of the palaeoshoreline. Evidence for large basinward or landward shifts in depositional environments as a consequence of relative sea level change is documented by extensive erosional or disconformable boundaries between successions in both marine and nonmarine settings. The amount of erosion and progradation or retrogradation of the shoreline is directly related to relative sea level change.

~~~~~~
~~~~~~

6. DEPOSITIONAL ENVIRONMENTS AND LITHOSTRATIGRAPHIC CORRELATION IN THE CENTRAL REGION: THE SHORELINE TO MIDDLE SHELF

6.1 INTRODUCTION

This chapter documents detailed lithostratigraphic correlation of isolated outcrops in the central region (Fig. 6.1). Cretaceous rocks exposed in the central region reflect dominantly marine depositional environments of a shoreline to middle shelf setting, and also include minor nonmarine and paralic facies successions in the western part of the region. The thicknesses, types, and relationships of facies successions in this region are similar to facies successions of the inner shelf and coastal plain (northern region) described in chapter 5. There are strong links between facies successions and depositional processes in both regions, even though important outcrops are separated by up to 500 km.

The geological and geographical setting of the central region is similar to the northern region; outcrops occur as isolated erosional remnants separated by large distances, and there is a general lack of detailed biostratigraphic data. Therefore, correlation of strata in the central region is based primarily on lithostratigraphic criteria. Local correlation again involves careful documentation of facies, recognition of facies successions and the bounding surfaces between successions, and detailed comparison of numerous measured sections and other field data. Local correlations documented in chapter 6 are utilised in chapter 8 in erecting a lithostratigraphic framework for the entire shelf.

6.2 DATABASE FOR DETAILED STRATIGRAPHIC CORRELATION DIAGRAMS

This chapter is based on the measurement of 49 outcrop sections and observations from numerous other field stations ranging from the "ruined city" in the north, to the western McArthur River in the south (Fig. 6.2). A series of 21 intersecting correlation diagrams was constructed to aid in preliminary correlation of Cretaceous rocks of the central region. These preliminary correlation diagrams were tested and refined, and combined with biostratigraphic, petrological, and geochemical data to construct 5 local to semi-regional correlation diagrams for

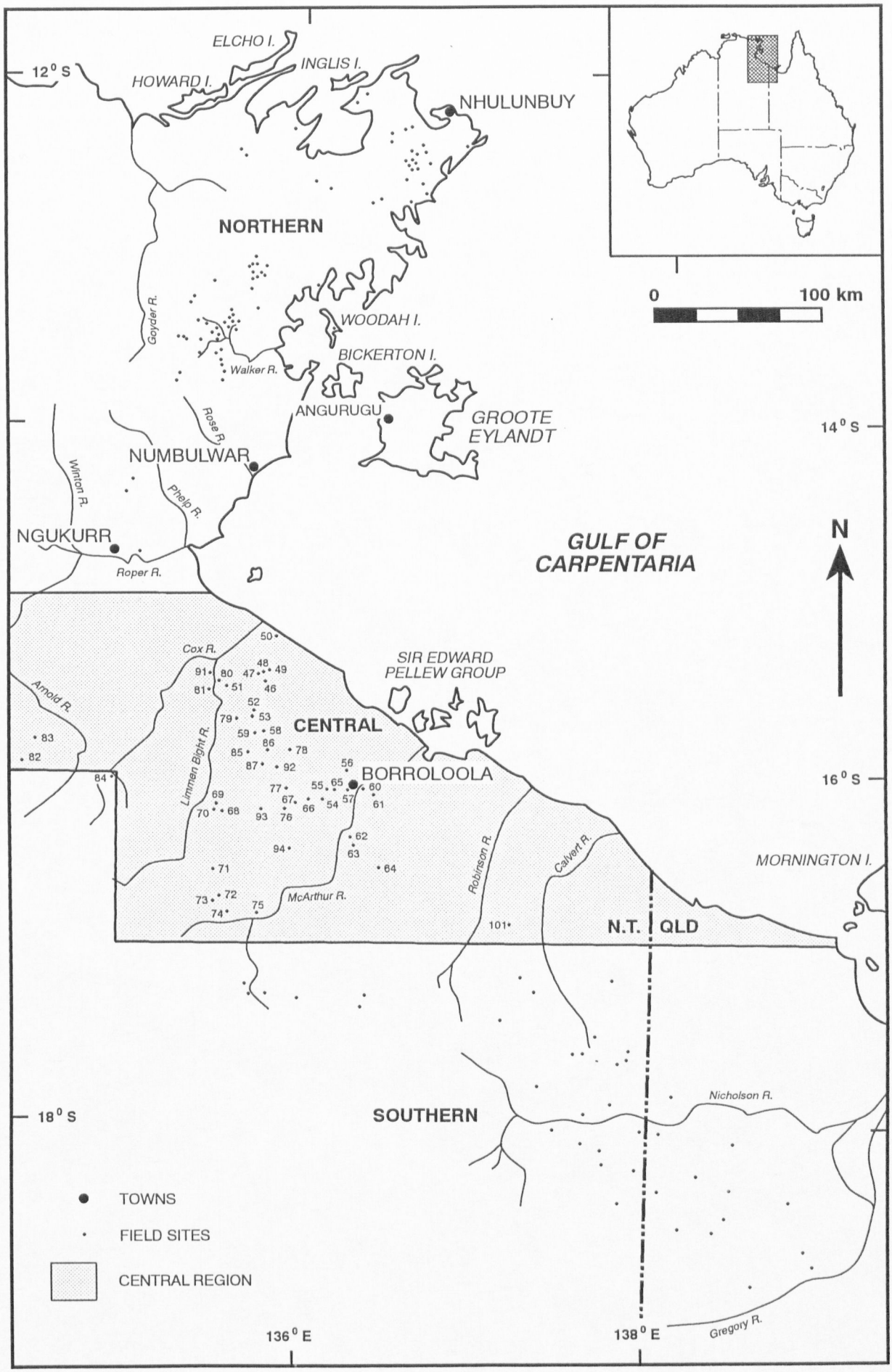

FIGURE 6.1. Location map for the central region showing field sites referred to in chapter 6.

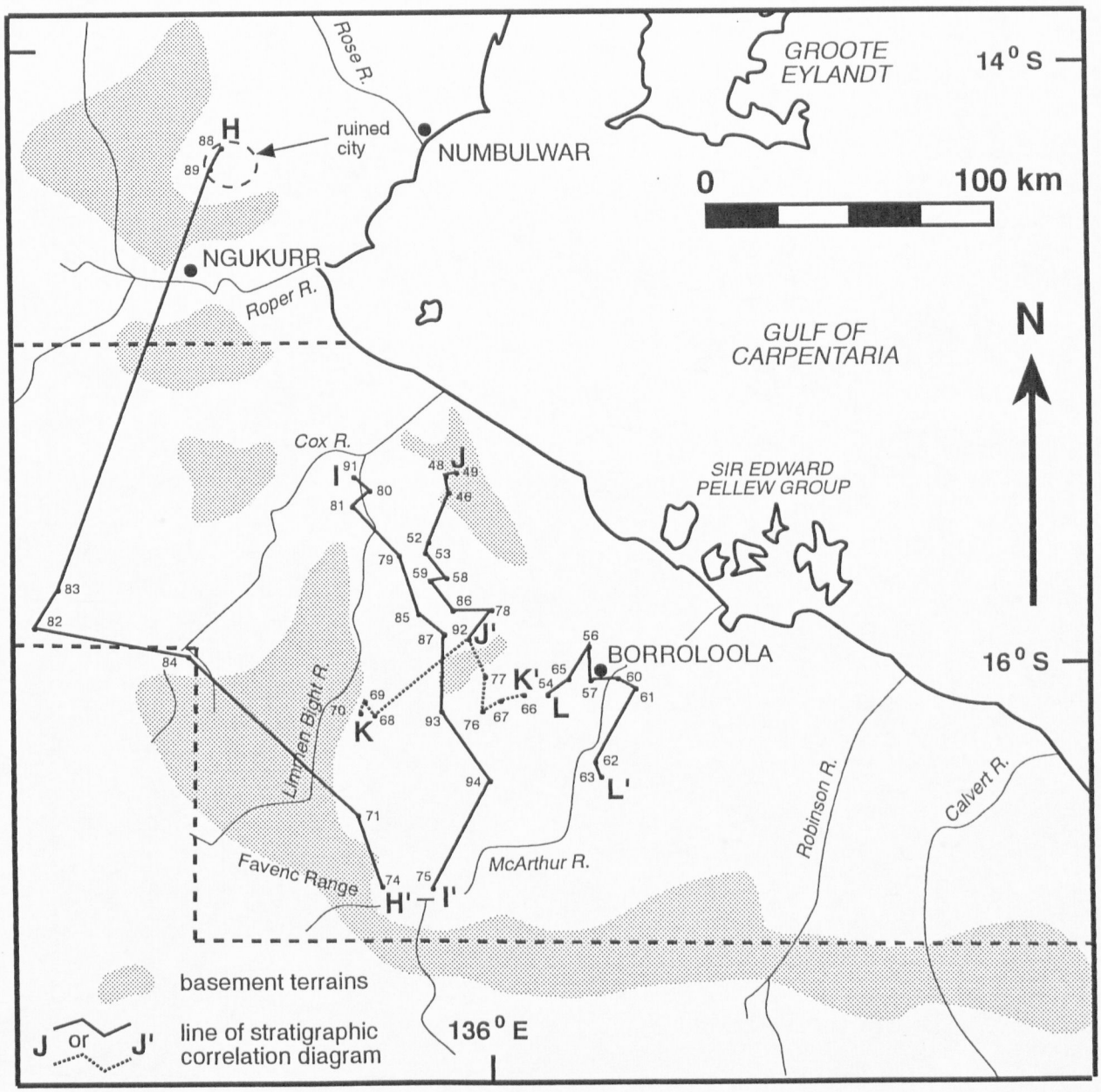

FIGURE 6.2. Location map for the central region showing field sites and location of correlation diagrams referred to in chapter 6.

the central region. For economy of space and clarity of correlation, these have been "condensed" from longer 'cross-sections'. The position of the correlation diagrams is located on a base map (Fig. 6.2), and all measured sections are drawn to the same scale.

Unlike the northern region, a reliable regional marker horizon is lacking in most Cretaceous outcrops in the central region. However, the relative stratigraphic position of most facies successions is apparent after laterally tracing more subtle marker beds, individual coarsening-upward and fining-upward cycles, and the few diagnostic fossil assemblages.

6.3 DETAILED STRATIGRAPHIC CORRELATION DIAGRAMS

6.3.1 Correlation diagram H - H' (Fig. 6.3)

This correlation diagram is unusual because it incorporates two sections from the southern part of the northern region. These sections (88 and 89) are isolated and problematic, but seemingly have a stronger affinity with successions in the central region than those of the northern region. The correlation diagram extends 310 km from the "ruined city" area in the vicinity of sections 88 and 89, to section 74 in the Favenc Range to the south.

Correlation diagram H-H' (Fig. 6.3) attempts to correlate widely spaced Cretaceous outcrops along the border of Skwarko's (1966) "Inland" and "Coastal" outcrop belts, which occurs at the western extremity of the central region in this study. According to Skwarko the border of his two outcrop belts marks the maximum westerly incursion of the Cretaceous sea in this area. There should be a clear change from nonmarine to marine depositional environments from west to east across this border if Skwarko's stratigraphic assignments are correct. However, the evidence for a regional nonmarine to marine transition is inconclusive, and correlation along H-H' is problematic using either Skwarko's data or lithostratigraphic data from this study. Relationships of nonmarine, paralic, and marine facies successions are only clear farther to the east.

Sections 88 and 89 in the northern part of H-H' have in common cross-bedded sandstones of presumable marine origin. In section 89 the sandstones exhibit a fining-upward trend, poorly preserved burrows, and some bioturbation. The sandstones are moderately sorted and texturally mature, and probably represent rocks of facies succession 5 from the shoreface to upper offshore zone, or the basal part of facies succession 4. In both measured sections the sandstones are overlain by a highly weathered, fine-grained facies with a high degree of

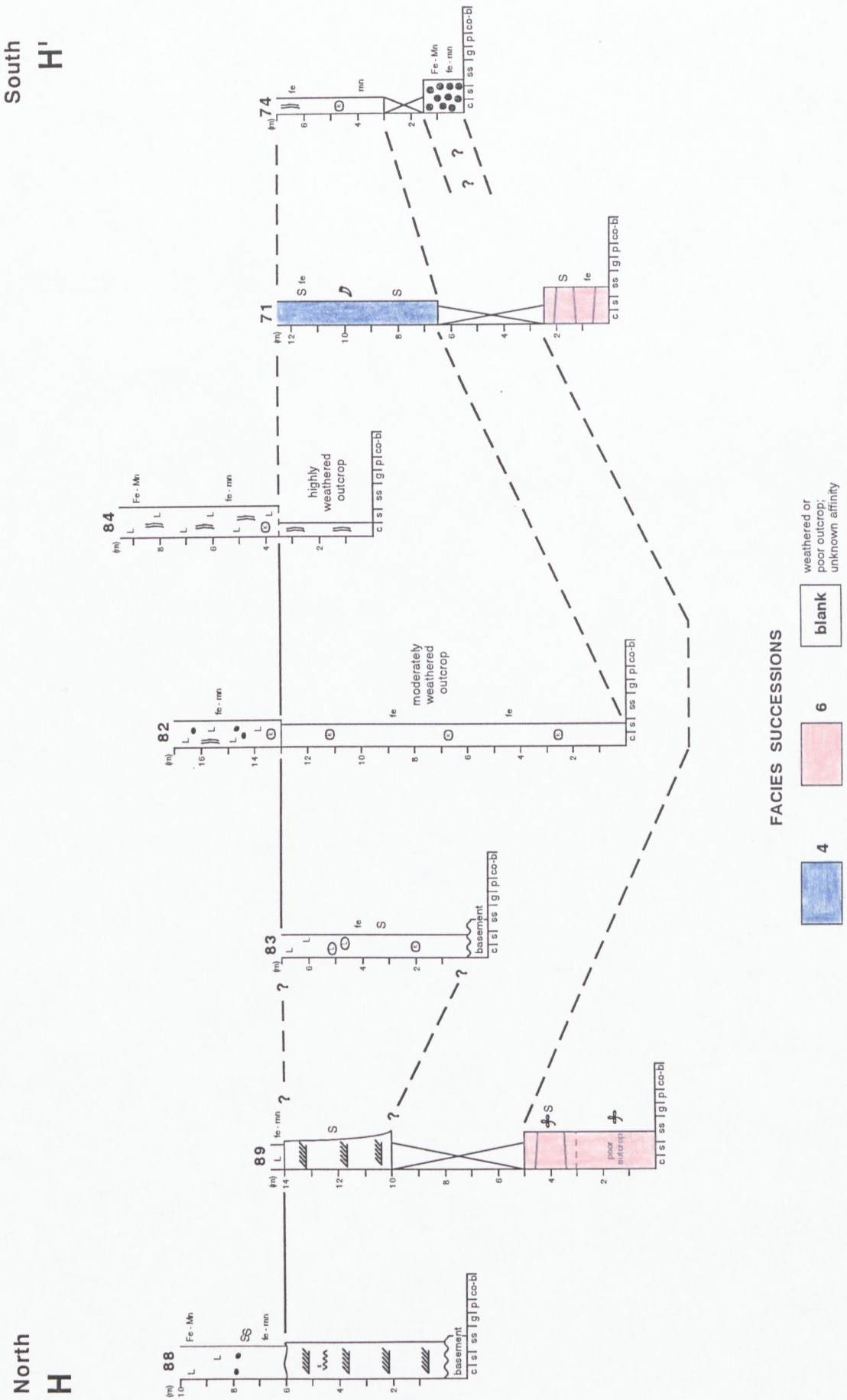

FIGURE 6.3. Stratigraphic correlation diagram along the western edge of the central region. Refer to Fig. 6.2 for location of sections along H-H'.

bioturbation in places. The upper facies possibly represents a deeper water marine environment, although this interpretation is tentative since there is a lack of marine body fossils in both sections. Five metres beneath the crossbedded sandstones in section 89, there are planar bedded and massive sandstones with plant fossils. These sandstones are correlative with facies in sections 68, 69, 70, 71, and 92 in the southern part of the central region (Fig. 6.2), and with facies in sections 32, 37, 139, 215, and 216 in the northern region (Fig. 5.2). The sandstones are assigned to facies succession 6, and are interpreted to represent a paralic depositional environment. This is supported by the stratigraphic position of similar sandstones between deltaic and offshore marine facies along K-K'.

Sandstones at the base of sections 71 and 89 along H-H' equate to "unit A" (Lees Sandstone) in terms of Skwarko's (1966) stratigraphic nomenclature. According to Skwarko (1966) this sandstone represents nonmarine environments only, but in the northern region the same unit contains a mixed assemblage of marine and nonmarine fossils. On the basis of fossil content and detailed lithostratigraphic correlation during this study, plant-bearing sandstones of facies succession 6 (equivalent to part of Skwarko's unit A) are considered to represent paralic (deltaic and brackish marine) depositional environments in close proximity to the palaeoshoreline.

On the far western edge of the central region along H-H', Cretaceous rocks are exposed intermittently as low ridges of highly weathered sandstone and siltstone (Plate 1e), capped by laterite and lateritic soils (*e.g.* sections 82, 83, and 84). Again, this region is interpreted to be close to the border of Skwarko's "Inland" and "Coastal" belts. In all three sections partly bioturbated siltstone is overlain by laterite/ferricrete, but recognition of the depositional environment of the siltstone is difficult due to the intense degree of weathering. Fossils were not recovered from any of the three measured sections here, but belemnites of indeterminate age were recovered close to section 84 in a previous study (Skwarko, 1961). The presence of belemnite fossils in the region, combined with the traces of bioturbation, suggest a marine depositional environment for the siltstone. Skwarko (1966) proposed that most Cretaceous strata in this area are composed of his marine "unit C" (Polland Shale), although lithostratigraphic correlation during this project tentatively assigns the siltstone to facies succession 4 (Fig. 6.3), which has more in common with Skwarko's "unit 6" in most places. Whichever assignment is correct, highly weathered fine-grained Cretaceous outcrops in this area on the western edge of the study area are regarded as marine in origin, and are correlated with fine-grained marine facies farther to the south and east.

To the south, the same fine-grained marine facies are exposed, but here the siltstones and sandstones are better preserved and their characteristics are more obvious (*e.g.* sections 71 and 74). Section 71 is the same as Skwarko's (1962c; 1966) fossil site TT 29 within his "unit 6", and corresponds to facies succession 4 of this study. The only fossils observed by Skwarko were unidentified worm trails, which have been identified as *Palaeophycus* burrows in this study. Whilst the presence of the trace fossils does not provide conclusive evidence for a marine origin for this facies succession, lithostratigraphic correlation with identical fine-grained facies with marine macrofossils farther to the east supports a marine origin for siltstones in this area.

In the southern area covered by Fig. 6.3 the youngest Cretaceous rock is siltstone of probable marine origin, which may belong to facies succession 4. The lower part of section 74 consists of an unusual facies similar to the anomalous facies of section 42 in the northern region. The anomalous facies in both sections 42 and 74 are highly mineralised by iron and manganese oxides, have a similar grain size and texture, and probably represent shallow-marine depositional environments. The lack of preserved sedimentary structures or fossils precludes a more detailed interpretation for the depositional environment of the lower pisolitic facies in section 74.

6.3.2 Correlation diagram I - I' (Fig. 6.4)

This correlation diagram extends along a 180.6 km line and illustrates dominantly marine deposits from near the junction of the Cox and Limmen Bight Rivers in the north close to section 91, to the western McArthur River near section 75 in the south (Fig. 6.2).

In the northern part of the area covered by correlation diagram I-I' (Fig. 6.4) the entire Cretaceous sequence is composed of fine-grained marine siltstone and sandstone of facies succession 4 (*e.g.* sections 80, 81, and 91). Siltstone and sandstone here are massive or subtly fining-upward, all facies are highly bioturbated, and bryozoan and bivalve fossils are common. Preserved sedimentary structures are limited due to the high degree of bioturbation, but ripple-lamination, thin graded beds, and discrete pods, lenses, and stringers (discontinuous laminae) of granule to pebble sized clasts are sometimes recognisable. In terms of Skwarko's (1966) nomenclature the facies here correspond to "unit 6" of his "Coastal" belt. Where the complete sequence is exposed, Cretaceous rocks overlie basement with a thin conglomeratic lag (*e.g.* section 81).

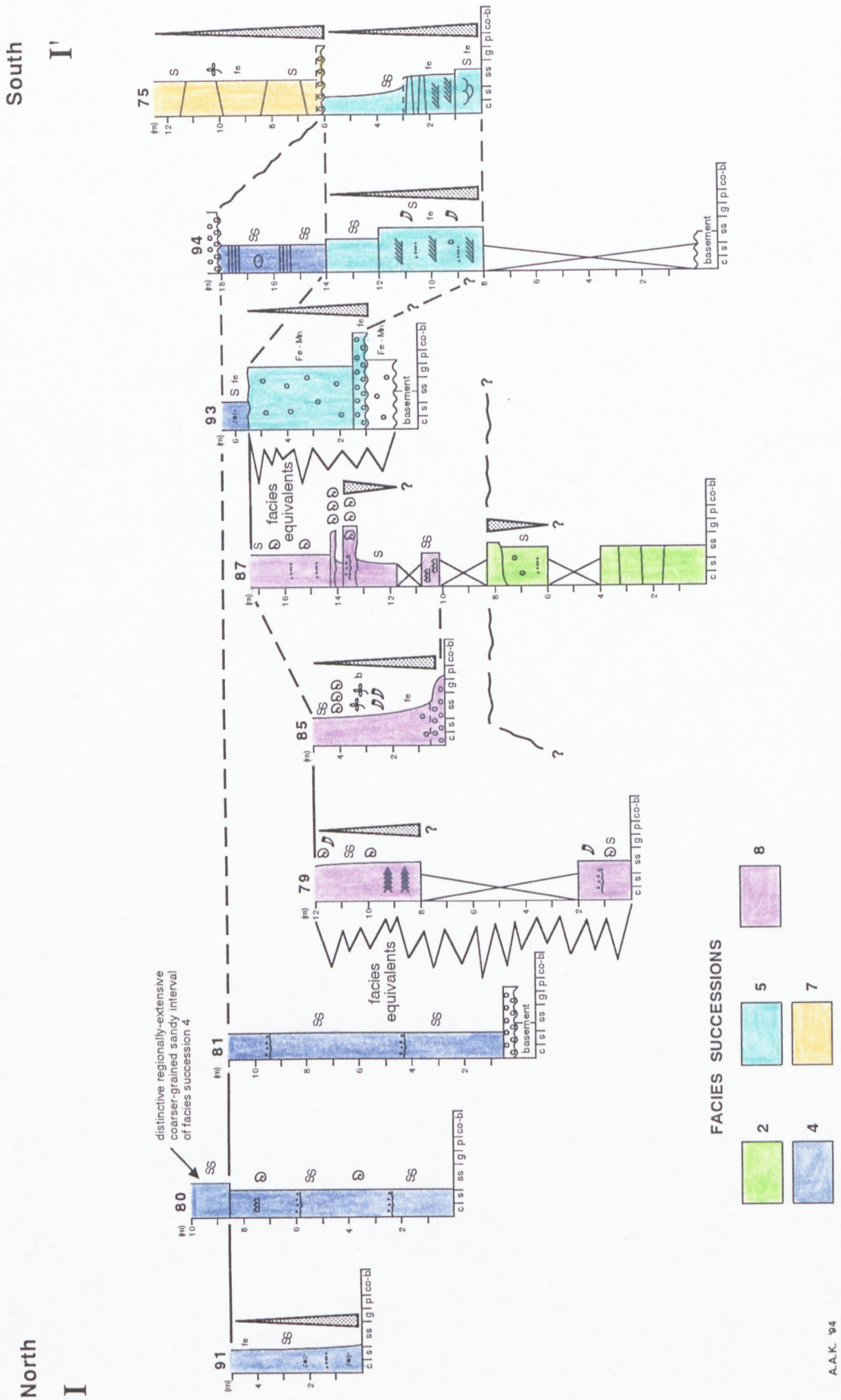

FIGURE 6.4. Stratigraphic correlation diagram for the central region. Refer to Fig. 6.2 for location of sections along I-I'.

Southeast of the junction of the Cox and Limmen Bight rivers in the area between sections 81 and 79, there is a significant facies change within the Cretaceous sequence. Overall, the southern facies (sections 79, 85 and 87) are similar to the northern facies of succession 4 (sections 80, 81, and 91), but there is an obvious increase in the diversity and abundance of fossils, and the grain-size and composition of the facies is far less uniform in the southern facies. In places (*e.g.* sections 79 and 85), the succession exhibits a fining-upward grain size trend, whereas in other exposures the grain size trend is irregular (*e.g.* section 87). The facies succession here contains evidence of storm deposition, including coquinas, irregular graded beds, and discrete stingers of poorly sorted clasts set in fine-grained matrix, and has similarities to facies succession 4.

The Cretaceous sequence in sections 79, 85, and the upper part of 87, is assigned to facies succession 8, which is interpreted as the deposit of a sheltered/restricted bay environment with an intermittent storm influence. The same facies succession occurs in correlation diagram J-J' to the east. In both I-I' and J-J' deposits of facies succession 8 occur in an area on the middle to inner shelf which was sheltered by an eastern barrier named as the topographically-high basement terrain of the Yiyintyi Range (shown as the shaded area around sections 46, 48, and 49 on Fig. 6.2). The Yiyintyi Range is exposed to the northeast of most exposures of facies succession 8 and seems to have formed a large island during the mid-Cretaceous. This interpretation is supported by the onlapping stratal relationship of Cretaceous facies with Yiyintyi Range Proterozoic units, and the corresponding facies change from succession 8 to open marine deposits of facies succession 4 away from the range to the north and south.

In places rocks of facies succession 8 overlie, presumably disconformably, thick coarsening-upward shoreface sandstone and conglomeratic sandstone (facies succession 2). These deposits are similar to facies near the base of the Cretaceous sequence in the BPRZ in the northern region. Indeed, the thicknesses and relationships of facies successions in section 87 are identical to those in the northern region. In terms of Skwarko's (1966) nomenclature, facies of succession 8 in sections 79, 85, and 87 and the surrounding area correspond to "unit 4" of his "Coastal" belt, whilst the underlying facies of succession 2 correspond to his "unit 2". The lack of marine fossils within facies succession 2 here is not overly problematic, since marine fossils are rare within identical shoreface deposits elsewhere, and Skwarko (1966, p. 26) also noted the same rarity of marine fossils within his "unit 2" in the area. Section 87 is equivalent to Skwarko's site TT 56, where he recorded in some detail the fossil content of facies succession 8 (his "unit 4"). For a diagrammatic representation of stratigraphic relationships

between my proposed stratigraphic scheme and Skwarko's (1966) scheme see Fig. 8.3. In section 87 (TT 56) facies succession 8 contains at least 6 different species of bivalves (Skwarko, 1966, p. 27). In the area around section 87 the diversity and abundance of fossils within facies succession 8 is much greater, and includes segmented plant fossils, unidentified vertebrate bone fragments, numerous trace fossils, a larger range of bivalves, and ammonite fragments.

In the southern area of I-I' the Cretaceous sequence is mostly composed of facies characteristic of unrestricted shallow-marine depositional environments. The oldest Cretaceous rocks in this area are fining-upward shoreface deposits of facies succession 5 (*e.g.* sections 75, 93, and 94). In most places this facies succession is composed of a basal sandstone or conglomeratic sandstone which fines upward over 5 to 6 m into siltstone and silty claystone. In section 93 facies succession 5 is very coarse-grained, and probably reflects high-energy deposition close to the palaeoshoreline. Farther offshore to the south, facies succession 5 is finer-grained and exhibits a more obvious fining-upward character (*e.g.* sections 75 and 94). In this area facies succession 5 does not contain any marine body fossils, but the sandstone and siltstone are highly bioturbated and contain marine trace fossils. The lack of body fossils in this succession is not uncommon, and is interpreted to be due to the inability of most infaunal organisms to tolerate the unstable, high-energy conditions of the depositional environment. The same situation is also apparent in many exposures of coarsening-upward shoreface deposits of facies succession 2.

In the southern part of the central region shoreface deposits of facies succession 5 are overlain by deeper-water offshore marine facies of succession 4 (*e.g.* sections 93 and 94), which can be confidently correlated along I-I' to the north. The contact between these two successions is sharp and is probably disconformable in most areas, although there are rarely any obvious signs of erosion at this surface. This contrasts markedly with nonmarine deposits which erosionally overlie facies succession 4 or 5 in this area; the contact between marine successions and nonmarine facies succession 7 is invariably marked by a conglomeratic lag, indicating significant erosion as fluvial deposits incised into underlying marine successions. Near section 94 the fluvial deposits have eroded down into facies succession 4, and only 4 m of facies succession 4 is preserved. Farther to the south, fluvial incision has apparently completely removed deposits of facies succession 4, and fluvial sandstones directly overlie facies succession 5 (*e.g.* section 75).

Sandstones of facies succession 7 (*e.g.* section 75) are massive and planar-bedded, poorly sorted, and contain rare segmented plant fossils and traces of bioturbation. Skwarko (1962c; 1966) recovered 4 main types of plant fossils from "unit A" (equivalent to facies succession 7) close to section 75, and did not record any marine fossils from the area.

6.3.3 Correlation diagram J - J' (Fig. 6.5)

This correlation diagram extends 94.6 km from the basement terrain of the Yiyintyi Range in the north, south to section 92 (Fig. 6.2). Most of the Cretaceous rocks in this region were deposited in marine environments of the middle and inner shelf, although nonmarine and paralic deposits occur in areas surrounding topographically high-standing basement ridges.

The oldest Cretaceous rocks in this part of the central region are composed of sandstone, pebbly sandstone, and conglomerate (Fig. 6.5). Facies have variable grain size, but typically have a coarsening-upward grain size trend (*e.g.* sections 52, 58, 78, and 92). Medium- to fine-grained sandstone is the main rock type, and the sandstone is typically moderately to well sorted, moderately to intensely bioturbated, and contains a sparse suite of fossils, including marine macrofossils, segmented plant fossils, and rare trace fossils. These rocks have been assigned to facies succession 2, which involves deposition in the shoreface to upper offshore zone. The facies are very similar to rocks of facies succession 2 in the BPRZ in the northern region.

In most places the fossil content of deposits interpreted as facies succession 2 does not give unequivocal support for a marine origin; a mixed marine / nonmarine fossil assemblage occurs in loose blocks at the base of section 48; the basal parts of sections 58 and 78 contain only plant fossils; the basal part of section 86 contains only marine fossils; elsewhere in correlation diagram J-J', facies succession 2 does not contain any body or plant fossils. Lithostratigraphic evidence strongly supports correlation of all of these facies as one succession of the same age, and also infers that the facies were deposited in a shallow-marine depositional environment.

The basic stratigraphic observations of Skwarko (1966) agree in general with correlations and interpretations of depositional environments presented in this study. However, in places Skwarko recognised a separate basal lacustrine facies, his "unit 1". This unit supposedly contains only plant fossils near the top, and grades upward into overlying marine sandstones of his "unit 2". Detailed local correlation in this study does not support the interpretation of a separate lacustrine facies for this region, and all facies have been grouped as marine facies

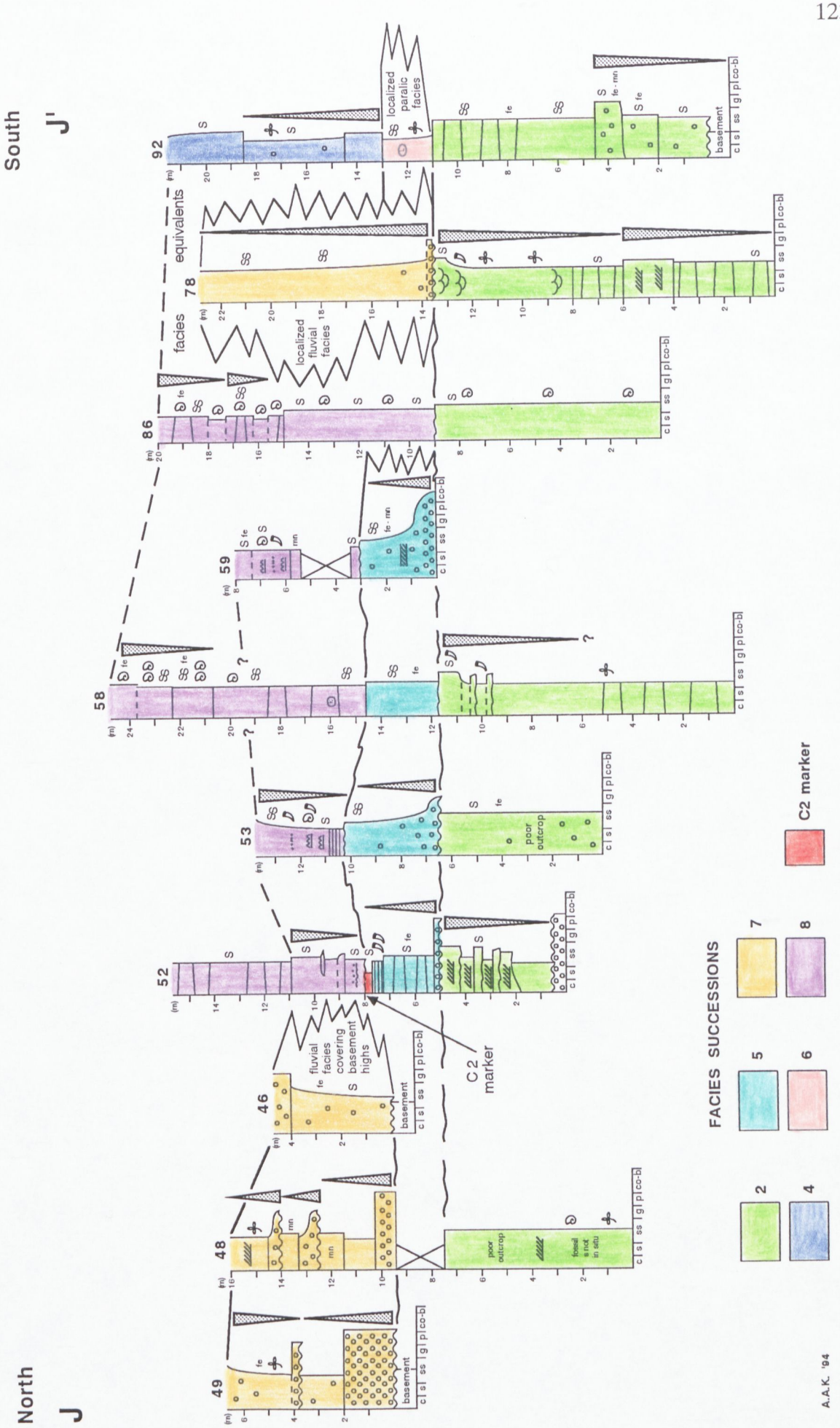

FIGURE 6.5. Stratigraphic correlation diagram for the central region. Refer to Fig. 6.2 for location of sections along J-J'.

succession 2. However, it is probable that some local exposures, especially coarse-grained facies overlying basement in topographically lower levels, represent a transitional depositional environment between brackish and full marine conditions (*e.g.* the bases of sections 52 and 92) during initial Cretaceous marine transgression in the area. This facies relationship was documented in chapter 5 for the BPRZ in the northern region (see Figs. 5.7, 5.8, 5.9, and 5.10), where thick marine sandstones of facies succession 2 gradationally overlie brackish sandstone and conglomerate. In the central region thick conglomeratic and brackish facies are missing at the base of the Cretaceous sequence, because significant nonmarine erosion was uncommon on this more distal part of the shelf, and the transition from nonmarine to marine sedimentation would have been rapid in this setting.

In the northern part of J-J' along the western flank of the Yiyintyi Range, poorly preserved outcrops of facies succession 2 are overlain by coarse-grained fluvial deposits of facies succession 7. The contact between marine facies of succession 2 and fluvial facies of succession 7 was not directly observed, but fluvial deposits occur less than 2 m above marine sandstone in section 48. Farther to the east in the Yiyintyi Range, fluvial deposits directly overlie Proterozoic basement and form patchy valley-fill deposits. The fluvial sandstones are poorly sorted, rarely bioturbated, and contain only rare plant fossils, including wood logs up to 50 cm long. These fluvial deposits are mostly fining-upward, and are similar in all respects to fluvial deposits in the northern region.

Fluvial sandstones of succession 7 accumulated on elevated basement highs in the central region, and incised into underlying middle to inner shelf deposits at the margins of the basement terrains after retreat of the sea from the region. Whilst a lack of marker beds and fossils makes correlation within the fluvial deposits tentative, all the fluvial deposits in the central region are younger than surrounding marine successions on the basis of stratigraphic position, and are considered to be equivalent in age. In the Yiyintyi Range area near sections 46 and 48, Skwarko (1962b; 1966) recovered a range of plant and marine body fossils, including 11 types of bivalves, 2 types of gastropods, an unidentified cephalopod, and numerous indeterminate plant fragments. Judging by the position of his site TT 55 it appears that the marine fossils were collected from the underlying facies succession 2 (Skwarko's "unit 2"), and the plant fossils belong to fluvial facies succession 7.

In the central area of correlation diagram J-J', coarsening-upward marine rocks of facies succession 2 are disconformably overlain by fining-upward rocks of facies succession 5. Facies succession 5 is composed of moderately to well sorted, rounded sandstone which fines

upward into silty sandstone, siltstone, and claystone. All of the facies are moderately to intensely bioturbated, and although no marine fossils were observed, marine trace fossils occur in places. The coarse grain size and lack of lithological contrast of much of the succession makes identification of individual trace fossils difficult, and there is a general lack of marine body fossils in this succession. The poorly fossiliferous nature of these shoreface facies successions was also documented in the northern region.

In section 52 the upper part of facies succession 5 contains the C 2 marker bed, which allows direct correlation and dating with the northern region and Groote Eylandt (Sects. 8.5.4 and 8.6.1, and Fig. 8.7). The C 2 marker bed is uncommon in the central region, because overlying facies of succession 8 have typically incised into succession 5 and removed the C 2 marker. However, even without the C 2 marker, these successions can be confidently correlated within the central region, and also with the northern region. In both the central and northern regions these facies successions exhibit identical relationships; thick deposits of facies succession 2 are disconformably overlain by relatively thin deposits of facies succession 5 which thin offshore, and are in turn overlain disconformably by thick deposits of facies succession 8. The disconformable contact between facies successions 2 and 5 involved transgressive erosion, and the underlying deposits of facies succession 2 may have been subaerially exposed in some areas close to the palaeoshoreline.

To the south in the vicinity of section 86, thick deposits of facies succession 8 directly overlie sandstones of facies succession 2 with a disconformable contact. Here, fining-upward sandstones of succession 5 were not deposited or have been completely removed by erosion. In this area facies succession 8 is up to 11 m thick, and is similar to succession 8 in correlation diagram I-I'. As in correlation diagram I-I', facies succession 8 is interpreted to have been deposited in a large bay to the west of a barrier island formed by the Yiyintyi Range. Again, the characteristic features of succession 8 are a great abundance and diversity of well-preserved marine fossils, an irregular facies stacking pattern, a high degree of bioturbation, storm-generated sedimentary structures overprinting indicators of quiet water deposition, and a finer grain size than underlying marine facies of successions 2 and 5.

In the southern part of correlation diagram J-J', localised fluvial and brackish facies directly overlie marine sandstones of facies succession 2 (Fig. 6.5). In section 78 the contact is disconformable, and subtly fining-upward fluvial sandstones of succession 7 overlie succession 2 with a thin basal conglomeratic lag. The fluvial sandstones at section 78 appear to have only local extent, they occur close to Proterozoic basement highs to the west, and are probably

correlative with fluvial succession 7 in the north (*e.g.* sections 46, 48, and 49). The moderate degree of bioturbation near the top of section 78 is unusual, and may indicate a brackish influence in the upper part of the fluvial succession.

In the southern area of correlation diagram J-J', the Cretaceous sequence is composed almost entirely of marine facies and is similar to parts of correlation diagram I-I'. In section 92 the basal half of the sequence is composed of thick marine sandstones of facies succession 2, which are sharply overlain by 2 m of massive, plant-bearing siltstone and very fine-grained sandstone. The facies here are moderately bioturbated, and are interpreted to represent localised transitional, paralic environments enclosed by marine facies above and below. It is envisaged that after shoaling and accumulation of the underlying coarsening-upward shoreface succession, quiet water paralic sedimentation would have occurred close to the palaeoshoreline. These paralic facies occur in a few localities surrounding basement highs in the Tawallah Pocket, and are sharply overlain, apparently conformably, by deepening-marine sandstone and siltstone of facies succession 4. These facies can be confidently correlated with similar successions throughout the central region on the middle shelf (*e.g.* sections 80, 81, and 91 correlation diagram I-I'), in areas away from the Yiyintyi Range barrier island. Facies of succession 4 in the southern part of J-J' (*e.g.* section 92) appear to be time equivalent to sheltered marine deposits of facies succession 8 to the north (*e.g.* sections 52, 53, 58, 59, and 86). The presence of plant fossils in succession 4 at section 92 is interpreted to indicate a more proximal position relative to other exposures of succession 4 to the north and east, where marine body fossils are prevalent.

6.3.4 Correlation diagram K - K' (Fig. 6.6)

Measured sections in correlation diagram K-K' occur along a 80 km line, which is approximately perpendicular to the palaeoshoreline. Correlation diagram K-K' joins with correlation diagram L-L', and illustrates the transition from paralic and nonmarine facies at the palaeoshoreline to marine successions of the middle and inner shelf. In this area there is no true marker bed that occurs in all exposures, but several conformable facies of constant thickness are common and can be used as marker beds for many sections.

Close to the palaeoshoreline in the western area of K-K', the oldest observed Cretaceous succession is composed of planar-bedded and cross-bedded sandstone with a thickness of 10 m (*e.g.* sections 68 and 69). Bioturbation is not obvious within this succession, but rare marine body fossils are present. Ripple-marks and abundant cross-bedding indicate a shallow-water

FIGURE 6.6. Stratigraphic correlation diagram for the central region. Refer to Fig. 6.2 for location of sections along K-K'.

depositional environment, whilst the nature of the fossils suggests marine to brackish conditions. This succession is interpreted to represent a deltaic shoreface, with sand probably derived from Proterozoic sandstone units nearby to the west. Cretaceous rocks are not well exposed in this area, so detailed palaeocurrent analysis is difficult, and mapping of the thickness and geometry of the deltaic sandbodies is not possible. Therefore, the planar-bedded and cross-bedded sandstones with a sparse marine body fossil assemblage have been assigned to facies succession 6, which encompasses all deltaic and/or estuarine facies.

Planar-bedded and massive plant-bearing sandstones overlie the deltaic shoreface deposits with a sharp, apparently disconformable contact. These sandstones are identical to sandstones in sections 71 and 89 (Fig. 6.3). The abundance of plant fossils suggests a nonmarine environment, but in most places the sandstones are moderately to intensely bioturbated, suggesting brackish conditions suitable for an abundant infauna. This is supported by the stratigraphic position of these plant-bearing sandstones; with deltaic-marine sandstones below and deeper-water marine siltstone above. The plant-bearing sandstone in sections 68 and 69 has also been assigned to facies succession 6, because it indicates a paralic depositional environment in close proximity to the palaeoshoreline.

The lower deltaic-marine sandstones of facies succession 6 equate to Skwarko's (1966) "unit 5", and the upper plant-bearing sandstones of facies succession 6 to his "unit A". At his fossil sites TT 31 and TT 32 (close to sections 69 and 68 respectively), Skwarko (1962c; 1966) collected 3 species of marine bivalves from unit 5, and 10 separate species of plant fossils from unit A, all of which give an indeterminate age for the strata. Skwarko noted an apparent alternation of marine and nonmarine rocks, but detailed lithostratigraphic analysis during the present study does not support this; rather, a thick deltaic-marine succession is overlain by plant-bearing brackish marine sandstone up to 4 m thick, which is in turn overlain by marine siltstone and sandstone. Disregarding minor differences between Skwarko's palaeontologically-based study and the present study, the overall interpretation is the same. There is agreement that these paralic (deltaic to brackish marine) facies only accumulated in localised areas along the palaeoshoreline, and were not observed (and presumably did not accumulate) east of section 92.

Offshore to the east of section 68, the base of the Cretaceous sequence is exposed (*e.g.* sections 66, 77, and 92). The rocks here consist of one or two coarsening-upward or massive cycles of facies succession 2, and are very similar to the deposits of facies succession 2 in Fig. 6.5. Coarsening-upward cycles of facies succession 2 can be confidently correlated over the whole

of the central region, and are regarded as being of the same age. It is also proposed that they are partly facies equivalents of the massive deltaic-marine sandstones in sections 68 and 69 to the west. This is supported by their related fossil assemblages, and the good correlation of overlying marine facies of succession 4 in all areas.

Fining-upward sandstone, conglomeratic sandstone, and siltstone of facies succession 5 occur stratigraphically above facies of succession 2 on the inner part of the shelf. The contact between the two successions is disconformable and features a conglomeratic lag in places (*e.g.* sections 66, 67, and 77). Deposits of facies succession 5 here can be confidently correlated with those to the north in Fig. 6.5, to the south in Fig. 6.4, and to the east in Fig. 6.7. Facies succession 5 becomes progressively finer-grained and thinner offshore to the east in correlation diagram L-L'. To the west, along I-I', facies succession 5 occurs in sections 93 and 75, and probably occupies the same stratigraphic level as plant-bearing sandstones of facies succession 6 in sections 68 and 69.

Throughout the area encompassed by correlation diagram K-K', the top of the Cretaceous sequence is composed of fining-upward rocks of facies succession 4 (Fig. 6.6). Deposits of facies succession 4 overlie facies succession 5 in the eastern part of K-K', and also occur directly above brackish marine plant-bearing sandstones of succession 6 between sections 69 and 92. Rocks of facies succession 4 along K-K' are correlative with facies succession 4 in the northern and southern parts of correlation diagram I-I', and comprise the bulk of the Cretaceous sequence on the middle shelf in the central region. Facies of succession 4 are moderately to intensely bioturbated, contain rare marine body and plant fossils, and show some sedimentary structures indicative of distal storm deposition. The contact between succession 4 and succession 5 or 6 is sharp and locally disconformable, and is typically marked by a thin, laterally extensive fine-grained sandstone bed (*e.g.* the base of section 76), which apparently thins to the west towards the palaeoshoreline. Another laterally extensive fining-upward or massive sandstone occurs at the top of facies succession 4 (*e.g.* the top 2 m of section 66 and the top 3 m of section 92). Both of these marker intervals are common in measured sections of the central region, and enable accurate correlation over distances of 50 to 150 km.

Near section 66, at sites TT 20 and 21, Skwarko (1962c; 1966) described the fossil content of rocks of facies succession 4, which are equivalent in most places to his "unit 6". Here facies succession 4 (his unit 6) contains at least 7 species of bivalves, a single species of gastropod, several species of cephalopods, unidentified plant fossils, and numerous trace fossils of the *Cruziana* ichnofacies. The same fossil assemblage occurs in part, or in its entirety, in other

exposures of facies succession 4 throughout the central region, and in this manner Skwarko's observations and detailed documentation of fossil assemblages support the lithostratigraphic correlations of this study.

6.3.5 Correlation diagram L - L' (Fig. 6.7)

Correlation diagram L-L' is a continuation of correlation diagram K-K', and extends along a 71.5 km line approximately perpendicular to the regional palaeoshoreline. The Cretaceous sequence in this middle shelf setting is composed of three facies successions, all of which are also exposed on more proximal parts of the shelf, and can be confidently correlated throughout the central region.

The oldest Cretaceous rocks are coarsening-upward cross-bedded, planar-bedded and massive sandstones of facies succession 2 (*e.g.* section 54). These facies are at least moderately bioturbated, contain very rare, poorly preserved marine body fossils, and marine trace fossils. This facies succession can be confidently correlated with the same facies succession in correlation diagrams K-K', J-J', and I-I' on the basis of similar lithology, lateral and vertical grain size trends, stratigraphic relationships with overlying rocks, and less commonly by fossil content. Marine body fossils were not observed in many isolated outcrops of facies succession 2 and other coarse-grained shoreface facies in the central region during this study.

The low abundance and poor preservation of body fossils within these coarse-grained facies requires detailed searching, description, and collection of fossils to prove a marine depositional environment for every outcrop, most of which is beyond the scope of the present study. However, these procedures were carried out by Skwarko at selected sites in the central region, and can be used as an aid and test for correlations made in this study. Skwarko (1962c; 1966) documented 6 species of bivalves, one species of belemnite, and one species of brachiopod from his "unit 2" at site TT 25, which corresponds exactly to facies succession 2 at section 54. This assemblage of marine body fossils is sparse compared with those of other parts of the central region, and those of finer-grained marine facies successions.

Correlation diagram L-L' illustrates the maximum seaward extent of deposits of facies succession 2, with the most easterly outcrop observed at section 54. Rocks of facies succession 2 may occur as far east as section 56, but the lower part of the Cretaceous sequence is covered here. East and south of section 56, younger Cretaceous marine rocks of facies

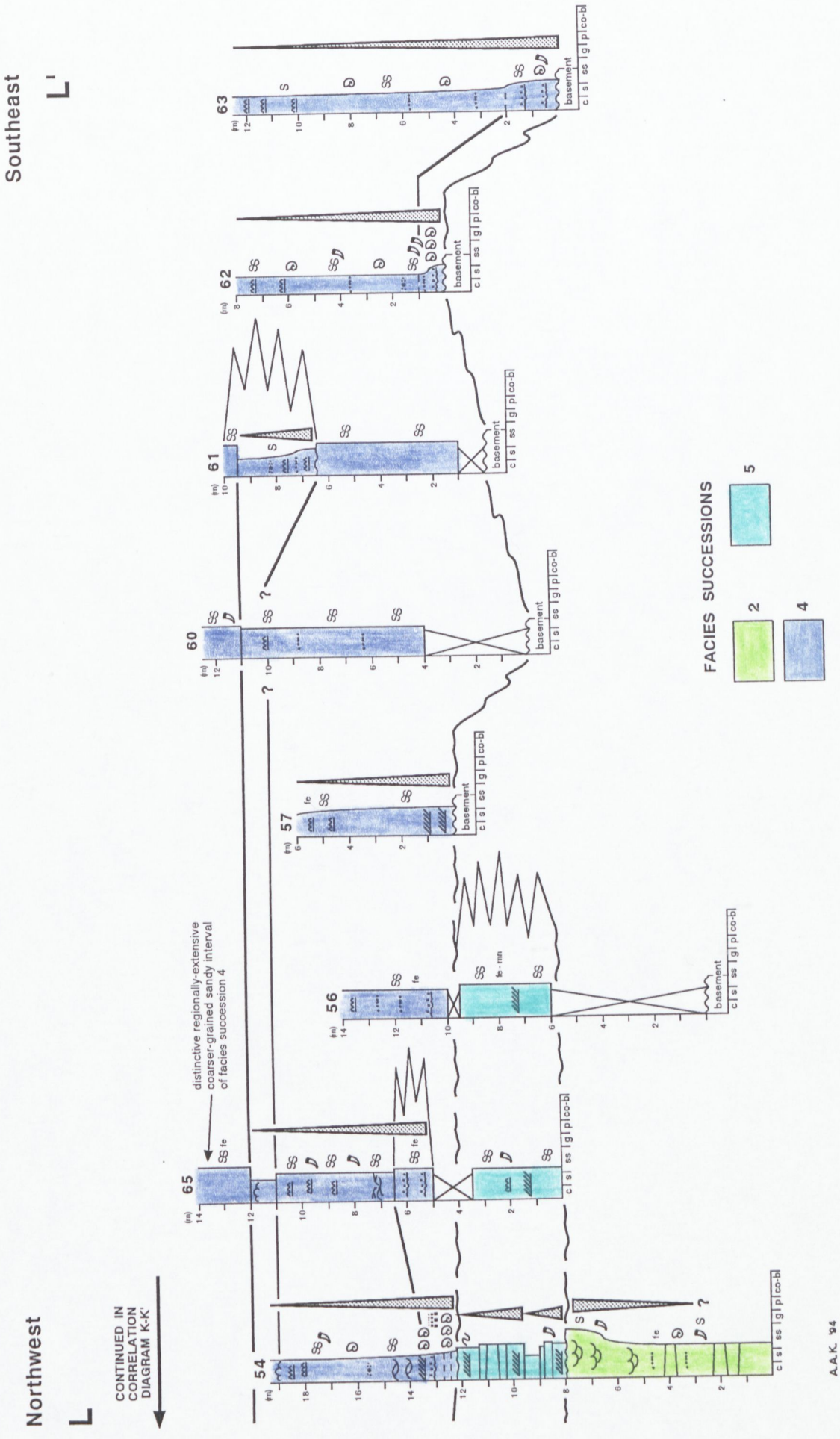

FIGURE 6.7. Stratigraphic correlation diagram for the central region. Refer to Fig. 6.2 for location of sections along L-L'.

succession 4 directly overlie basement, and it is interpreted that shallow-marine sandstones of succession 2 were not deposited this far from the palaeoshoreline.

Fining-upward shoreface to upper offshore rocks of facies succession 5 disconformably overlie facies succession 2 in the western part of L-L'. Rocks of facies succession 5 are finer-grained and thinner than facies succession 5 elsewhere in the central region, and the sedimentary structures indicate a moderate rather than high-energy depositional environment. East and south of section 56, shoreface sediments of facies succession 5 are not preserved, and probably did not accumulate farther offshore from this position on the shelf. Similar to coarse-grained shoreface deposits of facies succession 2, facies of succession 5 on this part of the shelf contain marine trace fossils, are significantly bioturbated, but no marine body fossils were observed. High rates of deposition and reworking during storms are indicated by slumping in these facies, and this type of environment is unlikely to have been a stable environment suitable for an abundant infauna.

Finer-grained marine sandstone and siltstone of facies succession 4 disconformably overlie rocks of facies succession 5 in the western part of correlation diagram L-L'. The base of facies succession 4 contains coquinas, graded beds, HCS, and cross-bedding indicative of an initially high-energy depositional environment affected by episodic storms. Facies of succession 4 fine upward in response to a change to a deeper-water distal depositional setting up-section. Rocks of facies succession 4 are invariably highly bioturbated, and contain numerous trace fossils and marine body fossils. The fine-grained top of the succession contains fine lamination and concretions, and this interval can be correlated across a wide area of the shelf in the central region. In some places (*e.g.* sections 60, 61, and 65), another fining-upward or massive cycle of facies succession 4 occurs at the top of the preserved Cretaceous sequence. This interval is also useful for correlation, and can be traced laterally along parts of K-K', J-J', and I-I'.

Deposits of facies succession 4 are the most extensive of all successions in the central region, and commonly the entire Cretaceous sequence is composed of this succession in offshore parts of the central region. Facies succession 4 corresponds to Skwarko's (1966) "unit 6" in most places, and contains at least 10 different species of marine bivalves and gastropods. Skwarko also recorded a few outcrops of plant-bearing siltstone of indeterminate age in the area covered by L-L', and classified them as a nonmarine facies ("unit B"). Correlation during this study does not support this interpretation, and it is likely that his "unit B" corresponds to parts of facies succession 4 which contain rare plant-fossils. These outcrops with plant fossils are

identical in all other respects to exposures of facies succession 4 elsewhere which contain marine body fossils.

6.4 BIOSTRATIGRAPHIC CONTROL

Most facies in the central region contain some type of fossil, whether marine body fossils, plant fossils, or trace fossils. None of the facies of the central region described in this study yielded any microfossils, and previous studies by Skwarko (1962a,b,c; 1966) also highlight the lack of preserved microfossils. Undoubtedly, microfossils were once present in some of the facies, but any such fossils would have been completely destroyed by the intense chemical and physical weathering which characterises outcrops in this region. The intense weathering has also affected macrofossils in the Cretaceous sequence, and the age and detailed systematics of some fossils are indeterminate beyond the most basic classification due to poor preservation. In this sense biostratigraphic control for Cretaceous rocks of the central region is poor, even though they are generally more fossiliferous than facies of the northern region.

In this study, correlation of facies from numerous different stratigraphic levels indicates that plant fossils and trace fossils of the central region are not useful for accurate biostratigraphic dating. However, characteristic accumulations of trace fossils or plant fossils can sometimes be traced along a particular stratigraphic interval, and may be useful as markers for correlation. These fossils have no specific age connotation, and cannot be used on their own for biostratigraphic correlation. This point is supported by Skwarko (1962c, p.5), who stated that "no accurate dating based exclusively on plants is possible, and individual floras indicate Upper Jurassic (?)-Lower Cretaceous age".

Marine macrofossils are the most important and abundant fossils in rocks of the central region. The situation regarding the biostratigraphic relevance of these marine macrofossils is exactly the same as in the northern region. That is, previous age assignments (Neocomian to Aptian, with rare Albian faunas) and regional interpretations (Skwarko, 1966) must be regarded as being doubtful, although comparison of Skwarko's macrofossil assemblages between individual outcrops is still useful for local correlation. Details of regional lithostratigraphic correlation in this study are presented in chapter 8, where, using correlations with sections and drillholes of known age, the age and extent of Cretaceous facies of the central region is presented in a regional framework.

6.5 SUMMARY OF FACIES SUCCESSIONS IN THE CENTRAL REGION

The oldest Cretaceous rocks observed in *outcrop* in the central region are sandstone and conglomeratic sandstone of facies succession 2, which occur in the basal parts of numerous measured sections on the inner shelf. In places their contact with Proterozoic basement rocks is exposed, but unlike facies in the northern region this unconformable surface is not mantled by a thick conglomerate. The succession typically consists of one or two coarsening-upward cycles, which accumulated in the lower shoreface to offshore zone. Facies succession 2 is limited in outcrop to a north-south trending zone, east of section 87 and west of section 54. This area is interpreted as the zone of accumulation of shoreface to upper offshore sediments on the inner shelf during major stages of Cretaceous marine incursion.

On the western (landward) edge of this shoreface zone, the Cretaceous sequence is composed of thick, massive sandstones of paralic (probably deltaic-marine) settings. This succession is restricted to an area surrounding sections 68, 69, and 70. Other paralic sandbodies may have been deposited elsewhere along the palaeoshoreline adjacent to basement highs, but none are preserved. All the facies here are regarded as belonging to facies succession 6, which includes deposits of various paralic environments. The 10 m thick sandstones which form the basal part of the succession are considered to be facies equivalents to sandstones of facies succession 2. The thin plant-bearing sandstone at the top of facies succession 6 occurs in several areas of the central region, most of which are close to the palaeoshoreline. This sandstone represents a transitional brackish marine environment and has only a localised lateral extent. All exposures of facies succession 6 are considered to be correlative, although only in the area of sections 68 and 69 are the facies relationships clear. Here, the thickness of the plant-bearing facies was observed to thin markedly basinwards, and was not observed east of section 92.

In most parts of the central region, paralic and nonmarine facies are uncommon, and the bulk of the Cretaceous sequence is composed of marine facies. In these areas the oldest rocks of facies succession 2 are typically disconformably overlain by fining-upward sandstone and siltstone of facies succession 5. The contact of these two successions is commonly defined by a conglomeratic lag, indicating significant erosion between accumulation of the successions. Fining-upward deposits of the shoreface have a maximum thickness of 6.5 m, include one or two fining-upward cycles, and are very similar to deposits of facies succession 2 in the northern region. Indeed, in section 52 the upper part of facies succession 5 contains the C 2 marker bed, and this enables direct correlation with the Cretaceous sequence in the northern region. Unfortunately, in most parts of the central region the C 2 marker bed has apparently been

removed by erosion prior to accumulation of overlying rocks of successions 4 and 8. Fining-upward shoreface deposits of facies succession 5 are much thinner and less extensive than deposits of facies succession 2 in the central area, and show a trend of decreasing thickness and grain size to the east (offshore). Shoreface deposits of succession 5 wedge out east of section 56, which is also close to the eastern limit of shoreface deposits of facies succession 2. This boundary between shoreface to upper offshore deposits in the west, and offshore deposits in the east is regarded as the break between the inner and middle parts of the shelf.

In most parts of the shelf, shoreface to upper offshore rocks of succession 5 are overlain by fining-upward, lower shoreface to offshore zone deposits of facies succession 4. The contact between successions 4 and 5 is sharp and locally disconformable, and transgressive erosion seemingly occurred at this surface. Along L-L' on the middle shelf, the entire Cretaceous sequence is composed of one or two fining-upward cycles of facies succession 4, which typically directly overlie Proterozoic basement with an angular unconformity. The maximum observed thickness of cycles of facies succession 4 is 12.5 m, but is likely to be greater since the top of the succession was not observed.

Within facies succession 4, subtle proximality trends are defined by lateral changes in grain size, thickness, abundance of plant fossils and conglomeratic clasts, the nature of vertical grain size trends, and the presence of storm-generated sedimentary structures versus offshore quiet-water structures such as fine lamination and concretionary horizons. In nearshore areas facies succession 4 contains plant fossils and intervals with dispersed pebble to granule sized clasts. Farther offshore in the area of correlation diagram L-L', facies succession 4 is thicker, has a more obvious fining-upward character, and most of the succession contains sedimentary structures indicative of deeper water and low to moderate energy depositional environments.

In the central part of the central region on the inner shelf, facies succession 5 is disconformably overlain by thick deposits of facies succession 8 instead of offshore marine facies of succession 4. The outcrop zone of facies succession 8 siltstones and sandstones occurs between the palaeoshoreline and the western, sheltered side of a large barrier island formed by the topographically-high, Yiyintyi Range basement terrain. To the north and south of this zone on the inner shelf, facies of succession 8 change laterally into equivalent unrestricted marine facies of succession 4. This significant facies change is most noticeable in correlation diagrams I-I' and J-J', where facies of successions 4 and 8 have an identical stratigraphic position, but are restricted to different palaeogeographical zones on the shelf.

Rocks of succession 8 exhibit important differences from those of succession 4; they are finer-grained, have a much greater abundance and diversity of fossils, show delicate preservation of fine lamination and fully-articulated fossils, have irregular vertical grain size trends, and contain sedimentary structures indicating a lower-energy depositional environment. Deposition of facies succession 8 occurred in a large bay, which was sheltered in the east and was apparently open to marine circulation to the north and south. The presence of rare storm-generated features within succession 8 indicates occasional high-energy deposition within the bay environment due to episodic storms, and supports the interpreted marine connection of the bay with the rest of the shelf.

Fluvial facies successions are rare in the central region, but occur in places on, or adjacent to basement highs. These successions are typically less than 5 m thick, and are exposed as irregular valley-fill deposits on basement terrains. Near the edges of basement terrains, fluvial deposits are incised into underlying marine facies successions, but direct contact between marine and nonmarine successions is rare. Where the contacts are exposed, fluvial facies invariably have an erosional relationship with underlying marine facies and basal conglomeratic lags are common. In places the fluvial successions have a linear, channel-like geometry. In the central region all of these deposits have been assigned to facies succession 7, and are similar in all respects to fluvial channel deposits in the northern region. The age of these fluvial deposits is problematic because of a lack of marker beds and scarcity of fossils, and the fact that the number of nonmarine exposures is low and they are spread widely across the western part of the central region. However, correlation is sometimes possible on a local scale within the one area (*e.g.* the Yiyintyi Range area in the northern part of J-J').

The last facies relationships of importance involve problematic facies at the northwest edge of the central region. In the area of correlation diagram H-H', highly weathered and isolated Cretaceous strata are exposed. The nature of these successions makes correlation difficult, but facies at the base of sections 71 and 89 are likely to be part of succession 6. In this area rocks of probable marine origin occur stratigraphically above plant-bearing sandstone of succession 6, and are most likely part of facies succession 4. It is probable that most fine-grained rocks in this area belong to facies succession 4, and overlie basement or brackish marine to nonmarine deposits of succession 6. The fact that facies succession 4 is the most laterally extensive succession in the entire region, and accumulated during a major transgression across the shelf, supports the interpretation of facies of succession 4 occurring in the area of correlation diagram H-H'.

6.6 CHAPTER SUMMARY

Cretaceous rocks of the central region are dominantly marine in origin, and represent a more distal shallow-marine setting than rocks of the northern region. In the central region nonmarine and paralic facies successions are rare, and are restricted to areas surrounding basement terrains. Marine successions in the western part of the central region contain sedimentary structures indicative of high-energy, shoreface to upper offshore depositional environments of the shoreline and inner shelf. In the eastern part of the central region, marine successions accumulated in deeper water under less energetic conditions, although in most areas the seafloor was still within the influence of storm waves.

Generally, rocks in the eastern part of the central region accumulated in an offshore marine setting characteristic of the middle shelf, and rocks in the western part of the central region accumulated on the inner shelf in the shoreface to upper offshore zone. Isolated deltaic deposits and localised facies changes indicate an irregular palaeoshoreline with deltaic protuberances, basement terrains as peninsulas, and basement highs as offshore barriers or islands.

The stacking patterns of coarsening- and fining-upward marine facies successions is internally consistent within the central region, and is correlative with the northern region. These successions or 'cycles' are again interpreted to reflect important changes in relative sea level which occurred across the shelf, and resulted in migration of the palaeoshoreline. Compared with the northern region, contacts between successions in the central region tend to have less obvious signs of major erosion and facies changes are more subtle. Lateral proximality trends are readily apparent in the central region after careful lithostratigraphic correlation, and document large shifts in depositional environments on the shelf over time.

~~~~~~
~~~~~~

7. DEPOSITIONAL ENVIRONMENTS AND LITHOSTRATIGRAPHIC CORRELATION IN THE SOUTHERN REGION: THE SHORELINE TO OUTER SHELF

7.1 INTRODUCTION

This chapter documents detailed lithostratigraphic correlation of isolated outcrops in the southern region (Fig. 7.1). Cretaceous rocks exposed in the southern region reflect dominantly marine depositional environments of a shoreline to outer shelf setting, but fluvial successions occur at the base of the Cretaceous sequence and above or adjacent to topographically-high basement terrains. Shoreface deposits also occur on this region of the shelf in areas close to basement terrains and near the base of the Cretaceous sequence. There preserved shoreface deposits record the passage of initial marine transgression across the shelf. The thicknesses, types, and relationships of facies successions in this region are broadly similar to those on more proximal parts of the shelf in the northern and central regions.

The geological and geographical setting of the southern region is similar to the northern and central regions; outcrops occur as isolated erosional remnants commonly separated by large distances, and there are limited subsurface data for Cretaceous rocks of the southern region. In contrast to the other regions, some outcrops in the southern region yield microfossils which are useful for biostratigraphic zonation, and provide limited age control for some Cretaceous successions. However, successions in the southern region are thinner and more numerous than in the northern and central regions, and correlation across the region is more complex and problematic. Correlation of strata in the southern region is based primarily on lithostratigraphic criteria and again involves careful documentation of facies, recognition of facies successions and the bounding surfaces between successions, and detailed comparison of numerous measured sections and other field data. Local correlations documented in chapter 7 are utilised in chapter 8 in erecting a lithostratigraphic framework for the entire shelf.

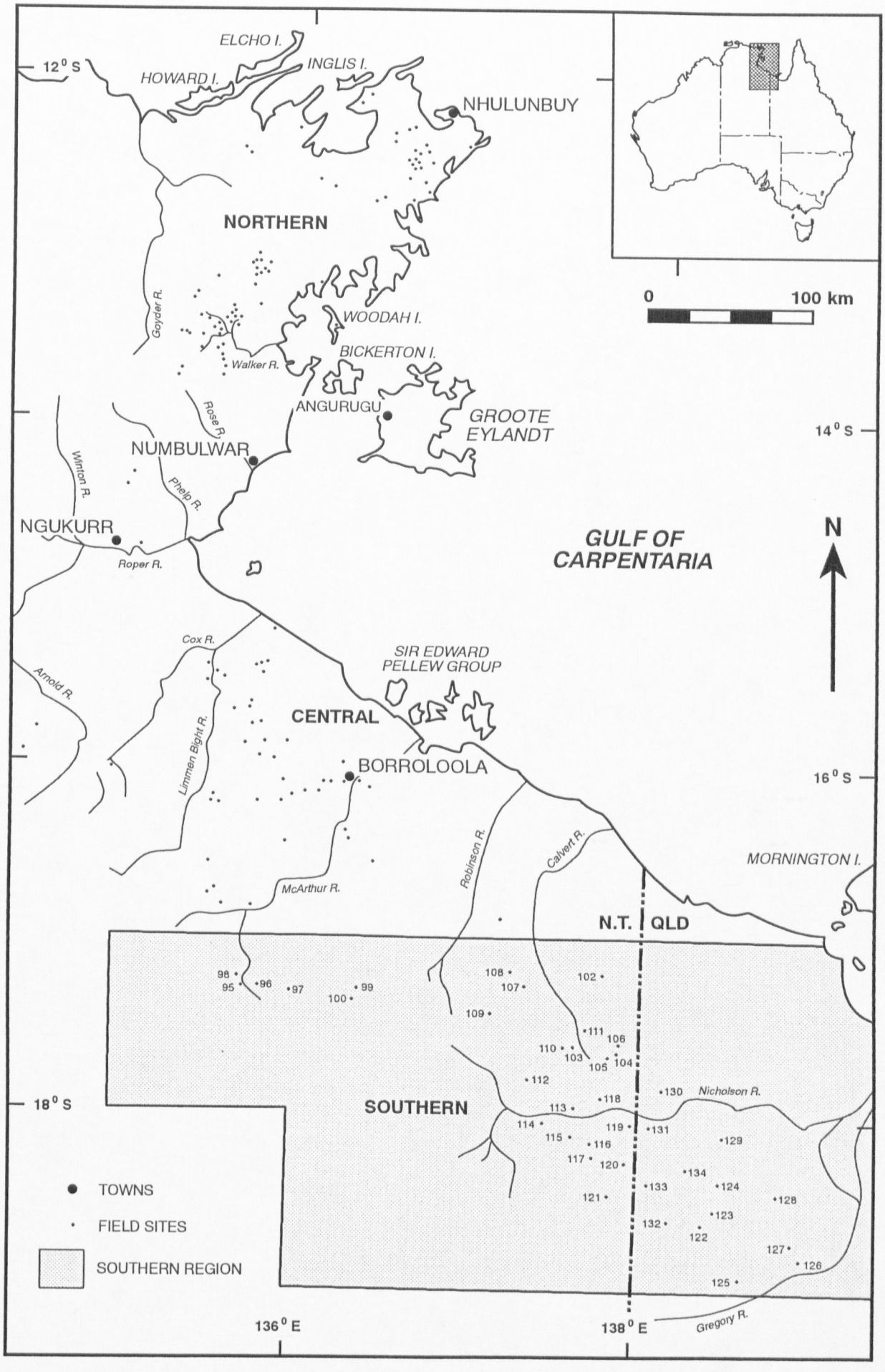

FIGURE 7.1. Location map for the southern region showing field sites referred to in chapter 7.

7.2 DATABASE FOR DETAILED STRATIGRAPHIC CORRELATION DIAGRAMS

This chapter is based on the measurement of 40 outcrop sections and observations from numerous other field stations ranging from the Wallhallow area in the northwest (near sections 96.97, and 98), to the Kamarga Dome area in the southeast (Fig. 7.2). A series of small-scale intersecting correlation diagrams was constructed to aid in preliminary correlation of Cretaceous rocks of the southern region. These preliminary correlation diagrams were tested and refined, and combined with biostratigraphic, petrological, and geochemical data to construct 5 local to semi-regional correlation diagrams (Figs. 7.3, 7.4, 7.5, 7.6, and 7.7) for the southern region. For economy of space and clarity of correlation, these have been "condensed" from longer 'cross-sections'. The positions of the correlation diagrams are located on a base map (Fig. 7.2), and all measured sections are drawn to the same scale.

Unlike the northern region, but similar to the central region, a reliable regional marker horizon is lacking in most Cretaceous outcrops in the southern region. Furthermore, similar facies successions tend to be repeated at different stratigraphic levels across the region, which makes correlation of incomplete measured sections difficult in places. However, the relative stratigraphic position of most facies successions is apparent after laterally tracing more subtle marker beds and individual grain size cycles, some of which are less than 0.5 m thick and can be correlated over more than 50 km between successive outcrops.

7.3 DETAILED STRATIGRAPHIC CORRELATION DIAGRAMS

7.3.1 Correlation diagram M - M' to N - N' (Figs. 7.3 and 7.4)

These two correlation diagrams join together to form a 410 km long line, from section 98 at the western end of a large east-west trending arm of the Cretaceous seaway on the Wallhallow and Calvert Hills map sheet areas, to section 134 on the outer southeastern part of the shelf on the Lawn Hill map sheet (Fig. 7.2).

In this area the base of the Cretaceous sequence and the contact with basement is rarely observed. Where the basal contact is exposed, the oldest Cretaceous deposits typically consist of conglomerate and conglomeratic sandstone. The basal facies are invariably fining-upward and have a thickness of up to 16 m, although the same succession has a thickness of at least 38 m farther to the north. The facies are massive and poorly sorted, contain only rare plant fossils,

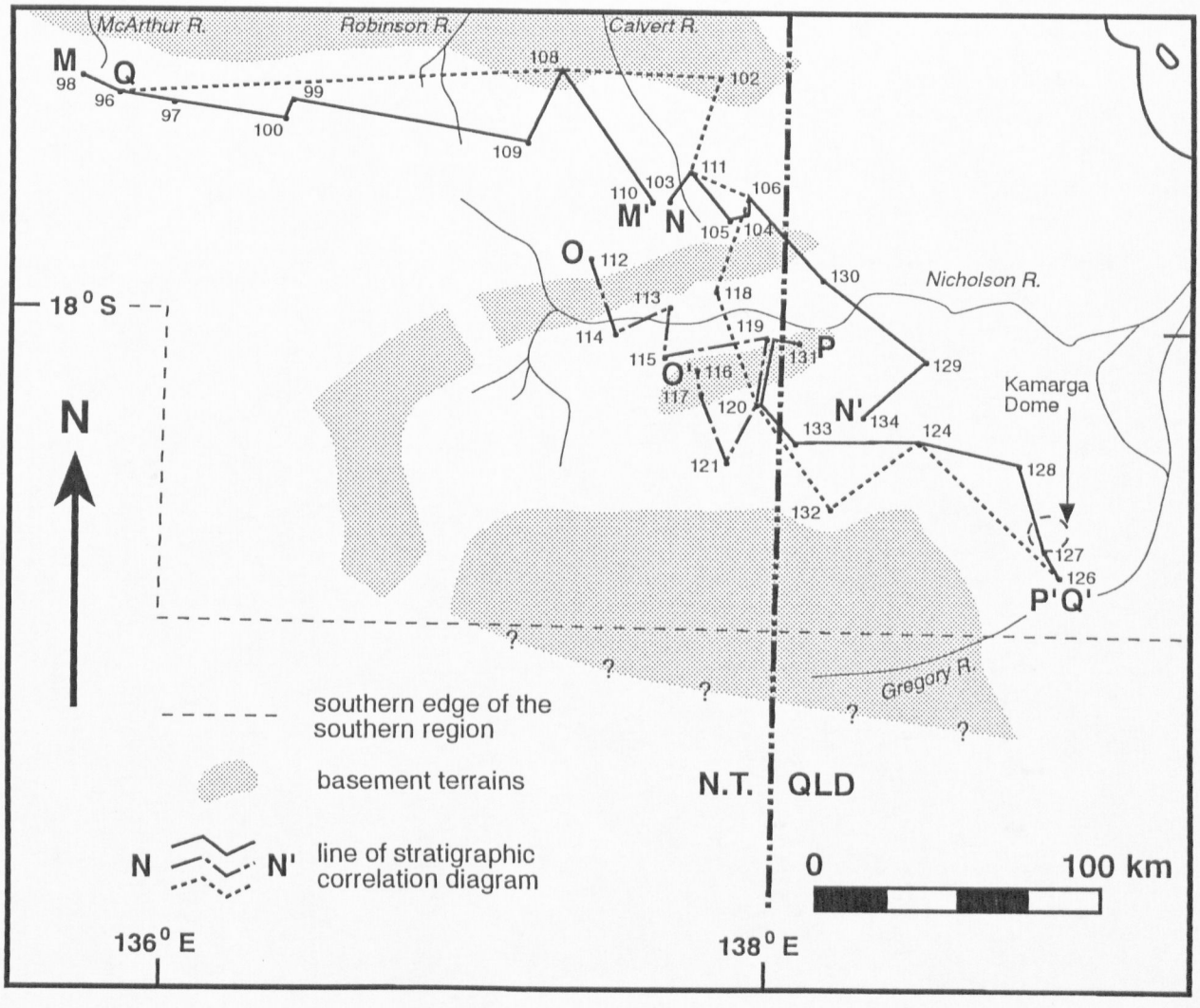

FIGURE 7.2. Location map for the southern region showing field sites and location of correlation diagrams referred to in chapter 7.

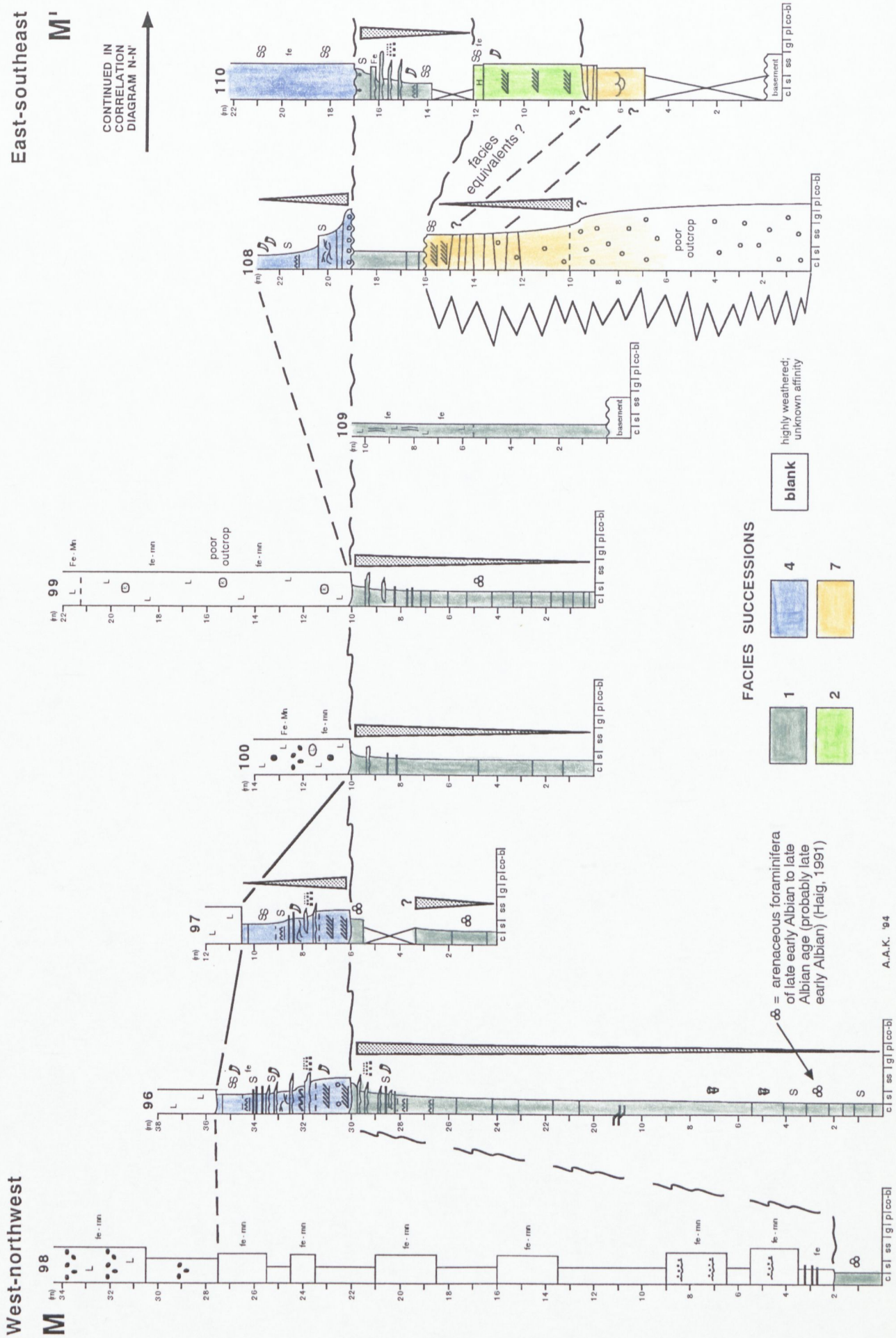

FIGURE 7.3. Stratigraphic correlation diagram for the northern part of the southern region. Refer to Fig. 7.2 for location of sections along M-M'.

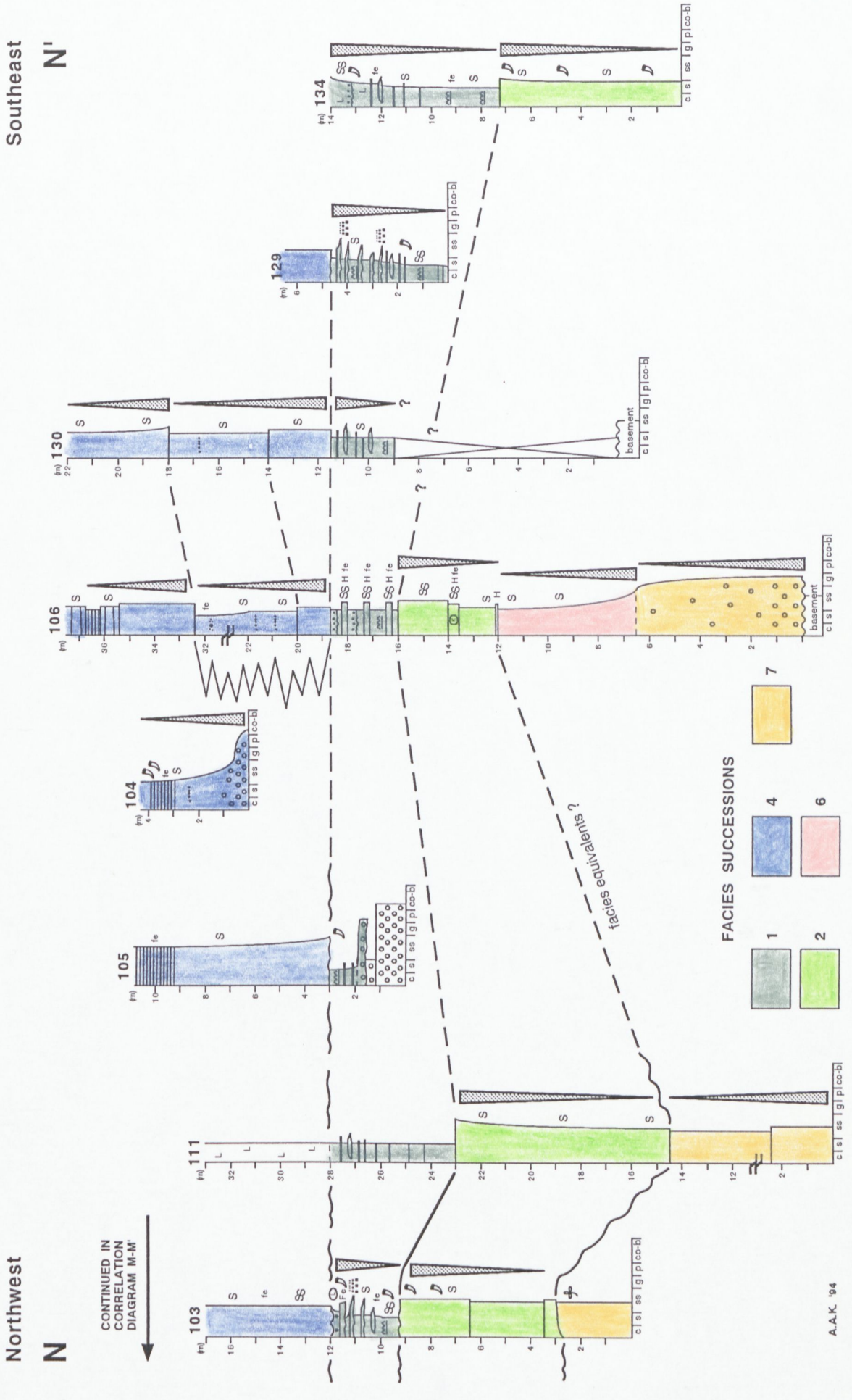

FIGURE 7.4. Stratigraphic correlation diagram for the central part of the southern region. Refer to Fig. 7.2 for location of sections along N-N'.

are not bioturbated, and are interpreted as fluvial deposits of facies succession 7. These fluvial deposits overlie basement with an angular unconformity and a thick conglomeratic lag, and their greatest thickness occurs adjacent to basement terrain and decreases markedly away from these topographically high-standing terrains, many of which formed islands on the shelf during the Cretaceous.

The age of the thick fluvial succession is problematic because the rocks contain only rare indeterminate plant fossils, and the base of the sequence may be of Jurassic age in basinal areas to the southeast. At section 103 (Skwarko's site TT 59) Skwarko (1966) recorded at least three different species of plant fossils in his "unit A" which corresponds to facies succession 7. The plant fossils have poor biostratigraphic resolution, and Skwarko proposed an age range of Neocomian to Aptian for unit A.

The upper contact of the thick fining-upward fluvial deposits is either disconformable with coarsening-upward shoreface marine facies of succession 2 (Fig. 7.3, section 110; Fig. 7.4, sections 103 and 111), or more rarely transitional with fining-upward, bioturbated brackish marine to paralic facies of succession 6 (Fig. 7.4, section 106). In section 106 the transition from fluvial sandstone to brackish marine sandstone and siltstone to shoreface marine sandstone is apparently conformable. This situation is rare; in most places post-succession 7 erosion has apparently removed all traces of brackish / paralic facies of succession 6.

Along the entire length of M-M' and N-N' interbedded clayey siltstone and coarse-grained sandstone overlie coarsening-upward shoreface deposits of succession 2. These bioturbated interbedded facies form coarsening-upward or massive facies succession 1, and represent an offshore to lower shoreface depositional environment. The thickness of this succession varies greatly, from at least 30 m in the west to only 3 m in the central part of this correlation diagram in nearshore zones where erosion between depositional episodes was common. In general there is a decrease in thickness towards the southeast (offshore), approximately perpendicular to the regional palaeoshoreline. Correlation of these interbedded deposits across such a large area is not always obvious, but the distinctive interbedded nature of this succession is recognisable in most exposures.

Offshore to the east and southeast, the coarsening-upward nature of this succession is typically subtle, and the succession tends to be thinner and contains only a few coarse-grained cemented interbeds which are interpreted as hardgrounds in this more distal setting (*e.g.* Fig. 7.4, section 106, 16 to 18.75 m level). In the western portion of the correlation diagram, the base of facies

succession 1 is relatively unweathered and yields arenaceous foraminifera of late early Albian to late Albian (probably late early Albian) age (Haig, 1991). Microfossils allow accurate correlation on biostratigraphic and lithostratigraphic grounds, but farther to the southeast deposits of facies succession 1 are thinner, more highly weathered, and do not yield any microfossils; their correlation with western outcrops is based on lithostratigraphic criteria.

The youngest Cretaceous facies in the correlation diagram consist of fining-upward and massive clayey sandstone, siltstone, and minor claystone of facies succession 4. These rocks are moderately to intensely bioturbated, and contain numerous marine trace fossils and rarer marine body fossils. The contact with underlying facies of succession 1 is disconformable in proximal areas near basement terrain, and commonly involved minor erosion and development of conglomeratic lags in these nearshore settings (*e.g.* Fig. 7.3, section 108). Away from basement "islands" deposition of facies succession 4 must have occurred only shortly after deposition and before lithification of underlying facies of succession 1, as indicated by a ball and pillow style contact (*e.g.* Fig. 7.3, section 110; Fig. 7.4, section 103). Balls and pillows composed of succession 4 sandstone have sunk up to 30 cm into underlying clayey siltstone and claystone of succession 1, and many of these structures are still attached to overlying beds by thin 'necks' (see Plates 11c and 13h).

Thus the contact between marine deposits of successions 1 and 4 is slightly diachronous across the region. In places deposition was essentially continuous and did not involve lithification or apparent subaerial exposure between depositional episodes, whereas in most places the older deposits of succession 1 were apparently partially lithified before erosion and incision (associated with the formation of the Arnhem Land Sequence Boundary). The contact between successions 1 and 4 is the most widely exposed and easily recognisable surface in the southern region, and in spite of the slightly variable nature of this contact it is used as a datum for correlation diagrams in the southern region.

Facies of succession 4 at the top of the Cretaceous sequence have a maximum thickness of 18.75 m, and consist of one or two major fining-upward cycles. In most places the thickness of individual fining-upward cycles is approximately 5 m, although in offshore areas grain size trends are more subtle and cycles tend to be thicker. Rocks of facies succession 4 occur widely across the southern region, and individual grain size cycles and beds can be confidently correlated over distances of hundreds of kilometres using lithostratigraphic characteristics. These deposits have close similarities with facies succession 4 in the central region.

Exposures of succession 4 in the southern region, unfortunately, do not contain any marine fossils which are useful for biostratigraphic zonation, and indeed body fossils are rare in most places. Only one of Skwarko's (1966) fossils sites is located near an exposure of succession 4 along M-M' to N-N'; site TT 60 corresponds to section 105 in this thesis (Fig. 7.4). Here, Skwarko (1966) recorded three species of bivalves, two belemnites, bryozoan fragments, and some plant remains. Skwarko assigned these facies and fossils to his marine "unit 7", which is supposedly Albian in age. No marine body fossils were discovered at section 105 in this study, but the Albian age proposed by Skwarko is consistent with the age of the basal facies based on lithostratigraphic correlation in this thesis. As thick deposits of facies succession 4 appear to lie on a disconformable surface that truncates succession 1 in places, rocks of succession 4 must be younger than late early Albian to late Albian in age, and through regional correlation an early Cenomanian age is proposed (Sect. 8.6.2)

In the far western portion of the correlation diagram at section 98 (Fig. 7.3), anomalous stacked facies of thickly interbedded fine- to medium-grained sandstone and clayey siltstone overlie fossiliferous siltstone of facies succession 1. The nature and depositional environments for the thickly interbedded facies are problematic due to the high degree of weathering, their lack of fossils, and their apparent dissimilarity to surrounding Cretaceous facies exposed at the same stratigraphic level. The basal 7 m of the thickly interbedded rocks contain irregularly graded sandstone beds interbedded with clayey, ferruginous siltstone. Lithologically these rocks resemble the lower part of succession 4, occupy the same stratigraphic position, *i.e.* overlying facies succession 1, and have been tentatively correlated with fining-upward sandstone and siltstone of facies succession 4 exposed 12.5 km to the east in section 96 (Fig. 7.3). Although the thickly interbedded rocks at section 98 do not show an obvious fining-upward grain size trend, the amount of silt and clay *vs.* sand does increase up section.

The thickly interbedded rocks were possibly deposited in a similar marine setting to facies succession 4 to the east, however it appears that the sediment supply was locally much greater in the vicinity of section 98. The large volume of sediment was probably derived from the large exposed Cambrian to Precambrian basement terrain just to the northeast of section 98, although there is a lack of palaeocurrent data and thickness trends to support this interpretation of provenance. The inferred high sediment supply for this area is highly unusual compared to the rest of the shelf for most depositional episodes.

Laterites are well developed in the western part of the correlation diagram on the Wallhallow map sheet area. These laterites are presumably of Tertiary age, and commonly cap the

Cretaceous sequence. In places the upper part of facies succession 4 has been intensely weathered and replaced by massive laterite or lateritic soil profiles.

7.3.2 Correlation diagram O - O' (Fig. 7.5)

Correlation diagram O-O' illustrates facies successions surrounding several basement terrains which are interpreted to have formed islands on the middle to outer shelf during the Cretaceous. The exact boundaries of the basement islands are not known in all areas, but can be interpreted from the position of topographically-high basement rocks and their relationships with onlapping Cretaceous facies. The isolated nature of some basement terrains as islands is also supported by the lateral continuity of Cretaceous facies on all sides of the basement terrains, inferring a similar depositional setting in all areas surrounding the islands.

Correlation diagram O-O' extends 184 km along an irregular line, from the northwest to the southeast, and illustrates stratigraphic relationships between dominantly marine successions of the offshore to lower shoreface zones (Fig. 7.5). Some facies successions in the southeastern part of the correlation diagram are fluvial in origin and were deposited on or adjacent to the basement islands.

The oldest Cretaceous deposits in the region are fining-upward fluvial facies of succession 7 (corresponding to Skwarko's "unit A"), which are identical to similar fluvial successions in Figs. 7.3 and 7.4 in terms of lithology, fossil content, and stratigraphic position. In section 113, close to one of the isolated basement terrains, fining-upward fluvial rocks of succession 7 are disconformably overlain by conglomerate (Fig. 7.5). The conglomerate represents a shoreface deposit (see discussion of lowstand shoreline deposits in Sects. 9.5.3 and 9.5.4), and can be traced laterally towards the southeast until it becomes unrecognisable amongst thin, coarse-grained interbeds east of section 120.

Away from basement highs, the oldest observed Cretaceous rocks are massive sandstone and conglomeratic sandstone (*e.g.* Fig. 7.5, base of sections 119 and 120). These rocks do not contain any fossils or sedimentary structures diagnostic of a particular depositional environment, but appear similar to coarsening-upward shoreface deposits of facies succession 2 to the north and south of correlation diagram O-O', and have the same stratigraphic position relative to overlying rocks. These shoreface sandstones are sharply overlain by up to 3 m of fining-upward, thinly interbedded siltstone or claystone and poorly sorted sandstone. The interbedded rocks contain thin graded beds, are highly bioturbated, and form at least two thin

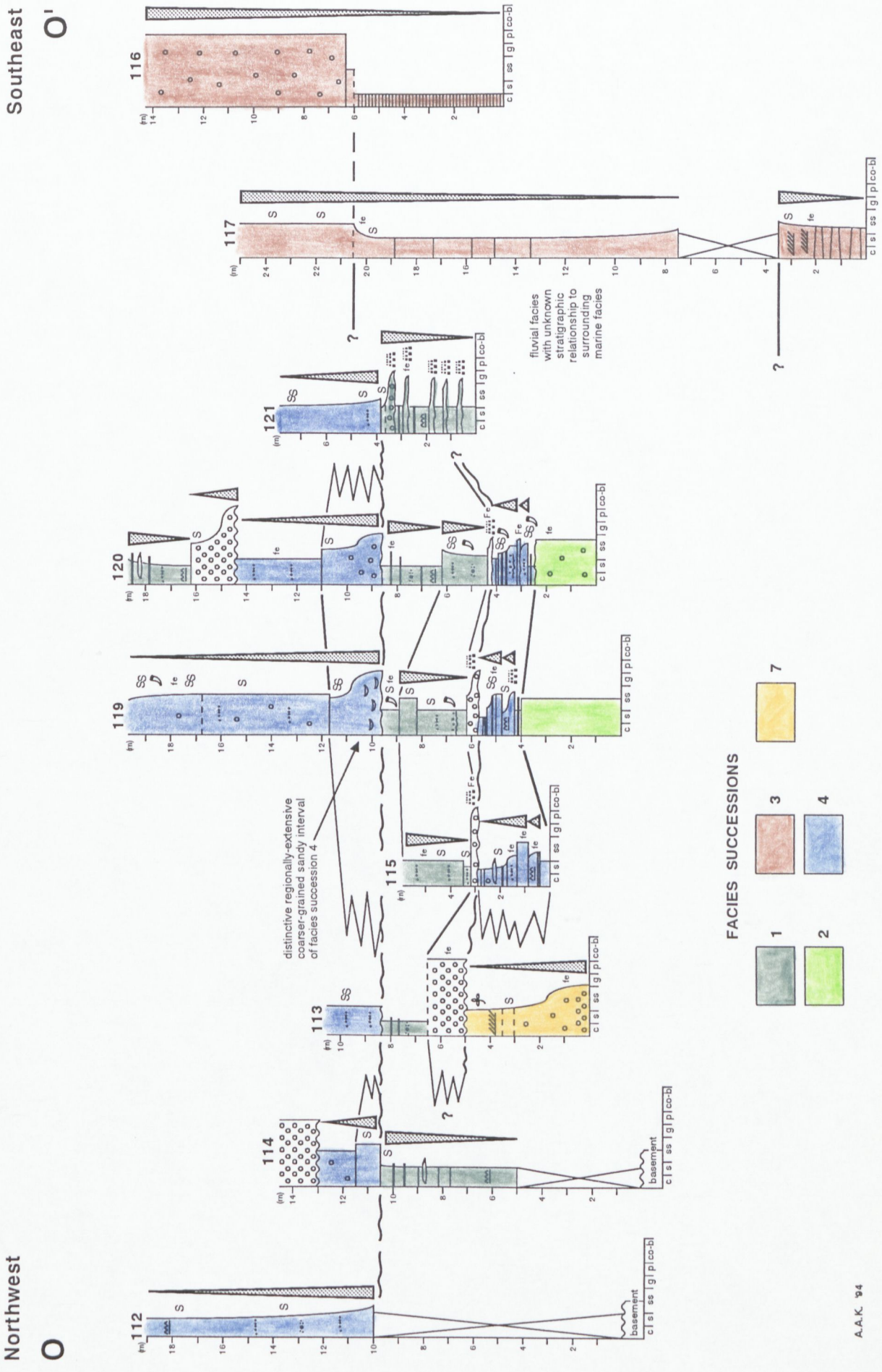

FIGURE 7.5. Stratigraphic correlation diagram for the central part of the southern region. Refer to Fig. 7.2 for location of sections along O-O'.

fining-upward cycles. Each of these cycles is interpreted as a separate facies succession, even though they are much thinner than is normal for succession 4. The delicate lamination, thinly interbedded nature, and small thickness of each succession is interpreted to reflect generally quiet, offshore deposition with water depth increasing up-section under the influence of episodic storms. Although individual beds within these cycles are very thin (< 0.25 m), subtle variations in texture, fabric, colour, and the abundance and grain size of clasts and matrix within graded storm beds enables correlation of discrete cycles over more than 40 km. The erosional feather edge of stacked, fining-upward deposits of succession 4 at this stratigraphic level is inferred to occur just to the northwest of section 115 (Fig. 7.5).

Rocks of facies succession 4 at this stratigraphic level are disconformably overlain by a conglomeratic lag, which rests on an erosion surface that can be traced over much of the southeastern part of the southern region (refer to Carpentaria SB in Sect. 9.4.3). This conglomerate thickens northward into a shoreface deposit (*e.g.* section 113), and diminishes to the southeast where it terminates south of section 120. Marine rocks of facies succession 2 underlying the shoreface conglomerate in the area of sections 115, 119, and 120 can be considered as facies equivalents of the fluvial succession in section 113.

In all areas of correlation diagram O-O' except the isolated basement terrains, the shoreface conglomerate is sharply overlain by coarsening-upward, thinly interbedded and massive units of facies succession 1. In this area rocks of facies succession 1 form one or two recognisable coarsening-upward cycles with a maximum combined thickness of 5.5 m, and are correlative with facies succession 1 in Figs. 7.3 and 7.4; where rocks of facies succession 1 form two stacked cycles, the upper cycle has the strongest similarity with rocks to the northwest in the previous two correlation diagrams.

Similar to Figs. 7.3 and 7.4, the youngest Cretaceous rocks in most areas encompassed by correlation diagram O-O' are fining-upward facies of succession 4 which exhibit a sharp, disconformable basal contact with rocks of facies succession 1. It should be noted that these deposits of facies succession 4 are separate and younger than similar deposits of the same succession at a lower stratigraphic level (*e.g.* the 2.5 to 4 m level in section 120). This relationship highlights the fact that particular depositional conditions were repeated on the shelf over time.

Facies succession 4 (at the higher stratigraphic level) has a maximum thickness of 10 m (top not exposed), and exhibits variations of internal grain size and sedimentary structures dependant on

proximity to isolated basement terrains. Close to basement, rocks of succession 4 are coarser-grained and contain dispersed clasts, exhibit a significant fining-upward trend, and have a conglomeratic or rip-up lag at their base (*e.g.* Fig. 7.5, sections 119 and 120). Away from basement, rocks of succession 4 are finer grained, exhibit a more subtle fining-upward trend, and their base displays more subtle evidence of erosion (*e.g.* section 121). At the top of section 120 there is another cycle of conglomerate overlain by interbedded rocks (facies succession 1?). Comparison of sections 119 and 120 indicates that this conglomerate is incised into underlying rocks of succession 4, and at least 4m of succession 4 is missing. This fining-upward conglomerate is also possibly correlative with the conglomerate which is incised into rocks of succession 4 in section 114. In this case, there is some evidence for late-stage erosion and accumulation of conglomerate, followed by marine transgression and accumulation of interbedded facies (possibly belonging to facies succession 1).

In the southeast along O-O', thick fluvial deposits of succession 3 are exposed and marine successions are not preserved. The fluvial successions consist of laminated claystone and clayey siltstone up to 13 m thick, which grades up into poorly sorted sandstone and conglomeratic sandstone. None of these facies contain fossils, only the upper parts are bioturbated, and they are considered to represent fluvial channel deposits (coarse-grained facies) overlying lacustrine or overbank deposits (finer-grained facies). Fluvial successions occur above or adjacent to basement terrains, and are probably equivalent in part to surrounding marine successions. Sandstones at the base of section 117 are similar to other fluvial sandstones at the base of the Cretaceous sequence (*e.g.* section 113), however, the lack of common marker beds or fossils makes accurate correlation between marine and nonmarine successions unreliable in this area.

7.3.3 Correlation diagram P - P' (Fig. 7.6)

Correlation diagram P-P' is partly a continuation of correlation diagram O-O', and extends from one of the basement terrains along the South Nicholson River in the northwest, to the outer shelf near the Kamarga Dome in the southeast. The correlation diagram extends for 175 km, and illustrates stratigraphic relationships between facies succession which are similar or identical to those in Fig. 7.5.

In the northern part of the correlation diagram, thick fluvial deposits of succession 3 surround basement highs (Fig. 7.6). These deposits are very similar to those in correlation diagram O-O', and consist of overbank or lacustrine fine-grained facies which grade upward into channel

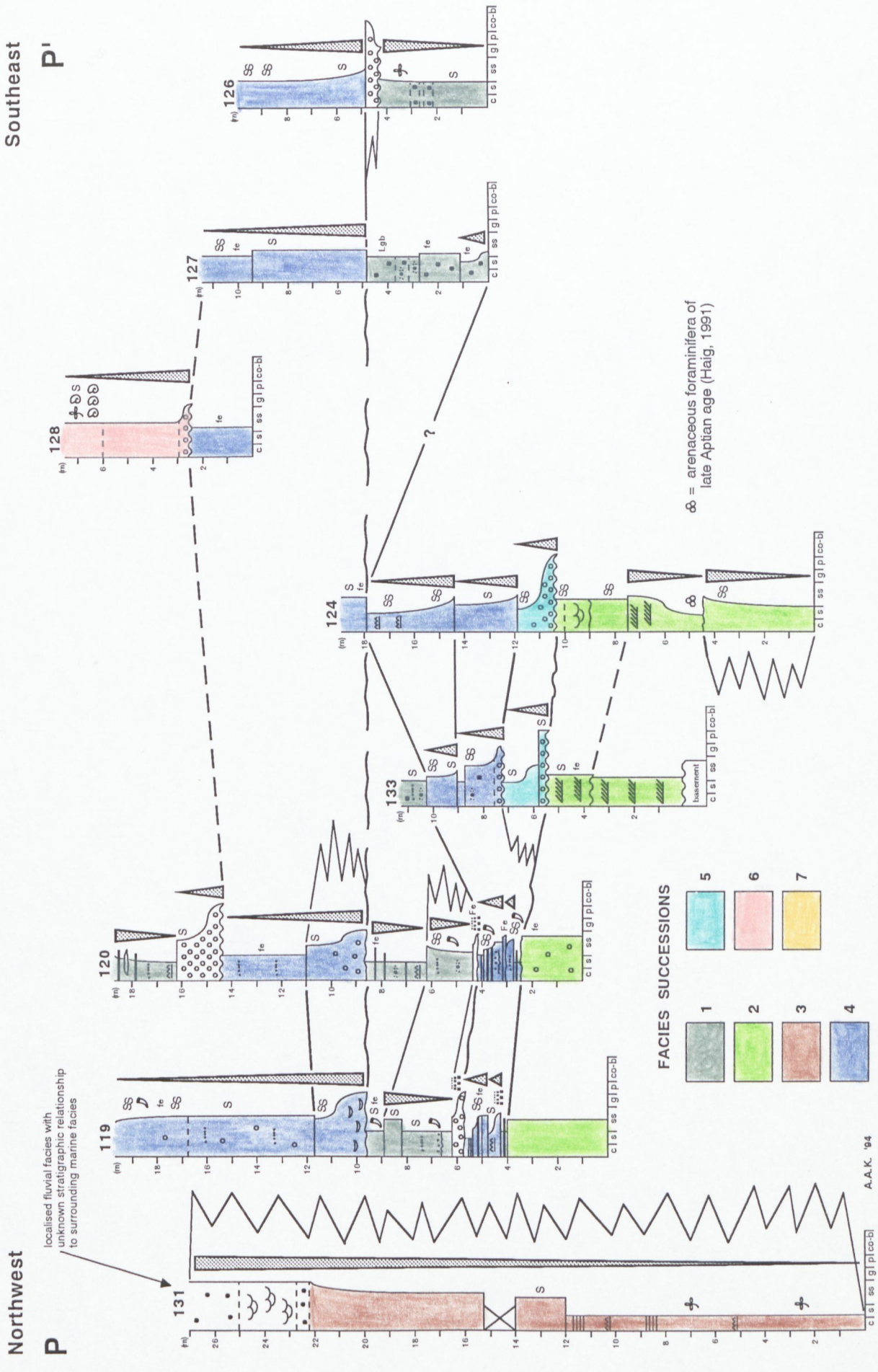

FIGURE 7.6. Stratigraphic correlation diagram for the southern part of the southern region. Refer to Fig. 7.2 for location of sections along P-P'.

sandstone and conglomeratic sandstone. The basal facies contain rare plant fossils composed of logs up to 30 cm long, which are similar to plant fossils of Late Jurassic to Early Cretaceous age in fluvial successions to the north (*cf.* Skwarko, 1962c, p. 5). The upper half of the fluvial succession consists of coarsening-upward sandstone, becoming conglomeratic towards the top. Facies in the upper part of the succession bear some similarity to brackish marine sandstones at other localities, and it is possible that the upper part of the succession in section 131 and surrounding areas represents a transitional nonmarine-paralic environment.

In the area of sections 126, 127, and 128 correlation between sections is inferred on the basis of a few recognisable facies, such as the basal boulder-bearing siltstone and claystone. The correlation of these rocks with more complete sections to the northwest must be regarded as tentative due to a complete lack of biostratigraphic control coupled with the incomplete nature of the measured sections, but the correlation of the sections illustrated along P-P' is duplicated throughout the southern region in areas with better control, and appears to be justified.

The oldest observed Mesozoic rocks in the area of correlation diagram P-P' occur in sections 124 and 133, where they may exhibit an angular unconformity with Proterozoic basement (see Plate 10b). This unconformity is probably the Walker River sequence boundary, but it is difficult to be sure because the unconformity is rarely exposed in the distal southern region. At the base of section 133 there are unfossiliferous cross-stratified shoreface sandstones of facies succession 2. These rocks are considered correlative with stacked fossiliferous crossbedded shoreface sandstones at the base of section 124 to the south, and are similar to numerous other exposures of succession 2 near the base of the Cretaceous sequence throughout the southern region.

Farther offshore in the vicinity of section 124, older stacked coarsening-upward successions are exposed, and these are also interpreted as shoreface deposits. In section 124 shoreface deposits form two coarsening-upward cycles and have a combined thickness of 10.5 m. Most of the facies here are intensely bioturbated, are commonly cross-stratified, and the base of the upper cycle contains arenaceous foraminifera proving a marine depositional setting for these facies. The microfossils give a late Aptian age for the strata (Haig, 1991), and confirm the evidence from local correlation which suggests that these rocks are older than surrounding successions, most of which are younger than late early Albian. Stacked coarsening-upward shoreface successions are restricted to more basinal parts of the southern region. North and west of section 124 the stack of shoreface successions is probably thinner, although their maximum thickness is unknown here because the contact with basement was not observed.

On the outer part of the shelf a thin fining-upward cycle of conglomerate, sandstone and siltstone disconformably overlies coarsening-upward shoreface deposits of succession 2 (*e.g.* Fig. 7.6, section 124, 10.5 m level and section 133, 5.5 m level). The intensely bioturbated facies here do not contain any fossils, but are correlated with similar facies of succession 5 in the central region (Figs. 6.6 and 6.7). The conglomeratic lag at the base of facies succession 5 in sections 124 and 133 attests to significant erosion at this level, erosion which involved an unknown amount of incision into underlying shoreface deposits. This surface of erosion (refer to China Wall SB in Sect. 9.4.2) can be correlated across 100 km or more, and eventually merges with other erosional surfaces to the northwest.

Overlying the fining-upward shoreface deposits of succession 5 are a series of stacked fining-upward rocks of facies succession 4. The stacked fining-upward cycles of succession 4 can be confidently correlated across a large part of the shelf in the southern region, although the thickness and style of individual successions changes across the shelf. In sections 119 and 120, close to basement terrain, deposits of succession 4 are thin, markedly fining-upward, and contain numerous coarser graded beds. The thinness of the successions is interpreted to be due to their relatively shallow-water depositional setting adjacent to basement islands, where only minor amounts of fine-grained material accumulated. Away from these basement islands on the outer shelf, deposits of succession 4 become progressively thicker, finer grained, more uniform, and show less evidence for storm reworking and deposition (*e.g.* Fig. 7.6, section 124, 12 to 18 m level). In this quieter, deeper-water, more distal setting the background sedimentation of fine-grained material was apparently constant and uninterrupted. The basal contact between succession 4 and underlying succession 5 is locally disconformable, and the contact can be traced laterally over large distances.

Overlying the stacked deposits of succession 4 are fine-grained facies of succession 1. In areas surrounding basement islands conglomerate separates successions 1 and 4, and represents a shoreface conglomerate. Southeast of section 120, in more basinal areas, succession 1 is finer-grained, is subtly coarsening-upward or massive, and contains large, randomly distributed cobble to boulder sized clasts enclosed within siltstone and claystone. The generally fine-grained nature of these rocks and their lack of storm-generated structures and interbeds is different to most exposures of succession 1 in more proximal areas and is consistent with a distal marine setting. However, the presence of the large isolated clasts within this succession is intriguing; are they the debris of storms, or were they emplaced by another mechanism? Frakes and Krassay (1992) propose that these deposits record ice-rafting in the Carpentaria

Basin, and that the large clasts were emplaced in distal, offshore seafloor muds (read fine-grained facies of successions 1 and 4) during the Cretaceous. This geological problem of the evidence for ice-rafting is discussed in Sect. 10.3.

Regardless of the presence and transport mechanism of the clasts in this area, the enclosing fine-grained facies typically correspond to facies succession 1. Facies succession 1 persists as a continuous horizon or 'blanket' in marine sections north and west of section 133, and can be correlated across most of the shelf. Facies succession 1 varies in thickness, and is locally absent as a result of variable erosion at the base of stratigraphically-higher deposits of succession 4 (*e.g.* section 124). Additional evidence for erosion at this stratigraphic level can be seen in the presence of a thin conglomerate in section 126 in a distal part of the shelf.

Rocks of facies succession 4 near the top of the Cretaceous sequence have been previously described in other correlation diagrams for the southern region, and typically consist of a thick fining-upward succession which becomes progressively finer-grained towards the southeast. In this part of the southern region correlation is difficult because most sections are incomplete and their relative stratigraphic position is not obvious, but rocks of succession 4 typically occur at the top of the preserved Cretaceous sequence across the shelf. The youngest succession along P-P', and probably the youngest Cretaceous succession in the entire region, consists of fining-upward sandstones with a conglomeratic base and a mixed plant and marine macrofossil assemblage (*e.g.* Fig. 7.6, section 128). This succession has not been identified elsewhere in the southern region, but has similarities in fossil content and lithology with paralic facies of succession 6 in the central and northern regions. The age of this succession is problematic because the macrofossils are not useful for biostratigraphic zonation, and the succession may be much younger than the rocks they overlie with a disconformable contact.

Along P-P' the erosion surface at the base of facies succession 6 (refer to Lawn Hill SB in Sect. 9.4.6) has been correlated with the erosion surface near the top of section 120, although the successions overlying the erosion surface are different in the two sections. There is no implied correlation of the upper successions in these two sections with those to the north, and these successions may be isolated remnants of younger Cretaceous strata which are not preserved elsewhere in the studv area.

7.4 BIOSTRATIGRAPHIC CONTROL

Compared with the northern and central regions Cretaceous marine and nonmarine body fossils are rare in the southern region. In many cases the only preserved fossils are marine trace fossils. This situation is not surprising, since most hard-shelled organisms were probably restricted to nearer shore zones, where higher wave energies and sandier substrates were the norm. In contrast the offshore shallow-marine setting of the southern region apparently was characterised by bioturbated, finer-grained substrates without pervasive shelly faunas. Fossil assemblages are the same as those in the northern and central regions, and they have poor biostratigraphic resolution for the same reasons as previously discussed in chapters 5 and 6.

Similarly, plant fossils recorded at the base of the Cretaceous sequence and in fluvial successions surrounding basement terrain in the southern region do not provide accurate biostratigraphic control for the successions. These plant fossils appear identical to those recorded in the northern and central regions, and according to Skwarko (1962c, p. 5) they have no specific age connotation beyond Late Jurassic to Early Cretaceous. Although macrofossils and trace fossils do not provide significant biostratigraphic control for rocks in the southern region, particular horizons with abundant macrofossils and/or trace fossils can be used as marker intervals for local correlation.

In contrast to the northern and central regions, isolated outcrops in the southern region yield marine microfossils. These microfossils afford the only reliable, documented biostratigraphic control over any outcrops of the shelf sequence throughout the entire study area. These microfossil assemblages are also highly useful because they can be correlated with microfossil assemblages described by previous workers (see Sect. 8.2.1). Altogether, six samples from five separate localities in the southern region yielded arenaceous foraminifera. Five samples contain foraminifera of the *Lingulogavelinella albiensis* biofacies and one contains foraminifera belonging to the *Ammobaculites australis* biofacies (Haig, 1991). Samples from the base of succession 1 in sections 96, 97, 98, and 99 contain fossils of the *Riyadhella crespinae* zone; they have an age range of late early Albian to late Albian, and probably represent the lower part of the zone, *i.e.* late early Albian (Haig, 1991). A single sample from the base of succession 2 in section 124 (5 m above the base of the section) contains fossils of the *Bigenerina pitmani* zone, which indicate a late Aptian age. Details of the documented foraminifera are presented in Table 8.4. and their palaeoenvironmental characteristics are discussed in Sect. 10.6.3.

Although biostratigraphic ages are available for only six samples over the entire southern region, these biostratigraphic ages are fundamental for age estimation of all successions of the southern region, and for correlation with biostratigraphically dated drillholes to the north (Sect. 8.5), and isolated outcrops in the central and northern regions.

7.5 SUMMARY OF FACIES SUCCESSIONS IN THE SOUTHERN REGION (Correlation diagram Q - Q', Fig. 7.7)

Correlation diagram Q-Q' is a summary correlation diagram illustrating the stratigraphic relationships for critical sections across the whole of the southern region. The correlation diagram extends 539 km from northwest to southeast, and encompasses all major rock types and successions. All but one type of the successions in this correlation diagram have been described and interpreted in previous correlation diagrams, and only a brief summary of each succession will be presented here. Of more importance is the correlation between successions on this middle to outer part of the shelf.

The contact of basement and Cretaceous successions is relatively rarely exposed in the southern region. Where the contact is exposed, a thick fining-upward fluvial succession typically overlies basement with an angular unconformity. Near basement terrains the entire Cretaceous sequence may be composed of fluvial rocks of successions 3 or 7 (*e.g.* Fig. 7.7, section 102), and parts of these fluvial deposits are interpreted to be equivalent to surrounding marine successions. In offshore basinal areas south and east of section 132, the base of the Cretaceous sequence is rarely exposed (*e.g.* section 133, but a lower series of stacked coarsening-upward shoreface successions (*e.g.* section 124) appears to correlate with basal fluvial deposits to the north and west. The stacked shoreface deposits are late Aptian in age based on biostratigraphy (see Sect. 8.2.1), and represent the oldest Cretaceous marine rocks in outcrop in the entire study region. The uppermost shoreface succession in this stacked series can be recognised across much of the middle shelf in the basal to intermediate part of the Cretaceous sequence. Shoreface successions are thicker, coarser-grained, and only subtly coarsening-upward to the northwest of section 120, and become thinner, repeatedly stacked, and finer-grained on more distal parts of the shelf in the southeast.

On most parts of the shelf, coarsening-upward shoreface rocks of succession 2 are sharply overlain by a thick 'blanket' of interbedded claystone or siltstone and graded sandstone of succession 1. Facies succession 1 varies in grain size and thickness across the shelf, and is thickest on the Wallhallow map sheet area where sedimentation occurred in a large east-west

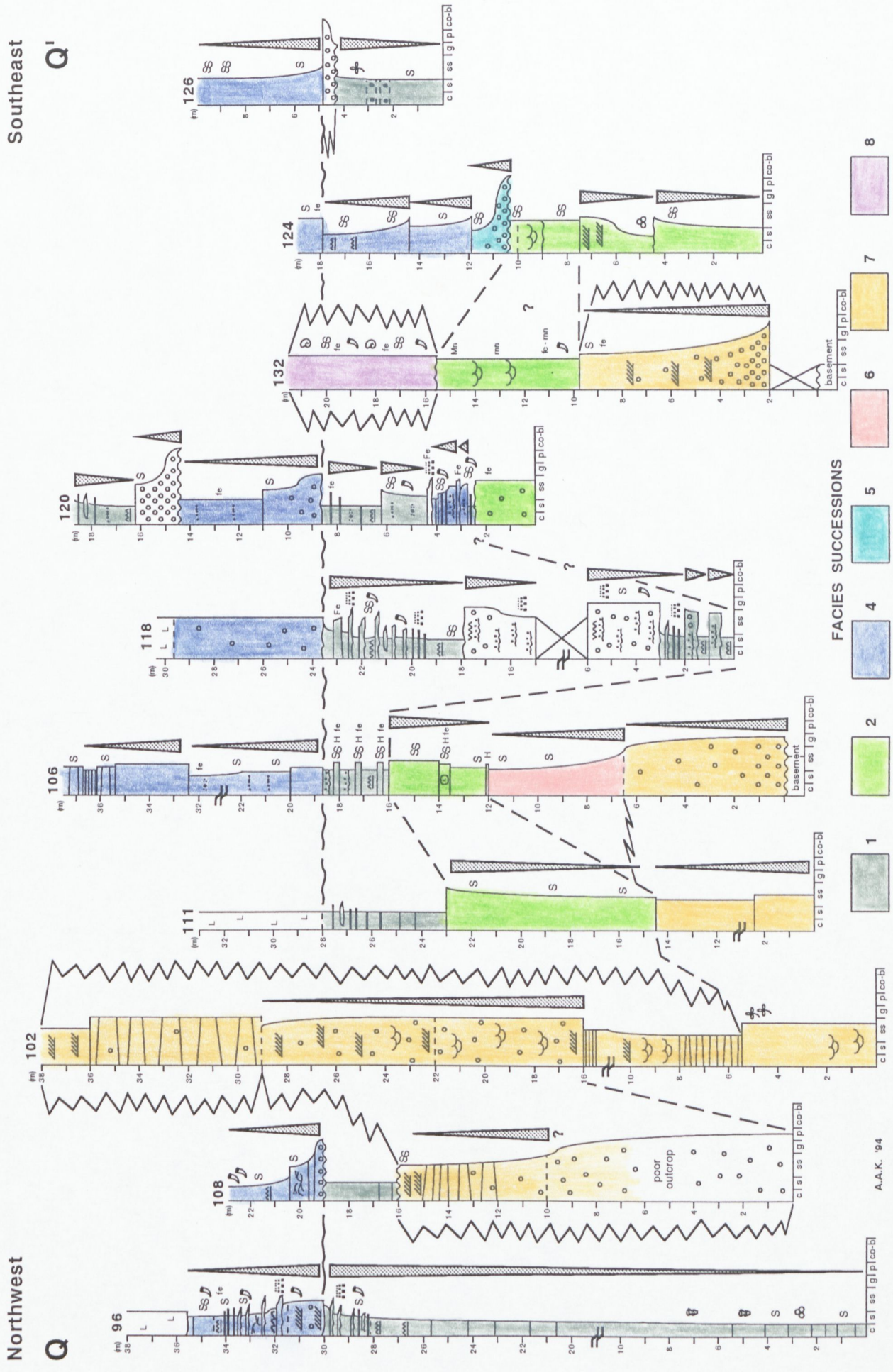

FIGURE 7.7. Stratigraphic correlation diagram for the entire southern region. Refer to Fig. 7.2 for location of sections along Q-Q'.

trending arm of the seaway. Facies succession 1 exhibits regional proximal-distal trends in terms of grain size, thickness, and most importantly in terms of sedimentary structures, with coarser-grained, graded storm beds becoming thinner and less frequent in distal exposures. Facies succession 1 typically comprises one coarsening-upward cycle, but in places a number of thinner, stacked coarsening-upward cycles are prominent (*e.g.* Fig. 7.7, sections 118 and 120). Correlation of individual cycles is difficult in this area due to rapid lateral changes in the thickness and grain size of some cycles, but the uppermost cycle of succession 1 has a similar morphology and thickness across the shelf.

The facies succession 1 'blanket' does not always overlie shoreface sandstones of succession 2 or fluvial facies of succession 7. East and south of section 115, in more complete marine sections (Fig. 7.5), a series of stacked fining-upward and graded facies occurs stratigraphically beneath facies succession 1. On the shelf surrounding section 120, these stacked, fine-grained fining-upward rocks of succession 4 are typically less than 2 m thick, and contain numerous coarser-grained graded beds. Farther offshore towards section 124, the fining-upward cycles of succession 4 become thicker, finer-grained, and contain far fewer coarser-grained interbeds. In this area the base of the stacked fining-upward rocks is conglomeratic and is considered as a shoreface deposit of succession 5. The thin shoreface conglomeratic facies have a disconformable contact with underlying rocks of succession 2, and erosion was locally significant at this stratigraphic level.

Across the entire shelf, the 'blanket' composed of facies succession 1 is disconformably overlain by fining-upward marine rocks of succession 4 (*e.g.* Fig. 7.7, sections 96, 106, 108, 118, 120, and 126). The contact between successions 1 and 4 is occasionally marked by a conglomeratic lag, or more commonly a fining-upward conglomeratic sandstone. These deposits occur stratigraphically higher than, and are significantly younger than thin, stacked cycles of succession 4 which occur elsewhere in the area (*e.g.* Fig. 7.7, 2.5 to 4 m level of section 120). The younger stratigraphic level of succession 4 rocks is composed of one or two thick fining-upward cycles, and shows proximal-distal trends in grain size, thickness, and sedimentary structures similar to underlying rocks of succession 1. However, the vertical changes within facies succession 4 occur in the reverse order in each succession.

7.6 PROBLEMS OF CORRELATION IN THE SOUTHERN REGION

In the southern region, particularly in the southeastern part, some assignments of depositional environments and correlations are tentative due to the lack of biostratigraphic control and the incomplete nature of many sections. There are a large number of individual successions repeated at several stratigraphic levels in the southern region, and lateral and vertical facies and thickness changes are more rapid and noticeable than in the northern and central regions. Stratigraphic relationships are complex, and impossible to define unequivocally in some areas from outcrops alone.

In the following section I have outlined the major uncertainties in correlation and assignment of depositional environments for the southern region. These comments relate to all correlation diagrams for the southern region:

1) The most important problem is the lack of an ideal marker bed in the southern region. In all five correlation diagrams the chosen datum is the contact of succession 1 with overlying rocks of succession 4. However, this contact is disconformable in most places, and has been shown to be slightly diachronous across the shelf. In spite of the uncertainty regarding the amount and timing of erosion at this contact, this is the only widely recognisable datum which is useful for correlation across the entire southern region.

2) The contact between the basal fluvial successions and the overlying shoreface rocks of succession 2 is typically sharp and shows some evidence for erosion, but in places the contact is apparently gradational and the intervening succession represents a paralic (?) / transitional environment (*e.g.* Fig. 7.7, section 106, 6.5 to 12 m level). Paralic rocks of succession 6 are interpreted to have been removed by transgressive erosion on most areas of the shelf.

3) The age and stratigraphic relationship of fluvial successions on basement highs compared to surrounding marine successions is problematic. In many cases correlation is not possible, and the exact age of the fluvial deposits is uncertain (*e.g.* Fig. 7.5, sections 116 and 117).

4) The extent of thin, stacked fining-upward cycles of facies succession 4 in sections 115, 119, 120, 133, and 124 is uncertain to the northwest of section 115. On the basis of local correlation it appears that these deposits thin rapidly, and wedge-out northwest of section 115, where their equivalents may be the basal fluvial deposits.

5) The thickness and morphology of facies succession 1 changes markedly across the shelf. The problem is, are all outcrops of facies succession 1 stratigraphically equivalent as shown, and are they all of the same late early Albian to late Albian age as defined by micropalaeontology? In most parts of Figs. 7.3, 7.4, and 7.5, outcrops of facies succession 1 are bounded above and below by the same successions, and are correlated with confidence. However, south of the line joining sections 121 and 134, sections are incomplete and fine-grained deposits at the base of sections 126 and 127 are correlated as succession 1 on the basis of their contact with overlying rocks. Even though the contact between the facies in this area is erosional, it appears that succession 1 can indeed be correlated across much of the shelf. Elsewhere rocks of succession 1 are anomalously thick and contain coarser-grained conglomeratic intervals (*e.g.* Fig. 7.7, section 118). The increased thickness and grain size of succession 1 here may be due to shedding of coarser clastics from the nearby topographically-high basement terrain. The same situation is suggested for succession 4 in section 98.

6) Correlation of trough- and planar-cross-stratified and massive sandstones of facies succession 2 between sections 124, 132, and 133 is problematic. There are few obvious similarities between sections 124 and 132, and the trough cross-stratified marine sandstones are the only direct lithostratigraphic link. Indirect evidence supporting this correlation involves the similar stratigraphic position of the basal fluvial succession in sections 106, 111, 118, and 132 across the shelf (see Fig. 7.7). The upper succession in section 132 is unique for the southern region, but is similar to facies succession 8 in the northern and central regions.

7.7 CHAPTER SUMMARY

The base of the Cretaceous sequence in the southern region is composed of coarse-grained fluvial successions, overlain by the first transgressive marine successions of the shoreface or upper offshore zone (successions 1 and 2). In the southeastern part of the southern region fluvial successions are not preserved, and older basinal marine successions occur near the base of the Cretaceous sequence. These basal marine successions are interpreted to increase in thickness to the south and east, and are considered correlative with thick Cretaceous marine formations of the central Carpentaria Basin (see chapter 8).

The intermediate and upper parts of the Cretaceous sequence in the southern region typically represent offshore shallow-marine successions of the middle to outer shelf. Compared to rocks of the northern and central regions, successions in the southern region tend to be finer-grained and exhibit sedimentary structures indicative of low-energy, distal sedimentation which was episodically interrupted by high-energy storm events.

The depositional setting of the southern region was not a simple, open marine shelf with a linear palaeoshoreline. The shoreline was highly irregular throughout much of the southern region, and several large basement islands and peninsulas featured on the middle part of the shelf. This complex palaeogeography resulted in multiple facies changes around the basement terrains, and correlation is difficult in some areas. However, the stratigraphic relationships between most successions are repeated across the shelf, and are broadly similar with those of the central region.

~~~~~~
~~~~~~

8. REGIONAL LITHOSTRATIGRAPHY AND BIOSTRATIGRAPHY: A STRATIGRAPHIC FRAMEWORK FOR THE WESTERN CARPENTARIA BASIN

8.1 INTRODUCTION

This chapter is designed to describe and illustrate the broad lithostratigraphic and biostratigraphic relationships on the western shelf of the Carpentaria Basin, and to present them in a coherent stratigraphic framework which is applicable across the entire study area. This stratigraphic framework is based primarily on lithostratigraphic correlations from chapters 5, 6, and 7, but also includes all known relevant biostratigraphic data.

Regional correlation involves the integration of three major data sources: First, and most importantly, are data collected and correlated during this project from "spot" outcrops of the Mullaman Beds in the three study regions. Second, are data from other onshore subsurface exploration and outcrop investigations along the western and southwestern margins of the Gulf of Carpentaria, including Groote Eylandt. Third, is the established data set from subsurface and outcrop investigations in the eastern Carpentaria Basin and Eromanga Basin.

After these data have been used to make regional correlations and construct a robust stratigraphic framework for the western Carpentaria Basin shelf, one can then attempt to relate the litho-, bio-, and sequence-stratigraphic history of the area to similar settings farther afield in northern Australia, Australasia, and the northern hemisphere. This chapter concentrates on the erection of a lithostratigraphic framework for the Carpentaria Basin.

8.2 REGIONAL BIOSTRATIGRAPHY

The major emphasis in this chapter is on lithostratigraphic correlation, but without biostratigraphic age control the overall age of the shelf succession would be unknown, and there is no external test for major lithostratigraphic correlations between isolated outcrops on different regions of the shelf. Therefore, it is necessary to reconcile the various biostratigraphic schemes, nomenclatures, and biostratigraphic age assignments for Cretaceous rocks of the Carpentaria Basin. Much of this information has been summarised in chapter 2, and only the important details and problems with the biostratigraphy are presented below.

8.2.1 Biostratigraphic dating on the mainland

The exact age of the Mullaman Beds exposed along the western and southwestern margins of the Gulf of Carpentaria has been the subject of repeated reappraisal. Sporadic attempts have been made over the last 25 years at constructing a biostratigraphic framework for the western margin of the Gulf of Carpentaria, but with minimal success. This has led to widespread confusion regarding the precise ages of Mesozoic sediments in the eastern Northern Territory and northwestern Queensland.

Factors that have contributed to the confusion are the rarity and poor preservation of micro-faunas and -floras, and the probability that many of the macro-faunas, upon which Skwarko (1966) dated the Mullaman Beds, were products of extremely localised conditions and hence are not representative of the area as a whole. Furthermore, the macrofossil assemblage cannot yet be readily correlated with Cretaceous reference taxa from the Canning and northern Canarvon Basins (Skwarko, 1962a; 1967). Similar problems exist with most woody plant fossils (Plate 7a-d) within the Mullaman Beds, and Skwarko (1962c, p.5) stated that "no accurate dating based exclusively on plants is possible, and individual floras indicate Upper Jurassic (?)-Lower Cretaceous age". Trace fossils are common (Plate 7e-h), but give no unique answer to problems of stratigraphic correlation unless the information they provide is combined with other characteristics such as contact relationships and stratigraphic level.

Prior to Skwarko's work there had been no attempt at a systematic study of the fossils within the Mullaman Beds. Identification and age determination of plant remains and marine macrofossils proceeded after each fossil discovery, but this work was unrelated to the detailed local stratigraphy and thus added little to an overall understanding of the region. Isolated outcrops and a poor understanding of the local stratigraphy have also hindered correlation and age determination from the outset.

Skwarko's (1966) palaeontological age determinations were obtained from molluscan macrofossils, which dominantly occur as poorly preserved moulds (Plate 8). Skwarko's biostratigraphic age assignments based of these macrofossils gave an age of Neocomian to Aptian for most rocks of his Coastal Belt (Table 8.1). Consulting palaeontologists for mineral-exploration companies (Paltech, 1980e; 1981b, c, d; 1982) suggested a revised mid to late Aptian age based on reassessment of Skwarko's molluscan faunas in rocks and core samples taken from the central region, in combination with a few isolated microfaunal age

PLATE 7

a External moulds of segmented plant fossils, mostly small fragments such as leaves, stems, and seed pods. These fossils are best preserved on silicified upper bedding planes within clean medium-grained quartz sandstone. The plant fossil-rich zones are commonly a few centimetres to 0.5 m thick, and may occur at several levels within any stratigraphic section. Site 33, northern region. Lens cap is 5.75 cm in diameter.

b Fossil log within fine-grained clayey quartz sandstone near the top of facies succession 6. Site 68, central region. Hammer is 32.5 cm long.

c Well-preserved manganese-stained external mould and part cast of a segmented log within sandstone of facies 6. Fossil shows preserved detail of the structure of the wood. The segmented nature of the plant species argues for a Mesozoic age. Site 33, northern region. Lens cap is 5.75 cm in diameter.

d Mixed plant and marine bivalve fossils (arrowed) as crude external moulds and rare casts within quartz sandstone of facies succession 2. Such mixed fossil assemblages occur in areas close to the palaeoshoreline, where the normal marine depositional environment was intermittently brackish or estuarine. Near site 49, central region. Pen is 13.5 cm long.

e Horizontal bedding plane exposure of *Planolites* burrow network and rarer *Palaeophycus* burrows within intensely bioturbated sandy siltstone of facies succession 8. Site 59, central region. Lens cap is 5.75 cm in diameter.

f Example of intense bioturbation within clayey siltstone and fine sandstone of facies succession 8. Trace fossil tiering is evident in these rocks, and most traces have been overprinted by successive trace fossil generations. The most obvious traces are straight burrows of *Planolites* and *Teichichnus*, but small branching *Thalassinoides* burrows are also apparent. Site 178, northern region.

g Impression of a fossil log (12 cm wide and 50 cm long) which has been almost completely bored by *Teredolites* trace fossils. The trace fossils form clusters of club-shaped borings, and occur only within the confines of the log. Some of the burrows show ornamentation relict from the plant fossil host. The log is enclosed by bioturbated clayey siltstone of facies succession 8. Site 85, central region. Pen is 15 cm long.

h Well-preserved *Rhizocorallium* burrows (one with ends of dwelling tube arrowed) occurring with positive relief (due to preferential cementation) on a bedding plane of clayey siltstone of facies succession 8. Site 140, northern region. Scale bar for reference.

CARL ZEISS
JENA

a

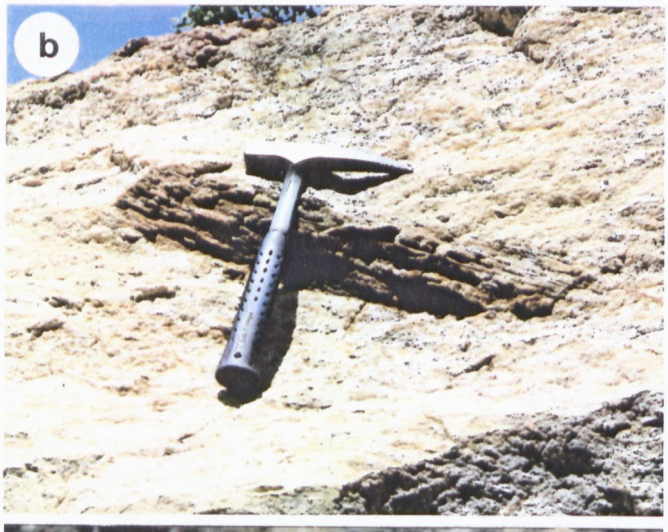

b

CARL ZEISS
JENA

c

d

e

2 4 6 8 10
1 3 5 7 9
CENTIMETERS

f

g

CENTIMETERS

h

determinations. Paltech's new age assignment of mid to late Aptian was then applied to the bulk of Skwarko's marine units of the Coastal Belt.

Table 8.1: Previous workers' biostratigraphic data from mainland macrofossils.

Literature Source	Area	Drillhole or sample number	Fossils	Suggested age
Skwarko (1966)	Coastal Belt	numerous outcrops	bivalves, ammonites, belemnites, gastropods	Neocomian to Aptian (Albian)
Paltech (1980e)	Limmen Bight	LB 21 @ 29-30m	1 belemnite, bivalves, gastropods	Aptian / Albian
	Limmen Bight	outcrop near LB47	bivalves, gastropods	mid-late Aptian
Paltech (1981a)	Limmen Bight	LB 35 @ 15-18m	bivalves	mid Aptian
Paltech (1981/c)	Numbulwar	RR 14 @ 13.5m	bivalves	Aptian (?)
	Numbulwar	RR 16 @ 14m	bivalves	Aptian (?)
	Numbulwar	RR 30 @ 8-9m	bivalves	Aptian (?)
Paltech (1981d)	Nathan River	outcrop	bivalves	mid-late Aptian

Only a few of the early attempts at biostratigraphic dating of the Mullaman Beds indicated an Albian age, and these dates were derived primarily from drillhole samples. Several Paltech samples from a single mainland drillhole (LB 8) yielded an age of Albian through to early Cenomanian (Table 8.2). However, this age assignment was considered to be anomalous and was disregarded in the context of Paltech's proposed mid to late Aptian age assignment for the Mullaman Beds.

Evans (in Dodson, 1967) documented a late Albian palynological assemblage in a drillhole near Gove in the northern region (Table 8.2), but this isolated sample within a thick fluvial to paralic succession was not cited by previous workers. However, this biostratigraphic age determination and corresponding palaeoenvironmental information is valuable for reconstruction of depositional environments of the northern region, and is discussed further in Sects. 8.5.1 and 8.5.2.

PLATE 8

a Bedding plane exposure typical of many fine-grained Mullaman Bed facies showing numerous articulated and disarticulated bivalve fossils as internal and external moulds. Some of the fossils are in life position. Matrix is a clayey siltstone. Site 174, northern region.

b Another typical shelly fossil assemblage of the Mullaman Beds; this time a death assemblage of disarticulated bivalve fossils, most convex-down. This fossil assemblage is dominated by one type of bivalve, and is typical of the low-diversity high-abundance assemblages within coarser-grained facies. Site 32, northern region. Lens cap is 5.75 cm in diameter.

c Cast of a large ammonite showing moderately preserved ornamentation (not sufficient for dating/taxonomic purposes). Collected by T. Madigan from near site 85, northern region. Lens cap is 5.75 cm in diameter.

d External mould of an ammonite within clayey sandstone of facies succession 2. Such external moulds are apparently preferentially preserved on silica-cemented bedding surfaces, but the process of silicification obliterates the fine details of fossil ornamentation. Site 34, northern region. Lens cap is 5.75 cm in diameter.

e Fully articulated (arrow) delicately preserved bivalve fossil within silty sandstone. Such fossils are not uncommon (see also plate 8h), and are taken to indicate a relatively low-energy depositional environment. Site 79, central region. Lens cap is 5.75 cm in diameter.

f Articulated trigonid fossil in life position within clayey sandstone of facies succession 8. Site 58, central region. Lens cap is 5.57 cm in diameter.

g Coquina or shell-hash bed with a large number of disarticulated and partly fragmented shells in a death assemblage. Valves have no preferred orientation. This rock is silica cemented, but may originally have been cemented by calcium carbonate derived from dissolution of the abundant shell material. Such coquinas are commonly associated with storm-generated sedimentary structures such as HCS and sandy graded beds. Site 36, northern region. Lens cap is 5.75 cm in diameter.

h Close up of fossils within quiet-water fine-grained deposits of facies succession 8. Note the fine detail of shell morphology above the lens cap, and the articulated bivalve to the right of the lens cap. Site 85, central region. Lens cap is 5.75 cm in diameter.

2 4 6 8 10
1 3 5 7 9
CENTIMETERS

a

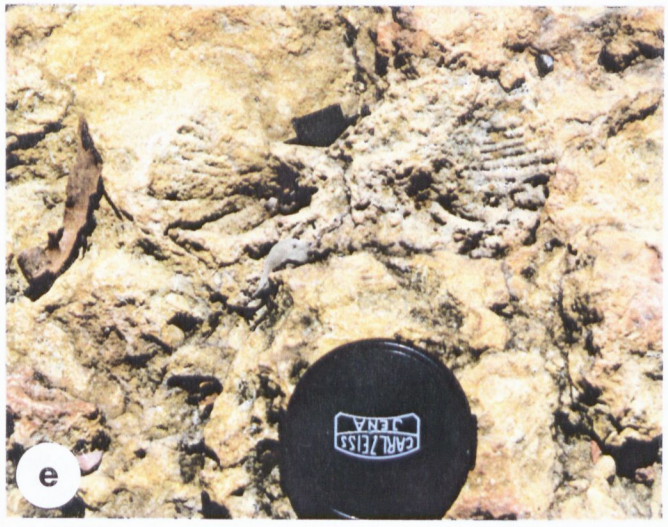
CARL ZEISS
JENA

e

CARL ZEISS
JENA

b

CARL ZEISS
JENA

f

CARL ZEISS
JENA

c

CARL ZEISS
JENA

g

CARL ZEISS
JENA

d

CARL ZEISS
JENA

h

Table 8.2: Previous workers' biostratigraphic data from mainland microfossils.

Literature Source	Area	Drillhole or sample number	Fossils	Suggested age
Plumb and Rhodes (1964)	Wallhallow	outcrop	ABF	Albian
Evans (in Dodson 1967)	Nhulunbuy	D.D.H. 2 @ 64m	D & S/P	late Albian
Paltech (1980b)	Seven Emus	SE 59 @ 39-54m	ABF	late Aptian (?)
	Seven Emus	SC 112 @ 33-36m	ABF	late Aptian to Albian (?)
Paltech (1980/d)	Limmen Bight	LB 8 @ 17-22m	ABF	Albian to early Cenomanian
Paltech (1980e)	Limmen Bight	LB 21 @ 29-30m	ABF	Aptian (?)
	Limmen Bight	LB 25 @ 14-25m	ABF	mid Aptian to Albian (?)
	Limmen Bight	LB 54 @ 31-32m	ABF	mid Aptian
	Limmen Bight	LB 59 @ 11-22m	ABF	Aptian / Albian
Paltech (1981c)	Numbulwar	RR 15 @ 14m	ABF	Aptian (?)
		RR 16 @ 13.5m	ABF	Aptian (?)
Paltech (1982)	Limmen Bight	LB 83 @ 30-50m	ABF	mid Aptian to early Albian (?)
Martin (1982)	Limmen Bight	LB 83 @ 30-50m	D & S/P	latest Albian
	Numbulwar	RR 38 @ 28-30m	D & S/P	mid Aptian to late Albian (?)

ABF = arenaceous benthonic foraminifera: D & S/P = dinoflagellates, spores and pollen:

8.2.2 Biostratigraphic dating on Groote Eylandt

While palaeontological age determination was in progress on the mainland, age dating of the Groote Eylandt manganese orebody was attempted (Table 8.3). Groote Eylandt is a large island which occurs 45 km offshore to the east of the mainland in the Gulf of Carpentaria, at about latitude 14^0 S (Fig. 2.2). The Cretaceous succession on Groote Eylandt has long been linked to the Mullaman Beds on the mainland, but this was not proven by correlation prior to biostratigraphic dating of Cretaceous rocks on the island.

Benthonic and planktonic foraminifera in samples enclosing the ore horizon on Groote Eylandt indicate an age of late Albian to early Cenomanian (Paltech, 1979a, b; 1981e), which was corroborated by palynological analyses suggesting an age of latest Albian to early Cenomanian (Ingram, 1981). Independent evidence of a latest Albian to early Cenomanian age for Cretaceous rocks surrounding the orebody on Groote Eylandt was obtained by K/ Ar dating of glauconite, which yielded a maximum age of 95 million years B.P. (Bolton, 1982).

Table 8.3: Biostratigraphic data from Groote Eylandt microfossils and macrofossils.

Literature Source	Drillhole or sample number	Fossils	Suggested age
Paltech (1979a)	R 41 @ 51.5-54.5m	ABF, CBF, CPF	late Albian-early Cenomanian
Paltech (1979b)	R 41 @ 39.5-42.5m	D & S/P	late Albian-early Cenomanian
	R 41 @ 51.5-54.5m	D & S/P	late Albian-early Cenomanian
	R 41 @ 57.5-64m	D & S/P	late Albian-early Cenomanian
Paltech (1979b)	R 39 @ 39-99m	ABF, CBF, CPF, bivalves, ostracods	early Cenomanian
	R 42/43/44/45/46/47	ABF, CBF, CPF	early Cenomanian
Ingram (1981)	4460 @ 27-27.5m	D & S/P	latest Albian
	4461 @ 25-25.5m	D & S/P	latest Albian
Paltech (1981e)	4460 @ 27-27.5m	CPF	early Cenomanian
	4461 @ 25-25.5m	CPF	early Cenomanian
	4471 @ 22-22.5m	CPF	early Cenomanian

ABF = arenaceous benthonic foraminifera: CBF = calcareous benthonic foraminifera:
CPF = calcareous planktonic foraminifera: D & S/P = dinoflagellates, spores and pollen:

The essential problem was then to explain the apparent age difference between the Groote Eylandt succession (latest Albian-early Cenomanian), and the similar succession of the Mullaman Beds (mid to late Aptian according to Paltech) to the west on the mainland. Paltech's dating regime of the time required the existence on the mainland of a non-depositional / erosional hiatus, encompassing the late Aptian and nearly all of the Albian.

8.2.3 Biostratigraphic dating in the present study

Age determinations of Mullaman Bed molluscan macrofossils on the mainland by Skwarko (Neocomian to Aptian, with rare Albian units) and Paltech (mid to late Aptian) are in conflict with ages yielded by previous and current dating of microfossil assemblages from both the mainland Mullaman Beds, and Groote Eylandt. To gain a better understanding of the age of the Mullaman Beds, and to provide improved biostratigraphic control for the Cretaceous Carpentaria Basin succession, a number of samples were analysed for microfossils in this study. The biostratigraphic ages and zonation yielded by these samples (Table 8.4) validate the age (Albian to Cenomanian) derived from some previous microfossil analyses of mainland samples in the central region, and are also in agreement with biostratigraphic ages previously suggested for the Cretaceous succession on Groote Eylandt.

In the present study fine-grained samples from three areas yielded microfossil assemblages which provided precise biostratigraphic zonation. Firstly, dinoflagellates and spores/pollen were recovered in samples from two U.S. Steel drillholes in the area north of Numbulwar (Fig. 8.1). The cores for these drillholes were logged and sampled in Darwin as part of this study. Secondly, arenaceous foraminiferal assemblages were recovered from four outcrop sections (96, 97, 98, and 99) on the Wallhallow map sheet in the southern region. Thirdly, an arenaceous foraminiferal assemblage was recovered from a sample from one outcrop section (124) in the far southeastern part of the study area on the Lawn Hill map sheet.

Table 8.4: Biostratigraphic data from mainland microfossils in this study.

Analysed by	Area	Drillhole or section number	Fossils	Suggested age
Alley (1991)	Numbulwar	RR 21 @ 35.5m	D & S/P	late Aptian to middle Albian
	Numbulwar	RR 38 @ 27m	D & S/P	middle Albian
Haig (1991)	Wallhallow	section 96 @ 4.5m	ABF	late early Albian-late Albian
	Wallhallow	section 97 @ 1.5m	ABF	late early Albian-late Albian
	Wallhallow	section 97 @ 5.5m	ABF	late early Albian-late Albian
	Wallhallow	section 98 @ 1m	ABF	late early Albian-late Albian
	Wallhallow	section 99 @ 6m	ABF	late early Albian-late Albian
	Lawn Hill	section 124 @ 5m	ABF	late Aptian

ABF = arenaceous benthonic foraminifera: D & S/P = dinoflagellates, spores and pollen:

Palynological analyses by Alley (1991) of two Mullaman Bed samples in the Numbulwar drillholes as part of the present study yielded an age of late Aptian to middle Albian for one sample, and a better-constrained age of middle Albian for another sample. This middle Albian age is consistent with the age-range of mid Aptian to late Albian defined for these Mullaman Bed drillhole samples by previous palynological analyses (Martin, 1982). Together, the biostratigraphic data of Martin (1982) and this study (Alley, 1991) refute the earlier tentative age of mid to late Aptian for the same stratigraphic level proposed by Paltech on the basis of molluscan macrofaunas.

Haig (1991) conducted foraminiferal analyses of outcrop samples collected from the Wallhallow map area in the present study (Fig. 8.1). The five samples from four separate measured sections all provided an age-range of late early Albian to late Albian, probably late early Albian (Haig, 1991). These biostratigraphic age determinations allow direct correlation with identical

FIGURE 8.1 Drillhole location map. In addition to the drillholes described in the text and tables, several shallow drilling programs were conducted on the mainland in the late 1970's and early 1980's, particularly in the northern part of the central region and in the area between the central and southern regions. Unfortunately, the information available from these drilling programs is of very poor quality. Core drilling was not used in any of these programs, and sampling and logging descriptions for most drillholes are not accurate enough for stratigraphic purposes in this study. In cases where the lithological descriptions are adequate and the holes have some biostratigraphic control, the data are included in this study. The location of the areas covered by these drilling programs (Limmen Bight, Yiyintyi, Seven Emus) is illustrated here, and the relevant biostratigraphic data from these drillholes is presented in Tables 8.1 and 8.2.

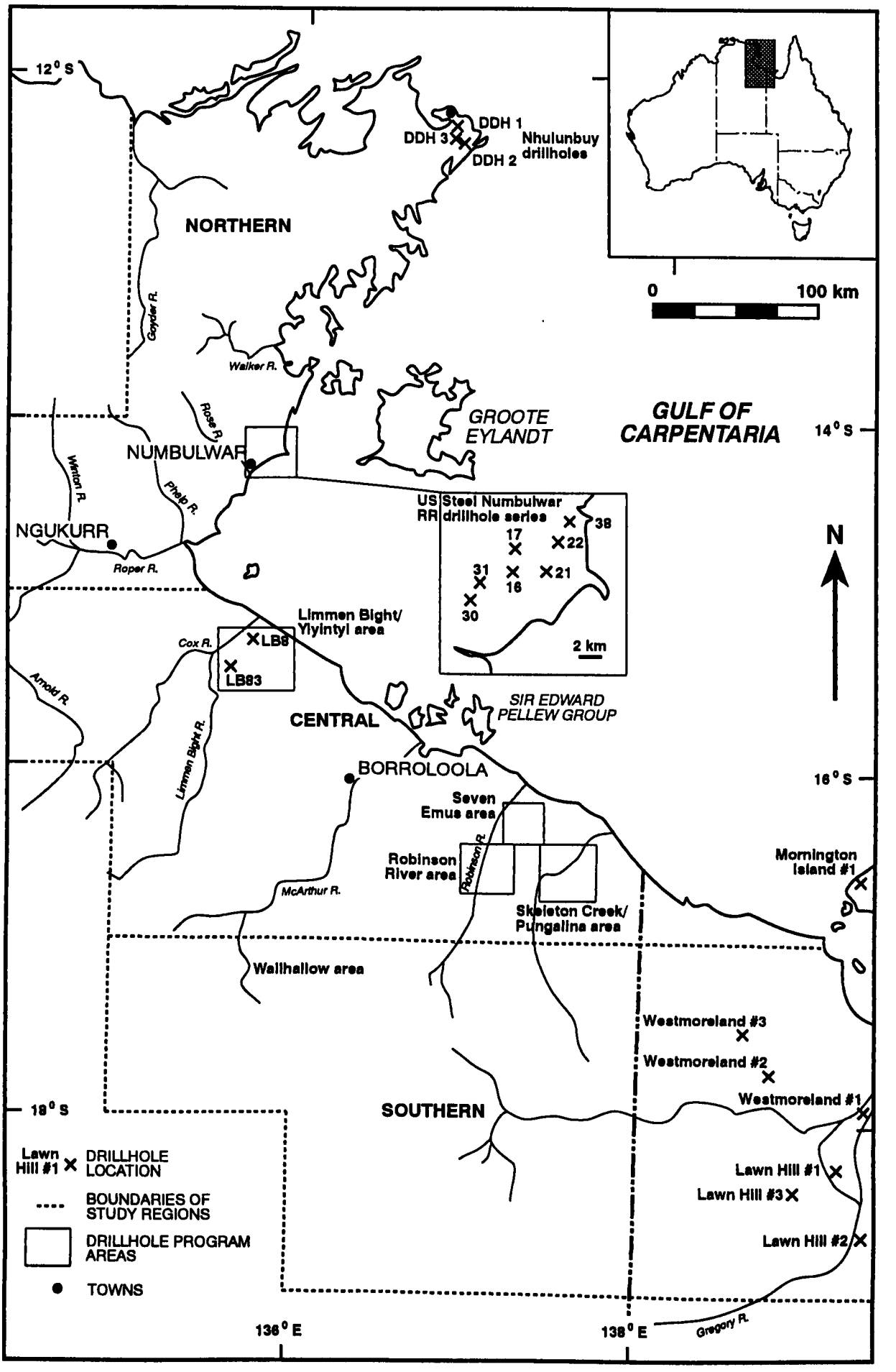
12° S
DDH 1
DDH 3
DDH 2
Nhulunbuy drillholes
NORTHERN
Goyder R.
Walker R.
Rose R.
GROOTE EYLANDT
GULF OF CARPENTARIA
14° S
NUMBULWAR
Wilton R.
Philip R.
US Steel Numbulwar drillhole series
38
17
22
31
21
16
30
2 km
NGUKURR
Roper R.
N
Limmen Bight/ Yiyintyi area
Cox R.
LB8
LB83
Arnold R.
CENTRAL
SIR EDWARD PELLEW GROUP
Limmen Bight R.
BORROLOOLA
16° S
Seven Emus area
Robinson River area
Robinson R.
McArthur R.
Mornington Island #1
Skeleton Creek/ Pungalina area
Wallhallow area
Westmoreland #3
Westmoreland #2
Westmoreland #1
18° S
SOUTHERN
Lawn Hill #1
Lawn Hill #3
Lawn Hill #2
Lawn Hill #1 DRILLHOLE LOCATION
BOUNDARIES OF STUDY REGIONS
DRILLHOLE PROGRAM AREAS
TOWNS
136° E
138° E
Gregory R.
0
100 km

FIGURE 8.1.

rocks of the Mullaman Beds in the Numbulwar drillholes to the north, and provide further evidence that the *exposed* Mullaman Beds are predominantly early Albian and younger in age.

In the entire study area there are only a few reliable biostratigraphic age determinations which document an Aptian age* for rocks of the Mullaman Beds. Haig (1991) identified late Aptian-aged arenaceous foraminifera in one sample from the far southeastern corner of the study area in section 124, near the base of the exposed Mullaman Beds succession. Paltech (1980e) dated numerous drillhole samples of the Mullaman Beds in the central region, and only one sample (from drillhole LB 54 near the Yiyintyi Range) provided a definite Aptian age (Table 8.2).

8.2.4 Summary of biostratigraphic dating and age control for the western shelf of the Carpentaria Basin

It is apparent from the tabulated data in prior sections that any age determinations based on the poorly preserved molluscan macrofossil assemblages of the Mullaman Beds, including those of Skwarko (1966) and Paltech (1980e; 1981b, c, d), must be considered as unreliable. In nearly all cases the tentative age assignments derived solely from molluscan macrofossils are in direct conflict with ages *and* age-ranges defined by the better-preserved and more diverse microfossil assemblages in the Mullaman Beds.

Although they provide rather limited biostratigraphic control in field-based studies of the Mullaman Beds, the only biostratigraphic age assignments that can be used with confidence are those determined from microfossil assemblages. In most outcrops in the northern and central region, microfossils were not found, and were either never present, or more likely have been destroyed by weathering and chemical diagenesis. Microfossils were only recorded in a few fresher outcrop samples in the southern region, and in relatively unweathered drillhole samples in the northern and central regions, and on Groote Eylandt.

---

* At the time of writing an Aptian-aged sequence (H. Barents, pers. comm. 1994) had just been documented from a few recent BHP drillholes in the Wallhallow area (southern region), in the area immediately north of Borroloola (central region), and near the Yiyintyi Range (central region). The dating of this sequence as mid to late Aptian is based on palynology and independent K/Ar dating of glauconite (M. Warne, pers. comm. 1994). The Aptian sequence lies at depths of about 20 to 80 m, and probably forms the basal part of the Mullaman Beds which accumulated during an initial transgressive pulse. Correlations between the various drillhole localities have yet to be proven, but it appears likely that these rocks are equivalent to Sequence *IA*, and are similar to other fine-grained deep-water marine rocks of facies succession 1 (Sequence *III*).

The best biostratigraphic control is afforded by samples with both benthonic and planktonic foraminifera and/or palynomorphs. In practice, most samples contain diverse assemblages of only one type of microfossil, typically benthonic arenaceous foraminifera which are resistant to weathering. Haig's (1979b) tripartite zonation based on the distribution of arenaceous-benthonic, calcareous-benthonic and planktonic foraminifera is the most useful scheme for biostratigraphic age control of the Mullaman Beds. By applying Haig's (1979b) scheme it is possible to position samples relative to the established lithologic sequence. In a similar way, palynological schemes of Morgan (1980) and Helby *et al.* (1987) are useful for positioning isolated Mullaman Bed outcrop samples containing dinoflagellates and spores/pollen.

In summary, the age of the Mullaman Beds along the western and southwestern margins of the Gulf of Carpentaria is defined by relatively few accurately dated samples. The only reliable biostratigraphic age control for the rocks is provided by microfossil assemblages, which are rarely preserved in outcrop. Detailed local correlation combined with biostratigraphic data above indicate that the bulk of the *exposed* Mullaman Beds are younger than Aptian in age (see previous footnote), and that marine deposition was common between the late Aptian and early Cenomanian on both Groote Eylandt and the mainland (see Sects. 8.6 and 8.7).

8.3 REGIONAL CORRELATION OF COMPOSITE OUTCROP SECTIONS

The following section documents lithostratigraphic correlations between the three regions of the study area. Each study area is divided into two distinct parts: the northern region encompasses the northeastern Arnhem Land Zone (ALZ) and the Bath and Parsons Ranges Zone (BPRZ), whilst each of the central and southern regions is divided into proximal and distal parts. In all, six composite stratigraphic sections (Fig. 8.2) have been constructed, and together these composite sections are representative of the entire western and southwestern parts of the Carpentaria Basin.

Construction of the composite sections was based on measured sections from isolated "spot" outcrops and their local correlation as presented in chapters 5, 6, and 7. Individual components of the composite sections in Fig. 8.2 represent the maximum thickness of a given succession on a particular region of the shelf, and were compiled to yield the stratigraphic section with the least interference by erosion. Even so, the amount of erosion on proximal parts of the shelf was high and many of the thicknesses shown in the composite sections are likely to be minimum values.

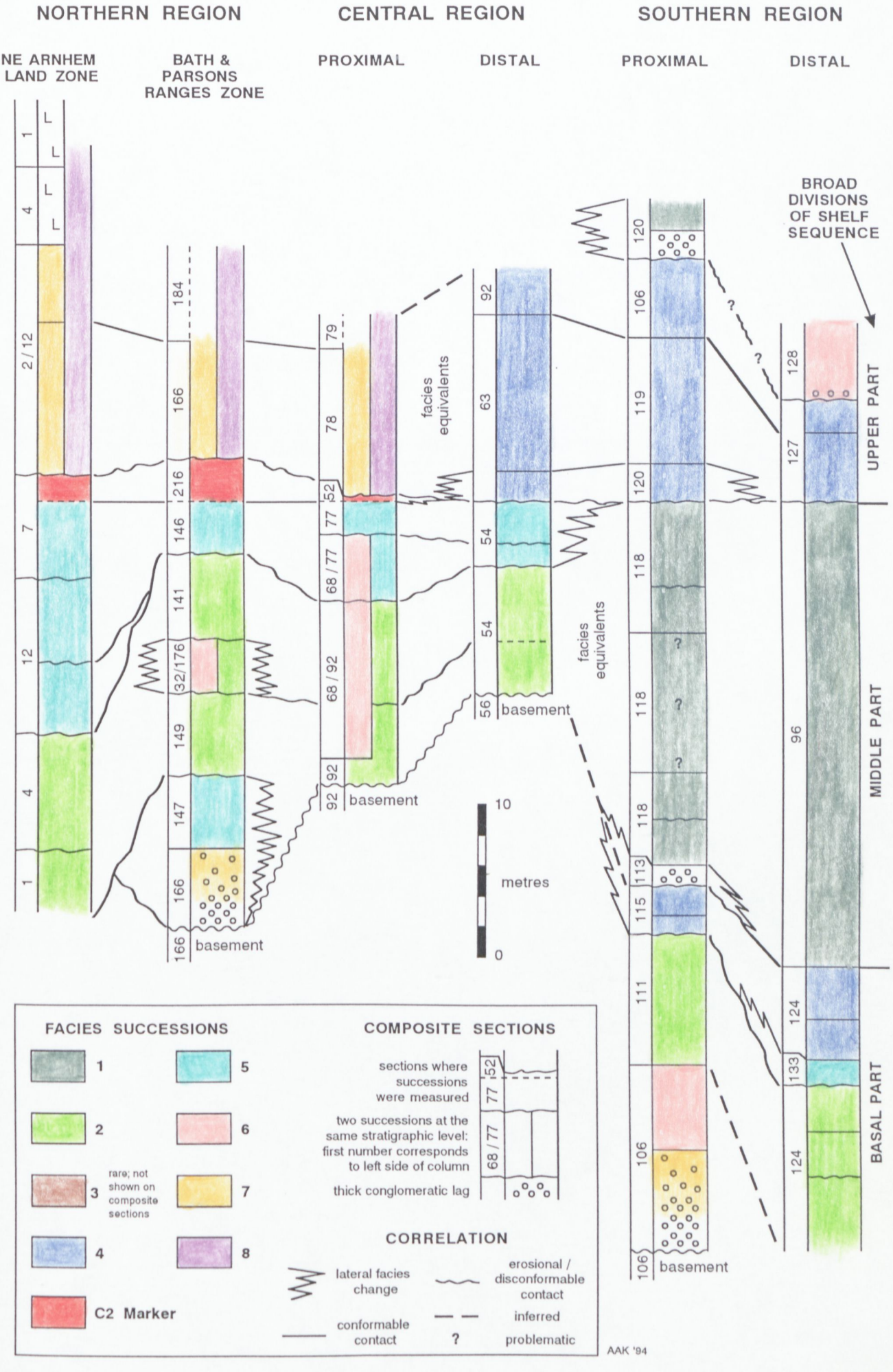

FIGURE 8.2. Regional correlation of composite outcrop sections across the three regions of the study area.

The shelf sequence can also be broadly subdivided into 3 parts on the basis of age (see Sect. 8.6.2), independent of the regions; the basal part is composed of relatively coarse-grained Early Cretaceous nonmarine and Aptian marine rocks; the intermediate part is composed of finer-grained marine and paralic rocks of Albian age; and the upper part is composed of fine-grained marine, restricted marine, and nonmarine rocks, mostly of Cenomanian age.

8.3.1 The basal (pre-Albian) part of the shelf sequence

The lowest stratigraphic level of the Cretaceous sequence is only exposed in the BPRZ and the proximal part of the southern region, although rocks interpreted to be near the base of the shelf sequence are also exposed in the distal part of the southern region. In the BPRZ and the proximal part of the southern region, a thick normally graded conglomerate representing the base of the shelf sequence unconformably overlies Proterozoic basement. Conglomerates and sandstones of successions 4 and 5 comprising the base of the Cretaceous shelf sequence are missing in the central region, and were probably never deposited across the basement highs of the central region. These regional variations are due to an irregular basement topography (see Sect. 8.6.1), which resulted in the preservation of Cretaceous rocks of varying ages overlying Proterozoic basement across the shelf.

In the proximal part of the southern region the basal conglomerate grades up into transitional/paralic rocks of succession 6, which are overlain by relatively thick sandstones of facies succession 2. Sandstones of succession 2 are also present at this stratigraphic level in the distal part of the southern region, but are not present to the north. Disconformably overlying succession 2 in the southern region are relatively thin, stacked deposits of successions 4 and 5. In the BPRZ rocks of succession 5 at the same stratigraphic level overlie the thick basal conglomerate with a sharp contact, and intervening transitional facies succession 6 and succession 2 are missing. The top of the basal part of the shelf sequence is marked by a prominent disconformity, and the local development of conglomeratic lags.

8.3.2 The middle (Albian) part of the shelf sequence

Across the whole shelf the rocks overlying basal successions 4 and 5 or basement (central region) belong to facies successions 1 and 2. In all areas these Albian-aged rocks (Sect. 8.6.2) have a disconformable contact with underlying successions, and form the middle part of the shelf sequence. In the ALZ these Albian-aged fine-grained marine siltstones and sandstones of

facies succession 2 are the oldest exposed rocks, and the base of the Cretaceous sequence must occur at depth.

In the proximal part of the southern region thick deposits of facies succession 1 overlie a basal conglomerate with a sharp contact, and succession 1 contains rare conglomeratic intervals which thin and wedge-out to the southeast. The total thickness of rocks of succession 1/2 varies from less than 10 m in the ALZ, to at least 30 m in the southern region and drillholes in the central region (Sect. 8.6). This middle part of the shelf sequence consists of up to four coarsening-upward successions, but typically only two coarsening-upward intervals were recognised. In the northern and central regions, deposition occurred in relatively shallow-water within the shoreface zone and deposits belong to facies succession 2. In the southern region sedimentation occurred in deeper water, generally more distal from the palaeoshoreline, and facies succession 1 accumulated in these areas. The same stratigraphic interval is represented in the northern and central regions by coarser-grained rocks of facies succession 2. In some proximal areas of the BPRZ and the central region, paralic rocks of facies succession 6 interdigitate with succession 2 offshore; estuarine and/or deltaic rocks can be seen to thin and wedge-out offshore to the east and southeast and are replaced by rocks of facies succession 2.

In all parts of the northern and central regions rocks of succession 2 are disconformably overlain by relatively thin shoreface deposits of facies succession 5 (Fig. 8.2), which also belong to the middle part of the shelf succession. The combined thickness of these shoreface deposits varies from 15 m in the ALZ to less than 5 m in the central region, where they wedge-out offshore to the east and southeast. Deposits of succession 5 consist of one to three stacked successions which are separated by disconformable contacts. On most parts of the shelf two stacked fining-upward cycles of succession 5 occur at this stratigraphic level. The uppermost fining-upward cycle of succession 5 grades up into the C2 marker bed.

8.3.3 The upper (post-Albian) part of the shelf sequence

The C2 marker bed, which marks the base of the upper part of the shelf sequence, is common in more complete outcrops in the northern region, and also occurs in rare places in the proximal part of the central region. The C2 marker bed is composed of silty claystone and very fine-grained siltstone and has a maximum thickness of 3 m in the BPRZ. The preserved thickness of the C2 marker varies across the shelf in response to the amount of erosion prior to deposition of overlying successions. Evidence for erosional thinning and truncation of the C2 marker bed is evident in numerous localities in the northern and central regions.

In the northern region and the proximal parts of the central region, the C2 marker is incised by fluvial rocks of facies succession 7. The amount of fluvial incision varies laterally, and the C2 marker bed and upper part of facies succession 5 have been completely eroded in places. At the same stratigraphic level in low-lying areas closer to the coast, such as in the BPRZ and the northwestern edge of the ALZ, thick restricted marine deposits of facies succession 8 are incised into the C2 marker.

In all areas the stratigraphic equivalence of rocks of successions 7 and 8 overlying the C2 marker can be clearly seen; lateral facies changes between the two successions are visible over distances of a few kilometres, and they both exhibit the same stratigraphic relationship with underlying marine successions (Fig. 8.2). This enables all the composite sections to be hung relative to the C2 marker level (Fig. 8.2), even though the C2 marker is not present in all areas. The assumption which underpins this construction is that the C2 marker once formed a thin 'blanket' of roughly constant thickness across the shelf, and was subsequently removed by erosion in the southern half of the study area. This assumption appears to be validated by the observed lateral continuity of successions above and beneath the C2 marker bed, and the way individual beds of only several metres thickness can be traced for over 300 km on the shelf.

Directly above the extrapolated stratigraphic level of the C2 marker in the southern region are relatively thick deposits of facies succession 4. The total thickness of these rocks is at least 15.5 m (the top is not visible in many places, and erosional in others) and is composed of two or three separate fining-upward cycles. The lower, coarsest-grained fining-upward succession disconformably overlies thick deposits of succession 1. This lower succession is present in the distal part of the central region and the proximal part of the southern region, but wedges-out to the southeast. Overall, rocks of facies succession 4 in the southern half of the study area appear to be contemporaneous with succession 7/8 in the northern half of the study area.

In the southern region conglomeratic units and paralic rocks of succession 6 locally lie on an erosion surface cut into rocks of succession 4, and probably represent the final Cretaceous depositional episode in the study region as the sea retreated from the western shelf (see Sects. 9.5.7 and 9.7.6). In the northern region, particularly in the ALZ, Cretaceous successions are capped by ferricretes and lateritic soil profiles up to 9.5 m thick.

8.4 COMPARISON OF STRATIGRAPHIC NOMENCLATURES

In this section the stratigraphy defined from outcrop in the present study is compared with the previous stratigraphic nomenclature for the Mullaman Beds by Skwarko (1966). Detailed comparisons of Skwarko's stratigraphy with stratigraphic successions in this study have been previously documented in correlation diagrams in chapters 5, 6, and 7. Therefore, only a brief overview of the data is presented here in the form of a summary diagram (Fig. 8.3).

8.4.1 Stratigraphic nomenclature in the northern region

In the northern region there is good correspondence between Skwarko's units and facies successions identified in this thesis. Some of the contact relationships between the units / successions are also interpreted to be similar, but the present study documents a larger amount of erosion and the formation of numerous disconformable contacts. The broad equivalence of the two stratigraphic schemes is as follows (see Fig. 8.3):

1) The basal conglomerate in the BPRZ is equivalent to Skwarko's unit 1, however the overlying sandstones of succession 5 do not fit into Skwarko's scheme.
2) Thick sandstones of succession 2 correspond to Skwarko's unit 2, although Skwarko makes no mention of interbedded / interdigitating paralic units which could be equivalent to rocks of facies succession 6 at this stratigraphic level.
3) Sandstone of facies succession 5, which fines up into the C2 marker bed, is equivalent to Skwarko's unit 3.
4) Overlying rocks of succession 8 correspond to Skwarko's unit 4.

8.4.2 Stratigraphic nomenclature in the central region

In the central region the stratigraphy is more complex, and the correspondence between the two stratigraphic schemes diminishes. The main points are (see Fig. 8.3):

1) Thick sandstones of facies succession 6 in the proximal part of the central region correspond in part with Skwarko's unit 5. However, in my scheme rocks of succession 6 are facies equivalents to unit 2 (instead of overlying unit 2), and occur beneath unit 3 (instead of above it).
2) In the distal part of the central region facies succession 4 is equivalent to most of Skwarko's unit 6, and all of Skwarko's unit 7. Skwarko's division of the rocks into unit 6 and unit 7 is not supported in the present study.

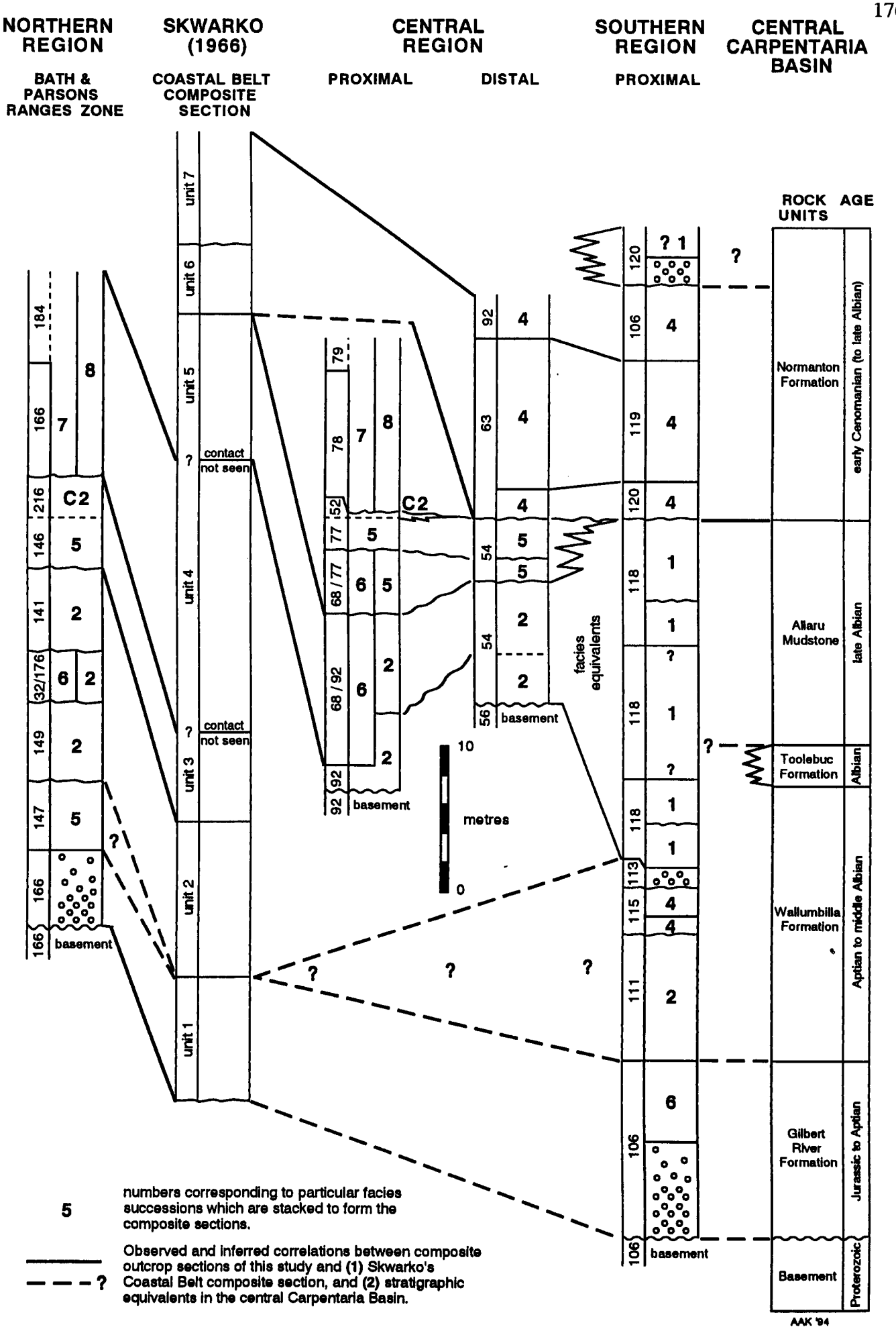

FIGURE 8.3. Comparison of composite outcrop sections in this study with (1) Skwarko's stratigraphic scheme, and (2) the central Carpentaria Basin stratigraphy, shown as bold correlation lines. Composite sections for the ALZ and distal part of the southern region are not included.

3) Similar to the northern region, restricted marine deposits of succession 8 in the proximal part of the central region correspond to Skwarko's unit 4. Fluvial rocks of succession 7 at the same stratigraphic level probably correspond to Skwarko's unit A of his Inland Belt, but this relationship does not hold in all areas.

8.4.3 Stratigraphic nomenclature in the southern region

Stratigraphic correlation between Skwarko's (1966) scheme and the stratigraphic scheme developed in this thesis becomes increasingly difficult in the southern region. The base of the Cretaceous sequence in the proximal part of the southern region probably corresponds to Skwarko's unit 1 (Fig. 8.3), but may also correspond to his inland unit A in places. Most overlying rocks do not fit into Skwarko's scheme in any repeatable or consistent pattern.

8.4.4 Discussion

Generally, Skwarko's (1963, 1966) work covered the northern and central regions of the study area in some detail, but his work in the southern region was not comprehensive. The stratigraphy of the northern and central regions is simpler than that of the southern region, and in the north there is relatively good correspondence and agreement between the two stratigraphic schemes in terms of lithostratigraphy (but not in age; see Sect. 8.2). Towards the south the correspondence between the two schemes diminishes markedly.

The main reason for the differences may lay in the fact that Skwarko's study was based primarily on palaeontology, whereas the current study is based mainly on lithostratigraphy. Skwarko constructed composite sections using his interpreted biostratigraphic ages from molluscan macrofossils, and in some cases (*e.g.* units 4 and 5) his units were stacked using his assigned ages with little or no lithostratigraphic control because he had not observed the contact relationships. In view of the reassignment of many of the original biostratigraphic age determinations in Skwarko's (1966) study (Sect. 8.2), the stratigraphic position of some of his units (*e.g.* unit 5) are probably not correct. These differences are highlighted by the redefinition of the age of the Mullaman Bed shelf sequence in the present study (Fig. 8.3; Sect. 8.6.2).

8.5 STRATIGRAPHIC DATA FROM THE SUBSURFACE

8.5.1 Drillholes near Nhulunbuy

During the mid 1960's a series of water bores was drilled near Nhulunbuy (Gove) in the ALZ. Several of these bores intersected coal, and three diamond drillholes, D.D.H.1, D.D.H.2, and D.D.H.3 (Fig. 8.1), were subsequently drilled to test for economic coal measures (Dodson, 1967). Information concerning the Cretaceous facies intersected in the three stratigraphic drillholes is important for three reasons:

1) The drillholes provide a complete record of, and the only subsurface data concerning, thick nonmarine Cretaceous deposits in close vicinity to measured sections in the ALZ.
2) Fine-grained rocks in the drillholes yield datable microfossils which were not recovered from weathered "spot" outcrops.
3) The well logs provide factual data about the composition of basement and its depth beneath the Cretaceous and Cainozoic cover sequences.

The Cretaceous sequence in each of the three drillholes is similar, although direct correlation between the drillholes is not obvious due to the massive nature of the sandstones, and the lack of lithological contrast in much of the sequence. The maximum drilling depth was 168 m in D.D.H. 1. In all three drillholes the sedimentary sequence overlies granitic basement, which occurs at a different depth in each of the drillholes (Dodson, 1967).

The Cretaceous sequence in the drillholes consists of massive, undifferentiated sandstone up to 53 m thick (commonly 9 to 14 m thick), alternating or interbedded with thinner intervals (typically < 1 m) of fine-grained micaceous siltstone, claystone, coaly claystone, and coal. The sandstone is unfossiliferous, highly arkosic, coarse-grained, and poorly sorted. Grains are typically angular to subangular and are composed of quartz, feldspar, and numerous heavy minerals (Dodson, 1967). Claystone and the rarer siltstone are pale grey or very pale brown, very fine-grained, and contain small quantities of heavy minerals similar to those in the arkosic sandstones. Low grade coal with pyrite is present as thin (maximum thickness of 7.6 cm), lens-shaped seams and carbonaceous partings within claystone.

Analysis of the well logs for the Nhulunbuy drillholes suggests that the Cretaceous succession was deposited largely in freshwater, in an interfluvial-distal deltaic region. This is confirmed by palaeoenvironmental analyses of fine-grained sediments and microfossils in D.D.H. 2 (Evans, in Dodson, 1967), which indicate that the siltstone is of lacustrine origin. The pyrite

within the coal is not detrital (Dodson, 1967), and the presence of sulphur-rich pyritic coal and coaly siltstone suggest a brackish marsh-like depositional environment (*cf.* Cohen, 1984; Postma, 1982) for the coaly parts of the Cretaceous sequence. The depositional model proposed here for the Cretaceous sequence in the Nhulunbuy drillholes involves rapid deposition of fluvial sediments in channels followed by episodic peat formation in interfluvial areas. This situation is typical of coastal lowlands or distal deltaic environments where peat formation is a short-lived process which is repeatedly interrupted by flooding (drowning) of the swamp by marine incursions and also by freshwater lakes deepening in interfluvial areas (Bless and Paproth, 1989).

8.5.2 Correlation of Nhulunbuy drillholes with outcrops in the ALZ

Sandstones in both outcrop and the three Nhulunbuy drillholes in the ALZ lack prominent marker beds or fossiliferous intervals, and bed by bed correlation is not possible. However, sandstones in both outcrop and the drillholes have identical grain size, sorting, texture, and composition. Sandstones at the surface contain relict feldspar (are sub-arkosic), and much of their clay content was probably derived from weathering of feldspars, which are better preserved in drillcore. All such fluvial successions are restricted to the same broad stratigraphic interval, though the succession in the drillholes is much thicker than that in outcrop. These arkosic outcrop and subsurface fluvial successions are strongly inferred to be equivalent in terms of facies and age, and are considered to have accumulated in the same fluvial depositional system.

Siltstone interbedded with coal in D.D.H.2 at 64 m depth has yielded a late Albian microflora (Evans, in Dodson, 1967). Outcrops of fluvial sandstone surrounding the drillholes in the ALZ occur topographically above the dated horizon in D.D.H. 2, and are therefore inferred to be younger than late Albian in age. This is supported by independent regional correlation which shows that fluvial sandstones in outcrop (*e.g.* Fig. 5.4, sections 7 and 10) are younger than latest Albian-early Cenomanian in age. This relationship is based on dating and correlation documenting that the C 2 marker bed is latest Albian to early Cenomanian in age (see Sect. 8.6; Fig. 8.7); older than overlying fluvial sandstones which truncate it.

In summary, the lithostratigraphic and temporal equivalence of fluvial successions in both outcrop and the subsurface is validated by the limited biostratigraphic data and the position of the regional C 2 marker bed. If, as seems likely, this correlation is correct there are three important conclusions that can be drawn:

1) It suggests that at least local fluvial deposition occurred in the interval from the late Albian to latest Albian - early Cenomanian, and probably over a much longer time period.
2) It confirms that the basement topography is very irregular (from the three drillhole depth to basement measurements), and suggests that the thickness of the Cretaceous sequence varies greatly in different areas in response to the underlying topography.
3) It confirms that a large part of the Cretaceous succession in the ALZ is indeed fluvial in origin, and provides positive evidence for subaerial exposure and nonmarine to slightly brackish sedimentation (in the form of coal), the evidence for which is lacking in outcrop.

8.5.3 Drillholes and quarries on Groote Eylandt

The stratigraphy and age (Table 8.3) of Cretaceous sedimentary rocks on Groote Eylandt are well known due to extensive quarrying and exploration drilling programs over the past 20 years. Extrapolation of detailed stratigraphic information from Groote Eylandt, offshore from the northern region, to the less well-known Mullaman Beds on the mainland is extremely important for regional correlation and age control. In this section the stratigraphy of Cretaceous rocks on Groote Eylandt is summarised, and correlations are made with Cretaceous shelf facies of the Mullaman Beds on the mainland to the west.

Groote Eylandt lies on the eastern edge of the Proterozoic McArthur Basin, and the basement for Mesozoic rocks on the island consists of Proterozoic feldspathic sandstone or quartzite known locally as the "Groote Eylandt Beds" (Plumb *et al.*, 1980). The basement is overlain unconformably by shallow-marine, glauconitic sandstones of probable late Aptian to early Albian age (Bolton, 1982), which are known as the "sand facies" (Fig. 8.4). Previous workers have noted that Upper Cambrian to Jurassic rocks are apparently absent (Bolton, 1982; Frakes and Bolton, 1984; Pracejus, 1989; Slee, 1976).

Overlying the "sand facies" with a locally disconformable contact is a thick sequence of claystone, siltstone, and minor sandstone of latest Albian to early Cenomanian age known as the "clay facies". The "pisolite facies" overlies the clay facies with a regional unconformity and is composed of a thick pisolitic/oolitic manganese oxide/carbonate unit (the main ore zone) which is overlain by a series of sandstones, siltstones, and claystones. The pisolite facies has a maximum age of late Albian-early Cenomanian based on radiometric dating of glauconite (Bolton, 1982), and is capped by a series of Tertiary or Late Cretaceous laterites and soil horizons known as the "alluvium and soil facies". Cretaceous sedimentary rocks have their

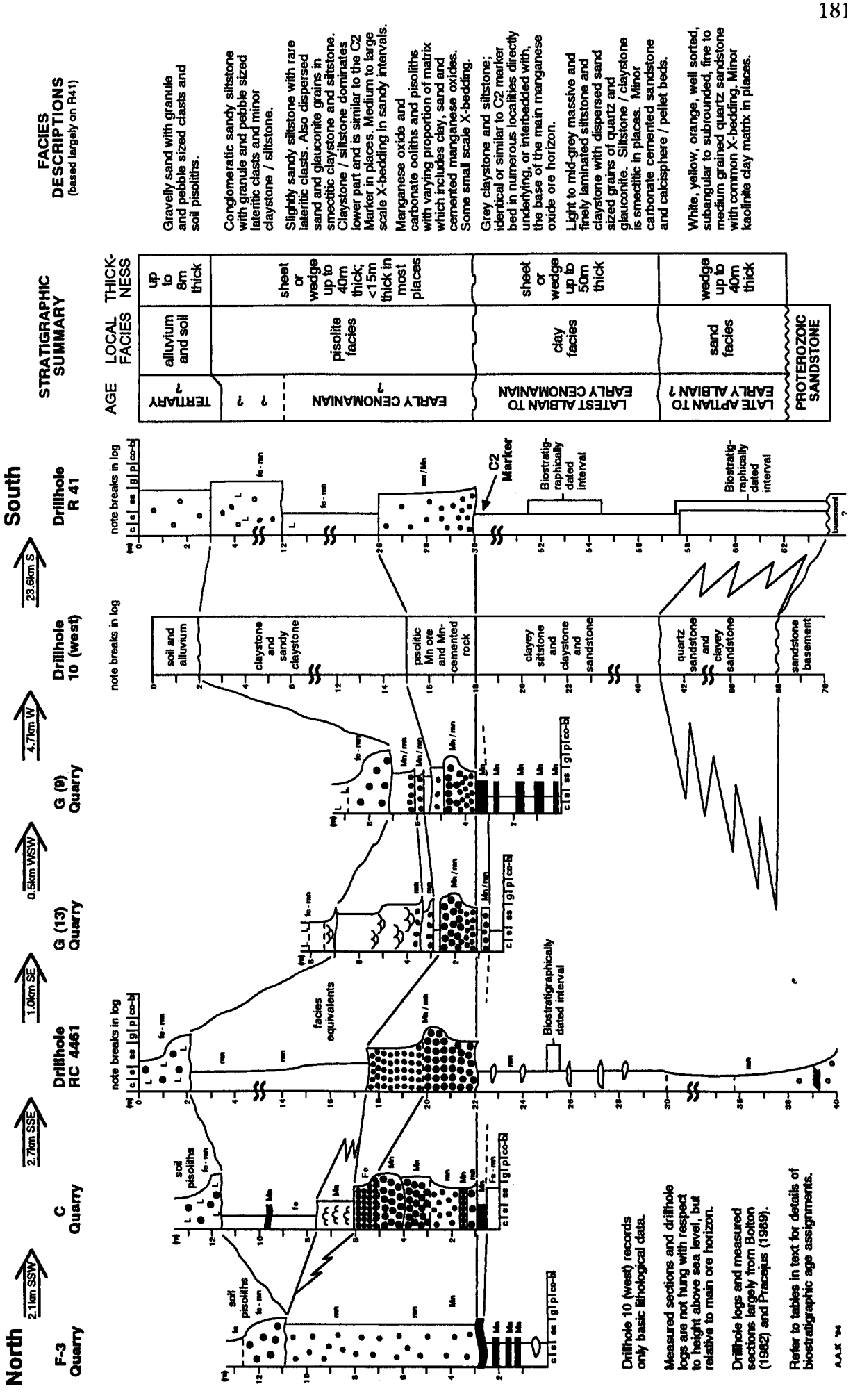

FIGURE 8.4. Stratigraphic correlation diagram of measured sections and drillhole sections through the Cretaceous sequence on Groote Eylandt. See Fig. 8.5 for location of sections.

greatest thickness of up to 100 m within two sub-basins on the western and southwestern parts of Groote Eylandt, which are separated by a prominent basement divide (Bolton, 1982).

Figure 8.4 illustrates the Cretaceous stratigraphy and correlation between important measured quarry-sections and drillholes on Groote Eylandt. The location of the drillholes and quarries is shown in Fig. 8.5. Only two of the drillholes (10 west and R 41) intersect basement, and most of the measured sections include only the pisolite facies and part of the underlying clay facies. The most important points to note from Fig. 8.4 are:

1) The basal sand facies thins markedly to the east and south, and commonly the lowest exposed Cretaceous rocks belong to the clay facies.
2) The clay facies directly underlies, and is sometimes interbedded with, the main ore horizon at the base of the pisolite facies.
3) There is good lateral continuity of normal and reverse graded intervals within the ore horizon, which allows confident correlation between quarry-sections and drillholes.
4) The thickness of the pisolite facies varies markedly due to erosion and formation of overlying soil horizons and laterites of the alluvium and soil facies. In particular, fine-grained rocks within the pisolite facies overlying the main ore horizon have highly irregular thicknesses and grain size across Groote Eylandt.

8.5.4 Correlation of Groote Eylandt drillholes with mainland outcrops

Correlation between the Mullaman Beds on the mainland and the Cretaceous sequence on Groote Eylandt is not obvious. Most facies successions on the mainland are thin and bounded by erosional or disconformable boundaries, whereas the successions on Groote Eylandt are much thicker and erosion between successive depositional episodes is less apparent in the more distal (palaeogeographical) marine setting of Groote Eylandt. However, recognition of the C2 marker bed in both the Groote Eylandt sequence and mainland outcrops during this study allows important lithostratigraphic and chronostratigraphic correlation between the two areas.

Some of the evidence for this regionally-significant correlation is presented in Fig. 8.4, but detailed supporting evidence from previous studies on Groote Eylandt is also presented. The main correlation is based on the nature of the upper part of the clay facies directly beneath the main ore horizon on Groote Eylandt. In numerous areas on Groote Eylandt, this upper part of the clay facies is composed of mid-grey silty claystone or claystone, and appears identical to the C2 marker bed on the mainland in terms of colour, grain size, composition, texture, sedimentary structures, and geochemistry (see Appendices 4, 6, and 7).

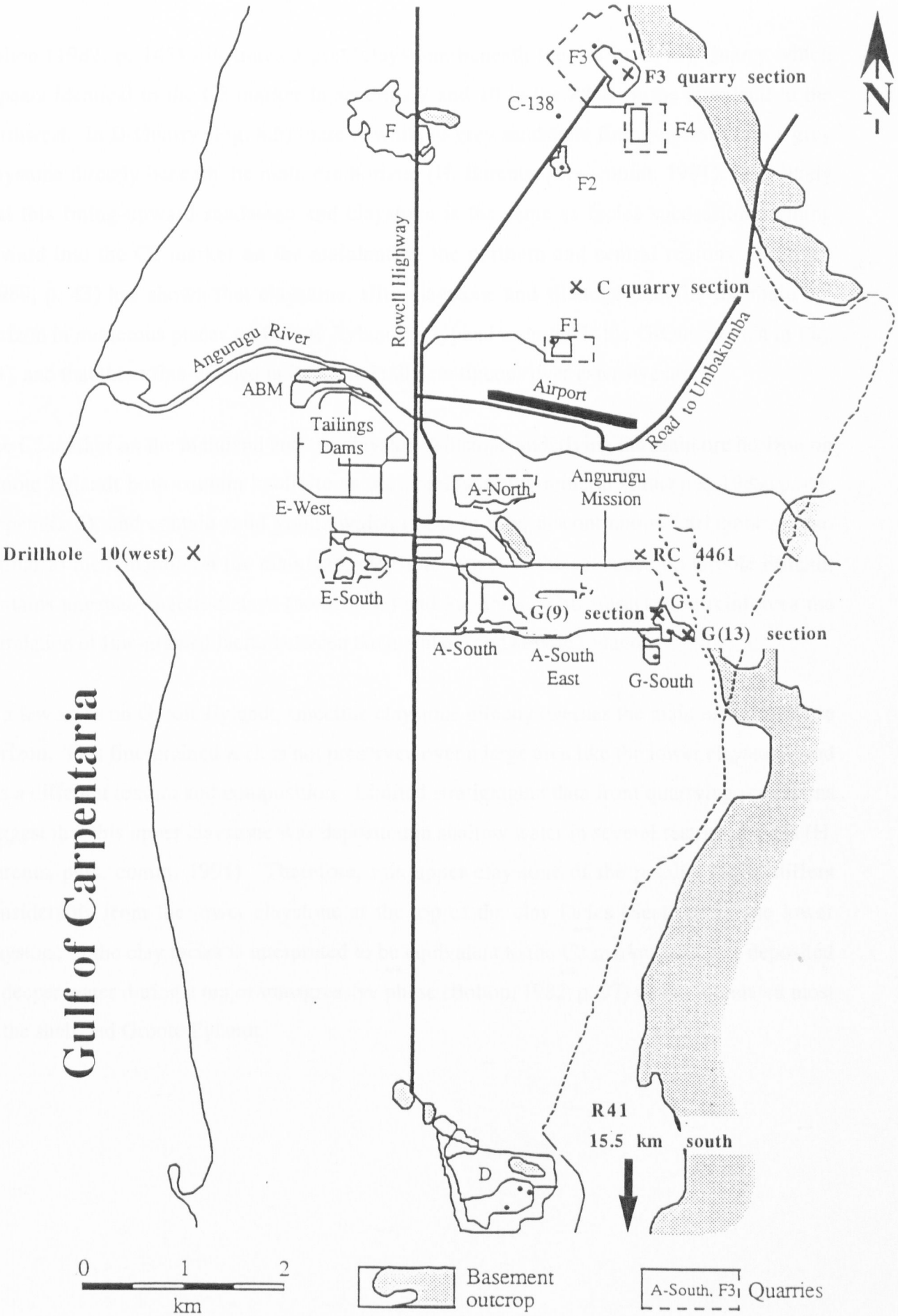

FIGURE 8.5. Location of stratigraphic drillholes and quarries on Groote Eylandt. Modified from Pracejus (1989).

Bolton (1982, p. 145) illustrates a grey claystone beneath the ore in G(13) Quarry which appears identical to the C2 marker in sections 7 and 10 in the ALZ on the mainland to the northwest. In D-Quarry (Fig. 8.5) there is white to grey sandstone fining-upward into a grey claystone directly beneath the main ore horizon (H. Barents, pers. comm. 1991). It is likely that this fining-upward sandstone and claystone is the same as facies succession 5 fining upward into the C2 marker on the mainland in the northern and central regions. Pracejus (1989, p. 43) has shown that claystone, silty claystone and siltstone underlie the main ore horizon in numerous places on Groote Eylandt (a typical example is the G-Quarry area in Fig. 8.4), and that these fine-grained units are laterally continuous over extensive areas.

The C2 marker on the mainland and the claystone/siltstone underlying the main ore horizon on Groote Eylandt both contain kaolinite as the dominant clay mineral (Pracejus, 1989, p. 43; Appendix 6), and contain sand grains which occur in thin, discontinuous "stringers". Also similar to the situation on the mainland, claystone lower in the sequence on Groote Eylandt contains unusual smectitic clays (nontronite) and kaolinite. This observation reinforces the correlation of fine-grained facies between the mainland and Groote Eylandt.

In a few areas on Groote Eylandt, smectitic claystone directly overlies the main manganese ore horizon. This fine-grained rock is not preserved over a large area like the lower claystone, and has a different texture and composition. Limited stratigraphic data from quarrying operations suggest that this upper claystone was deposited in shallow water in several restricted areas (H. Barents, pers. comm. 1991). Therefore, this upper claystone of the pisolite facies differs considerably from the lower claystone at the top of the clay facies (Sect. 10.5); the lower claystone of the clay facies is interpreted to be equivalent to the C2 marker, and was deposited in deeper water during a major transgressive phase (Bolton, 1982, p. 37) which inundated most of the shelf and Groote Eylandt.

8.5.5 Drillholes near Numbulwar (Rose River)

In 1971 the US Steel company conducted a drilling program in the area surrounding Numbulwar, near the coast on the mainland in the northern region and to the west of Groote Eylandt (Fig. 8.1). The objective of the program was to locate manganese mineralisation in a similar palaeogeographical setting to that of Groote Eylandt. Most of the holes were only drilled to shallow depth (< 38 m), and basement was not intersected. However, the stratigraphic information provided by this drilling program is very useful for four reasons:

1) Drillhole samples provide accurate biostratigraphic age zonations for the sequence in the drillholes and enable correlation with other areas, including outcrops in the study area.
2) The drillholes provide information in an area of very poor exposure, and fill in a gap of data which exists between the areas of good outcrop in the BPRZ and the central region.
3) The close spacing (~2 km) of the drillholes highlights subtle lateral and vertical proximality trends in grain size, the nature and extent of interbedding, and facies changes within the Cretaceous sequence that are commonly not evident in isolated "spot" outcrops.
4) They are the only closely spaced shallow drillholes on the mainland where Cretaceous rocks were cored successfully.

The stratigraphy, local correlations, and rock descriptions of the Numbulwar drillhole sequence are summarised in Fig. 8.6. There are two main Cretaceous rock types in the Numbulwar drillhole sequence. The basal part of the sequence is composed of massive and coarsening-upward silty claystone and siltstone, which contain an increasing number of thin, massive or graded sandstone interbeds towards the top of the unit. The upper part of the sequence is composed of stacked fining-upward clayey quartz sandstones. Figure 8.6 illustrates correlation between selected drillholes from the Numbulwar drilling program, and documents the lateral continuity of the main coarsening-upward and fining-upward facies successions. The boundaries between the various units in the drillholes were picked by detailed core-logging during the present study, in which particular attention was placed on subtle grain size variations and the nature of bedding contacts. The location of the drillholes is shown in Fig. 8.1, and details of the biostratigraphic data are presented in Tables 8.1, 8.2, and 8.4.

The basal part of the sequence is composed of one or two coarsening-upward cycles (Fig. 8.6, RR 21) which are identical in thickness, grain size, texture, sedimentary structures, clay mineralogy, and overall vertical morphology to facies succession 1 in outcrop in the southern region. Paltech (1981c) originally suggested that the basal fine-grained, coarsening-upward part of the drillhole sequence reflected "sedimentation under restricted, marginal marine

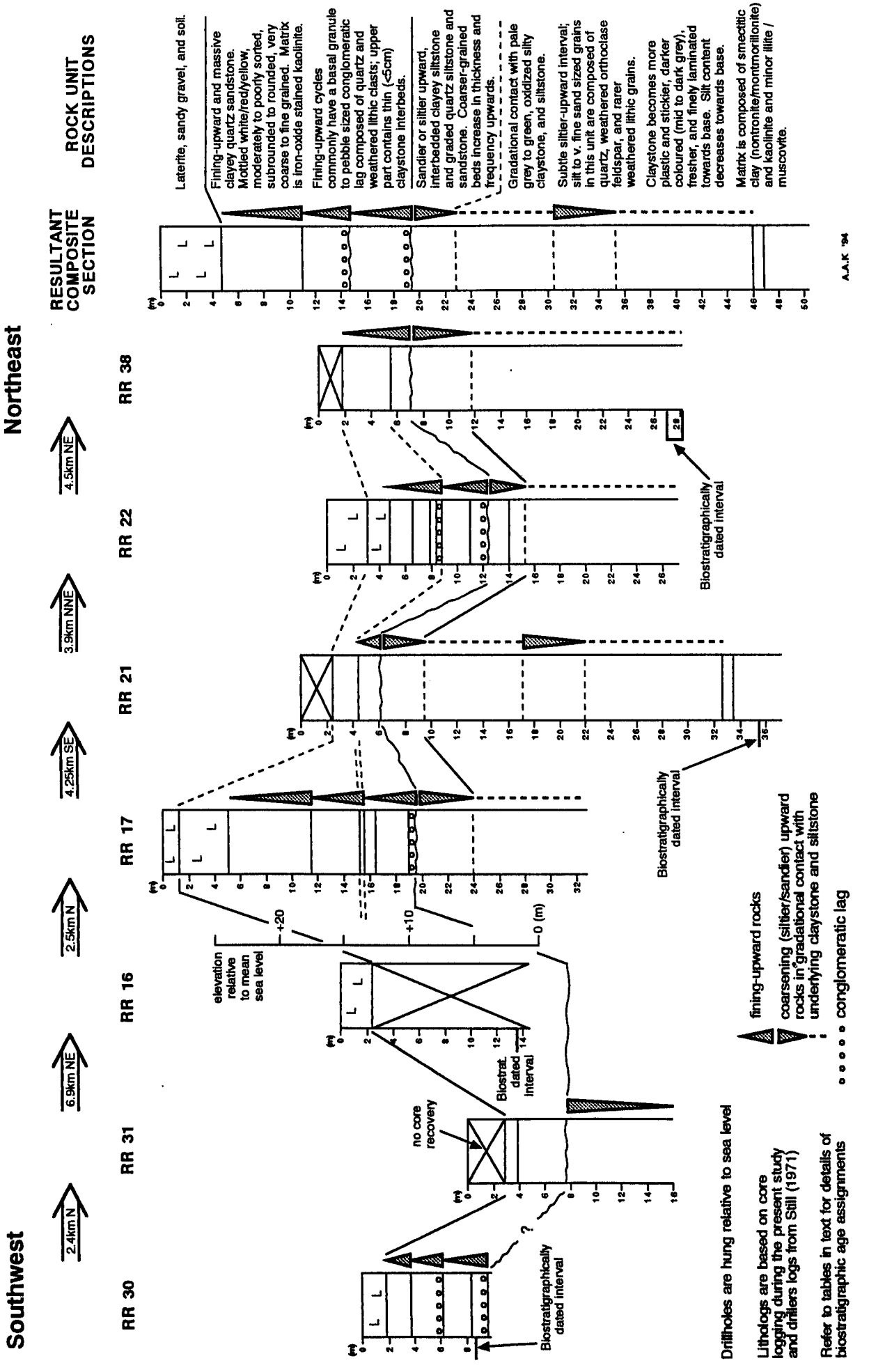

FIGURE 8.6. Stratigraphic correlation diagram of US Steel Inc. drillholes near Numbulwar in the northern region. See Fig. 8.1 for location of drillholes.

influence; possibly intertidal, delta front conditions in a situation distal to stream discharge". However, palaeoenvironmental analyses based on microfossil content and re-examination of the cores during this study suggest that the unit was deposited under relatively deep-water marine conditions, sufficiently distant from the land to receive very little in the way of land-plant debris, spores and pollen (Alley, 1991; Martin, 1982). These palaeoenvironmental parameters correspond closely to the depositional setting envisaged for facies succession 1; that is, the offshore shallow-marine zone beneath fair weather wave base and beyond the reach of most deltaic processes. There is a general decrease in grain size to the northeast in the Numbulwar drillhole sequence, and the preserved thickness of the basal coarsening-upward claystone/siltstone succession increases markedly offshore to the east, as would be expected for progressively more distal marine deposition on the shelf.

Coarsening-upward rocks of facies succession 1 are unconformably overlain in the drillhole sequence by fining-upward coarse- to medium-grained quartz sandstone. This sandstone commonly has a conglomeratic lag at its base (*e.g.* Fig. 8.6, RR 17 / 22), and grain size decreases upward as clay content increases upward above the conglomeratic lag. In all respects this lowest fining-upward cycle is similar to deposits of facies succession 5 seen in outcrop in the northern and central regions.

One or two distinct fining-upward cycles occur at higher levels (Fig. 8.6, RR 17 / 22 / 30). These cycles are finer grained, have better sorting, have a greater silt- and clay-sized component, and exhibit prominent parallel bedding and flat lamination. The upper stacked fining-upward cycles show a subtle decrease in average grain size to the northeast, and are very similar to deposits classified as facies succession 4 in outcrop exposures in the distal part of the central region, and in the southern region.

The texture and composition of fining-upward sandstones in the upper part of the Numbulwar drillhole sequence points to a marine depositional environment, and these sandstones have been interpreted as deposits of facies successions 4 and 5. There is no evidence within these sandstones for subaerial exposure, coal or peat formation, or very shallow-water tidal processes as inferred by Paltech (1981c). Furthermore, fining-upward sandstones in the upper part of the Numbulwar drillhole sequence contain microfossils and rare macrofossils (Tables 8.1 and 8.2) which prove their marine origin.

8.5.6 Correlation of Numbulwar drillholes with mainland outcrops

A composite section of the Numbulwar drillhole sequence, based on stratigraphic observations above, is illustrated in Fig. 8.6. The basal half of the sequence is composed of one or two coarsening-upward deposits of facies succession 1, with a total thickness of about 30 m (Fig. 8.6). Fining-upward sandstones of facies succession 4 and/or 5 overlie succession 1 with a disconformable contact which is defined locally by a conglomeratic lag. The combined thickness of the fining-upward sandstones is approximately 15 m, and the contact between the lower two fining-upward sandstone successions is also locally disconformable. This same stratigraphy is recognisable in outcrop in both proximal (*e.g.* Fig. 7.7, section 118) and distal (*e.g.* Fig. 7.3, section 96) parts of the southern region, and similar deposits occur in the distal part of the central region. Therefore, on the basis of lithostratigraphy the Numbulwar drillhole sequence can be correlated with composite outcrop sections in the central and southern regions.

In addition to the above lithostratigraphic similarities, biostratigraphic analyses have proven the age equivalence of the Numbulwar drillhole sequence and outcrops in the southern region. Microfossil analyses of the Numbulwar drillhole sequence have shown that the age of rocks of facies succession 1 in the basal half of the sequence is middle Albian and younger (Tables 8.1, 8.2, 8.4). Microfossil analyses from outcrops in the southern region yielded an age of late early Albian to late Albian for rocks of facies succession 1 (Table 8.4), and thus permit a positive biostratigraphic correlation with the thick deposits of facies succession 1 in the Numbulwar drillhole sequence, over 300 km to the north.

Correlation of the Numbulwar drillhole sequence with mainland outcrops is also possible using geochemical criteria; both mainland outcrops and Numbulwar drillcore samples contain unusual smectitic clays (nontronite and montmorillonite) as matrix, and significant amounts of orthoclase feldspar as small grains. These two components are not present together in any other unit of the Mullaman Beds, and provide a useful way to distinguish between this succession and various other fine-grained units. This is the only known case where geochemistry facilitated reliable correlation within the Mullaman Beds. The significance of these clay minerals is discussed in Sect. 10.5.

8.6 INTEGRATION OF THE STRATIGRAPHIC DATA: A STRATIGRAPHIC FRAMEWORK FOR THE SHELF

In this section all the stratigraphic data from the Mullaman Bed shelf and Groote Eylandt is used to erect a stratigraphic framework for the entire shelf. This framework is based on lithostratigraphy and biostratigraphy and documents all regional correlations and the ages of Cretaceous successions in the various parts of the study area. The correlations between composite outcrop sections and drillholes are illustrated in Fig. 8.7, which is a synthesis of the large amount of stratigraphic data presented earlier in this chapter (see Figs. 8.2, 8.4, and 8.6) and in preceding chapters. Some of the details have been discussed previously, and only the major points and conclusions are presented here.

8.6.1 Regional stratigraphic correlation of facies successions

Some individual facies successions (*e.g.* succession 5) occur at more than one stratigraphic level within the Mullaman Bed shelf sequence, and reflect duplication of conditions at different times during the depositional history of the shelf. Given this stratigraphic repetition within the shelf sequence, it is important to be able to place these rocks into the correct stratigraphic order by the use of marker beds and biostratigraphic zones (*e.g.* Haig's, 1979b scheme).

The C2 marker is the only areally extensive lithological unit in the study area which can be used as a marker bed. It is distinctive and easily recognisable amidst surrounding coarser-grained facies due to its hardness (silica cement) and resistance to weathering in outcrop. The C2 marker is flat-lying, has the same thickness (~2 m) over an enormous area, and is considered to represent a single time interval across the shelf.

The C2 marker is recognised throughout the northern region, on Groote Eylandt (where it is not silicified), and in the northern proximal part of the central region over a distance of at least 380 km (Fig. 8.2). However, south of about latitude 14^0 S in the southern part of the northern region, the C2 marker is rarely present; it is absent near the coast in the Numbulwar drillhole sequence at latitude 14^0 15' S, but is present as erosional remnants southward until about latitude 15^0 35' S in the central region.

There is an increase in the amount of erosion towards the south, so that the C2 marker bed and underlying rocks of succession 5 thin in that direction. Neither the C2 marker bed nor the immediately underlying shoreface deposits of succession 5 are present in the southern region.

SHELF-WIDE STRATIGRAPHIC FRAMEWORK

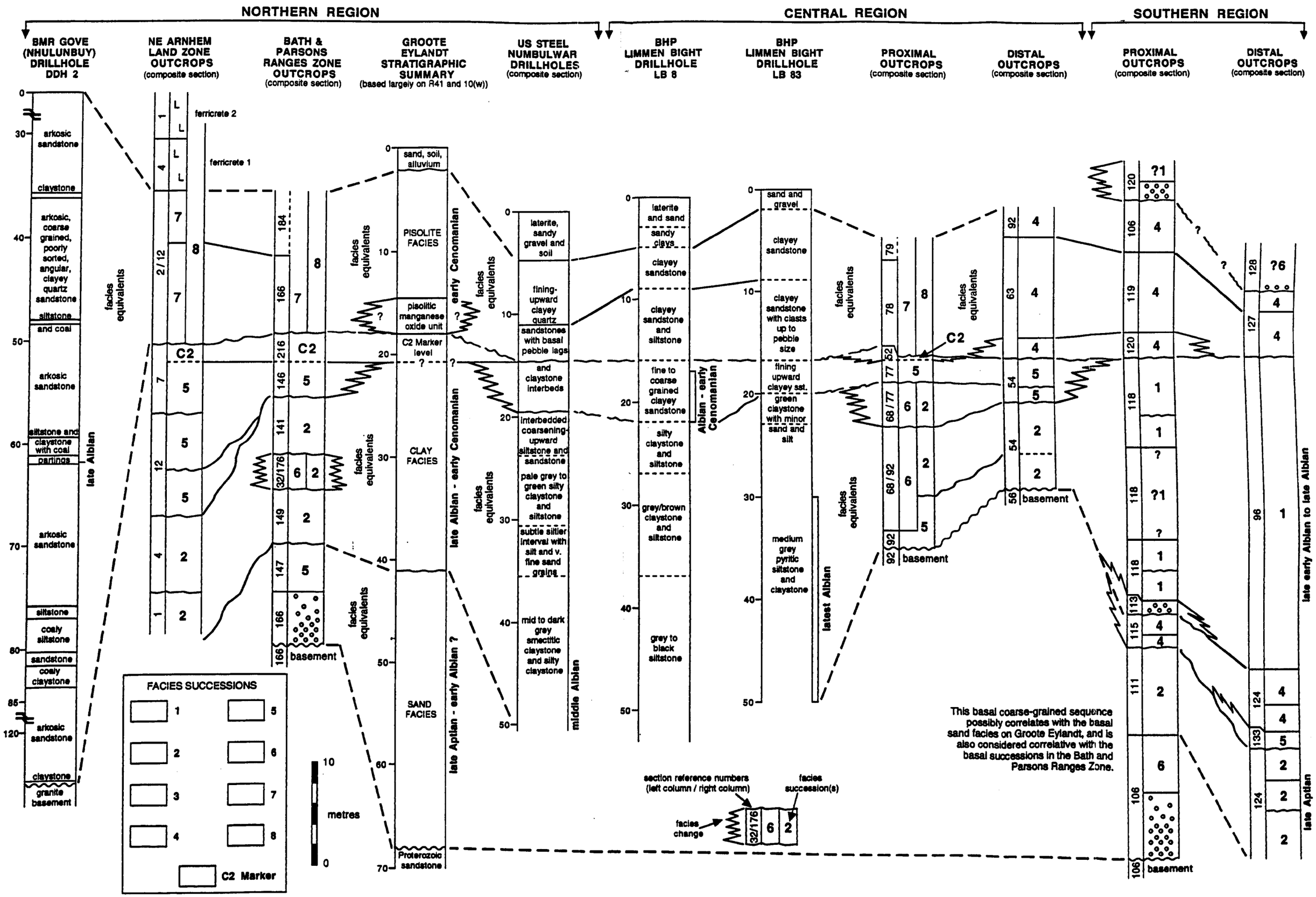

FIGURE 8.7. Stratigraphic framework for the western and southwestern shelf of the Carpentaria Basin.

However, it is possible to trace the C2 marker stratigraphic level into the southern region by comparing stratigraphic relationships in the southern region with the distal part of the central region, where the shoreface succession underlying the C2 marker is present. The absence of shoreface sandstones of facies succession 5 in the southern region reflects non-deposition and the position of the shoreface landward of the southern region, rather than thinning due to erosion.

In Fig. 8.7 all drillholes and composite sections are hung relative to the C2 marker interval. Assuming that this datum is correctly correlated, then Fig. 8.7 illustrates that the depth to basement varies greatly across the shelf. Figure 8.7 shows that basement is significantly higher in the central region, and consequently the Cretaceous sequence is much thinner here than on other parts of the shelf. In general, the basement topography becomes more obvious to the west where basement units are exposed and progressively younger marine rocks of the Mullaman Beds onlap basement terrain.

Further evidence for an irregular basement topography is given by the irregular exposure of basement highs across the region, and by the varying thickness of the Cretaceous sequence and depth to basement measurements in drillholes across the shelf. In the northern region, the Nhulunbuy drillhole logs indicate that the basement topography varies by as much as 123 m over a lateral distance of less than 5 km (Dodson, 1967). Seismic lines offshore from the northern and central regions also show irregular basement topography on the western shelf of the Carpentaria Basin (Burgess, 1984; Thomas *et al.*, 1992).

8.6.2 Age of facies successions of the Mullaman Beds

The oldest reliable age defined for the Mullaman Beds by biostratigraphy is mid Aptian, and represents a sample from the base of drillhole LB 54 (Table 8.2) near the Yiyintyi Range in the central region. This dated stratigraphic level cannot be accurately correlated with outcrops from the present study due to a lack of adequate stratigraphic information for the drillhole. However, this age is likely to represent rocks near the base of the Mullaman Beds which occupy lows in the basement topography to the east of the Yiyintyi Range; a proposition which is supported by recent drilling in the area (H. Barents, pers. comm. 1994).

An age of late Aptian was defined by biostratigraphy in the present study for rocks near the base of the exposed Mullaman Beds in the distal part of the southern region. It is inferred by correlation (Fig. 8.7) that basal normally-graded conglomerate and sandstones of successions 2

and 6 in the BPRZ and the southern region are late Aptian or older in age. The basal conglomerate in these regions is possibly somewhat older than late Aptian, and may represent a long period of nonmarine erosion during the Early Cretaceous (early Aptian?).

In the northern and southern regions, thin sandstones of succession 4 and 5 overlie the thick basal conglomerate and/or late Aptian sandstones. These successions are considered to be equivalent to the sand facies on Groote Eylandt, and are probably early Albian in age. Disconformably overlying these ?early Albian sandstones are thick deposits of sandstone and siltstone of facies succession 1 and 2. In the Numbulwar and Limmen Bight drillholes (between depths of ~20 to 50 m), and the southern region, rocks at this stratigraphic level belong to facies succession 1. In more proximal areas including the ALZ and BPRZ and the central region rocks of the same age belong to facies succession 2. Fine-grained rocks of the clay facies on Groote Eylandt are also considered equivalent to these facies successions (Fig. 8.7). The total thickness of these rocks is consistently about 30 m in distal areas (Fig. 8.7, the three drillholes and the southern region) and about 10-12 m in proximal areas (Fig. 8.7, northern and central regions).

The age of this interval is defined by several biostratigraphic analyses; late early Albian to late Albian in southern region outcrops; middle Albian at the base of the interval in the Numbulwar drillholes; latest Albian in drillhole LB 83 (Sect. 8.2). Therefore, by correlation (Fig. 8.7), the age range of these thick stacked marine rocks of successions 1 and 2 is late early Albian to latest Albian. This correlation is very significant and documents the long time interval of high relative sea level and marine deposition throughout much of the Albian.

Thick Albian marine rocks of successions 1 and 2 are disconformably overlain on the shelf by fining-upward shoreface rocks of succession 5 (except in the southern region). These shoreface sandstones are only locally present on Groote Eylandt, and wedge-out towards the southeast in the distal part of the central region. Their age is defined as latest Albian to early Cenomanian by biostratigraphic dating of samples in drillhole LB 8. The upper fining-upward shoreface succession 5 grades up into the C2 marker, which is dated as latest Albian to early Cenomanian on Groote Eylandt. Thus, the age range for shoreface sandstones and the overlying C2 marker is latest Albian to early Cenomanian.

In most parts of the shelf, except the northern region and the proximal part of the central region, thick marine sandstones of facies succession 4 overlie the C2 marker stratigraphic level with disconformity (Fig. 8.7). These rocks must be younger than latest Albian to early Cenomanian,

and are considered to be equivalent to the pisolite facies on Groote Eylandt of early Cenomanian age. The same age is proposed for equivalent rocks of facies succession 7 and 8 in the northern region and proximal outcrops in the central region. A minimum age for the top of these successions is unknown, but is unlikely to be younger than Cenomanian because marine deposition was terminated when the sea retreated from the shelf in the latter part of the Cenomanian (Sect. 9.7.6).

In the upper part of the Cretaceous sequence in the southern region there are several outcrops of conglomerate and overlying siltstone and sandstone which are incised into rocks of succession 4 (probable early Cenomanian age). These are probably the youngest rocks seen in outcrop, besides weathering horizons, but their exact age is unknown. These rocks represent paralic and nonmarine depositional environments, and were probably deposited in basinal areas during the final retreat of the sea in the Cenomanian-Turonian (*cf.* Dettmann *et al.*, 1992).

However, in inland parts of the northern region it is likely that nonmarine deposition occurred from at least the late Albian into the early Cenomanian. In Nhulunbuy drillhole DDH 2, the middle part of an approximately 125 m thick nonmarine sequence was dated as late Albian. Judging by the large thickness of these fluvial and lacustrine rocks it is likely that nonmarine deposition occurred over a long time period, possibly from the Aptian through to the Cenomanian (and younger). The nonmarine rocks in the Nhulunbuy drillholes are facies equivalents to rocks of succession 7 in surrounding outcrops in the northern region. The age of nonmarine deposits in outcrop has been documented as being younger than latest Albian to early Cenomanian, and so succession 7 in outcrop is probably only contemporaneous with the upper part of the nonmarine Nhulunbuy drillhole sequence. Ferricretes and soil horizons at the top of the Cretaceous sequence (best developed in the northern region) are probably Tertiary in age, although some weathering profiles are thought to have formed in the Late Cretaceous on the basis of stratigraphic correlation (Bardossy and Aleva, 1990; Grubb, 1970) and palaeomagnetic evidence (unpublished data, M. Idnurm, pers. comm. 1994).

8.7 SHELF-TO-BASIN REGIONAL CORRELATION: STRATIGRAPHIC TIES TO THE GREAT ARTESIAN BASIN

In this section stratigraphic correlations between the Mullaman Bed shelf sequence and the central Carpentaria Basin sequence are proposed. The correlations are based on information from seven deep stratigraphic drillholes, five of which are located onshore in the distal part of the southern region (Fig. 8.1), and two towards the central part of the Carpentaria Basin

(offshore). Correlation between most of the seven drillholes and other drillholes in the Carpentaria and Eromanga Basins is well established, and these correlations (Fig. 8.7) are based on descriptions and stratigraphic ties in Meyers (1969), Passmore (1979), Smart (1976), and Smart *et al.* (1980).

Correlation from the shelf to the basinal Cretaceous sequence in these drillholes is important in this study because the drillhole sequence has good biostratigraphic age control. Regional ties to the deep drillhole stratigraphy are also important because the stratigraphy of the drillhole sequence is continuous to the south across the Euroka Arch into the Eromanga Basin, to the north across the Merauke Rise into the Papuan Basin, and is also in probable lithologic continuity around the northern end of the Peninsula Ridge with the coastal Laura, Styx, and Maryborough Basins (Morgan, 1980). Thus, in effect, correlation from the shelf to the seven deep drillholes also documents important inter-basinal stratigraphic ties throughout northern Australia.

8.7.1 Carpentaria Basin shelf-to-basin regional correlation

Figure 8.8 illustrates the stratigraphic relationships of Precambrian through Quaternary sediments in the Carpentaria Basin. Detailed descriptions of the age and lithology of major rock units of the Carpentaria Basin (*e.g.* Wallumbilla Formation) are presented in the discussion of the Carpentaria Basin stratigraphy in chapter 2.

There is an obvious trend of rapid shallowing of basement to the west onto the shelf, so that Cretaceous rocks in outcrop and in Westmoreland # 2 and # 3 directly overlie Precambrian basement (Fig. 8.8). Palaeozoic rocks (unnamed) and Jurassic rocks (Gilbert River Formation) thin rapidly to the west, and are generally considered not to occur on the Mullaman Bed Shelf (*cf.* Meyers, 1969). However, the overlying thick Cretaceous sequence of the Rolling Downs Group (Wallumbilla Formation, Toolebuc Formation, Allaru Mudstone, and Normanton Formation) continue onto the Mullaman Bed shelf, and are equivalent in age to outcrops in this study.

8.7.2 Correlation between deep stratigraphic drillholes

The Toolebuc Formation is the key stratigraphic unit for correlation in the central Carpentaria Basin because it is thin, lithologically and geochemically distinctive, and because it separates the two, monotonous, very thick shales of the Wallumbilla Formation and Allaru Mudstone. In the

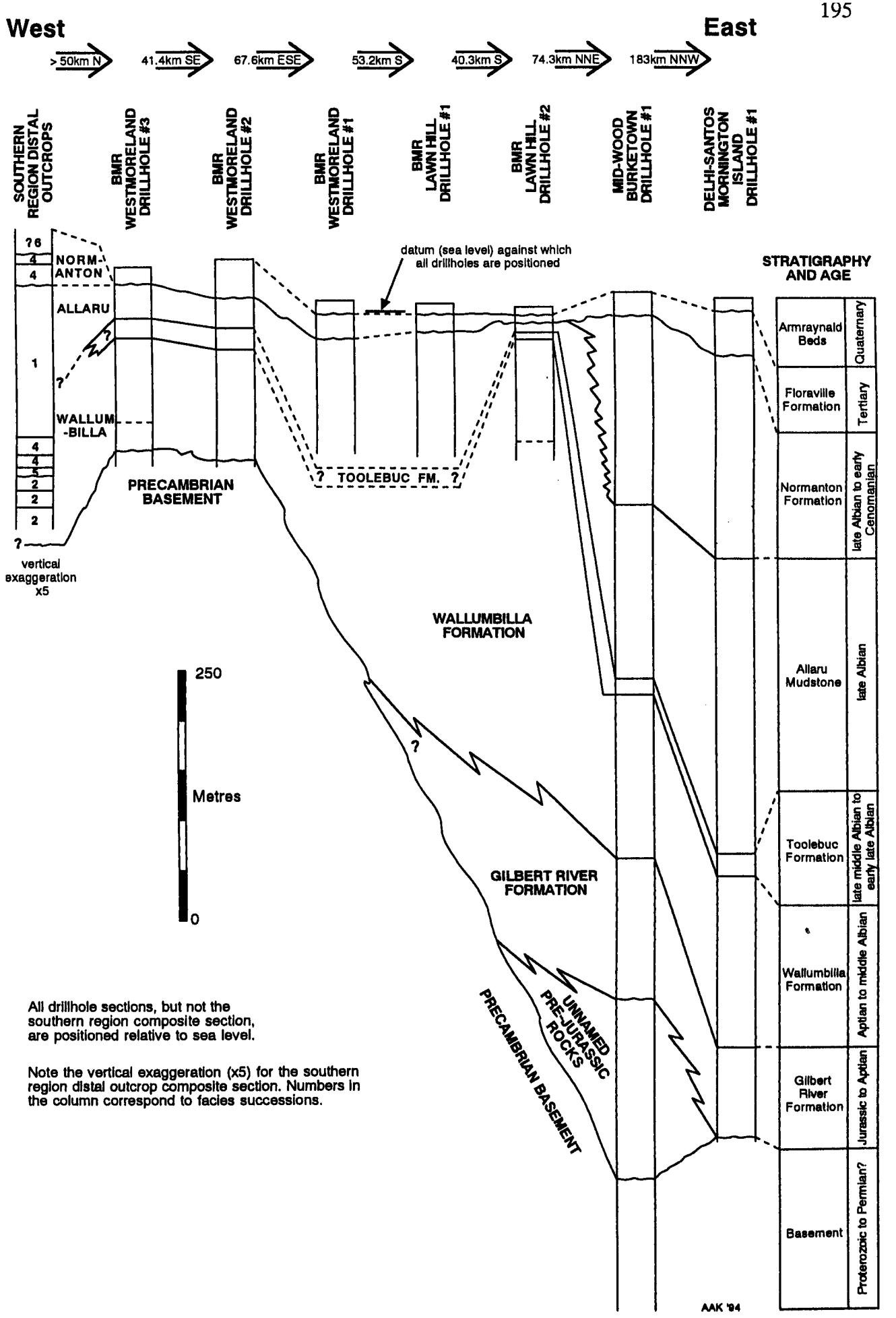

FIGURE 8.8. Shelf-to-basin regional correlation: correlation of the most southeasterly (distal) composite section of this study with deep stratigraphic boreholes along an approximate W-E line.

absence of the Toolebuc Formation, it is often very difficult to distinguish between these two shale sequences due to their lithological similarity and the lack of precise biostratigraphic control through the shale sequence.

Figure 8.8 clearly shows this situation: in five of the drillholes (Westmoreland #2 and #3, Lawn Hill #2, Burketown #1, and Mornington Island #1) the Toolebuc Formation was recognised, and the separation of the Wallumbilla Formation from the Allaru Mudstone is obvious. However, in Westmoreland #1 and Lawn Hill # 1 the Toolebuc Formation was not recognised, and hence correlation is more problematic. Needham *et al.* (1971) propose that the Toolebuc Formation was not intersected in these two drillholes and presumably lies at greater depth in the basin. To support their interpretation they relied on palynological analyses of the thick basal siltstone from Westmoreland #1, which were "largely inconclusive but suggested a post-Toolebuc age", *i.e.* Allaru Mudstone age (Needham *et al.*, 1971, p. 13). Palynological analyses from Lawn Hill # 1 are similar and also suggest a post-Toolebuc age on the basis of comparison with microfloras of the Eromanga Basin (Needham *et al.*, 1971) .

The stratigraphy of Westmoreland # 2 and #3, closest to outcrops of the Mullaman Beds in the southern region, is well-defined. Both the Wallumbilla Formation and Allaru Mudstone are present, and are separated by the Toolebuc Formation. Gibson *et al.* (1973) suggest that the Normanton Formation is missing through erosion, and that the Tertiary Floraville Formation disconformably overlies the Allaru Mudstone. Comparison with other drillholes in Fig. 8.8 and Meyers (1969) shows that the Normanton Formation is present in many drillholes in the Carpentaria Basin, but was removed by Tertiary erosion in places.

8.7.3 Correlation between deep drillholes and Mullaman Bed outcrops

The age-range of the exposed Mullaman Beds in the southern region (and the rest of the shelf) has been documented in this thesis as late Aptian to early Cenomanian. Comparison with the ages of various formations within the basinal sequence suggests that the Mullaman Beds are equivalent to the stratigraphic interval represented by the upper Gilbert River Formation and the Rolling Downs Group. Correlations between southern region outcrops and the basinal strata are illustrated in Figs. 8.3 and 8.8.

In the Mullaman Bed shelf succession the oldest exposed rocks are thick conglomerates which grade up into paralic and marine facies. The exact age of these successions is unknown, but they are older than late Aptian. These successions may be equivalent in part to the Gilbert River

Formation, and may be Early Cretaceous in age. Previous correlations (*e.g.* Meyer, 1969) suggest that the Gilbert River Formation does not extend west onto the shelf (Fig. 8.8), but it is likely that isolated remnants of the formation occur near the base of the Cretaceous shelf sequence in topographic lows. Rock exposures have been mapped as Gilbert River Formation on the central parts of the Lawn Hill 1:250,000 geological map (Hutton and Grimes, 1983), and these exposures are close to outcrops of the Mullaman Beds in the southern region. The base of the sequence in the BPRZ and proximal part of the southern region (Fig. 8.3) also have similarities with the Gilbert River Formation in terms of lithology and depositional environments.

Coarsening-upward sandstones overlying these rocks on the shelf have been dated as late Aptian and belong to the *Bigenerina pitmani* Zone (Haig, 1991). Judging by the biostratigraphic zonations of Haig (1979b), this interval corresponds to the lower Wallumbilla Formation, which is quite sandy in places. In the southern region these units are overlain by up to 8m of fining-upward siltstones and sandstones. The exact age of these facies is unknown, but they have been correlated in the present study with the sand facies on Groote Eylandt (Fig. 8.7, late Aptian to early Albian ?) and overlie late Aptian units. Given this age range, this stratigraphic interval of the Mullaman Beds corresponds to the lower to middle Wallumbilla Formation.

The overlying rocks on the southern region of the shelf are 30 m-thick siltstones and claystones of late early Albian to late Albian age, which belong to the *Riyadhella crespinae* Zone (Haig, 1991). According to Haig (1979b), this biostratigraphic zone covers the upper Wallumbilla Formation, Toolebuc Formation, and the Allaru Mudstone in the western Carpentaria Basin. The age of this interval in the central and northern regions is defined more accurately as middle Albian to latest Albian by comparison with palynological zones from the Numbulwar and Limmen Bight drillholes (Alley, 1991; Martin, 1982). Thus, the base of the 30 m-thick shelf succession probably corresponds to the Wallumbilla Formation, whilst the top of the 30 m-thick succession probably corresponds to the Allaru Mudstone.

Significantly, the Toolebuc Formation was not recognised anywhere on the shelf, and there are no bituminous and calcareous units within the Mullaman Beds that are obvious candidates as shelfal equivalents of this formation. Judging from correlation in this thesis the Toolebuc Formation does not extend onto the Mullaman Bed shelf. Other workers have noted the absence of the Toolebuc Formation at the margins of the Carpentaria Basin, and Haig and Lynch (1993) state that at latitudes north of 16^0 S the Wilgunya Subgroup cannot be subdivided

into formations (Wallumbilla versus Allaru) due to the absence of the lithologically distinctive Toolebuc Formation.

In the absence of the Toolebuc Formation on the Mullaman Bed shelf, the stratigraphic level of the contact between the Wallumbilla Formation and Allaru Mudstone is thought to occur somewhere within the 30 m-thick fine-grained succession (Sequence *III*) in the southern region (Figs. 8.3 and 8.8). I propose that this contact probably lies towards the base of the 30 m succession, because in drillhole LB 83 most of the succession is dated as latest Albian (Fig. 8.7).

On the shelf in the southern region, the 30 m-thick succession is disconformably overlain by up to 15 m of fine-grained sandstone and siltstone of facies succession 4. The age of these rocks is considered to be early Cenomanian (Fig. 8.7), and therefore they probably correspond to the Normanton Formation. The age of the Normanton Formation is late Albian to early Cenomanian (Burgess, 1984), and the base of this unit is erosional and represents a large regressive episode in the Carpentaria Basin (Morgan, 1980). The Normanton Formation is exposed in large areas on the southern part of the Burketown 1:250,000 geological map (Ingram, 1972) to the east of the southern region, but is not shown farther to the west.

The age-range of late Albian to early Cenomanian reported for the Normanton Formation is the same as the age of the C2 marker and underlying shoreface sandstones in the northern and central regions of the shelf (Fig. 8.7). However, I propose that the C2 marker bed and underlying fining-upward sandstones correspond to the transgressive Allaru Mudstone, whilst overlying fluvial and restricted marine rocks of successions 7 and 8 (early Cenomanian, Fig. 8.7) correspond to the regressive Normanton Formation.

Thus, in the northern region and proximal central region of the shelf, the C2 marker probably corresponds to the top of the Allaru Mudstone, and is incised by fluvial and nonmarine rocks equivalent to the Normanton Formation. Farther offshore on the shelf in the southern region, fine-grained marine rocks of succession 4 are equivalent to the Normanton Formation and disconformably overlie the 30 m-thick succession, the upper part of which is considered correlative with the upper Allaru Mudstone.

8.8 CHAPTER SUMMARY

The age of the Mullaman Bed shelf sequence has been defined by biostratigraphy and lithostratigraphic correlation in this study. Although there are only a few intervals that are precisely biostratigraphically dated, integration of these data in a stratigraphic framework provides broad age control for the entire shelf sequence.

Cretaceous rocks in mainland drillholes and on Groote Eylandt are confidently correlated, although these stratigraphic ties are not obvious without detailed stratigraphic analysis of numerous "spot" outcrops on the mainland. The Mullaman Bed stratigraphic scheme constructed in this thesis agrees in part with the previous scheme of Skwarko, but diverges and provides far more comprehensive and systematic stratigraphic ties to surrounding rocks of the Carpentaria Basin.

The base of the exposed shelf sequence is nonmarine and probably corresponds to the Gilbert River Formation. Overlying these units are late Aptian sandstones which are equivalent to the lower Wallumbilla Formation, and other marine successions which are probably equivalent to the lower to middle Wallumbilla Formation. The overlying 30 m-thick deposits of succession 1 or 2 of late early Albian to late Albian age are equivalent to the upper Wallumbilla Formation and the Allaru Mudstone. The Toolebuc Formation has no equivalent within the Mullaman Beds. The upper part of the Allaru Mudstone is represented on the shelf by the C2 marker, and the C2 marker corresponds to the top of the clay facies, underlying the ore horizon, on Groote Eylandt. Overlying nonmarine and marine deposits at the top of the Cretaceous shelf sequence are equivalent to the Normanton Formation of early Cenomanian age. The Cretaceous sequence is capped by ferricretes, duricrusts, and lateritic soil profiles probable Tertiary age.

~~~~~~
~~~~~~

9. SEQUENCE STRATIGRAPHY OF THE WESTERN CARPENTARIA BASIN

9.1 INTRODUCTION

This chapter is designed to analyse the Cretaceous sediments on the Mullaman Bed shelf with regard to major regional erosion surfaces and the large-scale sequences bounded by these surfaces. The nature, extent, thicknesses, duration, and lateral and vertical variations of these sequences and their bounding surfaces are documented. Discussion and interpretation of the origin and significance of these sequences follows, and is linked to previous and current studies of sea level fluctuation (relative and eustatic) and depositional processes in analogous shallow-marine shelf settings.

Sequence stratigraphy is the alternate model used to describe and interpret the depositional history and depositional processes of the Carpentaria Basin shelf. In this chapter the approach to the sedimentological and stratigraphic problems is from a different perspective to previous chapters, but relies heavily on the prior lithostratigraphic component of the study.

9.2 CONCEPTS, DEFINITIONS, AND RATIONALE FOR THIS CHAPTER

Besides classical lithostratigraphy there are essentially three main conceptual models for dividing and analysing outcrops of shallow-marine sedimentary rocks and sediments. The three concepts or models are *sequence stratigraphy* (Posamentier *et al.*, 1988; Posamentier and Vail, 1988; Vail *et al.*, 1977; Van Wagoner *et al.*, 1990), *genetic stratigraphic sequence analysis* (Galloway, 1989), and *allostratigraphy* (see review in Walker, 1992, p. 9). In these three models change in relative sea level controls sequence development and is considered to be related to changes in one or more of the following processes; eustatic sea level, the rate of sediment supply, and the rate of subsidence.

In essence, sequence stratigraphy and genetic stratigraphic sequence analysis are similar, the main difference being that in sequence stratigraphy (the Exxon Production Research model) unconformities are defined as the sequence boundaries, whereas in genetic stratigraphic sequence analysis (Galloway's model) maximum marine flooding surfaces are defined as the

sequence boundaries. Allostratigraphy is also similar to sequence stratigraphy but is more flexible, in that any type of bounding discontinuity (*e.g.* unconformity, flooding surface, disconformity) can be used as the sequence boundary (Walker, 1990).

In outcrops of the Mullaman Beds on the Carpentaria Basin shelf the most obvious regional sequence-bounding discontinuities are unconformities, whereas maximum marine flooding surfaces are less obvious and more difficult to trace laterally over large areas. In this sense genetic stratigraphic sequence analysis is not as readily applicable to the Mullaman Beds as either of the other 'sequence models'.

The principles and techniques of allostratigraphy can be applied to the Mullaman Beds, and the geological setting, thicknesses and style of cycles and sequences within the Mullaman Beds are similar to those documented in other allostratigraphic studies (*e.g.* Bhattacharya and Walker, 1991; Martinsen *et al.*, 1993; Plint and Norris, 1991). However, in stark contrast to the settings of previous allostratigraphic studies, there is a lack of precise biostratigraphic control on an outcrop scale in the Mullaman Beds. There is also little detailed subsurface data to link individual allomembers/parasequences/cycles/successions seen in outcrop to regional sandbody geometries and stacking patterns which are best documented by subsurface correlation. Allostratigraphy, as noted by Martinsen *et al.* (1993), is generally a more descriptive model and does not have the predictive potential of the sequence stratigraphic model.

In view of the detailed description of rocks already accomplished using lithostratigraphy (chapters 3-8), the sequence stratigraphic model is considered to be the most useful for this study. Another reason for choosing sequence stratigraphy would be the current wealth of detailed sequence stratigraphic studies in the published literature, and the numerous papers and texts (*e.g.* papers in C.K. Wilgus *et al.*(eds.), 1988; Van Wagoner *et al.*, 1990) dealing with sequence stratigraphy and problems inherent or implied with this model (*e.g.* Hunt and Tucker, 1992; Miall, 1986, 1991; Walker, 1990). Such a wealth of data does not yet exist for the other two methodologies, and comparison of the area with analogous settings would thus be more difficult if allostratigraphy or genetic stratigraphic sequence analysis were used.

It is beyond the scope of this study to compare and contrast the results of applying the three different stratigraphies (sequence- *vs.* allo- *vs.* genetic stratigraphic analysis) to the shallow-marine and coastal/alluvial-plain rocks of the Mullaman Beds. This is mainly due to the nature of the raw data, which consist of thin isolated 'spot' outcrops with sporadic biostratigraphic control. In this study, basic stratigraphic correlation between outcrops in order to construct a

continuous stratigraphic record is highly complex, and is the subject of detailed interpretation (see chapters 3-8). This is not the ideal situation for comparing and contrasting the three detailed stratigraphic models, because the models themselves would not be the prime focus of discussion and interpretation. Therefore, all of the following discussion and interpretation in this chapter is concerned with *sequence stratigraphy* and its application in defining depositional sequences, but also includes possible problems or inconsistencies of the model as indicated by analysis of the Mullaman Beds.

The following major definitions and terms of sequence stratigraphy are referred to in this chapter. The *depositional sequence* is the fundamental unit of sequence stratigraphy (Mitchum and Van Wagoner, 1991), and is defined as a relatively conformable succession of genetically related strata bounded by unconformities and their correlative conformities. Sequences are divided into *systems tracts* which link contemporaneous depositional systems (Brown and Fisher, 1977). *Sequence boundaries* define the upper and lower margins of sequences and two main types of sequence boundaries exist, *i.e.* type 1 and type 2 (Van Wagoner *et al.*, 1990). The fundamental building blocks of sequences and systems tracts are parasequences which are themselves composed of beds and bedsets (Mitchum and Van Wagoner, 1991). A *parasequence* is defined as a relatively conformable succession of genetically related beds or bedsets bounded by marine-flooding surfaces and their correlative surfaces (Van Wagoner *et al.*, 1990). Parasequences are typically stacked in progradational, aggradational, and retrogradational sets (Van Wagoner *et al.*, 1990).

In summary, a sequence is a genetically related succession of strata with no apparent internal unconformities, composed of parasequences and parasequence sets arranged in systems tracts, and bounded by unconformities and their correlative conformities. For more detailed explanations of sequence stratigraphic terms, definitions, and general concepts, the reader is referred to Mitchum and Van Wagoner (1991), Vail *et al.* (1977), and Van Wagoner *et al.* (1987; 1988; 1990).

9.3 METHODS

Correlation of sequences and surfaces (bounding discontinuities; Plate 9) and their interpretation on a regional-scale is based on the shelf-wide stratigraphic framework of composite sections (Fig. 9.1), as developed in chapter 8. However, sequence stratigraphic analysis can equally be applied to individual measured sections or small areas. Herein, sequence stratigraphic analysis at smaller scales (*e.g.* important individual beds, successions, or surfaces) is described where necessary to illustrate significant details.

The methodology of sequence stratigraphy requires certain logical steps in the analysis of any group of sedimentary strata. In an ideal case the steps should be broadly as follows (Vail, 1989):

1) The lithology and depositional environments of the rocks are documented.
2) Sequence boundaries and systems tract boundaries are 'picked' in the rock succession.
3) The nature of systems tracts are described and their internal stacking patterns are documented.
4) According to Vail (1989) one should then age date the sequence with ties to the global cycle chart (latest version of the chart is Haq *et al.*, 1988).
5) The 'picked' sequence boundaries are 'merged' with seismic boundaries.
6) Parasequences and markers are correlated.
7) Summary cross-sections are constructed.
8) 'Time slice' maps are then constructed by mapping lithofacies and/or chronostratigraphic units (*e.g.* a particular maximum flooding horizon) to show important boundaries (*e.g.* shorelines) and their change over time in response to relative sea level changes.

In practice, in real-life examples such as this study, not all of these steps are possible or necessary. In this study the first step of interpretation of depositional environments has already been accomplished (chapters 3-8). The age dating of the sequence (part of step 4) has been covered in Sects. 8.2 and 8.6.2, to the limits of the available data. Markers have already been correlated in Sects. 8.5,8.6, and 8.7 (part of step 6), and some parasequences have been correlated inasmuch as most coarsening-upward facies successions of the Mullaman Beds satisfy the definition of a parasequence (see Sect. 9.2). Construction of the lithostratigraphic framework (Fig. 8.7) using correlation diagrams in chapters 5-7 partly satisfies step 7.

Therefore the major tasks remaining are to pick the sequence boundaries and systems tracts (step 2), describe the systems tracts and their internal geometries (step 3), and integrate these

PLATE 9

Various types of parasequence boundaries:

a Hiatal surface illustrated by a shell pavement consisting of a life assemblage of numerous bivalve fossils which colonised this bedding surface during a time of low sedimentation. Site 128, southern region. Lens cap is 5.75 cm in diameter.

b Oblique view of a pale grey compacted and cemented shelly coquina (death assemblage). This surface sharply overlies sandstone (at top of photo), and forms the parasequence boundary at the base of a thick cycle of facies succession 4. Landward of this palaeogeographical position such boundaries are commonly marked by conglomeratic lags. Site 54, central region. Pen is 15 cm long.

c Upper surface of a sedimentary breccia which marks the parasequence boundary between stacked fining-upward cycles of facies succession 5 in the northern region. Breccia fragments are up to boulder size and are cemented by iron-oxide or rarer manganese-oxide. Note the pale coloured clayey sand filling spaces between the fragments; this matrix probably infiltrated from above after initial brecciation. Site 4, northern region.

d Silica-cemented *Skolithos*-burrowed hardground of highly bioturbated fine-grained marine siltstone (facies 21). This surface marks a regional condensed bed at the top of fining-upward facies succession 5. Note the numerous closely spaced burrows which earn this unit the local name of 'piperock'. Site 146, northern region. Hammer (in shadow) is 32.5 cm long.

e & f Marine flooding surfaces defined by intensely bioturbated intervals of clayey siltstone with numerous, intersecting horizontal burrows of the *Cruziana* ichnofacies. Sites 34 (northern region) and 66 (central region) respectively. Lens cap is 5.75 cm in diameter.

g & h Outcrop view and close-up of fine-grained marine flooding surface (hiatal surface) with abundant concretions. Plate g shows a large expanse of the bedding plane, whereas plate h shows one of the concretions in detail. Concretions are composed of very finely laminated, iron-oxide cemented clayey siltstone and claystone. Site 164, northern region. Hammer is 32.5 cm long.

a

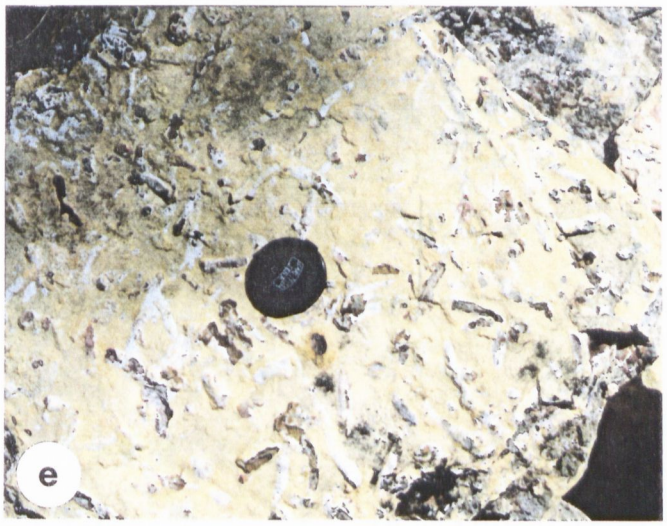
e

b

f

CENTIMETERS
c

g

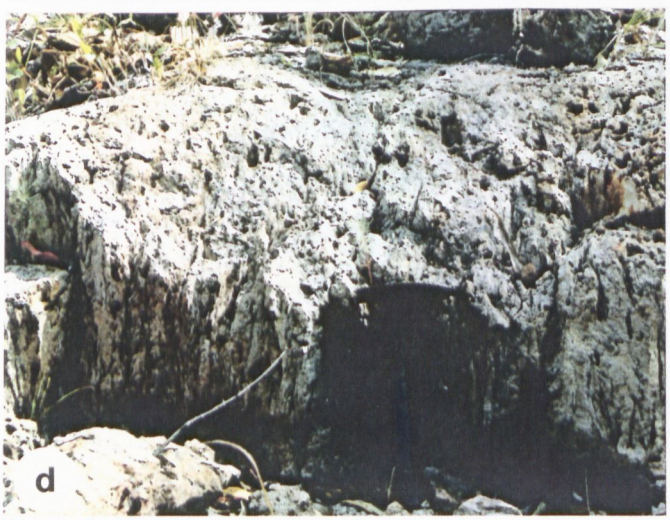
d

1 2 3 4 5 6 7 8 9 10
CENTIMETERS
h

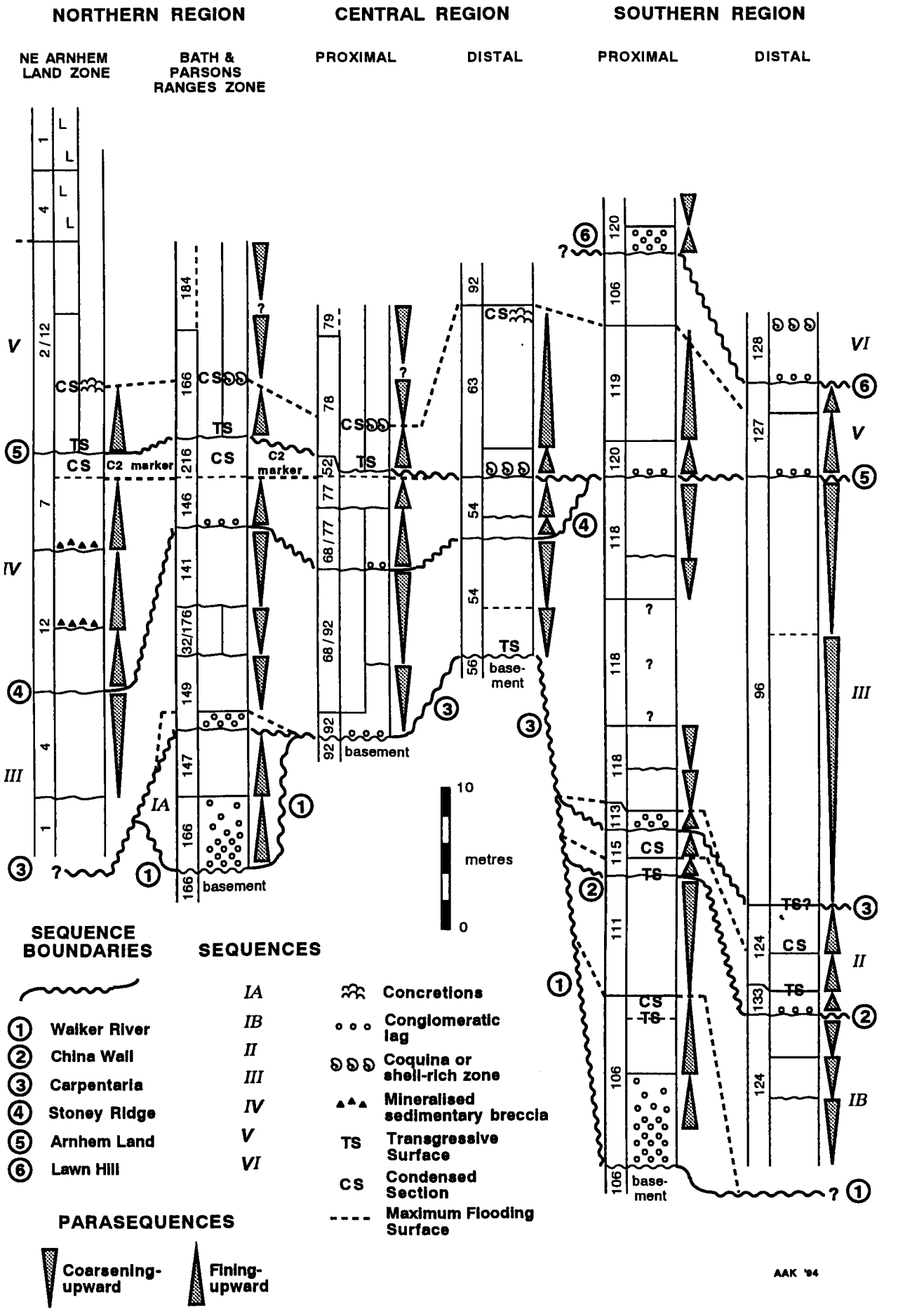

FIGURE 9.1. Regional sequence stratigraphic correlation on the western shelf of the Carpentaria Basin.

data with previous correlation diagrams to form maps for the various sequences (step 8). Correlation and comparison with the global sea level chart of Haq *et al.* (1988) and other sea level curves (step 4) is presented in section 9.8. In the present study step 5 is omitted because it is not possible to merge the outcrop data with seismic data; there is only a small amount of seismic coverage available (*e.g.* Burgess, 1984; Thomas *et al.*, 1992) and it is limited to the offshore areas; there is no documented correlation to rocks exposed onshore on the Mullaman Bed shelf.

To accomplish the above tasks as part of sequence stratigraphic analysis the stratigraphic position of conglomeratic lags, coquinas, condensed intervals with concretions, marine hardgrounds, sedimentary breccias, rip-up lags, and mineralised horizons are positioned on the previous lithostratigraphic and biostratigraphic framework (Fig. 9.1). These features enable the sequence boundaries to be picked in the three regions on the shelf, and to be correlated across the entire shelf. Recognition of vertical grain size variation, the thicknesses of successions (parasequences), and their vertical and lateral stacking patterns enables division of the rocks into systems tracts.

9.4 SEQUENCE BOUNDARY UNCONFORMITIES

Six regionally extensive sequence boundaries have been recognised within the Mullaman Beds during this study. The stratigraphic position, morphology, and lateral extent of these sequence boundaries are illustrated in Figs. 9.1 and 9.2. The composite sections in Figs. 9.1 and 9.2 are hung on the C2 marker or its equivalent stratigraphic interval, and these figures thus summarise the type and amount of erosional relief for each of the sequence boundaries across the shelf. The erosional relief for each sequence boundary unconformity by area (documented in stratigraphic diagrams in chapters 5-7) is presented in Table 9.1. Independent data on the nature and amount of erosion along each of these sequence boundaries are also presented from single outcrops, and localised areas. The six sequence boundaries have been named from local geographical localities where they were first recognised or are best exposed. They are described in order from oldest to youngest.

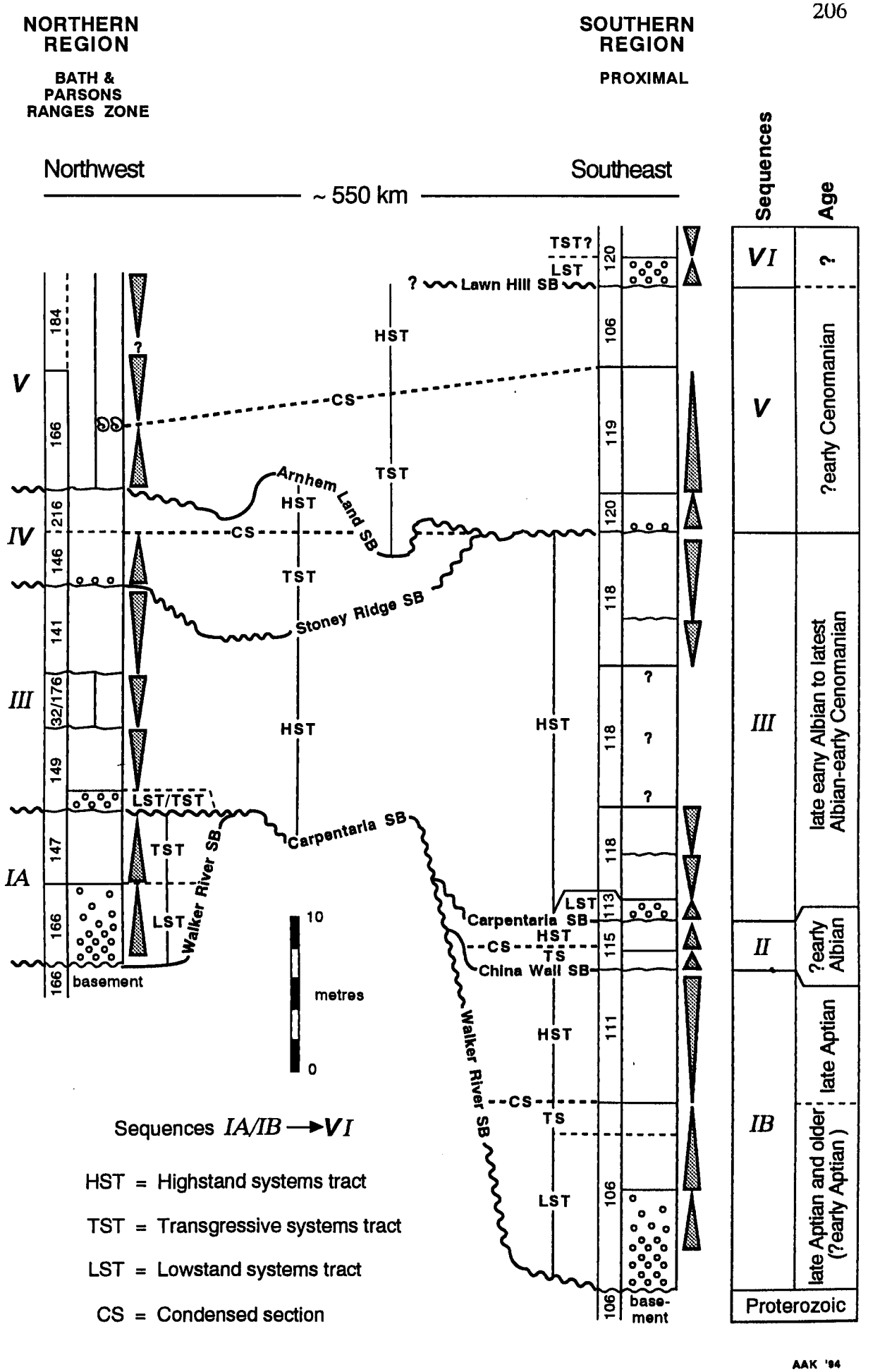

FIGURE 9.2. Systems tracts, age of sequences, and sequence stratigraphic correlation across the western shelf of the Carpentaria Basin.

Table 9.1: Erosional relief and nature of sequence boundary unconformities by area.

Area / Sequence Boundary	Nature of SBs *	NE Arnhem Land Zone	Bath-Parsons Ranges Zone	Central Region	Southern Region
Lawn Hill SB	type 1?	------	------	------	10+
Arnhem Land SB	type 1	10+	3+	4	2
Stoney Ridge SB	type 2	4	1.75	4	------
Carpentaria SB	type 1	------	9+	13+	19
China Wall SB	type 1	------	------	------	2.5+
Walker River SB	type 1	------	10+	------	8+

Erosional relief refers to maximum values in metres for each area, + indicates value is likely to be greater.

* Nature of sequence boundaries refers to assignment as type 1 or type 2 (*sensu* Van Wagoner *et al*, 1990).

9.4.1 Walker River sequence boundary

The Walker River sequence boundary is mapped in this study in both the BPRZ and in the southern region (Fig. 9.1; Plate 10a-b), although conclusive proof of a similar age for the unconformity in both areas is lacking. The correlation of the unconformity is based on the similar stratigraphic position at the base of the shelf deposits, and the identical nature and similar thickness of overlying deposits in both areas (as shown in Sect. 8.6). Although the unconformity in the two separate areas probably represents the formation of an erosional surface at the same time, its extent and classification is different in each area.

The sequence boundary in the Walker River area defines an incised valley and the base of the Cretaceous succession. In the southern region the same sequence boundary also marks the base of the Cretaceous succession in the distal region underlying the lowstand wedge, but was not formed by valley incision. The Walker SB is interpreted to extend over a large distance (possibly 100's km? farther offshore from the study area) where it may change into a correlative conformity.

In terms of Vail (1987) the Walker River SB is a type 1 sequence boundary and involved a significant amount of subaerial erosion. Near the Walker River the sequence boundary cuts down into dipping Proterozoic siltstones, which floor a large incised valley, and is overlain by thick fluvial and transitional-marine rocks consisting of cobble to granule conglomerate (Plate 10a) and poorly-sorted, coarse-grained quartz sandstone. The estimated *shelf-wide* relief on this unconformity is 30 m over a distance of approximately 500 km (Table 9.1), but is most noticeable within the confines of the incised valley in the BPRZ (Figs. 9.1 and 9.2).

PLATE 10

Sequence boundaries and associated Mullaman Bed facies:

a Thick chert cobble conglomerate filling a large incised valley and overlying a major sequence boundary (Walker River SB). The thickness of the conglomerate is greatest in the central part of the valley at its headward end, and decreases towards the valley edges. Note the crude normal grading of the conglomerate with the largest clasts near the level of the hammer. Site 155, northern region. Hammer is 32.5 cm long.

b The Walker River sequence boundary in the southern region (shown by thick white dashed line). Cretaceous transgressive marine facies directly overlie the sequence boundary and have an angular unconformable relationship with dipping Proterozoic siltstones (dip shown by white dotted lines). The basal Cretaceous facies (arrowed) is a transgressive quartz sandstone with dispersed chert pebbles, which is overlain by crossbedded shoreface sandstones. Site 133, southern region. Hammer is 32.5 cm long.

c Subtle expression of a major sequence boundary (merged Carpentaria and Arnhem Land SB's; the Stoney Ridge SB is not present in this distal zone) shown by arrows in a distal marine depositional setting. Here, the upper half of the photo illustrates orange Cretaceous fossiliferous clayey sandstone of facies succession 4 disconformably overlying slightly paler flat-lying Proterozoic sandstone. In the centre is a bivalve shell resting directly on the sequence boundary. Site 62, central region. Lens cap is 5.75 cm in diameter.

d More proximal exposure of the same regional surface as in plate 10c (merged Carpentaria and Arnhem Land sequence boundaries, see arrow). Here, the sequence boundary exhibits obvious scouring (arrow) and is overlain by a sandy conglomeratic pebble lag. Site 81, central region. Hammer is 32.5 cm long.

e Stoney Ridge sequence boundary (type 2) seen in outcrop (between two arrows) as a gently undulating sharp surface, possibly a cemented wave-rippled pavement. Thick shoreface marine sandstones of facies succession 2 occur directly beneath the disconformity, and interbedded marine siltstone and sandstone above it. There is no evidence for subaerial exposure. Site 154, northern region. Hammer is 32.5 cm long.

f The most obvious sequence boundary in the study region, the Arnhem Land SB (arrowed). Rocks beneath the unconformity belong to fining-upward marine facies succession 5. At the top of this fining-upward cycle is the C2 marker, which has been removed by erosion in places along the unconformity. Upper fluvial rocks of facies succession 7 have incised into the marine succession. Note the variable (but significant) amount of erosional relief along the unconformity. Site 7, northern region. Helicopter for scale. See also plate 6e for closer view.

g Another outcrop of the Arnhem Land sequence boundary (arrowed). Here, fluvial deposits of facies succession 7 directly overlie steeply dipping (see dashed lines) Proterozoic basement. Site 212, northern region. Hammer is 32.5 cm long.

a

d

b

e

f

c

g

As would be expected for an incised valley, the amount of erosion along the sequence boundary varies according to position in the valley. The greatest amount of local erosion (10 m) coincides with the thickest fluvial conglomerate (Plate 10a) overlying the unconformity, and occurs in the interpreted thalweg of the valley axis. The exact positions of the valley walls are difficult to define, but can be approximated by the regular decrease in thickness of the basal fluvial conglomerate in combination with a lessening in the amount of erosion and incision towards the valley walls. On the sides of the valley the sequence boundary is overlain by fining-upward marine deposits of facies succession 5, which form part of the transgressive systems tract. There is no indication of soil formation along the sequence boundary in response to subaerial exposure, but soils would be unlikely to be preserved in the valley walls due to erosion during the subsequent transgression (*cf.* Wright and Marriot, 1993).

The nature and size of this incised valley appears to be similar to those which formed in an analogous shelf settings, particularly those of the western edge of the Cretaceous Western Interior Seaway of North America. There, incised valleys and their fluvial and marine fills of the Dakota Formation in Utah have the same coarse-grained stream deposits overlying similar valley-floor unconformities, and grade upward into restricted-marine and shoreface marine facies (Ende, 1991). Moreover, the lower marine rocks contain a brackish fauna and probably accumulated in an initially lagoonal or estuarine environment, similar to rocks of facies succession 2 and 6 overlying the basal fluvial sandstone and conglomerate of the Walker River incised valley stratigraphy.

Most incised valleys have their axes oriented approximately perpendicular to the regional palaeoshoreline (Allen and Posamentier, 1993), but in the case of the Walker River incised valley the axis is approximately north-south, roughly parallel to the regional palaeoshoreline. However, when local palaeogeography is considered, the orientation of the valley-axis can be clearly seen to be controlled by the strike-length of high-standing basement terrain of the Bath Range. The incised valley axis is therefore perpendicular to the *local* palaeoshoreline (approximately E-W) defined by the joining of basement terrains of the Bath and Parsons Ranges (see base map for the BPRZ in Appendix 3 for geographical localities).

9.4.2 China Wall sequence boundary

This sequence boundary is only evident in the southern (basinal) region on the shelf, and apparently terminates to the northwest against the Walker River SB near the basement terrain known locally as the "China Wall". This unconformity represents a period of erosion on the

distal part of the shelf, and evidence for its presence as a separate surface is lacking on more proximal parts of the shelf (Fig. 9.1). Such evidence on proximal parts of the shelf may have been destroyed by erosion during formation of the major overlying, shelf-wide unconformity (the Arnhem Land SB).

The China Wall SB extends over at least 120 km and involves at least 12 m of erosional relief on a regional scale according to correlation in Fig. 9.1, although the maximum amount of erosional relief viewed in outcrop is 2.5 m (Table 9.1). In most places the unconformity is overlain by a thin conglomeratic lag and/or thin transgressive sandstones. In terms of Vail (1987) this unconformity is a type 1 sequence boundary, and it there was significant erosion and a subsequent significant basinward shift in facies belts at this surface. Similar to the underlying sequence boundary, evidence for subaerial exposure (*e.g.* soils, coal, karstification, desiccation cracks, anhydrite) are missing, but the coarse-grained lags regionally overlying the unconformity suggest significant erosion and lowering of base level with probable subaerial erosion on at least the inner parts of the shelf.

9.4.3 Carpentaria sequence boundary

This unconformity is the older of two shelf-wide erosional surfaces which have been documented throughout the study area. In the BPRZ in the northern region this unconformity truncates the top part of the Walker River incised valley deposit (Sequence *IA*). In the ALZ the sequence boundary was not recognised, but is interpreted to occur beneath the exposed Cretaceous succession. In the central region the Carpentaria SB marks the boundary between the Cretaceous succession and Proterozoic basement. In the southern region the Carpentaria SB has eroded down into Sequence *II* by up to 19 m (Table 9.1).

In the northern and central regions and the proximal part of the southern region, the Carpentaria SB is overlain by well-defined conglomeratic lags or thicker lowstand shoreline deposits. In the distal part of the southern region the sequence boundary is poorly exposed and evidence for erosion at this level is greatly diminished. On this part of the shelf the sequence boundary is essentially a sharp planar surface (Plate 10c), which is the correlative conformity of the landward, more erosive unconformity (Plate 10d). Overlying basement highs in places in the central region, the regional erosion surface between basement and the Cretaceous succession probably represents the merged Carpentaria, Stoney Ridge, and Arnhem Land sequence boundaries.

In terms of classical sequence stratigraphy this unconformity represents a type 1 sequence boundary (*cf.* Vail, 1987), as highlighted by the abrupt basinward shift in facies from beneath to above the unconformity, the evidence for significant erosion and incision along the unconformity in numerous localities, and the regional onlap of overlying marine strata onto the sequence boundary. In most places the unconformity is overlain by an erosional lag, thin transgressive deposits, and thick highstand deposits.

9.4.4 Stoney Ridge sequence boundary

This sequence boundary occurs in the northern and central regions, but was not recognised in the southern region. Unlike the older boundaries this unconformity involved only minor erosion on the shelf (<4 m, Table 9.1), and is not characterised by abrupt shallowing or a basinward shift in facies belts across the boundary. Therefore, the Stoney Ridge SB is classified as a type 2 sequence boundary (*cf.* Van Wagoner *et al.*, 1990).

On all parts of the shelf the unconformity has eroded down into underlying thick highstand deposits, and in most areas it is overlain by thin, transgressive conglomeratic lags at the base of the transgressive systems tract. The amount of erosion varies along the unconformity and is generally greatest and most obvious in the northern region. It becomes less obvious in the southern part of the northern region (Plate 10e), and the distal part of the central region where the Stoney Ridge SB merges with, or is truncated by, the younger Arnhem Land SB.

9.4.5 Arnhem Land sequence boundary

This sequence boundary is the second (younger) of two shelf-wide unconformities, and is the most obvious erosional surface in the study area. It is a type 1 sequence boundary and displays a major basinward shift in facies belts, abrupt shallowing across the boundary, and marine onlap onto the sequence boundary in distal parts of the shelf.

In the northern region and the proximal part of the central region the unconformity is typically defined by erosion and incision by overlying fluvial or restricted marine deposits into older fine-grained, offshore marine deposits (Plate 10f), including the C2 marker. The amount of incision varies along the unconformity but is up to 10 m over a lateral distance of 90 m in places (Table 9.1). There is a general decrease in the amount of erosion in an offshore direction (southeast); in the southern region and much of the distal part of the central region, marine deposits occur above and beneath the unconformity. In the northwest of the study area the sequence boundary

is highlighted by the unconformable contact of Cretaceous fluvial rocks and basement (Plate 10g). In offshore areas the unconformity is defined by a sharp change in grain size and the formation of marine hardgrounds and regionally-extensive shelly and conglomeratic lags overlying a slightly undulating erosional surface.

9.4.6 Lawn Hill sequence boundary

The youngest sequence boundary in the Mullaman Bed shelf succession is the Lawn Hill SB. The exact age and nature of this unconformity is least certain of all the sequence boundaries because it was only recognised in a few localities near the top of the Cretaceous succession in the southern region. Correlation of this sequence boundary over the entire shelf is not possible because the rocks overlying the sequence boundary are only present in the southern region. It is likely that the time of formation of this sequence boundary shortly preceded the final marine depositional episode in the Cretaceous before complete retreat of the Great Artesian Basin (GAB) seaway from the inland area of Australia in the late Cenomanian or Turonian (Frakes *et al.*, 1987).

The Lawn Hill SB exhibits a thick erosional lag, a moderate amount of subaerial erosion and incision (Table 9.1), and an abrupt shift in facies (offshore marine to nonmarine) across the unconformity. This unconformity truncates underlying deposits of the transgressive or highstand systems tracts (Sequence *V*) and qualifies as a type 1 sequence boundary.

9.5 SEQUENCES AND SYSTEMS TRACTS

The definition of systems tracts has previously been given as "linkages of contemporaneous depositional systems" (Brown and Fisher, 1977). These include lowstand, transgressive, highstand, and shelf margin systems tracts, all of which occur in predictable patterns within sequences (*e.g.* Van Wagoner *et al.*, 1988). More recently Hunt and Tucker (1992; 1993) proposed an additional systems tract, the "forced regressive wedge systems tract", after identifying conceptual problems with the EPR model for carbonate settings involving relative sea level falls. However, these authors admit that "In reality, this new scheme (forced regressive wedge systems tract) is academic and no easier to use than its predecessors for real geological situations, but it does eliminate the contradictions and ambiguities associated with falling and lowstands of relative sea-level in the previous models" (Hunt and Tucker, 1992, p. 5). An analogous "falling-stage systems tract" has been proposed for siliciclastic settings (Ainsworth, 1994).

Regardless of the exact number or type of systems tracts nominated in any sequence, the systems tracts do not necessarily say anything about eustatic fluctuation in sea level. As noted by Christie-Blick (1991, p. 40) "Although systems tracts are commonly interpreted in terms of eustatic fluctuation, as suggested by the names selected, they are actually descriptive entities and do not require any preconceived notions about the role of eustasy in the origin of sedimentary cyclicity".

Sequences and systems tracts are thus defined on the basis of stratal geometry and physical relationships, using objective criteria that do not depend on frequency of occurrence, thickness, lateral extent, or interpreted depositional mechanisms. In the following section, sequences and systems tracts are described and discussed without reference to eustatic sea level change; only relative sea level change is inferred. The thickness variations of sequences across the shelf is presented in Table 9.2. The origins and mechanisms of formation of the sequences and systems tracts are *interpreted* later in Sects. 9.8 and 9.9.

Table 9.2: Age, and thickness variation of sequences by area.

Age of Sequence	Area / Sequence	NE Arnhem Land Zone	Bath-Parsons Ranges Zone	Central Region	Southern Region
Cenomanian	Sequence *VI*	min. N/A max. N/A	min. N/A max. N/A	min. N/A max. N/A	min. 2 max. 5
? early Cenomanian	Sequence *V*	min. 2.5 max. 21.5	min. 1 max. 50	min. 1 max. 15	min. 0 max. 18.5
late Albian to latest Albian or early Cenomanian	Sequence *IV*	min. 6 max. 16.8	min. 1.5 max. 6.3	min. 0 max. 6.75	min. N/A max. N/A
late early Albian to late Albian	Sequence *III*	min. 5 max. 11.9	min. 4.5 max. 16.9	min. 0 max. 13.5	min. 0 max. 30
? early Albian	Sequence *II*	min. N/A max. N/A	min. N/A max. N/A	min. N/A max. N/A	min. 0 max. 7.5
Aptian (mid to late?)	Sequence *IB*	min. N/A max. N/A	min. N/A max. N/A	min. N/A max. N/A	min. 0 max. 20
? Aptian (mid to late?)	Sequence *IA*	min. N/A max. N/A	min. 0 max. 12.5	min. N/A max. N/A	min. N/A max. N/A

All thickness measurements in metres.

N/A = not applicable, *i.e.* the sequence was not observed at any locality on this region of the shelf.

Thickness value of 0 for any particular sequence indicates that overlying and underlying sequences were observed in direct contact.

9.5.1 Sequence *IA*

Lowstand systems tract

In this sequence the lowstand systems tract (LST) is composed of normally graded fluvial conglomerate of facies 1 and 2, which fine upward into pebbly sandstone (facies 5). The thickness of these fluvial rocks of the LST is up to 12.5 m. The basal conglomerate of the LST lies directly on the type 1 Walker River SB, which forms the floor of a large incised valley. The LST forms the lower part of the valley-fill in this area (Figs. 9.3A-B).

The top of the fluvial conglomerate is generally a gently undulating, relatively sharply defined surface which represents the transgressive surface. However, in places this contact is not sharply defined, and the fluvial conglomerate fines upward over ~0.25 m into a marine sandstone with dispersed pebbles. Here, the interpretation is that some fluvial clasts from the underlying LST were ripped-up and incorporated in the base of the transgressive systems tract (TST) during transgressive erosion as the valley was drowned.

Transgressive systems tract

Overlying the transgressive surface are fining-upward marine rocks of facies succession 5. The maximum preserved thickness of these rocks of the TST is 5.5 m, but commonly these rocks are thinner due to erosional incision along the Carpentaria SB at the base of Sequence *III*.

The rocks of facies succession 5 have been described previously (chapters 4-5), and record apparent transgression during an increase in relative sea level, which in this case caused drowning of the lowstand deposits in the incised valley (Fig. 9.3C). In the basal part of the TST some wave ravinement of the underlying fluvial deposits is apparent, but a sharp wave ravinement surface is lacking in most places. The TST is composed of only one fining-upward succession (parasequence), and so it is not possible to see any parasequence stacking pattern across the area which would absolutely confirm the classification as a TST (TSTs should show a retrogradational stacking pattern, *e.g.* Van Wagoner *et al.*, 1990). However, the patchy basal conglomeratic lag, transgressive surface, and sedimentary structures within succession 5 indicating an upward increase in water depth strongly support classification as a TST. The top of Sequence *IA* is defined by the Carpentaria SB, which truncates the TST at the top of the incised valley-fill.

FIGURE 9.3. Sequence stratigraphic evolution of the shelf succession. This figure illustrates the progressive evolution of sequences, systems tracts, and their bounding unconformities on the Carpentaria Basin shelf over time. Each panel (A-O) of the figure corresponds to a particular time interval in the history of the shelf. Each panel covers the width of the shelf. No vertical scale is implied, and the depositional slopes are greatly exaggerated.

A-C Initial erosion, valley incision, accumulation of Sequences *IA* and *IB*.

A Pre mid-Cretaceous lowstand; formation of the Walker River sequence boundary.

B Lowstand erosion and filling of incised valley(s) by coarse-grained clastics.

C Transgression, drowning of incised valley(s), accumulation of finer-grained transgressive fill in incised valley(s). Highstand, and accumulation of condensed marine beds.

D-F Development of Sequences *II* and *III*.

D Relative sea level fall, forced regression; formation of the China Wall sequence boundary. Lowstand erosion and accumulation of lowstand shoreface deposits.

E Relative sea level rise, transgression, and highstand.

F Relative sea level fall, forced regression; formation of the Carpentaria sequence boundary. Lowstand erosion and accumulation of lowstand shoreface deposits.

G-I Development of Sequences *III* and *IV*.

G Relative sea level rise, major transgression and extended highstand; accumulation of thick highstand systems tract.

H Minor relative sea level fall; formation of the Stoney Ridge sequence boundary without subaerial exposure or forced regression.

I Gradual step-wise transgression punctuated by stillstands or minor relative sea level falls. Accumulation of thick transgressive systems tract.

J-L Development of Sequences *IV* and *V*.

J Highstand; accumulation of a thick condensed bed (C2 marker) at the top of Sequence *IV*.

K Major relative sea level fall, subaerial exposure and erosion; formation of the Arnhem Land sequence boundary.

L Relative sea level rise, transgression and subsequent highstand; accumulation of thick transgressive and highstand systems tracts of Sequence *V*.

M-O Development of Sequence *VI*, followed by complete retreat of the sea.

M Major relative sea level fall, shelf-wide regression and lowstand; accumulation of coarse-grained lowstand systems tract.

N Minor relative sea level rise, minor transgression and accumulation of thin transgressive deposits. Subaerial exposure of proximal and intermediate parts of the shelf.

O Major relative sea level fall, terminal Cretaceous regression and retreat of the Carpentaria Sea from the Great Artesian Basin. Shelf-wide subaerial exposure and massive erosion.

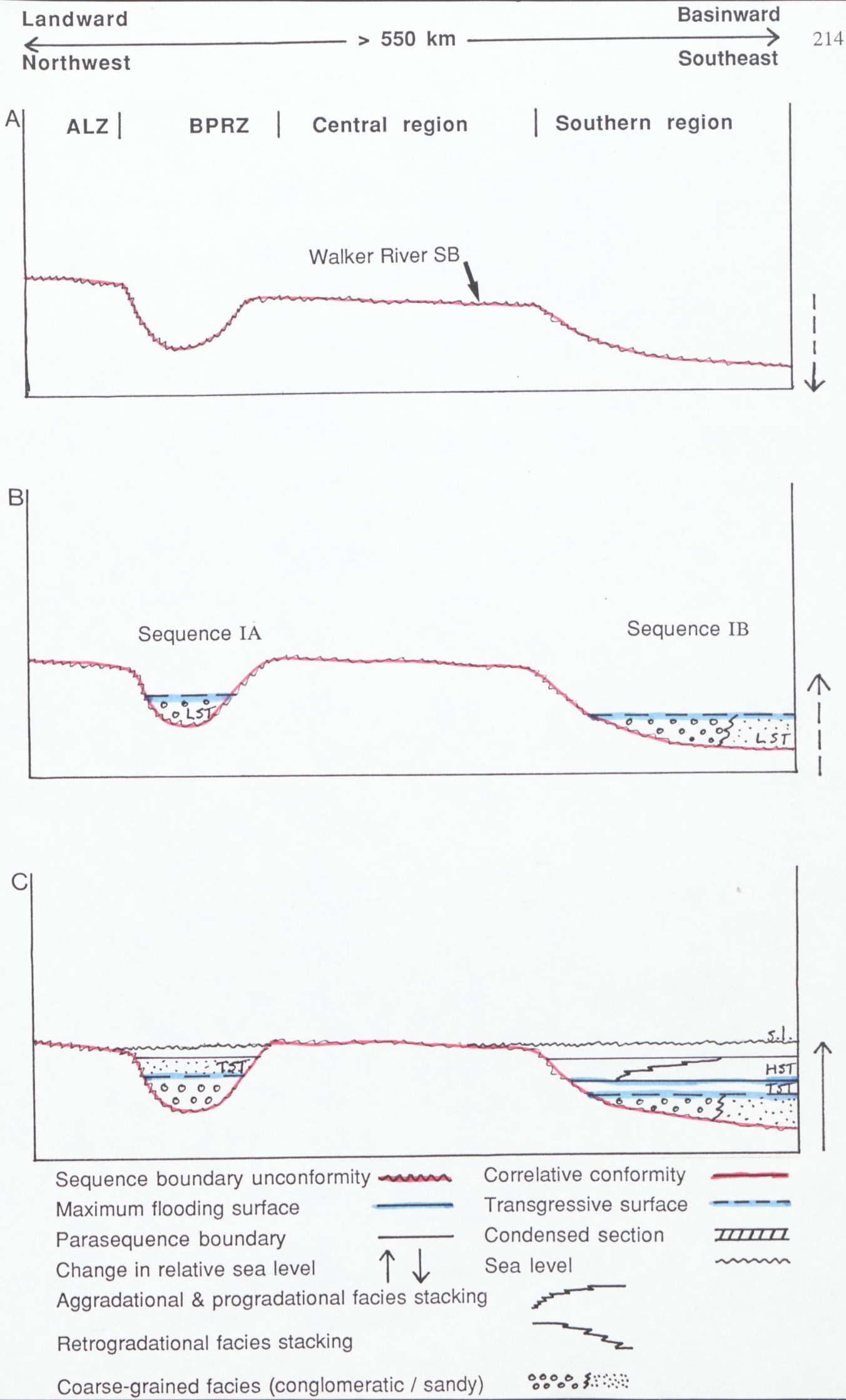
Landward
Northwest
> 550 km
Basinward
Southeast
A
ALZ
BPRZ
Central region
Southern region
Walker River SB
B
Sequence IA
Sequence IB
LST
LST
C
TST
S.l.
HST
TST
Sequence boundary unconformity
Correlative conformity
Maximum flooding surface
Transgressive surface
Parasequence boundary
Condensed section
Change in relative sea level
Sea level
Aggradational & progradational facies stacking
Retrogradational facies stacking
Coarse-grained facies (conglomeratic / sandy)

9.5.2 Sequence *IB*

In this chapter two sequences are regarded as closely related and have been termed as Sequence *IA* and *IB*. Lithostratigraphic correlation (chapter 8) has documented their similar morphology and stratigraphic position, but a common age is equivocal because similar biostratigraphic zonations are lacking. For this reason the rocks in the two areas (BPRZ and the southern region) have been designated as two related sequences (*IA* and *IB*) rather than two completely different sequences, or only one sequence. Their relationship is also shown by the fact that the same sequence boundary (Walker River SB) marks the base of both sequences, although deposition and erosion from proximal to distal parts of the shelf may have been slightly diachronous at this level (Fig. 9.2). Comparison of the systems tracts for both sequences shows their lithological equivalence at least, and adds qualified support for their approximate age equivalence because these deposits are unique to this level on the shelf. Sequence *IB* is the more complete of the two, and contains highstand deposits which are not preserved in Sequence *IA* (Fig. 9.2).

Lowstand systems tract

Sequence *IB* occurs on the distal part of the shelf, and the LST was only documented in the proximal part of the southern region. Offshore in the distal part of the southern region, the LST is interpreted to exist at depth beneath the exposed part of the Cretaceous succession.

Lowstand deposits in this region are similar to fluvial conglomerates at the base of Sequence *IA*, but they have smaller clast size (typically granules and small pebbles) and are thinner (<6.5 m). These rocks belong to facies 1, 2, 4, and 5 and have not been grouped into a specific facies succession. They are interpreted as representing high-energy fluvial channel deposition, and lack preserved fine-grained overbank deposits which would indicate a lower-energy (point bar) channel setting. The well-developed normal grading of these conglomerates and conglomeratic sandstones suggests decreasing energy in the channel environment concomitant with a rise in base level caused by transgression. Given the scarcity of outcrops of lowstand deposits in this area, it is difficult to see any evidence for progradation, which would be expected for lowstand deposits (*cf.* Christie-Blick, 1991; Van Wagoner *et al.*, 1990).

The upper surface of these fluvial rocks is a relatively sharp horizon defined by an abrupt decrease in grain size (no clasts are present), an increase in the amount of clayey matrix, and the

first appearance of significant bioturbation. This surface is interpreted as the transgressive surface (Fig. 9.3C). There is no evidence of wave ravinement at this level.

Transgressive systems tract

Transgressive deposits in Sequence *IB* overlie the transgressive surface and have a maximum thickness of 10.5 m, although they are commonly much thinner (Fig. 9.2). On this part of the shelf, transgressive deposits belong to facies succession 5 (fully marine) or facies succession 6 (brackish marine to deltaic). Regardless of which facies succession the transgressive rocks belong to, they all exhibit a deepening-upward marine character, as shown by decreasing grain size, increasing bioturbation, and the change in sedimentary structures (refer to Sects. 4.5.2 and 4.5.3). Similar to the underlying lowstand deposits, rocks of the TST are relatively poorly exposed and the backstepping stacking pattern expected for these deposits cannot be verified.

The upper 1 m of the TST contains several marine hardgrounds separated by 10 to 50 cm. In all cases the upper hardground is thickest, best developed, most laterally extensive, and shows the greatest degree of bioturbation. This hardground is interpreted as representing the maximum marine flooding surface on this part of the shelf; it probably also represents a surface of omission (*sensu* Banerjee and Kidwell, 1991). Although no condensed section is preserved here, it is likely (but unproven) that a condensed section was formed at this stratigraphic level in the offshore, shale-dominated part of the central basin in the manner envisaged by Loutit *et al.* (1988).

Highstand systems tract

Overlying the hardground is a series of coarsening-upward marine rocks of facies succession 2. Although all rocks of the highstand systems tract (HST) in this sequence belong to succession 2 and are similar, they exhibit differing vertical and lateral trends depending on their position on the shelf. The lower successions (parasequences) are fine-grained, and the overall grain size of the successions increases both in an offshore direction (progradational) and towards the top of the HST. The upper succession in the HST is typically thicker, coarser-grained and conglomeratic.

In some landward positions the upper part of highstand deposits (or rarely the entire HST) is composed of thick (8-9 m) prograding, coarsening-upward sandstone and conglomeratic sandstone. In these areas it is difficult to distinguish individual parasequences within the more

massive sandbody, but lateral correlation (see chapter 7) clearly shows the equivalence of these thicker sandbodies with stacked parasequences offshore from the interpreted palaeoshoreline.

HST rocks are the products of aggradation and progradation during highstand on this part of the shelf. They show the initially aggradational, then strongly progradational parasequence stacking patterns (Fig. 9.3C) diagnostic of highstand systems tracts (*cf.* Van Wagoner *et al.*, 1990). The age of the base of the middle parasequence in the HST has been documented as late Aptian (Haig, 1991; Sect. 8.2.3). On this part of the shelf rocks of the HST are truncated by the overlying China Wall SB, which marks the base of Sequence *II*.

9.5.3 Sequence *II*

Sequence *II* is thin and is one of the least extensive sequences in terms of areal distribution. It is restricted to the southern region, in the distal part of the study area near the shelf-basin transition. Sequence *II* is bounded below by the China Wall SB, and above by the Carpentaria SB. The China Wall SB merges with the Walker River SB to the northwest in the proximal part of the southern region, and these merged sequence boundaries in turn merge in the northwest with the Carpentaria SB (Fig. 9.2). Sequence *II* is composed mainly of thin condensed beds and thin facies successions (parasequences). It is difficult to assess the amount of Sequence *II* missing through erosion at the level of the Carpentaria SB, but it is likely to be small (possibly in the order of a few metres).

Lowstand systems tract

Lowstand deposits within Sequence *II* are unusual compared to most systems tracts of the Mullaman Beds in terms of thickness and lateral extent, but reflect the same extreme degree of progradation which affects the geometry, location, and stacking patterns of other late highstand and lowstand deposits on the shelf.

In the proximal part of the southern region there are no appreciable lowstand deposits overlying the China Wall SB, and this area of the shelf appears to have been a zone of sediment bypass (see discussion of lowstand shorelines below and in Sect. 9.5.4). However, in the distal part of the southern region lowstand deposits occur as isolated, coarse-grained shoreface successions (Fig. 9.3D). These lowstand shorefaces are relatively thin (2-3 m), and are composed of facies succession 5 sandstones and basal conglomeratic lags.

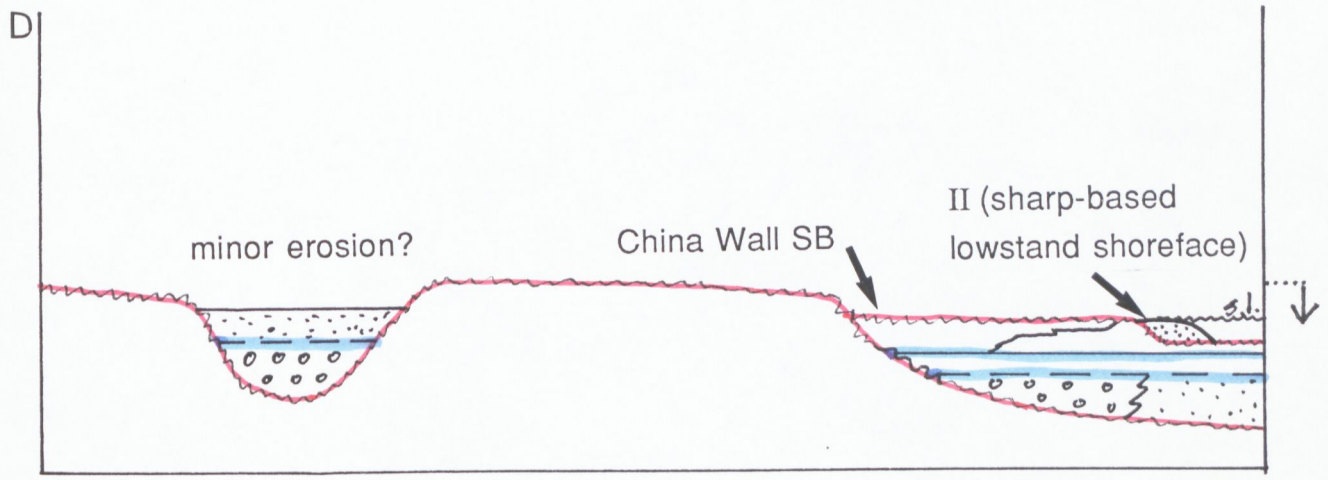
D
minor erosion?
China Wall SB
II (sharp-based
lowstand shoreface)
s.l.

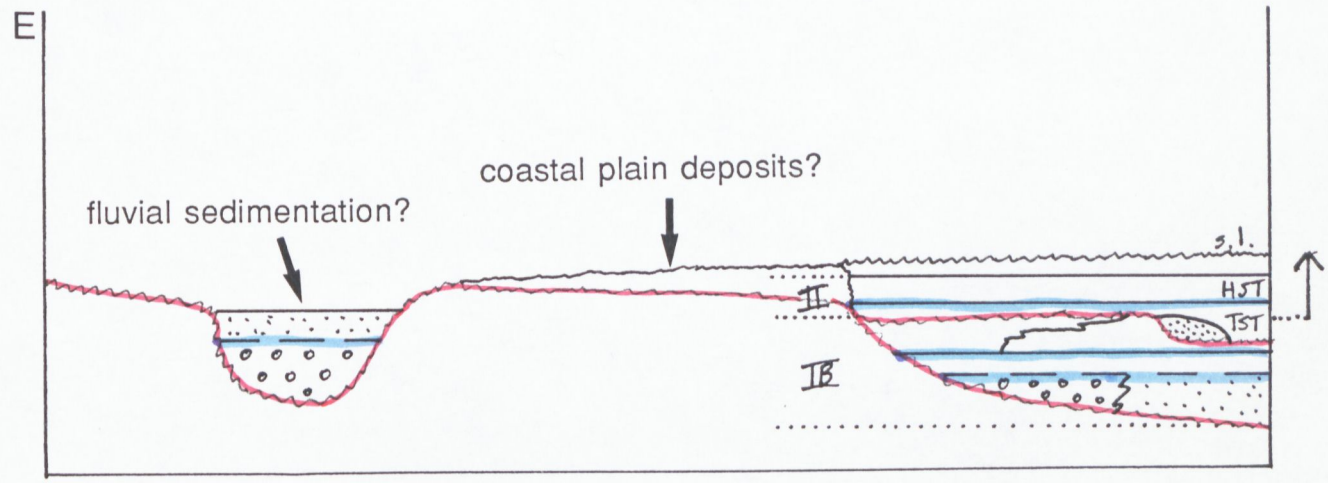
E
fluvial sedimentation?
coastal plain deposits?
s.l.
HST
TST
II
IB

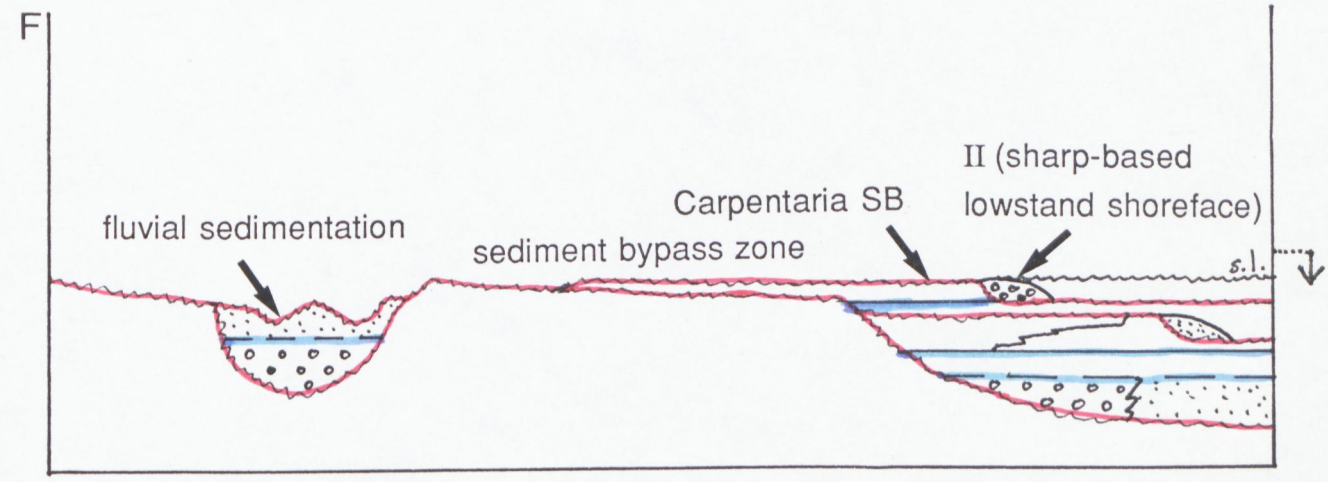
F
fluvial sedimentation
sediment bypass zone
Carpentaria SB
II (sharp-based
lowstand shoreface)
s.l.

Isolated shoreface deposits thin rapidly landward and seaward of a ~10 km wide zone, and to either side the coarse-grained shoreface deposits are enclosed by finer-grained transgressive marine rocks. In the proximal part of the southern region (to the northwest) these transgressive marine deposits directly overlie the sequence boundary and lowstand deposits are missing (Figs. 9.1 and 9.3E). The zone of outcrop of lowstand deposits is oriented approximately parallel to the regional palaeoshoreline, and probably reflects the development of a linear belt of shoreface deposits at the maximum basinward (lowstand) position of the shoreline.

These coarse-grained shoreface deposits satisfy the criteria of lowstand shorelines of Posamentier *et al.* (1992) including (Fig. 9.3E); coarse-grained and detached from preceding depositional systems; narrow zone of outcrop (typically < 12 km); transgressive deposits onlapping, and overlying, the lowstand deposits; landward lowstand pinch-out where the sequence-bounding unconformity is merged with a transgressive surface of erosion; and seaward of the lowstand shoreline, pinch-out of the sequence-bounding unconformity occurs below the lowstand shoreline and the transgressive surface of erosion occurs above the lowstand shoreline. No incised-valley feeder system for these proposed lowstand shoreline deposits is preserved, but this is common for many lowstand shorelines (Posamentier *et al.*, 1992).

Transgressive systems tract

Transgressive deposits occur directly above lowstand shoreline deposits in the distal part of the southern region, and directly above the sequence boundary in more landward areas in the proximal part of the southern region. The transgressive surface is commonly defined in these places by a thin, discrete conglomeratic lag up to 30 cm thick (Fig. 9.1). The lag is matrix supported, relatively well-sorted, and is composed of rounded small pebble and granule sized clasts in a sandy matrix. Preservation of this transgressive lag is patchy, and in places the transgressive surface is represented by a sharp, slightly undulating contact with no conglomeratic lag.

The bulk of the TST is composed of one or two thin (0.5 to 2.5 m), fining-upward 'parasequences' of facies succession 4. There is no strong retrogradational stacking pattern evident in these 'parasequences', as might be expected for a TST. However, considering their limited areal extent and relatively condensed nature, such 'parasequence' stacking patterns are probably too subtle to see without closer outcrop spacing. Beds become thinner and more

condensed towards the top of the TST along with a general decrease in grain size up to the interpreted maximum flooding surface.

Highstand systems tract

The HST is thin (< 3.5 m) and is composed of highly condensed, bioturbated, and locally mineralised siltstones belonging to facies succession 4. Similar to the underlying TST, highstand deposits do not show an obvious parasequence stacking pattern (progradational for a HST) as is expected in the sequence stratigraphic model (*cf.* Van Wagoner *et al.*, 1990). This is interpreted to be the result of slow hemipelagic deposition in a regime of generally low sediment supply in the basinal part of the study area, *i.e.* sediment supply was too low to create 'normal' sediment-driven progradation. However, major progradation occurred in response to relative lowering of sea level when deposits of the LST or late highstand were subjected to forced regression in the sense of Plint (1988) and Hunt and Tucker (1992). The top of the HST, and the upper limit of Sequence *II*, is defined by the Carpentaria SB.

9.5.4 Sequence *III*

This sequence was deposited across the entire shelf during a major transgression and subsequent highstand of relative sea level (Fig. 9.3G). The sequence is exposed in all six areas (Fig. 9.1), and is the thickest sequence on the shelf (≤ 30 m). The sequence is composed of up to 4 coarsening-upward parasequences which range in thickness from 3 to 15 m. In most places two thicker parasequences were recognised. In Sequence *III* lowstand deposits are rare, transgressive deposits are thin, and the bulk of the sequence consists of highstand deposits.

Lowstand and transgressive systems tracts

Thin lowstand deposits or early transgressive deposits are developed above the Carpentaria SB at the base of Sequence *III* in four areas (Fig. 9.1). Firstly, in the proximal part of the southern region the LST is represented by coarse-grained lowstand shoreline deposits up to 3 m thick. Secondly, in the BPRZ the LST or early TST is reflected by several outcrops of a pebble conglomerate up to 0.5 m thick. Thirdly, in the proximal part of the central region conglomerate of the LST or early TST is present, but it is thinner and its development is more patchy than in the BPRZ. Fourthly, several thin coarsening-upward facies successions (parasequences) probably represent the TST in the southern region.

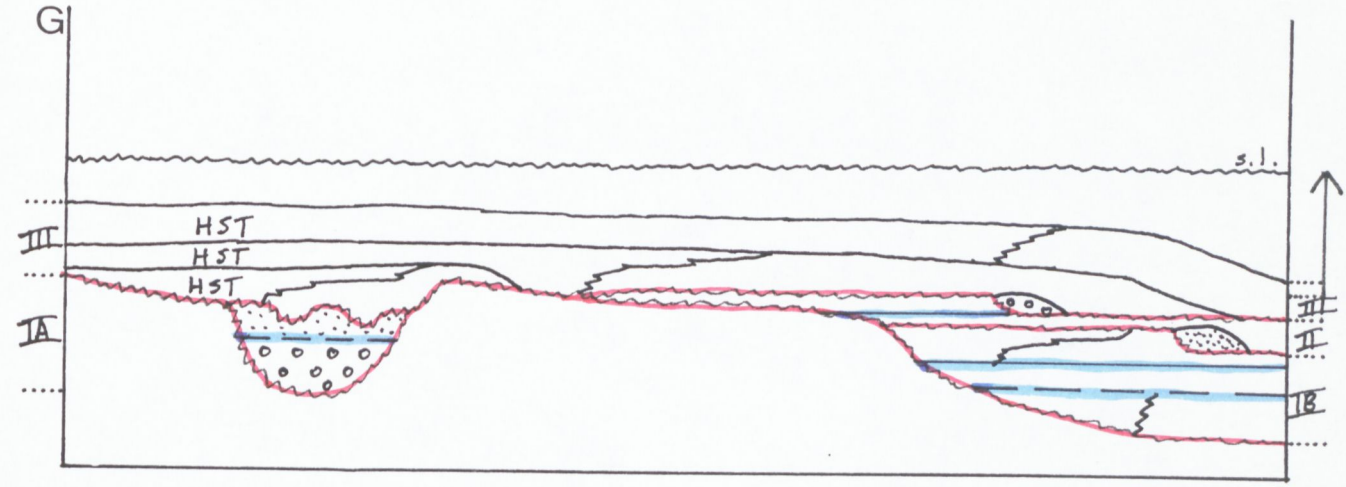
G
s.l.
HST
HST
HST
III
IA
III
II
IB

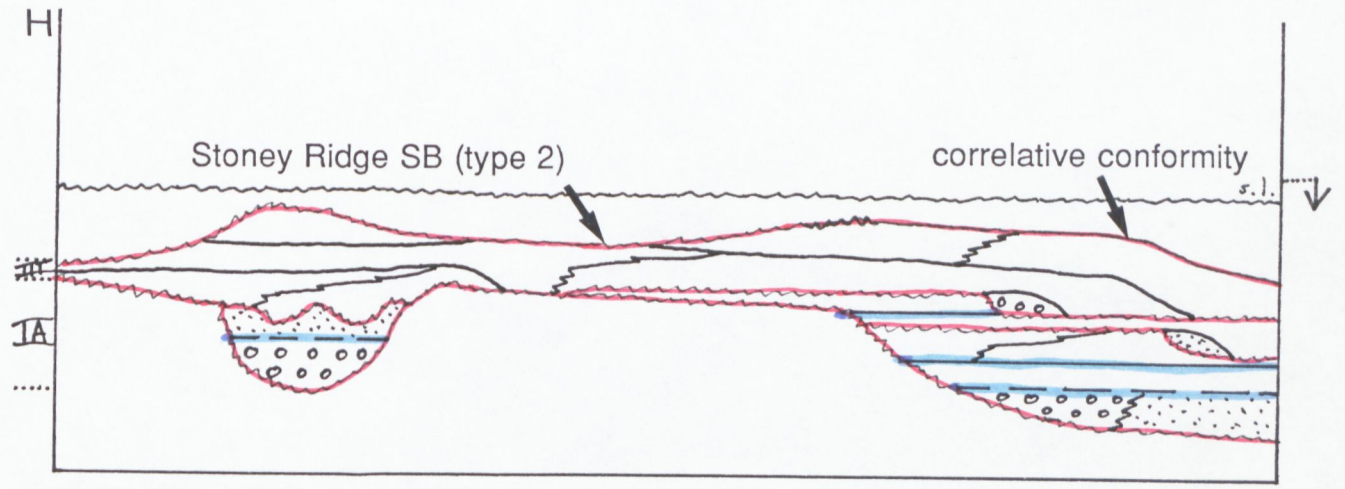
H
Stoney Ridge SB (type 2)
correlative conformity
s.l.
III
IA

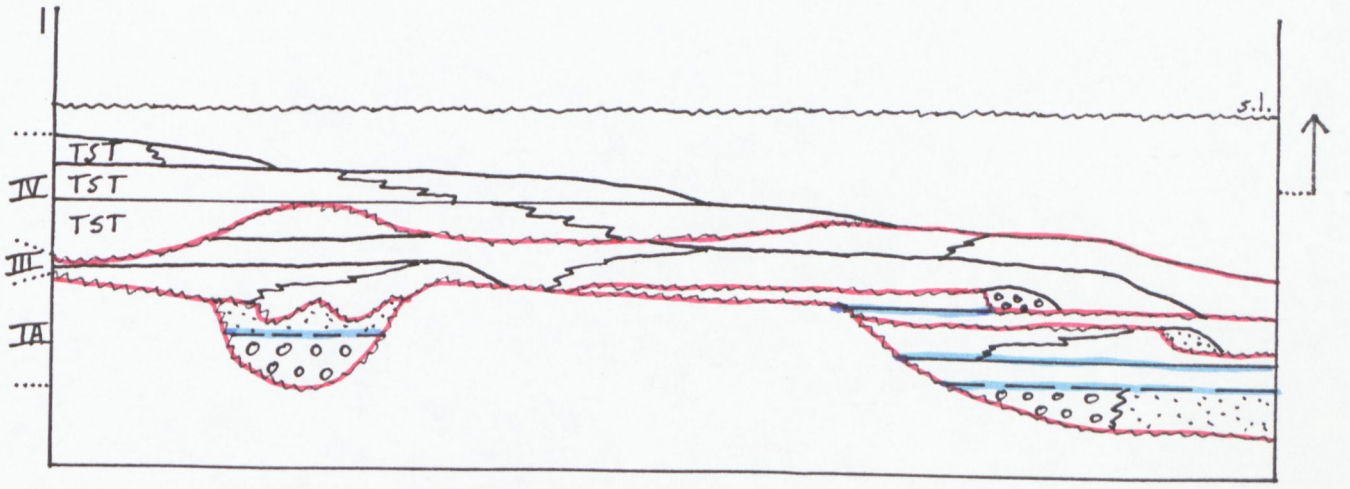
I
s.l.
TST
TST
TST
IV
III
IA

Lowstand deposits are missing in the distal part of the central region, and this is interpreted to indicate that this area of the shelf was a zone of sediment bypass and non-deposition during lowstand of sea level (Fig. 9.3F). Lowstand deposits are also missing in the distal part of the southern region, but this is due to the shoreline not having prograded that far out onto the shelf (the maximum basinward position of the lowstand shoreline occurs to the northwest in the proximal part of the southern region). Lowstand deposits may occur in the subsurface in the ALZ (the oldest exposed part of the Cretaceous succession is the HST of Sequence *III*), but were not observed during this study.

Lowstand shoreline deposits of Sequence *III* in the proximal part of the southern region are almost identical in facies geometry, thickness, and lateral extent to lowstand shoreline deposits of Sequence *II*. The Sequence *III* lowstand shoreline deposits differ in being slightly coarser-grained, they occur in a slightly more landward (northwest) position (Fig. 9.3F), and they show more clearly the stratigraphic relationships of typical lowstand shoreline deposits (as documented by Posamentier *et al.*, 1992). Most noticeably, the lowstand shoreline deposits occur in a relatively narrow NNE-SSW outcrop belt (thicker deposits occur in a zone ~15 km wide, but pinch-out into a thin lag over a further 20 km in places).

These lowstand deposits also exhibit other diagnostic criteria of lowstand shorelines, including:

1) sharp-based nature in proximal localities and a gradational nature in distal localities;
2) coarse grain size and isolated nature;
3) the fact that the TST onlaps the distal part of the shoreline deposit, and also overlies the deposit;
4) the fact that landward of the lowstand deposit the sequence boundary at the base of the shoreface merges with the transgressive surface (Figs. 9.1 and 9.3G);
5) the fact that seaward of the lowstand shoreline pinch-out the sequence boundary occurs below the lowstand deposit; and
6) the transgressive surface occurs above the lowstand deposit.

In the BPRZ and the proximal part of the central region, deposits of the LST or early TST are well-defined (if somewhat patchily distributed) conglomerates. These occur directly above the Carpentaria SB and are interpreted to have accumulated initially during a major period of subaerial erosion. Their thickness and areal distribution may once have been significantly greater than at present, *i.e.* these lags may have been modified or completely eroded in some areas during subsequent transgression (see discussion in Sect. 9.6.3), similar to other

documented cases of significant transgressive erosion in shallow-marine settings (*e.g.* Plint and Norris, 1991; Wadsworth and Walker, 1991).

In the case of Sequence *III*, the thin conglomeratic lags at the base of the sequence can be considered either as the LST or part of the early TST, depending on the extent of transgressive modification of coarse-grained clastic deposits. However, it is difficult to assess the amount of transgressive modification. The lags are well-sorted but show no imbrication or obvious marine cements. I regard the lags as having undergone some transgressive modification, which probably resulted in better sorting and controlled their patchy distribution (they are restricted to slight topographic lows on the Carpentaria SB surface in the BPRZ and the proximal part of the central region).

In the southern region, thin (typically < 0.5 m) coarsening-upward or massive strata of facies succession 1 form the TST. These transgressive deposits overlie the lowstand shoreline with a sharp contact, defining the transgressive surface, and are in turn overlain by thicker shoaling-upward parasequences of the HST. Rocks of the TST are distinguished from the overlying HST by their thinner parasequences, and by their position directly above coarse-grained lowstand shoreline deposits of the LST. In the distal part of the southern region the contact between Sequence *II* and Sequence *III* is poorly exposed, there are no basal conglomeratic lags, and no significant TST deposits were identified. The TST is probably defined in this area by claystone and very fine-grained siltstone of facies succession 1, even though there is no obvious maximum flooding surface separating the TST and the HST due to the lack of lithological contrast in these very fine-grained rocks.

In Sequence *III* thick TST deposits are not preserved, and the rise in relative sea level seems to have been rapid. In the BPRZ the conglomeratic lags are sharply overlain by fine-grained rocks of the HST, and this contact marks a marine flooding surface. I regard the conglomeratic lags underlying the marine flooding surface to belong to the late LST / early TST. Locally they may belong completely to the LST where a well-defined transgressive surface exists, or they may belong entirely to the TST where evidence of transgressive erosion and modification is more obvious (particularly in the central region).

Highstand systems tract

Overlying the conglomeratic lags and lowstand shoreline deposits in Sequence *III* are a series of stacked, coarsening-upward parasequences of the HST. These parasequences are composed of

facies succession 2 (Plate 11a-b) in proximal areas of the shelf (northern and central regions), and finer-grained facies succession 1 (Plates 4a, 5a, 11c) in more distal areas of the shelf (southern region). Each facies succession corresponds to a single parasequence, and there are up to 4 such stacked parasequences (Fig. 9.1). The age of the HST parasequences in the southern region has been documented as late early Albian to late Albian by biostratigraphy (Haig, 1991; Sect. 8.2.3).

The contact between parasequences is defined by sharp, typically undulating, regional marine flooding surfaces. These surfaces record an abrupt increase in water depth indicated by a significant decrease in grain size and changes in sedimentary structures and trace fossils. Minor submarine erosion characterises these surfaces on a regional-scale, although local storm erosion and scouring has created more prominent erosional relief of up to 2 m (typically <0.5 m) in places, commonly associated with large-scale hummocky beds and gutters (Krassay, 1994a).

Shallowing-upward facies successions become coarser towards the top of the HST, and also become coarser in an offshore direction within individual areas on the shelf. This is taken to indicate aggradation during the early and middle HST after maximum flooding across the shelf (lower parasequences), followed by progradation (upper parasequences) in the late HST as accommodation space progressively decreased.

It is not always easy to determine the direction and amount of progradation between outcrops because of the significant overprint of storm-generated coarse-grained deposition (Krassay, 1994a). Also, in some areas coarse-grained clastic debris was shed from basement islands on the shelf and incorporated into local parasequences. Thus some parasequences are anomalously coarse-grained in localised areas. However, the general trend is finer-grained and thinner parasequences in the early HST, and coarser-grained and thicker parasequences in the late HST.

The end result of progradation in clearly shown in the uppermost deposits of the HST of Sequence *III* (particularly in the BPRZ and central region) where conglomeratic upper shoreface deposits extend southeast across the shelf (basinwards) into the proximal part of the central region (Fig. 9.3G). Offshore from this position the top of the HST is not composed of upper shoreface deposits, but consists of shallowing- and coarsening-upward strata of the lower shoreface to offshore zone. The effects of progradation in this systems tract are also clearly illustrated by thin paralic or deltaic sandbodies in the BPRZ (see Fig. 5.7), and thicker deltaic sandbodies in the proximal part of the central region (see Fig. 6.6). In the BPRZ sandbodies of facies succession 6 up to 3 m thick prograde basinwards from the palaeoshoreline, where they

PLATE 11

Parasequences and facies successions within the Mullaman Beds:

a Stacked marine parasequences of Sequence III. Rocks beneath the top of the thick grey sandstone bed (arrowed) form two coarsening-upward cycles of facies succession 2. Planar bedded and interbedded sandstones above this level form one or two crude fining-upward cycles of facies succession 5. Site 77, central region. Grey sandstone ledge is 10 m above base of the cliff.

b Stacked coarsening-upward parasequences (arrowed) of facies succession 2 in the northern region. The bulk of each cycle consists of interbedded sandstone and siltstone, with sandstone beds increasing in frequency and thickness towards the top of each cycle. Site 174, northern region. Both parasequences are about 5 m thick.

c Sharp parasequence boundary at the top of a coarsening-upward cycle of facies succession 1. Upper coarser sandstone of facies succession 4 is 'loaded' down into the underlying succession and exhibits a 'ball and pillow' type contact (the contact and the outline of one large sandstone ball are dashed). Site 103, southern region. Pencap is 6 cm long.

d Marine crossbedded medium- to coarse-grained sandstones at the base of a fining-upward cycle of facies succession 5. Note the decrease in bedding thickness towards the top of the cycle (out of photo). Site 75, central region. Hammer is 32.5 cm long.

e Oblique aerial view of the stratal relationship of marine parasequences of a transgressive systems tract in the central region. The lower bench consists of fining-upward marine shoreface sandstones of facies succession 5 (4 m thick). The offshore depositional limit of the shoreface is shown where the two benches merge (arrowed). Note the divergence of the benches (retrogradational thickening of the lower shoreface rocks) to the left of photo. These coarse-grained shoreface rocks are overlain by finer-grained offshore marine parasequences (facies succession 4, the upper bench), which accumulated farther offshore. Sites 65 and 56, central region.

f Mesa showing lower fining-upward marine sandstones of facies succession 5 (arrow) disconformably overlain by a paler fluvial facies succession (7). Site 75, central region. Lower parasequence is 6 m thick.

g & h Coarse-grained, large-scale trough cross-stratified sandstones of facies succession 7 forming fining-upward fluvial channel sequences with erosive bases. In the case of plate g, the base of the succession is also a major sequence boundary, the Arnhem Land sequence boundary. In plate h, the bases of individual fining-upward cycles are defined by zones of weathered-out clasts. Sites 7 and 37 respectively, northern region. Hammer is 32.5 cm long. Person for scale in plate h.

a

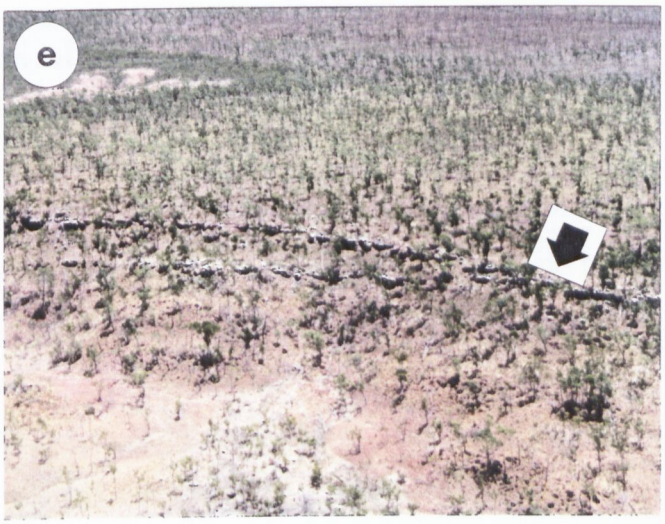
e

b

f

c

g

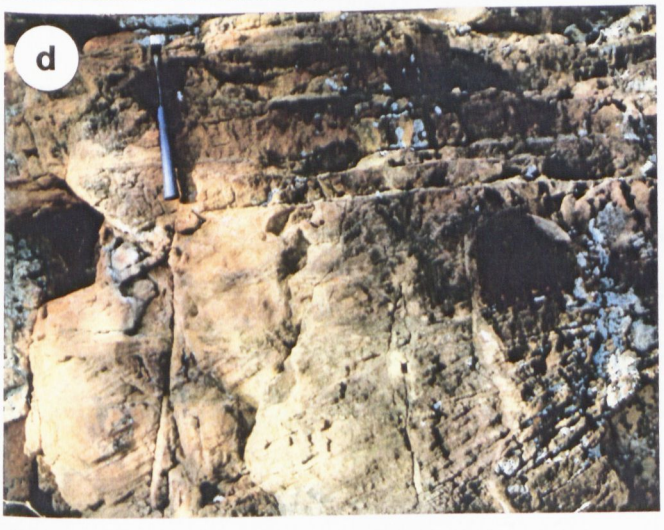
d

h

pinch-out and are enclosed by marine rocks of facies succession 2, which make up parasequences of the HST.

In the proximal part of the central region, sandbodies of facies succession 6 up to 10 m thick are equivalent to offshore fully marine, progradational parasequences of the HST. In all areas on the shelf the formation of coarse-grained deltaic / paralic sandbodies is limited to progradational episodes during the late part of HSTs. On most parts of the shelf the top of the HST, and the top of Sequence *III*, is defined by the Stoney Ridge SB which marks the base of Sequence *IV*. However, in the southern region Sequence *IV* has been completely eroded or was not deposited. Here the top of Sequence *III* is defined by the Arnhem Land SB, which also marks the base of Sequence *V*.

9.5.5 Sequence *IV*

Sequence *IV* is relatively thin on most parts of the shelf and is dominated by stacked fining- and deepening-upwards parasequences of the TST (Plate 11d-f). The TST is overlain by thin, condensed beds of the HST. Lowstand deposits did not form in Sequence *IV* because the sequence developed after a relatively minor fall in relative sea level which did not involve subaerial exposure of the shelf (Fig. 9.3H). Most erosion within Sequence *IV* is interpreted to have occurred during transgression and is probably due to wave scour at the active shoreface.

Sequence *IV* is composed mainly of shoreface rocks of facies succession 5, and as such the sequence only occurs landward (northwest) of the most basinal shoreface in the distal part of the central region. Sequence *IV* is not present offshore from this position, *i.e.* in the southern region. The upper part of the sequence (the HST and C2 marker deposited during maximum transgression and stillstand) may once have extended across the entire shelf, but are not preserved in the southern region and may be missing due to major lowstand erosion during the formation of the Arnhem Land SB.

Transgressive systems tract

The bulk of Sequence *IV* is composed of up to three stacked, fining-upward parasequences of the TST. Each such fining-upward parasequence is interpreted to record marine deposition in progressively deeper water. Stacked examples of these parasequences are interpreted to record an overall relative sea level rise punctuated by minor relative falls in sea level which involve some submarine erosion (but not subaerial exposure). In this sense the stacking patterns and

geometry of these parasequences can be interpreted via the sequence stratigraphic model as in other studies where fining-upward TST 'parasequences' are documented (*e.g.* Cheel and Leckie, 1992; Shanley and McCabe, 1991; Surlyk, 1991).

On most parts of the shelf the base of the TST is a thin, transgressive pebble lag (Fig. 9.1). The lag is less than 0.25 m-thick, and is sometimes only defined by a few scattered granule to small pebble sized clasts (*e.g.* in the BPRZ). The underlying Stoney Ridge SB coincides with the regional transgressive surface. The basal fining-upward transgressive succession is the coarsest-grained of the 'parasequences' in the TST, and shows the upward decrease in grain size, and changes in sedimentary structures and trace fossils indicative of progressive drowning (see description of facies succession 5 in Sect. 4.5.2).

The tops of fining-upward parasequences are defined by undulating surfaces of submarine erosion with erosional relief of tens of centimetres and marine hardgrounds (Plate 9d). Overlying these surfaces are the bases of younger fining-upward parasequences. These surfaces and corresponding TST deposits are best seen in the northern region, particularly the ALZ, where the number and thickness of fining-upward parasequences is greatest (Fig. 9.1). Here the base of each succession is defined by a thin conglomeratic lag (similar but thinner than the lag at the base of the TST), or a mineralised and brecciated sandy layer (Plate 9c).

There are 3 stacked TST fining-upward parasequences in the ALZ, and in most other places on the shelf there are 2 stacked fining-upward parasequences. There are a few trends in these successions across the shelf, the most obvious being their retrogradational (back-stepping) stacking pattern, *i.e.* both the number and thickness of TST parasequences increase regionally in a landward (northwest) direction (Fig. 9.3I). Also, the grain size of successions decreases towards the top of the TST across the entire shelf. This feature supports the interpretation of retrogradation in response to overall transgression during accumulation of TST deposits (*cf.* Van Wagoner *et al.*, 1990).

On all parts of the shelf within the TST of Sequence *IV* the uppermost fining-upward succession is the most complete, and contains the finest-grained rocks. In the northern region and the proximal part of the central region the grain size within this parasequence decreases upward to a relatively sharp layer, above which thin very fine-grained beds occur. This surface is the base of the C2 marker and forms a maximum flooding surface across the shelf.

Highstand systems tract

The HST of Sequence *IV* is thin (maximum of 3.5 m) and is only preserved in the northern half of the study area. Offshore from the proximal part of the central region the HST is missing. As previously stated (chapters 5-8), It is likely that the HST accumulated across the entire shelf (Fig. 9.3J), but is missing in the southern half of the study area due to significant erosion during formation of the Arnhem Land SB (Fig. 9.3K).

The HST is composed of a condensed section of fine-grained rocks including the C2 marker and facies 13, 16, 21, and 22 (Plates 6c, 6e, 10f). These rocks have not been grouped into any specific facies succession, but can be considered as one parasequence for the purpose of regional correlation. Due to the small thickness of the HST and its partial truncation by the overlying sequence boundary unconformity, it is not possible to recognise any parasequence stacking pattern within this systems tract. The top of the HST, and the top of sequence *IV*, is marked by the shelf-wide Arnhem Land SB.

9.5.6 Sequence *V*

Sequence *V* is the most complex, and probably most interesting, of all sequences on the shelf because it contains a large variety of facies successions encompassing fully marine, sheltered/restricted marine, and fluvial depositional environments. The sequence documents a large lateral shift in facies belts across the shelf and is bounded at its base by a type 1 shelf-wide unconformity (Arnhem Land SB). In places the top of Sequence *V* is marked by an unconformity and overlying ?Tertiary weathering profiles, but in many areas the top of Sequence *V* (as should be defined by a sequence boundary) is not preserved.

Fluvial, restricted marine, and nonmarine deposits in Sequence *V* are all considered to have been deposited during the TST and HST, not the LST. This observation seemingly contradicts the 'normal' interpretation that fluvial deposits in such a setting belong to the LST. Evidence for fluvial deposition within the Mullaman Beds during transgression is presented in Sect. 9.6.2. Sequence stratigraphic concepts and nomenclature can be applied to all rocks of Sequence *V* regardless of depositional environment.

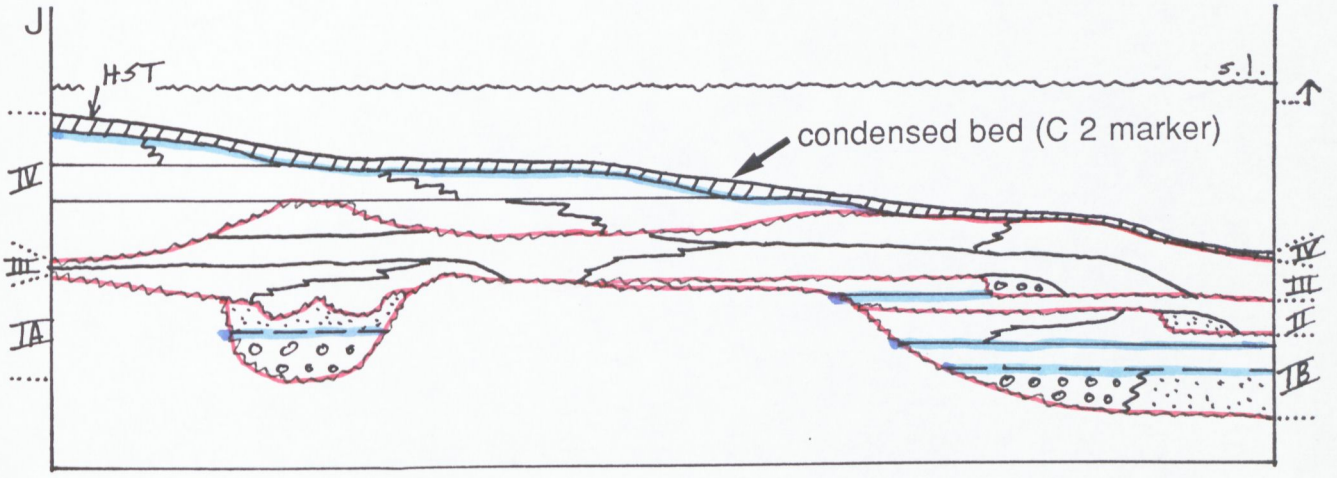
J
HST
s.l.
condensed bed (C 2 marker)
IV
III
IA
IV
III
II
IB

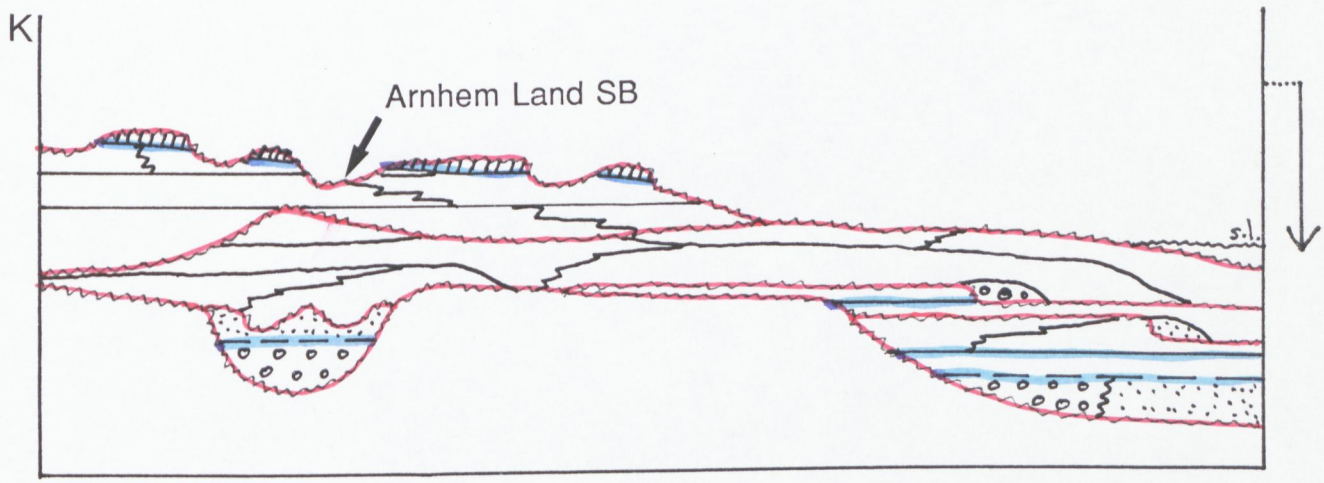
K
Arnhem Land SB
s.l.

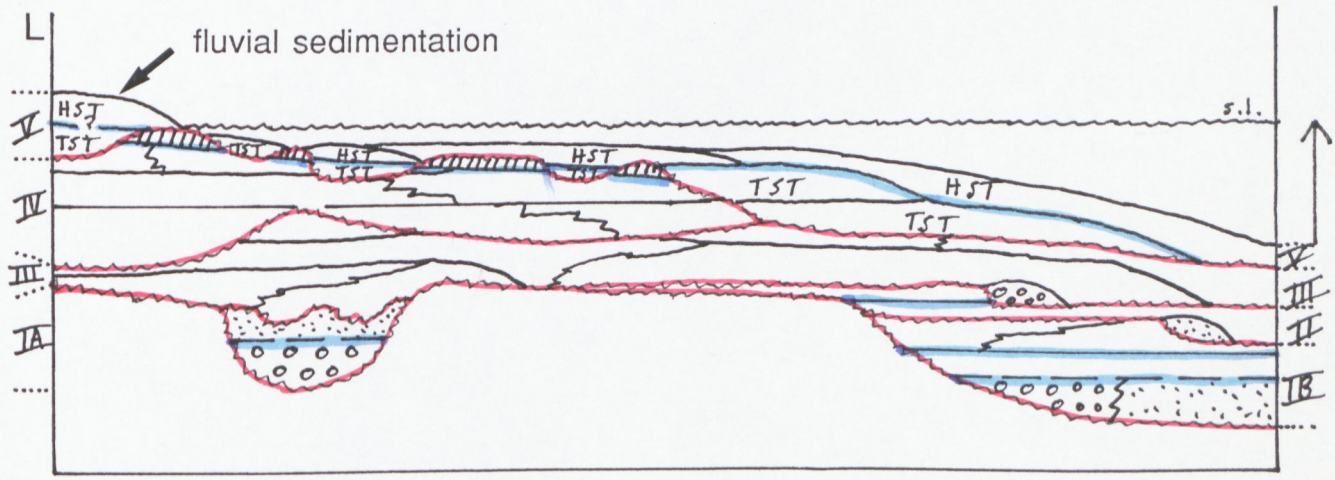
L
fluvial sedimentation
HST
TST
s.l.
V
IV
III
IA
TST
HST
TST
V
III
II
IB

Transgressive systems tract (northern nonmarine/restricted marine successions)

In the northern half of the study area the TST is composed of two major facies successions (Fig. 9.1); facies succession 7 which represents nonmarine deposition, mainly in fluvial channels (Plate 11g-h); and facies succession 8 which represents restricted marine deposition in large sheltered bays and lagoons where there was still some storm influence. These two facies successions do not occur together in the one location, but are related by regional lateral facies changes (Sect. 8.3). The presence or absence of each of these facies successions depends on local palaeogeography and (palaeodepositional) position on the shelf. Facies succession 7 is interpreted to occur landward of the palaeoshoreline, and facies succession 8 is interpreted to occur basinward of the regional palaeoshoreline, but separated from the open shelf by a barrier (back barrier/lagoon).

Correlation of systems tracts and surfaces is best between deposits of facies succession 4 (southern region offshore marine) and succession 8 (restricted marine). On a regional scale the thick restricted marine deposits of facies succession 8 overlie the Arnhem Land SB with a sharp erosional contact. Rarely, a thin conglomeratic lag is present at the base of succession 8. The grain size variation both laterally and vertically within succession 8 deposits is irregular, and appears to be controlled or strongly influenced by local palaeogeography and proximity to sources of coarse-grained clastics (topographically-high basement terrains). However, there are two main regional stratigraphic trends apparent in deposits of facies succession 8 in the northern half of the study area (Fig. 9.1):

1) The basal parts of the deposits exhibit fining-upward grain size and/or a change in sedimentary structures, indicating an apparent rise in relative sea level.
2) Regionally, a highly bioturbated zone rich in concretions (in the ALZ) and bivalve and ammonite shells (in the BPRZ and central region) occurs between 3 and 4.5 m (typically 4 m) above the sequence boundary. This zone or surface defines a change in sedimentary structures and grain size within succession 8 deposits across the northern half of the shelf (above this surface the grain size is coarser and sedimentary structures indicate progressive shallowing).

I regard the basal rocks of facies succession 8 (up to the 4.5 m level) as belonging to the TST. The evidence suggests a progressive rise in relative sea level up until the condensed shell-rich zone at the 3 to 4.5 m level, which is interpreted as the maximum flooding surface. Further evidence for transgressive deposition of facies succession 8 at this level is given by the local abundance of segmented plant fossils, including logs with *Teredolites* trace fossils (*e.g.* section

85, TST of Sequence *V*). Concentration of xylic substrates with allochthonous logs and/or *Teredolites* is indicative of transgressive shelf deposits, and the formation of log-grounds or plant-rich zones is controlled by relative sea level rise (Savdra, 1991; Savdra *et al.*, 1993).

There is no obvious retrogradational stacking pattern for the TST, but considering the thinness of TST rocks of succession 8 and their restriction to particular settings (*e.g.* bays) this is not surprising. Above the 3 to 4.5 m level (maximum flooding surface) thick, typically coarser-grained deposits of facies succession 8 are interpreted as belonging to the HST.

It is more difficult to correlate between marine (facies succession 4) and nonmarine (facies succession 7) deposits using sequence stratigraphic criteria because of the uniformly coarse grain size of the fluvial deposits and the lack of obvious surfaces defining base level changes. This situation is not unique to the Mullaman Beds, *i.e.* one of the greatest criticisms of the sequence stratigraphic model is its lack of applicability (perceived or proven) to nonmarine environments, and the fact that it is based almost entirely on marine case studies (*e.g.* Miall, 1986, 1991; Posamentier and Weimer, 1993). If simple 'one to one' correlation exists along the Arnhem Land SB, then fluvial deposits in the northern half of the study area are coeval with offshore marine rocks in the southern half, and they all belong to the TST.

Fluvial rocks of succession 7 in Sequence *V* are typically fining-upward, trough cross-bedded sandstones with basal conglomeratic lags. The maximum thickness of these deposits is 50 m, although this thickness is only reached in one locality in the BPRZ. Typically the total thickness of fluvial deposits is 8 to 12 m. The thickness of each fining-upward cycle (parasequence?) is less than 10 m (typically about 5 m). In outcrop the fluvial deposits are composed of up to four such stacked cycles, representing amalgamated coarse-grained channel deposits (Plates 6e and 11g). There are almost no fine-grained rocks within these fluvial deposits. Erosion at the base of the channels is common, and smaller-scale erosive surfaces are also present within each channel sequence (fining-upward cycle).

Transgressive systems tract (southern marine successions)

In the southern half of the study area, on intermediate to distal parts of the shelf, the TST is composed of two fining-upward parasequences, each consisting of a single fining-upward cycles of facies succession 4 (Fig. 9.1). The lower parasequence is coarser-grained, and directly overlies the Arnhem Land SB with a thin transgressive lag (Fig. 9.1). The clast size of the lag generally decreases in an offshore direction (southeast), and the amount of erosional

relief along the unconformity also decreases in this direction (Table 9.1). In places a correlative conformity is present, or the amount of erosion was minimal (Plate 11c).

The transgressive lag is regionally extensive and is composed of different components in different areas including, disarticulated bivalve shells, large shale rip-up clasts, and granule to rare pebble sized clasts in coarse sand. Rarely do these different components occur together in the lag, and the composition of the lag seems to have been dependent on the local availability of various coarse-grained material. The lag is 0.25 to 0.5 m thick, and typically has a gradational contact with overlying sandstone and siltstone. The top of this cycle is defined by a sharp regionally-extensive contact across which there is a decrease in grain size.

The upper parasequence is subtly fining-upward and is composed of sandy siltstone, siltstone and rare claystone. In places dispersed small-pebble to granule sized clasts are present amongst the finer-grained rocks in association with HCS, and are interpreted as storm-transported clasts (see Krassay, 1994a). Towards the top of this succession the degree of bioturbation increases, fine lamination becomes more prominent, and the top 0.5 to 1 m contains concretions. This thin condensed concretionary horizon, interpreted as the maximum flooding surface, separates the overlying HST deposits from the two underlying TST parasequences.

The TST in Sequence *V* exhibits a prominent retrogradational stacking pattern of parasequences, in the sense that in all areas in the southern region the grain size decreases offshore and towards the top of the TST. Successively younger parasequences were deposited farther landward during a progressive rise in relative sea level across the shelf (Fig. 9.3L).

Highstand systems tract (northern nonmarine/restricted marine successions)

Restricted marine rocks of the HST of Sequence *V* in the north belong to facies succession 8. As in the southern area, the difference between the HST and the underlying TST is not reflected by obvious changes in sedimentary structures, grain size, or fossil content. However, in the BPRZ the HST becomes thicker and coarser-grained to the south (offshore) in response to progradation, and can be separated on a regional scale from underlying finer-grained rocks of the TST. The key surface for separating the HST and TST is the concretionary or shell-rich zone about 4 m above the Arnhem Land SB (Fig. 9.1). This surface can be confidently correlated from the northern area (marginal marine) to the southern area (fully marine). Highstand deposits are thicker in the northern half of the study region, and this is interpreted to be due to preservation of the thickest prograding sandbodies near the regional palaeoshoreline.

In the ALZ the thickness of the HST rocks of facies succession 8 reaches a maximum of 17 m, but in many places the thickness is less than 10 m. It is difficult to correlate individual cycles ('parasequences') in the HST between different areas in the northern half of the study area. It is envisaged that this is due to local factors (sediment supply, degree of connectedness of the bays / lagoons, amount of incident wave energy) that controlled accumulation and progradation within the separate bays where facies succession 8 accumulated.

Within amalgamated coarse-grained fluvial deposits (facies succession 7) of Sequence *V* it is not possible to recognise the maximum flooding surface, and so it is not possible to precisely separate the TST and HST in the deposits. This fact is predicted in the model of Wright and Marriot (1993; Sect. 9.6.2), which suggests that during highstand the main process would be reworking of fluvial deposits rather than continued accumulation. Thus, any surfaces distinguishing the HST from the TST (*e.g.* flooding surfaces, condensed intervals) would probably not survive intense reworking (lateral accretion) on the coastal and alluvial plains during highstand.

Highstand systems tract (southern marine successions)

On offshore regions of the shelf the HST has a maximum preserved thickness of 5.5 m and is composed of sandstone and siltstone of facies succession 4. In the southern half of the study area the HST is only preserved in the distal part of the central region and the proximal part of the southern region. The HST overlies the regional maximum flooding surface defined by a condensed concretionary horizon. The HST is missing through erosion (at the Lawn Hill SB level) in the distal part of the southern region.

Compared to the HST of other sequences on the shelf, the HST of Sequence *V* is composed of relatively fine-grained rocks which do not show obvious stratal geometries or stacking patterns. The rocks of the HST are similar to the rocks of the underlying TST in terms of sedimentary structures, fossil content, and average grain size. Without the presence of the regional concretionary horizon it would be difficult to distinguish between rocks of the TST and HST.

9.5.7 Sequence *VI*

This sequence is the thinnest and least extensive of all the sequences. The nature and extent of this sequence is based on only a few outcrops, all in the southern region. For this part of the stratigraphy there is no biostratigraphic control on an outcrop scale, so it is possible that the

isolated outcrops at the top of the Cretaceous succession do not all belong to the one sequence. It is also possible that some of these rocks are Tertiary in age, and belong to the overlying Karumba Basin succession. However, considering that these rocks form similar facies successions and have similar thicknesses, sedimentary structures, and trace fossil content to underlying Cretaceous rocks they are assumed to be part of the Mullaman Beds.

Lowstand systems tract

Everywhere the base of Sequence *VI* is defined by a conglomerate up to 2 m thick (Fig. 9.1), but in the distal part of the southern region the conglomerate is preserved as a thin veneer. The conglomerate contains pebble to granule sized clasts (and rare cobbles), is massive or normally graded, poorly sorted, and directly overlies the Lawn Hill SB. The conglomerate reflects the same high-energy fluvial depositional environments as envisaged for thick conglomerates at the base of the Cretaceous shelf succession (Sequence *IA* and *IB*). The conglomerate does not contain any fossils, shows no imbrication or marine cementation, and is not bioturbated.

It is likely that these conglomerates formed in large and/or high-energy fluvial channels which incised across the shelf during lowstand. This interpretation is supported by the stratigraphic relationship of the conglomerate to underlying marine deposits of Sequence *V*; the Lawn Hill type 1 unconformity has incised down into underlying rocks of Sequence *V* by at least 10 m in places. Here the entire HST and much of the TST of the older Sequence *V* is missing through erosion (Fig. 9.3M). The amount of regional erosion along the Lawn Hill SB indicates deep incision by powerful streams during lowstand. The fill of these streams is preserved as the overlying fluvial conglomerate of Sequence *VI*.

The top of the conglomerate (LST) exhibits a sharp contact with overlying rocks on a regional scale. This contact marks the vertical change to finer-grained, fossiliferous, bioturbated brackish marine and ?lacustrine rocks of facies succession 6. The sharp contact is interpreted as the transgressive surface.

Transgressive systems tract

In the proximal part of the southern region the TST is represented by up to 3 m of coarsening-upward, ripple-laminated siltstone and interbedded fine sandstone. These rocks do not contain fossils and are slightly bioturbated. They most closely resemble facies succession 1 (shallowing-upward offshore marine), but due to their overall lack of fossils, limited lateral

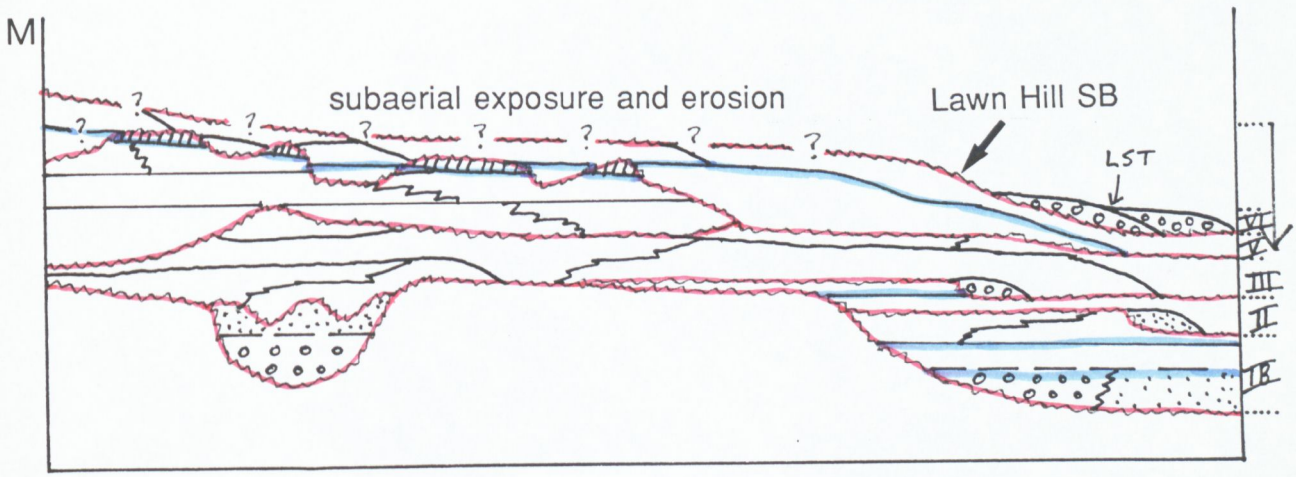
M
subaerial exposure and erosion
Lawn Hill SB
LST
VI
V
III
II
IB

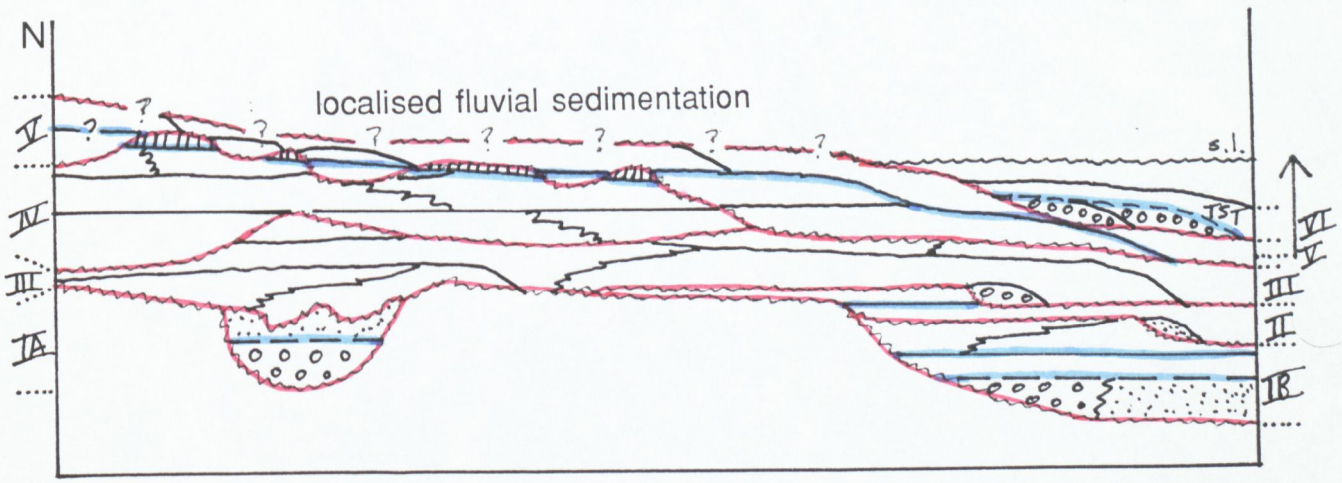
N
localised fluvial sedimentation
s.l.
LST
VI
V
IV
III
IIA
II
IB

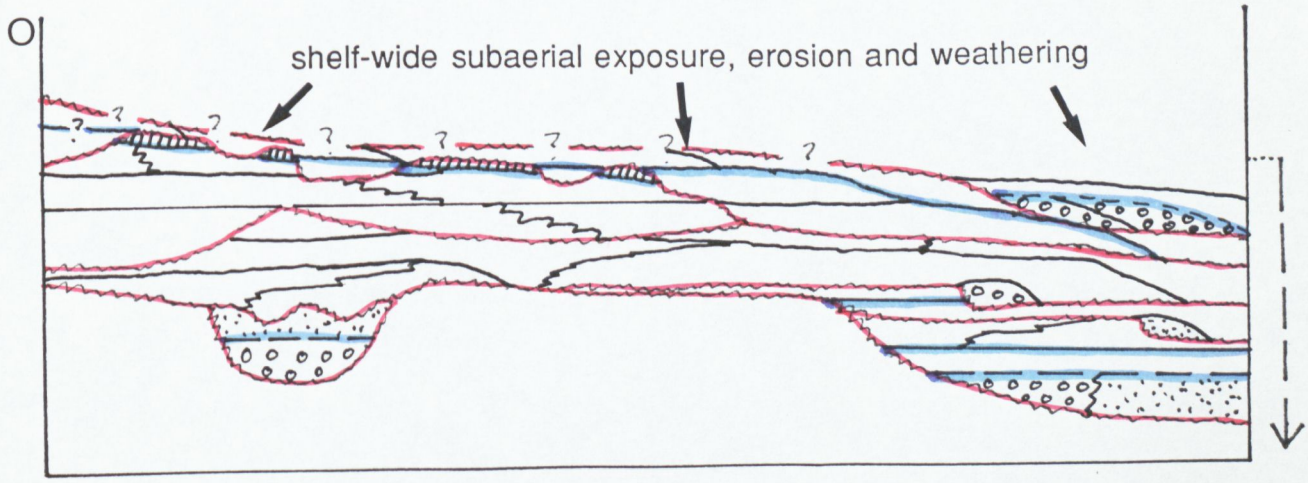
O
shelf-wide subaerial exposure, erosion and weathering

extent, and small thickness it is not possible to unequivocally define their depositional environment. However, it is possible to say that these rocks overlie LST coarse-grained fluvial conglomerate (Figs. 9.1 and 9.2) and seem to indicate deposition in deeper (probably marine) water (Fig. 9.3N).

Farther offshore, in the distal part of the southern region, the conglomerate (LST) is overlain by massive or subtly fining-upward, slightly bioturbated coarse- to medium-grained sandstone. The top two metres of this sandstone are moderately bioturbated and contain a great abundance of marine bivalves preserved as disarticulated whole valves. This sandstone also contains numerous segmented plant fossils preserved as moulds of small stems. In most places the bivalve and plant fossils occur together at the same stratigraphic level.

The lower sandstone (unfossiliferous and not bioturbated) and upper sandstone (fossiliferous and bioturbated) belong to facies succession 6. The lower (nonmarine?) sandstone overlies the LST conglomerate and grades up into the upper (brackish marine?) sandstone. The lower nonmarine(?) sandstone could be considered as part of the LST, but it overlies the conglomeratic lag with a well-defined, sharp contact interpreted as the transgressive surface. Therefore, both of these sandstones of facies succession 6 probably belong to the TST.

In summary, the TST of Sequence *VI* shows lateral variation in the southern region; in proximal areas the rocks are fine-grained and overlie a thick nonmarine conglomerate; in distal areas the rocks are coarser-grained, more obviously marine in character, and overlie a thinner conglomeratic lag. It is difficult to see stratigraphic geometry indicative of transgression (in the form of a retrogradational stacking pattern of parasequences/successions), but transgression is indicated by a sharp contact of fine-grained rocks with an increasing marine influence over coarser-grained nonmarine conglomerate.

The top of Sequence *VI* is not exposed, but this stratigraphic level is represented in the area surrounding Sequence *VI* outcrops by the contact with weathering horizons of probable Tertiary age. Here the ?Tertiary rocks are nonmarine, and the contact is regarded as a type 1 unconformity at the top of the Cretaceous shelf succession (Fig. 9.3O). However, as on all parts of the shelf the upper boundary of the Cretaceous shelf succession is poorly defined because preservation (or development) of the ?Tertiary rocks is patchy. No single regional unconformity which marks the top of the Cretaceous shelf succession was identified.

9.5.8 Summary of sequences on the Carpentaria Basin shelf

1) Most unconformities on the shelf are type 1 sequence boundaries involving a large amount of subaerial and/or submarine erosion, and a significant basinward shift in 'facies belts'.

2) LSTs are typically thin and are composed of prograding, coarse-grained nonmarine or shallow-marine clastic deposits (lowstand fans and fine-grained slope deposits are missing). On the inner shelf the LST occurs as incised valley fills, and on the distal shelf the LST is represented by thin, coarse-grained lowstand shorelines. The middle shelf was typically a zone of bypass, and the only LST deposits there are thin conglomeratic lags which have been modified by transgression.

3) Most TSTs are composed of fining- and deepening-upwards parasequences. Each parasequence equates to one facies succession (typically facies succession 4 or 5 for the marine shelf). The TST typically has a basal transgressive lag, and individual parasequences within the TST also commonly have a basal lag. The stacking pattern of parasequences within the TST (if recognised) is retrogradational, with parasequences becoming finer-grained landward and towards the top of the TST. There are no systematic parasequence thickness variations within the TST.

4) Most HSTs are composed of coarsening- and shoaling-upwards parasequences, where each facies succession (typically facies succession 1 or 2 for the marine shelf) corresponds to a single parasequence. HSTs overlie maximum flooding surfaces defined by thin, condensed intervals rich in fossils, ferruginous and manganiferous cement, and concretions. Where the TST is missing, the base of the HST may be defined by a thin conglomeratic lag. The upper part of HSTs exhibit subtle to extreme progradational parasequence stacking patterns, where parasequences become thicker and coarser-grained towards the top of the HST as the deposits build out into the basin. The basal and intermediate parts of HSTs typically show little or no evidence of progradation, and were formed by aggradation.

5) On many parts of the shelf transgressive surfaces coincide with sequence boundaries because LST deposits are missing (either due to erosion during subsequent transgression, or to non-deposition and sediment bypass on parts of the shelf).

6) Within restricted/marginal marine deposits (facies successions 6 and 8) and nonmarine deposits (facies successions 3 and 7) recognition of parasequences is more difficult, and these deposits commonly have irregular vertical grain size variation and stacking patterns.

9.6 SEQUENCE STRATIGRAPHIC DISCUSSION

9.6.1 Do fining- and deepening-upwards marine parasequences exist?

Parasequences are the fundamental building blocks of systems tracts and sequences, and their definition and documentation is vital in sequence stratigraphic analysis. The definition of a parasequence (see Sect. 9.2), is taken to mean coarsening- and shoaling-upward facies successions. Fining-upward parasequences do exist, but are mostly thought to be shoaling-upward and supposedly represent tidal or subtidal deposition in muddy, tide-dominated shallow-marine settings (*e.g.* Van Wagoner *et al.*, 1990).

Van Wagoner *et al.* (1990, p. 8-10) state that "If individual 'deepening-upward' parasequences do exist, they are assumed to be rare in the rock record". After documenting such fining- and deepening-upward marine parasequences in the Mullaman Beds I regard this assumption to be incorrect, at least in the case of the Carpentaria shelf system. Van Wagoner *et al.* (1990, p. 10) also believe that "most deepening-upward facies associations (read successions) probably are produced by a back-stepping set of parasequences...". Indeed, this is the case with such parasequences of the Mullaman Beds and the present study is in agreement with these authors on this point.

In their interpretive summary of the existence of fining- and deepening-upward parasequences, Van Wagoner *et al.* (1990) suggest that careful observation may reveal subtle evidence of flooding surfaces marking parasequence boundaries, *i.e.* they believe that the recognition of fining- and deepening-upward parasequences in the field signifies a lack of care in picking flooding surfaces, and that in reality the same rocks can be better divided into shoaling-upward parasequences. This is not the case for most fining-upward parasequences of the Mullaman Beds (*e.g.* facies successions 4 and 5; Plate 2h); there are well-documented, repeated trends within these parasequences which show a gradual vertical change from coarser-grained upper shoreface deposits (*e.g.* SCS sandstone) to finer-grained lower shoreface deposits (*e.g.* HCS sandstone; Plate 3f) to ripple-laminated interbedded rocks to fine-grained hemipelagic facies of the offshore region (Plate 6c). The bases of these parasequences are clearly defined in most places by transgressive lags or omission surfaces, and the only marine flooding surface (if preserved) occurs at the top of the parasequence.

I propose that fining- and deepening-upward parasequences do exist in the Mullaman Beds, and that they are an important component of the Cretaceous succession. Detailed description of

these parasequences (each commonly defined by a single facies succession) and evidence for my assertions above are presented in Sects. 4.5.1 and 4.5.2, and the stacking patterns of these parasequences to form systems tracts are documented in Figs. 9.1, 9.2, and 9.3 and Sect. 9.5.

9.6.2 Fluvial successions: deposition during the LST or TST/HST?

The response of fluvial systems to relative sea level fall has received significantly more attention than the response to relative sea level rise. Posamentier and Weimer (1993) suggest that this focus is likely to have occurred because the fluvial response to falling relative sea level is significantly faster and consequently more dramatic than the response to relative sea level rise. With this in mind some authors have questioned parts of the classical sequence stratigraphic model with regards to the timing of fluvial deposition (*e.g.* Miall, 1991), and have suggested that maximum alluvial sedimentation takes place during the TST and/or HST rather than the LST (*e.g.* Shanley and McCabe, 1991, 1994; Wright and Marriot, 1993).

In the northern half of the study area thick fluvial deposits directly overlie the Arnhem Land SB (Plates 6e and 10f). In the conventional sequence stratigraphic terminology of Posamentier and Vail (1988) these deposits would belong to the LST. However, offshore to the southeast along the same unconformity these fluvial deposits correlate with fining-upward marine rocks which obviously belong to the TST (Figs. 9.1 and 9.2). Sequence stratigraphic analysis of the Mullaman Beds seems to support the new theories on the timing of fluvial sedimentation, and it seems likely that most nonmarine deposits formed on the shelf during early transgression. In some inland regions (*e.g.* the thick fluvial deposits in ALZ near the Nhulunbuy drillholes) fluvial deposition probably occurred during most times of sequence development.

The process of widespread fluvial clastic deposition, documented by fluvial deposits such as facies succession 7 in Sequence *V*, is documented by three main sequence stratigraphic models which encompass various periods in sequence development. Posamentier *et al.* (1988) suggest that in type 1 sequences (*i.e.* sequences bounded beneath by an type 1 unconformity formed by subaerial erosion after a major relative fall of sea level involving a basinward shift of 'facies belts') widespread fluvial deposition on broad floodplains may occur after all incised valleys are filled, during the late HST. According to these authors fluvial deposition can also occur during lowstand (LST), but the resulting deposits are isolated and have a sinuous or linear distribution pattern. Clearly, this scenario for deposition during the late HST and early LST does not fit fluvial deposits on the Mullaman Bed shelf (amalgamated channels forming broad alluvial sheets).

Shanley and McCabe (1991, 1994) consider that fluvial deposits accumulate only when subaerial accommodation space is being created (particularly during the early TST). In a study of Upper Cretaceous strata of the Kaiparowits Plateau in Utah, these authors documented laterally and vertically amalgamated trough cross-bedded channel sandstones, with little preserved fine-grained overbank sediment, immediately overlying a regional sequence boundary. These deposits are almost identical to fluvial deposits in Sequence *V* overlying the Arnhem Land SB. Shanley and McCabe (1991) regard their fluvial deposits as belonging to the lowermost part of the TST, and propose that when viewed over limited areas such deposits could be confused as belonging to the LST, in a situation similar to that of the Mullaman Beds.

In the third model Wright and Marriot (1993) propose that minor fluvial deposition could occur during lowstand, followed by major fluvial deposition during transgression as accommodation space increased. These authors believe that lowstand fluvial deposition in marginal marine sequences is rare because lowstand is more likely to cause cessation of fluvial deposition and reworking in the main fluvial system.

Wright and Marriot (1993) suggest that with a large, rapid rise in relative sea level, fluvial deposits form during the TST and are characterised by isolated channels with weakly developed soils separated by thick floodplain 'fines'. This is dissimilar to fluvial deposits in Sequence *V*. Conversely, with a slower rise in relative sea level, fluvial deposits formed during the TST are characterised by more amalgamated channel sandbodies, similar to those in Sequence *V*. During the later stages of the TST and early HST the formation of accommodation space decreases, and this results in lateral accretion. Lateral accretion increases the channel (sandy) / floodplain (silty) ratio, increases the amalgamation and interconnectedness of the sandbodies, and decreases the preservation potential of soils due to significant erosion and reworking which accompanies channel migration (Shanley and McCabe, 1994; Wright and Marriot, 1993).

In summary, Wright and Marriot (1993) propose that maximum fluvial sediment accumulation occurs during the TST, and fluvial deposits are reworked during the HST. This contrasts directly with the model of Posamentier *et al.* (1988), who propose that maximum fluvial sedimentation occurs in the late HST. The characteristics of fluvial deposits of the Mullaman Beds in the northern half of the study area (particularly in Sequence *V*) best fit the model of Wright and Marriot (1993), and also closely resemble rocks documented and modelled by Shanley and McCabe (1991). In both these models the fluvial rocks accumulated during the highest rate of increase in subaerial accommodation space and belong to the TST. A similar

situation with regards to the timing of fluvial sedimentation may also hold for estuarine rocks overlying sequence boundaries (Ainsworth, 1994).

Thus, it is interpreted that rocks of facies succession 7 in Sequence *V* belong to the TST, and accumulated during transgression following a major fall in relative sea level which produced a type 1 unconformity across the shelf (Arnhem Land SB). Amalgamated sandy fluvial deposits of Sequence *V* appear to be very similar to fluvial sandbodies which accumulated in Triassic and Cretaceous interior basins in Argentina (Legarreta and Uliana, 1991). These deposits are considered to have accumulated in a fluvial system with limited accommodation space and a low surface gradient, similar to the alluvial/coastal-plain setting envisaged for parts of the northern region in the present study.

9.6.3 Origin of lags and breccias in the Mullaman Beds

Conglomeratic and shelly lags are common in parts of the Mullaman Beds overlying sequence boundaries and parasequence boundaries (basal lags), and within individual marine parasequences (intraformational lags). Similar lags also occur in the top part of coarsening- and shoaling-upwards parasequences (upper lags) beneath marine flooding surfaces which define the parasequence boundaries. Lags occur on all parts of the shelf, but are in greatest abundance in areas where marine deposition occurred between the upper shoreface and offshore transition zone within the influence of storm waves. All three types of lags are described in detail as facies 3 (Sect. 3.2.3), whilst their development in a sequence stratigraphic sense is discussed in the following sections.

Basal lags and breccias (base of parasequences)

Lags at the base of individual facies or at the base of a parasequence are typically 0.5 to 0.75 m thick, with a maximum thickness of 2 m. Basal lags (Plates 5e and 6a) contain numerous components, may be weakly normally graded, and display subtle erosive reactivation surfaces defined by laterally continuous variations in clast size (see Sect. 3.2.3).

The formation of thin basal lags (such as in Sequence *III*, *IV*, and *V*) can be envisaged as occurring by one of three main processes:

1) by erosion in a fully subaerial setting following a major lowering of relative sea level, in which case coarse-grained material would be transported across the shelf by incising streams. Here, conglomeratic lags would belong entirely to a LST;

2) by regional wave scouring in an open marine setting where a minor lowering of sea level results in wave erosion of the underlying marine substrate. Clasts incorporated in the lags could be derived both from erosion of underlying units, and from offshore-directed transport of coarse-grained shoreface conglomerate. Again the lags would belong to a LST; and
3) by a combination of the first two processes; where initial erosion and lag formation is due to subaerial exposure during lowstand, and is followed by submarine (wave) erosion during transgression.

Lags formed by the second process would tend to contain numerous components and display laterally extensive reactivation surfaces, multiple graded intervals, and small-scale scours. These features would be produced by successive reworking events, presumably related to large storm-generated waves and strong currents (*cf.* Banerjee and Kidwell, 1991). The problems with this process when applied to the Mullaman Beds areas follows; firstly, the lags overlie a significant shelf-wide sequence-bounding unconformity which implies more than a minor lowering of relative sea level; and secondly, the lags also overlie nonmarine rocks in places and so the erosion surface could not have been formed entirely by wave scour in an open marine setting.

Thin conglomeratic lags could be formed by the third process with a lowering of relative sea level followed immediately by a steady rise (*cf.* Wadsworth and Walker, 1991). Importantly, the coarse clastic component which accumulated during lowstand would remain on the unconformity as a transgressive lag and the transgressing shoreface would remove all(?) traces of subaerial exposure, *i.e.* soil, coal, desiccation cracks. Wadsworth and Walker (1991, p. 1517-1518) state that in this scenario "a shoreface would be expected to form at the point of maximum lowstand of sea level, before the transgression began". This is exactly what occurs on the Mullaman Bed shelf, where a lowstand shoreline occurs at the base of Sequence *III* in the proximal part of the southern region and is laterally correlative with a thinner lag to the northwest overlying the Carpentaria SB.

In the ALZ, mineralised and brecciated horizons (Plate 9c) occur at the base of both of the upper two fining-upward parasequences within the TST of Sequence *IV*. These mineralised and brecciated layers are regionally extensive and are identical in stratigraphic level to 'normal' conglomeratic lags at the base of similar successions in other areas. They are interpreted to have formed entirely by submarine erosion, and their fragments contain ferromanganese marine(?) cement. Possibly they represent marine hardgrounds at omission surfaces which

were brecciated in situ by wave scour (which also formed the basal transgressive surface of erosion), and were then loosely filled-in by clayey sand during ensuing transgression. In the case of Sequence *IV*, these mineralised sandy breccias are interpreted to have formed by minor falls in relative sea level (short stillstand or regression) during a major transgression.

Intraformational lags (within parasequences)

Intraformational conglomeratic lags are common within the Mullaman Beds, particularly in facies 15-19 (Plates 3g and 13f). Here, the lags are thin (0.5 to 3 cm), laterally continuous on an outcrop scale and crudely graded (see Sect. 3.2.3).

In view of the interpreted low gradient of the shelf (see Sect. 10.6.4), the most likely process for the development of intraformational lags is 'normal' marine transport and erosion on the shelf during stillstand or stable periods of sea level. The position of these lags within parasequences and their composition and lateral extent suggests that storm waves were occasionally capable of eroding the seafloor without a relative fall in sea level. Some thin intraformational lags contain only one major type, or size, of clast or skeletal material and probably represent true, single-event storm layers (see Sect. 3.2.3). This interpretation is supported by the normal grading of these beds, their upward change in stratification, and their association with small-scale HCS and interference wave-ripples, suggesting deposition of progressively finer sediment towards the top of the bed as flow strength waned (Krassay, 1994a).

The process envisaged for widespread formation of numerous thin, laterally semi-continuous pebble lags within facies 15-19 of the Mullaman Beds has been described by Plint and Norris (1991). For a setting in the Alberta Foreland Basin similar to the Carpentaria Basin, Plint and Norris (1991) suggest that erosion by storm waves concentrated intraclasts, and moved chert pebbles several tens of kilometres out to sea in water that was only 10 to 20 m deep. This model is supported by the evidence for storm-deposition and reworking within intraformational lags of the Mullaman Beds.

Upper lags and coquinas (top of parasequences)

Lags are also present near the top of coarsening-upward parasequences, where they form discontinuous lenses or pods (up to 60 cm thick), which are commonly associated with HCS beds and coarser-grained cross-bedded sandstone (facies 8 and 14; see Plate 13b)

Upper lags tend to be thinner and less laterally continuous than basal lags or coquinas. Discontinuous lenses and pods of conglomerate at the tops of coarsening-upward parasequences are closely associated with HCS beds. Indeed, in many places their local distribution appears to be restricted to swales and erosional hollows in the underlying HCS beds. This suggests that after formation of HCS beds during waning storm conditions, the flow was probably incapable of moving pebbles significant distances, but was still able to concentrate pebbles in local topographic lows, *i.e.* the swales and hollows of the underlying HCS beds.

Some conglomerate lenses pass upwards into HCS beds or cross-bedded medium- to coarse-grained sandstone. This provides further evidence that the concentration of pebbles into discontinuous lenses was not the result of long-term reworking due to a relative fall in sea level, but more likely was the result of reworking during peak and waning storm-stages or possibly between storms in regions with strong bottom currents such as rips (*cf.* Leithold and Bourgeois, 1984). Similar interstratified lenses of conglomeratic lag and shelly lag associated with HCS beds, high-angle cross-stratified pebbly sandstone, and coarse-grained megaripples have been described in other storm-influenced shallow marine successions (Brenchley, 1985; Craft and Bridge, 1987; Dott and Bourgeois, 1982; Leckie, 1988; Nottvedt and Kreisa, 1987).

9.7 A SEA LEVEL CURVE FOR THE WESTERN CARPENTARIA BASIN, AND COMPARISON WITH GREAT ARTESIAN BASIN SEA LEVEL CURVES

The generalised sedimentary succession of the GAB (including the Carpentaria Basin) has been described as a series of coarse-grained sandstone bodies separated by finer-grained, silty and argillaceous intervals (Burger, 1986). Most authors have attributed these sedimentary changes (from high-energy to low-energy depositional environments) to regional sea level fluctuations (Burger, 1986; Exon and Burger, 1981; Morgan, 1980). In the following section the relative sea level history of the Carpentaria Basin shelf is interpreted from data presented earlier in the chapter, and is summarised in Fig. 9.4 and Table 9.3.

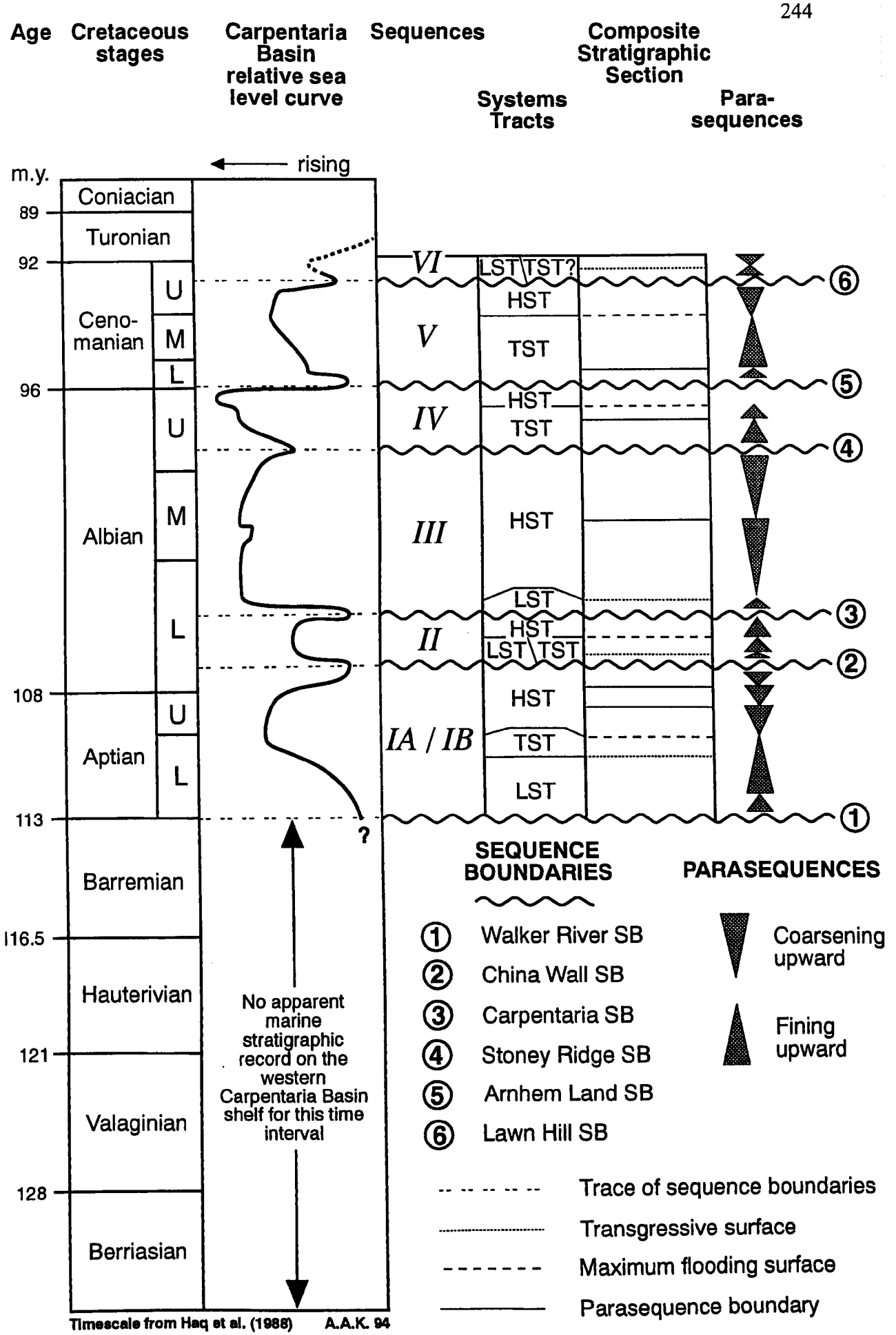

FIGURE 9.4. Cretaceous relative sea level curve for the western shelf of the Carpentaria Basin.

Table 9.3: Summary of depositional sequences and their internal composition and age.

Sequence	Status *	Estimated Age	Facies Successions (FS)	Basinal Equivalents
VI	- major regression - minor transgression in far southeastern part of shelf - terminal regression	Cenomanian (mid-late?)	LST = conglomerate + lower part of FS 6 TST = FS 6 + FS 1(?)	Normanton Formation (?)
V	- major rapid regression - step-wise transgression - max. flooding in central region	early (possibly earliest) Cenomanian	northern TST = FS 7 + 8 southern TST = FS 4 northern HST = FS 7 + 8 southern HST = FS 4	Normanton Formation
IV	- gradual transgression - max. flooding of northern shelf with extended highstand and thick condensed section	late Albian to latest Albian-early Cenomanian	TST = FS 5 HST = facies 13,16,21,22 and C 2 marker	upper Allaru Mudstone
III	- rapid major transgression - max. flooding of southern shelf and major highstand - minor regression	late early Albian to late Albian	LST = conglomerate HST = FS 1 + 2 late HST = FS 6	upper Wallumbilla Formation + Allaru Mudstone (Toolebuc missing)
II	- rapid minor transgression - rapid major regression	early Albian	LST = FS 5 + conglomerate TST and HST = FS 4	lower Wallumbilla Formation
IA / IB	- lowstand valley-filling - gradual transgression - slow regression	late Aptian and older (early Aptian?)	Valley Fill = FS 7 +fluvial facies TST = FS 4 + 6 HST = FS 2	Gilbert River Formation

Isolated fluvial deposition of facies successions 3 and 7 is not shown in this summary. Such deposition probably occurred mainly during the early TST and late HST of Sequences *IA / IB*, *II*, *V*, and *VI* (see Sect. 9.6.2). However, the exact ages of these fluvial deposits are unknown.

* The estimated timing and rates of relative sea level change are discussed in Sect. 9.7.

9.7.1 Pre-Aptian marine flooding of the western Carpentaria Basin shelf

The oldest age determined by biostratigraphy for the *exposed* Mullaman Beds in the present study is late Aptian, and the exact age of the base of the Mullaman Beds has not been directly established because there are a lack of suitable fossiliferous rocks at this level. In the absence of any biostratigraphically-dated Neocomian marine sediments within the Mullaman Beds (disregarding Skwarko's (1966) superseded palaeontological age determinations; see Sect. 8.2), there is no record of Early Cretaceous (pre-Aptian) relative sea level changes preserved in

the rocks. Regional correlations in this thesis have demonstrated that the bulk of the Mullaman Beds are younger than Aptian in age, and that it is likely that the base of the Mullaman Beds in most places (as defined by the Walker River SB) is no older than early Aptian (Figs. 9.2 and 9.4). A mid to late Aptian marine sequence has been documented recently in a few drillholes on the mainland in the central and southern regions (H. Barents, pers. comm. 1994), and this sequence is likely (but not proven) to represent the base of the Mullaman Bed succession.

Although Cretaceous marine rocks of Neocomian age may exist on the Mullaman Bed shelf, they probably only occur as a few isolated erosional remnants. Moreover, rocks of pre-late Aptian age are poorly exposed on the shelf, and the extent and nature of any pre-late Aptian relative sea level changes cannot be determined in the present outcrop-based study. However, a large and more complete database concerning the Neocomian to Aptian sea level history of the northern Australian region (including the Carpentaria Basin) is available from previous regional studies based in other northern Australian Basins (*e.g.* Eromanga). The evidence from these studies is discussed below.

Morgan's (1980) GAB sea level curve (Fig. 9.5A) shows only minor transgression in the Neocomian, followed by greater transgression from the basal Aptian onwards. A regional study by Paltech (1980c) in the Carpentaria and Eromanga Basins supports Morgan's findings, and again suggests only minor transgression in the Great Artesian Basin during the Neocomian (Fig. 9.5B). Paltech (1980c) propose that gradual transgression due to regional relative sea level rise began in the late Neocomian (Hauterivian), but increased markedly in the earliest Aptian.

Other evidence for Early Cretaceous (pre-Aptian) sea level changes in the Carpentaria Basin are documented in two major studies of Australian Cretaceous palaeogeography by Dettmann *et al.* (1992) and Frakes *et al.* (1987). Both of these studies involved the construction of palaeogeographic maps which illustrate the regional position of land and sea during various stages of the Cretaceous. From these assessments of emergent areas linked with relevant biostratigraphic data one can estimate the extent of transgression in the Carpentaria Basin at various times during the Neocomian.

The results of Dettmann *et al.*'s (1992) and Frakes *et al.*'s (1987) studies are in general agreement with each other, and with those of Morgan (1980), Paltech (1980c), and Burger (1973;1982) regarding regional sea level changes in the Neocomian in the GAB. They document only minor transgression onto the western Carpentaria Basin shelf from the

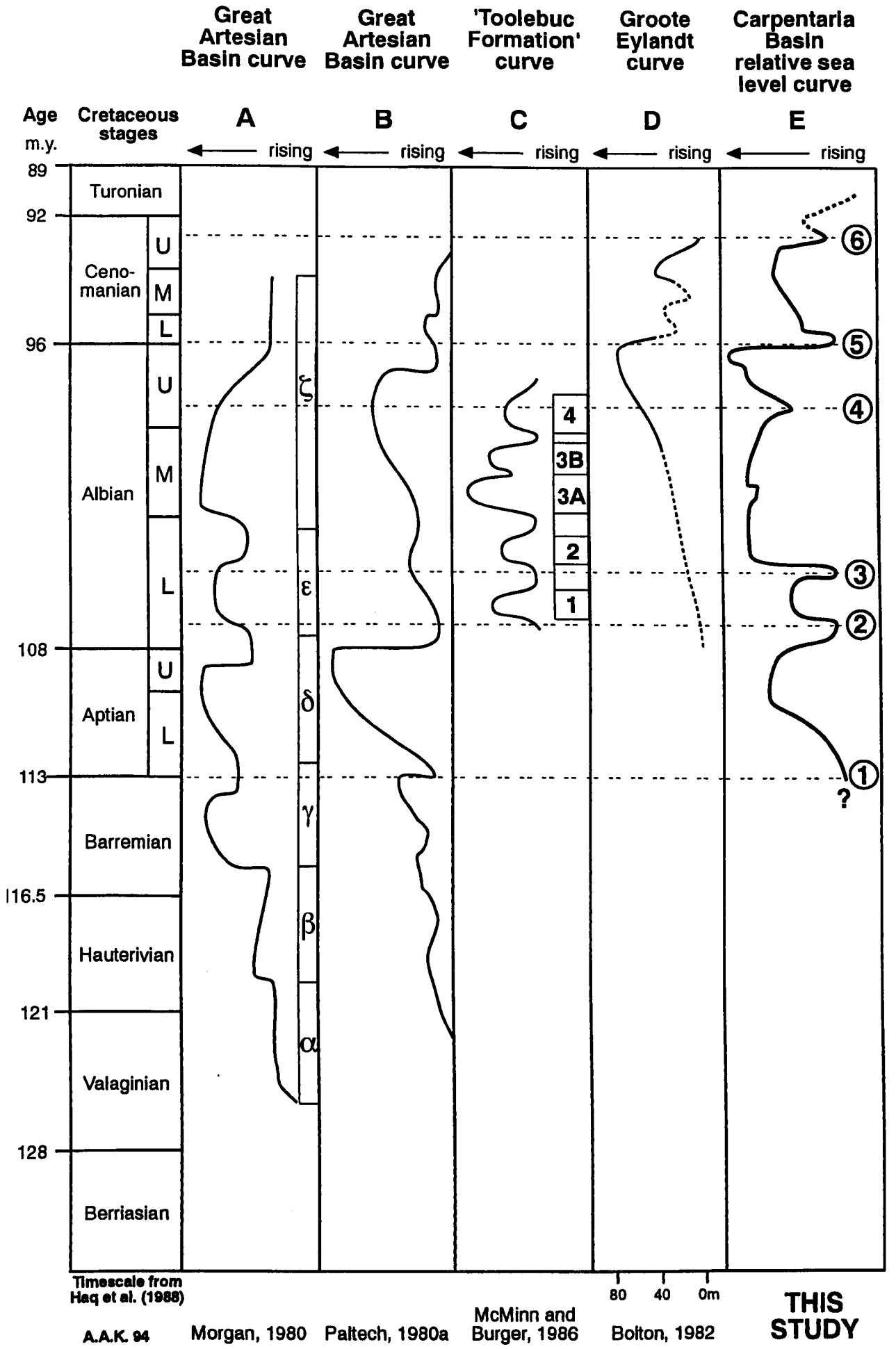

FIGURE 9.5. Comparison of northern Australian Cretaceous sea level curves.

Berriasian-earliest Valaginian to Barremian, followed by more extensive transgression from the basal Aptian onwards (Fig. 9.5A, B).

9.7.2 Aptian transgression

The first transgression recorded throughout the study area began at some time before the late Aptian (probably in the early Aptian, but the maximum age is unknown) after a significant period of erosion defined by the Walker River SB. The pre-late Aptian transgression seems to have been slow and steady and resulted in infilling of incised valleys of Sequence *IA* and accumulation of a thicker sedimentary succession (Sequence *IB*) on the outer shelf (Fig. 9.3B-C). Maximum transgression occurred in the middle to late Aptian (see ties between Aptian curves in Fig. 9.5A, B, and E) and preceded a relatively long period of high-water, resulting in the accumulation of thick HST deposits. The end of marine deposition and a major fall in relative sea level at the end of the Aptian is represented by the China Wall SB, which involved subaerial erosion on parts of the shelf. The relative sea level fall allowed steady progradation during the late highstand and must have been rather gradual. Subsequently, a lowstand shoreline was deposited above the sequence boundary during lowstand (Fig. 9.3D).

The timing of pre-late Aptian transgression on the Carpentaria Basin shelf (Fig. 9.5) has a good correlation with Morgan's (1980) "transgression δ", and also with the major Aptian transgression of Paltech (1980c; Fig. 9.5B). On Morgan's curve the regression ("minor regression γ") preceding the pre-late Aptian transgression corresponds closely in age to the Walker River SB, and also supports a tie between the curves.

Frakes *et al.* (1987) document major marine flooding over much of northern Australia in the Barremian-earliest Aptian, and high sea level supposedly occurred throughout much of the Aptian (*cf.* Dettmann *et al.*, 1992). However, judging by the rarity and small thickness of marine rocks of the Mullaman Beds which are late Aptian or older in age, it may be that the extent of Aptian transgression has been slightly overestimated in previous studies (see palaeogeographic reconstructions in chapter 10).

9.7.3 Early Albian (?) transgression

Following a period of subaerial erosion and formation of the China Wall SB, transgression occurred on the southeastern part of the Mullaman Bed shelf and surrounding Groote Eylandt. The age of this transgression is probably early Albian, but the exact age is unknown. This

transgression was short-lived and resulted in deposition of Sequence *II* in the southeastern part of the study area. Regression occurred towards the end of the early Albian and resulted in the formation of the Carpentaria SB (Fig. 9.5). This regression was caused by a rapid lowering of relative sea level, and involved a major basinward shift in facies across the shelf as the shoreline moved basinward (Fig. 9.3F).

The HST of Sequence *II* reflects the rapid nature of the regression because aggradational sediments are abruptly topped by a sequence boundary which lies beneath a lowstand shoreline deposit in the distal region (Fig. 9.2), *i.e.* slow and steady deposition proceeded for a time during the high water stage, and then HST deposition was abruptly terminated by a large, rapid fall in relative sea level. In this sense the lowering of relative sea level represents a 'forced regression' (*sensu* Hunt and Tucker, 1992; Posamentier *et al.*, 1992), and the lowstand shoreline deposit (at the base of Sequence *III*) overlying the Carpentaria SB could be considered as a 'forced regressive wedge systems tract' (Hunt and Tucker, 1992).

On the basis of foraminiferal evidence, Haig and Lynch (1993) document an early Albian sea level rise in the Carpentaria Basin which matches the timing of the rise on my curve, but could not determine the magnitude of the rise purely on the basis of the faunal records. Palaeogeographic reconstructions by Dettmann *et al.* (1992) suggest that this transgression was relatively small, in accordance with my observations, and resulted in inundation of parts of the northern and southern regions of the study area.

This proposed early Albian transgression corresponds well with Morgan's (1980) "minor transgression ε", "episode 1" of McMinn and Burger (1986), and the more gradual sea level rise in the early Albian on Paltech's (1980c) curve (Fig. 9.5). Given that the early Albian relative sea level rise on my curve can be tied to the other independent regional sea level curves, one can be confident that this early Albian rise was a regional event (at least), and is not simply an artefact of local processes within the Carpentaria Basin. Furthermore, on Fig. 9.5 the age and position of the China Wall SB (basal Albian) and Carpentaria SB (late early Albian), which formed before and after the early Albian rise respectively, also tally with major lowstands documented by Morgan (1980) and McMinn and Burger (1986) as eustatic lowstands.

9.7.4 Major marine flooding from the late early Albian to the late Albian: Maximum flooding of the southern shelf

Low relative sea level and subaerial erosion (Carpentaria SB) on the shelf towards the end of the early Albian were apparently short-lived, and were followed by major transgression which resulted in high relative sea level for much of the Albian (Figs. 9.3G and 9.4). Transgression is interpreted to have been rapid and widespread and caused sudden drowning of much of the shelf, particularly the southern half of the shelf (see Sect. 10.4.5). The rapidity of the transgression is suggested by the lack of well-defined TST deposits, abrupt drowning of lowstand shoreline deposits at the base of Sequence *III*, the large area inundated by the sea during this transgression, and the continuation of high water for a lengthy period after initial transgression. The age of the transgression is late early Albian to late Albian based on biostratigraphy of rocks of the Mullaman Beds (Haig, 1991). On the basis of regional correlation in the present study (Sect. 8.6), the transgressive pulse began on the western Carpentaria Basin shelf in late early Albian to early middle Albian time. The end of this major transgressive pulse occurred in the late Albian (just prior to Stoney Ridge SB time), but was followed almost immediately by another transgression (Fig. 9.5E).

The age, relative stratigraphic position, and duration of this major late early Albian transgression is supported in a detailed microfaunal study by Haig and Lynch (1993), although they did not produce a specific sea level curve. These authors have documented a major late early Albian transgressive pulse which affected the Papuan Basin and many northeastern Australian basins (Carpentaria, Eromanga, Surat, Laura). Haig and Lynch (1993) suggest that the sea level rise was Australia-wide, was partly controlled by eustatism, and may have been increasingly influenced in the late Albian by the tectonic climax along the eastern Australian margin (see Sect. 9.8 for discussion of eustasy and Sect. 9.9.3 for discussion of tectonic activity).

Initial relative sea level rise and major transgression on the western Carpentaria Basin shelf (beginning in the late early Albian to early middle Albian) can be tied to a similar rise of Paltech's (1980c) curve (Fig. 9.5B). Similarly, Haig and Lynch's (1993) late early Albian transgressive pulse corresponds to Morgan's (1980) "partial transgression ε" (Fig. 9.5A) and "episodes" 1 and 2 of McMinn and Burger (1986) (Fig. 9.5C). Haig and Lynch do not support the recognition of "minor regression ε" of Morgan (1980), and believe that sea level remained relatively high from the late early Albian to the late Albian. However, corroborating evidence

for a short-lived regression near the end of the early Albian (as shown by Morgan, 1980 and Paltech, 1980c) is present in the form of the Carpentaria SB on the shelf (Figs. 9.2 and 9.3G).

9.7.5 Major marine flooding from the late Albian to the latest Albian-early Cenomanian: Maximum flooding of the northern shelf

On the Carpentaria Basin shelf a minor lowering of relative sea level occurred in the late Albian, and resulted in minor submarine erosion and formation of the Stoney Ridge SB (Figs. 9.3H and 9.5). Supporting evidence for a major fall in relative sea level during the late Albian is shown by Morgan (1980; see Fig. 9.5A), McMinn and Burger (1986; see Fig. 9.5C), Paltech (1980c; see Fig. 9.5B), and Dettmann *et al.* (1992). However, none of these authors identified the subsequent transgression (Sequence *IV* transgression) which affected the Carpentaria Basin shelf. This transgression began in the late Albian and maximum transgression was reached in the latest Albian-early Cenomanian. This transgression is interpreted as the maximum flooding event for the Aptian-Cenomanian interval across the northern shelf (Fig. 9.5), and resulted in deposition of the C2 marker (Sequence *IV*) during relative highstand.

The timing of maximum flooding as latest Albian-early Cenomanian is supported by a detailed study of stratigraphic relationships, graded bedding and geomorphic features within the sedimentary sequence on Groote Eylandt by Frakes and Bolton (1984). They interpreted a series of benches cut into the Proterozoic bedrock on Groote Eylandt as being wavecut benches developed by near-shore processes at various times in the Cretaceous. Correlation of these topographically distinct benches with zones of normally- and inversely-graded pisoliths in quarries on the island were used by Bolton (1982) to construct an Albian to Cenomanian relative sea level curve for the Groote Eylandt region (Fig. 9.5D).

Frakes and Bolton's study also lends support for the major fall in relative sea level identified in the present study near the Albian-Cenomanian boundary (postdating the major sea level rise from the late Albian to the latest Albian-early Cenomanian). The exact timing of this fall in relative sea level is unknown, but it probably occurred in earliest Cenomanian time because the assigned age for the older HST deposits (latest Albian-early Cenomanian) is a *maximum* age derived from radiometric dating of glauconite (Sect. 8.2.2). Corroborating evidence for a major sea level fall after the late Albian is presented by Dettmann *et al.* (1992) based on palynology, and by Haig and Lynch (1993) based on marine microfaunas.

9.7.6 Early to middle (?) Cenomanian transgressions, terminal Cenomanian regression, and complete emergence in the Turonian

After the major fall in relative sea level at or near the Albian-Cenomanian stage boundary in the Carpentaria Basin (Fig. 9.5), there was another transgression which flooded the eroded landscape formed during lowstand (Arnhem Land SB time). This transgression probably began in earliest Cenomanian time and was apparently initially relatively rapid and affected most of the shelf. Rocks deposited during this transgression may be facies equivalents to the Cenomanian Bathurst Island Formation near Darwin. In particular, the Mookinu Member of the Bathurst Island Formation (see Hughes and Senior, 1973) is similar in lithology, age, and thickness to stacked deposits of facies succession 8 of Sequence *V*, and the Marligur Member of the same formation is similar to stacked deposits of facies succession 4 of Sequence *V*. Maximum transgression may have been reached as late as the middle (?) Cenomanian (no direct dating is available), and was followed by a moderate interval of high water before a major fall in relative sea level some time in the middle-late (?) Cenomanian (Lawn Hill SB time; Fig. 9.5E).

Bolton's (1982) data from Groote Eylandt (Fig. 9.5D) supports early Cenomanian transgression for the western Carpentaria Basin, and his final regression is tied to regression and lowstand (Lawn Hill SB) on my curve (Fig. 9.5E). Similarly, Paltech's (1980c) curve documents two minor transgressions in the early to middle Cenomanian which agree in principle with high relative sea level shown on my curve.

Not surprisingly, Morgan's (1980) curve is not in agreement with the present study (and Bolton, 1982) for the late Albian onwards; Morgan (1980) shows gradual regression in the late Albian and lowstand into at least the middle Cenomanian (Fig. 9.5A), whereas the present study documents regression at the beginning of the late Albian (Stoney Ridge SB time) followed by two additional major transgressions (Fig. 9.5E). However, it is important to realise that Morgan's curve is derived largely from microfossil data from the Eromanga Basin region, which was emergent in the Cenomanian (Dettmann *et al.*, 1992, fig. 10; Frakes *et al.*, 1987, fig. 8). Thus, relative sea level changes in the Carpentaria Basin which occurred in the Cenomanian did not affect the Eromanga Basin, and would not be recorded on Morgan's (1980) GAB sea level curve.

On the distal part of the Carpentaria Basin shelf, the Lawn Hill SB is overlain by lowstand conglomerate and interbedded rocks (Fig. 9.2). The interbedded rocks may be part of a TST which suggests another minor transgression, but the evidence is equivocal. After this possible

transgression (Fig. 9.5), it appears that terminal regression in the Carpentaria Basin began in the Cenomanian and the entire region was emergent by the Turonian (Frakes *et al.*, 1987). No record of younger Cretaceous marine rocks is preserved on the shelf, and it is likely that the entire shelf was subaerially exposed until the Tertiary (*cf.* Smart *et al.*, 1980).

9.8 COMPARISON WITH GLOBAL AND NORTHERN HEMISPHERE SEA LEVEL CURVES

9.8.1 Eustatic sea level curves

Haq et al.'s (1988) chart

Haq *et al.*'s (1987, 1988) global "eustatic" sea level curve (Fig. 9.6A) is probably the most widely accepted sea level record for the Mesozoic. On a broad scale there is agreement between the global "eustatic" curve and the Carpentaria Basin relative sea level curve; in both curves the Albian is a time of major transgression with maximum transgression at the Albian-Cenomanian boundary, marked regression near the beginning of the Cenomanian, and continued transgression in the early to middle Cenomanian. However, for the Aptian and the post-middle Cenomanian there is poor correspondence. This lack of correspondence of northern hemisphere and northern Australian Late Cretaceous sea level curves is taken to indicate either epeirogeny in the Late Cretaceous (Gurnis, 1994), or excess sediment supply (Gallagher and Lambeck, 1989), both of which could have resulted in overall apparent regression in Australia during a period of global transgression.

From the basal Aptian to the middle Cenomanian the Carpentaria Basin succession is composed of 5 complete sequences (not including Sequence *VI*) and six sequence boundaries (Fig. 9.6F). In comparison, for the same time interval the global "eustatic" chart records 11 sequences and 12 sequence boundaries (Haq *et al.*, 1988). With these figures in mind it seems that the two curves are not closely matched, although some of the important events are common to both curves. The mismatch in the number of sequences may be due in part to the proposed very low sedimentation rates for the Carpentaria Basin shelf, because low sedimentation rates tend to result in fewer and/or thinner sequences in most shallow-marine settings.

There are a number of ties between the curves, but the match (or mismatch) is irregular (Fig. 9.6A, F): the base of the Carpentaria succession (Walker River SB) matches exactly with the type 2 SB at 113.5 m.y. on the Haq *et al.* (1988) curve. However, the timing of transgression

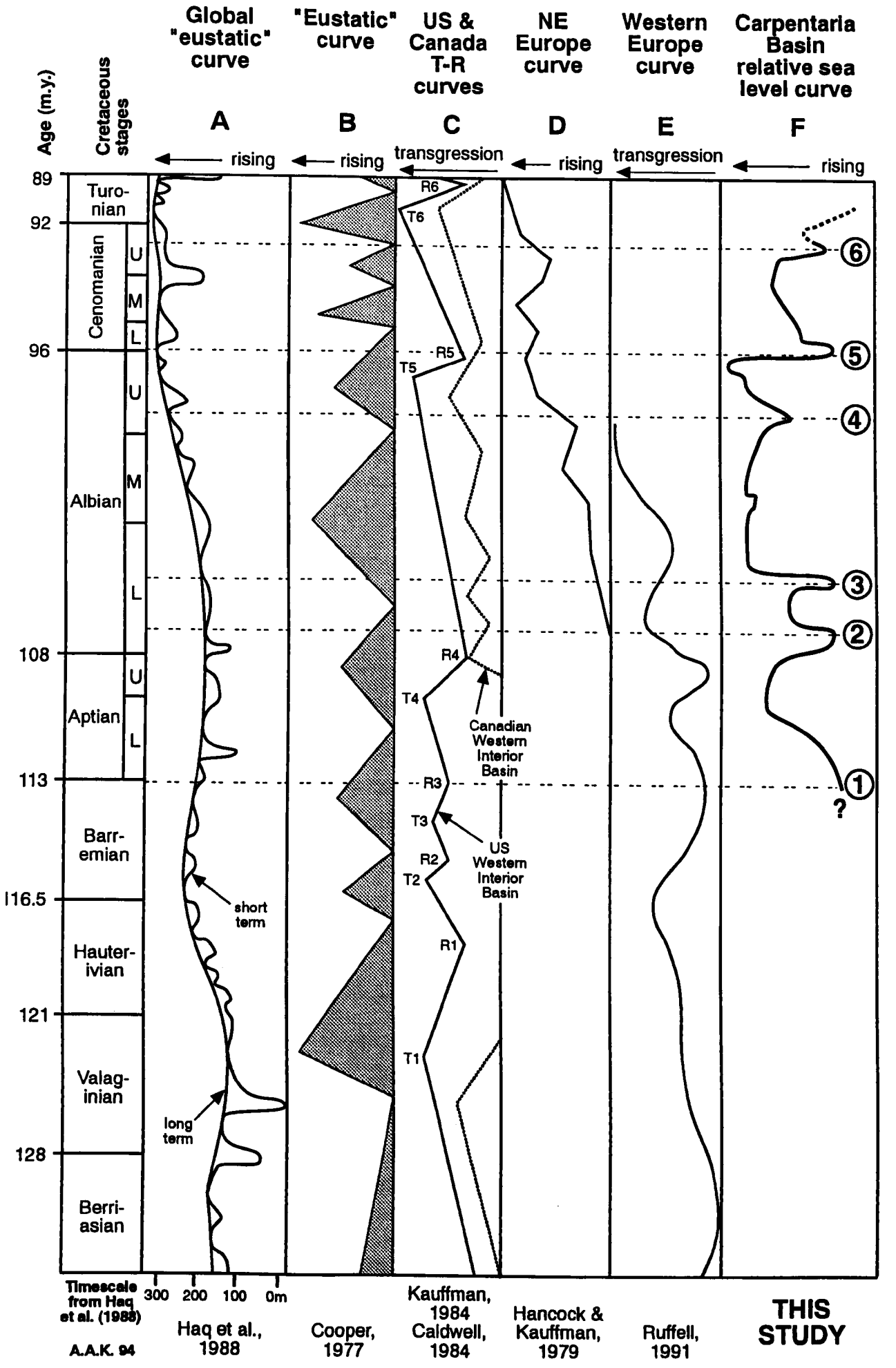

FIGURE 9.6. Comparison of Cretaceous Carpentaria Basin, northern hemisphere, and global sea level curves.

and maximum flooding during the Aptian are out of phase in the two curves. The China Wall SB does not match any SB on the global "eustatic" chart, but may be related to the type 1 SB at 107.5 m.y. Again, early Albian transgression and maximum flooding on the Carpentaria Basin curve do not match the global "eustatic" curve.

The position of the Carpentaria SB does not precisely match any sequence boundary on the global "eustatic" chart, but both curves show extensive transgression and highstand from the early to late Albian. The Stoney Ridge SB is close in position and age to the type 1 SB at 98 m.y., but I interpret the Stoney Ridge SB as a type 2 unconformity which only involved a minor lowering of relative sea level (possibly related to a low sedimentation rate and low subsidence rate, upon which a relatively minor sea level change was superimposed; see Sect. 9.9). There is a good match for late Albian transgression and stillstand leading up to maximum flooding in the latest Albian, which is followed by major regression in the latest Albian-early Cenomanian. At this level the Arnhem Land SB might correspond to the 95.5 m.y. type 2 SB on the global "eustatic" chart.

As with the Stoney Ridge SB, it is difficult to reconcile the differences in the type of sequence boundaries between the two curves, as the shelf-wide Arnhem Land SB is interpreted in this study as a type 1 unconformity (versus a type 2 SB on the global "eustatic" chart). Both curves show an early Cenomanian transgression, but in the Carpentaria Basin maximum flooding and subsequent regression occur at younger ages. The Lawn Hill SB seems to match the type 2 SB at 93 m.y. on the global "eustatic" chart.

Cooper's (1977) chart

Cooper's (1977) eustatic chart was palaeontologically-based and was compiled prior to and independently from early versions of the Exxon chart (*e.g.* Vail *et al.*, 1977), which is the precursor to Haq *et al.'s* (1988) chart. The close resemblance of Cooper's (1977) chart (Fig. 9.6B) to that in the present study (Fig. 9.6F) supports the proposition that these sea level changes are eustatic in origin (see further evidence for the eustatic nature of the sea level changes in Sects. 9.8.4 and 9.8.5).

Cooper's (1977) chart shows good correspondence with the curve for the Carpentaria Basin shelf with respect to the following (compare Fig. 9.6B to Fig. 9.6F):

1) major transgression in the late Aptian (and regression in the early Albian).
2) major transgression in the early-middle to late Albian.

3) regression at about the early late Albian (Stoney Ridge SB time).
4) renewed transgression in the late Albian.
5) regression near the Albian-Cenomanian boundary.
6) transgression in the early and middle Cenomanian, followed by major regression in the middle-late Cenomanian (Lawn Hill SB time).

The obvious difference is that Cooper's chart does not document an early Albian transgression, but this is not considered vitally important because the early Albian transgression was a relatively minor event on the Carpentaria Basin shelf anyway. The magnitude of some of Cooper's (1977) transgressive and regressive events differs from the present study because his regressions are all drawn to an arbitrary baseline, whereas in the present study a distinction is made regarding the magnitude of sea level falls (*e.g.* falls associated with a type 1 or type 2 sequence boundary). Also, Cooper (1977) showed the peaks of all his transgressions and regressions as sharp points joined by straight lines. His approach considers maximum flooding and lowstand as single points in time, whereas in reality these events occurred over some fixed time interval. Minor discrepancies aside, Cooper's (1977) chart has good correspondence and numerous apparent ties with the 'relative' sea level curve for the western shelf of the Carpentaria Basin.

9.8.2 Problems of precision for the sea level curves

The global "eustatic" curve of Haq *et al.* (1988) supposedly has a high level of biostratigraphic control which is supported by geochronology and magnetostratigraphy, whereas the Carpentaria Basin curve is constructed with a highly limited amount of biostratigraphic control, and the age of many of the sequence boundaries and other surfaces are therefore relatively poorly known. This on its own may bring about errors and make meaningful correlation difficult. However, the nature of biostratigraphic control in the present study does not allow a more detailed quantitative analysis of potential errors or mismatches in the correlations above.

Another potential problem is the time-scale used to construct the various curves. Early sea level curves of Morgan (1980) and Burger (1986) incorporated the time-scale of Van Hinte (1976). This varies significantly from Haq *et al.*'s (1988) time scale (which is used in Figs. 9.4, 9.5, and 9.6), which in turn varies from the most recent time-scale of Harland *et al.* (1990). Thus, the numbers assigned to the boundaries of Cretaceous international stages are not consistent for all studies, but this does not affect the biostratigraphic ages used in this study.

These factors suggest that direct correlation is difficult without a stable frame of reference, and ideally should depend on common biostratigraphic zones. In the absence of common precise biostratigraphy for both curves, most correlations should not be regarded as being unequivocal. Miall (1991; 1992b) takes the argument much further, and proposes that Haq *et al.*'s (1988) global "eustatic" curve cannot possibly be correct in its present form because the implied accuracy of the third-order eustatic cycle chart (short term curve in Fig. 9.6A) exceeds the error margins for various components used to construct the chart, *i.e.* global time-scale, ages of stage boundaries, biostratigraphic resolution. According to Miall (1992b) such errors are summed in the global "eustatic" chart, and so the Exxon global "eustatic" chart gives a false sense of precision for the timing and position of sequence boundaries, cycles and surfaces. This remains a highly contentious issue.

9.8.3 North American sea level curves

Figure 9.6C shows two summaries of transgressive-regressive cycles for North America; one for the western interior of the United States (from Kauffman, 1984), and one for the western interior of Canada (from Caldwell, 1984). Major features in both North American cycles show some positive correlation with the relative sea level curve for the Carpentaria Basin (Fig. 9.6F), but the matches are not exact.

On the US transgressive-regressive chart, R3 corresponds to the Walker River SB, T4 corresponds to the early Aptian transgression, T5 corresponds to latest Albian transgression, and R5 corresponds closely to major regression in the latest Albian-early Cenomanian. However, some early Albian regressions and transgressions in the Carpentaria Basin are not recorded on the US chart. The Canadian chart is interesting in that it resembles the US chart, but contains several more transgressive-regressive cycles in the early to middle Albian and thus has a better match with the Carpentaria Basin relative sea level curve. The Canadian chart shows a major regression from the Valaginian to the late Aptian. This agrees in principle with the situation in northern Australia, but the exact timing of transgression and regression are out of phase with the Carpentaria Basin curve (Fig. 9.6F) and other northern Australian curves (Fig. 9.5).

Both the US and Canadian western interior transgressive-regressive charts are similar in that they match moderately well with the Carpentaria Basin curve for the Aptian to middle Cenomanian interval. However, their younger record of high sea level is almost the reverse of the situation for the Late Cretaceous in northern Australia, where large areas were emergent (see

palaeogeographic maps of Dettmann *et al.*, 1992 and Frakes *et al.*, 1987). This discrepancy may be due to major Late Cretaceous tectonic activity along the southern and eastern Australian margins (see Sect. 9.9.3).

9.8.4 European sea level curves

Comparison of relative sea level curves for Europe (from Hancock and Kauffman, 1979; see Fig. 9.6D) and the Carpentaria Basin shelf shows good correlation from the middle Albian to Cenomanian, but poor correspondence for older and younger intervals. The two curves match with regard to minor regression in the late Albian (Stoney Ridge SB time) and subsequent transgression; regression in the latest Albian-early Cenomanian (Arnhem Land SB time); early Cenomanian transgression; and middle Cenomanian regression. The older parts of the curves show only superficial correspondence in that transgression is shown to have occurred gradually from the early Albian in northeastern Europe, but in the Carpentaria Basin significant changes in relative sea level occurred in both the Aptian and early Albian.

The northeastern European curve shows almost continuous transgression and high relative sea level from the Cenomanian to the Maastrichtian with maximum Cretaceous flooding in the late Campanian (not shown on Fig. 9.6D) and only a relatively short-lived lowstand in the Turonian. This is exactly the opposite to the situation in northern Australia where relative sea level peaked in the latest Albian-early Cenomanian and was apparently low from the late Cenomanian to the Tertiary (*cf.* Struckmeyer and Brown, 1990).

Ruffell (1991) produced a relative sea level curve for the Lower Cretaceous of NW Europe, based mainly on successions in Germany, France, and England (Fig. 9.6E). Ruffell's curve corresponds well with the curve for NE Europe of Hancock and Kauffman (1979), but shows some added details. Firstly, Ruffell (1991) documents one major transgression in the Aptian which corresponds well with the Aptian transgression in the Carpentaria Basin. Secondly, Ruffell (1991) indicates two major transgressions in the Albian, one in the early Albian, and one from the middle Albian onwards (Fig. 9.6E). The age and position of these transgressions and the intervening sequence boundaries can be confidently correlated between the two curves, and there are only minor discrepancies in the timing and interpreted rate of initial transgression between the curves.

Thus, there are good but variable matches in the relative sea level history for the Aptian-Albian interval between the two hemispheres, which supports (in principle at least) a eustatic origin for

these sea level changes. The sea level records for older and younger intervals show poor correspondence between the two curves, probably due to the tectonic 'overprint' which affected northern Australia in the Late Cretaceous (see Sect. 9.9.3) after a long period of quiescence during the mid-Cretaceous (Gurnis, 1994).

9.8.5 Russian (CIS) sea level curves

Sahagian and Holland (1991) have produced a eustatic sea level curve for the Russian platform based on the supposed tectonic stability of the platform. They used a back-stripping method to calculate sea level changes from stage-to-stage with support from the topographic elevation and the position of ancient shoreline deposits. These authors propose that there was a eustatic sea level rise of ~110 m from the middle Jurassic to the Albian. Of direct interest to this study are their results for the Aptian to Albian interval.

Sahagian and Holland's (1991) eustatic curve (not shown on Fig. 9.6) illustrates a ~45 m sea level rise from the basal to late Aptian, which corresponds well to the Aptian transgression (Sequence *IA / IB*) in the Carpentaria Basin. This is followed by a large fall at the Aptian-Albian boundary which may coincide with the China Wall SB. Considering the resolution of their curve and the lack of biostratigraphic precision in the Carpentaria Basin curve, this regression may also correspond to the Carpentaria SB because the two unconformities are closely spaced in time in the Carpentaria Basin.

The Aptian-Albian boundary sea level fall is followed by a large (~40-50 m) sea level rise throughout the Albian which seems to correspond with the early late Albian transgression (Sequence *III*) in the Carpentaria Basin. In this case the early Albian transgression (Sequence *II*) is missing on Sahagian and Holland's curve, as it also is on Cooper's (1977) eustatic chart. Although not shown on their curve, the Cenomanian is considered by Sahagian and Holland (1991) as a time of regression, with the formation of significant unconformities. This matches the situation in the Carpentaria Basin where the Cenomanian marks the time of final retreat of the seaway and the formation of two major unconformities (Arnhem Land SB and Lawn Hill SB).

Of particular interest is the interpreted amount of sea level rise from the basal Aptian to the late Albian in Sahagian and Holland's plot. They calculate a rise of 65-70 m, which compares favourably with the rise of ~75 m (relative to the present sea level) calculated by Bolton (1982, see Fig. 9.5D) for the same period in the Carpentaria Basin. Haq *et al.* (1988) show an overall

rise of ~80-85 m for the same period on their global "eustatic" chart (Fig. 9.6A), although their curve shows long-term low sea level during the Aptian and early Albian, in contrast to Sahagian and Holland (1991).

The eustatic curve of Sahagian and Holland (1991) documents sea level changes of similar age and magnitude to those which affected the Carpentaria Basin in the Aptian-Albian interval, and provides qualified support (considering the limited biostratigraphic correlation and resolution of the curves) for a eustatic origin for these sea level changes. The proposition of a eustatic origin for Aptian-Albian sea level changes was previously suggested by positive correlations between the sea level curves of the Great Artesian Basin and other intracratonic basins world-wide (Morgan, 1980, fig. 48 and p. 88). This proposition is reinforced in the present study by correlation of relative sea level curves between the Carpentaria Basin and Europe (see Sect. 9.8.4), and these ties have now also been extended to the Russian region.

9.9 SEQUENCE DEVELOPMENT: MECHANISTIC MODELS AND SPECULATION

9.9.1 Hierarchy of sequences and parasequences

On first appraisal, using the limited biostratigraphic data available, the sequences on the Carpentaria Basin shelf appear to have a duration of a few million years each. In order to obtain a more accurate estimate it is necessary to make several assumptions. I will assume that the reference time-scale of Haq *et al.'s* (1988) chart is accurate and is representative of both the northern and southern hemispheres. I will also assume that the base of the Cretaceous succession on the shelf coincides with the base of the Aptian stage as inferred on Fig. 9.1, although previously (Fig. 9.2, Sect. 9.7) it has been shown that the base is actually poorly dated and may be older than Aptian in places.

Using the time-scale on the Haq *et al.* (1988) chart, the time interval for accumulation of the Carpentaria shelf succession (from the basal Aptian to the middle Cenomanian) is approximately 20 m.y (Fig. 9.6). One can then calculate the theoretical duration of each of the complete sequences of the Carpentaria shelf succession: Sequences *IA/IB - V* have estimated durations of 5.8, 1.9, 6.2, 2.4, and 3.9 million years respectively (Fig. 9.5). Sequence *VI* is considered as incomplete, but has an estimated duration of at least 1 m.y. All of these sequences have a recurrence interval in the order of 1-10 m.y., and can therefore be considered as third-order cycles (Van Wagoner *et al.*, 1990).

The retrogradational, aggradational or progradational stacking of parasequences within each of the sequences is considered to represent a higher-order cyclicity, although some of these parasequences have an apparent cyclicity similar to short-lived third-order cycles. It is not possible to accurately define the duration of each and every parasequence within the Cretaceous succession due to the lack of adequate biostratigraphic control. However, the average duration of parasequences can be estimated relative to the time-scale of Haq *et al.* (1988). The Cretaceous succession, approximately 20 m.y. in duration, is composed of at least 25 parasequences (only 18 are shown on Fig. 9.5 due to the nature of the composite section). It is likely that more than 25 parasequences were originally present since erosion along sequence boundaries has probably removed all traces of some parasequences; the number of 25 is taken as a minimum value.

Simple arithmetic gives the duration of an average parasequence as about 800,000 years. However, as can be seen on Fig. 9.5 the parasequences do not all have the same thickness (and therefore probably different durations) and might have an average duration in the order of 500,000 years or less. This estimated duration is generally longer than that expected for 'normal' fourth-order cycles (0.2-0.5 m.y. Kauffman, 1988; 0.1-0.2 m.y Mitchum and Van Wagoner, 1991; 0.08-0.5 m.y. Posamentier and Weimer, 1993), but they still are considered to represent "high frequency sequences" (*sensu* Mitchum and Van Wagoner, 1991).

Parasequences on the Carpentaria Basin shelf are considered to reflect a higher-order cyclicity than the sequences. In numerous places individual parasequences (facies successions) are composed of smaller-scale coarsening- or fining-upward intervals which suggest a yet higher-frequency control. These higher-frequency cycles may correspond to fifth-order cycles or even higher-order cycles, but their duration is purely speculative given the present limited biostratigraphic control for this study.

The duration of the Carpentaria Basin shelf parasequences is similar to at least some other Jurassic and Cretaceous inner- to outer-shelf siliciclastic and carbonate sedimentary cycles (*e.g.* 735,000 to 850,000 year Mesozoic cycles at Svalbard, Dypvik, 1992). Many similarities exist between stacked Carpentaria Basin parasequences (particularly storm-dominated cycles) and other high-frequency shelf cycles (Sect. 10.9). In particular, the thicknesses of coarsening- or fining-upward parasequences on the Carpentaria Basin shelf has the same range as the thicknesses of "punctuated aggradational cycles" (1-5 m, Goodwin and Anderson, 1985) and a similar range to the thicknesses of other storm-influenced shelf and ramp sediments (1-3 m, Cotter, 1990; 1-3 m, Jennette and Pryor, 1993; 5 m, Plint, 1991).

9.9.2 Allocyclic versus Autocyclic processes

In considering the driving mechanism of sequence development and relative sea level change it is important to first assess the scale of sedimentary cyclicity: Are the depositional architecture and sedimentary cyclicity controlled by intra-basinal (autocyclic) processes, or do the depositional architecture and sedimentary cyclicity reflect an extra-basinal (allocyclic) control? Preserved within the Mullaman Beds on the Carpentaria Basin shelf are third-order cycles (Sequences *IA/IB - VI*), probable fourth-order cycles (25+ parasequences), and possibly higher-order cycles of unknown frequency and duration (smaller scale fining- and coarsening-upward cycles). In any one area on the shelf it is possible that localised processes (*e.g.* avulsion, delta-lobe switching, lateral migration of shoreline complexes, highly seasonal sediment supply and/or runoff) could control the local depositional architecture. On a small scale the sedimentary cycles produced by autocyclic processes might be similar to thin third- or fourth-order cycles reflecting an allocyclic control. However, many of the parasequences on the Carpentaria Basin shelf can be correlated along depositional strike for up to 500 km, and basinwards for up to 300 km. They are not considered to be the product of local autocyclic changes in sedimentation rate, and therefore this effect will not be considered further.

Not only can individual parasequences be traced across the shelf, but marine flooding surfaces and sequence boundaries can also be confidently traced over the entire length and width of the shelf. The regional extent of these features implies that their mechanism of formation is allocyclic in nature (*e.g.* major tectonic uplift or subsidence of the basin and/or hinterland, major climate changes controlling sediment flux), and that the mechanism affected the entire Carpentaria Basin. Furthermore, the lateral continuity and temporal equivalence of the strata and surfaces throughout the Great Artesian Basin (*cf.* Morgan, 1980) suggests that these allocyclic processes affected the entire northern margin of Australia, and may have been eustatic in origin. Positive correlation of sea level records between the two hemispheres (at least for the Aptian-Albian) has been identified in Sects. 9.8.4 and 9.8.5, and the main inference from these correlations is that the sea level changes were eustatic in origin.

If the driving mechanism for sequence development is allocyclic there are three main controlling mechanisms to consider; regional sediment supply, tectonism (basin-floor movements), and eustatic sea level change. In most basins these mechanisms act in combination, and it is typically difficult to identify and isolate the signal of each process by analysing the sedimentary record of a basin. In the case of the Carpentaria Basin the sediment supply variable is considered to be least important, because the rates of sediment supply were low during

accumulation of most of the Mullaman Beds and the shelf was characterised by reworking and cannibalisation of older sediments (refer to Sect. 10.6.4; Krassay and Frakes, 1992). Thus, the role of sediment supply is not elaborated upon in the following discussion on sequence development and depositional cyclicity.

9.9.3 Northern Australian tectonism

Tectonic processes which were active during the Cretaceous in the northern Australian region may have influenced sequence development on the western shelf of the Carpentaria Basin, either by controlling regional sea level or by producing basin-floor movements. In this sense, tectonic subsidence or epeirogeny may have amplified any eustatic sea level changes that occurred. Such a scenario has been proposed for the Cretaceous Western Interior Seaway of North America (Harrison, 1990), and might explain how inferred eustatic sea level changes in the order of tens of metres in that seaway resulted in relative sea level changes of hundreds of metres.

Senior *et al.* (1978) have suggested that uplift of the Euroka Arch may have initiated the terminal regression (throughout the Albian) by closing the northern seaway (separating the Carpentaria Basin from the Eromanga and Surat Basins). Similarly, Day *et al.* (1983) suggested that closure of the connection of the Eromanga and Surat Basins through uplift of the Nebine and Eulo Ridges occurred from the early Albian onwards. However, evidence presented in this thesis documents high relative sea level throughout much of the Albian and final regression in the Cenomanian, which is out-of-phase with these tectonic events. In addition, it has not been demonstrated that such tectonic movements could have occurred repeatedly in the mid-Cretaceous, nor that their frequency is high enough to explain the sedimentary cycles.

In a broad study of palaeogeography, relative sea level, and inundation curves for Australian basins, Struckmeyer and Brown (1990) suggest that comparison of marine flooding curves for various Cretaceous basins indicates that the shape of these curves depends very strongly on the tectonic setting of the basin during a particular time. For example, the Bonaparte Basin was relatively tectonically stable for the Cretaceous period and its sea level curve apparently shows good correlation with the Exxon global "eustatic" chart, whereas sea level curves for Australian intracratonic basins (*i.e.* the Great Artesian Basin) show overall poor correspondence with the Exxon chart. According to Struckmeyer and Brown (1990) and Frakes *et al.* (1987) this is due to a tectonic overprint in the relative sea level signal for each basin.

Although initial flooding in Australian intracratonic basins may have occurred as a result of eustatic sea level change (as proposed for the Aptian-Albian interval in the present study), the changes in sea level were probably enhanced by epeirogenic movement (*cf.* Gurnis, 1994; Harrison, 1990). The end result of this is the disparity between northern Australian sea level curves and global "eustatic" charts for the Late Cretaceous (see Fig. 9.6; Frakes *et al.*, 1987, p. 45; Dettmann *et al.*, 1992).

Haig and Lynch (1993) have suggested a significant tectonic influence or enhancement of Australian sea levels for the middle to late Albian, and their observations are in accordance with Veever's (1991) proposition of high tectonic activity along the eastern margin of the continent. Veevers' (1991) hypothesis involves a tectonic climax in the mid-Cretaceous (Cenomanian) of the Australian region leading to intense uplift, denudation and retreat of the epicratonic seas (*e.g.* Great Artesian Basin seaway). Supporting evidence is presented by Exon and Senior (1976) who recognised an increase in volcanic detritus in Albian and Cenomanian strata over a large area of northeastern Australia, which suggests high (or increasing) tectonic activity in eastern Australia. However, the frequency of Veevers' proposed vertical tectonic motions is not rapid enough to satisfactorily explain the repeated high-frequency (<1 m.y.) sedimentary cycles in the Carpentaria Basin.

Retreat of the sea and complete emergence of the entire Carpentaria Basin is the end result of this tectonic activity (mainly warping and regional uplift) according to Dettmann *et al.* (1992) and Frakes *et al.* (1987). In this sense the formation of the land bridge from northern Australia to Papua New Guinea in the Late Cretaceous would be due to tectonics. These results are interesting and seemingly fit well with my interpretation of relative sea level fluctuations in the Carpentaria Basin (*i.e.* major Aptian and Albian marine flooding, followed by major regression in the Cenomanian).

Relative sea level changes apparent in the upper part of the Carpentaria Basin sequence may have been influenced or driven by broader-scale tectonic processes such as changes in plate configuration and movement. Seafloor spreading is interpreted to have commenced along the southern margin of Australia in Cenomanian time (Veevers and Eittrem, 1988). In a similar manner, sea level rise in the Aptian (the first major Cretaceous flooding of the Mullaman Bed shelf) may have been related to major early Aptian mantle plume activity (Tarduno *et al.*, 1991) involving significant flood basalt volcanism at the Ontong Java Plateau to the northeast of the Carpentaria Basin. According to Tarduno *et al.* (1991) the eruption of flood basalts was rapid

(occurring over < 1 m.y.), and presumably this would translate to a rapid rate of rise in sea level.

9.9.4 Glacio-eustasy

Glacio-eustasy has been widely accepted as being a plausible mechanism to explain fourth- and higher-order cyclicity (*e.g.* Plint *et al.*, 1992; Rowley and Markwick, 1992), and a great deal of research has focused on the effects of glacio-eustasy driven by Milankovitch-band astronomical forcing (summaries in Fischer, 1986 and Kauffman, 1988). Milankovitch 'cycles' involve variations in the Earth's tilt and orbit which are caused by three processes of orbital variation: eccentricity, precession, and obliquity. In this model the waxing and waning of ice sheets is dependent on the seasonal amount of solar radiation at critical latitudes, which is controlled by Milankovitch cyclicity (Fischer and Bottjer, 1991; Imbrie and Imbrie, 1980).

The existence of Milankovitch cycles or rhythms has been demonstrated by detailed studies of oxygen isotope variations and relative sea level changes in the Quaternary (*e.g.* Chappell and Shackleton, 1986). High-frequency sedimentary rhythms apparently controlled by Milankovitch cycles have also been documented in numerous regions for strata of varying ages (*e.g.* numerous papers in Fischer and Bottjer (eds.), 1991; Maynard and Leeder, 1992). In spite of the apparent correspondence of Milankovitch cycles and the oxygen isotope record, there is generally poor agreement of the oceanic oxygen isotope record with the Exxon global "eustatic" chart (Williams, 1988).

Given this broad background of research into glacio-eustasy, *the essential question is whether glacio-eustasy is a plausible mechanism for explaining the development of third- and higher-order cycles within the Cretaceous Mullaman Beds.* Despite the general acceptance for a warm Cretaceous period without continental ice masses, there is evidence for the formation of seasonal ice in northern Australia (Frakes and Francis, 1988; Frakes and Krassay, 1992), and mid-Cretaceous Australian continental temperatures had a seasonal variation of -18^{0}C to +27^{0}C (Barron and Washington, 1982), and a low mean annual temperature of <5^{0}C (Rich *et al.*, 1988). Computer modelling by Olgesby (1989) also suggests that an ice mass may have developed in the Antarctic during the Mesozoic. The Cretaceous palaeoclimate of the northern Australian region is discussed in more detail in Sect. 10.2.

In spite of all these peripheral indicators, there is no direct evidence for continental glaciation during the Cretaceous. However, many Cretaceous shallow-marine strata (including the

Mullaman Beds) provide compelling evidence for high-frequency changes in relative sea level outside the normal periodicity associated with tectono-eustatic mechanisms. In these cases a glacio-eustatic control is an appealing mechanism to explain widespread, rapid, high-frequency changes in sea level and their attendant sedimentary cycles (*e.g.* Plint, 1991; Plint and Norris, 1991; Plint *et al.*, 1986; Wadsworth and Walker, 1991).

It is also possible that the absence of large continental ice masses does not rule out change in the volume of ocean water (the same principle as glacio-eustasy) as a plausible controlling mechanism for high-frequency sea level changes. Recent studies have highlighted the neglected potential of lakes, reservoirs, terrestrial aquifers (groundwater storage), and possibly even permafrost regions as traps for large volumes of water at certain times in earth history (*e.g.* Hay and Leslie, 1990; Jacobs and Sahagian, 1993). The release or trapping of water in these settings could cause moderate changes in eustatic sea level (a few tens of metres), and these factors may also be related to Milankovitch cycles and thus have similar frequencies to fourth- and higher-order cycles.

Fluctuation in groundwater storage, possibly in tandem with glacio-eustasy, is becoming increasingly attractive as a mechanism to explain high-frequency sea level changes in shallow-marine settings. Recent models based on this idea have focused on the Cretaceous Western Interior Basin of North America. There, Leithold (1994) documents a thick stack of parasequences, similar in all significant aspects to those of the Carpentaria Basin, which make up the Cenomanian to Turonian Tropic Shale and Mancos Shale. Leithold suggests the the timing, development, and stacking of the parasequences and the six corresponding sequences is related to a combination of glacio-eustasy, groundwater storage fluctuations, and possible additional climatic forcing in the Milankovitch band. It is envisaged that glacio-eustasy (and/or groundwater storage) is a possible mechanism for partial control of high-frequency depositional cycles (25+ parasequences) and sea level changes on the Carpentaria Basin shelf. However, the lack of direct evidence for glaciation, and the relatively poorly constrained periodicity of the Carpentaria Basin cycles (due at least in part to relatively poor biostratigraphic control) means that these models should be applied with caution to the Carpentaria Basin shelf.

9.10 CHAPTER SUMMARY

The sequence stratigraphic history of the western and southwestern margin of the Carpentaria Basin is complex, and involves multiple changes in relative sea level on the shelf over a time interval of approximately 20 m.y. Six major sequences were deposited on the shelf in the interval from the basal Aptian to the ?middle Cenomanian. These sequences are bounded by six regional unconformities and correlative conformities (sequence boundaries). Most sequence boundaries are type 1 examples, which record large basinward shifts in depositional 'facies belts' at times of major regression. From the position and style of strata overlying the sequence boundaries, it appears that many of these regressions were caused (or forced) by rapid falls in relative sea level.

The duration of sequences (about 1-6 m.y.) corresponds to third-order cycles, and the parasequences (<800,000 years) probably correspond to fourth-order cycles. The record of relative sea level change on the Carpentaria Basin shelf (interpreted from the depositional cycles) has some correspondence with the global "eustatic" curve of Haq *et al.* (1988), and much better correspondence with the "eustatic" chart of Cooper (1977). Moreover, there are notable similarities and matches with the sea level curves of northern Europe and Russia for the Aptian-Albian interval, but the sea level curves for the two hemispheres generally diverge in the Late Cretaceous (post-Cenomanian). For the Aptian-Albian interval the sea level curve in the present study also fits well with sea level changes recognised in other northern Australian basins.

These observations suggest a eustatic control for sea level changes in the Aptian-Albian interval, followed by a more regional tectonic overprint on sea levels in the northern Australian region from the Cenomanian onwards. The driving mechanisms of any eustatic sea level change which affected the western shelf of the Carpentaria Basin are unknown. This problem can only be resolved with greater biostratigraphic control for the rocks, which would enable more detailed ties between relative sea level curves in the northern Australian region and beyond.

~~~
~~~

10. PALAEOCLIMATE, PALAEOGEOGRAPHY, SHELF DYNAMICS, AND A DEPOSITIONAL MODEL FOR THE WESTERN SHELF OF THE CARPENTARIA BASIN

10.1 INTRODUCTION

This concluding chapter has five main purposes:

1) to combine the interpretations presented in chapters 3 through 9 into a regional summary of major depositional events on the western shelf of the Carpentaria Basin during the deposition of the Mullaman Beds. This history is treated in a series of interpreted time slices, which are illustrated in stage-by-stage shoreline maps and regional palaeogeographic reconstructions.
2) to attempt to define the dynamic processes that operated on the Mullaman Bed shelf over time, and to document their relative importance in the formation and preservation of the shelf sequence.
3) to address the problem of the origin of storm-cycles and 'ice-rafted' deposits under the broader context of the mid-Cretaceous palaeoclimate of northern Australia.
4) to derive a depositional model for the storm- (and wave-) dominated shelf sequence that may be applicable to other storm-dominated shallow-marine siliciclastic sequences, particularly those of broad, shallow epeiric seas.
5) to compare and contrast the Mullaman Bed depositional model with other storm- (and wave-) dominated sequences described in the literature, and to demonstrate the significance of the Mullaman Beds and the model developed here as a contribution to this literature.

10.2 CRETACEOUS PALAEOCLIMATES OF NORTHERN AUSTRALIA

10.2.1 Introduction

The Cretaceous Period is generally considered to have been one free of large ice caps, or even terrestrial ice. However, recent studies on sediments, vertebrate fossils, and on oxygen isotopes have suggested that the presumed warm and equable (ice-free) climates which may have characterised most of the Earth at this time did not affect Australia, nor other high-latitude sites (*e.g.* Frakes and Francis, 1988; Pirrie and Marshall, 1990). For this reason, and despite

the abundance of strata of Mesozoic age on the continent, the nature of the palaeoclimate of northern and central Australia during the Cretaceous is controversial (Dettmann and Playford, 1969; Douglas and Williams 1982; Gregory *et al.*, 1989; Rich *et al.*, 1988).

Computer modelling and statistical studies on Cretaceous climates have suggested that even with warm oceans, the interiors of high-latitude contents would tend to remain seasonally cold and suffer winter freezing (Barron, 1983; Barron *et al.*, 1981, 1985). It has been predicted that the low equator-to-pole temperature gradient would have produced very weak atmospheric circulation that would have been unable to transport heat to and from the oceans and inland areas, giving rise to extremes in seasonal temperatures (Sloan and Barron, 1990). An additional effect of Cretaceous relative sea level changes was to alter the land-sea distribution, and hence global albedo. This in turn had the potential to produce major climate changes over time and apparently promoted temperature differences over land vs. sea (Barron *et al.*, 1980; Crowley *et al.*, 1986). Such environmental conditions are likely to have existed in parts of the Great Artesian Basin seaway in the interior of the Australian continent, which lay mostly at latitudes between 55^0 and 80^0 S in the Cretaceous. During mid-Cretaceous (Aptian through Cenomanian) time the western shelf of the Carpentaria Basin in northern Australia lay at latitudes between 55^0 and 65^0 S (Embleton, 1984).

10.2.2 Palaeontological evidence for Cretaceous climates

Palaeontological evidence based on palynology and the diversity of molluscan faunas suggests that the climate during Neocomian to Aptian time was cool to temperate (Burger, 1973; Dettmann and Playford, 1969). Of more immediate interest to the present study are data obtained from the Aptian to middle Albian Wallumbilla Formation (one of the basinal equivalents of the Mullaman Beds). Faunal and floral assemblages of the Wallumbilla Formation suggest that a cool temperate climate prevailed over much of the GAB (Haig and Barnbaum, 1978). Furthermore, wood with narrow growth rings in the Aptian-Albian Bulldog Shale (Wallumbilla Formation equivalent) in the central part of the GAB imply that cool climates existed, and that there was marked seasonality (Frakes and Francis, 1988).

Microfaunal evidence suggests that cool surface water conditions continued from the Early Cretaceous up into at least the early Albian (Haig, 1992; Haig and Lynch, 1993), but palaeotemperatures are interpreted to have increased gradually through the middle and late Albian (Dettmann, 1973; 1981; Haig and Lynch, 1993). Similarly, the nature and distribution of land vegetation indicates warmer climates for the middle-late Albian than the Aptian, and the

existence of a temperature gradient (warmer to the north) in eastern Australia (Dettmann and Playford, 1969).

10.2.3 Isotopic evidence for Cretaceous climates

In southeastern Australia, which was situated at about 80^0 S, isotopic determinations on numerous carbonate nodules indicate that the mean annual temperature was as low as -2 to $+5^0$ C during the Aptian to early Albian (Gregory *et al.*, 1989; Rich *et al.*, 1988). According to Gregory *et al.* (1989, p. 37) the mean annual temperature estimate is likely to be the average of a highly variable temperature distribution, and "it is plausible that winter temperatures ... were considerably below zero (~ -20^0 C or less)". These observations support the proposition of Waldman (1971), that winter freezing occurred in southern Australia (at least), and that there was pronounced seasonality.

Oxygen isotope analyses of Cretaceous (Aptian) belemnites in the Lake Eyre region, south-western Eromanga Basin, indicate cool palaeotemperatures of 12.2^0 to 16.5^0 C (Dorman and Gill, 1959). Such values were initially dismissed as being too low by Lowenstam (1964), who compared them directly with northern hemisphere isotopic values. However, as noted by Stevens (1971), the isotopic values and associated low palaeotemperature estimates must be interpreted with regard to Australia's known high palaeolatitude at the time. Subsequent studies have proven the validity of a cool Eromanga Sea in Cretaceous time (Day, 1969; Dettmann *et al.*, 1992). Moreover, several of the original palaeotemperature estimates have since been reassessed downwards (see Dettmann *et al.*, 1992 for a full list of palaeotemperature estimates), and this strengthens the proposition of cool to cold surface temperatures with winter freezing in the Great Artesian Basin region.

10.2.4 Discussion of Cretaceous climate of northern Australia

The general global trend of oxygen isotope palaeotemperature estimates (and other data including the presence and distribution of ice-rafted deposits, and the diversity and types of pollen and nannofossils) show cooling in the Late Jurassic and Early Cretaceous, followed by warming from the late Albian up into the Cenomanian (Frakes *et al.*, 1992).

Australian earliest Cretaceous climates were apparently temperate with cool temperatures (0-12^0 C) and high precipitation levels in southern regions (Dettmann *et al.*, 1992). Winter freezing may have occurred during the Aptian, but evidence from land vegetation types and isotope

palaeotemperatures for the marine realm (Stevens and Clayton, 1971) indicates that warming occurred during the Albian. Palaeotemperature data for the Cenomanian are lacking, but climates similar to modern warm temperate ones have been postulated (Dettmann et al., 1992; Douglas and Williams, 1982). A strongly seasonal climate was predicted in computer models of the Cretaceous climate (Barron and Washington, 1984; Schneider *et al.*, 1985), and such models predict that the large continental land mass of Australia/Antarctica would have experienced summer temperatures as high as $+27^0$ C and winter temperatures of -18^0 C.

There is now a fair-sized body of evidence suggesting that strongly seasonal climates characterised Cretaceous high latitudes, and that winter freezing was a feature. The presence of reportedly ice-rafted boulders in mudrocks of Aptian age in the Eromanga Basin (Frakes and Francis, 1988), and in Aptian to Albian mudrocks of the Carpentaria Basin (Frakes and Krassay, 1992; Sect. 10.3), has been interpreted in terms of seasonally cold climates with freezing temperatures in winter. The presence of many glendonite nodules (pseudomorphs of crystal aggregates after ikaite, a mineral stable only in near-freezing temperatures; Kemper, 1987) in mudrocks of the Eromanga Basin provides additional evidence of cold temperatures within the GAB. Similar nodules reported in other ancient deposits (England, 1976; Kemper and Schmitz, 1975) and modern cold and/or high-latitude sites (Jansen *et al.*, 1987; Kennedy *et al.*, 1987; Shearman and Smith, 1985) have also been used to infer low (freezing) palaeotemperatures.

During the Early Cretaceous and early Middle Cretaceous, the southern part of the GAB seaway was situated very close to the South Pole (Dettmann *et al.*, 1992; Embleton, 1984). Parts of Australia at these high palaeolatitudes may have experienced periglacial conditions (Frakes and Francis, 1988; Frakes and Krassay, 1992), and it is possible that limited glacial conditions existed for landmasses at even higher palaeolatitudes (Barron *et al.*, 1981; Francis, 1986, 1989; Parrish and Spicer, 1988; Pirrie and Marshall, 1990). The proposition of freezing in Early to Middle Cretaceous time in Australia is still controversial, and some authors oppose this view (*e.g.* Jell and Duncan, 1986) on the basis of palaeontological considerations for local areas. However, new evidence is presented in this study (see also Frakes and Krassay, 1992) which supports the proposition of freezing and ice-rafting in Cretaceous time in Australia, from a part of the continent where it had not previously been recognised, the southwestern marginal shelf of the Carpentaria Basin (Sect. 10.3).

10.3 ICE-RAFTING OR STORM-TRANSPORT?

10.3.1 Introduction

Isolated rounded clasts up to small boulder size have been discovered in fine-grained sediments of Jurassic to Cretaceous age in the eastern Northern Territory and northwestern Queensland, between Borroloola in the central region and Burketown in the southern region. The dominantly silty strata have previously been assigned to the Mullaman Beds and the Gilbert River Formation and fossil evidence indicates a partial late Aptian age, but their full age range is uncertain.

The important question is whether these deposits were formed by ice-rafting, or storm transport and deposition? The short answer is that both processes appear to have been active on the shelf, possibly at the same time. However, in many places it is possible to distinguish between deposits containing storm-transported clasts and those containing ice-rafted clasts, particularly in the southern region where the influence of storms was reduced due to the deeper-water distal position on the shelf.

In many cases where isolated clasts are small (say granule and pebble size) and abundant, or form thin layers, it is likely that the clasts were transported or winnowed by storm currents. This is particularly true for intervals where other features of storm deposition and transport are present, *i.e.* HCS, megaripples, gutters, laterally continuous 'veneers' of pebbles erosively overlying fine-grained rocks (see Krassay, 1994a; and descriptions of facies and successions in chapters 3-4 for evidence of storm-influence). However, in more distal localities on the shelf, larger (cobble to boulder sized) clasts occur within thick mudstones, and there is no evidence for erosion or winnowing in these rocks. Moreover, the sedimentary structures (thin lamination, concretions, preserved horizontal burrows) and the fine grain size seem to indicate quiet deposition in relatively deep water, in areas which were beyond the influence of most storms. The mechanism of transport of these clasts into basin sediments is considered to have been rafting by ice, since fossil driftwood remains are small and there is no evidence of rafting in floating tree roots, or of lateral emplacement by swift currents.

10.3.2 Evidence for ice-rafting in the Mullaman Beds

Numerous rocks in the southern part of the central region and the southern region consist of large clasts (lonestones) enclosed in fine-grained matrix. Biostratigraphic correlation is not

possible, but the sequences can be correlated on lithological grounds as shown in chapters 5-8. Foraminifera in the dated section (124) belong to a sublittoral marine assemblage of late Aptian age (Haig, 1991). On the basis of regional correlation the age range of deposits containing lonestones is Aptian to early Albian.

The fine-grained host rocks in these sections were typically deposited subaqueously in the offshore zone. There is little trace of erosion or winnowing in association with clasts, suggesting they were not transported by fast flowing currents nor was intervening matrix material removed. However, they do occur in what are interpreted as storm-influenced facies successions, and the coarser-grained parts of these deposits do contain storm-generated sedimentary structures.

It is possible to recognise the effects of ice-rafting in the finer-grained parts of these facies successions. However, the coarser-grained parts represent deposition under progressively higher-energy conditions as the sediment surface was built up towards storm wave base; it is not possible to see preserved features of ice-rafting (*e.g.* penetration and drape structures) in these intervals. The effects of waves impinging upon the seafloor have probably obliterated any fragile indicators of ice-rafting in the coarser-grained parts of these facies successions, but it is possible that some of the clastic debris (particularly clasts larger than pebble size) which form storm-generated event layers was supplied to the basin by ice-rafting, and was then modified by storm activity.

Isolated clasts and pods of clasts are typically enclosed within pale-coloured, bioturbated, mudstone (Plate 12a). In the central region small pods and stringers (discontinuous layers) of outsized clasts are dispersed randomly throughout fine-grained offshore marine rocks of facies succession 4 (*e.g.* sections 67 and 91). The clasts in the pods range from granule to small pebble size, show a wide range in composition, and display a highly variable degree of rounding, suggestive of multiple provenance. The pods extend no more than about 30 cm, usually 5 - 8 cm, in any direction and are often irregularly elliptical or lens shaped (Plate 12b-d). The stringers comprise clasts of variable size set in poorly defined coarse sand layers up to 20 cm in length. Both the stringers and pods represent scatterings or concentrations of clasts along bedding planes.

Farther to the south, near the boundary of the central and southern regions, the size of the clasts increases and larger isolated 'lonestones' occur within mudstone. Similar to northern exposures, the host rock for the 'lonestones' is fine-grained facies succession 4 (*e.g.* sections

PLATE 12

Sedimentary features suggestive of ice-rafting within the Mullaman Beds:

a Typical outcrop view of slightly iron-oxide stained fine-grained offshore marine rocks that contain the best indicators of ice-rafting. Site 127, southern region. Thickness of the main outcrop in centre of photo is about 7 m.

b & c Small pods of granule sized clasts and coarse to very coarse sand grains enclosed within bioturbated marine claystone and siltstone. The pods typically have well-defined margins, no obvious indication of erosion, and only extend a few centimetres in any direction. Where lamination is visible in the fine-grained host rock, these pods appear to be scattered on bedding surfaces. Sites 76 and 91 respectively, central region. Pens for scale.

d Larger pod (delimited by arrows) of larger and more varied clasts. Clasts are poorly sorted and have highly variable composition and roundness, which suggests that they were not simply derived from local winnowing and concentration of coarse debris. Note large cobble sized rounded clast at the right edge of the pod. Host rock is bioturbated clayey marine siltstone and very fine-grained sandstone. Site 127, southern region. Lens cap is 5.75 cm in diameter.

e & f Lonestones within bioturbated fine-grained marine host rock. Clasts range from pebble size (plate e) to boulder size (plate f). Site 127, southern region. Hammer and lens cap for scale.

g Very poorly sorted lonestones within laminated fine-grained marine siltstone. Note the large range in clast size, shape and composition. At the base of the unit the lamination within the host rock (arrowed) appears to be disturbed by clasts, *i.e.* clasts appear to have been dropped into the siltstone. Such lamination is rare; in most outcrops the host rock is intensely bioturbated and it is not possible to see penetration or drape structures in association with the lonestones. Site 127, southern region. Pen is 13.5 cm long.

h Single lonestone (arrowed) with a near vertical orientation with respect to weak lamination in the host rock. This suggests that clasts were dropped onto a soft muddy substrate. Site 127, southern region. Lens cap is 5.75 cm in diameter.

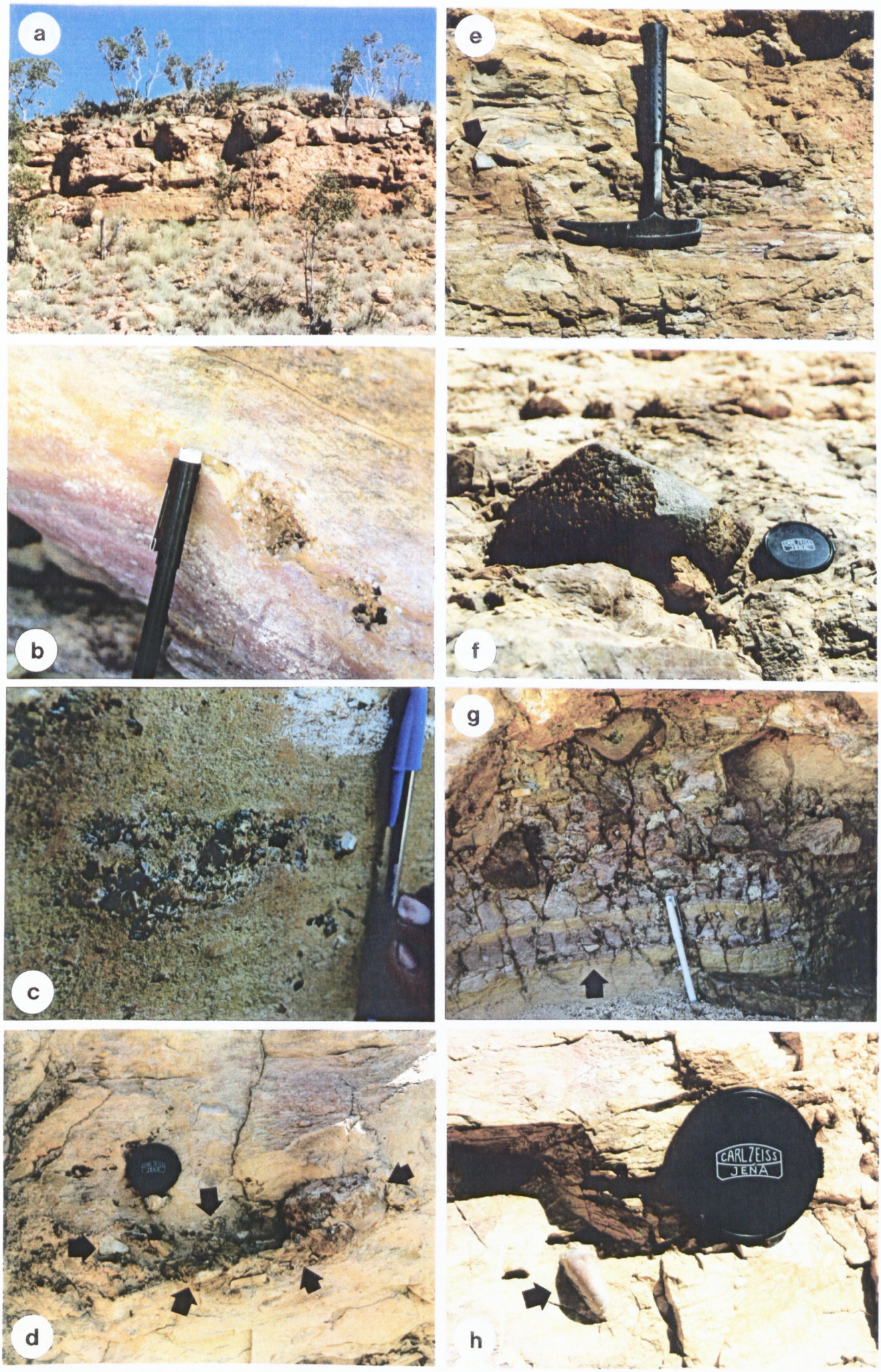
a
e
b
f
c
g
d
h
CARL ZEISS
JENA

105, 115). Clasts within the mudstone are rounded to subangular, and are mostly pebbles composed of fine-grained chert and siltstone (Plate 12e-h).

In the southern region isolated subrounded to rounded, coarse pebble to boulder sized clasts of various sedimentary compositions occur within siltstone or very fine sandstone. The best examples of large clasts within a fine grained matrix can be seen in sections 126 and 127, south of the Kamarga Dome in far northwestern Queensland, and in section 133. Section 127 contains the most diverse suite of lonestone clasts along with pods of clasts (less common) as described for sections 67, and 91. The observed lonestone clasts are granule to boulder size (Plate 12f), with the largest measuring 26 cm in diameter. Generally, clasts are sub-rounded to sub-angular and are composed of various sedimentary rock types. Section 126 is similar, except that the clasts are confined to two thin and poorly defined layers. The top metre of section 133 contains both large lonestones and pods of clasts. In all three sections the host rocks are fine-grained offshore marine facies of facies succession 1, which accumulated in a low-energy offshore shallow-marine environment.

The mudstones surrounding the lonestones are typically either bioturbated or poorly laminated and therefore it is not possible to determine unequivocally whether clasts penetrate layering and thus were dropped into the sediment (although traces of draping and penetration do occur in places; Plate 12g). Furthermore, some units contain elongate clasts orientated with their long-axes near vertical (Plate 12h); clasts within the coarser material tend to have random orientations. The former type of fabric suggests that stones fell from rafts and that the argillaceous substrate was unconsolidated upon deposition. These features are typical of vegetation-rafted and ice-rafted diamicts as distinct from tills and debris flows (Anderson, 1983). Examination of the larger clasts did not reveal any glacial striae or chatter marks, and the rare fossil wood observed in outcrop (*e.g.* sections 67 and 126) consists of small fragments nowhere near large enough to transport cobbles or boulders.

The general trend of increasing size and abundance of lonestones, stringers, and pods of clasts towards the south on the Carpentaria Basin shelf is in agreement with Cretaceous palaeogeographic information, which indicates a southerly change to higher palaeolatitudes (65^0 S or higher), colder surface temperatures, and presumably more common or more effective rafting of clasts by ice. This trend provides sedimentological evidence for ice-rafting as the preferred transport mechanism for the clasts, because the southerly increase in lonestone clasts is the reverse of that for storm-transported clastics, *i.e.* in the southern and southeastern parts of

the shelf, coarse-grained storm-influenced deposits are rare; their greatest abundance occurs to the north and northwest, the opposite trend to that of lonestone-rich intervals.

10.3.3 Discussion

As described previously (Sect. 10.2), parts of the GAB seaway lay at high palaeolatitudes and experienced cold climates, and there is good evidence for freezing in these areas. As shown by Frakes and Francis (1988, fig. 1), late Mesozoic clast-bearing shales in Arctic Canada, Spitsbergen, Siberia, and possibly Alaska occupied similar palaeolatitudes when formed. These circumstances lead to the conclusion that during parts of the late Mesozoic, the high latitudes suffered sufficiently cold winters to cause freezing along rivers and perhaps along marine shorelines, and summers were warm enough to allow the floes to drift into the basin, melt and drop their sediment load into the shelf sediments.

The occurrence of lonestone clasts in the mudstones is best explained by the dropping of the clasts from rafts of some sort, as any current strong enough to carry the clasts would have eroded the substrate significantly. Direct evidence as to the identity of the type of raft is completely lacking. The occurrence of similar deposits of equivalent age (Alley, 1988; Cambell *et al.*, 1985) in the Eromanga Basin, which also contain clasts (up to 3 m in length) penetrating laminated mudstone, has been explained on the basis of seasonal ice-rafting in high latitude locations (Frakes and Francis, 1988). Entrainment within the root masses of driftwood or attachment to floating algae (Gilbert, 1984) would be other possible modes of transport for the clasts, but the general scarcity of fossil wood in the Carpentaria Basin marginal shelf and the large size of many of the clasts suggests that this was unlikely. Concentration of clasts due to selective bioturbation and 'mining' of the sediment by infauna is a possible mechanism for forming pods of clasts. However, the preservation of delicate lamination adjacent to the pods in many areas makes the idea of highly selective and localised bioturbation unlikely. Also, this mechanism does not explain the presence of clasts within offshore mudstone to begin with. Rafting by ice is the most likely mechanism for clast emplacement.

Ice rafts can be of two principal types: glacial ice in the form of icebergs, or seasonal ice in the form of floes developed in rivers or along shorelines during cold winters. Glacial ice usually generates easily recognised sediment types, such as till (proximal to the glacier), and normal marine sediments containing pellets of till-like material and rare clasts (distal to the glacier, Mode *et al.*, 1983; Ovenshine, 1970). In the absence of till deposits and other characteristic features of glaciation such as glacially striated bedrock or clasts, ice rafting is best ascribed to

seasonal ice floes. As yet there are no known glacial tills of Mesozoic age in Australia or elsewhere; a few striated stones have been identified from the Bulldog Shale (David, 1950), but these were probable striated during pre-Cretaceous glaciations. It is therefore likely that clasts in the Carpentaria shelf sequences were transported by river or marine-shore ice of a seasonal nature ('fast ice' in the terminology of Anderson, 1983).

Seasonal ice floes would generally be expected to contain rounded to subrounded sand and coarser material typical of the high to moderate energy littoral and/or fluvial environments from whence they were derived, and would probably be lacking the abundant mud-size component associated with most glacial ice. As the ice floes drifted offshore their subaerial surface would have ablated and their debris would have been concentrated. The coarser debris then would have been deposited episodically offshore by tilting, fragmentation or overturning of the ice floes; whereas finer sediment was probably released from the ice and transported over the side by small meltwater rivulets (*cf.* Ovenshine, 1970), possibly giving rise to discontinuous layers of sand and clasts as observed in sections 67 and 91. Rolling and tilting of the floes due to mass imbalance may have dumped ablation debris as piles on the seafloor, to be preserved as lenses/pods in a stratigraphic section (Powell, 1983; Thomas and Connell, 1985), similar to features in sections 67, 91, 127, and 133.

10.4 CARPENTARIA BASIN PALAEOGEOGRAPHY

10.4.1 Introduction

The main marine connection of the Carpentaria Basin in its early history was to the north, over the Bramwell Arch into the Papuan Basin, and ultimately with the Cretaceous Pacific Ocean (Barron, 1987; Riccardi, 1991). Throughout most of the Aptian and Albian the narrowest part of the Great Artesian Basin epeiric seaway, at about the latitude of Weipa, had an east-west dimension of over 500 km (Frakes *et al.*, 1987). Farther to the south, along most of the shelf, the east-west dimension of the seaway exceeded 750 km. The western shoreline of the shelf had a regional north-northeast orientation in the mid-Cretaceous, changing to a north-northwest palaeoshoreline trend along the southern half of the shelf. However, at times of significant transgression--in the Aptian (limited data), middle Albian, late Albian, and early Cenomanian (see palaeogeographic sketches in this chapter)--the shoreline had a ragged irregular profile with arms of the seaway extending much farther to the west in some places than in others. The entire shelf was completely emergent from the Turonian onwards.

The size and shape of the sea during mid-Cretaceous time was greatly affected by the pre-existing topography of the landsurface across which it flooded. Many large high-standing basement terrains existed as islands and peninsulas along the western margin of the shelf, and formed at least partial barriers to westward transgression during times of Cretaceous inundation (Krassay and Frakes, 1991). The position, size, and type of these basement blocks is summarised in Table 10.1, and illustrated on Fig. 10.1. The local effects of these basement blocks upon the paths of transgression, positions of the palaeoshoreline, and the accumulation of Cretaceous sediments, are discussed in the following sections. In this chapter the Early to Middle Cretaceous palaeogeography of Australia as a whole are illustrated in Figs. 10.2 and 10.3, whereas the more detailed palaeogeography and shoreline positions of the western Carpentaria Basin are illustrated in Figs. 10.4 through 10.14. The Late Cretaceous palaeogeography of Australia is illustrated in Fig. 10.15.

10.4.2 Palaeogeography of the northern region (Arnhem Land Zone)

The three prominent palaeogeographic elements of the ALZ which influenced Cretaceous sedimentation are as follows (see Table 10.1 and Fig. 10.1):

1) the northeast-trending Mitchell Range (terrain #1) in the west;
2) a zone of northeast-trending Proterozoic sedimentary rocks (terrain #2) in the north; and
3) a belt of largely crystalline rocks (terrain #3) to the east trending north-northeast along the present Gulf of Carpentaria coastline.

Ridges of Proterozoic rocks and a belt of granitic inliers with a north-northeast structural trend were exposed in the ALZ and served as barriers to transgressions of the sea at various times during the mid-Cretaceous. Notable among these was the Mitchell Range, which restricted the sea on the west, except perhaps for maximum flooding during stage 5. The stratigraphic position of Mesozoic onlap, the regional lateral continuity of marginal shelf facies, and the localised nature of coarse-grained sediment wedges shed off the Proterozoic ridges, indicate that these ridges and granitic terrains had relatively low topographic elevations during the Cretaceous. These ridges and terrains probably would not have interrupted the flow of prevailing winds, although they were islands, but they provided partial barriers to marine circulation and resulted in the formation of several large palaeoembayments.

It is likely that the main Cretaceous inner shallow-marine basin in the ALZ lay between the Mitchell Range (terrain #1) and the granite island chain (terrain #3) during stages 3-5 (Figs. 10.7 through 10.12), with extensions to the open sea being mainly to the east through breaks in

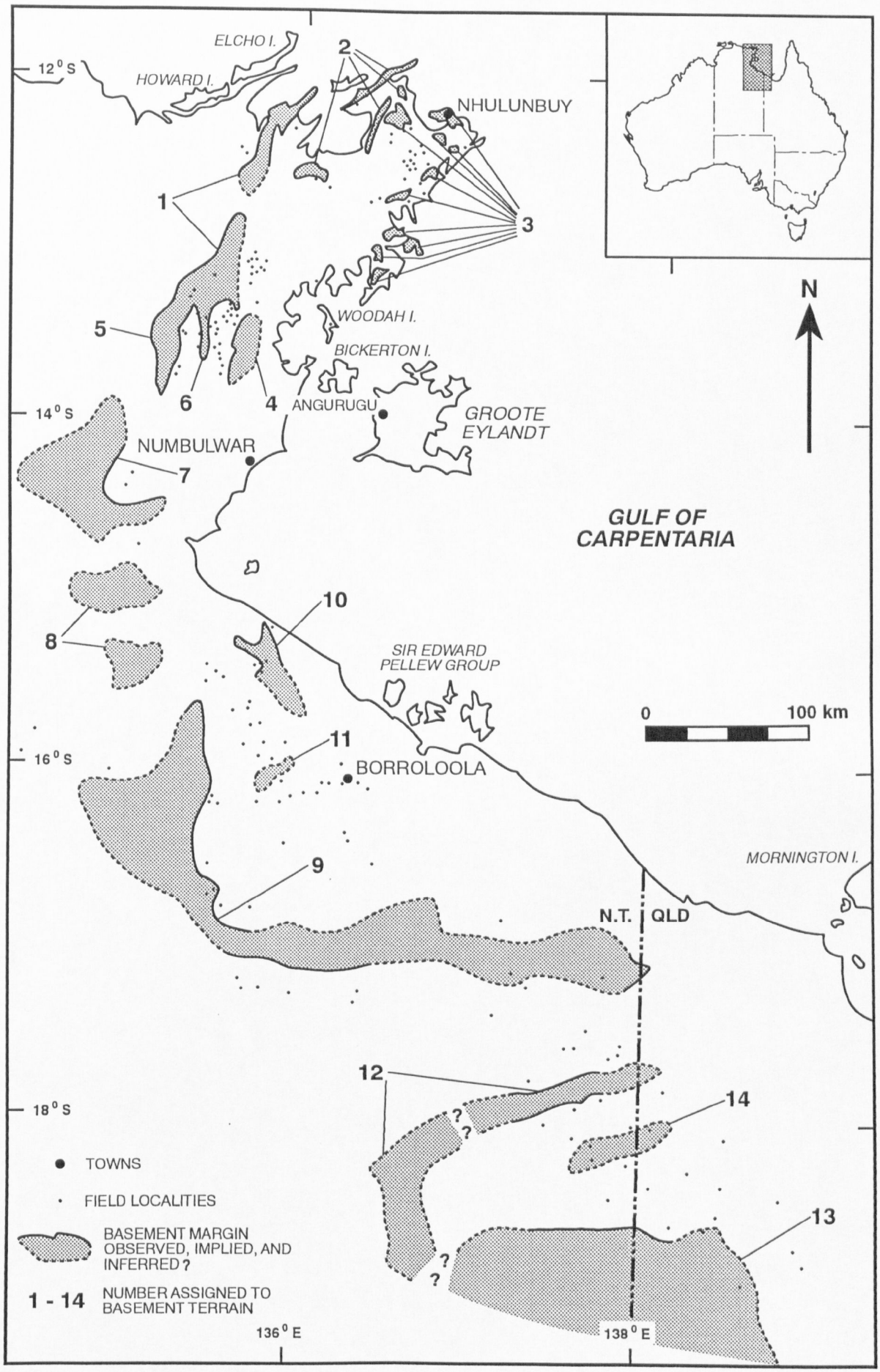

FIGURE 10.1. Location, size, and shape of major basement terrains that affected Cretaceous palaeogeography. In places Cretaceous sediments onlap these basement terrains, and many Cretaceous rocks were derived directly from erosion of basement rocks. Refer to Table 10.1 for details.

the granite chain in the Dalywoi Bay and Caledon Bay areas (at about latitudes 12^0 20' S and 12^0 50' S respectively). Maximum flooding of the northern shelf (stage 4, Figs. 10.9 and 10.10) came from the sea to the east and southeast, as indicated by lateral facies changes to finer-grained sedimentation in these directions. Arms of this sea are also interpreted to have extended to the Groote Eylandt area during stage 1 through 5 (Figs. 10.3 through 10.12).

TABLE 10.1: Major mainland basement blocks which affected Cretaceous palaeogeography.

Basement terrain #	Region	Local name (informal)	Shape/type of basement block	Exposed length x width (km)*	Composition and age
1	northern	Mitchell Range	elongate strike range	115 x 15	Proterozoic sed. rocks
2	ALZ	Dhalingbuy area blocks	elongate ridges	various < 30 x 8	Proterozoic sedimentary rocks
3	ALZ	granite island chain	linear NE-trending chain of small blocks	various < 15 x 12	Archean and Proterozoic granites
4	BPRZ	Bath Range block	NNE-trending strike range	40 x 15	Proterozoic McArthur Group
5	BPRZ	Parsons Range block	NNE-trending strike range	75 x 15	Proterozoic Parsons Range Gp. sedimentary rocks
6	BPRZ	central spur	NNE-trending ridge	25 x 15	Proterozoic Parsons Range Gp. sedimentary rocks
7	northern	Jalboi block	irregular crescent shaped block	90 x 55	Proterozoic Roper Gp. sedimentary rocks
8	central	Roper River blocks	two semi-rectangular blocks	57 x 25 & 30 x 22	Proterozoic Roper & McArthur Groups
9	central & southern	Limmen Bight-Mallapunyah block	large L-shaped block	380 x 75	Proterozoic McArthur, Roper, Tawallah Groups
10	central	Yiyintyi Range	large Y-shaped block	45 x 15	Proterozoic Tawallah Gp.
11	central	Tawallah Pocket block	elongate	28 x 8	Proterozoic Tawallah Gp.
12	southern	China Wall block	L-shaped block	230 x 25	Proterozoic/Archean sedimentary/igneous rocks
13	southern	Littles/Bluff/Carrara Ranges block	block of multiple E-W trending strike ridges	180 x 80	Proterozoic South Nicholson Group
14	southern	Nicholson River block	elongate ENE -trending block	65 x 15	Proterozoic igneous and sedimentary rocks

* The length and width are estimates of maximum values; the exact area of basement terrains cannot be calculated from these figures because most basement blocks have irregular widths along their length.

FIGURE 10.2. Stage 0: regional shorelines of latest Jurassic and Neocomian time. The known areas of Cretaceous sedimentation shown on the series of palaeogeographic maps in this chapter, and as seen in exposure areas on geologic maps, are not large as a result of having been covered by younger deposits and because of post-depositional erosion. Deducing palaeogeography and the exact position of shorelines from such limited information is difficult and it has been necessary to adopt a conservative approach, *i.e.* the extent of the sea at any time is generalised from the known distribution of rocks of a particular unit that has been dated by the best available biostratigraphy. The simplest interpretation is followed, and thus the full extent of the sea at any time may be underestimated. This is particularly true for areas where marine rocks grade into paralic or marginal marine facies.

There are few, if any, exposed rocks of Early Cretaceous age on the Mullaman Bed shelf. However, other regional studies have shown that transgressions and regressions did affect the study area in Early Cretaceous times. In the interests of continuity a series of these previously published regional palaeogeographic maps showing the position of land and sea is presented here. These maps were not intended to give detailed information on a particular area, rather they provide a regional overview, and complement the more detailed palaeogeographic maps in this study which are specific to the western shelf of the Carpentaria Basin.

In the following palaeogeographic reconstructions shaded areas represent land, and shorelines are shown as solid lines when control is good, as long-dashed lines where less certain, and as short-dashed lines where problematic. All three parts of Fig. 10.2 are from Frakes *et al.* (1987)

Part A

During the latest Jurassic to early Neocomian (latest Tithonian to Berriasian) none of the shelf was innundated, although an arm of the sea did extend to the area near Groote Eylandt. This embayment near Groote Eylandt persisted throughout much of Cretaceous time.

Part B

The extent of marine transgression supposedly increased in Valaginian to Hauterivian time, and the southern and western parts of the shelf may have been inundated (although there is no direct evidence in the form of dated marine sediments).

Part C

Continued transgression in Barremian and earliest Aptian time resulted in further inundation of the study area, and the extent of the seaway was apparently similar to stage 4 (see Fig. 10.9).

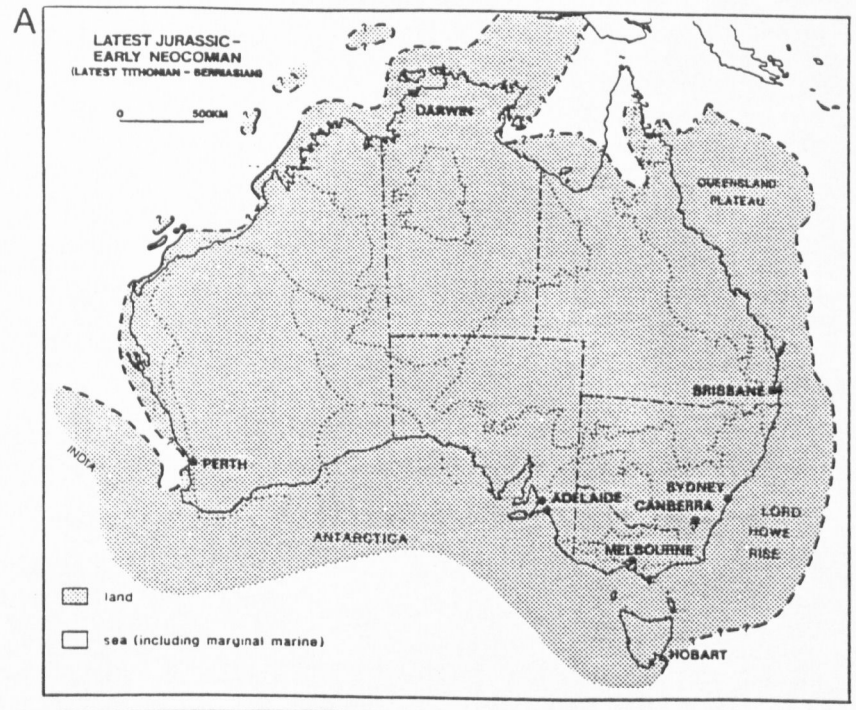
A
LATEST JURASSIC –
EARLY NEOCOMIAN
(LATEST TITHONIAN – BERRIASIAN)
0 500KM
DARWIN
QUEENSLAND
PLATEAU
BRISBANE
INDIA
PERTH
ADELAIDE
SYDNEY
CANBERRA
LORD
HOWE
RISE
ANTARCTICA
MELBOURNE
land
sea (including marginal marine)
HOBART

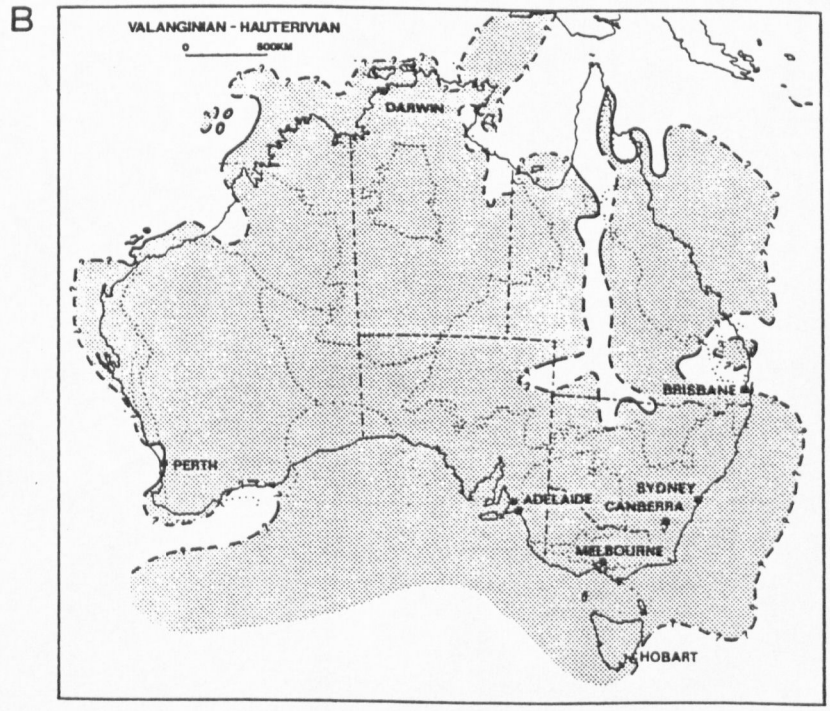
B
VALANGINIAN - HAUTERIVIAN
0 800KM
DARWIN
BRISBANE
PERTH
ADELAIDE
SYDNEY
CANBERRA
MELBOURNE
HOBART

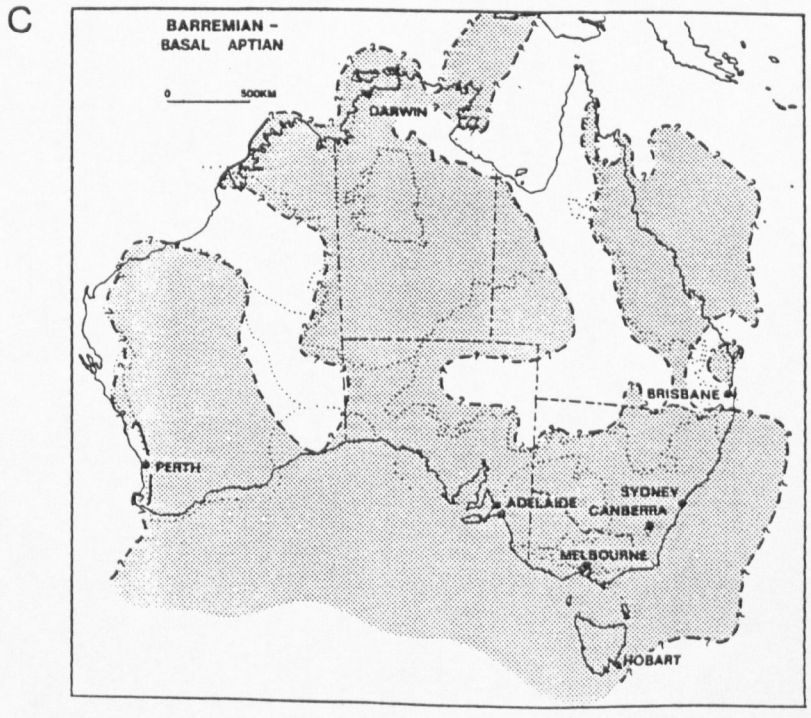
C
BARREMIAN –
BASAL APTIAN
0 500KM
DARWIN
BRISBANE
PERTH
ADELAIDE
SYDNEY
CANBERRA
MELBOURNE
HOBART

Landward of the intermittent belt of granitic islands, deposition on the mainland was restricted by basement ridges in the Dhalingbuy (terrain #2) and Mitchell Range areas, and there was thus limited deposition in areas in the north of the Arnhem peninsula and in western Arnhem Land (Figs. 10.7 through 10.12). Cretaceous sediments in these more distant areas (Arnhem peninsula) are thin and patchy in their distribution and probably relate to transgressions of unknown ages from the Arafura Sea to the north (west of the Mitchell Range). Relatively little is known about the nature and distribution of onshore Cretaceous rocks in the area between Arnhem Land and the Darwin region.

Sediments derived from the bounding ridges in the Dhalingbuy and Mitchell Range areas were deposited relatively rapidly, and thin sheets of marine sandstone were spread over most northern parts of the shelf; these were later eroded and reworked by fluvial systems, primarily during stage 5. Ferruginous and/or manganiferous sandstone of facies successions 2 lies adjacent to and southeast of the basement ridge near Arnhem Bay in the Dhalingbuy area, and the basement ridge probably blocked marine transgression any farther to the southwest.

The dominant marine rock type in the ALZ is sandstone, except for interbedded siltstones in facies succession 8 and siltstone-claystone developed at the top of facies succession 5. This relatively coarse-grained material was apparently derived from the basement terrains surrounding marine Cretaceous deposits (see petrological evidence in Sect. 10.6.4 and Appendix 4). Energy conditions were high, and judging from occurrences of HCS and gutters, storm waves were generated at times.

The sediment supply rate was not high however (Sect. 10.6.4), because the sediment cover on this broad shelfal platform is thin and discontinuous. Disconformities throughout the sequence indicate that this was a "cannibalising" shelf (Krassay, 1992), with just-deposited sediments being reworked through subaerial erosion during regressions and submarine erosion during transgressions.

Nonmarine and restricted marine deposits of facies successions 7 and 8 respectively occur only in proximal areas that were close to the palaeoshoreline (Fig. 10.12). They extend south from the northern region to about latitude 18^0 S; however they are not present within this region in more distal areas such as the Numbulwar and Limmen Bight drillhole sequences, or on Groote Eylandt. South and east of latitude 17^0 S, nonmarine deposits of successions 3 and 7 occur only locally near basement highs.

FIGURE 10.3. Regional and local shorelines in Australia during the ?middle to late Aptian.

Part A

This regional map shows that the extent of marine transgression had increased markedly by Aptian time, and most of the study area was apparently inundated. However, the distribution of marine facies of the Mullaman Beds suggests a more conservative estimate of the area flooded during the Aptian; compare the different sizes of the Aptian flooded area in part A vs. part B. Most likely the true extent of Aptian flooding is somewhere between the two estimates presented here. From Frakes *et al.* (1987).

Part B

Part B of Fig. 10.3 is the first in a series of six stage-by-stage shoreline maps specific to the western shelf of the Carpentaria Basin. This stage encompasses the time from deposition of the basal exposed Mullaman Beds (based on stratigraphic correlation) through to the late Aptian (based on direct biostratigraphic dating).

Based *solely* on preserved Aptian-aged rocks in outcrop, it is only possible to discern that the seaway occupied the eastern part of the southern region in the more basinal part of the Gulf, and some of the BPRZ. There is a complete lack of preserved Aptian-aged outcrops on the rest of the shelf, which suggests that there was only minor transgression onto the western mainland in the Northern Territory. However, older Aptian marine rocks have been documented farther inland in recent drillholes (M. Warne, pers. comm., 1994), signaling more extensive Aptian transgression than suggested solely by the distribution of outcrops of the Mullaman Beds.

STAGE 1 Regional shorelines: Aptian

A

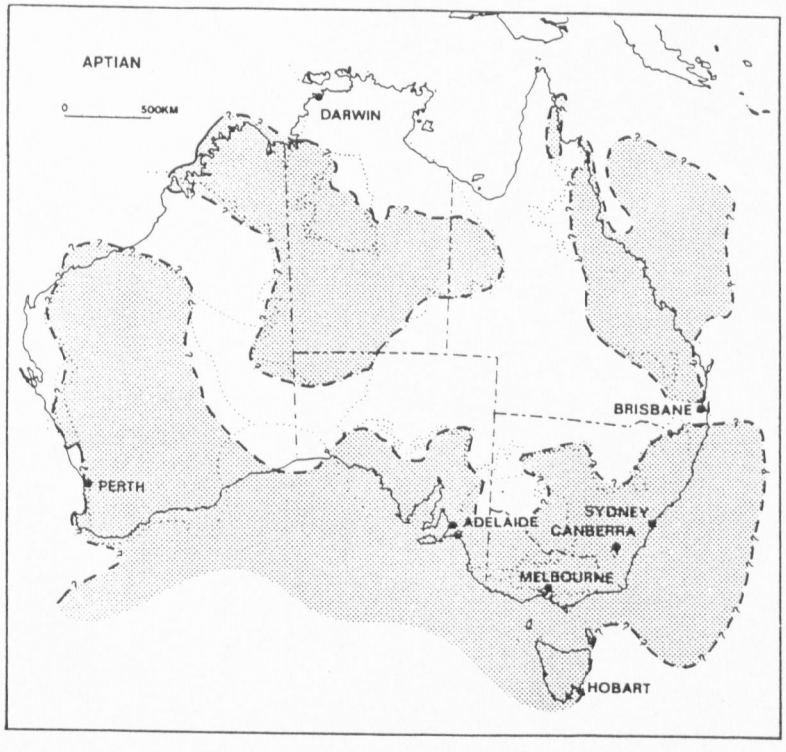

STAGE 1 Shorelines: Aptian (?mid to late)

B

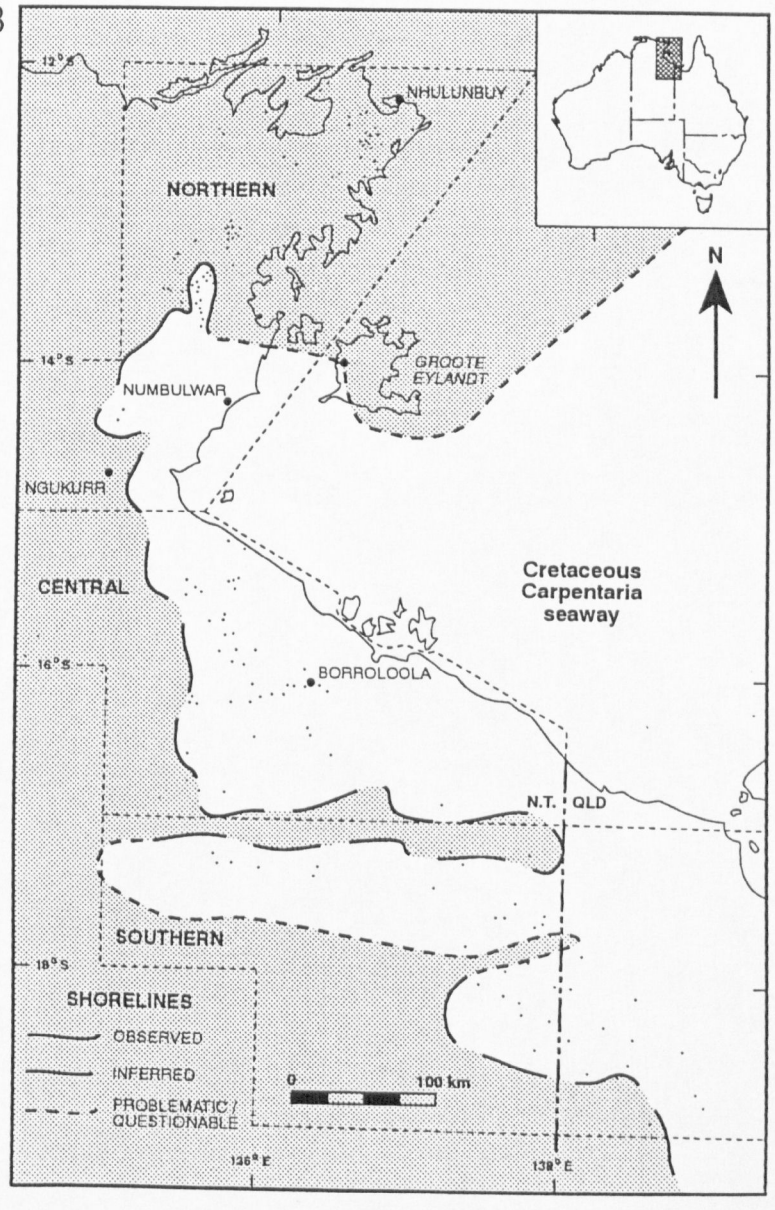

The directions of sediment transport during transgression and regression can be generalised as nonmarine and marine progradation towards the east and southeast during times of regression, and coastal onlap towards the north and northwest during transgression. Sedimentary facies suggest only a slight decrease in grain size from west to east in the ALZ, but this trend becomes more pronounced farther south along the shelf. The ALZ has abundant palaeogeographical parallels with the Groote Eylandt area during the early Cretaceous in that it was characterised by shallow-marine embayments with low sedimentation rates.

10.4.3 Palaeogeography of the northern region (Bath and Parsons Ranges Zone)

The BPRZ and surrounding areas display three significant areas of exposed Cretaceous rocks. The first is a sizeable embayment (approximate area of 2400 km^2) between the Bath and Parsons Ranges, which was flooded in stage 1 (Fig. 10.4) and stages 3-5 (Figs. 10.7 through 10.12). Here, Cretaceous sediments onlap the flanks of both ranges and the area where the ranges converge in the vicinity of section 33. Sections examined along these ancient shorelines consist of conglomerates and sandstones, with only minor siltstone and claystone. The sandstones, of facies successions 2 and 5, contain coarse and angular grains directly derived from the adjacent source rocks, and clasts in the conglomerates show a local provenance (especially chert).

Near the central spur (terrain #6), the sandstones are very coarse-grained (*e.g.* section 152). On the western side of the palaeoembayment small sandstone 'deltas' composed of facies succession 6 are preserved in smaller embayments in the Parsons Range (*e.g.* sections 37, 208-210). This all constitutes strong evidence that conditions here were quite different from the ALZ; erosion was active and sedimentation was comparatively rapid. Even near the centre of the embayment accumulation of sand dominated, and finer-grained material is present only in minor amounts. The stratigraphic repetition of fossiliferous sandstones of facies succession 2 reflects the unusual palaeogeography in the northern end of the Bath and Parsons Range embayment, which resulted in rapid facies changes and large-scale interbedding of marine and non-marine rocks in the proximal part of the embayment (Fig. 10.8).

This large palaeoembayment was connected to the open sea in the south, in the area north of Numbulwar. No other link to the sea is possible owing to the elevated terrain (>300 m a.s.l.) surrounding the Bath-Parsons Ranges Cretaceous outcrops, which lie at elevations of less than

FIGURE 10.4. (this caption also applies to Figs. 10.6, 10.8, 10.10, 10.12, and 10.14).

Figure 10.4 is the first of six regional palaeogeographic reconstructions illustrated as a series of timeslices (stages 1-6); the same stages are illustrated in the stage-by-stage shoreline maps. The simple patterns on the maps show the extent of various marine facies successions on the shelf. Here, unlike the stage-by-stage shoreline maps, patterned areas represent sea and the plain (white) areas represent land.

The position of the palaeoshoreline for each of these reconstructions is taken from the corresponding stage-by-stage shoreline map, and is shown as a single solid line. For greater detail on the 'confidence level' in assigning the position of shorelines refer to the stage-by-stage shoreline maps. For more detailed explanations of features noted on the palaeogeographic reconstructions refer to the main text. For the positions of basement terrains from which the Cretaceous sediments were derived refer to Fig. 10.1.

STAGE 1 Palaeogeographic sketch map: Aptian

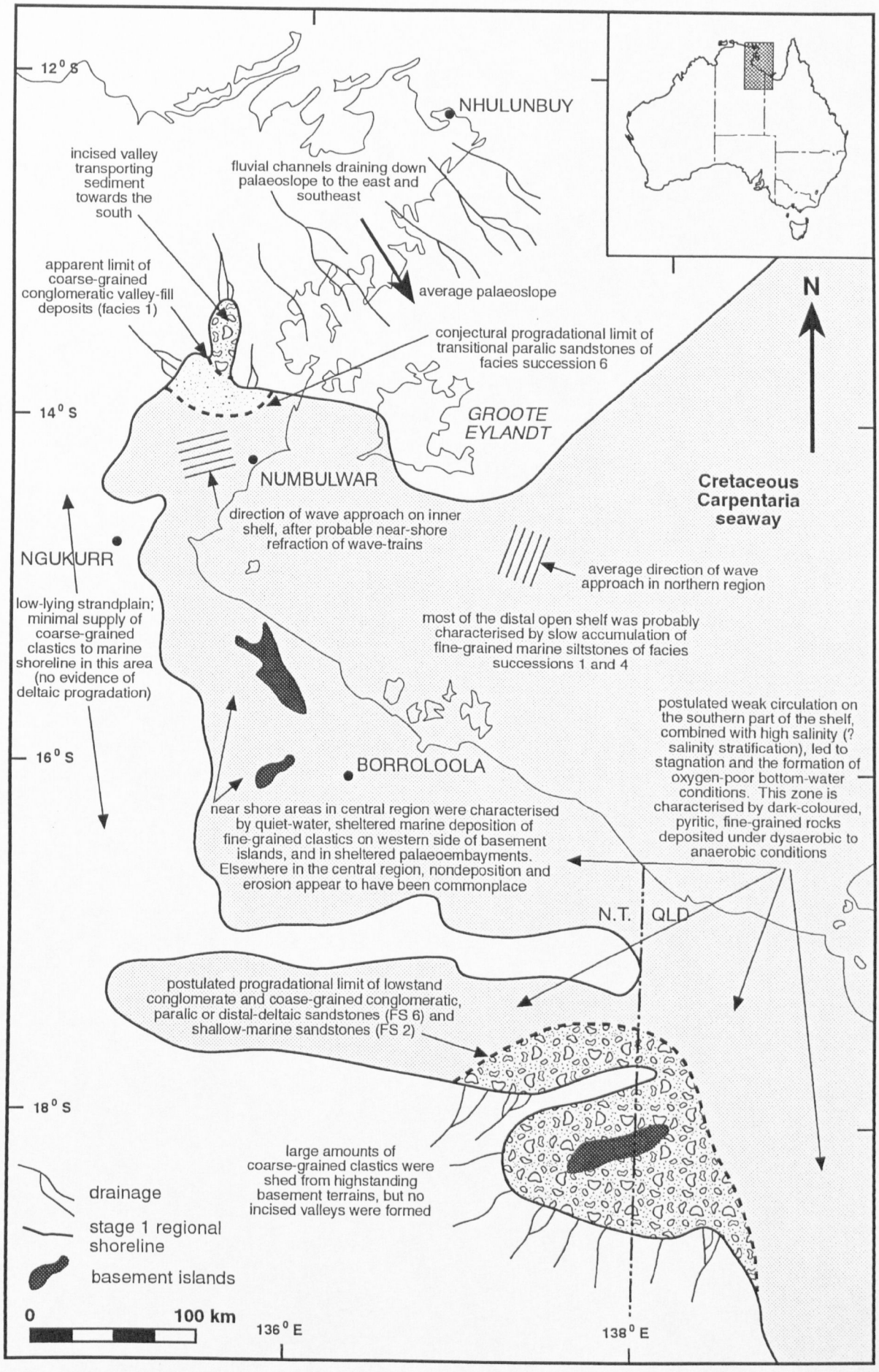

FIGURE 10.4.

130 m a.s.l.. Over time this seaway deepened, as indicated by upward fining of the sequence and the presence of thick highstand and transgressive deposits (Sects. 9.5.4, 9.5.5, and 9.7.4).

The second area of Cretaceous sedimentation lies much farther south, near the Rose River. This area near Numbulwar was drilled by U.S. Steel to reveal a fine-grained sequence deposited predominantly in the offshore zone. Cyclic deposition is apparent, and there is a suggestion that grain size decreases towards the east and northeast (Sect. 8.5.5). The age and sedimentary architecture of deposits in this area are similar to those in the BPRZ, but sediment accumulation occurred in a quieter, deeper-water offshore though shallow-marine environment, which was relatively distant from the palaeoshoreline and basement ridges to the west and north.

The third area of major Cretaceous marine deposition on the mainland in the northern region is rather poorly defined; the extent of Cretaceous marine flooding in this area is extrapolated from previous descriptions by Skwarko (1966) of marine fossiliferous strata in the western part of the Urapunga map sheet. Fossiliferous marine sandstones in this area appear to correlate with marine rocks of facies succession 2 in the BPRZ on the basis of their fossil content and stratigraphic position. Therefore, it is suggested that an arm or lobe of the seaway extended west and then southwest at about latitude 14^0 S around a large basement block (terrain #7) during stage 3 (Figs. 10.7 and 10.8), and possibly also during stage 4 (Figs. 10.9 and 10.10). The westward limit of this part of the seaway is not precisely known, but is thought to lie near the boundary of the Urapunga map sheet at about longitude 134^0 E.

Accepting an age of early Albian to early Cenomanian for rocks in the northern region in this study (as proposed in Sect. 8.2) leads to a reasonable reinterpretation of the palaeogeography of the western and southern basin margins, including the Groote Eylandt region. There is no longer a need, for example, for a continuous "barrier" between the so-called coastal and inland belts of Skwarko (1966), sedimentary evidence for which is lacking in the northern region in any case. Instead, each facies succession is seen to have been deposited within the confines of an embayment or sub-basin. Several of these large embayments existed at various times on the broad shallow shelf which deepened eastward into the Carpentaria Basin.

FIGURE 10.5. After the late Aptian highstand (represented by Fig. 10.3B) there was a major regression, followed by a smaller transgression of the sea (illustrated here) at some time between the late Aptian and the late early Albian; this is considered here as early Albian on the basis of stratigraphic correlations.

The early Albian sea was smaller and more restricted than the sea during stage 1. A lobe of the sea occupied the same southern part of the southern region as the Aptian sea, and also extended northwest in the vicinity of Groote Eylandt. The extent of marine inundation between these two areas in early Albian time is unknown due to the complete lack of early Albian-aged outcrops in the area, but it is likely that the early Albian sea did not cover the northern or central regions.

STAGE 2 Shorelines: ?early Albian

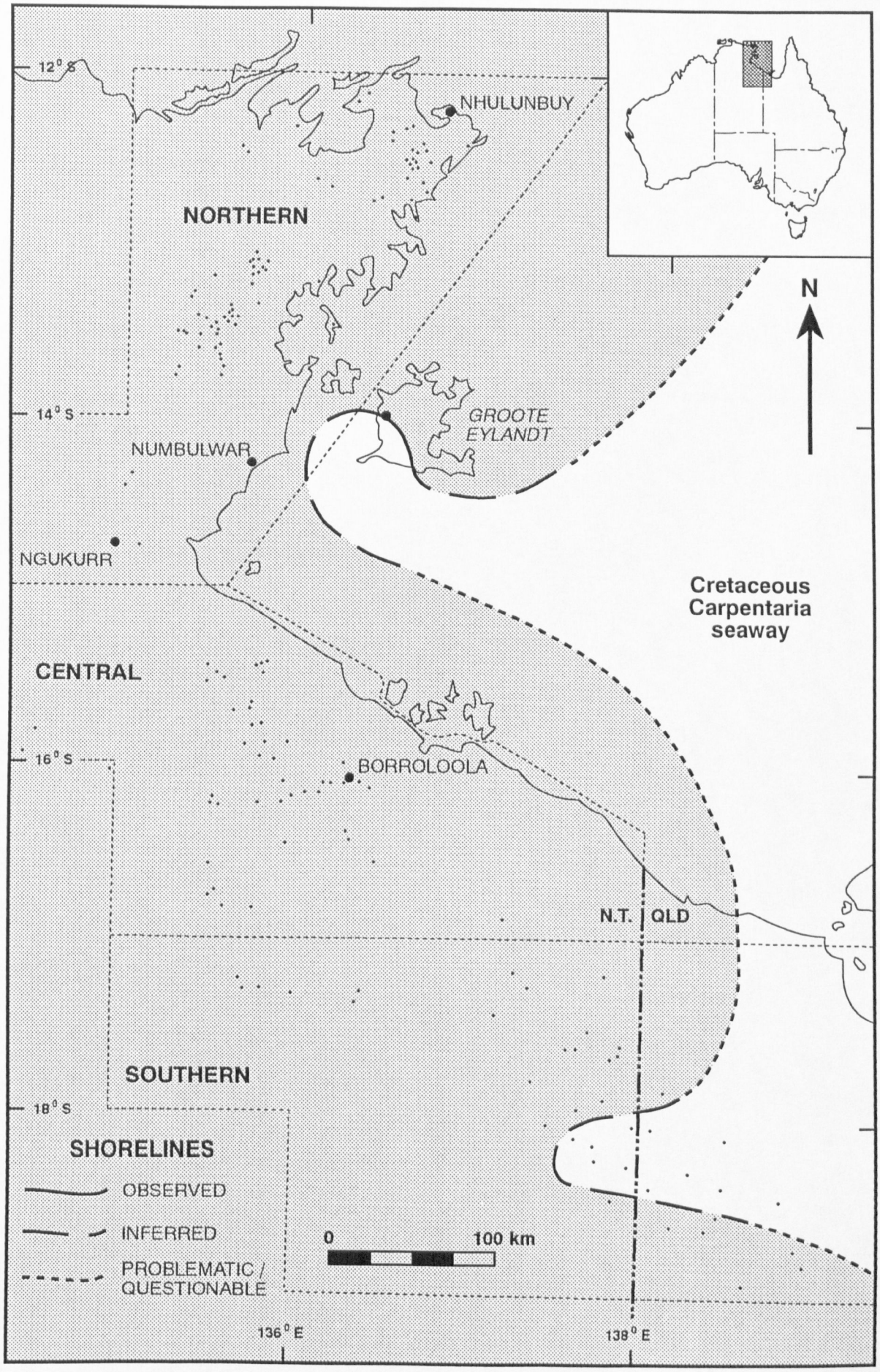

FIGURE 10.5.

STAGE 2 Palaeogeographic sketch map: ?early Albian

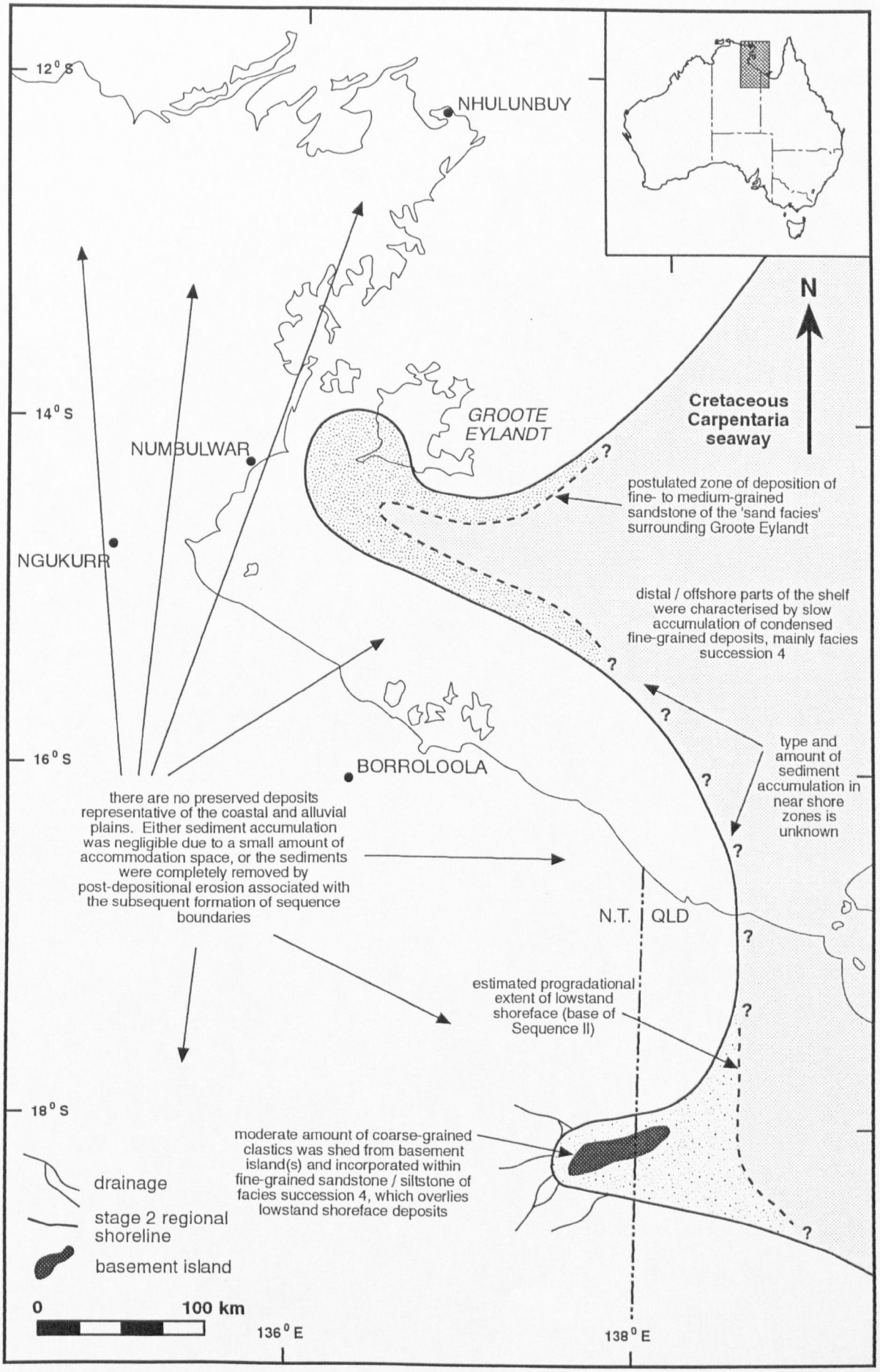

FIGURE 10.6.

10.4.4 Palaeogeography of the central region

In the central region there are three major basement terrains which exerted some influence upon Cretaceous depositional systems (see Table 10.1 and Fig. 10.1):

1) There are two moderately sized (~50 km wide) basement blocks (terrain #8) which were emergent in the northern part of the central region, south of Ngukurr.
2) There is a large ?continuous basement block (terrain #9) comprising ancient mountain ranges which occupied the southeastern and southern parts of the central region.
3) The Yiyintyi Range (terrain #10) in the northeastern part of the central region formed a barrier or large island during most times of sediment accumulation in the mid-Cretaceous.

The exact size and shape of the basement blocks of terrain #8 are poorly known, but these areas appear to have been emergent during major flooding of the shelf, although the sea intruded between these two basement highlands during stages 4 and 5 (Figs. 10.9 through 10.12). The largest basement terrain in the central region, which affected Cretaceous sedimentation and the configuration of the seaway, is composed of a series of linked basement highlands, minor mountain ranges, and lower ridges in the southeastern and southern parts of the central region (Fig. 10.1). Part of this large basement block (terrain #9) probably covered most of the area between latitudes 16^0 and 17^0 S. The Cretaceous palaeoshoreline formed a north-south trend along the eastern margin of this basement terrain, approximately coincident with the present course of Limmen Bight River. The southern end of this basement highland is linked to a series of low-lying east-west trending basement ridges along the southern part of the central region.

At times during the mid-Cretaceous these basement ridges formed one emergent "L-shaped" landmass, and in many places Cretaceous rocks onlap and thin rapidly onto basement terrain #9. There are no preserved Cretaceous exposures on the elevated parts of this basement terrain, and it is unlikely that basement was ever completely inundated, even during maximum flooding on the shelf. However, it is possible that not all of the basement blocks were joined to form a single landmass during all stages, and that minor Cretaceous flooding occurred to the west and southwest through gaps in basement terrain #9.

The third major basement block is the Yiyintyi Range (terrain #10) in the northeastern part of the central region. Evidence for Cretaceous emergence of the range is given by the onlap of marine Mullaman Bed strata exposed in the area surrounding the lower part of the range. Shallow drilling on the western side of the range (Sands, 1979) indicates that the Cretaceous marine sequence thins rapidly toward the range (onlap). Upper shoreface deposits of facies

FIGURE 10.7. The late early to middle Albian (stage 3) was a time of major transgression on the western shelf of the Carpentaria Basin; the time of maximum flooding of the southern half of the shelf for the Aptian-Cenomanian interval.

The sea had six main lobes or arms: the two southern lobes occurred in approximately the same position as during stage 1. However, relative sea level was higher in the Albian, and this enabled the sea to break through the topographically high Proterozoic barriers in some areas, facilitating transgression farther westward in these areas. One such arm of the sea in stage 3 extended up to 200 km in a west-east direction at latitude 17^0 20' S (similar to the Aptian embayment which previously existed in this area).

The largest part of this Albian seaway occupied the area from south of Borroloola to the northern end of the Bath and Parsons Range embayment. Flooding occurred up to a distance of 175 km inland from the present gulf coast, and the sea also encompassed the western and southwestern parts of Groote Eylandt. Again, the western extent of this lobe was controlled by the position of the generally north-northeast trending Proterozoic ridges on the mainland. In the northern part of this large sub-basin one arm of the sea extended up to 80 km farther inland at about latitude 14^0 S, whilst another arm extended 50 to 60 km into the BPRZ.

The fifth lobe of the Albian sea covered a portion of Arnhem Land from just north of Groote Eylandt to about 20 km south of Nhulunbuy. The palaeoshoreline of this lobe was close to the present gulf coast, but the sea penetrated the chain of granite islands near the present coast in several places and extended up to 20 km farther inland. The sixth, and northernmost, lobe occupied part of the present day Arnhem and Buckingham Bays west of Nhulunbuy, plus a small area of the mainland. The extent of this lobe was controlled by the Wessel Island trend lying to the northwest, and north-northeast trending basement ridges to the east and south.

STAGE 3 Shorelines: late early Albian to middle Albian

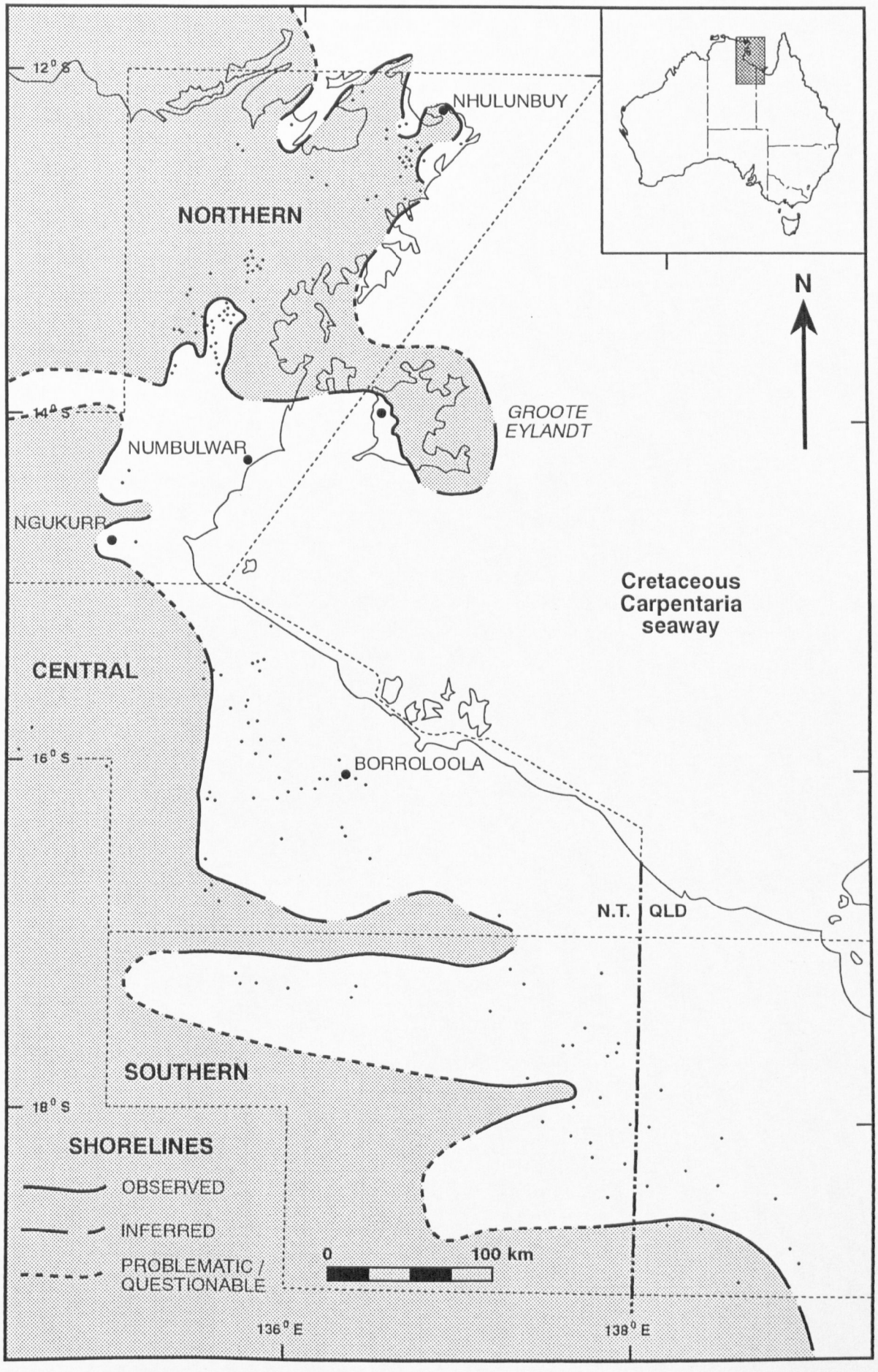

FIGURE 10.7.

STAGE 3 Palaeogeographic sketch map: late early Albian to middle Albian

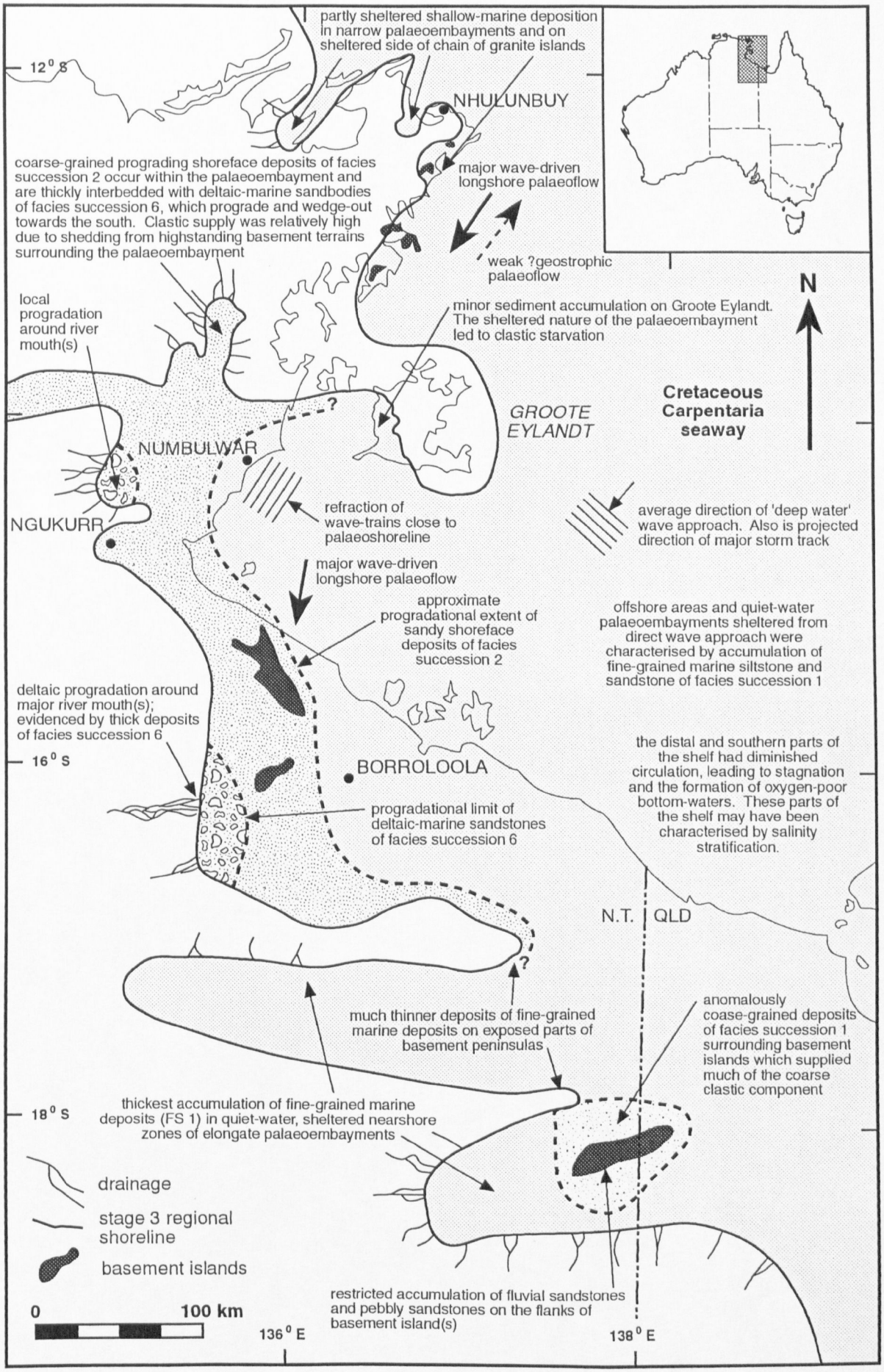

FIGURE 10.8.

succession 2 are exposed intermittently around the base of the range and mark the position and relative stratigraphic height of the palaeoshoreline. Patchy coarse-grained fluvial valley-fill deposits of probable mid-Cretaceous age in the middle to upper parts of the range also provide evidence for fluvial deposition, indicating that the Yiyintyi Range was emergent during the Cretaceous.

The central region of the shelf was at least partly inundated in Aptian time (Figs. 10.3 and 10.4; based on limited recent drillhole data, H. Barents, pers. comm. 1994), but was emergent in the early Albian (Figs. 10.5 and 10.6). However, extensive marine flooding of the shelf occurred during middle Albian to early Cenomanian time, and marine sediments accumulated in large embayments or sub-basins in the central region during stage 3 through 5 (Figs. 10.8 and 10.12). During these stages the western shoreline of the Cretaceous seaway in the central region had a regional north-northwest trend, which was broken in places by arms of the sea which extended farther westward. The most westward marine incursion occurred during stage 5 in the Cox River area, where an arm of the sea extended between basement terrains #8 and #9 at about latitude 16^0 S (Fig. 10.11).

The main marine basin in the central area during stages 3-5 lay to the west of the Sir Edward Pellew Islands, which were apparently submerged during the Cretaceous, and east of the short arm of the "L-shaped" basement terrain #9. The Yiyintyi Range formed a large island on the inner part of the shelf at these times, and resulted in partly restricted marine circulation and deposition in more sheltered environments, as shown by a regional lateral facies change from fully-marine facies succession 4 to restricted-marine facies succession 8 (Fig. 10.12). The existence of isolated Cretaceous fluvial deposits, and the trend of the palaeoshoreline (defined by upper shoreface deposits within facies succession 2), indicate that at least one more basement block (terrain #11) was emergent about 50 km west of Borroloola, within the large embayment between the Sir Edward Pellew Islands and terrain #9 to the west. The long (east-west) arm of terrain #9 separated the central and southern regions of the shelf, but related contemporaneous deposits exist on both regions of the shelf, and deposition appears to have been relatively continuous on either side of this large basement highland.

FIGURE 10.9. After an extended period of high water throughout much of the Albian (stage 3), there was a minor regression which was followed by another major transgression from late Albian to latest Albian (possibly earliest Cenomanian) time (stage 4). This was the time of accumulation of marine sandstones and siltstones capped by the C2 marker.

During stage 4 the sea occupied a similar area to that earlier in the Albian, but flooding was more extensive in the northern region. The main differences are that the sea transgressed at least 75 km farther westward in the northern region in the latest Albian, and there was a marine connection between the BPRZ and the northern region through the Blue Mud Bay area. The northern and central parts of Groote Eylandt and the area around Bickerton Island were probably joined to form a large island at this time. Farther to the north, a large part of the ALZ was inundated south of Arnhem Bay.

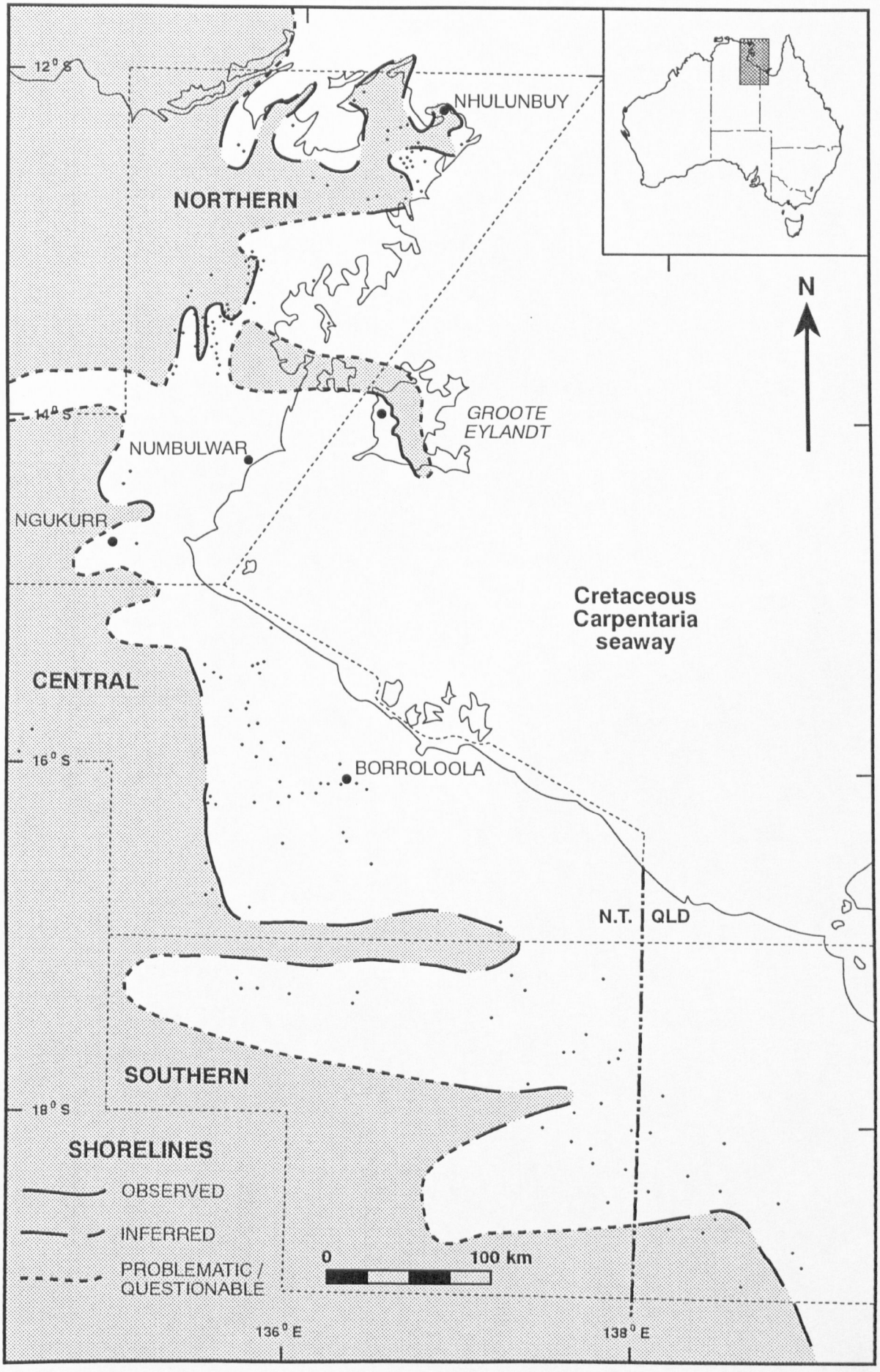
12° S
NHULUNBUY
NORTHERN
14° S
NUMBULWAR
GROOTE
EYLANDT
NGUKURR
N
Cretaceous
Carpentaria
seaway
CENTRAL
16° S
BORROLOOLA
N.T.
QLD
SOUTHERN
18° S
SHORELINES
OBSERVED
INFERRED
PROBLEMATIC /
QUESTIONABLE
0
100 km
136° E
138° E

FIGURE 10.9.

STAGE 4 Palaeogeographic sketch map: late Albian to latest Albian

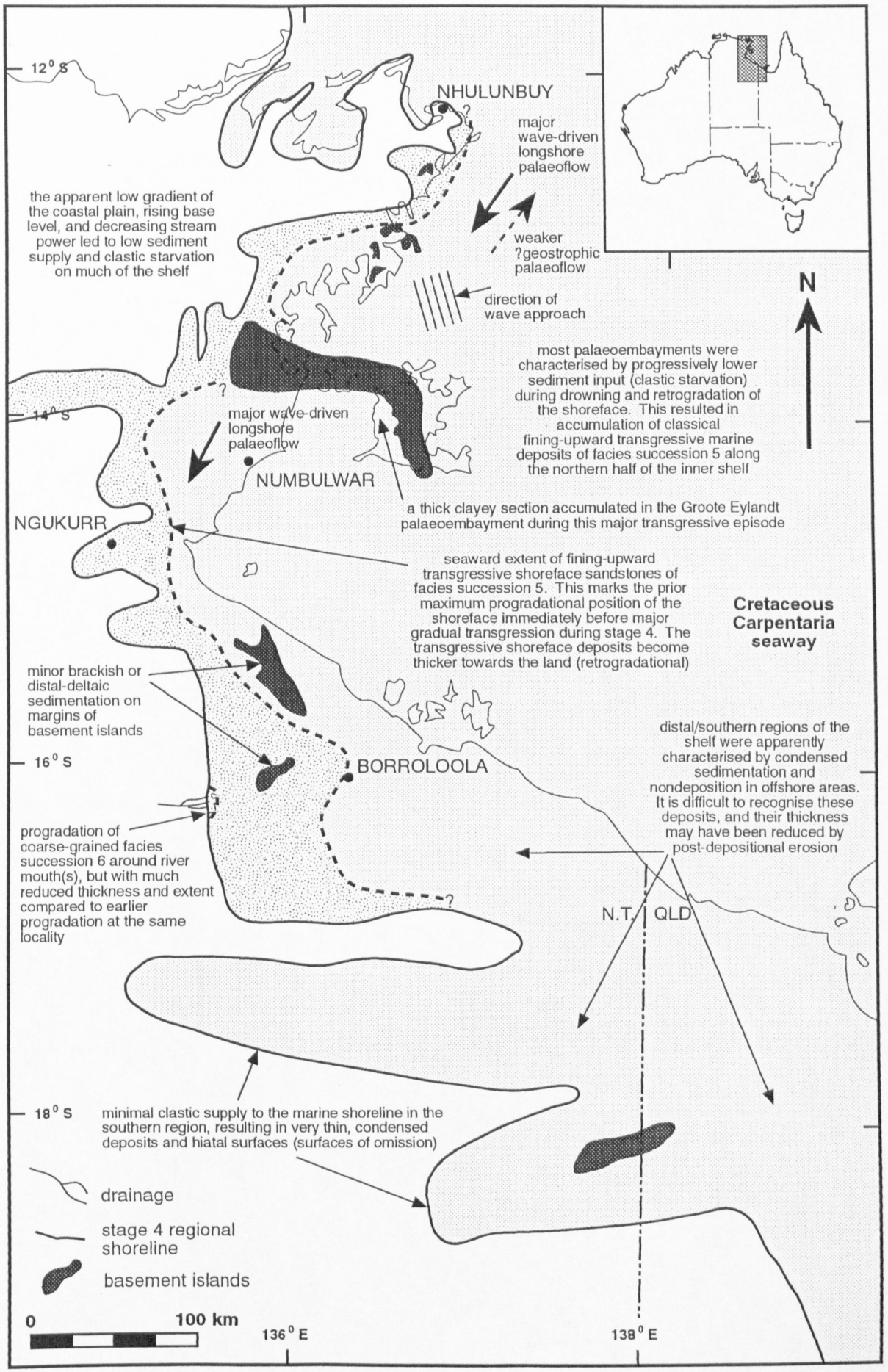

FIGURE 10.10.

10.4.5 Palaeogeography of the southern region

The main palaeogeographic elements in the southern region are (see Table 10.1 and Fig. 10.1):

1) The long east-west trending part of terrain #9 in the northern part of the southern region, whose southern margin acted as a barrier to northward transgression.
2) A large elongate west-southwest trending basement block known as the 'China Wall", which was linked to another (poorly defined) north-south trending basement block. Together they define basement terrain #12.
3) A large basement block (terrain #13) whose northern and eastern margins defined the east-west and north-south palaeoshorelines (respectively) at the southern edge of the study area.
4) A northeast trending basement block (terrain #14) in the central part of the southern region, which was an island during most times of transgression.

The long east-west part of the "L-shaped" terrain #9 is a highland (typically >170 m a.s.l.) which blocked northward transgression into the central region. This terrain formed the northern east-west trending palaeoshoreline of an elongate embayment on the Wallhallow map sheet during stages 3-5 (Figs. 10.7 through 10.12), and probably also during stage 1 (Figs. 10.3B and 10.4). Initial flooding and deepening of this seaway was probably rapid as indicated by the relatively thick outcrop of fine-grained facies succession 1, and a similar basal Aptian-aged sequence in the subsurface (T. Bernecker, pers. comm. 1994). The position of the western end of the embayment is not exactly known, but probably occurs just to the west of section 98 on the Wallhallow map sheet. Cretaceous facies successions in this palaeo-embayment show onlap geometries to the north and west with basement, and the grain size of Cretaceous rocks increases markedly towards these basement highlands. These facies changes document the high-energy, shallow-marine depositional processes which occurred along the edge of terrain #9; again most of the Cretaceous clastics were derived locally from erosion of basement rocks.

The elongate 'China Wall' basement highland (terrain #12) is elevated (> 200 m a.s.l.) and was emergent throughout the Cretaceous. No marine Cretaceous deposits lie directly above this basement highland, but marine facies successions 1, 2, and 4 were deposited around its lower parts (<100 m a.s.l.). The size and abundance of clasts decreases away from basement , and clasts are composed of Proterozoic basement rock types (indicating local provenance).

The southwestern end of the 'China Wall' joins another north-south trending basement block (also a part of terrain #12), which has significant topographic elevation (up to 300 m a.s.l.) and forms the eastern boundary of the Barkly Tableland. This basement highland marks the

FIGURE 10.11. Shortly after accumulation of the C2 marker bed during latest Albian highstand (stage 4) there was regression, which was followed by transgression some time in the early Cenomanian.

Significant parts of the western and southwestern margins of the Gulf of Carpentaria were flooded. However, in most areas the sea had retreated from its position during the latest Albian highstand. There was no longer a marine connection of the northern region and BPRZ through the Blue Mud Bay area, and the Groote Eylandt-Bickerton Island area was no longer an island. Also, the sea had retreated from the east-west trending embayment at about latitude 14^0 S. The exception to this overall retreat of the sea in early Cenomanian time occurred in the central region, where westward transgression of up to 110 km occurred in the vicinity of the Cox River between latitudes 15^0 40' and 16^0 S.

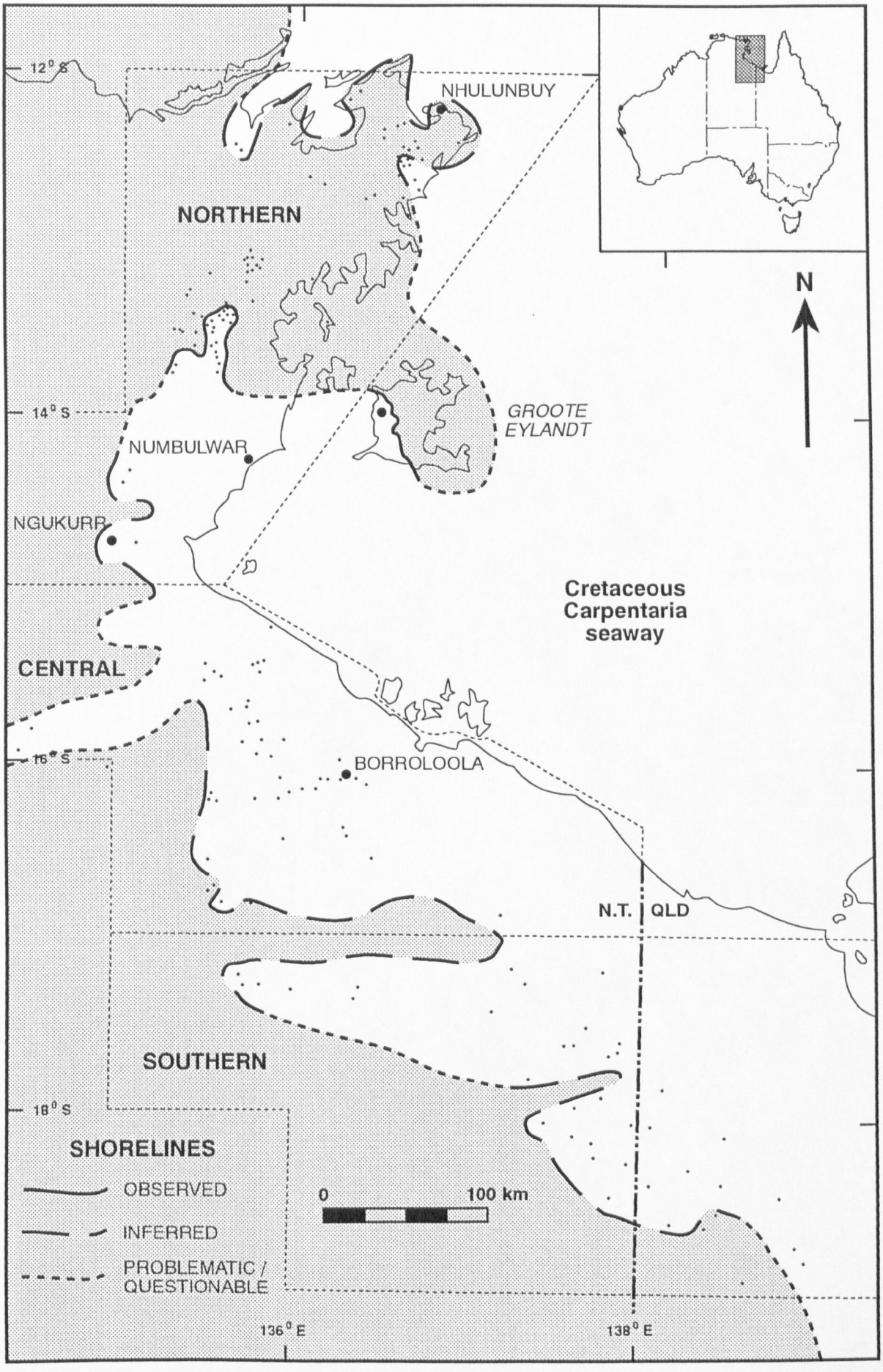
12° S
NHULUNBUY
NORTHERN
N
14° S
GROOTE
EYLANDT
NUMBULWAR
NGUKURR
Cretaceous
Carpentaria
seaway
CENTRAL
16° S
BORROLOOLA
N.T.
QLD
SOUTHERN
18° S
SHORELINES
OBSERVED
INFERRED
PROBLEMATIC /
QUESTIONABLE
0
100 km
136° E
138° E

FIGURE 10.11.

STAGE 5 Palaeogeographic sketch map: ?early Cenomanian

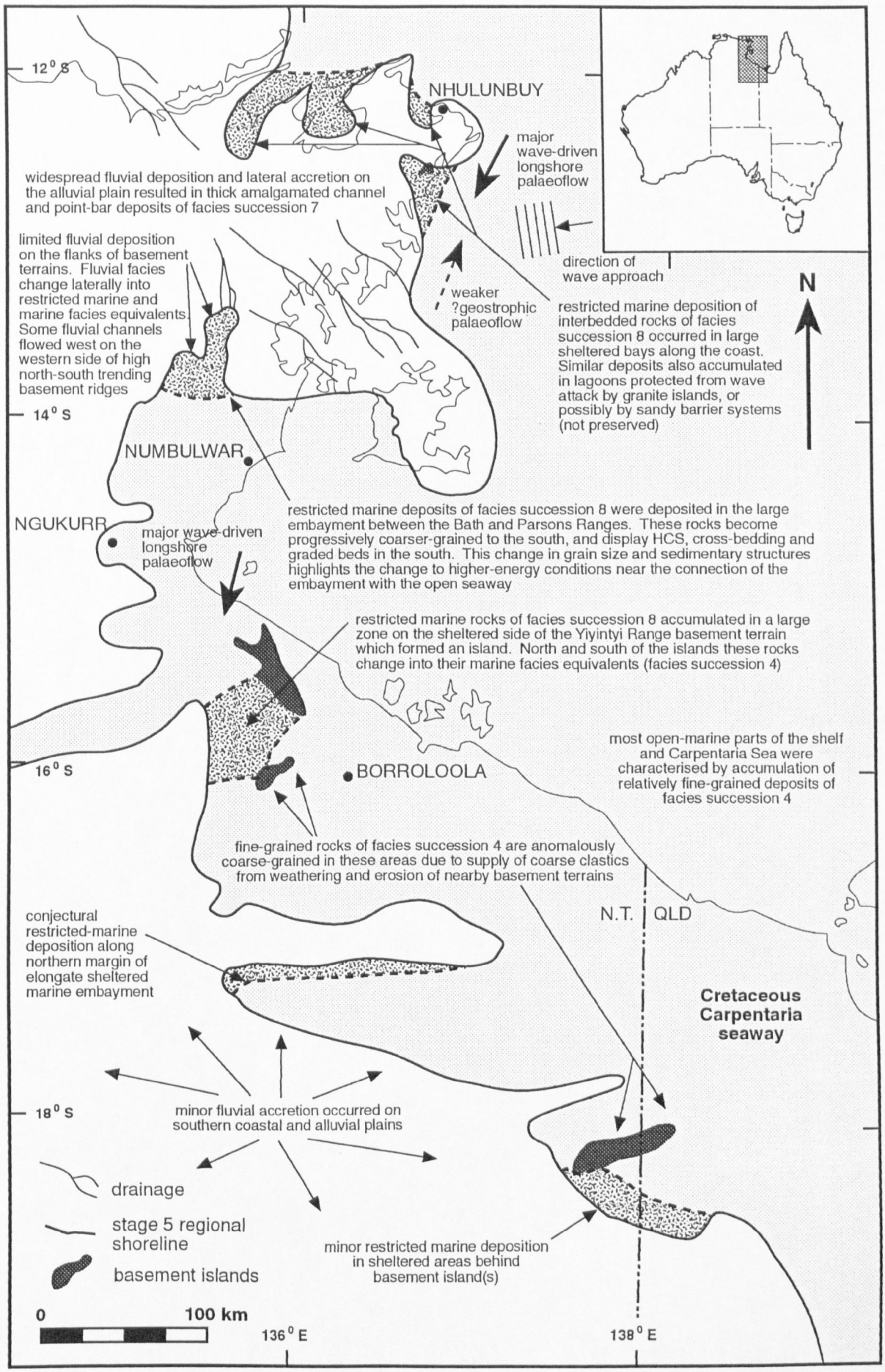

FIGURE 10.12.

westward limit of transgression in the Cretaceous. However, Cretaceous rocks are rarely preserved in this region, and are limited to several outcrops of facies succession 2 (*e.g.* site 52; Skwarko, 1966) which are correlative with similar deposits in the central region and BPRZ, and were deposited during stage 3. On Fig. 10.1 the basement blocks of terrain #12 are considered to have formed one single emergent landmass in the Cretaceous, although it is possible that gaps in the basement terrain were partially flooded during stages 3-5 (Figs. 10.7 through 10.12).

Cretaceous rocks onlap along the northern and eastern margins of basement terrain #13, and lack of any preserved marine Cretaceous deposits in the ranges, combined with the observed onlap geometry, suggest that this basement terrain was emergent in the Cretaceous and blocked southward transgression in the southern part of the southern region.

In summary, the Cretaceous sea covering the southern region during stages 3-5 was divided into two large embayments, with maximum flooding occurring during stage 3 (late early to middle Albian, Figs. 10.7 and 10.8). The northern embayment had an east-west dimension of about 200 km and was between 25 to 75 km wide (narrowing toward the west). Its northern shoreline was defined by the southern edge of terrain #9, and its southern shoreline was defined by the northern edge of terrain #12.

The southern embayment also had an east-west axis, but was not as narrow as the northern embayment. The northern and western shorelines of the embayment were defined by the southern edge of terrain #12, whilst the southern shoreline of the embayment occurred along the northern edge of terrain #13. During maximum flooding in stage 3, this embayment had a west-southwest to east-northeast dimension of about 100 km, and a width of 60-70 km.

In both of these embayments shoreface deposits at the palaeoshoreline are defined by relatively coarse-grained Cretaceous rocks (commonly facies succession 2) abutting basement terrains, whereas finer-grained rocks (typically facies successions 1 and 4) were deposited several to tens of kilometres offshore from the palaeoshoreline. Most deposits in the southern region are finer-grained than contemporaneous deposits in the central and northern regions, indicating the distal position of most depositional environments on the southern region of the shelf.

FIGURE 10.13. By the final transgressive pulse in about middle Cenomanian time (stage 6), the sea covered only a fraction of the area previously flooded during the Albian. The sea was restricted to a single embayment in the central part of the southern region, similar in area and position to the southern part of the sea during stage 2. This situation was the result of progressive retreat of the sea from early to middle Cenomanian time, beginning in the north, as the sea contracted south and east towards the basin centre due to a progressive fall in relative sea level.

STAGE 6 Shorelines: ?middle Cenomanian

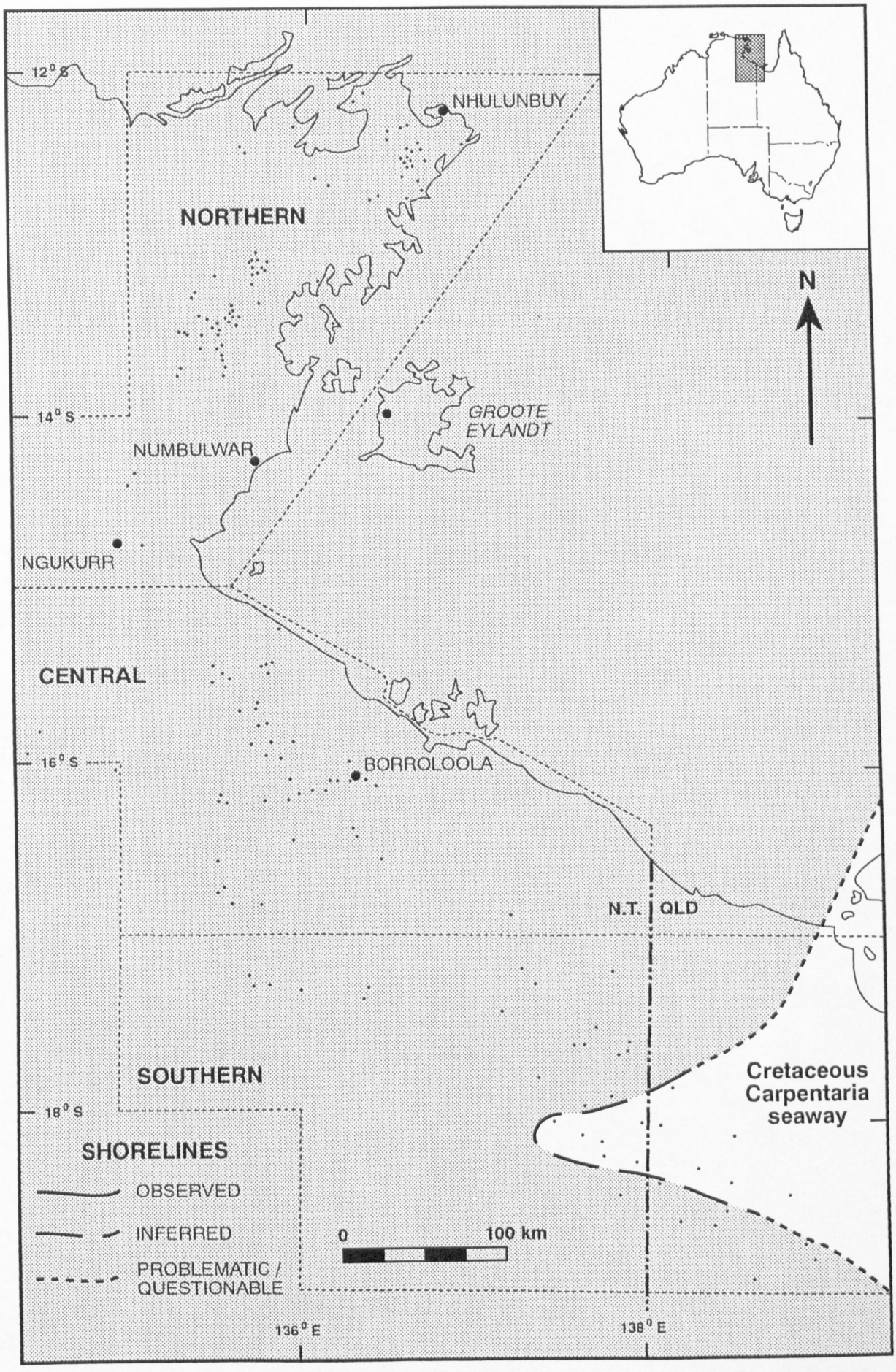

FIGURE 10.13.

STAGE 6 Palaeogeographic sketch map: ?middle Cenomanian

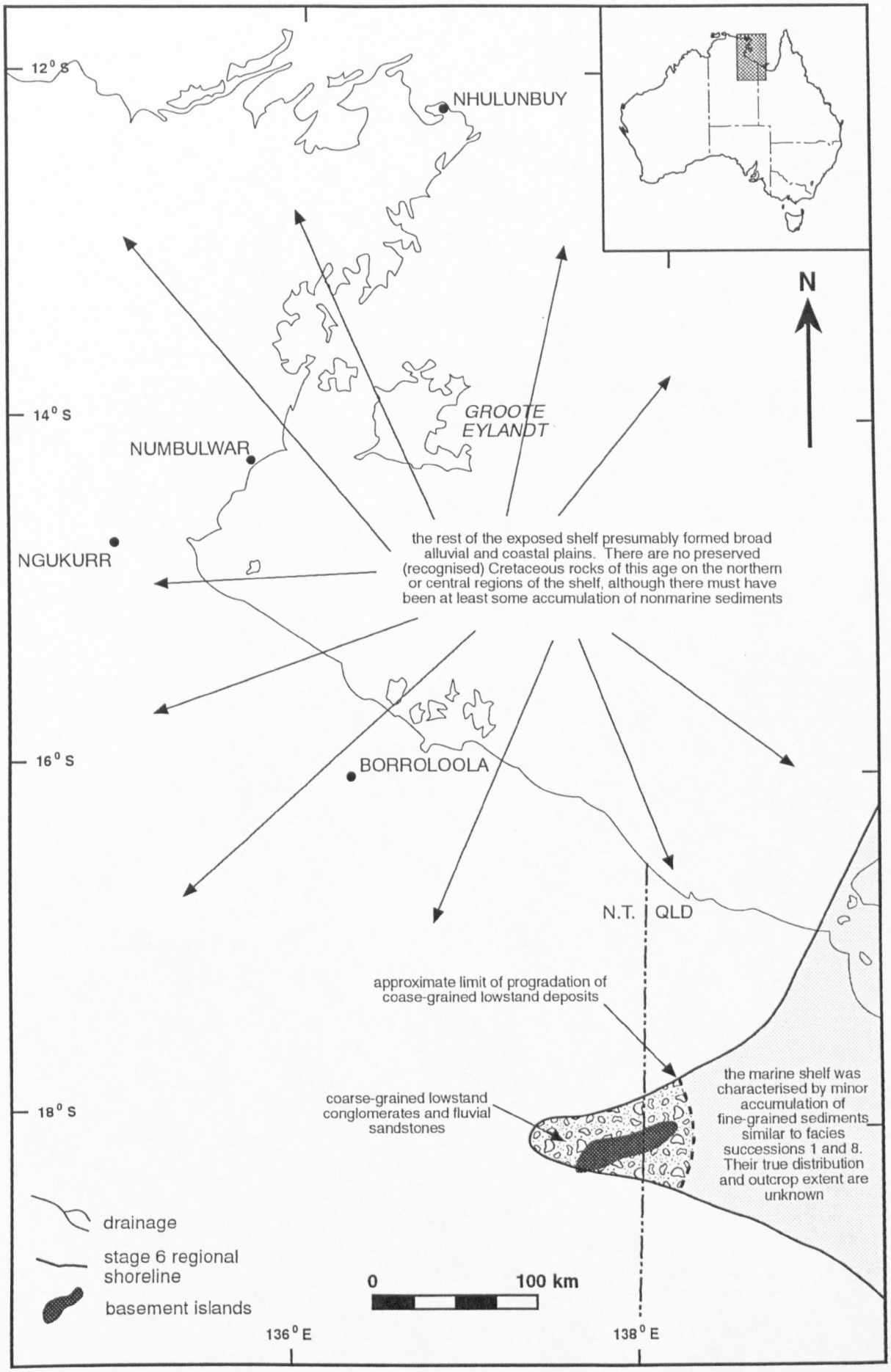

FIGURE 10.14.

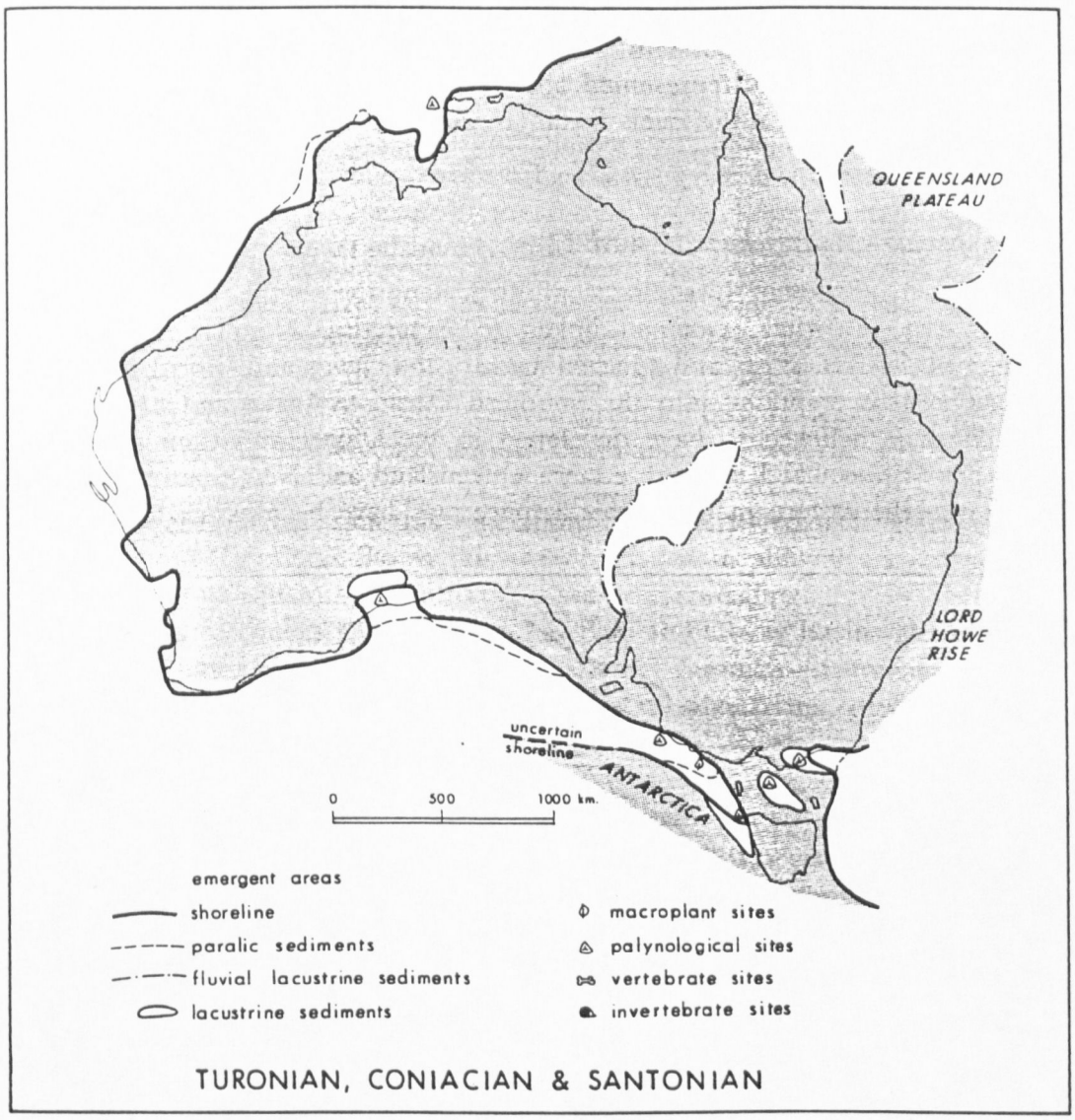

FIGURE 10.15. The end of accumulation of the Mullaman Beds occurred in about middle Cenomanian time, judging by the rocks preserved on the shelf. The end of sedimentation coincides with retreat of the sea from the western shelf of the Carpentaria Basin some time in the middle to late Cenomanian. Regional studies have shown that the entire Carpentaria Basin and surrounding areas were emergent for the Turonian stage and the remainder of the Cretaceous Period. The lack of any preserved Late Cretaceous marine sediments on the Carpentaria Basin shelf, combined with regional palaeontological criteria from previous studies, indicate that the sea did not return to the area in the Late Cretaceous, and that a land connection with Papua New Guinea existed in the north. From Dettmann *et al.* (1992).

10.5 PALAEOGEOGRAPHICAL SIGNIFICANCE OF THE CLAY MINERALOGY OF THE MULLAMAN BEDS

10.5.1 Trends of clay mineral distribution in the marine Mullaman Beds

Analyses of clay mineralogy provide additional insights into fine-grained marine sedimentation near the western margin of the seaway. XRD analyses of numerous fine-grained samples from the mainland and Groote Eylandt in the present study have resulted in some important discoveries concerning the mineralogy, distribution, and palaeoenvironmental significance of fine-grained marine rocks on the shelf (Table 10.2 and Appendix 6).

TABLE 10.2: Clay-mineral trends in marine facies successions of the Mullaman Beds.

Sequence (=age) [1]	Facies succession [2]	Depositional environment	Proximality	Clay minerals *		
				kaolinite	illite	smectites [4]
III [3]	FS 1 (base)	lower offshore marine	distal	r [5]	p	c
III [3]	FS 1 (middle)	offshore marine	distal	p [5]	r	c
III [3]	FS 1 (top)	upper offshore/lower shoreface	intermediate	c [5]	p	----
III	FS 2 (base)	lower shoreface/upper offshore	intermediate	p	p	----
III	FS 2 (middle)	middle shoreface	proximal	p	r	----
III	FS 2 (top)	upper shoreface/foreshore	proximal	p	p	----
IV	FS 5 (base)	upper shoreface/foreshore	proximal	p	r	----
IV	FS 5 (middle)	middle shoreface	proximal	c	p	----
IV	FS 5 (top)	lower shoreface/upper offshore	intermediate	c	p	----
IV	C 2 Marker	offshore marine	intermed.-distal	c	p	----
V	FS 4 (base)	upper-middle shoreface	proximal	p	r	----
V	FS 4 (middle)	lower shoreface	intermediate	p	r	----
V	FS 4 (top)	upper offshore to offshore	intermed.-distal	p	p	----
III	FS 1 equivalent	Groote Eylandt embayment	distal	p [5]	p	c
IV	C 2 Marker	Groote Eylandt embayment	intermed.-distal	c	p	----
V	FS 1? equivalent	G.E. quiet shallow marine	intermed.-distal	p	p	c

* c = common p = present r = rare ---- = absent

1 For details of Sequences and their ages refer to chapter 9.

2 For details of Facies Successions refer to chapter 4.

3 Based on both mainland and Numbulwar (US Steel) drillhole sample analyses.

4 Montmorillonite and nontronite are the two types of smectitic clay in the Mullaman Beds.

5 Denotes that at least some kaolinite is authigenic and is derived from weathering of detrital feldspar.

The main observations relating to the clay mineralogy of the rocks are:

1) samples of lower facies succession 1 from both the Numbulwar and Wallhallow areas have an identical, distinctive mineralogy, comprising smectitic clay (mostly montmorillonite), quartz, subordinate kaolinite and illite with minor unaltered orthoclase feldspar;
2) the C2 marker throughout the study area and Groote Eylandt (*cf.* Bolton, 1982) contains kaolinite as its dominant clay mineral, and a minor amount of illite;
3) other Cretaceous rocks of facies successions 2, 4, and 5 contain various clay mineral suites, depending on their proximity to the palaeoshoreline; and
4) on Groote Eylandt there are 3 main clay mineral suites: the base of the 'clay facies' (equivalent to Sequence *III*) contains montmorillonite and is similar to the base of facies succession 1; the top of the 'clay facies' (equivalent to the top of Sequence *IV*) directly underlying the main ore horizon contains kaolinite and illite, and is closely related in texture and composition to the C2 marker on the mainland, and; the claystone of the 'pisolite facies' (equivalent to Sequence *V*) which encloses the ore horizon contains nontronite (a type of iron-rich montmorillonite), kaolinite, and minor illite and is similar to facies succession 1 on the mainland.

These observations can be generalised as the following trends in the distribution and relative abundance of clay minerals (see Table 10.2):

1) Most proximal and coarse-grained rocks (*e.g.* shoreface sandstones of facies successions 2 and 5) contain only a minor amount of clay, typically kaolinite.
2) Slightly finer-grained rocks (*e.g.* the lower parts of facies succession 2), still in proximal localities relative to the palaeoshoreline, contain a significant amount of kaolinite and a minor amount of illite.
3) Progressively finer-grained and more distal rocks (*e.g.* fine-grained parts of facies successions 4 and 5) contain lower amounts of kaolinite and higher amounts of illite.
4) Truly distal shallow-marine deposits (*e.g.* facies succession 1 and Groote Eylandt equivalents) contain more illite than kaolinite, and a significant amount of smectitic clay (typically montmorillonite and nontronite).

10.5.2 Models to account for the observed clay mineral trends

There are probably three main alternatives to explain the trends of clay mineralogy, distribution, and abundance within the Mullaman Beds, or any similar fine-grained marine sequence:

1) *Local provenance model*: there may have been original (Cretaceous) variations in the distribution (deposition) patterns of locally derived clays (due to differing floc size).

2) *Remote provenance model*: there may have been episodic/periodic delivery of particular clay minerals by water currents (or airfall) from a remote source area.
3) *Palaeoclimate control model*: there may have been differences in the absolute amounts of clay (particularly illite/smectitic clays) delivered by local rivers to the proximal seaway during wet versus dry periods.

In the *local provenance model*, clays would have been derived primarily from weathering of basement rocks of the McArthur Basin, and supplied to the seaway by rivers. After delivery to the marine environment, clays would have settled-out of suspension at different rates due to their varying floc size (Gibbs, 1977); floc size increases from smectite (and mixed-layer smectite/illite clays) to kaolinite to illite (Edzwald and O'Melia, 1975). Thus, flocs composed of smectite and/or mixed-layer smectite/illite clays may have been held in suspension (and transported farther offshore by shelf flows in the seaway), whereas kaolinite flocs fell out of suspension at a more rapid rate, in areas closer to the palaeoshoreline.

The *remote provenance model* presents the proposition that there may have been input of clay from the volcanic chains to the north (in Papua New Guinea; Paltech, 1980c) and to the east (along the eastern margin of northern Australia; Veevers, 1991). Fine-grained clays from these sources could have been transported into the Carpentaria Basin by currents or winds.

In the *palaeoclimate control model*, changes in precipitation rates may have affected the amount of fluvial runoff, and hence the type and amount of river-transported clays entering the seaway over time. This model has been proposed as a controlling mechanism for clay-mineral suites within a thick Turonian siliciclastic and carbonate sequence in an analogous setting in the Western Interior Seaway of North America (Sethi and Leithold, 1994). These authors propose that during dry climatic phases, characterised by diminished rainfall and lower rates of fluvial avulsion and downcutting, kaolinite (which dominates the uppermost parts of soil horizons; Weaver, 1989) would have been mobilised chiefly by surface runoff and delivered to the seaway. At such times the model predicts that sediments in proximal localities (*e.g.* ALZ and BPRZ) would have been relatively poor in illite/smectite clays, and relatively rich in discrete kaolinite and illite.

Conversely, during wet periods of increased rainfall and fluvial runoff, a larger proportion of mixed-layer smectite/illite clays may have been mobilised and delivered to the seaway due to higher rates of fluvial avulsion and downcutting into lower illite/smectite-rich parts of soil

horizons. This increased input of illite/smectite may have led to concentration of illite/smectite clays in the seaway (even its proximal parts) during wet periods.

10.5.3 Discussion

It is difficult to assess the relevance of the *remote provenance model* because it is impossible to quantify the input of clay from a distant source, or indeed, whether any clay was supplied from such a source. The absence of distinctive accessory minerals such as biotite, sphene, and cristobalite, or glass shards in the smectitic clays of the Mullaman Beds argues against a primary volcanogenic source. More likely, smectitic clays were largely derived from erosion of nearby Precambrian McArthur Basin volcanogenic units along the western margin of the seaway, and were transported to the basin by local rivers.

It is also difficult to assess the importance of the *palaeoclimate control model* in explaining the distribution of clay minerals in the Mullaman Beds. Firstly, there is no direct evidence for changes in precipitation rates in northern Australia during the Cretaceous. The climate was generally cool, but was humid (Dettmann *et al.*, 1992; Haig and Lynch, 1993), and would have been suitable for deep weathering and the formation of significant amounts of clay, particularly kaolinite. Secondly, chemical diagenesis during pedogenesis and ferricrete/laterite formation (there are well-developed ?Late Cretaceous and/or Tertiary laterites in many parts of the study area) may have transformed some of the original clay mineral assemblages, thus erasing any climatic signal recorded by detrital clay mineral abundances (*cf.* Singer, 1988). The model predicts an abundance of smectitic and mixed smectite/illite clays throughout the seaway (even in proximal localities) during wet periods. However, smectitic clays are only preserved in a few distal localities within the Mullaman Beds. Thus, it appears unlikely that cyclical climate variations were responsible for clay mineral distribution on the shelf.

As shown in Table 10.2, kaolinite is a major component of the clay-mineral suites in the shelf sequence. The kaolinite is probably detrital, and its abundance largely reflects original proximity to the shoreline, although kaolinite can also form authigenically; there is obvious kaolinitic alteration associated with the formation of lateritic profiles and soils in the upper part of the shelf sequence, and in some parts of the lower sequence the kaolinite in thin sections and hand specimens can be seen to be derived from weathering of detrital feldspar (Appendix 4). However, throughout the bulk of the shelf sequence the increased percentage of kaolinite in near-shore deposits appears to reflect the original depositional pattern, as documented in other marine settings (*e.g.* Hallam *et al.*, 1991; Singer, 1984).

The observed clay-mineral distribution pattern corresponds closely to that predicted by the *local provenance model*, where abundant kaolinite occurs in proximal deposits (*e.g.* in the ALZ and BPRZ), mixed kaolinite/illite in intermediate deposits, and smectitic and illite clays in distal deposits (*e.g.* in the Numbulwar, Wallhallow, and Groote Eylandt areas). There is no need (or evidence) to invoke either the *remote provenance model* or the *palaeoclimate control model*, although some (an unspecified amount) of clay may have been derived from distant sources.

10.6 SHELF DYNAMICS

10.6.1 Introduction

It has been documented that fluctuations in relative sea level and climatic conditions caused key oceanographic parameters to vary throughout the history of the Cretaceous Western Interior Seaway of North America (Ericksen and Slingerland, 1990). There are many similarities between this relatively shallow epeiric seaway and the Great Artesian Basin seaway of Australia, including: their large size and long north-south axes; the 5 or 6 major transgressive-regressive cycles which characterised the seaways; the cyclical nature of mudstone- and sandstone-dominated stratigraphic intervals; and their general intracratonic setting and Cretaceous palaeogeography (despite the lack of large marginal mountain belts in the GAB).

Considering the broad palaeogeographical similarities of the two seaways, it is probable that fluctuations in relative sea level and climate also controlled oceanographic parameters in the Great Artesian Basin seaway of Australia. Such fluctuations, in turn, would have caused variations in circulation and sediment-transport regimes, but these were not documented in previous studies. It is interesting to note that the Carpentaria Basin (Arafura Sea) is also considered as a Holocene analogue for the Cretaceous Western Interior Seaway of North America (Klein and Ryer, 1978). It seems that the configuration of the Carpentaria Basin has not changed greatly since the Mesozoic, and there have been no profound tectonic events to alter the shallow-intracratonic depression which forms the Carpentaria Basin and marks the present-day Gulf of Carpentaria.

In this section an attempt is made to model the depositional processes which formed the Mullaman Beds. The controlling factors in the development of the shelf sequence include the following: relative sea level fluctuation; rates of sediment supply; basin subsidence and tectonics; palaeoclimates; palaeogeography of the shelf; winds and tides; basin circulation patterns, and so on. The interplay of these factors and their interpreted effects are discussed

below, and much of this discussion follows on from data and ideas introduced in previous chapters.

10.6.2 Storm generation potential

Considering the regional extent and great abundance of interpreted storm-influenced deposits and storm-generated structures (Plate 13) in the Mullaman Beds on the Carpentaria Basin shelf (Krassay, 1994a), it is important to assess the actual potential or likelihood for storm generation in and around northern Australia in mid-Cretaceous time. Integration of the major information sources (palaeogeographic reconstructions, palaeoclimate simulations, and computer modelling of circulation patterns) might yield estimates for the type, intensity, and occurrence interval of storms which affected the Mullaman Bed shelf.

Judging by preserved sedimentary structures the type of storm activity that affected the western shelf of the Carpentaria Basin is that which was capable of significantly affecting shallow-marine depositional environments. Such storms include severe tropical cyclones (hurricanes) and intense winter storms (*cf.* Duke, 1985), but not normal rough water conditions which occur on a weekly to monthly basis near modern ocean margins.

When considered over geological time, hurricanes have been responsible for the majority (73%) of global storm deposits (Duke, 1985, as documented by HCS occurrences), and intense winter storms have been responsible for the remainder (27%). It may be that storm deposits in the Mullaman Beds were produced exclusively by hurricanes, but there is no direct evidence for this, and it is not sufficient to consider storm intensity and type purely on the basis of latitudinal distribution, *i.e.* intense winter storms at high palaeolatitudes and hurricanes dominating lower palaeolatitudes (Barron, 1989). Sea surface temperatures are important, but climate and geography induce significant variability in storm-generation rates and the distribution of storms. Hurricane activity (modelled from the present) is seasonal and is restricted to areas with warm sea surface temperatures (>26-27^0 C, Barron, 1989). Other conditions conducive for hurricane genesis involve circulation variables (*e.g.* high Coriolis force and increased low-level vorticity). According to Barron (1989) such parameters would have combined favourably for hurricane genesis as a matter of probability on geological time scales, and hurricanes *would have* occurred, particularly during times of warm sea-surface temperature (the most essential requirement for hurricane genesis) as expected for the Albian to Cenomanian ocean lying to the north of Australia.

PLATE 13

Sedimentary features of storm-dominated sedimentation within the Mullaman Beds:

a Medium- to large-scale (wavelength > 2 m) hummocky cross-stratification in amalgamated fine-grained sandstone (facies 14). Bundles of laminae in the upper part of the hummocks are defined by parting along slightly finer-grained layers. Site 148, northern region. Scale bar is 12 cm wide. (See plate 3f for another view of HCS).

b Discontinuous metre-scale lenses (arrowed) of pebble conglomerate in the upper part of a coarsening-upward facies succession (2). Conglomeratic lenses are enclosed by interbedded sandstone and siltstone exhibiting HCS, wave ripples, and graded beds. Site 148, northern region. White scale bar at centre left of one of the lenses is 12 cm wide.

c Thinly interbedded bioturbated siltstone and sandstone with a sharp-based coarser sandstone bed (just above scale bar), which has been partly reworked into a *Thalassinoides* burrow network. Originally this sandstone bed probably comprised a lenticular (starved) sandy wave ripple. Site 176, northern region.

d Similar rocks to those in plate 13c, but here the sandstone is coarser-grained and contains foresets of crossbeds that are mantled by granule to small pebble sized chert clasts. Also prominent are sand-filled gutters (arrowed) and complex erosional scours. Site 168, northern region. Hammer is 32.5 cm long.

e Massive coquina consisting almost entirely of fragmented and disarticulated bivalve shells. This coquina occurs amidst low-energy sandy siltstone of facies succession 8, and suggests that strong currents were episodically active. The coarse size of the shells and their concentration into death assemblages indicates significant reworking. Site 87, central region. Lens cap is 5.75 cm in diameter.

f Storm-emplaced veneer of coarse sand, granules and small pebbles (arrowed) parallel to top of scale bar. Note 2 cm diameter clast next to top left-hand corner of scale bar. This veneer is an intraformational lag and occurs within interbedded ripple-laminated sandstone and clayey siltstone of facies succession 2. Site 154, northern region.

g Thin graded beds (coarse sand and granules) interbedded with offshore laminated clayey siltstone and hemipelagic claystone. Such graded rhythmites have sandstone beds with erosional bases and even tops, and indicate the presence of storm currents which episodically disturbed the seafloor in distal areas. Site 118, southern region. Hammer is 32.5 cm long.

h Rapidly deposited sandstone which was loaded down into previously deposited (but only semi-lithified) fine-grained rocks. Sandstone from the overlying bed has formed balls and pillows, which are attached (or detached by tens of centimetres) to the source bed by thin necks (arrowed). Site 103, southern region. Sandstone pillow is 9 cm across.

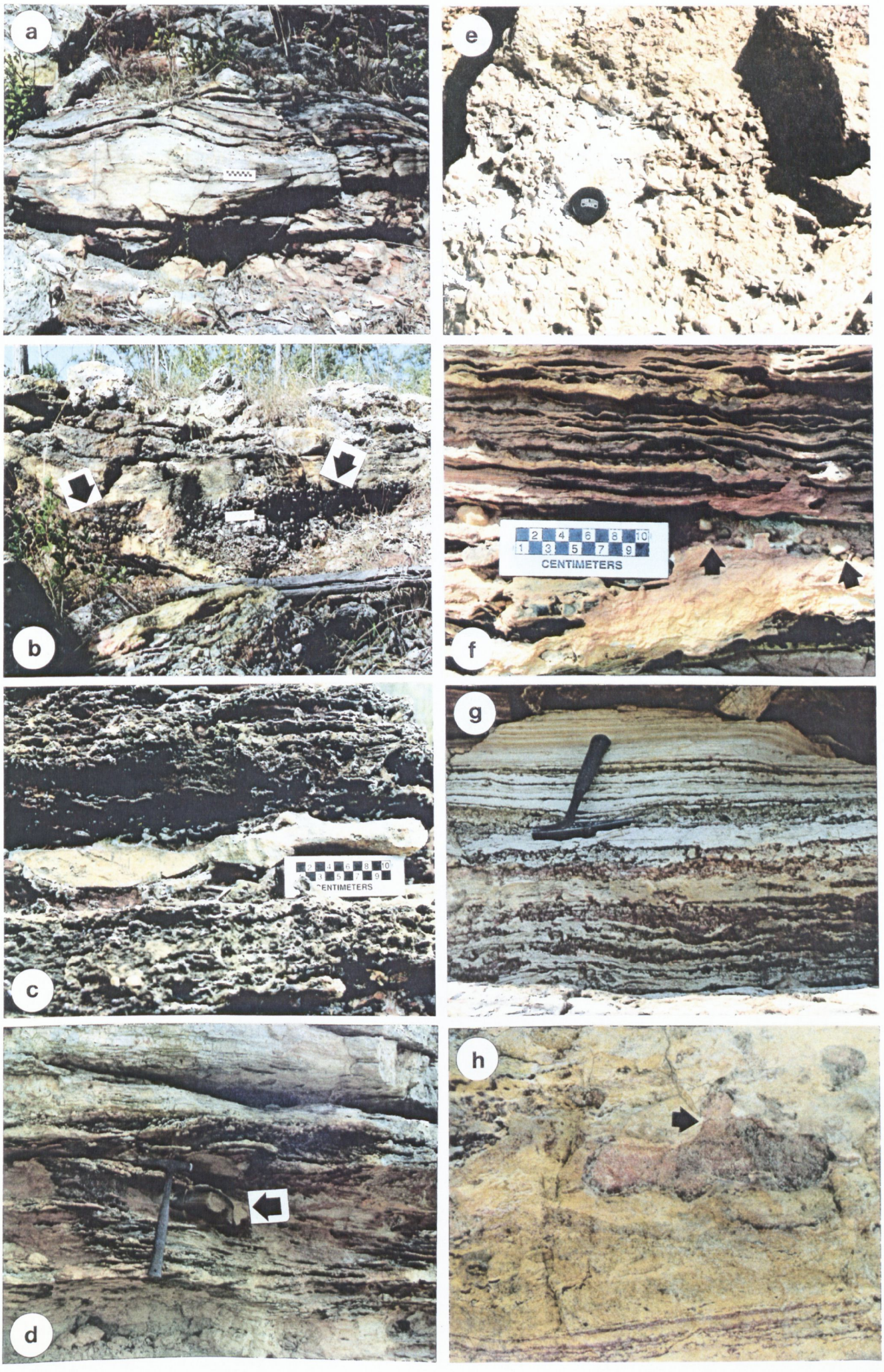
a
e
b
f
CENTIMETERS
c
g
d
h

Winter storms tend to form near the atmospheric jet stream in regions with large temperature contrasts (fronts), and the strongest temperature contrasts between air masses offer areas of greatest frequency and intensity of winter storms (Barron, 1989). The greatest temperature contrast, and hence the greatest storminess, is expected at the boundary of polar continental climate and lower-latitude oceanic conditions. The interpreted cold (to periglacial) conditions of the interior of northern Australia during some parts of the Cretaceous, particularly the Aptian, would have provided just such a temperature contrast with warmer equatorial conditions in the Cretaceous Pacific ocean. Thus, the formation of intense winter storms during the mid-Cretaceous was likely, considering the regional palaeogeography and palaeoclimate of northern Australia.

Palaeoclimate modelling shows a Pacific Ocean high pressure zone at latitude 30^0 S during the peak hurricane generation period for the mid-Cretaceous (Barron, 1989, fig. 9). This high pressure zone would have been relatively close (several hundred kilometres) to the northern marine connection with the Great Artesian Basin, and may have been responsible for large storms that affected the western epeiric shelf of the Carpentaria Basin. Increasing sea-surface temperatures from the Albian through into the Cenomanian in the northern Australian region (*cf.* Dettmann, 1981; Dettmann *et al.*, 1992) would have been ideal for hurricane generation in the mid-Cretaceous Pacific Ocean, and hurricane formation was probably substantially more frequent than at present due to the broad areas of the mid-Cretaceous oceans, their warm sea-surface temperatures, and the lower poleward temperature gradient (Barron, 1989; Duke, 1985). This should have enabled hurricanes to range into higher latitudes in the Cretaceous compared to times when global climate was similar to that of today. Documented occurrences of high-latitude hurricane-generated HCS in Cretaceous deposits (Duke, 1985) support this proposition.

Model predictions for winter storms in the southern hemisphere (Barron, 1989, fig. 10) show a winter storm belt at latitudes between 40^0 and 70^0 S, but it is poorly developed and highly zonal. However, there may have been potential for some winter storm generation just to the northeast of the northern oceanic connection of the Carpentaria Basin.

On a regional scale the Cretaceous Great Artesian Basin seaway involved a large, uninterrupted marine connection to the northwest and northeast with storm centres in the mid-Cretaceous Pacific Ocean, and the major centre of winter storminess modelled for the mid-Cretaceous is the Pacific Ocean in the northern hemisphere. It is likely that the large width of the seaway enabled storm systems to track southward into the Carpentaria Basin without impedance during intervals

of high relative sea level, particularly in Albian to Cenomanian time. However, according to Barron (1989) the record of storms for the Albian to Cenomanian is much reduced compared to storm-influenced deposits for the Campanian to Maastrichtian (at least in the northern hemisphere). He proposes that this apparent difference is due to palaeogeography, *i.e.* increased landfall of hurricanes during the Late Cretaceous, but the computer models used to estimate the 'storminess' parameter did not have much input from sedimentological data from the southern hemisphere.

The apparent reduced storminess between the different Cretaceous stages is quite possibly a function of a lack of documentation of Albian to Cenomanian aged storm deposits, rather than any real variation in storminess from mid to late Cretaceous time due to palaeoclimate or circulation. As such, the documentation of storm deposits on the Carpentaria Shelf in the present study may help to better constrain the paths of storms in the southern hemisphere during the mid-Cretaceous, but more data are needed before southern hemisphere storm tracks can be accurately documented.

10.6.3 Palaeobathymetry

There are three main lines of evidence for interpreting the palaeobathymetry of the Mullaman Bed shelf:

1) lithological data combined with preserved physical sedimentary structures;
2) microfaunal assemblages which are characteristic of particular water depths and environmental settings; and
3) trace fossils which occur commonly (but not exclusively) in certain bathymetric zones.

Wave-generated structures are common in sediments of the western marginal shelf of the Carpentaria Basin. This indicates that water depth was less than about 100 m, and probably less than 50 m during most depositional episodes. Limited lithological data (grainsize, sorting, sedimentary structures *etc.*) from stratigraphic boreholes in the onshore part of the central Carpentaria Basin (Smart *et al.*, 1980) indicate that the water depth in the depocentre was considerably greater, and probably about 150 m.

On the basis of foraminiferal evidence Haig and Lynch (1993) have suggested water depths of 150 m for the northern Carpentaria Basin, and 50-100 m for the southeastern Carpentaria Basin during maximum flooding in the late early Albian to late Albian (stage 3). Somewhat lesser water depths are envisaged for the Mullaman Bed shelf along the western and southwestern

margin of the Carpentaria Basin, probably less than 50 m in most places. The change in bathymetry during the transgressive pulse was greatest in the northern marginal basins (possibly a deepening of 100 m or more), and decreased to the southeast (about 10-20 m) where sand deposition occurred (Haig and Lynch, 1993).

All of the foraminiferal assemblages recovered from the Mullaman Beds in this study belong to the *Ammobaculites* benthonic association, which is characterised by non-calcareous agglutinated foraminifera of shallow land-locked epicontinental seas with oxygen-deficient bottom waters (Haig, 1991). Benthic assemblages belonging to the *Ammobaculites* association are represented in three biofacies defined by Haig (1979b) within the epeiric basins (Fig. 10.16): the innermost neritic *Ammobaculites australis* biofacies; inner neritic *Lingulogavelinella albiensis* biofacies; and the outer neritic *Neobulimina albertensis* biofacies (which was only developed during the Albian and was not observed within the Mullaman Beds). Foraminiferal assemblages in the upper Wallumbilla Formation in the southern Carpentaria Basin suggest water depths in the outer part of the inner neritic zone (based on the biofacies recognised by Haig, 1979b).

Trace fossils of the Mullaman Beds belong almost exclusively to the *Skolithos* and *Cruziana* ichnofacies (see chapters 3 and 4). Not surprisingly, these two ichnofacies are commonly associated with shallow-marine environments (Fig. 10.17), particularly in epicontinental seas (*e.g.* Ekdale, 1988; Pemberton and Frey, 1984; Pemberton *et al.*, 1992). The *Skolithos* ichnofacies typifies rather high-energy hydrodynamic conditions in clean winnowed sediments that are subject to abrupt erosion or deposition (Ekdale, 1988). Indeed, this is the case in the Mullaman Beds where trace fossils of the *Skolithos* ichnofacies are abundant within high-energy shallow marine deposits of facies successions 2 and 5. The *Cruziana* ichnofacies typically occurs below normal wave base (but not necessarily below storm wave base, Fig. 10.17) in environments of somewhat lower-energy hydrodynamic conditions in muddy and clean sands and silts (Ekdale, 1988). Such trace fossils and substrates exist in deposits of facies successions 1 and 4 in the Mullaman Beds.

Typical ichnofacies models (*e.g.* Seilacher, 1967 and numerous other publications) can be used broadly as a guide to conditions in marine (and in a more restricted sense in nonmarine) environments. For example, the change from the *Skolithos* to *Cruziana* to *Zoophycos* ichnofacies is commonly taken to indicate increasing water depth (from the foreshore to offshore zone) in a 'normal' shelf-slope-basin setting (Fig. 10.17). However, the predicted environmental setting of a particular ichnofacies can vary widely in a marine environment which

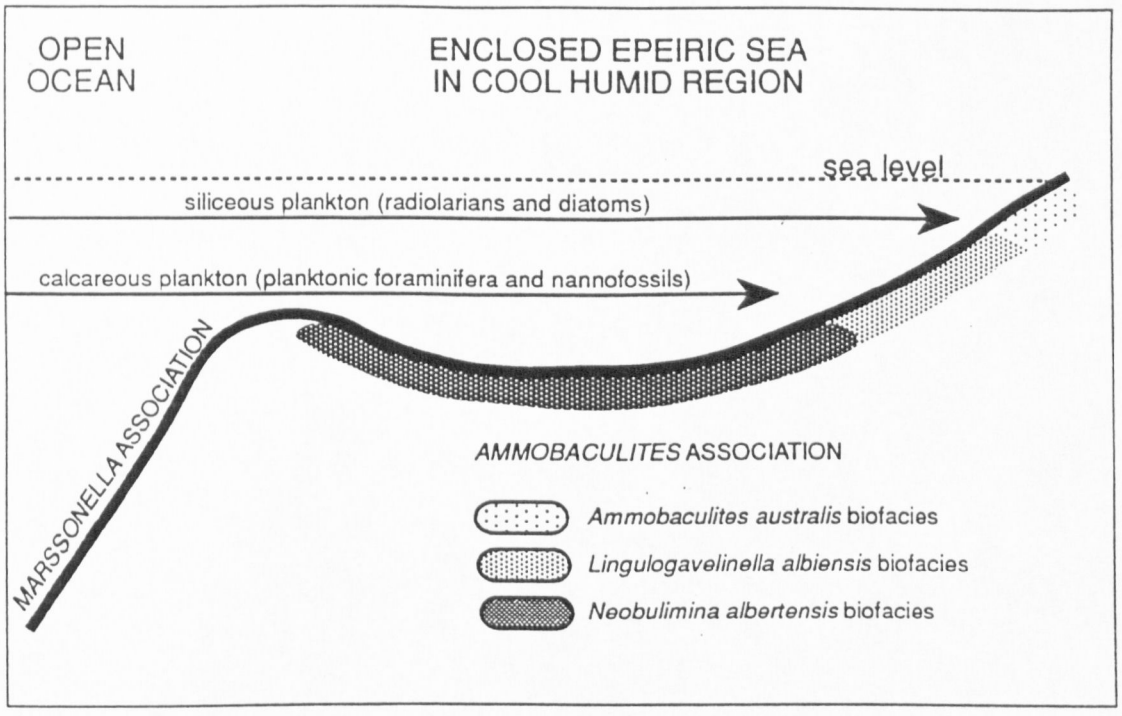

FIGURE 10.16. Biofacies model for Aptian-Albian basins of northeastern Australia (including the Carpentaria Basin). Illustrates the relative palaeobathymetry and depositional settings of *Marssonella* and *Ammobaculites* foraminiferal associations. Arenaceous foraminifera of the Mullaman Beds recovered in the present study all belong to the *Ammobaculites* association. From Haig and Lynch (1993).

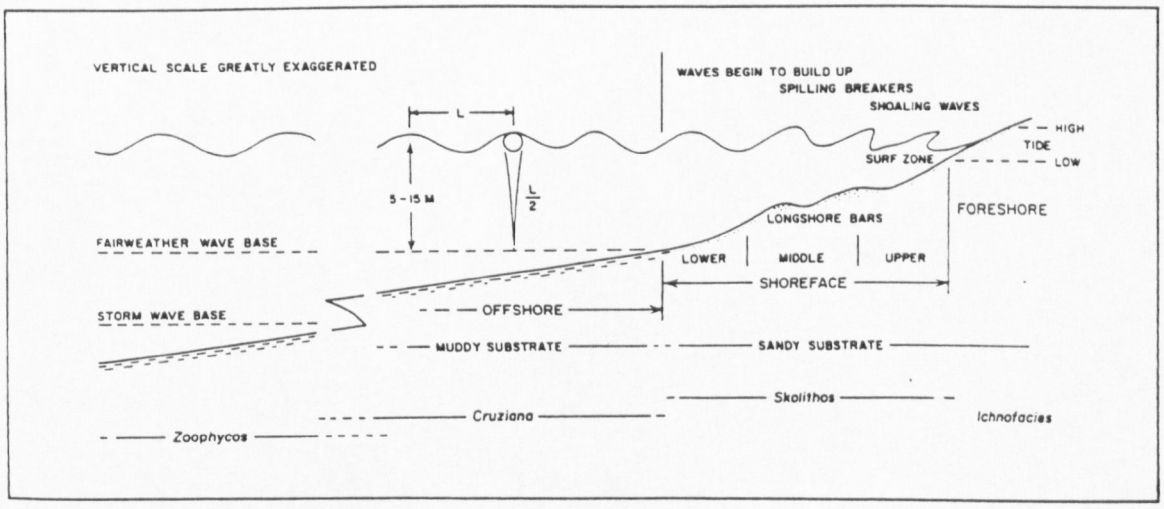

FIGURE 10.17. Typical shallow-marine profile. Locates foreshore, shoreface and offshore areas, as well as fairweather wave base and the approximate zones occupied by different ichnofacies. Fairweather waves of wavelength L cannot impinge upon the sea floor at depths greater than approximately L/2. Fairweather wave base lies at depths of about 5-15m. From Walker (1992).

is characterised by unusual or fluctuating salinity, oxygenation, substrate composition, or changes in other local factors such as turbidity and food supply (Ekdale, 1988; Pemberton *et al.*, 1992). In the case of the Mullaman Bed shelf, substrate conditions are considered to have been typical of shallow marine settings, but the degree of bottom water oxygenation varied widely between depositional episodes. A large oxygen-depleted zone existed in many parts of the basin during maximum flooding in the Albian and also during the initial transgressive pulse in the Aptian. Salinities apparently also varied over time (*cf.* Haig and Lynch, 1993).

Particular trace fossils (ichnocoenoses) can help constrain the palaeoenvironment. For example, *Diplocraterion* burrows, which occur in abundance within marine sandstones of facies succession 2 in the BPRZ, are thought to be confined to the high-energy intertidal and shallow subtidal zone (Dam, 1990; Ekdale, 1988). Similarly, *Planolites* burrows, which occur in offshore deposits of facies succession 1 and 4 in the Mullaman Beds, are characteristic of distal storm-dominated shelf deposits (Dam, 1990). However, palaeobathymetric interpretations cannot be based solely on the presence of absence of particular trace fossils, and ichnology should be linked with physical sedimentary structures and stratigraphic position in order to assess the potential water depth. In this sense, the trace fossils documented on the Carpentaria Basin shelf provide additional evidence consistent with a depth of an intertidal to inner neritic setting.

10.6.4 Sediment supply and shelf profile

During the mid-Cretaceous the depositional setting of the western Carpentaria Basin was a broad shelf with a width of more than 200 km in places, and an estimated gradient of less than one degree. The very low gradient of the shelf is extrapolated from the depositional gradient and bedding attitude of Cretaceous strata from offshore shallow seismic lines (*e.g.* Passmore *et al.*, 1992; Thomas *et al.*, 1992; Ward, 1981), and from variations in stratigraphic height of the C2 marker bed in the northern and central regions.

A very shallow, broad, gently-sloping shelf such as the western margin of the Carpentaria Basin produces a conceptual problem in terms of the rate of sediment supply across the shelf. Given a high sediment supply in such a setting, the shoreface would rapidly prograde, fill in the accommodation space available on the shelf, and potentially narrow the seaway (*cf.* Cotter, 1990). This would occur even with most rates of relative sea level rise. However, the shelf appears to have maintained a low gradient throughout the mid-Cretaceous without the formation

of many thick, regionally extensive, prograding sandbodies; *i.e.* at most times accommodation space was not filled.

There are three important reasons for this: Firstly, the low sediment supply and reworking of older sedimentary rocks is documented by the local provenance of much of the Mullaman Beds, where clear trends in the lateral extent and thickness of coarse-grained sediment wedges shed-off Proterozoic and Cambrian landmasses are apparent along the western margin of the shelf. The intense degree of bioturbation of most marine sediments also provides evidence for low sedimentation rates (except for episodic storm sedimentation) on the shelf. The low-diversity trace fossil assemblages of the Mullaman Beds, combined with the high degree of bioturbation, lead to the inference that sedimentation was slow and there was little physical reworking (*cf.* Maples and Suttner, 1990), except during storms when there was intense physical reworking and rapid deposition.

Secondly, nearly all of the sandstones (and most finer-grained rocks) on the shelf have supermature to mature compositions and mature to supermature textures. The maturity of the rocks is indicated by their high ratio of quartz + chert grains compared to feldspar + rock fragments, their negligible matrix content, their moderate to good sorting, and the subrounded to rounded nature of the grains (Plates 14 and 15; Appendix 4). This suggests that sediment delivered to the shelf was reworked extensively by shallow-marine processes, including during storms, and that rapid burial and removal (isolation) of sediment from the cycle of erosion and deposition on the shelf was uncommon.

Thirdly, subsidence appears to have been steady and slow (with little structural displacement), and was limited to gentle sagging away from basement highs (Passmore, 1979; Passmore *et al.*, 1993; Smart *et al.*, 1980). The low rate of sediment supply, the intense storm reworking of accumulated sediment, and the postulated dominance of sea level fluctuation over and above subsidence, appear to have combined to maintain the shelf as a stable feature and to keep the seaway open. Judging by the preserved sedimentary structures, the depositional surface of the shelf was maintained approximately between average storm wave base and sea level. This combination of parameters has been reported in other shallow marine shelves and ramps where the depositional gradient is very gentle (*e.g.* Cotter, 1990), and has resulted in the formation of thin, small-scale coarsening- and shallowing-upwards sequences similar to those of the Mullaman Beds.

PLATES 14 & 15

a Rounded and subrounded quartz grains within shoreface sandstone. Many of the larger grains have prominent quartz overgrowths. Smaller quartz grains tend to be more angular due to corroded and embayed margins. Opaque iron-oxide cement occurs in places between the smaller quartz grains. Sample at 25 ft depth in drillhole US Steel RR19.

b Claystone (facies 22) showing two distinct grainsize components. First is silt sized and smaller relatively well-sorted quartz grains amidst a greenish-grey clay matrix. Second is larger, corroded more angular quartz grains (towards bottom left of photo) which tend to occur in pockets or lenses. Sample AL2-18.

c Moderately sorted and packed subrounded to subangular (rarer) quartz grains within facies 12. Many grains have embayed and corroded margins and point contacts. Some grains have a thin orange coating of iron-oxide. Greenish-grey clay partly fills the larger porespaces. Sample AL2-16.

d Thin quartz lamination of fine- to medium-grained quartz grains within a clayey matrix. Nearly all of the quartz grains are highly corroded and embayed, giving an artificial angularity to the grains. The quartz-rich band is preferentially cemented or stained by isotropic iron-oxide. Sample AL4-26.

e Well sorted and well rounded moderately to tightly packed coarse quartz grains with large quartz overgrowths. The outlines of the original grains are clearly shown by hematite dust and inclusions. Small rounded heavy mineral grains occur in some larger pore spaces. Sample AL3-77.

f Iron-oxide cemented quartz arenite (facies 6) showing well rounded single quartz grains with simple extinction, and rarer, corroded, more angular quartz with undulose extinction. Sample AL3-3B.

g Coarse rounded and subrounded quartz grains with large quartz overgrowths (see arrow) and silica cement in the porespaces. Both the grains and the overgrowths are corroded in places. Very small heavy minerals are clustered in some of the larger porespaces, see top right-hand corner of photo. Sample AL3-1.

h Crudely zoned pisolites within ferricrete 2. Pisolites have irregular semi-spherical shapes, and may be hollow or have a iron-cemented core. Sample AL3-47.

---

a Thin quartz bed with normal grading; base of bed is toward base of photo. Top of bed is defined by dark clay-rich (organic-rich?) band. Sample AL3-49.

b Thin vein-like quartz-rich bands cutting across a quartz siltstone (facies 16). The quartz grains within the 'veins' are tightly packed, have long sutured contacts, and have probably been altered by local dissolution and reprecipitation of silica. The 'veins' may originally have been thin coarser-grained beds within the siltstone, or may reflect silicification of some form of biogenic lamination. Sample AL2-31B.

c Tightly packed, moderately sorted thin bed of quartz silt to fine sand sized grains within a claystone. The coarser-grained layer is preferentially stained and partly cemented by isotropic iron-oxides due to its high porosity and permeability compared to the surrounding claystone. Sample B023.

d Normally-graded quartz-rich bed within thinly interbedded rocks of facies 15. Note the decrease in grain size towards the top of the photo, and the concentration of flat, platy mica fragments near the top of the graded bed (upper arrow). The bed has a sharp based (lower arrow). Sample AL4-8.

e & f Fragmented and weathered feldspar laths (arrowed in plate e) surrounded by yellowish zones of sericitic alteration. Other weathered feldspar laths are visible near the bottom edge of plate e. Sample at 36.5 ft in US Steel drillhole RR22, and sample AL4-67 respectively.

g Tightly packed well sorted subrounded medium quartz grains with grain to grain contacts in facies 10 sandstone. Many grains have undergone minor dissolution as evidenced by their corroded and embayed margins. Sample AL2-6.

h Rounded, moderately to well sorted, loosely packed medium quartz sand grains with simple extinction and thin coatings of iron-oxides. This type of fabric is typically of many proximal marine facies of the Mullaman Beds. Sample AL3-42.

Width of view for photomicrographs in Plate 14 and 15a,c,d,e, g,and h is 2.6 mm.
Width of view for photomicrographs 15b and f is 1.25 mm.
Photomicrographs 14b and 15a, b, and g show view with crossed-polars, all others are plane polarised.

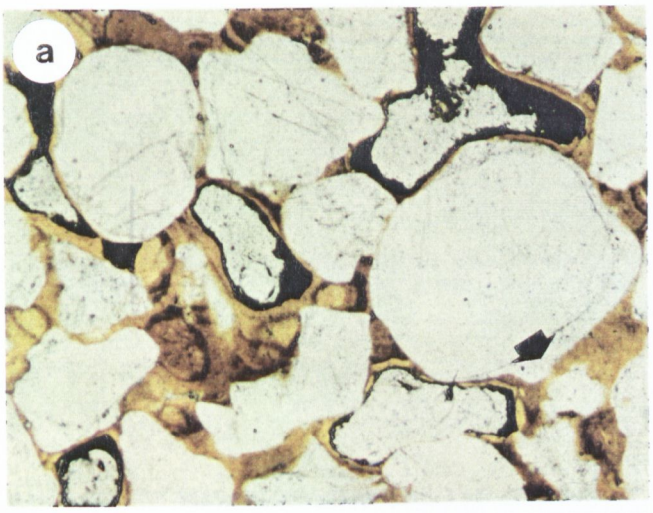
a

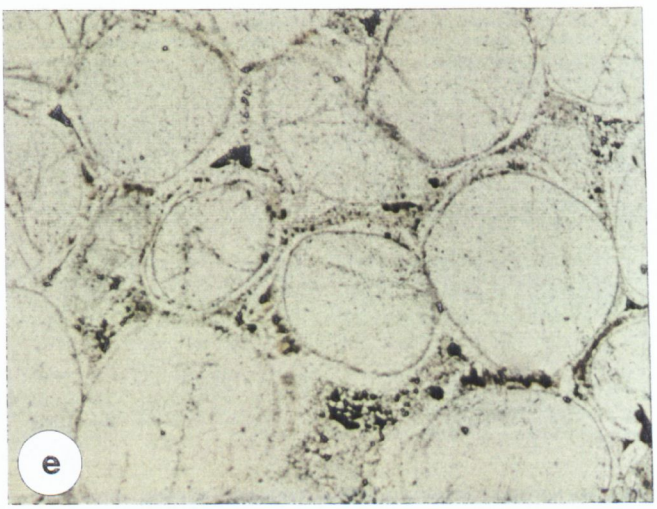
e

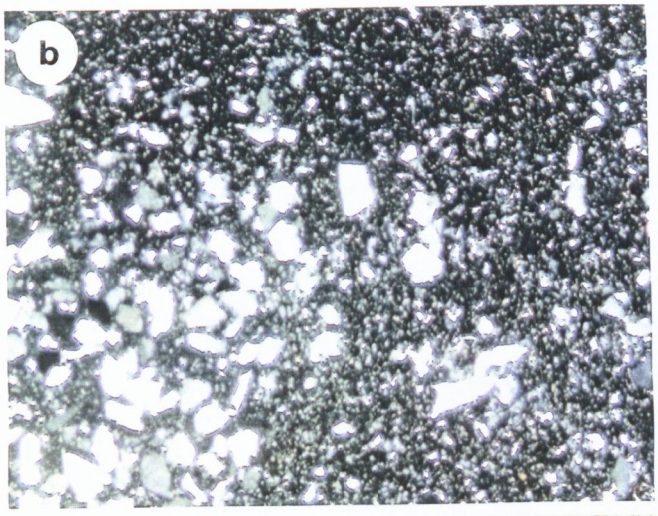
b

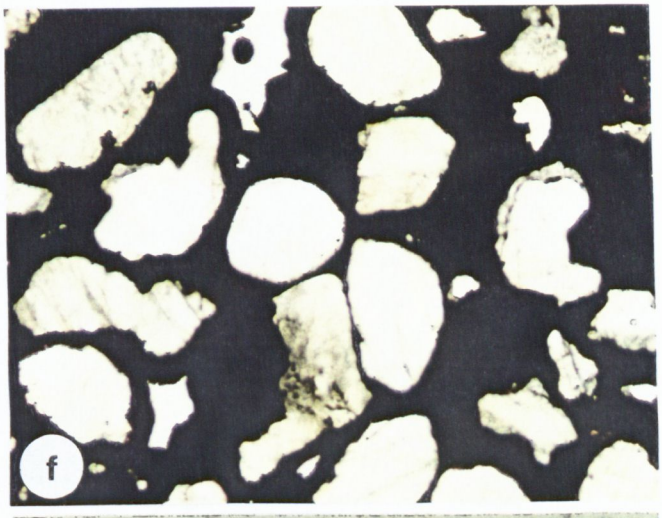
f

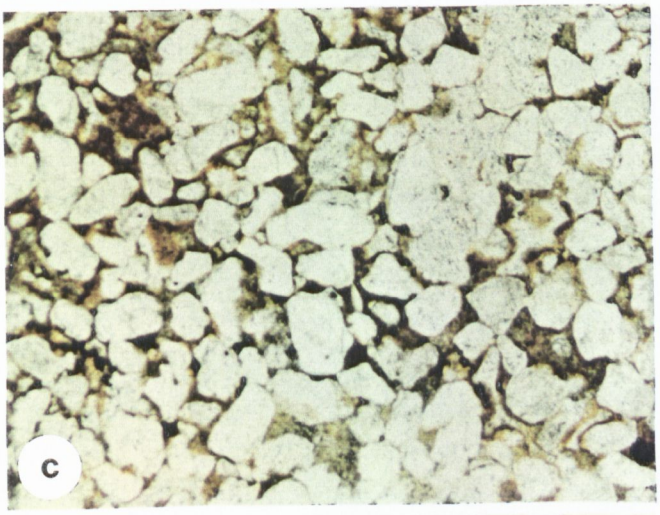
c

g

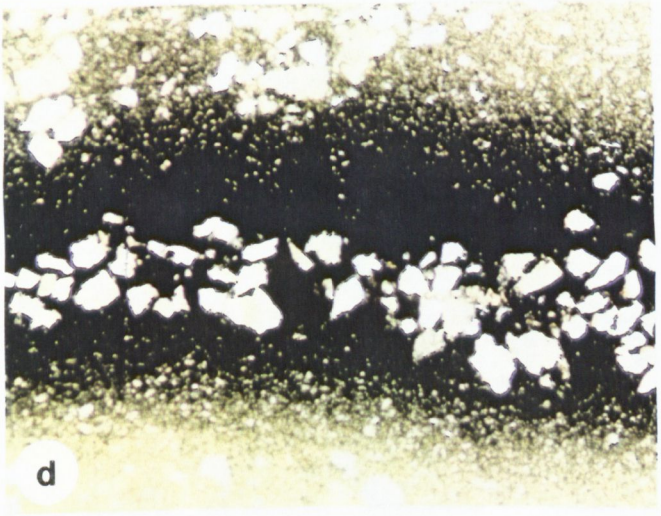
d

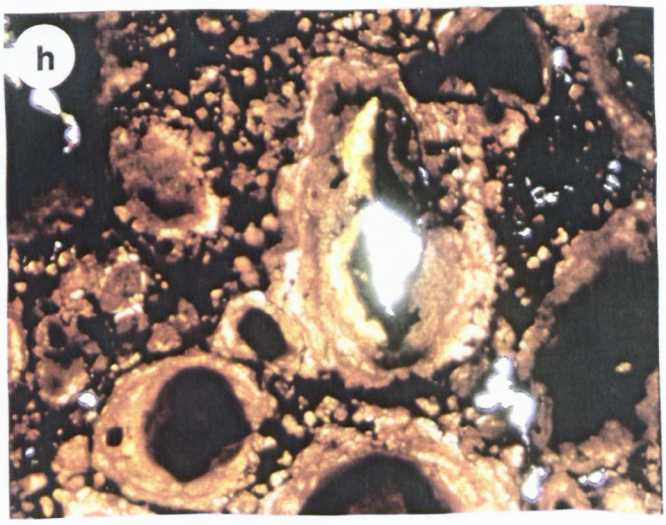
h

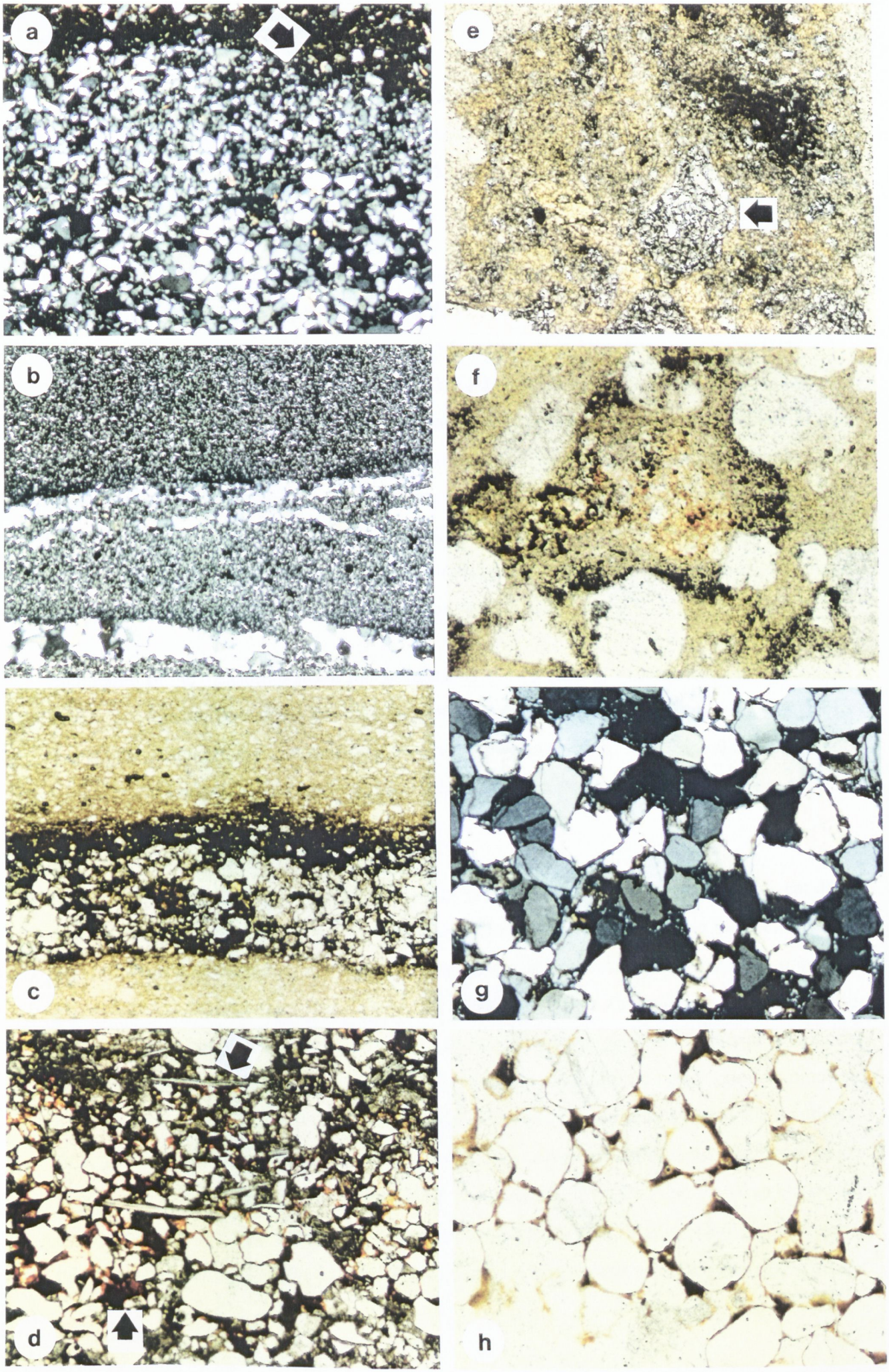
a
e
b
f
c
g
d
h

10.6.5 Palaeocurrents

Due to the regional scope of the study and the large distances between outcrops there is a general lack of closely-spaced palaeocurrent data. Summaries of the pertinent palaeocurrent data are presented in this section and are linked to the regional stratigraphic framework for the Carpentaria Basin shelf.

Given the limitations in the type of outcrop exposure (and hence palaeocurrent data), particularly for rocks of stages 2 and 6 which were deposited during minor transgressions, detailed palaeocurrent analysis is presented only for times of major marine inundation (stages 3-5); some palaeocurrent measurements were also taken from rocks of Sequence *IA* (stage 1), which were deposited during initial mid-Cretaceous transgression. Palaeocurrent indicators are not present in equal abundance on all parts of the shelf. The northern region provides the bulk of palaeocurrent data because measurable current and wave indicators are most common and best preserved within the coarse-grained, shallow-marine rocks in this region. Farther offshore, particularly in the southern region, reliable palaeocurrent indicators such as tool marks and planar crossbedding are rare within offshore marine rocks.

Summaries of the measurements of the orientations of sedimentary structures and the associated estimates of palaeoflow directions for rocks of the various stages are presented in Figs. 10.18 and 10.19. Although the data coverage is restricted, palaeocurrent directions show systematic variation and are considered to reflect the regional circulation patterns on the western shelf of the Carpentaria Basin.

Marine and deltaic rocks of Sequence *III* (stage 3) yield the most abundant palaeocurrent data. Marine cross-bedding within these rocks indicates dominant palaeoflow along the shelf towards the southwest approximately parallel to the regional palaeoshoreline, with a smaller opposing palaeoflow towards the northeast (Fig. 10.18c). The southwest directed flow is considered to indicate the direction of wave approach, and probably also corresponds to the direction of storm approach (see later discussion of gutter orientations). The plot of ripple cross-lamination palaeocurrent directions similarly shows a significant part of the flow towards the southwest (Fig. 10.18e). However, there is a major palaeoflow component towards the northwest which may be due to refraction of wave-trains close to the palaeoshoreline (Fig. 10.8), as evidenced by the orientation of near-shore grooves and gutters (Fig. 10.18a). Such a relationship between the palaeocurrent orientation of large-scale cross-bedding *versus* smaller-scale ripple cross-

Palaeocurrent plots for shallow marine rocks of Sequence III (STAGE 3)

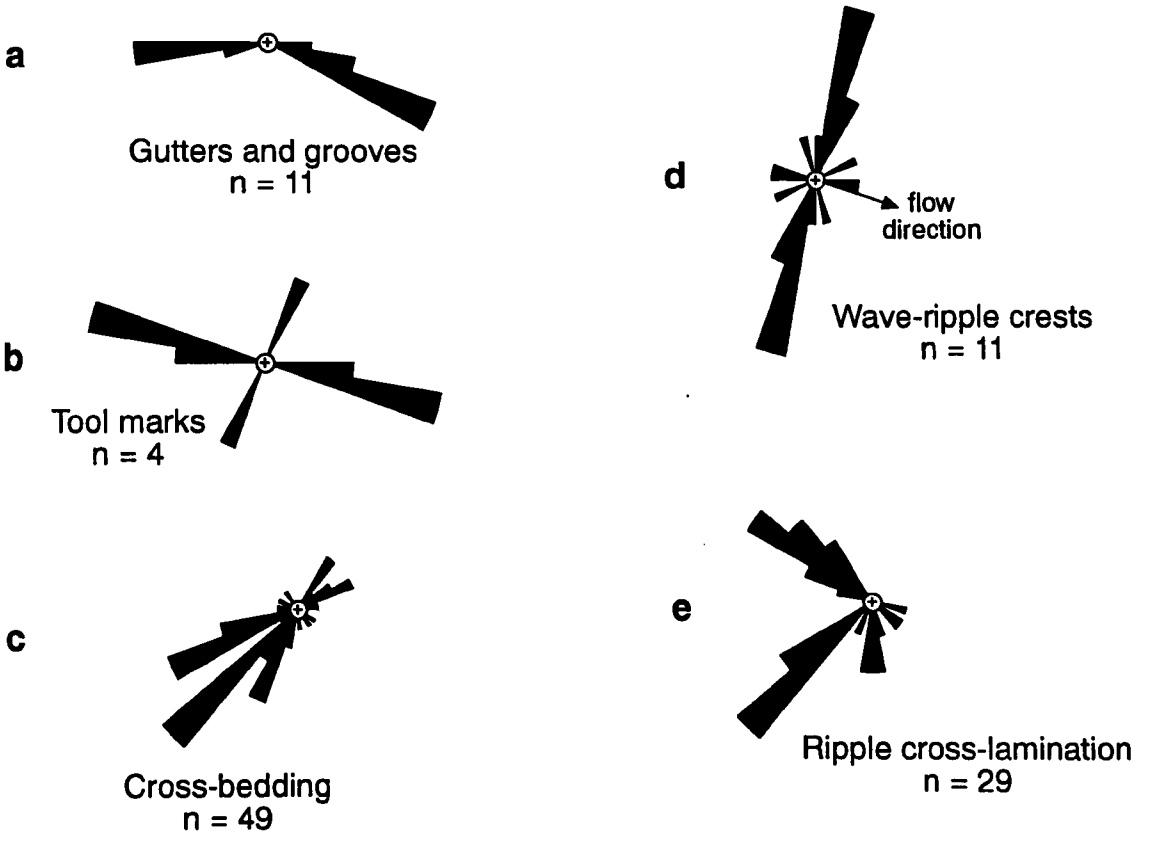

Palaeocurrent plots for deltaic-marine rocks of Sequence III (STAGE 3)

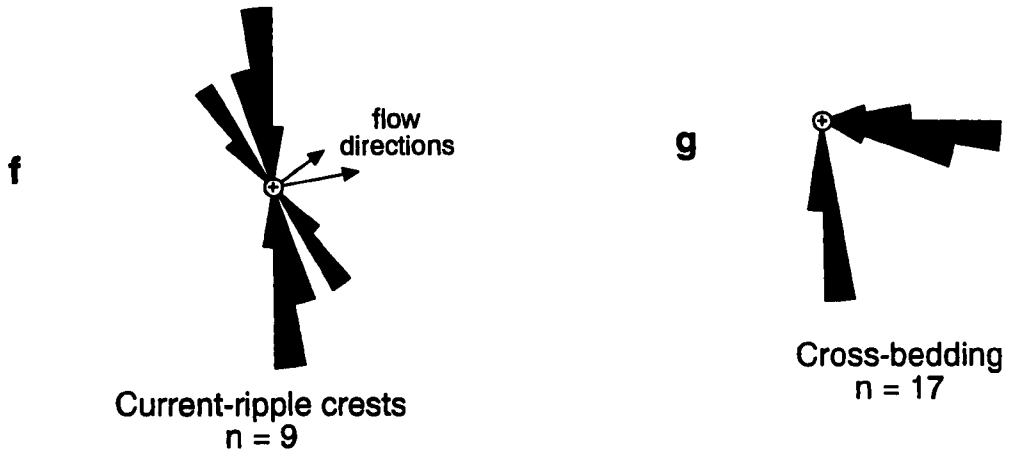

FIGURE 10.18. Measurements of the orientation of sedimentary structures and associated palaeocurrent directions within shallow-marine and deltaic-marine rocks which accumulated during stage 3 (late early Albian to middle Albian). The data are grouped as measurements from different types of sedimentary structures, which each record components of the palaeoflow. Refer to text (Sects. 10.6.5 and 10.6.6) for discussion. North is toward the top of the page for all plots.

lamination has been previously assigned to refraction of wave-trains in other shallow-marine settings (*e.g.* Plint and Norris, 1991).

Indicators of smaller and lower-energy flows (*e.g.* ripple cross-lamination) also record offshore palaeoflow oblique or perpendicular to the palaeoshoreline (towards the south and southeast, Fig. 10.18e), which may be related to waning storm circulation. Similar offshore-directed palaeoflow towards the east-southeast is evidenced by internal stratification of storm-generated coarse-grained wave-ripples (megaripples), whose crests are aligned predominantly parallel to the palaeoshoreline (Fig. 10.18d). Tool markings in HCS beds and associated gutters within rocks of Sequence *III* show offshore palaeocurrent directions, normally to the east-southeast, but to the west for palaeoembayments with an eastern barrier (Fig. 10.18a and b).

Palaeocurrent directions for deltaic-marine rocks of Sequence *III* are related to, but differ from, palaeoflow in fully-marine rocks of the same sequence. Cross-bedding within deltaic facies succession 6 indicates a strong bipolarity in the palaeoflow (Fig. 10.18g). The main palaeoflow is interpreted to indicate easterly progradation of most deltaic deposits on the shelf, whilst palaeoflow towards the south is related to peculiar progradation in the northern end of the Bath and Parsons Ranges embayment. Current ripples occurring towards the top of the deltaic deposits are oriented with their crests trending north-south or northwest-southeast (Fig. 10.18f). Asymmetry within some of these current ripples (shown by the arrows on Fig. 10.18f) indicates unidirectional flow mainly to the east, with lesser flows to the northeast.

Figure 10.19b shows the major direction of fluvial transport for rocks of Sequence *IA* (stage 1) at the base of the Cretaceous sequence. The plot is almost unimodal and indicates fluvial transport (and palaeoslope) broadly towards the east-southeast to southeast (Fig. 10.4). Overlying transgressive deposits of Sequence *IA*, which form part of the fill of the Walker River incised valley, contain marine cross bedding indicating palaeocurrent directions towards the west-northwest and north-northwest (Fig. 10.19a), and a minor offshore component to the southeast. The north-northwest palaeoflow is interpreted to reflect the more northerly directed transgression which occurred within the confines of the Bath and Parsons Range embayment.

There is only a limited amount of palaeocurrent data available for Sequence *IV* (stage 4), and most palaeocurrent measurements were taken from large to medium scale planar cross-bedding near the base of facies succession 5. The plot of these data shows a moderate spread in palaeoflow direction, but the dominant component is towards the west and southwest (Fig. 10.19c). This is similar to the palaeocurrent plot for marine cross-bedding within Sequence *III*

Palaeocurrent plots for rocks of Sequence IA (STAGE 1)

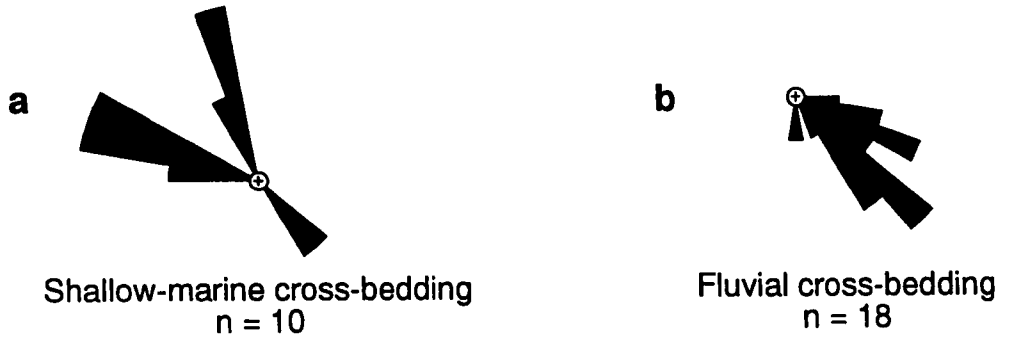

Palaeocurrent plot for shallow-marine rocks of Sequence IV (STAGE 4)

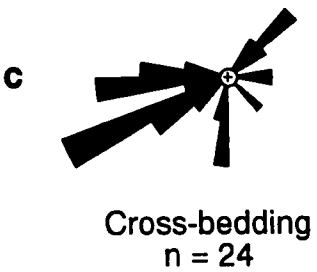

Palaeocurrent plots for rocks of Sequence V (STAGE 5)

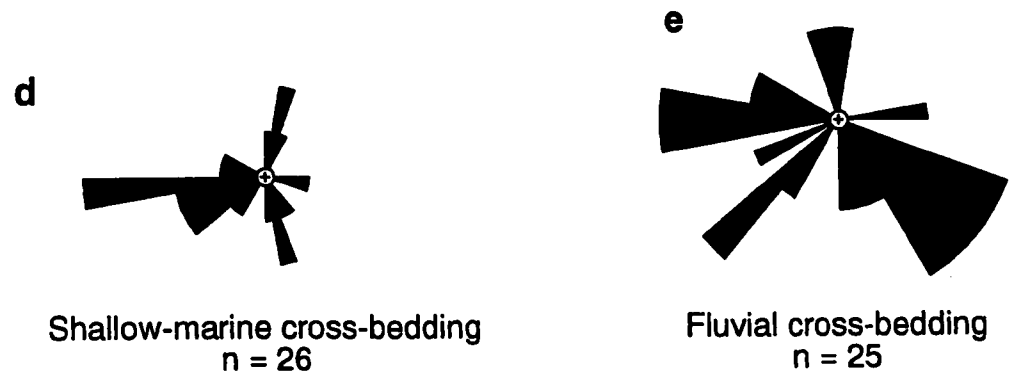

FIGURE 10.19. Measurements of the orientation of sedimentary structures and associated palaeocurrent directions within shallow-marine and fluvial rocks which accumulated during stage 1 (Aptian), stage 4 (late Albian to latest Albian), and stage 5 (?early Cenomanian). The data are grouped as measurements from different types of sedimentary structures, which each record components of the palaeoflow. Refer to text (Sects. 10.6.5 and 10.6.6) for discussion. North is toward the top of the page for all plots

(stage 3), and the southwesterly palaeoflow is similarly interpreted to indicate that wave approach was from the northeast, and that shelf-currents generally were directed along-shore or oblique-to-shore towards the southwest (Fig. 10.8). The presence of a smaller but consistent opposing palaeoflow towards the northeast along the shelf (Fig. 10.19c) during stage 4 is almost identical in orientation to the palaeocurrent plot for stage 3 (Fig. 10.18c).

Evidence for wave approach from the northeast also occurs in offshore rocks of the central and southern regions, which were deposited tens of kilometres to over a hundred kilometres from the palaeoshoreline. Here isolated unidirectional scours and minor, small-scale cross-bedding (not shown on palaeocurrent plots) indicate that the direction of wave approach was roughly from the northeast to east-northeast.

Cross-bedding within marine facies succession 4 and restricted marine facies succession 8 of Sequence *V* (stage 5) indicates dominantly westerly directed palaeoflow (Fig. 10.19d). This is similar to the palaeoflow during high sea level in stages 3 and 4, but during stage 5 the palaeoflow was directed slightly more towards the west. Again there was a smaller opposing palaeoflow to the north-northeast along the shelf parallel to the palaeoshoreline, and some palaeoflow was directed obliquely offshore to the east and south (Fig. 10.19d).

The record of fluvial palaeocurrents for stage 5 (Sequence *V*) was obtained mostly by measurement of large-scale planar and trough cross-bedding in deposits of facies succession 7 in the ALZ and the BPRZ. The plot of these palaeocurrent data shows a large spread in palaeoflow directions (probably due to high sinuosity of the fluvial channels), but there are two major orientations (Fig. 10.19c). The main palaeoflow (and the palaeoslope) are directed to the southeast and east-southeast, but significant palaeoflow within fluvial channels also occurred towards the west (Fig. 10.19e). Westerly-directed palaeocurrent indicators are interpreted as showing the major drainage divide on the coastal and alluvial plains, as fluvial channels drained towards the west on the western side of large highstanding north-northeast to south-southwest trending basement ridges. The other palaeoflow directions on this plot probably indicate subordinate channel axes surrounding local basement highs, but given enough channel length to diverge around basement highs, most fluvial systems would have drained down the palaeoslope towards the east-southeast and southeast.

10.6.6 Regional palaeoflow and shelf circulation

Palaeocurrent directions above indicating along-shore or slightly oblique-to-shore palaeoflow, mostly towards the south and southwest, were probably formed by long-term, time-averaged flow reflecting the net along-shore transport direction. In contrast, tool markings, gutter casts, grooves, and internal stratification of coarse-grained megaripples were likely to have been formed by offshore-directed instantaneous bed shear stresses during peak storm conditions (*e.g.* Duke *et al.*, 1991). This type of relationship where gutters, gutter casts, parting lineation, and tool marks are all oriented approximately offshore and perpendicular to the palaeoshoreline has been well documented in other shallow-marine storm-dominated settings (*e.g.* Dott and Bourgeois, 1982; Leckie, 1988; Leckie and Krystinik, 1989; Plint and Norris, 1991). In these studies it was also recognised that most wave-ripple crests and megaripple crests are oriented nearly parallel to the palaeoshoreline, and that their internal stratification is typically directed perpendicularly offshore.

The relationship of 'normal' cross-bedding palaeocurrent directions to other palaeocurrent trends is less unique, and depends largely on the palaeogeographical setting, the nature of winds and tides, and the direction of geostrophic flow. In the case of the Mullaman Bed shelf it appears that the palaeoflow was typically along-shore towards the south or southwest on the western side of the Carpentaria Basin, and that smaller or less frequent (?) opposing palaeoflow occurred along-shore towards the northeast (Figs. 10.8, 10.10, and 10.12).

It is interesting here to consider the high southerly Cretaceous palaeolatitude of the Mullaman Bed shelf in view of the fact that the strength of the Coriolis force increases with increasing latitude (Open University Course Team, 1989, p. 32). The theory of shelf circulation with regard to the Coriolis force is as follows; during storms a coastal set-up is created; that is, positive elevation of the water surface towards the land as water is 'piled up'. This induces a *seaward* pressure gradient, which in turn produces an *offshore* flow (pressure relaxation flow). This offshore-directed flow is then deflected due to the Coriolis force (deflected to the left in the southern hemisphere) and evolves into a geostrophic flow.

In the case of the western shelf of the Carpentaria Basin, one would have expected the Coriolis force to have deflected an offshore pressure-relaxation flow to the left, resulting in a northeast directed geostrophic current. However, most inner shelf palaeocurrent indicators show that the dominant current on the shelf was towards the southwest and there is only a minor (although consistent) northeast palaeoflow indicated by some crossbedding (Figs. 10.18c and 10.19c).

This subordinate palaeoflow to the northeast may have been a weak geostrophic current created after storms, but it appears either that the circulation pattern on the western shelf of the Carpentaria Basin was not dominated by geostrophic currents, or that the record of such currents is not preserved in high-energy shelf environments, as suggested by study of other shelf settings (Leckie and Krystinik, 1989).

At most times (between storms) when the coastal set-up was negligible, the dominant current on the western shelf was apparently a wave-driven longshore flow towards the southwest in response to wave approach from the northeast (Fig. 10.8). At times of shore-parallel winds the dominant ocean current would have been obliquely-onshore or obliquely-offshore (depending on the direction of the wind), and may explain minor cross-bedding and ripple cross-lamination palaeocurrent trends at variance with the direction of the main wind-driven longshore flow and geostrophic flow. Stages 3-5 (possibly also stage 1) represent the times of major marine inundation along the western and southwestern margins of the Gulf of Carpentaria, and it is considered likely that circulation patterns during these stages are similar to those which existed for most times of transgression and highstand in the Carpentaria Basin throughout the mid-Cretaceous.

Supporting evidence for southerly (or southwesterly) directed regional palaeoflow on the Mullaman Bed shelf is documented by regional analysis of sedimentary facies of the Carpentaria and Eromanga Basins for the middle to late Albian (Ozimic, 1986, fig. 9), which shows a regional north to south bottom flow along the western shelf of the Carpentaria Basin. This flow presumably would have trended slightly to the west of south in the northern part of the shelf where the palaeoshoreline also trends west of south. Similarly, computer modelling of the mid-Cretaceous by Barron and Peterson (1990) predicts consistent counter-clockwise surface circulation in the Cretaceous Pacific Ocean to the north of the Carpentaria Basin; within the confines of the Carpentaria sea such counter-clockwise circulation would have produced southwesterly directed palaeoflow along the western shelf, in accordance with the palaeocurrent trends documented in this thesis. In an apparently opposing view, Haig and Lynch (1993) propose that palaeoflow in the Great Artesian Basin occurred towards the south along the eastern margins of the Great Artesian Basin seaway, changing to a southwesterly palaeoflow in the southern part of the seaway. However, these authors do not describe any palaeoflow trends for the western shelf.

The circulation models of Ozimic (1986) and Haig and Lynch (1993) are based largely on data from the Eromanga Basin and the eastern margin of the Carpentaria Basin, and they do not give

a detailed account of potential circulation patterns along the western Carpentaria Shelf. Palaeocurrent data in this thesis are seemingly more compatible with Ozimic's circulation pattern which is supported by Barron and Peterson's computer modelling, although palaeocurrent trends documented in this thesis do not contradict Haig and Lynch's model, so long as it does not require northerly-dominant return flows along the western margin of the epeiric seaway.

Qualitative support for significant shore-parallel palaeoflows on the Carpentaria Basin shelf comes from computer modelling of circulation patterns in the analogous setting of the Western Interior Seaway of North America. Ericksen and Slingerland (1990) suggest that wind-driven and storm-driven circulation in large epeiric seas was largely controlled by coastline-constrained currents flowing parallel to the shoreline, and that such circulation was not greatly affected by Coriolis forces (at least not in North America). This might explain the apparently weak geostrophic palaeoflow in the western Carpentaria Basin.

10.6.7 Cretaceous Oceanic Anoxic Events: Links to Carpentaria Basin stagnation and anoxia during the Albian (stage 3)?

The Cretaceous Period is characterised by unusually widespread distribution of black shales in both deep- and shallow-marine settings. Stratigraphic studies over the last 20 years, especially since the beginning of the Deep Sea Drilling Project, have indicated that the times of globally important organic-carbon burial (Oceanic Anoxic Events, OAEs) in the Cretaceous include the Aptian-Albian, the Cenomanian-Turonian boundary, and the Coniacian-Santonian (Jenkyns, 1980). Of particular interest in the present study are Aptian-Albian OAEs numbered 1A to 1C, which are prominent in the northern hemisphere (Arthur *et al.*, 1990).

The temporal variation in $\delta^{13}C$ in connection with OAEs has been well documented (Scholle and Arthur, 1980), and global correlation of organic carbon-rich stratigraphic levels and $\delta^{13}C$ spikes to within a few 100 ka is possible (Arthur *et al.*, 1990). However, data on the variation of carbon isotope values through time in the mid-Cretaceous invariably centres on data from the northern hemisphere (*cf.* Weissert, 1989). The only stratigraphic sequences outside Europe and America which are thought to contain a widespread late Albian "oceanic anoxic subevent" (OASE) are the Toolebuc Formation in the Carpentaria and Eromanga Basins of Australia, and unnamed rocks drilled on the Hess Rise (DSDP Sites 465 and 466) (Arthur *et al.*, 1990).

The Carpentaria-Eromanga occurrences of black shales represent the extreme southern palaeolatitudinal extent of organic-carbon rich rocks, and are important in a global context for an

understanding of the distribution, timing and nature of OAEs. However, it is not yet possible to determine whether the accumulation of Cretaceous organic-rich deposits in the northern hemisphere (*e.g.* Scisti A Fucoidi and Scaglia Bianca Formations of northern Italy; Erba and Premoli-Silva, 1992), was synchronous with accumulation of the organic-rich Toolebuc Formation or other similarly-aged organic-rich rocks on the western shelf of the Carpentaria Basin, *i.e.* rocks of facies succession 1 in Sequence *III*. Studies to resolve this problem are beyond the scope of this thesis, but the world-wide nature of such OAEs is intriguing to consider in relation to the presence of organic-rich Aptian and Albian aged rocks of the Mullaman Beds as documented in this thesis (see below).

During high sea level and stillstand, particularly in stage 3 (late early to middle Albian), there was diminished circulation in the central and southern parts of the Carpentaria Basin (Fig. 10.8). This weak circulation led to stagnation and oxygen-poor conditions towards the bottom of the water column, and these conditions may have been enhanced by a slight salinity gradient (more brackish to the south) as described by Haig and Lynch (1993). Similar conditions probably existed on the distal parts of the Mullaman Bed shelf, and are thought to have been prominent locally in the formation of sedimentary ore deposits on Groote Eylandt. There, oxygen deficiency in the water column was a precursor to concentration of dissolved manganese species in the water column and their subsequent precipitation upon oxygenation concurrent with regression (*cf.* Frakes and Bolton, 1984). Preliminary investigations of an Aptian-aged (stage 1) deep-water marine sequence similar to facies succession 1 in recent drillholes on the shelf also indicate dysaerobic to anaerobic bottom water conditions and abnormally high salinities during the initial Aptian transgressive pulse (unpublished data, H. Barents, pers. comm. 1994).

Primary field evidence for oxygen-poor conditions in the Carpentaria Basin are the dark colouration, high organic content (Alley, 1991), and presence of pyrite (now generally weathered to gypsum) in muddy offshore rocks of facies succession 1 (stage 3) in the central and southern areas. The obvious lack of carbonate within these rocks also implies that basin waters were depleted in oxygen (*cf.* Jewell, 1993). The highly organic-rich nature of late middle to earliest late Albian (stage 3) Toolebuc Formation in the basin centre strongly suggests that stagnant, oxygen-poor conditions existed (at least in bottom water) throughout much of the basin at this time.

Additional evidence for oxygen-deficient waters is suggested by the peculiar low-diversity, non-calcareous nature of benthonic foraminifera within offshore rocks of facies succession 1 on

the distal shelf, and elsewhere in the basin. According to Haig and Lynch (1993) these microfossil assemblages indicate that waters of the Great Artesian Basin sea (including the Carpentaria Basin) were hyposaline (slightly brackish in places) and cool, with dysaerobic to anaerobic bottom waters in quiet areas overlying mud substrates (*e.g.* the conditions envisaged for accumulation of facies successions 1 and 4).

Another factor that may have been important in forming dark coloured organic-rich sediments is high productivity in the euphotic zone. High productivity has the potential to increase the amount of organic-rich detritus accumulating on the sea floor in addition to causing oxygen deficiency due to high oxygen consumption by abundant organisms. Pederson and Calvert (1990) suggest that this mechanism may account for the production of black shales in many Cretaceous deposits, especially where vigorous thermohaline circulation is predicted and thus a stratified water column due to sluggish circulation is unlikely as the cause of anoxia. However, in the intracratonic setting of the Carpentaria Basin the palaeogeography would have promoted reduced circulation in embayments during high sea level, and a stratified water column is considered as the most likely cause of significant oxygen depletion or anoxia at the sea floor and the base of the water column.

The evidence for a stratified water column in the Carpentaria Basin during periods of high sea level in the mid-Cretaceous is seemingly at odds with the evidence for significant wind- and wave-generated circulation, particularly when related to large storms. However, Jewell (1993) has shown that for much of the depositional history of the analogous Western Interior Seaway of North America, wind-driven and even storm-driven circulation was ineffective in destroying any stratification that developed during periods of high sea level and stillstand. A similar situation is envisaged for the Carpentaria Basin.

10.7 SHALLOW-MARINE DEPOSITIONAL SYSTEMS

A depositional system is defined as "a three dimensional assemblage of lithofacies, genetically linked by active or inferred processes and environments" (Posamentier *et al.*, 1988, p. 110). The term is designed to incorporate various depositional environments and their active (characteristic) processes. Implicit within the description of depositional environments and the correlation of facies successions in chapters 5, 6, and 7 is an understanding of depositional systems on the Carpentaria Basin shelf. That is, detailed lateral correlation of the vertical facies successions in previous chapters provides a three dimensional view of the rock relationships on

the shelf, and the accompanying interpretation of depositional environments identifies the characteristic processes of the depositional systems.

The remainder of this chapter concentrates on the two major shallow-marine depositional systems on the shelf because rocks of these systems comprise by far the largest part of the preserved shelf sequence. The geographical positions of preserved outcrops of the main shallow-marine depositional systems on the shelf are summarised in Table 10.3, along with their descriptive titles and component facies successions. The genetic links within each system and their main characteristics are summarised in Table 10.4.

The elements of a typical shallow-marine profile are illustrated in Fig. 10.17, and the distribution of Mullaman Bed facies in such a setting is shown in Fig. 10.20. The vertical stacking patterns of these facies is illustrated in Figs. 10.21 and 10.22, and is discussed in the following sections.

TABLE 10.3: Shallow-marine depositional systems on the shelf.

Depositional Systems	Palaeogeographical position on the shelf	Components
Coarsening- & shoaling-upwards	Proximal (BPRZ, central region) =	FS 2
storm-(and wave-) dominated	Intermediate (basal units in ALZ / southern region) =	FS 1 / FS 2
offshore to shoreface	Distal (central & southern regions) =	FS 1
Fining- & deepening-upwards	Proximal (ALZ, BPRZ) =	FS 5
storm-(and wave-) dominated	Intermediate (proximal part of central region) =	FS 5 / FS 4
foreshore to offshore	Distal (distal central region & southern region) =	FS 4

Evidence for the stratigraphic equivalence and genetic links of contemporaneous facies successions which are grouped to form each depositional system is presented in Sects. 8.3 and 8.6, and is illustrated by detailed stratigraphic correlation diagrams (chapters 5-7) and the stratigraphic framework (Figs. 8.2 and 8.7). All these genetic links of depositional environments and facies successions are further reinforced by sequence stratigraphic analysis in chapter 9 (see Figs. 9.1 and 9.2) because, by definition, each systems tract recognised in chapter 9 is "a linkage of contemporaneous depositional systems" (Posamentier *et al.*, 1988, p. 110).

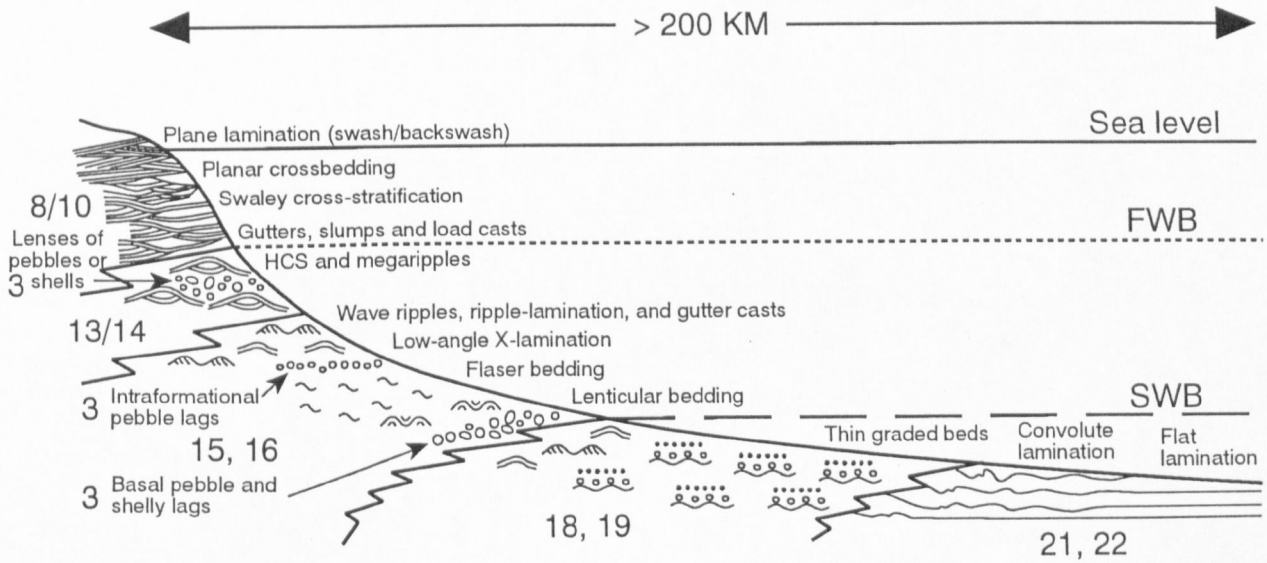

3,8,10,13,14,15,16,18,19,21,22 = Storm-influenced facies of the Mullaman Beds

3 Conglomeratic and shelly lags
8 Planar, swaley, and trough cross-stratified sandstone
10 Bioturbated clayey sandstone
13 Bioturbated silty sandstone
14 Hummocky cross-stratified sandstone
15 Interbedded sandstone and siltstone
16 Thinly-bedded graded sandstone and siltstone
18 Laminated clayey siltstone and sandy siltstone
19 Weakly bioturbated laminated siltstone
21 Intensely bioturbated siltstone
22 Silty claystone

Planar cross-bedding
Swaley cross-stratification
Hummocky X-stratification
Wave-ripple lamination
Micro-hummocky beds
Flaser bedding
Lenticular bedding
Thin graded beds
Convolute lamination
Flat lamination

FIGURE 10.20. Schematic shelf profile illustrating the relative position of facies and their characteristic sedimentary structures in a shallow-marine storm- (and wave-) dominated depositional system; in this case, a prograding coarsening- and shoaling-upwards system. FWB = fair-weather wave base. SWB = storm wave base.

TABLE 10.4: Rock type/processes within shallow-marine depositional systems on the shelf.

Depositional System	Genetic linkages of facies successions across varying depositional sites on the shelf: Proximal	to Intermediate	to Distal	Processes & depositional settings
Coarsening- and shoaling-upwards shallow -marine	coarse-grained blocky to massive cross-bedded and planar laminated bioturbated sparsely fossiliferous sandstones (FS 2)	finer-grained coarsening-upward bioturbated cross-bedded / HCS fossiliferous sandstones with intraformational lags (FS 2 / 1)	intensely bioturbated dark-coloured coarsening- and thickening upwards interbedded siltstone and sandstone with thin graded beds (FS 1)	aggradation and formation of sandier -upward cycles, followed by progradation
Fining- and deepening-upwards shallow -marine	coarse-grained planar laminated, trough cross-bedded / SCS sandstone with basal conglomeratic lags (FS 5)	slightly finer-grained fining-upward bioturbated fossiliferous cross-bedded/HCS silty sandstone (FS 5 / 4)	finer-grained intensely bioturbated slightly fining-upward sandy siltstone with minor X-bedding (FS 4)	progressive drowning and retrogradation of the shoreface

10.8 DEPOSITIONAL MODEL

10.8.1 Introduction

This section is subdivided into 3 main parts. The first part is an extrapolation of the ideal vertical and lateral trends of both fining- and coarsening-upward cycles (facies successions) on the Mullaman Bed shelf. These ideal cycles are based on complete successions exposed at various localities on the shelf, and are generalised to highlight the major characteristics of the successions. The second part provides an interpretive summary of the processes and mechanisms which are envisaged to have formed the ideal coarsening- and fining-upwards facies successions in this particular shelf setting. The third part describes the real variation and range in depositional architecture which is observed within facies successions on the shelf, and attempts to explain variations from the 'norm' (ideal cycles) in terms of local depositional processes.

Together, the three parts encompass the 'nuts and bolts' descriptive aspect, idealised aspect, and predictive aspect of a depositional model. Combined with a comparison of modern and ancient examples in the following section (Sect. 10.9), this concluding part of the thesis provides a facies model for storm- (and wave-) dominated shallow-marine siliciclastic

deposition. Figures 10.21 and 10.22 summarise the depositional model of the Mullaman Bed siliciclastic shallow-marine shelf sequence. They attempt to express the basic depositional architecture of the evolving sequence, and are based on the vertical and lateral variability of facies within facies successions 1-2 and 4-5, which compose the shallow-marine depositional systems on the shelf. These figures and most of the following sections emphasise vertical trends within the evolving depositional systems.

Because of erosion and nondeposition, no single measured section displays every aspect of the interpreted ideal vertical cycles, rather they have been constructed by superposition of what are considered to be typical examples of each laterally synchronous facies obtained from a number of localities. For both coarsening- and fining-upward successions, the ideal vertical cycle relies heavily on the correct identification and correlation of contemporaneous facies successions. The ideal vertical cycles are approximately 5 m-thick, and are repeatedly stacked to form the shelf succession (interstratified with less common rocks of other facies successions (3, 6, 7, and 8)).

10.8.2 Ideal vertical and lateral trends for coarsening- and shoaling-upwards facies successions

This section documents the ideal trends within a coarsening- and shoaling-upwards shallow-marine depositional system on the shelf, and is based on storm- (and wave-) dominated shallow-marine rocks of facies successions 1 and 2. After examination of numerous individual sections and outcrops which are considered to be broadly synchronous across the shelf, the lateral variations have been broadly documented as follows; the proximal (shoreface zone) and intermediate (offshore transition zone) parts of the depositional system are composed dominantly of facies succession 2, whereas contemporaneous distal (offshore zone) deposits are composed of facies succession 1. These lateral trends are detailed in Tables 10.3 and 10.4.

Close to the palaeoshoreline coarsening-upward successions are very coarse-grained and relatively thin (*e.g.* measured sections 148, 149, 154, and 168 in the BPRZ). Here HCS, lenses of conglomerate, and thick graded beds are prominent features. Contacts between successions are sharp and irregular, and commonly involve visible erosional relief and scouring. An ideal coarsening-upward cycle from this position on the shelf (Fig. 10.21A) begins with interbedded units of facies 15-16 overlying a basal lag related to a prior depositional episode; facies 18-19 and 21-22 are commonly missing. Intermediate parts of the cycle contain ripple lamination, flaser bedding, and sandstone beds with bioturbated tops. Upper parts of the

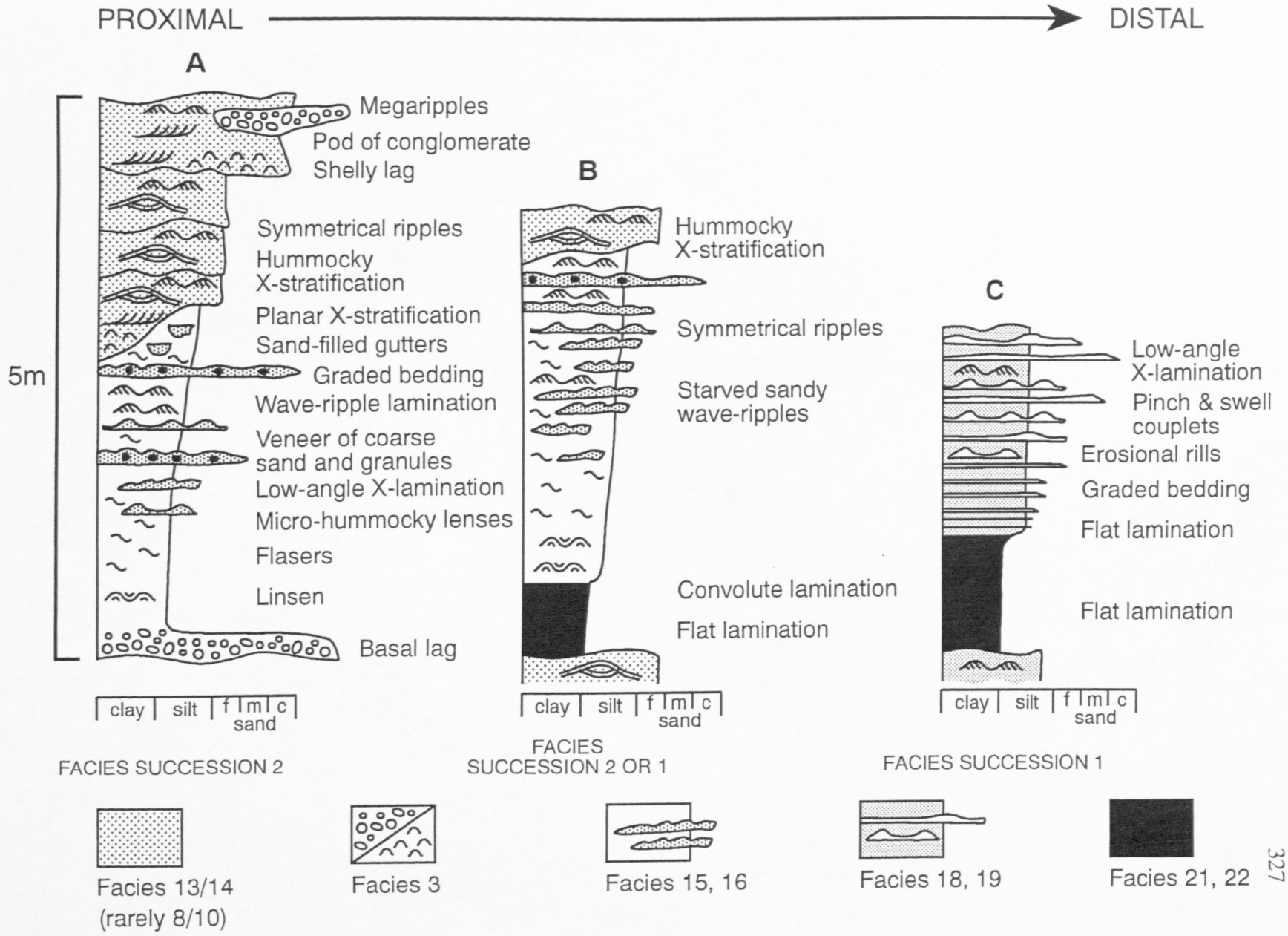

FIGURE 10.21. Generalised illustration of the depositional architecture of the idealised shallow-marine coarsening- and shoaling-upwards depositional system on the shelf. Diagram is based on descriptions of facies successions 2 and 1, and shows the variation in facies, sedimentary structures and grain size. Refer to main text for discussion.

cycle are mostly hummocky cross-stratified (facies 13/14), but coarser sand-sized intervals are planar or trough cross-stratified. Capping the cycle are coarse sandstone or discontinuous lags (facies 3 and 8).

Farther offshore there is an increase in the thickness of coarsening-upward successions, the amount of coarse-grained material is reduced, and interbedded facies (15-16) and fine-grained facies (21-22) are thicker (*e.g.* basal succession of measured section 149, and measured sections 176 and 178 in the BPRZ). Coarse-grained material is commonly present as intraformational lags within facies 15-16, and thin lags at the top of coarsening-upward successions. The ideal cycle for this intermediate part of the shelf is shown in Fig. 10.21B.

Still farther offshore, to the east and southeast, numerous stacked coarsening-upward storm-dominated successions are preserved. Here successions commonly begin with a thin, bioturbated clayey siltstone layer (facies 21-22), which grades into a relatively thick interval of thinly laminated and graded beds (facies 18-19) (*e.g.* measured sections 103, 118, and 121 in the southern region); other facies are missing. The ideal coarsening- and shoaling-upwards cycle on distal regions of the shelf is shown in Fig. 10.21C. In general, contacts between facies on distal parts of the shelf tend to be gradational, and involve little or no large-scale erosion of the substrate. This contrasts markedly with the situation in proximal regions, where the boundaries between facies are typically defined by sharp, eroded surfaces which mark sites of reworking and event scouring and deposition.

10.8.3 Ideal vertical and lateral trends for fining- and deepening-upwards facies successions

Fining-upward storm-dominated successions are thinner and less common than coarsening-upward successions within the Mullaman Beds, and they tend to cap series of stacked coarsening-upward successions. The vertical change in grain-size is more pronounced for fining-upward successions. Description of the ideal fining- and deepening-upwards shallow-marine cycles of the depositional system on the shelf is based on storm- (and wave-) dominated shallow-marine rocks of facies successions 4 and 5. The proximal (foreshore zone) and intermediate (middle-lower shoreface zone) parts of the depositional system are composed dominantly of facies succession 5, whereas contemporaneous distal (offshore zone) cycles are composed of facies succession 4. The trends are detailed in Tables 10.3, 10.4 and Fig. 10.22.

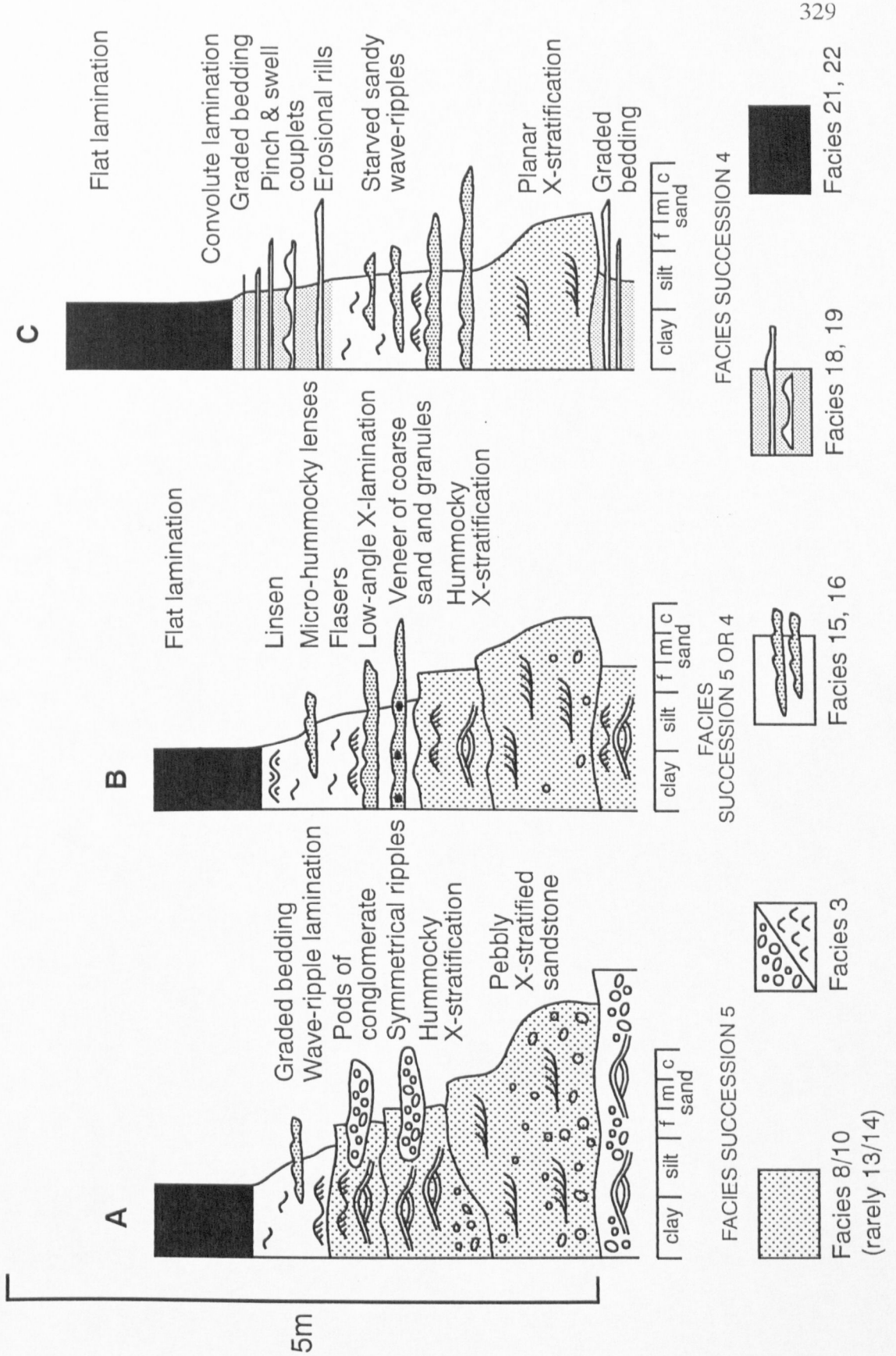

FIGURE 10.22. Generalised illustration of the depositional architecture of the idealised shallow-marine fining- and deepening-upwards depositional system on the shelf. Diagram is based on descriptions of facies successions 5 and 4, and shows the variation in facies, sedimentary structures and grain size. Refer to main text for discussion.

In most proximal fining-upward successions (*e.g.* measured sections 148, 149, 154, and 168 in the BPRZ), the thicknesses of facies 21-22 are increased and the thicknesses of facies 15-16 decreased compared to those in proximal coarsening-upward successions. The base of fining-upward successions in proximal regions is commonly medium to coarse-grained cross-stratified sandstone (facies 8/10). Intermediate parts of the succession contain fine-grained HCS sandstone with lenses of pebble lag. HCS sandstone passes abruptly upward into interbedded facies (15-16), which grade into intensely bioturbated or thinly laminated clayey siltstone (facies 21-22) at the top of the succession. Thin graded beds of facies 18-19 are missing. The ideal fining- and deepening-upwards cycle for proximal parts of the shelf is shown in Fig. 10.22A.

Farther offshore on the shelf fining-upward successions commonly contain less coarse-grained sediment, HCS is less common, and dispersed pebble-sized clasts are rarer. Here the thicknesses of the interbedded facies (15-16) and siltstone or claystone (facies 21-22) are marginally greater, and the overall grain-size of the succession is finer. Thin graded beds (facies 18-19) are not present. The ideal cycle for intermediate parts of the shelf is shown in Fig. 10.22B.

At distal localities on the shelf the thicknesses of facies 21-22 are significantly greater and thin graded beds (facies 18-19) are prominent within fining-upward successions (*e.g.* measured sections 96 and 97). Here facies 8/10 is thin and facies 3 is missing. Compared to more proximal localities, the thicknesses and grain-size of facies 15-16 are not significantly changed, and facies 15-16 grade upward into an even finer-grained interval of thin graded beds (facies 18-19). The thin graded beds are in turn overlain by a relatively thick interval of siltstone or claystone (facies 21-22). The ideal cycle for distal parts of the shelf is shown in Fig. 10.22C.

10.8.4 Development of coarsening- and shoaling-upwards facies successions: shoreface drowning and rapid nondepositional transgression, followed by aggradation and limited progradation

The following discussion and Fig. 10.23 provide an interpretive summary of the formation of coarsening- and shoaling-upwards facies successions (parasequences) which compose the most common depositional system on the shelf, and also typically form systems tracts (particularly HSTs) of the six sequences. Details of the lithology, fossil content, and sedimentary structures of these facies successions are presented in chapter 4 under separate headings for each succession.

FIGURE 10.23. Generalised illustration showing possible sequence of events in the origin of coarsening- and shoaling-upwards facies successions on the Mullaman Bed shelf.

(A) during stillstand or stable periods of relative sea level, minor progradation takes place.

(B) rapid landward movement of the shoreline occurs in response to a rapid rise in relative sea level and the very low gradient of the shelf. Sediment accumulation is initially negligible. A transgressive lag mantles the transgressive erosion surface. A blanket of transgressive mud accumulates, and is thickest in intermediate and distal localities.

(C) when the rate of relative sea level rise decreases or becomes zero, the shoreline position is stabilised, and gradual shoreface progradation commences.

(D) typically the end of a depositional episode is characterised by a fall in relative sea level, which due to the low shelf gradient, results in rapid basinward movement of the shoreline and formation of a new sharp-based erosional shoreface profile.

The positions of idealised vertical facies successions from Fig. 10.21 are shown on the diagram. The slope of the shelf is exaggerated. For all stages the rate of sediment supply is interpreted to have been low compared to other shelf settings. This figure is based in part on Plint (1988).

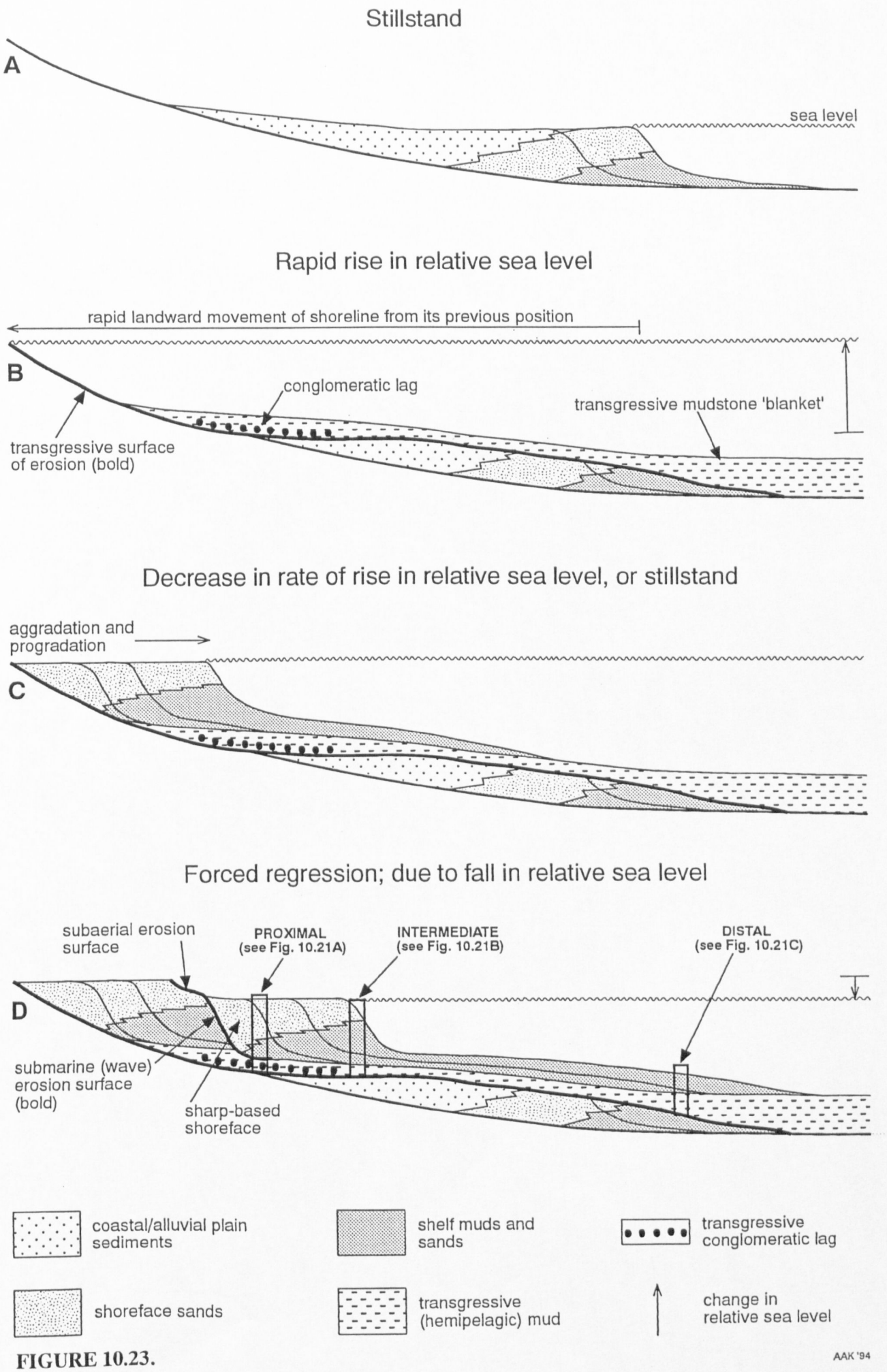
Stillstand
A
sea level
Rapid rise in relative sea level
rapid landward movement of shoreline from its previous position
B
conglomeratic lag
transgressive mudstone 'blanket'
transgressive surface
of erosion (bold)
Decrease in rate of rise in relative sea level, or stillstand
aggradation and
progradation
C
Forced regression; due to fall in relative sea level
subaerial erosion
surface
PROXIMAL
(see Fig. 10.21A)
INTERMEDIATE
(see Fig. 10.21B)
DISTAL
(see Fig. 10.21C)
D
submarine (wave)
erosion surface
(bold)
sharp-based
shoreface
coastal/alluvial plain
sediments
shelf muds and
sands
transgressive
conglomeratic lag
shoreface sands
transgressive
(hemipelagic) mud
change in
relative sea level
AAK '94

FIGURE 10.23.

Initial accumulation of a typical coarsening-upward marine cycle (facies succession 1 or 2) involved deposition of laminated clayey siltstone or claystone (facies 21-22). Occasionally this unit overlies a basal lag, which was probably produced by subaerial exposure (stream incision and concentration of coarse clastic debris) followed by, or related exclusively to, submarine (wave) erosion during transgression (Sect. 9.6.3).

After deposition of claystone or siltstone a relatively long period of sediment accumulation is represented by a thick package of interbedded facies (15-16). These facies show a range of wave-generated features, which indicate that low-energy, quiet-water sedimentation was overprinted by episodic storm deposition. During peak storm conditions oscillatory wave and shelf (geostrophic) currents would have combined to scour the seabed (*cf.* Aigner, 1985), after which graded beds were deposited from suspension as turbulence waned.

The upward increase in wave and current energy during accumulation of facies 15-16 due to shoaling is indicated by the vertical change from lenticular bedding at the base, to flaser bedding in the intermediate parts, to amalgamated units of ripple-laminated sandstone with rare finer-grained drapes in the upper parts of these facies. Other structures were sporadically formed in these facies by storms, including micro-hummocky cross-stratified beds and rare cross-bedded intervals with coarse-grained foresets. The vertical changes in sedimentary structures and grain-size within this part of the cycles reflect continuing sedimentation concurrent with decreasing accommodation space. The proportion of clayey siltstone versus coarser-grained rocks varies primarily as a function of distance from the palaeoshoreline, with a higher percentage of coarser-grained rocks and lags in more proximal areas.

With continued aggradation or progradation the sea floor was affected by progressively higher energy processes and thick, amalgamated sandstone beds with hummocky cross-stratification were formed. The hummocky bedforms have a moderate to long wavelength and low amplitude, typically 4 to 6 m and 0.5 to 0.75 m respectively. According to Dott and Bourgeois (1982) and Duke *et al.* (1991) the presence of these bedforms in any shallow marine setting attest to the presence of large waves (presumably storm-generated).

The top of a coarsening- and shallowing-upwards cycle (succession) is represented by amalgamated hummocky sandstone beds or a lag (Sect. 9.6.3). Final deposition produced discontinuous lags at the top of the cycle in response to maximum energy conditions and reworking by numerous storms. After formation of HCS beds at the top of coarsening- and shoaling-upwards cycles during waning storm conditions, the flow was probably incapable of

moving pebbles significant distances, but was still able to concentrate pebbles in local topographic lows (*i.e.* the swales and hollows of the underlying HCS bed). Some of these lags, or the laterally equivalent coarse sandstone tops, have been subsequently filled in by sediment or cemented to form hardgrounds, which are overlain by uncemented Cretaceous marine facies of similar overlying cycles.

Accumulation of coarsening-upward successions on the shelf is interpreted as taking place by aggradation after a *rapid* rise in relative sea level (Fig. 10.23), similar to the process described by Plint (1988). In this scenario it seems possible that the transition from stillstand to greatest rate of change (in relative sea level) is geologically instantaneous and insignificant on a geological scale, as inferred in the present study and others (*e.g.* Kamola and Huntoon, 1994). Aggradation was followed in places by a progradational shift in lateral facies boundaries caused by falling relative sea level. Relative sea level fall resulted in decreased accommodation space, which led to fairweather waves impinging on the seafloor; a situation which is highlighted by thin sharp-based shoreface sandstones overlying offshore sediments on distal to intermediate parts of the shelf (*e.g.* the bases of Sequences *II* and *III*, Sect. 9.7.3), and by coarse-grained upper shoreface deposits at the top of the HST building out into the basin in more proximal areas (*e.g.* the top of Sequence *IB* in the southern region, and the top of Sequence *III* in the BPRZ).

Aggradation gradually built the sediment surface progressively upward, until it became affected by stronger wave energies, storm waves being the most energetic. During aggradation, penecontemporaneous scouring created sandstone-filled gutters and truncated the margins of earlier storm beds. The infilling of gutters (mostly by fine sand) probably took place under the combined influence of oscillatory wave motion and flows parallel to shore (*cf.* Aigner, 1985; Duke, 1990; Plint and Norris, 1991).

10.8.5 Development of fining- and deepening-upwards facies successions: gradual shoreface incision and retrogradation

The processes of formation of some fining- and deepening-upwards cycles on the shelf are less well understood than are those of coarsening- and shoaling-upwards cycles. However, fining-upward cycles (facies succession 5) at the tops of Sequence *IA* (BPRZ) and *IB* (southern region) can be explained simply by transgression. That is, these cycles represent classical fining-upward cycles which formed by inundation of previously emergent areas or drowning of shoal areas (see Fig. 10.24).

FIGURE 10.24. Generalised illustration showing possible sequence of events in the origin of fining- and deepening-upwards facies successions on the Mullaman Bed shelf.

(A) during stillstand or stable periods of relative sea level, minor progradation takes place.

(B) a gradual rise in relative sea level begins. The shoreface advances landward and forms a transgressive ?barrier shoreface. The offshore area is characterised by nondeposition, and a pebbly and/or shelly lag is spread over the transgressive erosion surface.

(C) as the shoreface stabilises or the rate of landward incision steadies, sand is derived from erosion of underlying rocks during shoreface incision and is spread as a thin 'envelope' over the transgressive erosion surface. Farther offshore sand changes laterally into thin sandy silt and mud.

(D) with continuing rise in relative sea level, the shoreface continues to incise landward, leaving behind another transgressive erosion surface mantled by gravel lag and overlain by another thin layer of eroded sand (from older units). The various shoreface positions can be considered as points along a continuum which forms a smooth stepped surface of erosion (shoreface envelope) with a relatively low angle. The surface of transgressive erosion is mantled by thin transgressive lags, and is overlain by a thin layer of sand derived from shoreface incision.

(E) At maximum flooding and highstand, clastic starvation occurs and most of the shelf is draped by a blanket of hemipelagic transgressive mud.

The positions of idealised vertical facies successions from Fig. 10.22 are shown on the diagram. The slope of the shelf is exaggerated. For all stages the rate of sediment supply is interpreted to have been low compared to other shelf settings. See Fig. 10.23 for legend.

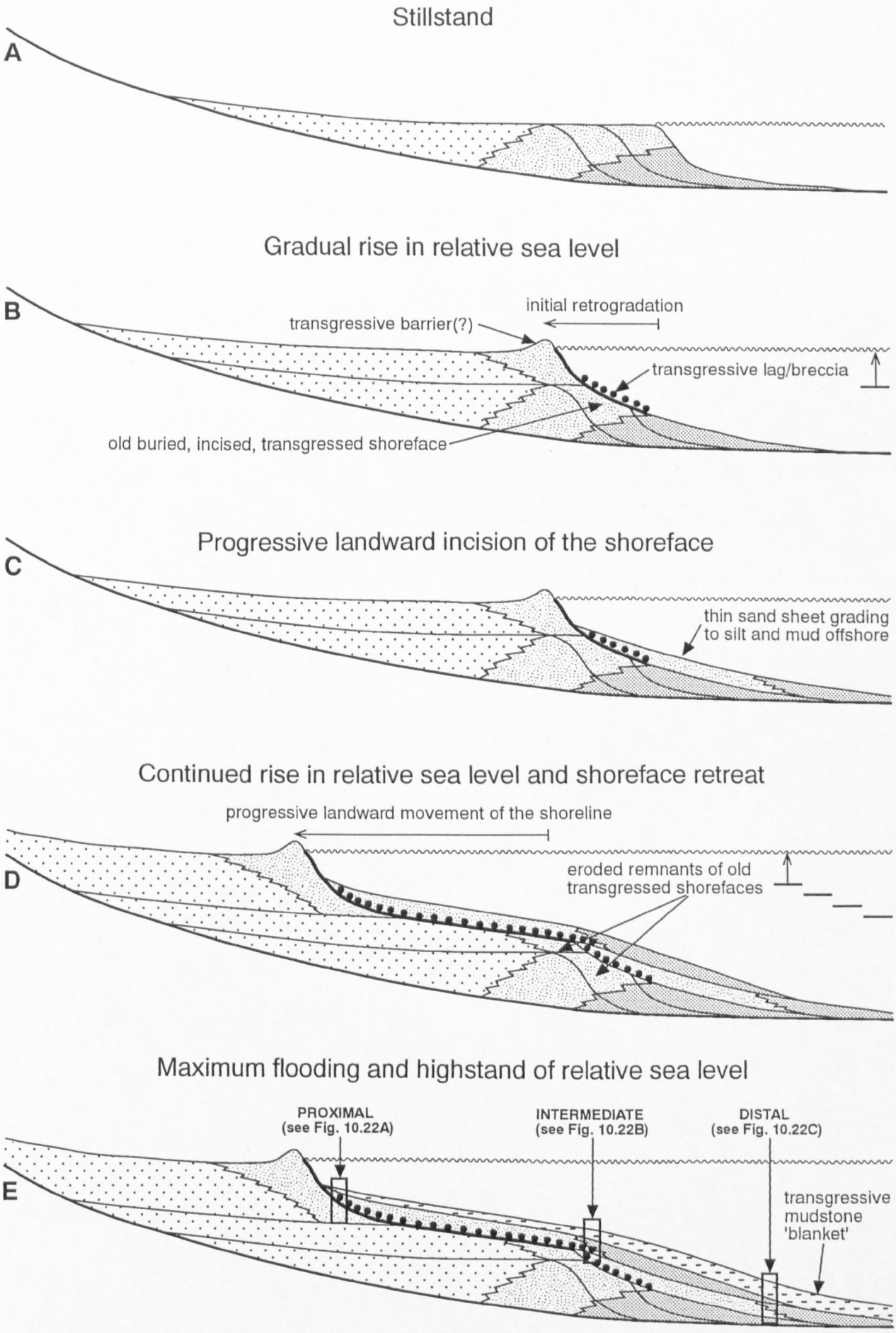

FIGURE 10.24.

AAK '94

The changes in sedimentary structures in these cycles (large-scale cross-bedding to small-scale cross-bedding/HCS to thinly interbedded units to graded laminae to flat lamination) indicate progressively increasing water depth towards the top of the cycles. Furthermore, these cycles typically have a basal transgressive lag or coquina and overlie normally-graded conglomerates or other paralic or shallow subtidal to intertidal facies, and document an upward increase in marine influence. The lags may be normally-graded where they are thick (<0.75 m), but tend to be defined by a layer only a few clasts thick. Lags are typically composed of well-rounded granule to small-pebble sized chert and lithic clasts. This type of lag is typical of those produced by erosion and transgression in siliciclastic shallow-marine settings (Sect. 9.6.3). Fining- and deepening-upwards (transgressive) cycles similar to those of Sequence *IA* and *IB* occur on other parts of the shelf overlying the major sequence boundaries (*e.g.* facies succession 4/5 overlying the China Wall SB at the base of Sequence *II*; facies succession 5 overlying the Stoney Ridge SB at the base of Sequence *IV*; facies succession 4 overlying the Arnhem Land SB at the base of Sequence *V*).

More problematic is the origin of stacked fining- and deepening-upwards cycles which overlie the basal transgressive fining-upward cycles in Sequences *II*, *IV*, and *V*. In most cases there is little evidence for significant erosion at the contacts between cycles, and there is no evidence of subaerial exposure, *i.e.* thin coals, palaeosols, dessication cracks, root casts *etc.*. It is therefore likely that the disconformities between these fining-upward cycles were formed in a submarine environment. The best evidence for this is found in the ALZ, where measured sections contain 2 to 3 stacked fining- and deepening-upwards cycles of facies succession 5 (*e.g.* measured sections 4 and 12). Here, the basal fining-upward cycle is a typical transgressive cycle with a thin (locally developed) conglomeratic lag. In many places the top of the basal transgressive cycle is defined by fine-grained rocks (facies 21-22) disconformably overlain by a sedimentary breccia (which forms the base of the next fining-upward cycle).

The sedimentary (intraformational) breccias (0.3 to 0.5 m-thick) which mark the bases of the overlying fining-upward shallow-marine cycles are composed of clast-supported pebble to cobble sized angular fragments set in a matrix of clayey sand. The breccia fragments have an irregular shape, are poorly sorted, and can be tightly packed; the matrix content is low because the there are only small gaps between the fragments. The fragments are composed of a similar material (moderately-sorted, subrounded to rounded, fine-medium to medium grained quartz arenite) as the matrix. The fragments are dark brown to black in colour, and are heavily stained and cemented (in places) by ferromanganese oxides. In contrast, the matrix is uncemented and

has a high clay content. These observations suggest that the breccias were formed by in-situ brecciation in a marine environment, and that the breccia fragments were not transported any significant distance. It seems likely that the breccias (at the base of fining- and deepening-upwards cycles) represent former mineralised and cemented marine hardgrounds that were broken-up by wave erosion during renewed transgression and storms. Each breccia horizon probably represents a submarine erosion surface (second diastem, *sensu* Nummedal *et al.*, 1993).

If this interpretation is correct, as seems likely from the various lines of evidence, then stacked fining- and deepening-upwards shallow-marine cycles would have been produced during major periods of transgression punctuated by shorter times of stillstand or minor regression. The situation envisaged for formation of stacked cycles of facies succession 5 and 4 (in Sequences *IV* and *V* respectively) is as follows (see Fig. 10.24); initial *gradual* transgression and advance of the shoreface would have produced the lower fining-upward transgressive cycle with a basal conglomeratic lag or coquina. It is likely that the thin sandy shoreface sediments, which lie *above* the transgressive erosion surface and form the basal parts of most proximal fining- and deepening-upwards cycles, were derived locally from erosion (through shoreface incision) of previously-deposited rocks. Such coarse-grained clastics grade upwards into finer-grained sediments indicative of deposition in progressively deeper-water environments away from the shoreface (which was actively incising landward).

As the water depth increased, and the shoreface moved landward, the rate of sediment supply (from fluvial incision) would have gradually decreased with the rise in base level. Recent flume experiments (*e.g.* Koss *et al.*, 1994) support the intuitive relationship of falling coarse sediment load in streams with rising base level, but show that base level changes have greater effects on marine shelves and lesser effects on fluvial drainage in the hinterland than previously thought. In any case, successively finer grained sediments were deposited in progressively deeper water giving the classical fining-upward cycle. The top of a transgressive cycle represents a marine starvation surface (fifth diastem, *sensu* Nummedal *et al.*, 1993).

The initially steady rise in relative sea level decreased (stillstand) or was temporarily reversed (leading to minor regression). During such intervals one would expect that accommodation space would have been filled as the sediment surface was built up by the continuing supply of sediment (resulting in a coarsening-upward cycle). However, the western shelf of the Carpentaria Basin had a low sediment supply at most times (Sect. 10.6.4), which would have been even further reduced during times of major transgression when base level was high and

the stream-gradient was significantly decreased; the inner shelf was characterised by clastic starvation during major transgressive episodes (especially their latter parts), and the only significant supply of sediment was from cannibalisation of older sediments in the zone of the actively incising shoreface. The existence of the brecciated hardgrounds at the contacts between cycles on the inner shelf supports the proposition of very low sedimentation rates because hardgrounds represent surfaces of omission (nondeposition) (*sensu* Banerjee and Kidwell, 1991). Farther offshore, condensed hemi-pelagic sediments would have been deposited from suspension as a blanket of transgressive mud across much of the offshore area (*e.g.* condensed fine-grained concretionary horizons at the top of fining- and deepening-upwards cycles within Sequence *V* in the central and southern regions).

During these intervals of stillstand or minor slow falls in relative sea level, the rate of sediment supply would have begun to increase. At the same time the affect of storms upon deposition and transport would have increased as the water depth decreased. Local scouring and remobilisation and offshore transport of coarse-grained sediment and clasts would have become increasingly common, and wave scour was probably also responsible for the brecciation of the marine hardgrounds (Sect. 9.6.3). Renewed slow and steady rise in sea level, and continuing retrogradation, is interpreted to have repeated the process to form the next fining- and deepening-upwards cycle (sandstone overlain by interbedded facies steadily fining-upward into thin graded beds and mudstone) overlying the sedimentary breccia.

In this interpretive summary the potential lag time for changes in rates of sediment supply in response to different rates of change in relative sea level is intriguing. That is, why are these transgressive cycles fining-upward instead of coarsening-upward? During other times (*e.g.* Sequence *III*) a rapid rise in relative sea level completely drowned the shelf, and previously deposited coarse-grained shoreface sediments were disconformably overlain by a blanket of transgressive mud. Such 'mud on sand' contacts between coarsening-upward cycles represent marine flooding surfaces (parasequence boundaries). The sediments overlying these flooding surfaces become progressively coarser-grained in response to decreasing accommodation space after an initial rapid rise.

However, fining-upward cycles represent times of *gradual* transgression, where the rate of sediment supply appears to have decreased gradually over time as the shoreface moved progressively landward. In this case, in contrast to coarsening-upward cycles, foreshore and shoreface sandstones were formed at the base of the sequence because the local supply of sediment (from erosion of underlying rocks) occurred relatively steadily near the actively

incising shoreface, and did not cease immediately upon transgression. That is, the palaeoshoreline moved slowly landwards over time due to progressive shoreface incision (*e.g.* Fig. 10.24), rather than 'jumping' tens of kilometres landward due to a very rapid rise in relative sea level such as that which occurred during Sequence *II* and *III* time (*e.g.* Fig. 10.23).

The increasingly landward onlap of successive stacked fining- and deepening-upwards cycles (*e.g.* Sequence *IV*) suggests that the overall regime was landward-stepping or transgressive, and that the rate of creation of accommodation space occurred over and above any increase in the rate of sediment supply (this concept is well illustrated by Shanley and McCabe, 1994, fig. 2). In general (when viewed over the entire period), it appears that the relative rises in sea level which formed fining- and deepening-upwards cycles are actually composed of shorter periods of relative sea level rise and stillstand, as noted in other settings which were affected by major transgressions (*e.g.* Kamola and Huntoon, 1994).

The rate of sediment supply apparently decreased gradually to a minimum during the time of maximum flooding (and stillstand). The dominance of finer-grained rocks in the middle and upper parts of fining- and deepening-upwards cycles suggests increasing deposition from suspension as the delivery of coarse-grained clastics from the hinterland and shoreface incision was reduced.

Thus, given a rise in relative sea level on the Mullaman Bed shelf, the major factor which controlled the depositional architecture of shallow-marine depositional systems appears to have been the rate of change in relative sea level; rapid rises produced coarsening-upward cycles, and gradual rises typically produced fining-upward cycles. Rate of transgression has previously been recognised as having significant influence on the character and preservation of stratigraphic sequences (Sanders and Kumar, 1975). Possibly, the discontinuous nature of transgression (gradual transgression punctuated by intermittent stillstands or minor regressions) may have been the product of fourth- and fifth-order relative sea level cycles superimposed on the rising limb of a third-order ?eustatic cycle, as envisaged by Van Wagoner *et al.* (1990).

10.8.6 Deviations from the model: The real Mullaman Beds

Any facies model must be able to be used as a template or norm against which individual examples or deviations from the norm can be measured and interpreted, even within the study area or sequence from which the model is derived. The following section describes, and attempts to explain, deviations from the norm in this shelf setting.

Variations on coarsening- and shoaling-upwards facies successions

Several important variations on the basic coarsening- and shoaling-upwards cycle (facies successions 1 and 2) occur. In places coarsening- and shoaling-upwards cycles are composed entirely of coarse-grained crossbedded sandstone (facies 8) and associated intraformational conglomeratic lags overlying a basal erosion surface; finer-grained facies are absent. This variation on the ideal cycle (*e.g.* Fig. 10.21) is probably due to progradation of shoreface sandbodies into water which was too shallow to allow preservation of finer-grained heterolithic facies and offshore muds.

A second, rare, variation on the ideal cycle is expansion of the amalgamated hummocky sandstone beds (facies 14), such that the entire cycle is dominated by this facies with very little fine-grained material (facies 15-16 or 21-22) at the base, and only minor amounts of coarse-grained material (facies 3) in the upper part of the cycle. This situation occurs in nearshore zones, where most coarser material (facies 3) and coarse to medium sand, was presumably bypassed offshore during peak storm conditions (*cf.* Plint, 1988). Subsequently fine sand (facies 14) was deposited as hummocky bedforms in the zone between storm wave base and the lower shoreface; finer-grained sediment (facies 15-16, 18-19 and 21-22) was still in suspension farther offshore.

On more distal parts of the shelf some cycles begin with a thin, intensely bioturbated siltstone layer (facies 21), which grades up into a relatively thick interval of thinly laminated and graded beds (facies 16 and 18-19). Interbedded wave-rippled units (facies 15), and coarse material (facies 3) are missing and only rarely do the upper parts of the cycle contain hummocky sandstone (facies 14). This deviation from the model is considered to represent areas where generally quiet, pelagic distal sedimentation was interrupted by episodic storms which formed the coarser-grained, graded beds (*cf.* Reineck and Singh, 1972). In places facies 18-19 are coarser-grained and contain dispersed clasts and irregular graded beds (*e.g.* middle parts of section 118). These coarser intervals occur at localities near basement islands on the shelf where anomalously coarse-grained clastics were apparently shed-off the basement terrains, and were incorporated within the otherwise fine-grained storm-influenced cycles.

Another variation on the model for coarsening- and shoaling-upwards cycles (facies succession 1) is where the upper interbedded facies (16), if present, is very thin and the bulk of the succession consists of dark grey, laminated siltstone and silty claystone of facies 19 (*e.g.* measured section 109 in the southern region). At these localities the exposed thicknesses of

cycles is between 5 and 10 m. This deviation from the model probably represents the most distal portion of the shelf, where even major storms did not disturb the depositional surface.

Variations on fining- and deepening-upwards facies successions

Variations from the model for ideal fining- and deepening-upwards cycle in proximal localities (*e.g.* Fig. 10.22A) involve changes in the relative thicknesses of facies 8/10, 15-16, and 21-22, or successions where facies (3 and 15-16) are missing. Cycles at localities near the maximum landward position of the shoreface are composed almost entirely of coarse- to medium-grained sandstone, with very little fine-grained material present near the top of the succession. Here, most fine-grained sediment was probably transported farther offshore in suspension.

Slightly farther offshore (but still proximal) the base of a fining- and deepening-upwards cycle may be represented by an interval of the interbedded facies (15-16), which grades upward into very fine-grained sandstone and siltstone with HCS (*e.g.* measured section 154). Here facies 10 has an unusually fine grain-size; in the model facies 15-16 only occurs overlying HCS sandstone. Elsewhere, coarse-grained planar cross-stratified sandstone (facies 8/10) is thin and grades rapidly upward into clayey siltstone (facies 21-22), and facies 3, 15-16 and 18-19 are missing (*e.g.* measured sections 75 and 168). These variations from the model are also interpreted to represent areas where most coarse-grained sediment was bypassed offshore during storms, and finer-grained sediment was subsequently deposited from suspension.

At a few distal localities, interbedded facies (15-16) are thin and pass upward into graded facies (16) which is capped by bioturbated siltstone (facies 21). Here, coarse- to medium-grained sandstone is missing and this cycle is considered to have been deposited in the offshore zone, where deposition of fine-grained sediment was episodically interrupted by large storms, which deposited coarser graded beds. Even farther offshore, rare fining-upward successions are composed almost entirely of fine-grained facies (21-22) and the graded facies (18-19), with only a small thickness of interbedded facies (15-16). This type of succession reflects slow, hemipelagic sedimentation of finer-grained material in areas distal from the palaeoshoreline, in water depth beyond the influence of all but the largest storms.

In some distal localities fining- and deepening-upwards cycles comprise thin (2-3 m), stacked fining-upward sub-cycles (*e.g.* measured sections 124 and 133). These sub-cycles involve several different facies which are not included in the model. The base of each sub-cycle is a thin lag which grades into bioturbated clayey sandstone (facies 10), which grades into offshore

silty sandstone (facies 13). As the grain size continues to decrease, silty sandstone grades into bioturbated siltstone (facies 21-22) or laminated very fine siltstone and claystone (facies 18-19). The upward transition from medium-fine sandstone to fine siltstone and claystone in each sub-cycle occurs gradationally over 1 or 2 metres. The overall grain size and thickness of the sub-cycles in such distal localities is much reduced compared to the ideal cycle. The lack of wave-formed structures in most of the sub-cycles suggests deposition beneath average storm wave base in the lower offshore zone. The stacking of thin, fine-grained rapidly fining-upward sub-cycles is consistent with an offshore marine setting, and suggests condensed sedimentation in distal regions.

10.9 COMPARISONS OF THE DEPOSITIONAL MODEL WITH OTHER STUDIES

The extensive application of sequence stratigraphy as a tool to assess and explain the depositional geometries and processes of formation of marine sequences in the last decade or so has also benefited more classical methods of sedimentological analysis. The application of this relatively new methodology has brought about renewed appreciation of the cyclicity and repetition of certain sedimentary cycles in many rock sequences, regardless of their age, and has led to a more process-oriented view of sedimentology and stratigraphy.

In this context, there has also been an increasing recognition of the role that storm-related processes play in controlling depositional architecture when they are superimposed on other higher-order variables (*e.g.* relative sea level change, sediment supply, subsidence) for a particular basin. A significant number of storm-dominated sedimentary sequences have now been documented from around the world, emphasising the importance of storms in sedimentary environments (about 80% of modern shelves are thought to be storm-dominated, Walker, 1984). This is a relatively new field of sedimentology because the recognition of ancient storm-dominated deposits has been hindered by the difficulty in observing modern storm sedimentation in action, and then relating this to the rock record.

The large body of literature now in existence for storm deposits has allowed a number of storm-related facies models to be developed for typical storm beds (tempestites). These classical models of Aigner (1982, 1985), Brenchley (1985), and Einsele and Seilacher (1982) are based on the proximality concept (analogous to the lateral variation in bed thickness and sedimentary structures in the turbidite facies model); proximal storm-beds (or cycles) in shallow water are typically thick-bedded and amalgamated, commonly display HCS, but are associated with

relatively little interbedded mudstone, whereas distal storm-beds (or cycles) in deeper water display thinner graded beds enclosed by mudstone with relatively few wave-generated sedimentary structures, and only very rare HCS.

In more recent times there has been a realisation that storms affected other related environments such as lakes (Dam and Surlyk, 1993; Duke, 1984; Higgs, 1991; Walker (in Duke, 1985)), deltas (Bhattacharya, 1993; Reynolds, 1992), estuaries, and tidal flats (Cotter, 1990), and that the record of storms in these settings provides important clues as to the evolution of the depositional systems. On a regional scale the facies trends described within most of these storm-dominated depositional environments have significant similarities (taking into account the varying scales of the deposits). This leads to the conclusion that a facies model developed for storm-dominated shallow-marine depositional systems (such as the model developed in this thesis) may have wider utility in the analysis of numerous different but related sedimentary environments.

In terms of the vertical sequence, the depositional model for the Mullaman Beds shelf sequence (Figs. 10.20 through 10.24) bears many similarities to typical storm-dominated siliciclastic rocks within other epeiric seaways, particularly the Cretaceous Western Interior Basin (WIB) of North America. In most cases these storm-dominated depositional systems are regressive (*cf.* Harms *et al.*, 1975), and are composed of coarsening- and thickening-upwards cycles deposited during shoaling events.

Such deposits include the Campanian Mesaverde Group of northwestern Colorado (Hadley and Elliot, 1993; Martinsen *et al.*, 1993), the Turonian Cardium Formation in Alberta, Canada (Hart and Plint, 1993; Plint, 1988; Walker and Eyles, 1988; Wright and Walker, 1981), the Upper Cretaceous Dakota, Ferron, and Price River Formations in Colorado and Utah (Dott and Bourgeois, 1982), the Coniacian to Santonian Muskiki and Marshybank Formations in Alberta, Canada (Plint, 1990, 1991; Plint and Norris, 1991), the Upper Albian Viking Formation in Alberta, Canada (Amajor and Lerbekmo, 1990; Posamentier *et al.*, 1992), the Turonian to Campanian Tropic Shale and Straight Cliffs Formation in Utah (Shanley and McCabe, 1991), and the Upper Cretaceous Tocito Sandstone in New Mexico (Jennette *et al.*, 1991).

Sequences with similar regressive/coarsening-upward storm-cycles (besides those in the WIB of North America) include the Upper Ordovician Kope and Fairview Formations in Ohio and Kentucky (Jennette and Pryor, 1993), the thick Jurassic Fernie and Kootenay Formations in Alberta, Canada (Hamblin and Walker, 1979), the Late Devonian West Falls Group in New

York, USA (Craft and Bridge, 1987), the Upper Eocene/Lower Oligocene Annot sandstones of southeastern France (Sinclair, 1993), the Silurian shelf sediments of Pennsylvania (Cotter, 1990), the Silurian to Devonian Sierra Grande Formation in southern Argentina (Spalletti, 1993), the Triassic Raibl Group in Austria (Bechstadt and Schweizer, 1991), the Jurassic to Cretaceous Janusfjellet Subgroup in Spitsbergen (Dypvik *et al.*, 1991), and similar (but thinner) finer-grained turbiditic sequences such as the Upper Silurian Kendal Group of northwest England (King, 1994).

Retrogradational and/or transgressive storm-dominated sequences, which incorporate fining and/or deepening-upward cycles, are less common than regressive (aggrading/prograding) sequences in the rock record. However, there are a number of well-studied examples of such sequences (which commonly occur in association with, and overlying, stacked coarsening- and shoaling-upwards cycles) including the Upper Cretaceous Cape Sebastian Sandstone in Oregon (Bourgeois, 1980), the retrogradational Cenomanian Kaskapau Formation in Alberta, Canada (Wallace-Dudley and Leckie, 1993), the Lower Palaeocene Clayton Formation of western Alabama (minor storm influence, Savrda *et al.*, 1993), and Jurassic-Early Cretaceous formations in the Jameson Land and Wollaston Forland basins of East Greenland (Surlyk, 1991).

The above lists of largely siliciclastic storm-dominated (or storm-influenced) sequences which are similar to the Mullaman Beds are by no means exhaustive, and it is beyond the scope of this thesis to compare all of these occurrences in detail; for a comprehensive review of storm-influenced deposits characterised by HCS refer to Duke (1985). All of the sequences cited above have at least some affinity with shallow-marine storm-dominated cycles of the Mullaman Beds in terms of thickness (relative thicknesses of various parts of the cycles), vertical and lateral changes in grain size and sedimentary structures, bedding contacts and internal stratification, changes in bioturbation and faunal assemblages, or broad depositional architecture.

10.9.1 Analogues

Probably the best analogues for coarsening- and shoaling-upwards storm cycles in the Mullaman Beds are 5 to 10 m-thick coarsening- and shoaling-upwards (aggrading / prograding) cycles within Upper Cretaceous foreland basin/shelf sequences in Alberta, Canada (*e.g.* Plint, 1988). In both Canada and northern Australia complete proximal cycles are composed of basal bioturbated mudstone which gradually coarsens upward into interbedded (flaser and lenticular

bedded) wave-rippled mudstone and sandstone, through HCS sandstone up into coarser-grained SCS and trough cross-bedded sandstone +/- conglomerate (Plint, 1988). Farther offshore, cycles become slightly thinner, and thin graded beds and wave-rippled interbedded facies are the major components of the cycles. Cycles in the WIB accumulated under higher sedimentation rates, and so generally their thicknesses are slightly greater than in the model developed in this thesis.

A good analogue for fining- and deepening-upwards storm cycles in the Mullaman Beds is the 4 to 5 m-thick fining- and deepening-upward coarse-grained storm-dominated cycle at the top of the Campanian Chungo Member of the Wapiabi Formation in southern Alberta, Canada (Cheel and Leckie, 1992). The cycle has a base of interbedded (somewhat lenticular) conglomerate and sandstone overlying a disconformity; the conglomerate is moulded into coarse-grained ripples (megaripples *sensu* Leckie, 1988). The conglomeratic interval is overlain by a fining-upward series of HCS sandstone and wave-rippled very fine- to fine-grained sandstone, which in turn is overlain by marine shale (Nomad Member).

A closely related sequence occurs in fining- and deepening-upwards storm cycles of the Mullaman Beds, the only difference being that megaripples were not observed at the base of the cycle. However, gritty lags and laterally equivalent sedimentary breccias occur at this position (base) of the cycles, and are probably equivalent in an energy-dynamic sense to megaripples formed in the North American example; it is likely that there was simply not enough coarse clastic debris available to be concentrated into megaripples on the Mullaman Bed shelf during transgression, although megaripples did form on the shelf at other times (in regressive sequences). In both the Canadian and Australian cases the upper fine-grained marine shale of the storm cycles (Nomad Member in Canada; facies 21-22 and/or C2 marker bed in the Mullaman Beds) represents the end result of transgression, with distal deposition of fine-grained sediment beneath storm wave base.

As a final note on the comparison of storm cycles, attention is drawn to the similarity between the Mullaman Beds and some carbonate storm-cycles described in the literature, particularly where the carbonate in the sequences occurred as particles which behaved hydraulically in a similar fashion to siliciclastic particles (*e.g.* Cotter, 1990). In this sense storm-cycles on some carbonate ramps and shallow shelves (*e.g.* 1 to 5 m-thick punctuated aggradational cycles, Goodwin and Anderson, 1985) have similar vertical and lateral trends to coarsening- and shoaling-upwards storm cycles on the western shelf of the Carpentaria Basin, and the same

interpretation holds for their formation, *i.e.* rapid nondepositional transgressions followed by slow, progradational regressions.

10.10 CHAPTER SUMMARY

During a time of high global sea level in the mid-Cretaceous, the western shelf of the Carpentaria Basin was flooded in a series of major transgressive pulses which affected most of the large epeiric seaway from Aptian to Cenomanian time. Over this time interval the northern and central parts of Australia lay at high palaeolatitudes, and were apparently characterised by strong seasonality and winter freezing (at least in the Aptian). The high palaeolatitudinal setting combined with the regional palaeogeography of the seaway created some unusual conditions; the sea was characterised by high salinities and typically dysaerobic bottom waters (except above fair-weather wave base), and was cool to cold in its early history, as shown by interpreted ice-rafted deposits within the Mullaman Beds and by palaeontological and isotopic evidence.

The palaeogeography and paths of transgression were largely controlled by the pre-existing land surface along the western margin of the shelf. There, basement terrains acted as barriers, peninsulas and islands throughout the history of the seaway. The rates of sediment supply were almost universally low during accumulation of the Mullaman Beds, and the large number of stratal discontinuities, together with the observed textural and compositional maturity of the rocks, indicates that erosion, transport, and redeposition were common.

That subsidence was slow and steady is a first-order assumption, based on the lack of any detected structural deformation of the exposed Mullaman Bed sequence, on regional structural analyses of the basin in previous studies, and on extrapolation of low-gradients and lack of evidence for structural discordance from offshore seismic data. Considering that subsidence appears to have been slow and sediment supply was minimal, the major mechanism for controlling the depositional architecture of the Mullaman Beds (and maintaining the shelf profile) is considered to have been change in relative sea level. Superimposed on these shelf dynamics were the episodic but important affects of storms on the shelf; storm-dominated shallow-marine depositional systems comprise the greater part of the shelf sequence.

After rapid rises in relative sea level, accumulation of coarsening- and shoaling-upwards cycles occurred by aggradation and progradation; at times this progradation was driven by 'normal' sediment supply, whereas at other times progradation was forced by relative falls in sea level,

resulting in sharp-based isolated coarse-grained shoreface deposits at distal localities. During more gradual rises in relative sea level, accumulation of fining- and deepening-upwards cycles was common. In both these cases accommodation space created by changes in relative sea level was rarely filled. Relatively short time breaks occurred between deposition of the stacked cycles, and these time breaks are evidenced by scouring on the order of a few metres and regional disconformities. After major falls in relative sea level, much of the shelf was subaerially exposed and major sequence boundaries formed during erosion and lowstand of sea level.

On an outcrop-scale the depositional model for shallow-marine rocks of the Mullaman Beds has many similarities with trends and cycles documented in other storm-dominated sequences. However, the depositional model developed here involves a more systematic approach, which attempts to place the role of storms in influencing depositional architecture into a sequence stratigraphic framework, where the effects of changes in relative sea level and sediment supply in the shallow-marine depositional systems are also addressed.

The similarity of storm-dominated depositional systems in many shallow-marine basins affords the possibility that the model outlined in this thesis, for Cretaceous rocks of the western shelf of the Carpentaria Basin, may have more widespread application. In particular, evidence from some of these other settings (especially the well-known sequences in the Cretaceous Western Interior Basin of North America) may be able to further substantiate or negate the ideas put forward in this thesis regarding the role of the rate of change of relative sea level in controlling the depositional architecture of storm-dominated systems.

~~~~~~
~~~~~~

REFERENCES

Aigner, T., 1982. Calcareous tempestites: storm-dominated stratification in Upper Muschelkalk limestones (Middle Trias, SW-Germany). *In* G. Einsele and A. Seilacher (editors), Cyclic and Event stratification. *Springer-Verlag, Berlin*, 180-198.

Aigner, T., 1985. Storm depositional systems. *In* G.M. Friedman, H.J. Neugebauer and A. Seilacher (editors), Lecture Notes in Earth Sciences. *Springer-Verlag, Berlin*, 174 pp.

Ainsworth, R.B., 1994. Marginal marine sedimentology and high resolution sequence analysis; Bearpaw-Horseshoe Canyon transition, Drumheller, Alberta. *Bulletin of Canadian Petroleum Geology*, 42, 26-54.

Ainsworth, R.B. and Crowley, S.F., 1994. Wave-dominated nearshore sedimentation and 'forced' regression: post-abandonment facies, Great Limestone Cyclothem, Stainmore, UK. *Journal of the Geological Society, London*, 151, 681-695.

Allen, G.P. and Posamentier, H.W., 1993. Sequence stratigraphy and facies models of an incised valley fill: The Gironde Estuary, France. *Journal of Sedimentary Petrology*, 63, 378-391.

Alley, N.F., 1988. Age and correlation of palynomorphs from the type Cadna-owie Formation, southwestern Eromanga Basin. *In* P.A. Jell and G. Playford (editors), Palynological and palaeobotanical studies in honour of Basil E. Balme. *Memoirs of the Association of Australasian Palaeontologists*, 5, 187-194.

Alley, N.F., 1991 (unpublished). Palynology of selected samples from the western Carpentaria Basin, Northern Territory. Report to A.A. Krassay and L.A. Frakes, 4pp.

Amajor, L.C. and Lerbekmo, J.F., 1990. The Viking (Albian) Reservoir sandstones of central and south-central Alberta, Canada - Part II. Lithofacies analysis, depositional environments and palaeogeographic setting. *Journal of Petroleum Geology*, 13, 421-436.

Anderson, J.B., 1983. Ancient glacial-marine deposits: their spatial and temporal distribution. *In* B.F. Molnia (editor), Glacial-Marine Sedimentation. *Plenum Press, New York*, 3-92.

Arthur, M.A., Jenkyns, H.C., Brumsack, H.J. and Schlanger, S.O., 1990. Stratigraphy, geochemistry, and palaeogeography of organic carbon-rich Cretaceous sequences. *In* R. Ginsburg and B. Beaudoin (editors), Cretaceous Resources, Events and Rhythms. *Kluwer Academic Press, Dordrect*, 63-119.

Banerjee, I. and Kidwell, S.M., 1991. Significance of molluscan shell beds in sequence stratigraphy: an example from the Lower Cretaceous Mannville Group of Canada. *Sedimentology*, 38, 913-934.

Bardossy, G. and Aleva, G.J.J., 1990. Lateritic Bauxites. Developments in economic geology 27. *Elsevier, Amsterdam*, 624 pp.

Barron, E.J., 1983. A warm equable Cretaceous: The nature of the problem. *Earth Science Reviews*, 19, 305-338.

Barron, E.J., 1987. Cretaceous plate tectonic reconstructions. *Palaeogeography, Palaeoclimatology, Palaeoecology*, 59, 3-29.

Barron, E.J., 1989. Severe storms during Earth history. *Geological Society of America, Bulletin* 101, 601-612.

Barron, E.J., Arthur, M.A. and Kauffman, E.G., 1985. Cretaceous rhythmic bedding sequences: a plausible link between orbital variations and climate. *Earth and Planetary Science Letters*, 72, 327-340.

Barron, E.J. and Peterson, W.H., 1990. Mid-Cretaceous ocean circulation: results from model sensitivity studies. *Paleoceanography*, 5, 319-337.

Barron, E.J., Sloan, J.C., III and Harrison, C.G.A., 1980. Potential significance of land-sea distribution and surface albedo variations as a climatic forcing factor; 180 m.y. to the present. *Palaeogeography, Palaeoclimatology, Palaeoecology*, 30, 17-40.

Barron, E.J., Thompson, S.L. and Schneider, S.H., 1981. An ice-free Cretaceous? Results from climate model simulations. *Science*, 212, 501-508.

Barron, E.J. and Washington, W.M., 1982. Cretaceous climate: a comparison of atmospheric simulations with the geologic record. *Palaeogeography, Palaeoclimatology, Palaeoecology*, 40, 103-133.

Barron, E.J. and Washington, W.M., 1984. The role of geographic variables in explaining paleoclimate: Results from Cretaceous climate model sensitivity studies. *Journal of Geophysical Research*, 9, 1267-1279.

Bechstadt, T. and Schweizer, T., 1991. The carbonate-clastic cycles of the East-Alpine Raibl Group: result of third-order sea-level fluctuations in the Carnian. *Sedimentary Geology*, 70, 241-270.

Berner, R.A., 1981. A new geochemical classification of sedimentary environments. *Journal of Sedimentary Petrology*, 51, 359-365.

Bhattacharya, J., 1993. The expression and interpretation of marine flooding surfaces and erosional surfaces in core; examples from the Upper Cretaceous Dunvegan Formation, Alberta foreland basin, Canada. *In* H.W. Posamentier, C.P. Summerhayes, B.U. Haq and G.P. Allen (editors), Sequence Stratigraphy and Facies Associations. *International Association of Sedimentologists, Special Publication* 18, 125-160.

Bhattacharya, J. and Walker, R.G., 1991. River- and wave-dominated depositional systems of the Upper Cretaceous Dunvegan Formation, northwestern Alberta. *Canadian Society of Petroleum Geologists, Bulletin* 39, 165-191.

Bless, M.J.M. and Paproth, E., 1989. Diachronism and tripartition of peat accumulation in paralic palaeoenvironments, Carboniferous and Cenozoic sequences in NW Europe. *International Journal of Coal Geology*, 12, 349-364.

Bolton, B.R., 1982 (unpublished). An investigation of Groote Eylandt Manganese Deposits. Final Report to B.H.P. Co. Ltd., 141pp.

Bourgeois, J., 1980. A transgressive shelf sequence exhibiting hummocky cross-stratification: the Cape Sebastian Sandstone (Upper Cretaceous), Southwestern Oregon. *Journal of Sedimentary Petrology*, 50, 681-702.

Brenchley, P.J., 1985. Storm influenced sandstone beds. *Modern Geology*, 9, 369-396.

Brown, D., 1993. Final sea level say sought: researchers can't find the yo-yo. *American Association of Petroleum Geologists, Explorer*, May 1993, p. 1 and 14-15.

Brown, L.F. and Fisher, W.L., 1977. Seismic-stratigraphic interpretation of depositional systems: examples from Brazilian rift and pull-apart basins. *In* C.E. Payton (editor), Seismic Stratigraphy-Applications to Hydrocarbon Exploration. *American Association of Petroleum Geologists, Memoir* 26, 213-248.

Burger, D., 1973. Spore zonation and sedimentary history of the Neocomian, Great Artesian Basin, Queensland. *In* J.E. Glover and G. Playford (editors), Mesozoic and Cainozoic Palynology: Essays in honour of Isabel Cookson. *Geological Society of Australia, Special Publication* 4, 87-118.

Burger, D., 1982. A basal Cretaceous dinoflagellate suite from northeastern Australia. *Palynology*, 6, 161-192.

Burger, D., 1986. Palynology, cyclic sedimentation, and palaeoenvironments in the Late Mesozoic of the Eromanga Basin. *In* D.I. Gravestock, P.S. Moore and G.M. Pitt (editors), Contributions to the Geology and Hydrocarbon Potential of the Eromanga Basin. *Geological Society of Australia, Special Publication* 12, 53-70.

Burgess, I.R., 1984. Carpentaria Basin: A regional analysis with reference to hydrocarbon potential. *APEA Journal* 1984, 7-18.

Burgess, I.R. and Reford, L., 1982 (unpublished). Farmout brochure NT/P30 and P31, Gulf of Carpentaria, offshore Northern Territory. Report for Canada Northwest Australia Oil NL and Ampol Exploration Ltd.

Caldeira, K. and Rampino, M.R., 1991. The mid-Cretaceous superplume, carbon dioxide, and global warming. *Geophysical Research Letters*, 18, 987-990.

Caldwell, W.G.E., 1984. Early Cretaceous transgressions and regressions in the Southern Interior plains. *In* D.F. Scott and D.J. Glass (editors), The Mesozoic of Middle North America. *Canadian Society of Petroleum Geologists, Memoir* 9, 173-203.

Cambell, K.S.W., Rogers, P.A. and Benbow, M., 1985. Fossiliferous Lower Devonian boulders from the Cretaceous of South Australia. *Geological Survey of South Australia, Quarterly Geological Notes* 62, 9-13.

Cathles, L.M. and Hallam, A., 1991. Stress-induced changes in plate density, Vail sequences, epeirogeny, and short-lived global sea level fluctuations. *Tectonics*, 10, 659-671.

Chappell, J. and Shackleton, N.J., 1986. Oxygen isotopes and sea level. *Nature*, 324, 137-140.

Cheel, R.J. and Leckie, D.A., 1992. Coarse-grained storm beds of the Upper Cretaceous Chungo Member (Wapiabi Formation), Southern Alberta, Canada. *Journal of Sedimentary Petrology*, 62, 933-945.

Christie-Blick, N., 1991. Onlap, offlap, and the origin of unconformity-bounded depositional sequences. *Marine Geology*, 97, 35-56.

Cloetingh, S., 1988. Intraplate stresses: A tectonic cause for third-order cycles in apparent sealevel? *In* C.K. Wilgus, B.S. Hastings, C.G.St.C. Kendall, H.W. Posamentier, C.A. Ross and J.C. Van Wagoner (editors), Sea-level Changes-An Integrated Approach. *Society of Economic Paleontologists and Mineralogists, Special Publication* 42, 19-29.

Cloetingh, S., Kooi, H. and Groenewoud, W., 1989. Intraplate stresses and sedimentary basin evolution. *In* R.A. Price (editor), Origin and Evolution of Sedimentary Basins and their Energy and Mineral Resources. *International Union of Geodesy and Geophysics, Geophysical Monograph* 48, 1-16.

Cloetingh, S., McQueen, H. and Lambeck, K., 1985. On a tectonic mechanism for regional sea level variations. *Earth and Planetary Science Letters*, 75, 157-166.

Cohen, A.D., 1984. The Okefenokee swamp: a low sulphur end-member of a shoreline-related depositional model for coastal plain coals. *In* R.A. Rahmani and R.M. Flores (editors), Sedimentology of Coal and Coal bearing Sequences. *International Association of Sedimentologists, Special Publication* 7, 231-240.

Cooper, M.R., 1977. Eustasy during the Cretaceous: its implications and importance. *Palaeogeography, Palaeoclimatology, Palaeoecology*, 22, 1-60.

Cotter, E., 1990. Storm effects on siliciclastic and carbonate shelf sediments in the medial Silurian succession of Pennsylvania. *In* T. Aigner and R.H. Dott (editors), Processes and Patterns in Epeiric Basins. *Sedimentary Geology*, 69, 245-258.

Cotter, E. and Graham, J.R., 1991. Coastal plain sedimentation in the late Devonian of southern Ireland; hummocky cross-stratification in fluvial deposits? *Sedimentary Geology*, 72, 201-224.

Craft, J.E. and Bridge, J.S., 1987. Shallow-marine sedimentary processes in the Late Devonian Catskill Sea, New York State. *Geological Society of America, Bulletin* 98, 338-355.

Crespin, I., 1963. Lower Cretaceous arenaceous foraminifera of Australia. *Bureau of Mineral Resources, Australia, Bulletin* 66, 110pp.

Crowley, T.J., Short, D.A., Mengel, J.G. and North, G.R., 1986. Role of seasonality in the evolution of climate during the last 100 million years. *Science*, 231, 579-584.

Curtis, C.D., 1977. Sedimentary geochemistry: environments and processes dominated by involvement of an aqueous phase. *Philosophical Transactions of the Royal Society of London*, A286. 353-372.

Dalrymple, R.W., Zaitlin, B.A. and Boyd, R., 1992. Estuarine facies models: conceptual basis and stratigraphic implications. *Journal of Sedimentary Petrology*, 62, 1130-1146.

Dam, G., 1990. Palaeoenvironmental significance of trace fossils from the shallow marine Lower Jurassic Neill Klinter Formation, East Greenland. *Palaeogeography, Palaeoclimatology, Palaeoecology*, 79, 221-248.

Dam, G. and Surlyk, F., 1993. Cyclic sedimentation in a large wave- and storm-dominated anoxic lake; Kap Stewart Formation (Rhaetian-Sinemurian), Jameson Land, East Greenland. *In* H.W. Posamentier, C.P. Summerhayes, B.U. Haq and G.P. Allen (editors), Sequence Stratigraphy and Facies Associations. *International Association of Sedimentologists, Special Publication* 18, 419-448.

David, T.W.E., 1950. The geology of the Commonwealth of Australia, by Sir T.W.E. David and edited by W.R. Browne, Volume 1. *Arnold, London.*

Davies, G.F., 1988. Role of the lithosphere in mantle convection. *Journal of Geophysical Research*, 93-B9, 10451-10466.

Davis, H.R. and Byers, C.W., 1989. Shelf sandstones in the Mowry Shale: evidence for deposition during Cretaceous sea level falls. *Journal of Sedimentary Petrology*, 59, 548-560.

Davis, H.R., Byers, C.W. and Pratt, L.M., 1989. Depositional mechanisms and organic matter in Mowry Shale (Cretaceous), Wyoming. *American Association of Petroleum Geologists, Bulletin* 73, 1103-1116.

Day, R.W., 1969. The Lower Cretaceous of the Great Artesian Basin. *In* K.S.W. Campbell (editor), Stratigraphy and Palaeontology, Essays in honour of Dorothy Hill. *Australian National University Press, Canberra,* 140-143.

Day, R.W., Whitaker, W.G., Murray, C.G., Wilson, I.H. and Grimes, K.G., 1983 (unpublished). Queensland Geology. *Geological Society of Queensland, Publication* 383, 639pp.

Deighton, I., 1985 (unpublished). Foraminiferal age and palaeoenvironmental analysis of Duyken-1, Carpentaria Basin. Report to Canada Northwest Australia Oil NL, 5pp.

Dettmann, M.E., 1973. Angiospermous pollen from Albian to Turonian sediments of eastern Australia. *In* J.E. Glover and G. Playford (editors), Mesozoic and Cainozoic Palynology: Essays in honour of Isabel Cookson. *Geological Society of Australia, Special Publication* 4, 3-34.

Dettmann, M.E., 1981. The Cretaceous Flora. *In* A. Keast (editor), Ecological Biogeography of Australia, vol. 1. *Junk, the Hague,* 357-375.

Dettmann, M.E., Molnar, R.E., Douglas, J.G., Burger, D., Fielding, C., Clifford, H.T., Francis, J., Jell, P., Rich, T., Wade, M., Rich, P.V., Pledge, N., Kemp, A. and Rozefelds, A., 1992. Australian Cretaceous terrestrial faunas and floras: biostratigraphic and biogeographic implications. *Cretaceous Research,* 13, 207-262.

Dettmann, M.E. and Playford, G., 1969. Palynology of the Australian Cretaceous: a review. *In* K.S.W. Campbell (editor), Stratigraphy and Palaeontology, Essays in honour of Dorothy Hill. *Australian National University Press, Canberra,* 174-210.

Devlin, W.J., Rudolph, K.W., Shaw, C.A. and Ehman, K.D., 1993. The effect of tectonic and eustatic cycles on accommodation and sequence-stratigraphic framework in the Upper Cretaceous foreland basin of southwestern Wyoming. *In* H.W. Posamentier, C.P. Summerhayes, B.U. Haq and G.P. Allen (editors), Sequence Stratigraphy and Facies Associations. *International Association of Sedimentologists, Special Publication* 18, 419-448.

Devoy, R.J.N. (editor), 1987. Sea surface studies, a global view. *Croom Helm, New York,* 649pp.

Dodson, R.G., 1967. Coal at Gove Peninsula. *Bureau of Mineral Resources, Australia, Record* 1967/87.

Dorman, F.H. and Gill, E.D., 1959. Oxygen isotope palaeotemperature measurements of Australian fossils. *Proceedings of the Royal Society, Victoria,* 71, 73-98.

Dott, R.H., Jr. and Bourgeois, J., 1982. Hummocky stratification: Significance of its variable bedding sequences. *Geological Society of America, Bulletin* 93, 663-680.

Douglas, J.G. and Williams, G.E., 1982. Southern polar forests: the Early Cretaceous floras of Victoria and their palaeoclimatic significance. *Palaeogeography, Palaeoclimatology, Palaeoecology*, 39, 171-185.

Doutch, H.F., 1976. Petroleum potential of the Carpentaria Basin, Queensland. *In* Economic geology of Australia and Papua New Guinea, Vol. 3, Petroleum. *Australasian Institute of Mining and Metallurgy, Melbourne.*

Duke, W.L., 1984. Paleohydraulic analysis of hummocky cross-stratified sands indicates equivalence with wave-formed flat bed: Pleistocene Lake Bonneville deposits, northern Utah. *American Association of Petroleum Geologists, Bulletin* 68, 472 (abstract).

Duke, W.L., 1985. Hummocky cross-stratification, tropical hurricanes, and intense winter storms. *Sedimentology*, 32, 167-194.

Duke, W.L., 1990. Geostrophic circulation or shallow marine turbidity currents? The dilemma of paleoflow patterns in storm-influenced prograding shoreline systems. *Journal of Sedimentary Petrology*, 60, 870-883.

Duke, W.L., Arnott, R.W.C. and Cheel, R.J., 1991. Shelf sandstones and hummocky cross-stratification: New insights on a stormy debate. *Geology*, 19, 625-628.

Dypvik, H., 1992. Sedimentary rhythms in the Jurassic and Cretaceous of Svalbard. *Geological Magazine*, 129, 93-99.

Dypvik, H., Nagy, J., Eikeland, T.A., Backer-Owe, K. and Johansen, H., 1991. The Bathonian to Hauterivian Janusfjellet Subgroup in Spitsbergen-depositional conditions as reflected in field appearance and sediment composition. *Sedimentary Geology*, 72, 55-78.

Edzwald, J.K. and O'Melia, C.R., 1975. Clay distributions in recent estuarine sediments. *Clays and Clay Minerals*, 23, 39-44.

Einsele, G. and Seilacher, A., 1982. Cyclic and Event Stratification. *Springer-Verlag, Berlin*, 550pp.

Ekdale, A.A., 1988. Pitfalls of paleobathymetric interpretations based on trace fossil assemblages. *Palaios*, 3, 464-472.

Ekdale, A.A. and Mason, T.R., 1988. Characteristic trace-fossil associations in oxygen-poor sedimentary environments. *Geology*, 16, 720-723.

Embleton, B.J.J., 1984. Australia's global setting: past global settings. *In* J.J. Veevers (editor), Phanerozoic Earth history of Australia. Oxford Geological Science Series 2. *Clarendon Press, Oxford*, 11-17.

Ende, B.A. am, 1991. Depositional environments, palynology, and age of the Dakota Formation, south-central Utah. *In* J.D. Nations and J.G. Eaton (editors), Stratigraphy, Depositional Environments, and Sedimentary Tectonics of the Western Margin, Cretaceous Western Interior Seaway. *Geological Society of America, Special Paper* 260, 65-83.

England, B.M., 1976. Glendonites, their origins and description. *The Mineralogical Record*, 7, 60-68.

Erba, E. and Premoli-Silva, I., 1992 (unpublished). Apticore-Albicore Workshop Field Guide, 44pp.

Ericksen, M.C. and Slingerland, R., 1990. Numerical simulations of tidal and wind-driven circulation in the Cretaceous Interior Seaway of North America. *Geological Society of America, Bulletin* 102, 1499-1516.

Evans, P.R., 1966. Contribution to the palynology of northern Queensland and Papua. *Bureau of Mineral Resources, Australia, Record* 1966/198.

Exon, N.F. and Burger, D., 1981. Sedimentary cycles in the Surat Basin and global changes in sea level. *BMR Journal of Australian Geology and Geophysics*, 6, 153-159.

Exon, N.F. and Senior, B.R., 1976. The Cretaceous of the Eromanga and Surat Basins. *BMR Journal of Australian Geology and Geophysics*, 1, 33-50.

Fischer, A.G., 1986. Climatic rhythms recorded in strata. *Annual Reviews of Earth Planetary Science*, 14, 351-376.

Fischer, A.G. and Bottjer, D.J. (editors), 1991. Orbital forcing and sedimentary sequences. *Journal of Sedimentary Petrology (Special Issue)*, 61, 1063-1252.

Frakes, L.A. and Bolton, B.R., 1984. Origin of manganese giants: sea-level change and anoxic-oxic history. *Geology*, 12, 83-86.

Frakes, L. A., Burger, D., Apthorpe, M., Wiseman, J., Dettmann, M., Alley, N., Flint, R., Gravestock, D., Ludbrook, N., Backhouse, J., Skwarko, S., Scheibnerova, V., McMinn, A., Moore, P. S., Bolton, B. R., Douglas, J. G., Christ, R., Wade, M., Molnar, R. E., McGowran, B., Balme, B. E. and Day, R. A., 1987. Australian Cretaceous shorelines, stage by stage. *Palaeogeography, Palaeoclimatology, Palaeoecology*, 59, 31-48.

Frakes, L.A. and Francis, J.E., 1988. A guide to Phanerozoic cold polar climates from high-latitude ice-rafting in the Cretaceous. *Nature*, 333, 547-549.

Frakes, L.A., Francis, J.E. and Syktus, J.I., 1992. Climate modes of the Phanerozoic. *Cambridge University Press, Cambridge, England,* 274pp.

Frakes, L.A. and Krassay, A.A., 1992. Discovery of probable ice-rafting in the Late Mesozoic of the Northern Territory and Queensland. *Australian Journal of Earth Sciences*, 39, 115-119.

Francis, J.E., 1986. Growth rings in Cretaceous and Tertiary wood from Antarctica and their paleoclimatic implications. *Palaeontolgy*, 29, 665-684.

Francis, J.E., 1989. Palaeoclimatic significance of Cretaceous-early Tertiary fossil forests of the Antarctic Peninsula. *In* M.R.A. Thomson, J.A. Crane and J.W. Thomson (editors), Geological Evolution of Antarctica. *Cambridge University Press, Cambridge, England*, 623-627.

Frey, R.W. and Goldring, R., 1992. Marine event beds and recolonization surfaces as revealed by trace fossil analysis. *Geological Magazine*, 129, 325-335.

Gallagher, K.G. and Lambeck, K., 1989. Subsidence, sedimentation, and sea-level changes in the Eromanga Basin. *Basin Research*, 2, 115-131.

Galloway, W.E., 1989. Genetic stratigraphic sequences in basin analysis I: architecture and genesis of flooding-surface bounded depositional units. *American Association of Petroleum Geologists, Bulletin* 73, 125-142.

Gibbs, R.J., 1977. Clay mineral segregation in the marine environment. *Journal of Sedimentary Petrology*, 47, 237-243.

Gibson, D.L., Powell, B.S., Doutch, H.F., Smart, J. and Grimes, K.G., 1973. Shallow stratigraphic drilling in the Carpentaria and Laura Basins, 1972. *Bureau of Mineral Resources, Australia, Record* 1973/77.

Gilbert, R., 1984. The movement of gravel by the alga *Fucus Vesiculosus* (L.) on an Arctic intertidal flat. *Journal of Sedimentary Petrology*, 54, 463-468.

Giunchi, C., Sabadini, R. and Zerbini, S., 1993. Basal drag and laterally varying lithosphere: implications for sea-level fluctuations and intraplate deformation. *Global and Planetary Change*, 8, 127-134.

Goodwin, P.W. and Anderson, E.J., 1985. Punctuated aggradational cycles: A general hypothesis of episodic stratigraphic accumulation. *Journal of Geology*, 93, 515-533.

Gravestock, D.I., Moore, P.S. and Pitt, G.M. (editors), 1986. Contributions to the Geology and Hydrocarbon Potential of the Eromanga Basin. *Geological Society of Australia, Special Publication* 12, 384pp.

Gregory, R.T., Douthitt, C.B., Duddy, I.R., Rich, P.V. and Rich, T.H., 1989. Oxygen isotopic composition of carbonate concretions from the Lower Cretaceous of Victoria, Australia: implications for the evolution of meteoric waters on the Australian continent in a paleopolar environment. *Earth and Planetary Science Letters*, 92, 27-42.

Grimes, K.G., 1974. Mesozoic and Cainozoic geology of Lawn Hill, Westmoreland, Mornington, and Cape Van Diemen 1:250,000 Sheet areas, Queensland. *Bureau of Mineral Resources, Australia, Record* 1974/106.

Grubb, P.L.C., 1970. Mineralogy, geochemistry, and genesis of bauxite deposits on the Gove and Mitchell Plateaux, northern Australia. *Mineralium Deposita*, 5, 248-272.

Gurnis, M., 1990. Ridge spreading, subduction, and sea level fluctuations. *Science*, 250, 970-972.

Gurnis, M., 1993. Depressed continental hypsometry behind oceanic trenches: a clue to subduction controls on sea-level change. *Geology*, 21, 29-32.

Gurnis, M., 1994. Vertical motion of Australia in the Cretaceous: a mantle dynamics perspective. *Geological Society of Australia, Newsletter* 19, 3-7.

Hadley, D.F. and Elliott, T., 1993. The sequence stratigraphic significance of erosive-based shoreface sequences in the Cretaceous Mesaverde Group of northwestern Colorado. *In* H.W. Posamentier, C.P. Summerhayes, B.U. Haq and G.P. Allen (editors), Sequence Stratigraphy and Facies Associations. *International Association of Sedimentologists, Special Publication* 18, 521-535.

Haig, D.W., 1979a. Global distribution patterns for mid-Cretaceous foraminiferids. *Journal of Foraminiferal Research*, 9, 29-40.

Haig, D.W., 1979b. Cretaceous foraminiferal biostratigraphy of Queensland. *Alcheringa*, 3, 171-187.

Haig, D.W., 1991 (unpublished). Micropalaeontological analyses of samples from the onshore Carpentaria Basin and Eromanga Basin. Report to L.A. Frakes, 8pp.

Haig, D.W., 1992. Aptian-Albian foraminifera from Ocean Drilling Program Site 766, Cuvier Abyssal Plain, and comparison with coeval faunas from the Australian region. *Proceedings of the Ocean Drilling Program, Scientific Results* 123, 271-297.

Haig, D.W. and Barnbaum, D., 1978. Early Cretaceous microfossils from the type Wallumbilla Formation, Surat Basin, Queensland. *Alcheringa*, 2, 159-178.

Haig, D.W. and Lynch, D.A., 1993. A late early Albian marine transgressive pulse over northeastern Australia, precursor to epeiric basin anoxia: Foraminiferal evidence. *Marine Micropalaeontology*, 22, 311-362.

Hallam, A., 1984. Continental humid and arid zones during the Jurassic and Cretaceous. *Palaeogeography, Palaeoclimatology, Palaeoecology*, 47, 195-223.

Hallam, A., Grose, J.A. and Ruffell, A.H., 1991. Palaeoclimatic significance of changes in clay mineralogy across the Jurassic-Cretaceous boundary in England and France. *Palaeogeography, Palaeoclimatology, Palaeoecology*, 81, 173-187.

Hamblin, A.P. and Walker, R.G., 1979. Storm-dominated shallow marine deposits: the Fernie-Kootenay (Jurassic) transition, southern Rocky Mountains. *Canadian Journal of Earth Sciences*, 16, 1673-1690.

Hancock, J.M. and Kauffman, E.G., 1979. The great transgressions of the Late Cretaceous. *Journal of the Geological Society, London*, 136, 175-186.

Haq, B.U., Hardenbol, J. and Vail, P.R., 1987. Chronology of fluctuating sea levels since the Triassic. *Science*, 235, 1156-1167.

Haq, B.U., Hardenbol, J. and Vail, P.R., 1988. Mesozoic and Cenozoic chronostratigraphy and eustatic cycles. *In* C.K. Wilgus, B.S. Hastings, C.G.St.C. Kendall, H.W. Posamentier, C.A. Ross and J.C. Van Wagoner (editors), Sea-level Changes-An Integrated Approach. *Society of Economic Paleontologists and Mineralogists, Special Publication* 42, 71-108.

Harland, W.B., Armstrong, R.L., Cox, A.V., Craig, L.E., Smith, A.G. and Smith, D.G., 1990. A geologic time scale 1989. *Cambridge University Press, Cambridge, England,* 263pp.

Harms, J.C., Southard, J.B., Spearing, D.R. and Walker, R.G., 1975. Depositional environments as interpreted from primary sedimentary structures and stratification sequences. *Society of Economic Paleontologists and Mineralogists, Short Course* 2, 161pp.

Harrison, C.G.A., 1990. Long-term eustasy and epeirogeny in continents. *In* R. Revelle (editor), Sea Level Change. National Research Council, Studies in Geophysics. *National Academy Press, Washington, D.C.*, 141-158.

Hart, B.S. and Plint, A.G., 1993. Origin of an erosion surface in shoreface sandstones of the Kakwa Member (Upper Cretaceous Cardium Formation, Canada): importance for reconstruction of stratal geometry and depositional history. *In* H.W. Posamentier, C.P. Summerhayes, B.U. Haq and G.P. Allen (editors), Sequence Stratigraphy and Facies Associations. *International Association of Sedimentologists, Special Publication* 18, 451-467.

Hay, W.W. and Leslie, M.A., 1990. Could possible changes in global groundwater reservoir cause eustatic sea level fluctuations? *In* R. Revelle (editor), Sea Level Change. National Research Council, Studies in Geophysics. *National Academy Press, Washington, D.C.*, 161-170.

Helby, R.J., Morgan, R. and Partridge, A.D., 1987. A palynological zonation of the Australian Mesozoic. *In* P.A. Jell (editor), Studies in Australian Mesozoic Palynology. *Memoirs of the Association of Australasian Palaeontologists*, 4, 1-94.

Hem, J.D., 1972. Redox processes at surfaces of manganese oxide and their effects on aqueous metal ions. *Chemical Geology*, 21, 199-218.

Higgs, R., 1991. The Bude Formation (Lower Westphalian), SW England: siliciclastic shelf sedimentation in a large equitorial lake. *Sedimentology*, 38, 445-469.

Hughes, R.J., 1978. The geology and mineral occurrences of Bathurst Island, Melville Island, and Cobourg Peninsula, Northern Territory. *Bureau of Mineral Resources, Australia, Bulletin* 177, 72pp.

Hughes, R.J. and Senior, B.R., 1973. Progress report on the geology of the Bathurst Island, Melville Island, Cobourg Peninsula and Fog Bay 1:250,000 Sheet areas, Northern Territory. *Bureau of Mineral Resources, Australia, Record* 1973/52.

Hunt, D. and Tucker, M.E., 1992. Stranded parasequences and the forced regressive wedge systems tract: deposition during base-level fall. *Sedimentary Geology*, 81, 1-9.

Hunt, D. and Tucker, M.E., 1993. Sequence stratigraphy of carbonate shelves with an example from the mid-Cretaceous (Urgonian) of southeastern France. *In* H.W. Posamentier, C.P. Summerhayes, B.U. Haq and G.P. Allen (editors), Sequence Stratigraphy and Facies Associations. *International Association of Sedimentologists, Special Publication* 18, 307-341.

Hutton, L.J. and Grimes, K.G., 1983. Lawn Hill 1:250,000 geological map, Queensland. *Department of Mines, Queensland.*

Imbrie, J. and Imbrie, J.Z., 1980. Modeling the climatic response to orbital variations. *Science*, 207, 943-953.

Ingram, B., 1981 (unpublished). Palynological report on two samples from Groote Eylandt. Report to B.H.P. Co. Ltd., 2pp.

Ingram, B., 1985 (unpublished). Palynology report AP68, Duyken No. 1 Cretaceous. Report to Canada Northwest Australia Oil NL, 17pp.

Ingram, J.A., 1972. Burketown, Queensland - 1:250 000 Geological Series. *Bureau of Mineral Resources, Australia, Explanatory Notes* SE/54-6.

Jackson, M.J., Muir, M.D. and Plumb, K.A., 1987. Geology of the southern McArthur Basin, Northern Territory. *Bureau of Mineral Resources, Australia, Bulletin* 220, 163pp.

Jacobs, D.K. and Sahagian, D.L., 1993. Climate-induced fluctuations in sea level during non-glacial times. *Nature*, 361, 710-712.

Jansen, J.H.F., Woensdregt, C.F., Kooistra, M.J. and van der Gaast, S.J., 1987. Ikaite pseudomorphs in the Zaire deep-sea fan: an intermediate between calcite and porous calcite. *Geology*, 15, 245-248.

Jell, P.A. and Duncan, P.M., 1986. Invertebrates, mainly insects, from the freshwater, Lower Cretaceous, Koonwarra Fossil Bed (Korumburra Group), South Gippsland, Victoria. *In* P.A. Jell and J. Roberts (editors), Plants and Invertebrates from the Lower Cretaceous Koonwarra Fossil Bed, South Gippsland, Victoria. *Memoirs of the Association of Australasian Palaeontologists*, 3, 111-205.

Jenkyns, H.C., 1980. Cretaceous anoxic events: from continents to oceans. *Journal of the Geological Society, London*, 137, 171-188.

Jennette, D.C., Jones, C.R., Van Wagoner, J.C. and Larsen, J.E., 1991. High-resolution sequence stratigraphy of the Upper Cretaceous Tocito Sandstone: the relationship between incised valleys and hydrocarbon accumulation, San Juan Basin, New Mexico. *In* J.C. Van Wagoner, C.R. Jones, D.R. Taylor, D. Nummedal, D.C. Jennette and G.W. Riley (editors), Sequence Stratigraphy Applications to Shelf Sandstone Reservoirs, Outcrop to Subsurface Examples. *American Association of Petroleum Geologists, Field Conference Guidebook.*

Jennette, D.C. and Pryor, W.A., 1993. Cyclic alteration of proximal and distal storm facies: Kope and Fairview Formations (Upper Ordovician), Ohio and Kentucky. *Journal of Sedimentary Petrology*, 63, 183-203.

Jewell, P.W., 1993. Water-column stability, residence times, and anoxia in the Cretaceous North American seaway. *Geology*, 21, 579-582.

Kamola, D.L. and Huntoon, J.E., 1994. Changes in rate of transgression across the Permian White Rim Sandstone, Southern Utah. *Journal of Sedimentary Research*, B64, 202-210.

Karner, G.D., 1986. Effects of lithospheric in-plane stess on sedimentary basin stratigraphy. *Tectonics*, 5, 573-588.

Kauffman, E.G., 1984. Paleobiogeography and evolutionary response dynamic in the Cretaceous Western Interior Seaway of North America. *In* G.E.G. Westermann (editor), Jurassic-Cretaceous Biochronology and Palaeogeography of North America. *Geological Association of Canada, Special Paper* 27.

Kauffman, E.G., 1988. Concepts and methods of high-resolution event stratigraphy: *Annual Review of Earth and Planetary Sciences*, 16, 605-654.

Kemper, E., 1987. Das klima der kreide-Zeit. *Geologisches Jahrbuch,* A96, 5-185.

Kemper, E. and Schmitz, H.H., 1975. Stellate nodules from the Upper Deer Bay Formation (Valaginian) of Arctic Canada. *Geological Survey of Canada, Paper* 75-1C, 11pp.

Kennedy, G.L., Hopkins, D.M. and Pickthorn, W.J., 1987. Ikaite, the glendonite precursor, in estuarine sediments at Barrow, Arctic Alaska. *Geological Society of America, Abstracts* 19, 725.

King, L.M., 1994. Turbidite to storm transition in a migrating foreland basin: the Kendal Group (Upper Silurian), northwest England. *Geological Magazine*, 131, 255-267.

Klein, G.deV. and Hsui, A.T., 1987. Origin of cratonic basins. *Geology*, 15, 1094-1098.

Klein, G.deV. and Ryer, T.A., 1978. Tidal circulation patterns in Precambrian, Paleozoic, and Cretaceous epeiric and mioclinal shelf seas. *Geological Society of America, Bulletin* 89, 1050-1058.

Kominz, M.A. and Bond, G.C., 1991. Unusually large subsidence and sea-level events during middle Palaeozoic time: New evidence supporting mantle convection models for supercontinent assembly. *Geology*, 19, 56-60.

Koss, J.E., Ethridge, F.G. and Schumm, S.A., 1994. An experimental study of the effects of base-level change on fluvial, coastal plain and shelf systems. *Journal of Sedimentary Research*, B64, 90-98.

Krassay, A.A., 1992. Litho-stratigraphy and sequence stratigraphy of a mid-Cretaceous shelf environment from scattered 'spot' outcrops in the Carpentaria Basin, Northern Territory, Australia. *American Association of Petroleum Geologists, Annual Convention Abstracts* 1992, 84.

Krassay, A.A., 1994a. Storm features of siliciclastic shelf sedimentation in the mid-Cretaceous epeiric seaway of northern Australia. *Sedimentary Geology*, 89, 241-264.

Krassay, A.A., 1994b. The Cretaceous geology of northeastern Arnhem Land, Northern Territory. *Australian Geological Survey Organisation, Australia, Record* 1994/40, 85pp.

Krassay, A.A. and Frakes, L.A., 1991 (unpublished). Western and southern margins, Gulf of Carpentaria 1989-90 field investigations - part 2. Report to B.H.P. Co. Ltd., 11pp.

Krassay, A.A. and Frakes, L.A., 1992. Litho-stratigraphy and sequence stratigraphy of a mid-Cretaceous shelf environment in the Gulf of Carpentaria. *Geological Society of Australia, Abstracts* 32, 108-109.

Kreisa, R.D., 1980. Storm-generated sedimentary structures in subtidal marine facies with examples from the Middle and Upper Ordovician of southwestern Virginia. *Journal of Sedimentary Petrology*, 51, 823-848.

Larson, R.L., 1991a. Latest pulse of Earth: Evidence for a mid-Cretaceous superplume. *Geology*, 19, 547-550.

Larson, R.L., 1991b. Geological consequences of superplumes. *Geology*, 19, 936-966.

Leckie, D.A., 1988. Wave-formed, coarse-grained ripples and their relationship to hummocky cross-stratification. *Journal of Sedimentary Petrology*, 58, 607-622.

Leckie, D.A. and Krystinik, L.F., 1989. Is there evidence for geostrophic currents preserved in the sedimentary record of inner to middle-shelf deposits? *Journal of Sedimentary Petrology*, 59, 862-870.

Leckie, D.A. and Walker, R.G., 1982. Storm- and tide-dominated shorelines in Late Cretaceous Moosebar-Lower Gates interval - outcrop equivalents of deep basin gas trap in western Canada. *American Association of Petroleum Geologists, Bulletin* 66, 138-157.

Legarreta, L. and Uliana, M.A., 1991. Jurassic-Cretaceous marine oscillations and geometry of back-arc basin fill, central Argentine Andes. *In* D.I.M. Macdonald (editor), Sedimentation, Tectonics, and Eustasy. *International Association of Sedimentologists, Special Publication* 12, 429-450.

Leithold, E.L. and Bourgeois, J.E., 1984. Characteristics of coarse-grained sequences deposited in nearshore wave-dominated environments - examples from the Miocene of south-west Oregon. *Sedimentology*, 31, 749-775.

Leithold, E.L., 1994. Stratigraphical architecture at the muddy margin of the Cretaceous Western Interior Seaway, southern Utah. *Sedimentology*, 41, 521-542.

Loutit, T.S., Hardenbol, J., Vail, P.R. and Baum, G.R., 1988. Condensed sections: the key to age dating and correlation of continental margin sequences. *In* C.K. Wilgus, B.S. Hastings, C.G.St.C. Kendall, H.W. Posamentier, C.A. Ross and J.C. Van Wagoner (editors), Sea-level Changes-An Integrated Approach. *Society of Economic Paleontologists and Mineralogists, Special Publication* 42, 183-213.

Lowenstam, H.A., 1964. Palaeotemperatures of the Permian and Cretaceous Periods. *In* A.E.M. Nairn (editor), Problems in Palaeoclimatology. *Interscience, London*, 227-252.

Ludbrook, N.H., 1966. Cretaceous biostratigraphy of the Great Artesian Basin in South Australia. *Geological Survey of South Australia, Bulletin* 40, 223pp.

MacEachern, J.A. and Pemberton, S.G., 1992. Ichnological aspects of Cretaceous shoreface successions and shoreface variability in the western interior seaway of North America. *In* S.G. Pemberton (editor), Applications of Ichnology to Petroleum Exploration. *Society of Economic Paleontologists and Mineralogists, Core Workshop Notes* 17, 57-84.

Maples, C.G. and Suttner, L.J., 1990. Trace fossils and marine-nonmarine cyclicity in the Fountain Formation (Pennslyvanian: Morrowan/Atokan) near Manitou Springs, Colorado. *Journal of Paleontology*, 64, 859-880.

Martin, H.A., 1982 (unpublished). Palynological investigations of Cretaceous sediments from the Carpentaria Basin. Report 1982/26 to the B.H.P. Co. Ltd., 12pp.

Martinsen, O.J., Martinsen, R.S. and Steidtmann, J.R., 1993. Mesaverde Group (Upper Cretaceous), Southeastern Wyoming: Allostratigraphy versus sequence stratigraphy in a tectonically active area. *American Association of Petroleum Geologists, Bulletin* 77, 1351-1373.

Maynard, J.R. and Leeder, M.R., 1992. On the periodicity and magnitude of Late Carboniferous glacio-eustatic sea-level changes. *Journal of the Geological Society, London*, 149, 303-311.

McMinn, A. and Burger, D., 1986. Palynology and palaeoenvironments of the Toolebuc Formation (sensu lato) in the Eromanga Basin. *In* D.I. Gravestock, P.S. Moore and G.M. Pitt (editors), Contributions to the Geology and Hydrocarbon Potential of the Eromanga Basin. *Geological Society of Australia, Special Publication* 12, 139-154.

Meyers, N.A., 1969. Carpentaria Basin. *Geological Survey of Queensland, Australia, Report* 34.

Miall, A.D., 1985. Architectural-element analysis: a new method of facies analysis applied to fluvial deposits. *Earth Science Reviews*, 22, 261-308.

Miall, A.D, 1986. Eustatic sea level changes interpreted from seismic stratigraphy: a critique of the methodology with particular reference to the North Sea Jurassic record. *American Association of Petroleum Geologists, Bulletin* 70, 131-137.

Miall, A.D., 1991. Stratigraphic sequences and their chronostratigraphic correlation. *Journal of Sedimentary Petrology*, 61, 497-505.

Miall, A.D., 1992a. Alluvial models. *In* R.G. Walker and N.P. James (editors), Facies Models, Response to Sea Level Change. *Geological Association of Canada, Saint Johns, Newfoundland*, 119-142.

Miall, A.D., 1992b. Exxon global cycle chart: an event for every occasion. *Geology*, 20, 787-790.

Mitchum, J.R. and Van Wagoner, J.C., 1991. High frequency sequences and their stacking patterns: sequence stratigraphic evidence of high frequency eustatic cycles. *Sedimentary Geology*, 70, 131-160.

Mode, W. N., Nelson, A. R. and Brigham, J.K., 1983. A facies model of Quaternary glacial-marine cyclic sedimentation along eastern Baffin Island, Canada. *In* B.F. Molnia (editor), Glacial-Marine Sedimentation. *Plenum Press, New York*, 495-533.

Monaco, P., 1992. Hummocky cross-stratified deposits and turbidites in some sequences of the Umbria-Marche area (central Italy) during the Toarcian. *Sedimentary Geology*, 77, 123-142.

Morgan, R., 1980. Eustasy in the Australian Early and Middle Cretaceous. *New South Wales Geological Survey, Bulletin* 27, 105 pp.

Needham, R.S., Smart, J., Grimes, K.G. and Doutch, H.F., 1971. Stratigraphic drilling in the southern Carpentaria Basin, 1970. *Bureau of Mineral Resources, Australia, Record* 1971/142.

Noakes, L.C., 1949. A geological reconnaissance of the Katherine-Darwin region, Northern Territory. *Bureau of Mineral Resources, Australia, Bulletin* 45, 54pp.

Nottvedt, A. and Kreisa, R.D., 1987. Model for the combined-flow origin of hummocky cross-stratification. *Geology*, 15, 357-361.

Nummedal, D., Riley, G.W. and Templet, P.L., 1993. High-resolution sequence architecture: a chronostratigraphic model based on equilibrium profile studies. *In* H.W. Posamentier, C.P. Summerhayes, B.U. Haq and G.P. Allen (editors), Sequence Stratigraphy and Facies Associations. *International Association of Sedimentologists, Special Publication* 18, 55-68.

Oglesby, R.J., 1989. A GCM study of Antarctic glaciation. *Climate Dynamics*, 3, 135-156.

Open University Course Team, 1989. Ocean Circulation. *Pergamon Press, Oxford, England*, 238pp.

Ovenshine, A. T., 1970. Observations of iceberg rafting in Glacier Bay, Alaska, and the identification of ancient ice-rafted deposits. *Geological Society of America, Bulletin* 81, 891-894.

Ozimic, S., 1986. The geology and petrophysics of the Toolebuc Formation and its time equivalents, Eromanga and Carpentaria Basins. *In* D.I. Gravestock, P.S. Moore and G.M. Pitt (editors), Contributions to the Geology and Hydrocarbon Potential of the Eromanga Basin. *Geological Society of Australia, Special Publication* 12, 119-139.

Pain, C.F. and Ollier, C.D., 1992. Ferricrete in Cape York Peninsula, North Queensland. *BMR Journal of Australian Geology and Geophysics*, 13, 207-212.

Paltech 1979a (unpublished). Micropalaeontological studies of the Groote Eylandt mid-Cretaceous. Report 1979/4 to B.H.P. Co. Ltd., 17pp.

Paltech 1979b (unpublished). Age and palaeobiology of the Groote Eylandt manganiferous sediments. Report 1979/9 to B.H.P. Co. Ltd., 75pp.

Paltech 1980a (unpublished). Marine Cretaceous Sequence: Carpentaria Basin-with emphasis on sedimentary mineral accumulation. Report 1980/2 to B.H.P. Co. Ltd., 28pp.

Paltech 1980b (unpublished). Bio and litho stratigraphy of BHP 1979 drillholes on southwestern margins of Carpentaria Basin-Northern Territory. Report 1980/3 to B.H.P. Co. Ltd., 19pp.

Paltech 1980c (unpublished). Review of sedimentary mineral potential in the Cretaceous cover on the Australian Plate. Report 1980/6 to B.H.P. Co. Ltd., 34pp.

Paltech 1980d (unpublished). Dobbyn and Limmen Bight-Drillholes 1980. Report 1980/15 to B.H.P. Co. Ltd., 10pp.

Paltech 1980e (unpublished). Palaeontological and lithological report on BHP/1980 drillholes from Limmen Bight, Koolpinyah/Hope Inlet, and Groote Eylandt. Report 1980/17 to B.H.P. Co. Ltd., 10pp.

Paltech 1981a (unpublished). Cretaceous bio and litho stratigraphy of selected samples from 1980 manganese drillhole series, eastern Arnhem Land. Report 1981/4 to B.H.P. Co. Ltd., 6pp.

Paltech 1981b (unpublished). Review of marine Cretaceous stratigraphy in Arnhem Land; with particular reference to Limmen Bight drillholes. Report 1981/8 to B.H.P. Co. Ltd., 4pp.

Paltech 1981c (unpublished). Stratigraphic relationships: Cretaceous sediment at Numbulwar, Arnhem Land. Report 1981/13 to B.H.P. Co. Ltd., 7pp.

Paltech 1981d (unpublished). Aptian (Early Cretaceous) molluscan fauna from Nathan River Crossing, Arnhem Land. Report 1981/14 to B.H.P. Co. Ltd., 3pp.

Paltech 1981e (unpublished). Probable early Cenomanian planktonic foraminifera in Groote Eylandt 1981 drillholes. Report 1981/18 to B.H.P. Co. Ltd., 5pp.

Paltech 1982 (unpublished). Palaeontological samples, 1981 series from Mt. Young and Robinson River 1:250,000 Sheet areas. Report 1982/10 to B.H.P. Co. Ltd., 7pp.

Parrish, J.T. and Spicer, R.A., 1988. Late Cretaceous terrestrial vegetation: A near-polar temperature curve. *Geology*, 16, 22-25.

Passmore, V.L., 1979. Carpentaria and Karumba Basins, explanatory notes and stratigraphic columns. *Bureau of Mineral Resources, Australia, Record* 1979/22.

Passmore, V.L., Maung, T.U., Gray, A.R.G., Williamson, P.E., Lavering, I.H., Blake, P., Wellman, P., Vuckovic, V. and Miyazaki, S., 1992. Gulf of Carpentaria petroleum prospectivity study. *Bureau of Mineral Resources, Australia, Record* 1992/20.

Passmore, V.L., Williamson, P.E., Maung, T.U. and Gray, A.R.G., 1993. The Gulf of Carpentaria - a new basin and new exploration targets. *APEA Journal* 1993, 297-314.

Pederson, T.F. and Calvert, S.E., 1990. Anoxia vs. Productivity: what controls the formation of organic-carbon-rich sediments and sedimentary rocks. *American Association of Petroleum Geologists, Bulletin* 74, 454-466.

Pemberton, S.G. and Frey, R.W., 1984. Ichnology of storm-influenced shallow marine sequence: Cardium Formation (Upper Cretaceous) at Seebe, Alberta. *In* D.F. Scott and D.J. Glass (editors), The Mesozoic of North America. *Canadian Society of Petroleum Geologists, Memoir* 9, 281-304.

Pemberton, S.G., MacEachern, J.A. and Frey, R.W., 1992. Trace fossil facies models: environmental and allostratigraphic significance. *In* R.G. Walker and N.P. James (editors), Facies Models, Response to Sea Level Change. *Geological Association of Canada, Saint Johns, Newfoundland,* 47-72.

Pettijohn, F.J., Potter, P.E. and Siever, R., 1987. Sand and Sandstone. *Springer-Verlag, New York,* 553 pp.

Pietsch, B.A., Wyche, S., Rawlings, D.J., Creaser, P.M. and Findhammer, T.L.R., 1991. McArthur River Region 6065-6165 1:100,000 Series, Northern Territory. *Northern Territory Geological Survey, Explanatory Notes.*

Pirrie, D. and Marshall, J.D., 1990. High-palaeolatitude Late Cretaceous palaeotemperatures: new data from James Ross Island, Antarctica. *Geology*, 18, 31-34.

Pitman, W.C., III, 1978. Relationship between eustacy and stratigraphic sequences of passive margins. *Geological Society of America, Bulletin* 89, 1389-1403.

Plint, A.G., 1988. Sharp-based shoreface sequences and "offshore bars" in the Cardium Formation of Alberta: their relationship to relative changes in sea level. *In* C.K. Wilgus, B.S. Hastings, C.G.St.C. Kendall, H.W. Posamentier, C.A. Ross and J.C. Van Wagoner (editors), Sea-level Changes-An Integrated Approach. *Society of Economic Paleontologists and Mineralogists, Special Publication* 42, 357-370.

Plint, A.G., 1990. An allostratigraphic correlation of the Muskiki and Marshybank formations (Coniacian-Santonian) in the foothills and subsurface of the Alberta Basin. *Bulletin of Canadian Petroleum Geology*, 38, 288-306.

Plint, A.G., 1991. High-frequency relative sea-level oscillations in Upper Cretaceous shelf clastics of the Alberta foreland basin: possible evidence for a glacio-eustatic control? *In* D.I.M. Macdonald (editor), Sedimentation, Tectonics and Eustasy. *International Association of Sedimentologists, Special Publication* 12, 409-428.

Plint, A.G., Eyles, N., Eyles, C.H. and Walker, R.G., 1992. Control of sea level change. *In* R.G. Walker and N.P. James (editors), Facies Models, Response to Sea Level Change. *Geological Association of Canada, Saint Johns, Newfoundland,* 15-26.

Plint, A.G. and Norris, B., 1991. Anatomy of a ramp margin sequence: facies successions, palaeogeography, and sediment dispersal patterns in the Muskiki and Marshybank formations, Alberta Foreland Basin. *Bulletin of Canadian Petroleum Geology*, 39, 18-42.

Plint, A.G. and Walker, R.G., 1987. Cardium Formation 8. Facies and environments of the Cardium shoreline and coastal plain in the Kakwa Field and adjacent areas, northwestern Alberta. *Bulletin of Canadian Petroleum Geology*, 25, 48-64.

Plint, A.G., Walker, R.G. and Bergman, K.M., 1986. Cardium Formation 6. Stratigraphic framework of the Cardium in subsurface. *Bulletin of Canadian Petroleum Geology*, 34, 213-225.

Plumb, K.A., Derrick, G.M. and Wilson, I.H., 1980. Precambrian geology of the McArthur River-Mount Isa region, northern Australia. *In* R.A. Henderson and P.J. Stephenson (editors), The Geology and Geophysics of Northeastern Australia. *Geological Society of Australia, Queensland Division*, 4, 71-88.

Plumb, K.A. and Rhodes, J.M., 1964. Wallhallow, Northern Territory - 1:250,000 Geological Series. *Bureau of Mineral Resources, Explanatory Notes*, SE/53-7.

Posamentier, H.W., Allen, G.P., James, D.P. and Tesson, M., 1992. Forced regressions in a sequence stratigraphic framework: concepts, examples, and exploration significance. *American Association of Petroleum Geologists, Bulletin* 76, 1687-1709.

Posamentier, H.W., Jervey, M.T. and Vail, P.R., 1988. Eustatic controls on clastic deposition I - conceptual framework. *In* C.K. Wilgus, B.S. Hastings, C.G.St.C. Kendall, H.W. Posamentier, C.A. Ross and J.C. Van Wagoner (editors), Sea-level Changes-An Integrated Approach. *Society of Economic Paleontologists and Mineralogists, Special Publication* 42, 109-124.

Posamentier, H.W. and Vail, P.R., 1988. Eustatic controls on clastic deposition II - sequence and system tract models. *In* C.K. Wilgus, B.S. Hastings, C.G.St.C. Kendall, H.W. Posamentier, C.A. Ross and J.C. Van Wagoner (editors), Sea-level Changes-An Integrated Approach. *Society of Economic Paleontologists and Mineralogists, Special Publication* 42, 125-154.

Posamentier, H.W. and Weimer, P., 1993. Siliciclastic sequence stratigraphy and petroleum geology - where to from here? *American Association of Petroleum Geologists, Bulletin* 77, 731-742.

Postma, D., 1982. Pyrite and siderite formation in brackish and freshwater swamp sediments. *American Journal of Science*, 282, 1151-1183.

Powell, R.D., 1983. Glacial-marine sedimentation processes and litho-facies of temperate tidewater glaciers, Glacier Bay, Alaska. *In* B.F. Molnia (editor), Glacial-Marine Sedimentation. *Plenum Press, New York*, 185-232.

Pracejus, B., 1989 (unpublished). Nature and formation of supergene manganese deposits on Groote Eylandt, Northern Territory, Australia. *University of Adelaide*, Ph.D. thesis, 231pp.

Reineck, H.E. and Singh, I.B., 1972. Genesis of laminated sand and graded rhythmites in storm-sand layers of shelf mud. *Sedimentology*, 18, 123-128.

Reynolds, A.D., 1992. Storm, wave and tide-dominated sedimentation in the Dintian Middle Limestone Group, Northumbrian Basin. *Proceedings of the Yorkshire Geological Society*, 49, 135-148.

Riccardi, A.C., 1991. Jurassic and Cretaceous marine connections between the Southeast Pacific and Tethys. *In* J.E.T. Channell, E.L. Winterer and L.F. Jansa (editors), Paleogeography and Paleoceanography of Tethys. *Palaeogeography, Palaeoclimatology, Palaeoecology*, 87, 155-190.

Rich, P.V., Rich, T.H.V., Wagstaff, B.E., McEwan Mason, J., Douthitt, C.B., Gregory, R.T. and Felton, E.A., 1988. Evidence for low temperatures and biologic diversity in Cretaceous high latitudes of Australia. *Science*, 242, 1403-1406.

Rowley, D.B. and Markwick, P.J., 1992. Haq et al eustatic sea level curve: Implications for sequestered water volumes. *Journal of Geology*, 100, 703-715.

Ruffell, A., 1991. Sea-level events during the Early Cretaceous in Western Europe. *Cretaceous Research*, 12, 527-551.

Sabadini, R., Doglioni, C. and Yuen, D., 1990. Eustatic sea level fluctuations induced by polar wander. *Nature*, 345, 708-710.

Sahagian, D.L., 1987. Epeirogeny and eustatic sea level changes since the mid-Cretaceous. Application to central and western United States. *Journal of Geophysical Research*, 91, 6678-7645.

Sahagian, D.L. and Holland, S.M., 1991. Eustatic sea-level curve based on a stable frame of reference: preliminary results. *Geology*, 19, 1209-1212.

Sanders, J.E. and Kumar, N., 1975. Evidence of shoreface retreat and in-plane "drowning" during Holocene submergence of barriers, shelf off Fire Island, New York. *Geological Society of America, Bulletin* 86, 65-76.

Sands, D., 1979 (unpublished). Report on exploration at Nathan River, Northern Territory, exploration licence 1744. Report to Nord Resources (Pacific) Pty. Ltd., 4pp + enclosures.

Savdra, C.E., 1991. *Teredolites*, wood substrates, and sea level dynamics. *Geology*, 19, 905-908.

Savdra, C.E., Ozalas, K, Demko, T.H., Huchison, R.A. and Scheiwe, T.D., 1993. Log-grounds and the ichnofossil *Teredolites* in transgressive deposits of the Clayton Formation (Lower Palaeocene), Western Alabama. *Palaios*, 8, 311-324.

Scheibnerova, V., 1976. Cretaceous foraminifera of the Great Artesian Basin. *Geological Survey of New South Wales, Memoir* 17, 265pp.

Schieber, J., 1990. Significance of styles of epicontinental shale sedimentation in the Belt basin, Mid-Proterozoic of Montana, U.S.A. *Sedimentary Geology*, 69, 297-312.

Schneider, S.H., Thompson, S.L. and Barron, E.J., 1985. Mid-Cretaceous continental surface temperatures: are high CO_2 concentrations needed to simulate above-freezing winter conditions? *In* E.T. Sundquist and W.S. Broecher (editors), The Carbon Cycle and Atmospheric CO_2 : Natural Variations Archean to Present. *American Geophysical Union, Geophysical Monograph* 32, 554-559.

Scholle, P.A. and Arthur, M.A., 1980. Carbon isotope fluctuations in Cretaceous pelagic limestones: Potential stratigraphic and petroleum exploration tool. *American Association of Petroleum Geologists, Bulletin* 64, 67-87.

Seilacher, A., 1967. Bathymetry of trace fossils. *Marine Geology*, 5, 413-428.

Senior, B.R., Mond, A. and Harrison, P.L., 1978. Geology of the Eromanga Basin. *Bureau of Mineral Resources, Australia, Bulletin* 167, 102pp.

Sethi, P.S. and Leithold, E.L., 1994. Climate cyclicity and terrigenous sediment influx to the early Turonian Greenhorn Sea, Southern Utah. *Journal of Sedimentary Research*, B64, 26-39.

Shanley, K.W. and McCabe, P.J., 1991. Predicting facies architecture through sequence stratigraphy - an example from the Kaiparowits Plateau, Utah. *Geology*, 19, 742-745.

Shanley, K.W. and McCabe, P.J., 1994. Perspectives on the sequence stratigraphy of continental strata. *American Association of Petroleum Geologists, Bulletin* 78, 544-568.

Shearman, D.J. and Smith, A.J., 1985. Ikaite, the parent mineral of jarrowite-type pseudomorphs. *Proceedings of the Geological Association*, 96, 305-314.

Sinclair, H.D., 1993. High resolution stratigraphy and facies differentiation of the shallow marine Annot Sandstones, south-east France. *Sedimentology*, 40, 955-978.

Singer, A., 1984. The paleoclimatic interpretation of clay minerals in sediments - a review. *Earth Science Reviews*, 21, 251-293.

Singer, A., 1988. Illite in aridic soils, desert dusts and desert loess. *Sedimentary Geology*, 59, 251-259.

Skwarko, S.K., 1961. Progress report on the field activities in the Northern Territory during 1961 field season. *Bureau of Mineral Resources, Australia, Record* 1961/153.

Skwarko, S.K., 1962a. Notes on Australian Lower Cretaceous palaeogeography. *Bureau of Mineral Resources, Australia, Record* 1962/11.

Skwarko, S.K., 1962b. The Mesozoic strata of Mt. Young 1:250,000 Sheet area. *Bureau of Mineral Resources, Australia, Record* 1962/83.

Skwarko, S.K., 1962c. The Mesozoic strata of Bauhinia Downs 1:250,000 Sheet area. *Bureau of Mineral Resources, Australia, Record* 1962/85.

Skwarko, S.K., 1963. Observations on occurrences of Cretaceous rocks in Queensland and Northern Territory: Progress Report 1962. *Bureau of Mineral Resources, Australia, Record* 1963/11.

Skwarko, S.K., 1966. Cretaceous stratigraphy and palaeontology of the Northern Territory. *Bureau of Mineral Resources, Australia, Bulletin* 73, 135pp.

Skwarko, S.K., 1967. Cretaceous stratigraphy of the Wiso Basin, Northern Territory. *Bureau of Mineral Resources, Australia, Record* 1967/47.

Slee, K.J., 1976 (unpublished). The setting, geology and origin of the Groote Eylandt manganese deposits, Australia. Report to B.H.P. Co. Ltd., 191pp.

Sloan, L.C. and Barron, E.J., 1990. "Equable" climates during Earth history? *Geology*, 18, 489-492.

Smart, J., 1976. Stratigraphic correlations in the southern Carpentaria Basin and Eromanga Basin. *Queensland Geology and Mining Journal*, 77, 171-178.

Smart, J., Grimes, K.G. and Doutch, H.F., 1972. New names and revised stratigraphic names, Carpentaria Basin. *Queensland Government Mining Journal*, 73, 190-201.

Smart, J., Grimes, K.G., Doutch, H.F. and Pinchin, J., 1980. The Carpentaria and Karumba Basins, North Queensland. *Bureau of Mineral Resources, Australia, Bulletin* 202, 73pp.

Smart, J., Morrissey, J.A. and Hassan, S.E., 1975. Index to drill-hole data - Carpentaria, Laura, and Karumba Basins, Queensland. *Bureau of Mineral Resources, Australia, Record* 1975/167.

Southard, J.B., Lambie, J.M., Federico, D.C., Pile, H.T. and Weidman, C.R., 1990. Experiments on bed configurations in fine sands under bidirectional purely oscillatory flow, and the origin of hummocky cross-stratification. *Journal of Sedimentary Petrology*, 60, 1-17.

Spalletti, L.A., 1993. An iron-bearing wave-dominated siliciclastic shelf: facies analysis and palaeogeographic implications (Silurian-Lower Devonian Sierra Grande Formation, southern Argentina). *Geological Journal*, 28, 137-148.

Stevens, G.R., 1971. Relationships of isotopic temperatures and faunal realms to Jurassic-Cretaceous palaeogeography, particularly of the south-west Pacific. *Journal of the Royal Society of New Zealand*, 1, 145-158.

Stevens, G.R. and Clayton, R.N., 1971. Oxygen isotope studies on Jurassic and Cretaceous belemnites from New Zealand and their biogeographic significance. *New Zealand Journal of Geology and Geophysics*, 14, 829-897.

Still, G.K., 1971 (unpublished). Northern Territory manganese project; 1971 Rose River exploration programme (prospecting authority 2166). Report to United States Steel International (New York) Incorporated, 46pp.

Struckmeyer, H.I.M. and Brown, P.J., 1990. Australian sealevel curves, Part 1: Australian inundation curves. *Bureau of Mineral Resources, Australia, Record* 1990/11.

Surlyk, F., 1991. Sequence stratigraphy of the Jurassic-lowermost Cretaceous of East Greenland. *American Association of Petroleum Geologists, Bulletin* 75, 1468-1488.

Tarduno, J.A., Sliter, W.V., Kroenke, L., Leckie, M., Mayer, H., Mahoney, J.J., Musgrave, R., Storey, M. and Winterer, E.L., 1991. Rapid formation of Ontong Java Plateau by Aptian mantle plume volcanism. *Science*, 254, 399-403.

Thomas, B.M., Stamford, P., Hanson, P., Taylor, L. and Stainforth, J.G., 1992. Petroleum geology and exploration history of the Carpentaria Basin, Australia, and associated infrabasins. *In* M.W. Leighton, D.R. Kolata, D.F. Oltz and J.J. Eidel (editors), Interior Cratonic Basins. *American Association of Petroleum Geologists, Memoir* 51, 709-724.

Thomas, G. S. P. and Connell, R. J., 1985. Iceberg drop, dump, and grounding structures from Pleistocene glacio-lacustrine sediments, Scotland. *Journal of Sedimentary Petrology* 55, 243-249.

Tucker, M.E., 1991. Sedimentary Petrology: An Introduction to the Origin of Sedimentary Rocks. *Blackwell, Oxford*, 260 pp.

Vail, P.R., 1987. Seismic stratigraphy interpretation procedure. *In* A.W. Bally (editor), Atlas of Seismic Stratigraphy. *American Association of Petroleum Geologists, Studies in Geology* 27, 1, 1-10.

Vail, P.R., 1989 (unpublished). At the frontiers of sequence stratigraphy. Notes from the Australian Cretaceous Eustacy Workshop (August 1989). *Bureau of Mineral Resources, Australia.*

Vail, P.R., Mitchum, R.M., Jr., Todd, R.G., Widmier, J.M., Thompson, S., III, Sangree, J.B., Bubb, J.N. and Hatlelid, W.G., 1977. Seismic stratigraphy and global changes of sea level (11 parts). *In* C.E. Payton (editor), Seismic Stratigraphy - Applications to Hydrocarbon Exploration. *American Association of Petroleum Geologists, Memoir* 26, 49-212.

Van Hinte, J.E., 1976. A Cretaceous time scale. *American Association of Petroleum Geologists, Bulletin* 60, 498-516.

Van Wagoner, J.C., Mitchum, R.M., Jr., Campion, K.M. and Rahmanian, V.D., 1990. Siliciclastic sequence stratigraphy in well logs, cores, and outcrops. *American Association of Petroleum Geologists, Methods in Exploration Series* 7, 55pp.

Van Wagoner, J.C., Mitchum, R.M., Jr. and Posamentier, H.W., 1987. Seismic stratigraphic interpretation using sequence stratigraphy, Part 2. Key definitions of sequence stratigraphy. *In* A.W. Bally (editor), Atlas of Seismic Stratigraphy. *American Association of Petroleum Geologists, Studies in Geology* 27(1), 11-14.

Van Wagoner, J.C., Posamentier, H.W., Mitchum, R.M., Jr., Vail, P.R., Sarg, J.F., Loutit, T.S. and Hardenbol, J., 1988. An overview of the fundamentals of sequence stratigraphy and key definitions. *In* C.K. Wilgus, B.S. Hastings, C.G.St.C. Kendall, H.W. Posamentier, C.A. Ross and J.C. Van Wagoner (editors), Sea-level Changes-An Integrated Approach. *Society of Economic Paleontologists and Mineralogists, Special Publication* 42, 39-46.

Veevers, J.J., 1991. Mid-Cretaceous tectonic climax, Late Cretaceous recovery and Cainozoic relaxation in the Australian region. *In* M.A.J. Williams, P.De. Deckker and A.P. Kershaw (editors), The Cainozoic in Australia: A Reappraisal of the Evidence. *Geological Society of Australia, Special Publication* 18, 1-14.

Veevers, J.J. and Eittrem, S.L., 1988. Reconstruction of Antarctica and Australia at breakup (95 +/- 5Ma) and before rifting (160Ma). *Australian Journal of Earth Sciences*, 35, 355-362.

Wadsworth, J.A. and Walker, R.G., 1991. Morphology and origin of erosion surfaces in the Cardium Formation (Upper Cretaceous, Western Interior Seaway, Alberta) and their implications for rapid sea level fluctuations. *Canadian Journal of Earth Sciences*, 28, 1501-1520.

Waldman, M., 1971. Fish from the freshwater Lower Cretaceous of Victoria, Australia, with comments on the palaeoenvironment. *Special Papers in Palaeontology*, 9, 1-124.

Walker, R.G., 1984. Shelf and shallow marine sands. *In* R.G. Walker (editor), Facies Models, 2nd edition. *Geological Association of Canada, Geoscience Canada, Reprint Series* 1, 141-170.

Walker, R.G., 1990. Facies modelling and sequence stratigraphy. *Journal of Sedimentary Petrology*, 60, 777-786.

Walker, R.G., 1992. Facies, Facies Models and Modern Stratigraphic Concepts. *In* R.G. Walker and N.P. James (editors), Facies Models, Response to Sea Level Change. *Geological Association of Canada, Saint Johns, Newfoundland*, 1-14.

Walker, R.G. and Eyles, C.H., 1988. Geometry and facies of stacked shallow marine sandier upward sequences dissected by erosion surface: Cardium Formation, Willesden Green, Alberta. *American Association of Petroleum Geologists, Bulletin* 72, 1469-1494.

Wallace-Dudley, K. and Leckie, D., 1993. The Lower Kaskapau Formation (Cenomanian): A multiple-frequency retrogradational shelf system, Alberta, Canada. *American Association of Petroleum Geologists, Bulletin* 77, 414-435.

Ward, I.G., 1981 (unpublished). Final report HC80 seismic survey, Gulf of Carpentaria, permit Q/19P. Report for Hematite Petroleum Pty. Ltd.

Weaver, C.E., 1989. Clays, Muds and Shales. Developments in Sedimentology, 44. *Elsevier, Amsterdam*, 819pp.

Weissert, H., 1989. C-isotope stratigraphy, a monitor of paleoenvironmental change: a case study from the Cretaceous. *Surveys in Geophysics*, 10, 1-61.

Wheatcroft, R.A., 1990. Preservation potential of sedimentary event layers. *Geology*, 18, 843-845.

Whitehouse, F.W., 1926. The correlation of the marine Cretaceous deposits of Australia. *Report of the Australian Association for the Advance of Science*, 18, 275-280.

Whitehouse, F.W., 1954. Geology of the Queensland portion of the Great Artesian Basin. Appendix G: Artesian water supplies in Queensland. *Department of Co-ordinator of Public Works, Queensland.*

Wilgus, C.K., Hastings, B.S., Kendal C.G.St.C., Posamentier, H.W., Ross, C.A. and Van Wagoner, J.C., 1988. Sea-level Changes: An Integrated Approach. *Society of Economic Paleontologists and Mineralogists, Special Publication* 42, 407pp.

Williams, D.F., 1988. Evidence for and against sea-level changes from the stable isotopic record of the Cenozoic. *In* C.K. Wilgus, B.S. Hastings, C.G.St.C. Kendall, H.W. Posamentier, C.A. Ross and J.C. Van Wagoner (editors), Sea-level Changes-An Integrated Approach. *Society of Economic Paleontologists and Mineralogists, Special Publication* 42, 31-36.

Wright, V.P. and Marriot, S.B., 1993. The sequence stratigraphy of fluvial depositional systems: the role of floodplain sediment storage. *Sedimentary Geology*, 86, 203-210.

Wright, M.E. and Walker, R.G., 1981. Cardium Formation (U. Cretaceous) at Seebe, Alberta - storm-transported sandstones and conglomerates in shallow marine depositional environments below fair-weather wave base. *Canadian Journal of Earth Sciences*, 18, 795-809.

Yagishita, Y., Arakawa, S. and Taira, A., 1992. Grain fabric of hummocky and swaley cross-stratification. *Sedimentary Geology*, 78, 181-189.

APPENDIX 1:
FIELD TECHNIQUES & DETAILS OF THE STUDY AREA

1.1 FIELD TECHNIQUES

A large part of the project is based on data collected from the field. A brief description of techniques is included here in order that the quality and detail of the work may be assessed.

Due to the enormous field area covered in the study, and taking into account the discontinuous nature of Cretaceous exposures, the only practical means of regional study of Cretaceous rocks was to use previously published 1:250,000 geological sheets as base maps. This method proved to be adequate in pinpointing most if not all of the major areas of Cretaceous exposure, and enabled detailed study of such areas. The 1:250,000 geological maps also provided valuable information on the nature and geographical distribution of basement lithologies and their broad relationships to Cretaceous strata. Further detail on location and elevation of field stations was gained from 1:100,000 scale topographic maps for the northern and central regions, and from the use of a portable satellite-based global positioning system when in the field in the northern region.

Initial reconnaissance photo-interpretation and planning was carried out prior to and during the field studies in the northern part of Arnhem Land with the aid of 1:84,000 scale RC-9 black and white airphotos supplied courtesy of B.H.P. Co. Ltd. However, due to the immense area covered, the age and rather poor quality of the airphotos, and the dense vegetation cover, this proved to be of little use in delineating areas of particular interest with respect to Cretaceous sediments. A later field trial with more recent 1:25,000 scale colour airphotos supplied by the N.T.G.S. proved to be more useful for specific areas. The scale of the airphotos would have required the use of thousands of such photos to cover the study area, and these resources not being available, geological interpretation through the use of airphotos was only used for smaller areas where Cretaceous rocks are abundant, such as the Blue Mud Bay and Mt Young 1:250,000 sheet areas.

Most Cretaceous rocks in the study area are horizontal, or have very gentle dips $<<1^0$ (except for channel fills and very large-scale cross-bedded units). Therefore, most sections were measured using a Brunton compass as a hand level, or by visual estimation of thickness backed up by tape measurements. Sections recorded in the field were plotted at a scale of 1 cm: 1 m whilst in the field or at base camp. The sampling interval in the field varied according to the type and number of lithologies within any particular section, but generally occurred in the range of one representative hand sample taken for every 0.25 m to 5 m of section, including

occasional sampling of problematic ?basement lithologies. Larger samples of fine-grained rocks were collected for micropalaeontological and XRD analysis.

1.2 LOCATION OF THE STUDY AREA

Investigations were carried out along the entire western margin and a large part of the south-western margin of the Gulf of Carpentaria in the Northern Territory and Queensland, in a belt stretching 80 km to 150 km inland from the present gulf coast. This area encompasses nearly all of the main exposures of Cretaceous sedimentary marine rocks, and a representative portion of the nonmarine sequence. The area occupies approximately 150,000 km^2 and is bounded by latitudes 12^0 08' S and 18^0 57' S, and longitudes 134^0 15' E and 138^0 58' E. Field work was carried out during dry seasons from October, 1988 to August, 1991.

1.3 LAND ACCESS

The northern half of the study area is situated within the Arnhem Land Aboriginal Reserve. Much of this region, excluding the area immediately around the mining town of Nhulunbuy (Gove), is poorly serviced by roads and is inaccessible during the wet season. Travel by road outside of the Nhulunbuy area is restricted to a few rough tracks joining the aboriginal outstations and to the unsealed Nhulunbuy-Katherine-Darwin highway. The vegetation is dense, and thus ground-vehicle based studies are seriously disadvantaged by the difficult terrain and the scarcity of tracks. South of the Arnhem Land Aboriginal Reserve, the vegetation cover becomes less dense and the number of access tracks also increases. Helicopters are the only practical means of transport for large-scale studies in this region, although the dense tree cover and lack of landing places is still a considerable hindrance.

1.4 LAND USE, TENURE, AND MINING

The Arnhem Land Aboriginal Reserve is owned and managed by the traditional land owners through the local community centres and the Northern Lands Council. Travel and study within the aboriginal reserve are by permit only, and are liable to constant appraisal and reassessment. Permits to companies for exploration or mining ventures within the aboriginal reserve are similarly controlled by the Northern Lands Council, and company activities in the area have been severely restricted in recent times.

South of the Arnhem Land Aboriginal Reserve the area is covered by large pastoral leases, dominantly used for cattle ranches. Land in the immediate vicinity of the major towns such as Borroloola is divided into freehold blocks. The pastoral industry is the main industry in the area and is supplemented by tourism. In past times the area was prospected extensively for mineral occurrences and many old workings are still visible, especially near the Northern Territory-Queensland border. Active exploration for manganese, base-metals, heavy minerals

and diamonds is presently occurring along with the operation of several mines, including the McArthur River 'HYC' base metal deposit in the Bauhinia Downs 1:250,000 map sheet area in the Northern Territory, and the Musselbrook Mining Camp in the Lawn Hill 1:250,000 map sheet area in Queensland. Large Cretaceous-aged sedimentary manganese deposits are currently being exploited on Groote Eylandt, about 50 km offshore from the southern part of the northern region.

1.5 PHYSIOGRAPHY AND VEGETATION

The study area contains a number of mountain ranges composed of Proterozoic rocks, particularly in the northern and central regions. Local drainage patterns are controlled by these generally northeast to north-northeast trending ranges characterised by high ridges and steep tree-filled valleys. Most major rivers exploit the major northeast structural trend, or drain eastwards toward the coast. Mesa 'badlands' topography is created by the considerable relief of the thin scattered Cretaceous remnants over the flat plains of Cenozoic sediments. The mesas and plateaux abut against, and in places impinge upon, the pre-existing mountain ranges which were formed by large structural movements pre-Jurassic (probably mainly Precambrian) times (Passmore, 1979).

In northeastern Arnhem Land the development of extensive bauxite and laterite horizons has led to the formation of large Tertiary plateaux underlain by Cretaceous strata. Elsewhere the Cretaceous remnants are generally scattered and discontinuous, except for the northwest trending Cretaceous escarpment about 100 km inland from the coast which separates the tablelands to the west from the plains to the east. Skwarko (1966) believed that this feature was the divide between the Coastal Belt to the east and the Inland Belt to the west. Extensive low-relief alluvial plains occupy the areas between the ranges and the mesas.

Vegetation in Arnhem Land is very dense due to the sub-tropical conditions which prevail, although the influence of the wet season on plant growth decreases southward and thus the amount of vegetation also decreases slightly to the south. Even in areas with relatively sparse tree cover there is usually a dense bushy scrubland or a tall grass cover.

APPENDIX 2:
NEW STRATIGRAPHIC NAMES & DEFINITIONS

2.1 WALKER RIVER FORMATION (new definition: A.A. Krassay)

DERIVATION OF NAME

From the Walker River, in the west-central part of the BLUE MUD BAY 1:250,000 Sheet. The headwaters of the river occur at approximately 13^0 20' S, 135^0 22' E, and the river enters the Gulf of Carpentaria at 13^0 35' 30" S, 135^0 50' 00" E.

DISTRIBUTION

The unit is extensively distributed along the western and south-western margins of the Gulf of Carpentaria, mostly within the Northern Territory but also within far northwestern Queensland. The unit is preserved as erosional remnants in the form of mesas, plateaux and low-lying rubbly hills occupying a broad zone up to 150 km inland from the present Gulf coastline. The erosional remnants commonly form outliers resting directly on Proterozoic rocks of the McArthur Basin. The area encompassed by this unit is in the order of 120,000 km^2, but the western and southern margins of the outcrop belt are relatively poorly defined, as the unit tends to thin in these directions. The main outcrop belt lies east of about 134^0 30' E, west of 138^0 50' E, south of 12^0 05' S, and north of about 18^0 55' S. The outcrop belt covers a large part of the eastern Northern Territory along the margin of the Gulf of Carpentaria, and occupies all or part of sixteen 1:250,000 Sheet areas.

TYPE SECTION

23 m of sandstone and silty sandstone (measured section 174), thinly interbedded with clayey siltstone and thin intraformational chert pebble conglomerate, forming a tiered cliff exposure at the edge of a large dissected Cretaceous plateau, about 5 km southwest of the northern arm of the Walker River, at 13^0 34' 07" S, 135^0 29' 25" E in the BLUE MUD BAY sheet area. The base is identified by a normally-graded, clast-supported chert cobble conglomerate, unconformably overlying laminated, shallowly-dipping Proterozoic siltstone. The top is the flat top of the erosional landform (plateau) which forms the outcrop, the upper surface of which is densely vegetated.

REFERENCE SECTION

Reference sections exist along the edge of dissected plateaus and large mesas in the areas surrounding the Walker River, within the boundaries of what was a large palaeoembayment in Cretaceous time between latitudes 13^0 21' S and 13^0 40' S, and longitudes 135^0 23' E and 135^0 31' E. Good reference sections also exist along the entire length of the

outcrop belt of this marine shelfal formation, and the lithological character of the unit changes in response to facies changes away from the palaeoshoreline. For completeness, the locations of three reference sections are included here, covering proximal, intermediate, and distal (palaeogeographical) depositional settings of the unit. In order (proximal to distal) their locations are; measured section 149, at 13^0 25' 51" S, 135^0 26' 54" E on the BLUE MUD BAY 1:250,000 Sheet, measured section 52, at 15^0 36' 45" S, 135^0 36' 30" E on the MOUNT YOUNG 1:250,000 Sheet, and measured section 96, at 17^0 14' 00" S, 135^0 38' 30" E on the WALLHALLOW 1:250,000 Sheet.

LITHOLOGY

The bulk of the unit is weathered sandstone: white to dark orange, moderately to well sorted, well rounded to subangular, coarse/medium- to fine-grained quartz arenite with iron-oxide staining. Interbedded with the sandstone are flaser and lenticular interbeds of white to pale yellow, silica-cemented, finely laminated clayey siltstone. Thin, sharp-based intraformational chert and lithic pebble lags occur parallel or slightly discordant to bedding, and more rarely pebbles are concentrated into metre-wide lenses. In distal palaeogeographical localities the overall amount of sandstone is less, and the bulk of the unit consists of laminated siltstone with sandy interbeds. The unit forms both fining-upward and coarsening-upward grain size cycles, typically 5 to 10 m-thick. Where the base of the unit is exposed, it consists of a thick, normally graded, chert cobble to pebble conglomerate which grades up into marine sandstones containing molluscan macrofossils and marine trace fossils.

Sedimentary structures within this heterolithic unit include hummocky cross-stratification, planar cross-bedding (0.25 to 2 m), wave and current ripples, gravelly ripples, ripple-lamination, convolute lamination, slump structures, gutters and gutter casts and other complex erosional scours and tool marks, graded beds, coquinas, and various styles of lamination.

The unit contains abundant to rare, moderately to poorly preserved specimens of molluscan macrofossils, mainly bivalves, but also rare ammonites and belemnites. Rare stratigraphic intervals have segmented plant fossils mixed with the molluscan fossils. Marine trace fossils of the *Skolithos* and *Cruziana* ichnofacies are common, and are characteristic of the high-energy shallow-marine depositional environment of the unit (Pemberton *et al.*, 1992). Fine-grained outcrops (and drillcore) that are not extensively weathered yield low-diversity microfloras (spores, pollen), dinoflagellates, and marine arenaceous foraminifera of the *Ammobaculites* Association (Haig, 1979b).

THICKNESS

Range 2 to 38 m in outcrop. At least 55 m in the subsurface (*e.g.* Bolton, 1982; Sands, 1979). Construction of composite sections indicates that the overall maximum thickness of the unit in outcrop is greater than 70 m.

PALAEOENVIRONMENT

The unit generally represents high-energy deposition in the foreshore to offshore shallow-marine zone. Some interbedded stratigraphic intervals represent distal deltaic to deltaic-marine depositional environments.

RELATIONSHIPS AND BOUNDARY CRITERIA

In outcrop and subsurface the unit overlies older Cretaceous nonmarine units with disconformity, or Palaeoproterozoic sedimentary rocks with angular unconformity. The unconformity surface is marked by a prominent chert cobble conglomerate in most places.

AGE & EVIDENCE

Skwarko (1966) collected marine molluscan macrofossils from these rocks and proposed an age range of Neocomian to Aptian, with rare Albian aged rocks. However, these biostratigraphic age determinations have now been refined (Krassay, 1994a), and the age of the unit is considered as late Aptian to early Cenomanian. Palynomorphs in the lower part of this unit, in US Steel drillholes near Numbulwar, belong to the *Coptospora paradoxa* spore-pollen Zone and the *Canninginopsis denticulata* microplankton Zone and, give an age of middle Albian (Alley, 1991). Correlative outcrops contain arenaceous foraminifera belonging to the *Riyadhella crespinae* Zone, which give an age range of late early Albian to late Albian for the lower to middle part of the unit (Haig, 1991). Arenaceous foraminifera belonging to the *Bigenerina pitmani* Zone in rocks from the lowest exposed stratigraphic interval of the unit give an age of late Aptian (Haig, 1991).

Preliminary results from recent drilling in the onshore northeastern Northern Territory, south and west of the Yiyintyi Range on the MOUNT YOUNG 1:250,000 Sheet, suggest that the base of this unit may be as old as early Aptian (M. Warne, pers. comm., 1994). On the basis of correlation to dated stratigraphic intervals on Groote Eylandt, the upper part of this unit is considered to be early Cenomanian in age. The full age range of the unit is likely to be Aptian to Cenomanian.

REMARKS

This unit occupies a large part of Skwarko's (1966) "Coastal Belt", and was previously placed within the Mullaman Beds. In terms of Skwarko's (1966) informal stratigraphic nomenclature, this unit is equivalent in part to Skwarko's 'units 2-7', and possibly also to 'unit B and C' of his "Inland Belt".

Skwarko's (1966) informal stratigraphic nomenclature is now superseded, and usage of his informal names ('belts' and 'units') should be discontinued. Further mapping is likely to extend the known westward limit of the Walker River Formation, and an aim of such mapping should be to replace the old terminology (Mullaman Beds, and Skwarko's informal terminology) on the basis of the new stratigraphic definition proposed here.

2.2 YIRRKALA FORMATION (new definition: A.A. Krassay)

DERIVATION OF NAME

From, Yirrkala, the old mission site on the Gove Peninsula in far northeastern Arnhem Land, at 12^0 15' 05" S, 136^0 53' 20" E on the ARNHEM BAY-GOVE 1:250,000 Sheet.

DISTRIBUTION

The unit occurs in two main areas. Firstly, as a broad semi-continuous low-lying plateau in the northeastern part of the ARNHEM BAY-GOVE 1:250,000 Sheet area, between Melville Bay and Wanyamera Point, and Arnhem Bay and Dalywoi Bay. The exposed area of this plateau (now partly dissected) is about 1500 km^2. The greatest thickness and extent of the Yirrkala Formation occurs on the ARNHEM BAY-GOVE 1:250,000 Sheet, in an area within about 50 km to the southwest of Nhulunbuy.

Secondly, the unit occurs as thinner, patchy palaeovalley fill and terraced deposits in the elevated parts of high-standing basement ranges. The unit has been recognised on the upper flanks of the Mitchell Range and Parsons Range on the BLUE MUD BAY 1:250,000 Sheet, and also in the elevated parts of the Yiyintyi Range on the MOUNT YOUNG 1:250,000 Sheet at about latitude 15^0 25' S.

TYPE SECTION

50 m of white sandstone (composite section 208-210) exposed along the banks and to the sides of 'Tiger Creek', at approximately 13^0 31' 30" S, 135^0 14' 50" E on the eastern flank of the Parsons Range on the BLUE MUD BAY 1:250,000 Sheet. The base is identified by a chert cobble and pebble conglomeratic lag, mantling a well developed angular unconformity on the Palaeoproterozoic Parsons Range Group. The top is the uppermost part of the sequence of flat-lying Cretaceous rocks which overlie shallowly to moderately dipping Proterozoic rocks of the Parsons Range.

REFERENCE SECTION

Reference sections (*e.g.* measured sections 7 and 161) occur along Wonga Creek, about 40 km southwest of Nhulunbuy, on the ARNHEM BAY-GOVE 1:250,000 Sheet, from approximately 12^0 26' 00" S, 136^0 34' 00" E to 12^0 29' 30" S, 136^0 39' 00" E. Here, the thickness of the unit varies from a few metres to over 15 m, with an average thickness of 8 to 10 m. In the Wonga Creek area the unit is incised into older marine rocks of the Walker River Formation, and the amount of fluvial incision decreases towards the modern coastline.

LITHOLOGY

Sandstone: white to pale grey, poorly to moderately sorted, fine- to very coarse-grained: Massive to thickly planar bedded, with large-scale trough cross-bedding with set thicknesses up to 2 m at the base, and planar cross-bedding in the middle and upper parts with rare dispersed

rounded pebble-sized chert clasts. Commonly forms fining-upward grain-size cycles, with chert pebble lags overlying local base-of-channel scours. Upper, finer-grained parts of the unit (or sub-cycles within the unit) contain rare, moderately to poorly preserved, external moulds of segmented plant fossils on upper bedding surfaces.

THICKNESS

Range 5 to 50 m: typically 8 to 15 m in outcrop, but probably much thicker in the subsurface, as shown in drill logs for three stratigraphic drillholes in the area surrounding Nhulunbuy (Dodson, 1967).

PALAEOENVIRONMENT

The unit generally represents high-energy fluvial deposition in channels, and coarse-grained nonmarine valley fills. Most outcrops conform to sandy bedform, channel, and gravel bar architectural elements in Miall's (1985) classification of fluvial deposits.

RELATIONSHIPS AND BOUNDARY CRITERIA

In outcrop, the unit overlies older Cretaceous marine units with disconformity or Palaeoproterozoic sedimentary rocks with angular unconformity. In the subsurface the unit overlies Proterozoic metasediments and granites with nonconformity (Dodson, 1967).

AGE & EVIDENCE

Plant macrofloras are relatively poorly preserved and consist of long-ranging forms, which may only be considered as Late Mesozoic in age (Skwarko, 1966, p. 32). For a full list of plant fossils, that have been previously collected from this unit, refer to Skwarko (1966, p. 32). The unit is correlated with the nonmarine sequence in three stratigraphic drillholes near Nhulunbuy; siltstone interbedded with the arkosic sandstones in drillhole D.D.H. 2 at 64 m depth has been dated by palynology as late Albian (Evans, in Dodson, 1967). Furthermore, on the basis of regional lithostratigraphic correlations, outcrops of the unit in the Wonga Creek area, about 40 km southwest of Nhulunbuy, disconformably overlie marine Cretaceous rocks of Albian age. The likely age of the unit in most places is Albian or younger (up to Cenomanian).

REMARKS

In places this unit is similar to that described by Skwarko (1966) as 'unit 1' of his "Coastal Belt" or 'unit A' of his "Inland Belt", and is included within the Mullaman Beds. The name Yirrkala Formation was initially proposed to describe nonmarine rocks in Arnhem Land, but it also applies to rocks distributed much farther to the south along the western margin of the Gulf of Carpentaria, to the vicinity of the Northern Territory-Queensland border. It is anticipated that further mapping will extend the known westward distribution of the unit.

APPENDIX 3:
FIELD SITE TABLE & EXPANDED BASE MAPS

SAMPLE #	ROCK TYPE	LOCAL SITE NAME	SITE #	1:250,000 MAP SHEET	LATITUDE degrees minutes	LONGITUDE degrees minutes
AL1-1A	QTZ ARENITE	Yangunbi	2	Arnhem Bay...	12 19	136 35.75
AL1-1B	GRANITE	Katherine Rd	3	Arnhem Bay...	12 36	136 32.5
AL1-1	CLAYEY SANDSTONE	Stoney Ridge	4	Arnhem Bay...	12 24.49	136 51.50
AL1-2	BRECCIA	Stoney Ridge	4	Arnhem Bay...	12 24.49	136 51.50
AL1-3	CLAYEY SANDSTONE	Stoney Ridge	4	Arnhem Bay...	12 24.49	136 51.50
AL1-4	QTZ ARENITE	Stoney Ridge	4	Arnhem Bay...	12 24.49	136 51.50
AL1-5	CLAYSTONE	Stoney Ridge	4	Arnhem Bay...	12 24.49	136 51.50
AL1-6	QTZ ARENITE	Mt Harold NW	5	Arnhem Bay...	12 27.75	136 40
AL1-7	CLAYSTONE	Wonga Ck	7	Arnhem Bay...	12 29.25	136 34
AL1-8	QTZ ARENITE	Wonga Ck	7	Arnhem Bay...	12 29.25	136 34
AL1-9	QTZ ARENITE	Wonga Ck	7	Arnhem Bay...	12 29.25	136 34
AL1-10	CLAYEY SANDSTONE	Wonga Ck	7	Arnhem Bay...	12 29.25	136 34
AL1-11	CLAYEY SANDSTONE	Wonga Ck	7	Arnhem Bay...	12 29.25	136 34
AL1-12	LATERITE	Dhalingbuy	8	Arnhem Bay...	12 24	136 28.25
AL1-13	QTZ ARENITE	Holly Inlet N	9	Arnhem Bay...	12 32	136 42.25
AL1-14	LATERITE	Holly Inlet N	9	Arnhem Bay...	12 32	136 42.25
AL1-15	CLAYEY SANDSTONE	Wonga Ck W	10	Arnhem Bay...	12 30.5	136 32
AL1-16	CALC ARENITE	Gathalala	11	Arnhem Bay...	12 44.25	136 35.5
AL1-17	QTZ ARENITE	Gathalala	11	Arnhem Bay...	12 44.25	136 35.5
AL1-18	QTZ ARENITE	Holly Inlet S	12	Arnhem Bay...	12 38	136 40
AL1-19	SILTSTONE	Holly Inlet S	12	Arnhem Bay...	12 38	136 40
AL1-20	SILTSTONE	Mt Alexander N	13	Arnhem Bay...	12 40.5	136 40.5
AL1-21	Mn CEMENTED ROCK	Woodah Isl	14	Blue Mud Bay...	13 27	136 11
AL1-22	PISOLITIC Mn ROCK	Woodah Isl	14	Blue Mud Bay...	13 27	136 11
AL1-23	PISOLITIC Mn ROCK	Woodah Isl	14	Blue Mud Bay...	13 27	136 11
AL1-24	Mn CEMENTED ROCK	Round Hill Isl	15	Blue Mud Bay...	13 18.5	136 5.5
AL1-25	Mn CEMENTED ROCK	Round Hill Isl	15	Blue Mud Bay...	13 18.5	136 5.5
AL1-26	PISOLITIC LATERITE	Round Hill Isl	15	Blue Mud Bay...	13 18.5	136 5.5
AL1-27	PISOLITIC LATERITE	Grindall Bay	16	Blue Mud Bay...	13 12.5	136 4.5
AL1-28	Mn CEMENTED ROCK	Slippery Ck	17	Arnhem Bay...	12 17.5	135 57
AL1-29	SILTSTONE	Slippery Ck	17	Arnhem Bay...	12 17.5	135 57
AL1-30	SILTSTONE	Slippery Ck	17	Arnhem Bay...	12 17.5	135 57
AL1-31	PISOLITIC ARENITE	Slippery Ck	17	Arnhem Bay...	12 17.5	135 57
AL1-32	PISOLITIC ARENITE	Slippery Ck	17	Arnhem Bay...	12 17.5	135 57
AL1-33	QTZ ARENITE	Cato R	18	Arnhem Bay...	12 21	136 27.5
AL1-34	PISOLITIC Mn ROCK	Frederick Hills	19	Arnhem Bay...	12 43.5	136 24
AL1-35	PISOLITIC Mn ROCK	Frederick Hills	20	Arnhem Bay...	12 46	136 20.5
AL1-36	CALC ARENITE	Point Alexander	21	Arnhem Bay...	12 49.5	136 36.5
AL1-37	LATERITE	Burungbirinung R	23	Arnhem Bay...	12 8	136 19.5
AL1-Misc A	manganiferous rock	various		Arnhem Bay...		
AL1-Misc B	manganiferous rock	various		Arnhem Bay...		
AL1-Misc C	manganiferous rock	various		Arnhem Bay...		
AL2-1	QTZ ARENITE	Kalarwoi R	24	Arnhem Bay...	12 26	135 37.5
AL2-2	CLAYEY SANDSTONE	Kalarwoi R	24	Arnhem Bay...	12 26	135 37.5
AL2-3	QTZ ARENITE	Kalarwoi R	25	Arnhem Bay...	12 24.5	135 36.25
AL2-4	CLAYEY SANDSTONE	Kalarwoi R	25	Arnhem Bay...	12 24.5	135 36.25
AL2-5	LATERITE	Goromuru R	26	Arnhem Bay...	approx 12 40	approx 136 07
AL2-6	QTZ ARENITE	Nilipitchi	28	Blue Mud Bay...	13 34.5	135 27.5
AL2-7	QTZ ARENITE	Nilipitchi	28	Blue Mud Bay...	13 34.5	135 27.5
AL2-8	QTZ ARENITE	Nilipitchi	28	Blue Mud Bay...	13 34.5	135 27.5
AL2-9	SHALE	Nilipitchi	28	Blue Mud Bay...	13 34.5	135 27.5
AL2-10	QTZ ARENITE	Marura Ck	31	Blue Mud Bay...	13 23.25	135 30.5
AL2-11	QTZ ARENITE	Marura Ck	31	Blue Mud Bay...	13 23.25	135 30.5
AL2-12	CONGLOMERATE	Marura Ck	31	Blue Mud Bay...	13 23.25	135 30.5
AL2-13	QTZ ARENITE	Marura Ck	31	Blue Mud Bay...	13 23.25	135 30.5
AL2-14	CLAYSTONE	Marura Ck	31	Blue Mud Bay...	13 23.25	135 30.5
AL2-15	QTZ ARENITE	Marura Ck	32	Blue Mud Bay...	13 22	135 29.5
AL2-16	QTZ ARENITE	Marura Ck	32	Blue Mud Bay...	13 22	135 29.5
AL2-17	QTZ ARENITE	Marura Ck	32	Blue Mud Bay...	13 22	135 29.5
AL2-18	CLAYSTONE	Marura Ck	32	Blue Mud Bay...	13 22	135 29.5
AL2-19	QTZ ARENITE	Marura Ck	33	Blue Mud Bay...	13 22.95	135 31
AL2-20	SILTSTONE	Marura Ck	33	Blue Mud Bay...	13 22.95	135 31
AL2-21	QTZ ARENITE	Central Spur S	34	Blue Mud Bay...	13 36	135 20.5
AL2-22	QTZ ARENITE	Central Spur S	34	Blue Mud Bay...	13 36	135 20.5
AL2-23	QTZ ARENITE	Central Spur	35	Blue Mud Bay...	13 32	135 21

AL2-24	QTZ ARENITE	Central Spur	35	Blue Mud Bay...	13 32	135 21
AL2-25	QTZ ARENITE	Parsons Ra S	36	Blue Mud Bay...	13 42.25	135 11
AL2-26	QTZ ARENITE	Parsons Ra S	36	Blue Mud Bay...	13 42.25	135 11
AL2-27	QTZ ARENITE	Parsons Ra N	37	Blue Mud Bay...	13 31.75	135 15.5
AL2-28	CLAYSTONE	Walker R	39	Blue Mud Bay...	13 32	135 26.5
AL2-29	PISOLITIC Mn ROCK	Strawbridge Ck	42	Blue Mud Bay...	13 18	135 36
AL2-30	QTZ ARENITE	Strawbridge Ck	42	Blue Mud Bay...	13 18	135 36
AL2-31	CLAYSTONE	Koolatong R	44	Blue Mud Bay...	13 01	135 37.5
AL2-32	LATERITE	Wonga Ck	7	Arnhem Bay...	12 29.25	136 34
AL2-Misc A	manganiferous rock	various		Blue Mud Bay...		
AL2-Misc B	manganiferous rock	various		Blue Mud Bay...		
AL2-Misc C	manganiferous rock	various		Blue Mud Bay...		
AL2-Misc D	manganiferous rock	various		Blue Mud Bay...		
AL2-Misc E	manganiferous rock	various		Blue Mud Bay...		
AL2-Misc F	manganiferous rock	various		Blue Mud Bay...		
AL2-Misc G	manganiferous rock	various		Blue Mud Bay...		
AL2-Misc H	manganiferous rock	various		Blue Mud Bay...		
AL3-1	LITH ARENITE	Yiyintyi Ra	46	Mt Young	15 26	135 42.5
AL3-2	CONGLOMERATE	Yiyintyi Ra	46	Mt Young	15 26	135 42.5
AL3-3	QTZ ARENITE	Yiyintyi Ra	47	Mt Young	15 25	135 40.5
AL3-3B	QTZ ARENITE	Yiyintyi Ra	49	Mt Young	15 24.5	135 41.25
AL3-4	CALC ARENITE	Mt Young E	50	Mt Young	15 10	135 45.5
AL3-5	CLAYSTONE	Kalampirri Ck	52	Mt Young	15 36.75	135 36.5
AL3-6	QTZ ARENITE	Kalampirri Ck	52	Mt Young	15 36.75	135 36.5
AL3-7	QTZ ARENITE	Bukalara Plateau	54	Bauhinia Downs	16 6.5	136 09
AL3-8A	SILTSTONE	Bukalara Plateau	54	Bauhinia Downs	16 6.5	136 09
AL3-8B	QTZ ARENITE	Bukalara Plateau	54	Bauhinia Downs	16 6.5	136 09
AL3-8C	QTZ ARENITE	Bukalara Plateau	54	Bauhinia Downs	16 6.5	136 09
AL3-8D	QTZ ARENITE	Bukalara Plateau	54	Bauhinia Downs	16 6.5	136 09
AL3-9	SILTSTONE	Bukalara Plateau	54	Bauhinia Downs	16 6.5	136 09
AL3-10	CLAYEY SANDSTONE	Batten Ck E	55	Bauhinia Downs	16 3.75	136 10
AL3-11	SILTSTONE	Batten Ck E	55	Bauhinia Downs	16 3.75	136 10
AL3-12	QTZ ARENITE	Batten Ck	56	Mt Young	15 58	136 17.5
AL3-13	QTZ ARENITE	Batten Ck	56	Mt Young	15 58	136 17.5
AL3-14	QTZ ARENITE	Watertower	57	Bauhinia Downs	16 03	136 18
AL3-15	QTZ ARENITE	Rosie Ck	58	Mt Young	15 43.75	135 40
AL3-16	QTZ ARENITE	Rosie Ck	58	Mt Young	15 43.75	135 40
AL3-17	QTZ ARENITE	Rosie Ck	58	Mt Young	15 43.75	135 40
AL3-18	QTZ ARENITE	Rosie Ck	58	Mt Young	15 43.75	135 40
AL3-19	QTZ ARENITE	Rosie Ck	58	Mt Young	15 43.75	135 40
AL3-20	QTZ ARENITE	Rosie Ck	58	Mt Young	15 43.75	135 40
AL3-20B	QTZ ARENITE	Rosie Ck	59	Mt Young	15 43.75	135 37.5
AL3-21	QTZ ARENITE	Rosie Ck	59	Mt Young	15 43.75	135 37.5
AL3-22	SILTSTONE	Mcleod Ra	60	Bauhinia Downs	16 3.75	136 21.5
AL3-23	QTZ ARENITE	Mcleod Ra	60	Bauhinia Downs	16 3.75	136 21.5
AL3-24	QTZ ARENITE	Borroloola W	65	Bauhinia Downs	16 3.5	136 11.5
AL3-25	QTZ ARENITE	Borroloola W	65	Bauhinia Downs	16 3.5	136 11.5
AL3-26	QTZ ARENITE	Borroloola W	65	Bauhinia Downs	16 3.5	136 11.5
AL3-27	QTZ ARENITE	Batten Ck	66	Bauhinia Downs	16 6.5	136 04
AL3-28	SILTSTONE	Emu Fault	67	Bauhinia Downs	16 7.75	135 59.5
AL3-29	CONGLOMERATE	Emu Fault	67	Bauhinia Downs	16 7.75	135 59.5
AL3-30	QTZ ARENITE	Emu Fault	67	Bauhinia Downs	16 7.75	135 59.5
AL3-31	CLAYSTONE	Emu Fault	67	Bauhinia Downs	16 7.75	135 59.5
AL3-32	QTZ ARENITE	Bauhinia Downs	68	Bauhinia Downs	16 10	135 26.5
AL3-33	QTZ ARENITE	Bauhinia Downs	68	Bauhinia Downs	16 10	135 26.5
AL3-33A	QTZ ARENITE	Bauhinia Downs	68	Bauhinia Downs	16 10	135 26.5
AL3-34	SOIL	Bauhinia Downs	68	Bauhinia Downs	16 10	135 26.5
AL3-35	QTZ ARENITE	Bauhinia Downs	68	Bauhinia Downs	16 10	135 26.5
AL3-35A	QTZ ARENITE	Bauhinia Downs	68	Bauhinia Downs	16 10	135 26.5
AL3-36	SOIL	Bauhinia Downs	68	Bauhinia Downs	16 10	135 26.5
AL3-37	QTZ ARENITE	Bauhinia Downs	69	Bauhinia Downs	16 9.5	135 25.5
AL3-38	QTZ ARENITE	Bauhinia Downs	69	Bauhinia Downs	16 9.5	135 25.5
AL3-39	QTZ ARENITE	Bauhinia Downs	69	Bauhinia Downs	16 9.5	135 25.5
AL3-40	QTZ ARENITE	Bauhinia Downs	70	Bauhinia Downs	16 10	135 22.5
AL3-41	SILTSTONE	Balbirini Ck	71	Bauhinia Downs	16 33.5	135 21
AL3-42	QTZ ARENITE	Balbirini Ck	71	Bauhinia Downs	16 33.5	135 21
AL3-43	SILTSTONE	Favenc Ra	72	Bauhinia Downs	16 42	135 23

AL3-44	CLAYSTONE	Favenc Ra	73	Bauhinia Downs	approx 16 43	approx 135 22
AL3-45	PISOLITIC LATERITE	Favenc Ra	74	Bauhinia Downs	approx 16 45	approx 135 24
AL3-46	CLAYSTONE	Favenc Ra	74	Bauhinia Downs	approx 16 45	approx 135 24
AL3-47	PISOLITIC LATERITE	Favenc Ra	74	Bauhinia Downs	approx 16 45	approx 135 24
AL3-48	QTZ ARENITE	Paddy Spring Ck	75	Bauhinia Downs	16 46.5	135 38
AL3-49	QTZ ARENITE	Paddy Spring Ck	75	Bauhinia Downs	16 46.5	135 38
AL3-50	LITH ARENITE	Paddy Spring Ck	75	Bauhinia Downs	16 46.5	135 38
AL3-51	QTZ ARENITE	Paddy Spring Ck	75	Bauhinia Downs	16 46.5	135 38
AL3-52	SILTSTONE	Yalco Ck	76	Bauhinia Downs	16 09	135 57.75
AL3-53	CONGLOMERATE	Yalco Ck	77	Bauhinia Downs	16 2.75	135 50
AL3-54	QTZ ARENITE	Yalco Ck	77	Bauhinia Downs	16 2.75	135 50
AL3-55	QTZ ARENITE	Festing Ck	78	Mt Young	15 51.5	135 49.5
AL3-56	QTZ ARENITE	Festing Ck	78	Mt Young	15 51.5	135 49.5
AL3-57	QTZ ARENITE	Nathan R	79	Mt Young	15 39	135 30.5
AL3-58	SILTSTONE	Four Archers	80	Mt Young	15 27.75	135 25
AL3-59	SHALE	Four Archers	80	Mt Young	15 27.75	135 25
AL3-60	LITH ARENITE	Surprise Ck	81	Mt Young	15 31.5	135 22.5
AL3-61	LATERITE	Anderson Ck	82	Hodgson Downs	15 55.5	134 15
AL3-62	CLAYSTONE	Anderson Ck	82	Hodgson Downs	15 55.5	134 15
AL3-63	SILTSTONE	Arnold R	83	Hodgson Downs	15 46.75	134 20
AL3-64	Fe CONCRETION	Arnold R	83	Hodgson Downs	15 46.75	134 20
AL3-65	LATERITE	Cox R	84	Hodgson Downs	approx 15 58	approx 134 45
AL3-66	SILTSTONE	Cox R	84	Hodgson Downs	approx 15 58	approx 134 45
AL3-67	CLAYSTONE	Cox R	84	Hodgson Downs	approx 15 58	approx 134 45
AL3-68	CLAYEY SANDSTONE	Limestone Ck	85	Mt Young	15 53	135 34
AL3-69	CLAYEY SANDSTONE	Limestone Ck	85	Mt Young	15 53	135 34
AL3-70	BONE FRAGMENT	Limestone Ck	85	Mt Young	15 53	135 34
AL3-71	QTZ ARENITE	Tawallah Ra	86	Mt Young	15 51.5	135 39
AL3-72	QTZ ARENITE	Tawallah Ra	86	Mt Young	15 51.5	135 39
AL3-73	QTZ ARENITE	Tawallah Ra	86	Mt Young	15 51.5	135 39
AL3-74	QTZ ARENITE	Ruined City	88	Urapunga	14 17	134 55
AL3-75	QTZ ARENITE	Ruined City	88	Urapunga	14 17	134 55
AL3-76	QTZ ARENITE	Ruined City S	89	Urapunga	14 21.75	134 50
AL3-77	QTZ ARENITE	Ruined City S	89	Urapunga	14 21.75	134 50
AL3-78	QTZ ARENITE	Roper R	90	Urapunga	14 44	134 58.5
AL3-79	CONGLOMERATE	Piker Ck	91	Mt Young	15 26	135 22
AL3-80	CLAYEY SANDSTONE	Tawallah Pocket	92	Mt Young	15 57	135 42.5
AL3-81	QTZ ARENITE	Tawallah Pocket	92	Mt Young	15 57	135 42.5
AL3-82	QTZ ARENITE	Tawallah Pocket	92	Mt Young	15 57	135 42.5
AL3-83	CONGLOMERATE	Scrutton Ck	93	Bauhinia Downs	approx 16 09	approx 135 39
AL3-84	SILTSTONE	Barney Ck	94	Bauhinia Downs	approx 16 24	approx 135 50
AL3-85	SILTSTONE	Barney Ck	94	Bauhinia Downs	approx 16 24	approx 135 50
AL3-86	QTZ ARENITE	Barney Ck	94	Bauhinia Downs	approx 16 24	approx 135 50
AL3-87	CLAYEY SANDSTONE	Barney Ck	94	Bauhinia Downs	approx 16 24	approx 135 50
AL3-88	QTZ ARENITE	Barney Ck	94	Bauhinia Downs	approx 16 24	approx 135 50
AL4-1	SILTSTONE	Bostock Ck	96	Wallhallow	17 14	135 38.5
AL4-2	EVAPORITE	Bostock Ck	96	Wallhallow	17 14	135 38.5
AL4-3	SILTSTONE	Bostock Ck	96	Wallhallow	17 14	135 38.5
AL4-4	QTZ ARENITE	Bostock Ck	96	Wallhallow	17 14	135 38.5
AL4-5	CLAYSTONE	Bostock Ck	96	Wallhallow	17 14	135 38.5
AL4-6	CALC SILTSTONE	Bostock Ck	96	Wallhallow	17 14	135 38.5
AL4-7	SILTSTONE	Spear Ck	97	Wallhallow	17 17.5	135 50.5
AL4-8	CLAYSTONE	Spear Ck	97	Wallhallow	17 17.5	135 50.5
AL4-9	SILTSTONE	Spear Ck	97	Wallhallow	17 17.5	135 50.5
AL4-10	CLAYSTONE	Bostock Ck	98	Wallhallow	17 14	135 31.5
AL4-11	Mn CEMENTED ROCK	Lancewood Ck	99	Wallhallow	17 16	136 14.75
AL4-12	CLAYSTONE	Lancewood Ck	99	Wallhallow	17 16	136 14.75
AL4-13	CLAYSTONE	Rocky Ck	100	Wallhallow	17 20.5	136 13.5
AL4-14	LATERITE	Rocky Ck	100	Wallhallow	17 20.5	136 13.5
AL4-15	CLAYEY SANDSTONE	Mcarthur R	62	Bauhinia Downs	16 17.5	136 16.75
AL4-15A	CLAYEY SANDSTONE	Mcarthur R	62	Bauhinia Downs	16 17.5	136 16.75
AL4-15B	CLAYEY SANDSTONE	Mcarthur R	62	Bauhinia Downs	16 17.5	136 16.75
AL4-15C	CLAYEY SANDSTONE	Mcarthur R	62	Bauhinia Downs	16 17.5	136 16.75
AL4-16	QTZ ARENITE	Mcarthur R	62	Bauhinia Downs	16 17.5	136 16.75
AL4-17	CLAYEY SANDSTONE	Frazer Ck	63	Bauhinia Downs	16 19.5	136 18.5
AL4-18	CLAYEY SANDSTONE	Kangaroo Ck	101	Robinson Rr	16 54.5	137 7
AL4-19	CONGLOMERATE	Echo Gorge	102	Calvert Hills	17 11	137 43

AL4-20	QTZ ARENITE	Echo Gorge	102	Calvert Hills	17 11	137 43
AL4-21	LITH ARENITE	Echo Gorge	102	Calvert Hills	17 11	137 43
AL4-22	QTZ ARENITE	Echo Gorge	102	Calvert Hills	17 11	137 43
AL4-23	QTZ ARENITE	Seigals Ck HS	103	Calvert Hills	17 36.5	137 34
AL4-24	CLAYEY SANDSTONE	Seigals Ck HS	103	Calvert Hills	17 36.5	137 34
AL4-25	CLAYSTONE	Seigals Ck HS	103	Calvert Hills	17 36.5	137 34
AL4-26	CLAYSTONE	Seigals Ck HS	103	Calvert Hills	17 36.5	137 34
AL4-27	Fe CEMENTED ROCK	Seigals Ck HS	103	Calvert Hills	17 36.5	137 34
AL4-28	CLAYSTONE	Seigals Ck HS	103	Calvert Hills	17 36.5	137 34
AL4-29	SILTSTONE	Seigals Ck HS	103	Calvert Hills	17 36.5	137 34
AL4-30	CLAYEY SANDSTONE	Debbil Debbil Ck	105	Calvert Hills	17 38.5	137 46
AL4-31	SILTSTONE	Debbil Debbil Ck	105	Calvert Hills	17 38.5	137 46
AL4-32	CONGLOMERATE	Debbil Debbil Ck	105	Calvert Hills	17 38.5	137 46
AL4-33	CLAYSTONE	Debbil Debbil Ck	105	Calvert Hills	17 38.5	137 46
AL4-34	CLAYEY SANDSTONE	Debbil Debbil Ck	105	Calvert Hills	17 38.5	137 46
AL4-35	CLAYEY SANDSTONE	Debbil Debbil Ck	106	Calvert Hills	17 35.5	137 49
AL4-36	CLAYSTONE	Debbil Debbil Ck	106	Calvert Hills	17 35.5	137 49
AL4-37	SILTSTONE	Debbil Debbil Ck	106	Calvert Hills	17 35.5	137 49
AL4-38	SILTSTONE	Debbil Debbil Ck	106	Calvert Hills	17 35.5	137 49
AL4-39	QTZ ARENITE	Debbil Debbil Ck	106	Calvert Hills	17 35.5	137 49
AL4-40	SILTSTONE	Debbil Debbil Ck	106	Calvert Hills	17 35.5	137 49
AL4-41	CLAYEY SANDSTONE	Debbil Debbil Ck	106	Calvert Hills	17 35.5	137 49
AL4-42	CLAYEY SANDSTONE	Debbil Debbil Ck	106	Calvert Hills	17 35.5	137 49
AL4-43	CLAYEY SANDSTONE	Debbil Debbil Ck	106	Calvert Hills	17 35.5	137 49
AL4-44	SILTSTONE	Debbil Debbil Ck	106	Calvert Hills	17 35.5	137 49
AL4-45	CONGLOMERATE	Debbil Debbil Ck	106	Calvert Hills	17 35.5	137 49
AL4-46	CLAYEY SANDSTONE	Debbil Debbil Ck	106	Calvert Hills	17 35.5	137 49
AL4-47	CLAYSTONE	Bluey Ck	108	Calvert Hills	17 10.25	137 10.5
AL4-48	CLAYEY SANDSTONE	Bluey Ck	108	Calvert Hills	17 10.25	137 10.5
AL4-49	CLAYSTONE	Bluey Ck	108	Calvert Hills	17 10.25	137 10.5
AL4-50	CLAYSTONE	Blackfella Ck	109	Calvert Hills	17 24.75	137 3.25
AL4-51	SILTSTONE	Nicholson R	112	Calvert Hills	17 47.5	137 17.25
AL4-52	QTZ ARENITE	Wallis Ck	113	Calvert Hills	17 56.5	137 34
AL4-53	CLAYSTONE	Wallis Ck	113	Calvert Hills	17 56.5	137 34
AL4-54	CONGLOMERATE	Wallis Ck	113	Calvert Hills	17 56.5	137 34
AL4-55	QTZ ARENITE	Nicholson R	114	Mt Drummond	18 1	137 23
AL4-56	SILTSTONE	Bauhinia Ck	115	Mt Drummond	18 7	137 34
AL4-57	CLAYSTONE	Bauhinia Ck	115	Mt Drummond	18 7	137 34
AL4-58	SILTSTONE	Bauhinia Ck	115	Mt Drummond	18 7	137 34
AL4-59	CLAYSTONE	Bullock Ck	116	Mt Drummond	18 9	137 40.75
AL4-60	QTZ ARENITE	Bullock Ck	116	Mt Drummond	18 9	137 40.75
AL4-61	SILTSTONE	Return Ck	117	Mt Drummond	18 13.75	137 41
AL4-62	Fe CEMENTED ROCK	Fish River HS	118	Calvert Hills	17 55.25	137 48.5
AL4-63	QTZ ARENITE	Border Ck	119	Mt Drummond	18 2.25	137 56
AL4-64	SILTSTONE	Border Ck	120	Mt Drummond	18 15.75	137 53.75
AL4-65	CLAYSTONE	Fish Hole WH	124	Lawn Hill	18 23	138 27.25
AL4-66	CONGLOMERATE	Bellbird Ck	125	Lawn Hill	18 57	138 35
AL4-67	SILTSTONE	Horse Ck	126	Lawn Hill	18 50	138 57.75
AL4-68	SILTSTONE	Horse Ck	126	Lawn Hill	18 50	138 57.75
AL4-69	QTZ ARENITE	Horse Ck	126	Lawn Hill	18 50	138 57.75
AL4-70	SILTSTONE	Sandy Ck	127	Lawn Hill	18 43.75	138 55.25
AL4-71	SILTSTONE	Sandy Ck	127	Lawn Hill	18 43.75	138 55.25
AL4-72	QTZ ARENITE	Jenny Ck	128	Lawn Hill	18 27.5	138 48.75
AL4-73	QTZ ARENITE	Accident Ck	129	Lawn Hill	18 7	138 28
AL4-74	SILTSTONE	Accident Ck	129	Lawn Hill	18 7	138 28
AL4-75	SILTSTONE	Gorge Ck	130	Westmoreland	17 52.25	138 6.5
AL4-76	CLAYSTONE	Accident Ck	131	Lawn Hill	18 4	138 4.5
AL4-77	CLAYEY SANDSTONE	Musselbrook Ck	132	Lawn Hill	18 36.5	138 9.25
AL4-78	QTZ ARENITE	Musselbrook Ck	132	Lawn Hill	18 36.5	138 9.25
AL4-79T	QTZ ARENITE	Bull Ck	64	Bauhinia Downs	16 29	136 26
AL4-79B	SILTSTONE	Bull Ck	64	Bauhinia Downs	16 29	136 26
AL4-80T	CLAYSTONE	Stott Ck	61	Bauhinia Downs	16 5.5	136 24
AL4-80B	SILTSTONE	Stott Ck	61	Bauhinia Downs	16 5.5	136 24
AL4-81	QTZ ARENITE	Tawallah Pocket	87	Mt Young	15 56	135 38
AL4-82	QTZ ARENITE	Tawallah Pocket	87	Mt Young	15 56	135 38
AL4-83	CLAYEY SANDSTONE	Tawallah Pocket	87	Mt Young	15 56	135 38
AL4-84T	SILTSTONE	Tawallah Pocket	87	Mt Young	15 56	135 38
AL4-84B	SILTSTONE	Tawallah Pocket	87	Mt Young	15 56	135 38

AL4-85T	QTZ ARENITE	Kalampirri Ck	53	Mt Young	15 37.5	135 37
AL4-85B	SILTSTONE	Kalampirri Ck	53	Mt Young	15 37.5	135 37
AL4-86	SILTSTONE	Marura Ck	33	Blue Mud Bay...	13 23.75	135 31
AL4-87	PISOLITIC LATERITE	Matta Murta Ck	45	Blue Mud Bay...	13 10	135 26.5
AL4-X1	Mn DOLOMITE	Calvert Hills HS	107	Calvert Hills	17 12.5	137 19.75
AL4-X2	Mn DOLOMITE	Calvert Hills HS	107	Calvert Hills	17 12.5	137 19.75
AL4-X3	Mn DOLOMITE	Calvert Hills HS	107	Calvert Hills	17 12.5	137 19.75
AL4-X4	Mn DOLOMITE	Calvert Hills HS	107	Calvert Hills	17 12.5	137 19.75
AL4-X5	Mn DOLOMITE	Calvert Hills HS	107	Calvert Hills	17 12.5	137 19.75
AL4-X6	Mn DOLOMITE	Calvert Hills HS	107	Calvert Hills	17 12.5	137 19.75
AL4-X7	Mn DOLOMITE	Calvert Hills HS	107	Calvert Hills	17 12.5	137 19.75
AL4-X8	Mn DOLOMITE	Calvert Hills HS	107	Calvert Hills	17 12.5	137 19.75
AL4-X9	Mn DOLOMITE	Calvert Hills HS	107	Calvert Hills	17 12.5	137 19.75
B-1	SILTSTONE	Marura Ck	33	Blue Mud Bay...	13 22.95	135 31
B-2	SILTSTONE	Marura Ck NE	138	Blue Mud Bay...	13 21.27	135 30.1
B-3	QTZ ARENITE	Marura Ck NE	138	Blue Mud Bay...	13 21.27	135 30.1
B-4	QTZ ARENITE	Marura Ck NE	138	Blue Mud Bay...	13 21.27	135 30.1
B-5	QTZ ARENITE	Marura Ck N	139	Blue Mud Bay...	13 21.25	135 29.88
B-6	SANDSTONE	Marura Ck N	140	Blue Mud Bay...	13 21.73	135 29.88
B-7	SILTSTONE	Marura Ck N	140	Blue Mud Bay...	13 21.73	135 29.88
B-8	SILTSTONE	Marura Ck	141	Blue Mud Bay...	13 22.33	135 30.17
B-9	QTZ ARENITE	Walker R	143	Blue Mud Bay...	13 23	135 28.42
B-10	SANDSTONE	Walker R	144	Blue Mud Bay...	13 23.1	135 27.42
B-11	SANDSTONE	Walker R	144	Blue Mud Bay...	13 23.1	135 27.42
B-12	SILTSTONE	Walker R	146	Blue Mud Bay...	13 23.34	135 26.95
B-13	CLAYEY SANDSTONE	Walker R	146	Blue Mud Bay...	13 23.34	135 26.95
B-14	SANDSTONE	Walker R	146	Blue Mud Bay...	13 23.34	135 26.95
B-15	QTZ ARENITE	Walker R	146	Blue Mud Bay...	13 23.34	135 26.95
B-16	CLAYEY SANDSTONE	Walker R	146	Blue Mud Bay...	13 23.34	135 26.95
B-17	QTZ ARENITE	Walker R	147	Blue Mud Bay...	13 23.68	135 27.02
B-18	QTZ ARENITE	Walker R	147	Blue Mud Bay...	13 23.68	135 27.02
B-19	QTZ ARENITE	Walker R	147	Blue Mud Bay...	13 23.68	135 27.02
B-20	SANDSTONE	Walker R	147	Blue Mud Bay...	13 23.68	135 27.02
B-21	SILTSTONE	Walker R	147	Blue Mud Bay...	13 23.68	135 27.02
B-22	CONGLOMERATE	Walker R	148	Blue Mud Bay...	13 24.23	135 26.12
B-23	SILTSTONE	Walker R	148	Blue Mud Bay...	13 24.23	135 26.12
B-24	SANDSTONE	Walker R	148	Blue Mud Bay...	13 24.23	135 26.12
B-25	SANDSTONE	Walker R	148	Blue Mud Bay...	13 24.23	135 26.12
B-26	SILTY SANDSTONE	Walker R	148	Blue Mud Bay...	13 24.23	135 26.12
B-27	CLAYEY SANDSTONE	Walker R	148	Blue Mud Bay...	13 24.23	135 26.12
B-28	QTZ ARENITE	Walker R	148	Blue Mud Bay...	13 24.23	135 26.12
B-29	SILTSTONE	Walker R	149	Blue Mud Bay...	13 25.86	135 26.9
B-30	CLAYSTONE	Walker R	149	Blue Mud Bay...	13 25.86	135 26.9
B-31	SILTY SANDSTONE	Walker R	149	Blue Mud Bay...	13 25.86	135 26.9
B-32	QTZ ARENITE	Walker R W	150	Blue Mud Bay...	13 26.04	135 25.38
B-33	SILTSTONE	Walker R	154	Blue Mud Bay...	13 27.25	135 27.32
B-34	MN SANDSTONE	Stoney Ridge	4	Arnhem Bay...	12 24.49	136 51.50
B-35	RUBBLY LATERITE	8km Bulman Rd	157	Arnhem Bay...	12 21.15	136 44.95
B-36	QTZ ARENITE	Wonga Ck	161	Arnhem Bay...	12 27.15	136 34.75
B-37	QTZ ARENITE	Pt Bradshaw Rd	164	Arnhem Bay...	12 32.60	136 36.30
B-38	SILTSTONE	Pt Bradshaw Rd	164	Arnhem Bay...	12 32.60	136 36.30
B-39	SILICIFIED WOOD	Conway Ck	166	Blue Mud Bay...	13 30.75	135 26
B-40	QTZ ARENITE	Conway Ck	170	Blue Mud Bay...	13 30.25	135 25.75
B-41	QUARTZITE	Walker R	171	Blue Mud Bay...	13 31.5	135 28
B-42	CLAYSTONE	Walker R	171	Blue Mud Bay...	13 31.5	135 28
B-43	CLAYEY SANDSTONE	Walker R	172	Blue Mud Bay...	13 33	135 28.5
B-44	SILTY SANDSTONE	SSW Nulapitji	173	Blue Mud Bay...	13 33.75	135 29
B-45	SILTY SANDSTONE	SSW Nulapitji	173	Blue Mud Bay...	13 33.75	135 29
B-46	SILTY SANDSTONE	SSW Nulapitji	173	Blue Mud Bay...	13 33.75	135 29
B-47	SILTY SANDSTONE	SSW Nulapitji	173	Blue Mud Bay...	13 33.75	135 29
B-48	CONGLOMERATE	SSW Nulapitji	173	Blue Mud Bay...	13 33.75	135 29
B-49	SILTSTONE	SSW Nulapitji	174	Blue Mud Bay...	13 34	135 29.5
B-50	SANDSTONE	SSW Nulapitji	174	Blue Mud Bay...	13 34	135 29.5
B-51	SILTY SANDSTONE	SSW Nulapitji	174	Blue Mud Bay...	13 34	135 29.5
B-52	QTZ ARENITE	SSW Nulapitji	174	Blue Mud Bay...	13 34	135 29.5
B-53	SILTY SANDSTONE	S Nulapitji	177	Blue Mud Bay...	13 34.5	135 30.75
B-54	SILTY SANDSTONE	S Nulapitji	178	Blue Mud Bay...	13 36	135 30.25

B-55	SILTY SANDSTONE	S Nulapitji	178	Blue Mud Bay...	13 36	135 30.25
B-56	SILTY SANDSTONE	S Nulapitji	178	Blue Mud Bay...	13 36	135 30.25
B-57	SILTY SANDSTONE	S Nulapitji	178	Blue Mud Bay...	13 36	135 30.25
B-58	CONGLOMERATE	S Nulapitji	179	Blue Mud Bay...	13 37	135 30.25
B-59	SANDSTONE	S Nulapitji	179	Blue Mud Bay...	13 37	135 30.25
B-60	SANDSTONE	S Nulapitji	179	Blue Mud Bay...	13 37	135 30.25
B-61	SILTY SANDSTONE	S Nulapitji	179	Blue Mud Bay...	13 37	135 30.25
B-62	SANDSTONE	S Nulapitji	179	Blue Mud Bay...	13 37	135 30.25
B-63	CONGLOMERATE	S Nulapitji	179	Blue Mud Bay...	13 37	135 30.25
B-64	CONG SANDSTONE	S Nulapitji	180	Blue Mud Bay...	13 37.5	135 30
B-65	CLAYEY SANDSTONE	S Nulapitji	181	Blue Mud Bay...	13 37.75	135 29.25
B-66	CLAYEY SANDSTONE	S Nulapitji	181	Blue Mud Bay...	13 37.75	135 29.25
B-67	CLAYEY SANDSTONE	S Nulapitji	182	Blue Mud Bay...	13 38	135 29
B-68	CLAYEY SANDSTONE	S Nulapitji	182	Blue Mud Bay...	13 38	135 29
B-69	SILTY SANDSTONE	S Nulapitji	182	Blue Mud Bay...	13 38	135 29
B-70	CONG SANDSTONE	S Nulapitji	182	Blue Mud Bay...	13 38	135 29
B-71	CONGLOMERATE	S Nulapitji	182	Blue Mud Bay...	13 38	135 29
B-72	CONGLOMERATE	S Nulapitji	182	Blue Mud Bay...	13 38	135 29
B-73	SILTY SANDSTONE	S Nulapitji	184	Blue Mud Bay...	13 39.25	135 28.75
B-74	SANDSTONE	S Nulapitji	184	Blue Mud Bay...	13 39.25	135 28.75
B-75	SANDSTONE	S Nulapitji	184	Blue Mud Bay...	13 39.25	135 28.75
B-76	QTZ ARENITE	Pt Bradshaw Rd	187	Arnhem Bay...	12 32	136 41
B-77	QTZ ARENITE	Pt Bradshaw Rd	189	Arnhem Bay...	12 30.75	136 36.25
B-78	LATERITE	NNE Dhalingbuy	196	Arnhem Bay...	12 19.25	136 31.5
B-79	CLAYSTONE	Wonga Ck NW	197	Arnhem Bay...	12 24.7	136 33.4
B-80	QTZ ARENITE	S Koolatong R	198	Blue Mud Bay...	13 11.89	135 35.12
B-81	SILTSTONE	S Koolatong R	198	Blue Mud Bay...	13 11.89	135 35.12
B-82	CONG SANDSTONE	S Koolatong R	200	Blue Mud Bay...	13 07.25	135 37.1
B-83	SANDSTONE	S Koolatong R	201	Blue Mud Bay...	13 05.6	135 36.5
B-84	SANDSTONE	S Koolatong R	206	Blue Mud Bay...	13 05.9	135 38.25
B-85	CONGLOMERATE	S Koolatong R	207	Blue Mud Bay...	13 06	135 38.6
B-86	CONG SANDSTONE	Vaughton Ck	212	Blue Mud Bay...	13 40	135 11
B-87	CLAYEY SANDSTONE	Vaughton Ck	213	Blue Mud Bay...	13 39.7	135 11.5
B-88	QTZ ARENITE	Vaughton Ck	213	Blue Mud Bay...	13 39.7	135 11.5
B-89	QTZ ARENITE	Vaughton Ck	213	Blue Mud Bay...	13 39.7	135 11.5
B-90	SILTY SANDSTONE	Vaughton Ck	213	Blue Mud Bay...	13 39.7	135 11.5
B-91	SANDSTONE	Vaughton Ck	213	Blue Mud Bay...	13 39.7	135 11.5
GE-1	CLAYSTONE	C Quarry - G.E.	-	Blue Mud Bay...	13 57.5	136 27.75
GE-2	CLAYSTONE	C Quarry - G.E.	-	Blue Mud Bay...	13 57.5	136 27.75
GE-3	Mn CEMENTED ROCK	C Quarry - G.E.	-	Blue Mud Bay...	13 57.5	136 27.75
Drillhole			Depth			
US 17	CLAYSTONE	Numbulwar N	96.8	Roper River...	14 7.75	136 47
US 19	QTZ ARENITE	Numbulwar N	25	Roper River...	14 06	136 48
US 19	CLAYSTONE	Numbulwar N	66	Roper River...	14 06	136 48
US 19	CLAYSTONE	Numbulwar N	97.6	Roper River...	14 06	136 48
US 21	SILTSTONE	Numbulwar N	117	Roper River...	14 9.25	136 49
US 22	CLAYSTONE	Numbulwar N	36.5	Roper River...	14 07	136 49.5
US 22	CLAYEY SILTSTONE	Numbulwar N	40.8	Roper River...	14 07	136 49.5
US 28	CLAYSTONE	Numbulwar N	66	Roper River...	14 08	136 45.5
US 30	SILTSTONE	Numbulwar N	18	Roper River...	14 11.75	136 44
US 33	CLAYSTONE	Numbulwar N	26	Roper River...	14 11.25	136 49
US 34	CLAYSTONE	Numbulwar N	27	Roper River...	14 11.5	136 49
US 37	SILTSTONE	Numbulwar N	57	Roper River...	14 6.5	136 53
US 37	CLAYSTONE	Numbulwar N	62	Roper River...	14 6.5	136 53
US 38	CLAYSTONE	Numbulwar N	88.5	Roper River...	14 06	136 52.25
US 40	SILTSTONE	Numbulwar N	33	Roper River...	14 5.5	136 50.5
US 41	CLAYSTONE	Numbulwar N	83	Roper River...	14 5.5	136 49.5
US 41	CLAYSTONE	Numbulwar N	93	Roper River...	14 5.5	136 49.5

Sample depth for drillholes in feet.

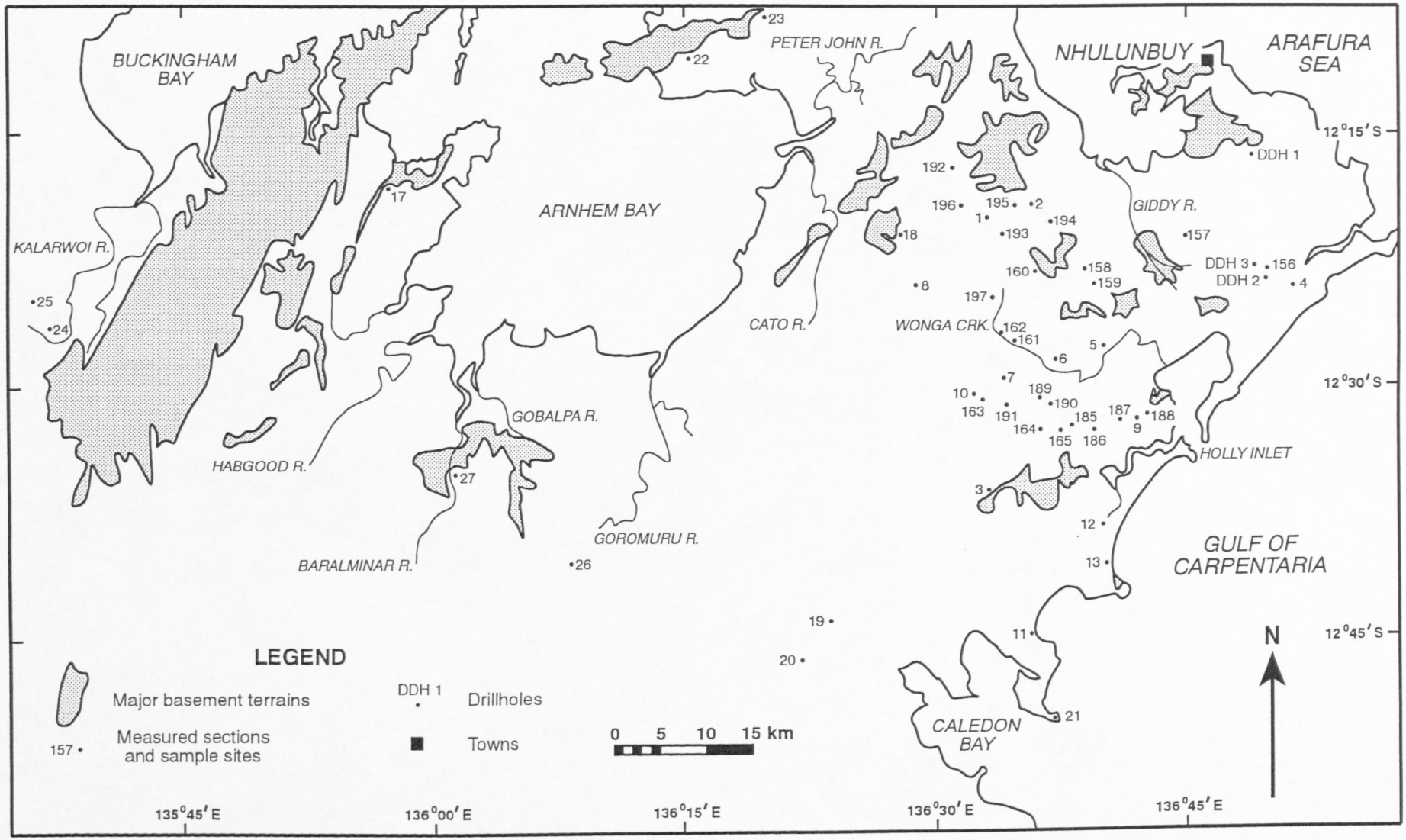

Detailed base map for the Arnhem Land Zone.

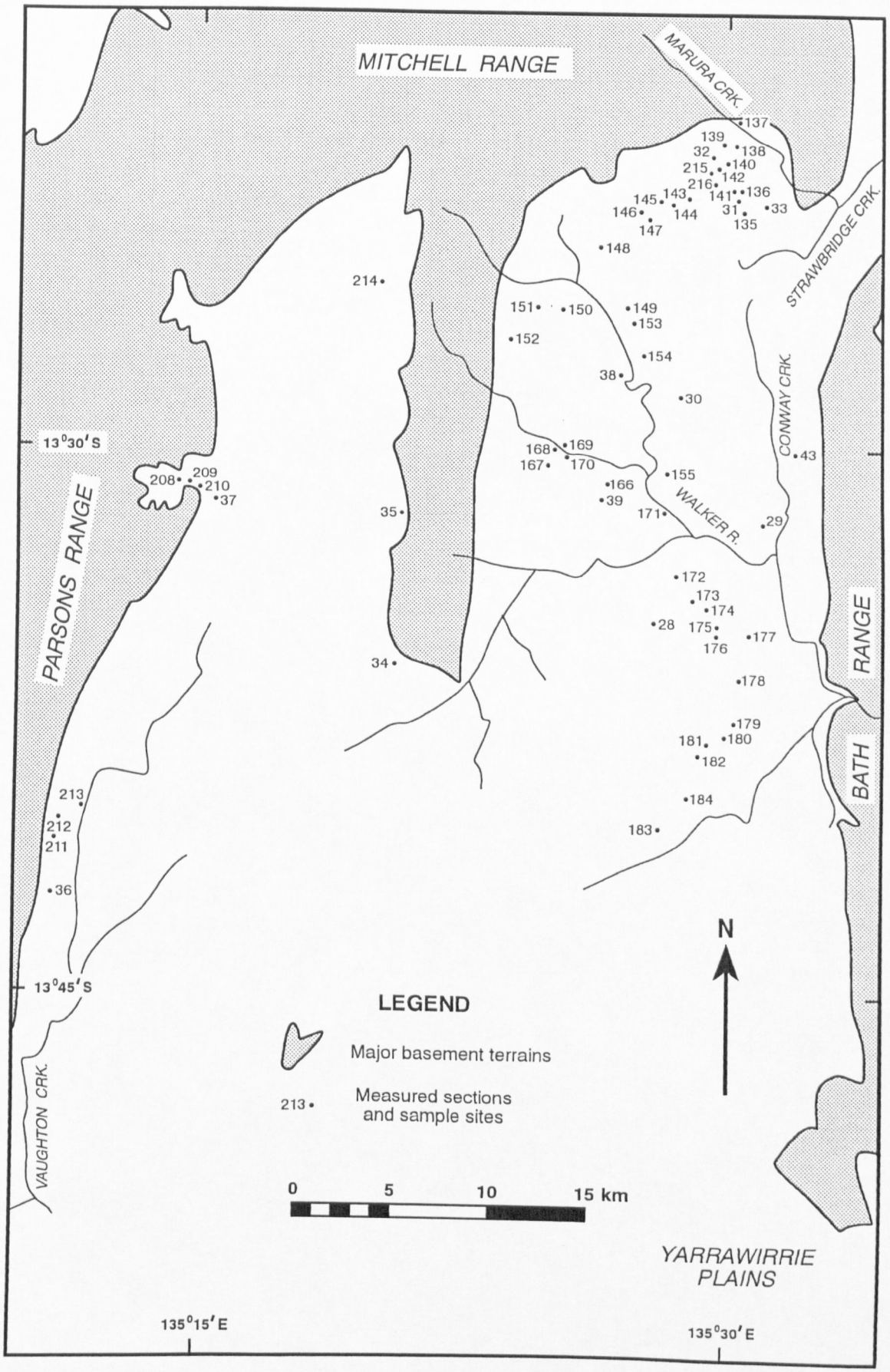

Detailed base map for the Bath and Parsons Ranges Zone.

APPENDIX 4:
PETROGRAPHIC DESCRIPTIONS

4.1 INTRODUCTION

This appendix focuses on the petrographic description of thin sections from a representative suite of samples from the Cretaceous sequence. Most of the samples described herein are coarser than silt size because the study of finer-grained rocks is best left to other methods such as XRD (see Appendix 6). The rocks described here generally represent marine depositional environments of the inner and middle shelf and were mostly collected from the northern and central regions of the study area.

4.2 SUMMARY

The petrology and mineralogy of rocks throughout the shelf succession in the study area are not especially distinctive. Regardless of grain size, thickness, stratigraphic position, or depositional (palaeogeographical) location on the shelf, petrological examination and XRD analyses (Appendix 6) of samples throughout the shelf succession has documented their rather simple mineralogies.

Most of the marine rocks are texturally and compositionally mature or supermature, although the degree of sorting and roundness vary between facies. Nonmarine rocks are massive and have similar compositions. These features are described in the petrological reports for particular samples that follow, but are probably best illustrated in photomicrographs interspersed with the main text. The facies are ordered by sample / thin section number and most of the facies are described, but emphasis is placed on the marine facies.

Quartz is the dominant framework grain component of the rocks, lithics are relatively rare, and weathered feldspar is an even less common framework grain component. Matrix is composed dominantly of kaolinite, silty and sandy clays, and less common muscovite and illite. The other significant components of the rocks are hematite and goethite as grain coatings, microscopic 'dust', and cement. Ferromanganese- or manganese-oxides are present as thin stainings or grain coatings, and more rarely as cement. Silica cement and large quartz overgrowths also feature prominently, especially in coarser-grained sandstones. The rocks do not appear to have been affected by any significant compaction or burial diagenesis, and many late-stage petrological features can be ascribed to the significant amount of near-surface chemical diagenesis and weathering that the rocks have suffered in the humid tropical environment of the Northern Territory.

Sample Number: AL1-4 **Facies:** 9
Section Number: 4 **Area:** Stoney Ridge
Stratigraphic distance from base of section: 12 m
Location: **latitude** 12° 24.49' **longitude** 136° 51.5'

Grainsize Name: very fine grained iron-cemented litharenite.

Hand Specimen: Brown, slightly friable, porous fine-grained sandstone with widely spaced irregular lamination and heavy iron-oxide staining.

Micro Description: A highly porous rock with the porosity derived from the dissolution of a primary sedimentary component, probably feldspar. The majority of the pores are angular and range in size from 0.08 to 0.3 mm. The irregular lamination (laminae up to 2 mm thick) is defined by more porous zones. The other components are highly altered and iron stained lithic clasts set in iron-oxide cement with pockets of hematitic clay in places, along with rare 'book like' masses of another clay, probably illite.

Framework Grains (grainsize, sorting, roundness):
0.1-0.5 mm (av 0.12), moderately-well sorted, subrounded-subangular, iron-oxide stained lithic fragments.

Matrix (grainsize, sorting, roundness):
Very fine-grained hematitic clay.

Cement:
Iron-oxide cements (possibly 2 generations); one is bright orange in PPL (plane polarised light) and the other is isotropic.

Composition (%):		
	Quartz	<15
	Feldspar	5
	Lithic/Rock Fragments	25
	Opaques/Accessories	
	Matrix	10-15
	Cement	15
	Porosity	25

Sample Number: AL1-10 **Facies:** 14
Section Number: 7 **Area:** Wonga Creek
Stratigraphic distance from base of section: 3 m
Location: **latitude** 12° 29.25' **longitude** 136° 34'

Grainsize Name: Very coarse-grained (silt) quartzwacke

Hand Specimen: White, very coarse-grained, clayey siltstone with traces of crossbedding.

Micro Description: Large, randomly oriented, fractured composite quartz grains are the framework of the fabric. These grains are corroded and show deeply embayed concavo/convex and sutured grain boundaries and numerous poikilitic inclusions. The quartz grains are set in a uniform, pure very fine-grained clay (kaolinite) matrix. Large irregular masses of illite/muscovite up to 1.5 mm in diameter are associated with the large quartz grains in places, and were probably derived authigenically by replacement of feldspar.

Framework Grains (grainsize, sorting, roundness):

0.2-2.5 mm (av 1.75), moderately sorted, rounded, corroded and fractured quartz.

Matrix (grainsize, sorting, roundness):

<0.005 mm structureless clay (kaolinite).

Aggregates of illite/sericite with a mottled appearance, 1 perfect cleavage and 1st orde birefringence.

Cement:

Composition (%):		
	Quartz	45 - 50
	Feldspar	2-3 (very highly altered)
	Lithic/Rock Fragments	
	Opaques/Accessories	<1 spinel (euhedral, 0.01-0.2 mm)
	Matrix	40 kaolinite
		5 - 8 illite/sericite
	Cement	
	Porositv	

Sample Number: AL1-18 **Facies:** 12
Section Number: 12 **Area:** Holly Inlet South
Stratigraphic distance from base of section: 1.25 m
Location: **latitude** 12° 38' **longitude** 136° 40'

Grainsize Name: Medium-grained quartz arenite

Hand Specimen: Mottled brown, medium- to fine/medium-grained, thinly bedded sandstone with traces of crossbedding.

Micro Description: Fabric is dominated by medium-grained, well sorted slightly corroded quartz grains, mostly with point contacts, small inclusions and simple extinction under XPL. Grain boundaries are defined by thin rims of brown/orange iron-oxides and hematitic clay in PPL. This iron oxide coating is not present where the quartz is in grain to grain contact. Aggregates of muscovite occur in the larger pore spaces. In places the sample has irregular bands (2-3 mm wide) of silica cement incorporating small quartz grains.

Framework Grains (grainsize, sorting, roundness):
0.2-0.75 mm (av 0.4), well sorted, subrounded-rounded quartz.
Rare 0.3 mm, moderately sorted, subangular lithic fragments.

Matrix (grainsize, sorting, roundness):
Clots of muscovite (0.15-0.3 mm) with 1 perfect cleavage.
0.05-0.1 mm, moderately sorted, subrounded quartz.

Cement:
Amorphous silica (chert).
Hematitic clay as a late stage overprint.

Composition (%):

Quartz	60
Feldspar	
Lithic/Rock Fragments	1 - 2
Opaques/Accessories	1 rutile (subhedral, 0.15-0.25 mm)
Matrix	10
Cement	10 - 15
Porosity	10 - 12

Sample Number: AL1-19 **Facies:** 10
Section Number: 12 **Area:** Holly Inlet South
Stratigraphic distance from base of section: 3 m
Location: **latitude** 12° 38' **longitude** 136° 40'

Grainsize Name: Fine/medium-grained subarkose.

Hand Specimen: Pale brown/pink/yellow, hard, thinly planar laminated/ripple cross-laminated, fine/medium-grained sandstone.

Micro Description: Lamination up to 1.5 mm wide is defined by iron-oxide staining and concentration of larger quartz grains. Most of the framework grains are fine-medium grained quartz with undulose extinction. A few highly altered relict feldspar (?microcline) grains are visible and have been partly or completely replaced by muscovite/sericite. The size of the muscovite aggregates indicates that the original size of the feldspar grains was 0.5-0.8 mm. Neither the quartz or the feldspar grains are in contact and they are cemented by silica and a semi-opaque structureless clay with dispersed very fine grains of hematite.

Framework Grains (grainsize, sorting, roundness):
0.3-0.6 mm (av 0.45), well sorted, subrounded quartz.
0.5-0.8 mm (av 0.6), highly altered microcline feldspar/muscovite.

Matrix (grainsize, sorting, roundness):
<0.005 mm brown hematitic clay.

Cement:
Amorphous silica.
Isotropic hematite.

Composition (%):		
	Quartz	45 - 50
	Feldspar	≥5
	Lithic/Rock Fragments	
	Opaques/Accessories	1 - 2 rutile (subhedral, <0.4 mm)
		<1 anhedral, rounded ilmenite <0.15 mm
	Matrix	5 - 8
	Cement	35
	Porosity	<1

Sample Number: AL2-1 **Facies:** 13
Section Number: 24 **Area:** Kalarwoi River
Stratigraphic distance from base of section: 4.5 m
Location: **latitude** 12° 26' **longitude** 135° 37.5'

Grainsize Name: Ferruginous lithic fine-grained greywacke.

Hand Specimen: Mottled red/brown, heavily bioturbated, ferruginous, fine/medium-grained lithic sandstone. Contains impressions (external and internal moulds) of cephalopod and bivalve shells.

Micro Description: The components have been moved/reworked extensively by bioturbation so that all primary structures have been destroyed, although the bioturbation has produced a pseudo-layering in places. The bulk of the sample is silty hematitic clay throughout which are scattered, poorly sorted quartz grains, rare lithic fragments, authigenic micas and possibly fragments of the siliceous casts of shelly fossils.

Framework Grains (grainsize, sorting, roundness):

0.03-0.25 mm, moderately sorted, angular-subrounded quartz.
0.02-0.03 mm, moderately sorted, subrounded, unidentifiable lithic fragments.
0.8-1.2 mm, gently curved muscovite bundles (replacing fossils as casts ?).

Matrix (grainsize, sorting, roundness):

<0.01 casts of shell fragments.
<0.005 mm, dark brown hematitic clay.

Cement:

Dark red hematite cement rims around some of the altered lithic fragments.

Composition (%):		
	Quartz	30
	Feldspar	
	Lithic/Rock Fragments	15
	Opaques/Accessories	5 hematite (anhedral)
	Matrix	5 - 8
	Cement	40
	Porosity	<2

Sample Number: AL2-3 **Facies:** 13
Section Number: 25 **Area:** Kalarwoi River
Stratigraphic distance from base of section: 19.5 m
Location: **latitude** 12° 24.5' **longitude** 135° 36.25'

Grainsize Name: Ferruginous lithic fine-grained greywacke.

Hand Specimen: Mottled orange/red, heavily bioturbated, argillaceous very fine-grained sandstone with numerous irregular, short/stubby, horizontal burrows. Partly laterised in places with the development of incipient solution pipes.

Micro Description: Majority of the sample consists of small, moderately-poorly sorted quartz grains scattered irregularly throughout a highly ferruginised (very fine specs of hematite dust) clay matrix. In places quartz grains have been concentrated by bioturbation to form zones (burrow infillings ?) up to 2 mm wide and 8 mm long. The quartz grains in these zones are preferentially cemented by isotropic hematite in a random pattern. The rest of the sample has a hematitic clay matrix but only rarely is it cemented by hematite. Lithic clasts and muscovite bundles are also present within the hematitic clay.

Framework Grains (grainsize, sorting, roundness):

0.05-0.3 mm (av 0.2), moderately-poorly sorted, subangular quartz.
0.25-0.4 mm, poorly sorted, subrounded, highly altered lithic grains.
0.2-0.4 mm, elongate aggregates of muscovite.

Matrix (grainsize, sorting, roundness):

Very fine grained clay with scattered, rounded, grains (0.005-0.02 mm) of hematite.

Cement:

Isotropic amorphous hematite.

Composition (%):		
	Quartz	25 - 30
	Feldspar	
	Lithic/Rock Fragments	15 - 20
	Opaques/Accessories	<1 rutile (equant, 0.1-0.2 mm)
	Matrix	40
	Cement	5 - 8
	Porositv	<2

Sample Number: AL2-4 **Facies:** 10
Section Number: 25 **Area:** Kalarwoi River
Stratigraphic distance from base of section: 2 m
Location: **latitude** 12° 24.5' **longitude** 136° 36.25'

Grainsize Name: Fine/medium-grained quartzwacke.

Hand Specimen: Pale brown/white, bioturbated clayey fine-grained sandstone with minor iron-oxide staining. Burrows are highlighted since they have been infilled by the paler, argillaceous component.

Micro Description: The fabric is typically matrix supported with small quartz grains scattered throughout a very fine grained clayey matrix. The clay matrix is slightly hematitic (very fine grains <0.001 mm of hematite) and has minor iron-oxide cement in places. Rare seritised shell fragments also occur amongst the matrix along with large detrital hematite grains. Bioturbation has concentrated the quartz grains and large hematite grains between burrows so that they are moderately-tightly packed with point contacts. The burrows themselves are filled with clay and the burrow walls are quite distinct.

Framework Grains (grainsize, sorting, roundness):

0.15-0.35 mm (av 0.2), moderately-poorly sorted, subangular quartz.
0.1-0.2 mm, muscovite aggregates (replacing shell casts ?).
0.008-0.15 mm, moderately sorted, subhedral hematite grains.

Matrix (grainsize, sorting, roundness):

Very fine grained clay with numerous small (<0.001 mm) dispersed hematite grains.

Cement:

Rare isotropic hematite cement.

Composition (%):		
	Quartz	35
	Feldspar	
	Lithic/Rock Fragments	<1
	Opaques/Accessories	<1 sphene (yellowish, square, 0.2 mm)
		<<1 rutile (subhedral, 0.08-0.1 mm)
	Matrix	55 hematitic clay
		3 hematite grains 1 - 2 muscovite
	Cement	<2 isotropic hematite
	Porositv	<5

Sample Number: AL2-6 **Facies:** 10
Section Number: 28 **Area:** Nilipitchi
Stratigraphic distance from base of section: 1.5 m
Location: **latitude** 13° 34.5' **longitude** 135° 27.5'

Grainsize Name: Medium/fine-grained ferruginous quartz arenite.

Hand Specimen: Brown/orange, ferruginous and slightly manganiferous, very fine-grained sandstone with numerous cavities caused by weathering-out of original shell material. Some of these cavities/voids have been filled by goethite.

Micro Description: Tightly packed mosaic of medium-grained, well sorted quartz grains with grain to grain contacts which have undergone minor dissolution as evidenced by the corroded and embayed margins of many of the grains. Grains are invariably coated by iron-oxides up to 0.02 mm thick, except where the grains are in contact, there the iron-oxide coating is missing. Pore spaces are angular, elongate voids up to 0.9 mm long and are often surrounded by isotropic hematite cement. Heavily weathered and altered feldspar (plagioclase) grains and muscovite bundles are also present.

Framework Grains (grainsize, sorting, roundness):

0.2-0.5 mm (av 0.3), well-moderately sorted, subangular-subrounded quartz with rare authigenic quartz overgrowths which predate the iron-oxide cement.

Matrix (grainsize, sorting, roundness):

0.25-0.3 mm, highly altered plagioclase.

0.1-0.2mm, somewhat fibrous aggregates of sericite.

Cement:

Amorphous isotropic hematite cement lining large pore spaces.

Composition (%):		
	Quartz	80
	Feldspar	<2
	Lithic/Rock Fragments	<1
	Opaques/Accessories	1 sphene (anhedral, 0.1-0.15 mm)
	Matrix	5 quartz overgrowths
	Cement	5 isotropic hematite
		2 hematitic clay
	Porosity	5 - 8

Sample Number: AL2-8 **Facies:** 8
Section Number: 28 **Area:** Nilipitchi
Stratigraphic distance from base of section: 16 m
Location: **latitude** 13° 34.5' **longitude** 135° 27.5'

Grainsize Name: Medium-grained quartz arenite

Hand Specimen: Pale grey, slightly friable, well sorted, medium-grained quartz arenite with crossbedding. Upper section is heavily silicified, elsewhere it has a thin manganiferous coating.

Micro Description: Sample is a very tightly packed almost pure quartz arenite. Fabric comprises medium/fine-grained quartz grains with smooth concavo/convex contacts and almost zero porosity. Angular chert fragments and pyroxene grains are present with the quartz and some of the grains are cemented by hematite around the larger pore spaces. The tight packing, concavo/convex contacts and overgrowths around the quartz grains are the result of dissolution and reprecipitation events which took place along grain boundaries during early diagenesis.

Framework Grains (grainsize, sorting, roundness):

0.16-0.5 mm (av 0.32), well sorted, rounded-subrounded quartz.
0.15-0.2 mm, moderately sorted, subangular chert fragments.
0.2-0.3 mm, moderately sorted, rounded (subhedral) pyroxene.

Matrix (grainsize, sorting, roundness):

Cement:

Minor isotropic hematite cement.
Quartz overgrowths.

Composition (%):		
	Quartz	95
	Feldspar	
	Lithic/Rock Fragments	<1 Chert
		0.5 Pyroxene
	Opaques/Accessories	1 sphene (anhedral, 0.08-0.18 mm)
		1 ilmenite (rounded, 0.05-0.2 mm)
	Matrix	
	Cement	1 Isotropic hematite
	Porosity	<<1

Sample Number: AL2-10 **Facies:** 12
Section Number: 31 **Area:** Marura Creek
Stratigraphic distance from base of section: 11 m
Location: **latitude** 13° 23.25' **longitude** 135° 30.5'

Grainsize Name: Medium/fine-grained quartz arenite.

Hand Specimen: Pale orange, slightly friable, slightly manganiferous, bioturbated, irregularly/thinly laminated, well sorted, fossiliferous medium-grained quartz arenite.

Micro Description: Lamination is defined by iron-oxide staining in bands (1.5-2.8 mm thick). Fabric is a moderately to tightly packed mosaic of well-moderately sorted, medium grained quartz grains. Grain to grain contacts are most common, although point contacts and concavo/convex contacts do occur. Rare quartz grains show the affects of dissolution and exhibit embayed edges. A few chert fragments and composite quartz grains are present and are similar in size and shape to the single quartz grains. Some of the larger pore spaces are rimmed by iron-oxide cement while the rest of the rock contains dispersed very small hematite grains. Small pockets (<0.75 mm) of the framework grains are cemented by brown, very fine grained hematitic clay.

Framework Grains (grainsize, sorting, roundness):
0.17-0.45 mm (av 0.26), well-moderately sorted, rounded quartz grains with minor authigenic quartz overgrowths. Same for chert fragments.

Matrix (grainsize, sorting, roundness):

Cement:
Very fine-grained hematitic clay (authigenic ?).
Rare isotropic iron-oxide cement around pore spaces.

Composition (%):		
	Quartz	85 - 90
	Feldspar	
	Lithic/Rock Fragments	1 Chert
	Opaques/Accessories	1 sphene (anhedral, 0.08-0.1 mm)
		1 ilmenite (subhedral, 0.05-0.09 mm)
	Matrix	
	Cement	<5 hematitic clay
		1 isotropic hematite
	Porosity	5

Sample Number: AL2-11 **Facies:** 9
Section Number: 31 **Area:** Marura Creek
Stratigraphic distance from base of section: 4.5 m
Location: **latitude** 13° 23.25' **longitude** 135° 30.5'

Grainsize Name: Coarse/medium-grained ferruginous quartz arenite.

Hand Specimen: Orange, fossiliferous, massive, friable, ferruginous, moderately sorted, medium- to coarse-grained, lithic quartz arenite.

Micro Description: Fabric comprises two randomly distributed grainsize modes. Firstly, framework grains are coarse, fractured, corroded and embayed quartz grains with undulose extinction under XPL, and a dusty appearance caused by numerous very small inclusions within the quartz. Rare chert grains and composite quartz grains of a similar size and shape are present along with a few highly altered feldspar grains. Secondly, the matrix grainsize fraction comprises smaller, more angular, cleaner/less corroded quartz grains. All grains are surrounded by a thin rim of brown/red iron-oxide except where quartz is in grain to grain contact.

Framework Grains (grainsize, sorting, roundness):
0.5-1 mm (av 0.7), moderately sorted, subrounded, corroded quartz.

Matrix (grainsize, sorting, roundness):
0.08-0.2 mm (av 0.15), moderately-poorly sorted, subangular-subrounded quartz.

Cement:
Brown anisotropic hematite cement surrounding grains.

Composition (%):		
	Quartz	45
	Feldspar	2
	Lithic/Rock Fragments	3 Chert
	Opaques/Accessories	0.5 ilmenite (anhedral)
	Matrix	35 as above only finer
	Cement	8 - 10 hematite cement
	Porositv	5 - 7

Sample Number: AL2-14 **Facies:** 21
Section Number: 31 **Area:** Marura Creek
Stratigraphic distance from base of section: 16 m
Location: **latitude** 13° 23.25' **longitude** 135° 30.5'

Grainsize Name: Sandy mudstone

Hand Specimen: White, hard, clayey siltstone with dispersed fine/medium-grained, angular quartz sand grains and small, red/purple streaks where the larger quartz grains are concentrated. The purple streaks/lenses are discontinuous and probably represent micro-bedding surfaces.

Micro Description: Medium sand-sized grains of quartz and rarer composite quartz grains all with slightly embayed boundaries are concentrated in elongate lenses parallel to bedding. The outer parts of these lenses (more porous than the matrix) are cemented by amorphous isotropic hematite which forms a relatively sharp boundary to the lenses. The larger quartz grains (both within the lenses and single dispersed grains elsewhere) are floating in a matrix of small dispersed quartz grains and rare clots of radiating, slightly fibrous illite in a very fine-grained clay. Several of the larger quartz grains have concavo/convex contacts and corroded rims indicating dissolution and reprecipitation of silica.

Framework Grains (grainsize, sorting, roundness):

0.25-0.8 mm (av 0.45), moderately sorted, subrounded quartz.
0.5-1.2 mm (av 1.2), moderately sorted, subrounded composite quartz.
0.3-0.75 mm, poorly sorted, illite.

Matrix (grainsize, sorting, roundness):

0.03-0.12 mm (av 0.05), moderately-poorly sorted, subangular-subrounded quartz.
Very fine-grained white/brown clay (kaolinite).

Cement: Isotropic hematite.

Composition (%):		
	Quartz	≤20
	Feldspar	
	Lithic/Rock Fragments	
	Opaques/Accessories	<1 ilmenite (subhedral, 0.02-0.05 mm)
	Matrix	50 - 55 Kaloinite
		20 quartz
		<3 Illite
	Cement	5 - 7 isotropic hematite
	Porosity	1 - 2

Sample Number: AL2-16 **Facies:** 12
Section Number: 32 **Area:** Marura Creek
Stratigraphic distance from base of section: 11 m
Location: **latitude** 13° 22' **longitude** 135° 29.5'

Grainsize Name: Fine/medium-grained quartz arenite.

Hand Specimen: Orange, slightly mottled, bioturbated, crossbedded, ferruginous, fine/medium-grained quartz sandstone. Contains preserved burrows and moulds of molluscan shelly fossils.

Micro Description: Fabric is grain supported and moderately-tightly packed with short grain to grain contacts (slightly concavo/convex) between corroded quartz grains with large authigenic quartz overgrowths. The original grain boundaries are outlined by hematite dust and inclusions. Amongst the quartz grains there are rare lithic grains which have been partially altered to muscovite/sericite. All grains are completely surrounded by a thin (0.03 mm) rim of anisotropic iron-oxide, except where the quartz has grain to grain contact. Overall the grains are well sorted, although there are several coarse, fresh/non-corroded quartz grains present.

Framework Grains (grainsize, sorting, roundness):

0.1-0.45 mm (av 0.25), well sorted, subrounded-rounded corroded quartz.
0.2-0.3 mm, moderately-well sorted, subrounded lithic grains.
0.6-0.9 mm, poorly-moderately sorted, subrounded, non-corroded quartz.

Matrix (grainsize, sorting, roundness):

Cement:

Composition (%):			
	Quartz	65 - 70 grains	3 - 4 overgrowths
	Feldspar		
	Lithic/Rock Fragments	<2	
	Opaques/Accessories	1 - 1.5 ilmenite (rounded, 0.05-0.15 mm)	
		<0.5 rutile (rounded, 0.15-0.18 mm)	
	Matrix		
	Cement	5 - 8 anisotropic hematite	
	Porosity	10 - 15	

Sample Number: AL2-17A **Facies:** 11
Section Number: 32 **Area:** Marura Creek
Stratigraphic distance from base of section: 8 m
Location: **latitude** 13° 22' **longitude** 135° 29.5'

Grainsize Name: Fine/medium-grained quartz arenite

Hand Specimen: Pale grey, thickly bedded, hard, well sorted, saccharoidal, fine/medium-grained quartz arenite. Contains abundant impressions of segmented wood fossils and molluscan macrofossils.

Micro Description: Fabric is a tightly packed grain supported network dominantly comprising single, well sorted, medium/fine-grained, quartz grains with simple to slightly undulose extinction in XPL, and concavo/convex and grain to grain contacts. Large quartz overgrowths are prominent with the original relict grain outlines being delineated by lines of microinclusions and hematite staining. Rare grains have numerous, small, elongate inclusions of spinel and hematite. In several of the larger pore spaces small, elongate, authigenic muscovite aggregates are visible.

Framework Grains (grainsize, sorting, roundness):
0.18-0.4 mm (av 0.24), very well sorted, rounded quartz.

Matrix (grainsize, sorting, roundness):

Cement:
Authigenic quartz overgrowths up to 0.05 mm thick.
0.04-0.06 mm, elongate aggregates of muscovite.

Composition (%):		
	Quartz	90
	Feldspar	
	Lithic/Rock Fragments	
	Opaques/Accessories	<1 ilmenite/hematite (<0.15 mm)
	Matrix	
	Cement	5 - 8 quartz
		<1 muscovite
	Porositv	2 - 3

Sample Number: AL2-18 **Facies:** 22
Section Number: 32 **Area:** Marura Creek
Stratigraphic distance from base of section: 15.5 m
Location: **latitude** 13° 22' **longitude** 135° 29.5'

Grainsize Name: Sandy mudstone

Hand Specimen: White, bioturbated, hard claystone with dispersed, fine-grained quartz and purple/red, discontinuous lenses/streaks.

Micro Description: Comprises a very fine-grained clay matrix with quartz grains scattered throughout. The quartz grains occur in two broad size ranges; rarer medium quartz grains tend to be elongate, moderately-poorly sorted, subrounded with slightly undulose extinction under XPL. The second size fraction contains fine, more angular quartz grains with better sorting. In several areas the medium and fine quartz grains and accessory grains are concentrated into sharply defined pockets and less well defined lenses/streaks. In rare places these lenses are partially cemented by isotropic hematite and hematitic clay. The lenses may have been formed by disruption of primary sedimentary layering by bioturbation or by some intermittant control on current strength during deposition (such as periodic storms). Coarse slightly fibrous aggregates of illite also occur in the matrix.

Framework Grains (grainsize, sorting, roundness):

Fraction 1 0.25-0.45 mm (av 0.35), moderately-poorly sorted, subrounded quartz.
Fraction 2 0.002-0.12 mm (av 0.09), moderately sorted, subangular quartz.

Matrix (grainsize, sorting, roundness):

<0.004 mm, pure kaolinite.
0.9-1.6 mm, subfibrous aggregates of illite.

Cement:

Rare isotropic hematite.

Composition (%):

Quartz	15	
Feldspar		
Lithic/Rock Fragments		
Opaques/Accessories	5 rutile (elongate)	
	2 hematite (<0.003 mm)	
Matrix	75 kaolinite	2-3 illite
Cement	<1 isotropic hematite	
Porosity	<1	

Sample Number: AL2-21 **Facies:** 15
Section Number: 34 **Area:** Central Spur South
Stratigraphic distance from base of section: 6.75 m
Location: **latitude** 13° 36' **longitude** 135° 20.5'

Grainsize Name: Bioturbated fine-grained quartzwacke.

Hand Specimen: Mottled yellow/brown, intensely bioturbated, hard, massive, clayey very fine-grained quartz sandstone thinly interbedded with white to pale orange, clayey siltstone. Coarser quartz grains are concentrated into semi-continuous layers parallel to bedding. These laminae are more porous and more extensively cemented by iron-oxides.

Micro Description: Fabric dominated by crude layering which is laterally semi-continuous. The layering is divided into 1) clay-rich (matrix) bands typically 1-2 mm thick but up to 10 mm thick which alternate with 2) quartz rich bands up to 7 mm thick, typically 2-3 mm. Quartz grains do occur within the clay-rich bands, but only rarely. The quartz is fine- to very fine- grained, well sorted, subangular-subrounded and has slightly undulose extinction under XPL. Each grain is matrix supported, with rare grains in point contact. Quartz overgrowths are common in the quartz-rich bands and small muscovite filaments are common in the clay-rich bands. The quartz rich-bands are cemented in varying amounts by dark brown to opaque iron-oxide which accounts for the varying colours of the laminae.

Framework Grains (grainsize, sorting, roundness):
0.18-0.3 mm (av 0.2), moderately sorted, subrounded-subangular quartz with inclusions and overgrowths (these grains are only found in quartz-rich bands).

Matrix (grainsize, sorting, roundness):
0.02-0.12 mm (av 0.1), moderately-poorly sorted, subangular quartz with rare overgrowths (these grains are found in both the quartz- and clay-rich bands).
0.08-0.25 mm, poorly sorted, elongate filaments of muscovite.

Cement: Isotropic/anisotropic hematite and hematitic clay.

Composition (%):

Quartz	40
Feldspar	
Lithic/Rock Fragments	<0.5 actinolite (equant, 0.1-0.12 mm)
Opaques/Accessories	1 ilmenite (elongate, 0.08-0.15 mm)
Matrix	45 hematitic clay 2 muscovite
Cement	5 - 8 hematite
Porosity	4 - 5

Sample Number: AL2-22 **Facies:** 15
Section Number: 34 **Area:** Central Spur South
Stratigraphic distance from base of section: 1.75 m
Location: **latitude** 13° 36' **longitude** 135° 20.5'

Grainsize Name: Fine/medium-grained quartzwacke.

Hand Specimen: Mottled yellow/brown, ferruginous, heavily bioturbated, hard, massive, very clayey, fine-grained sandstone. Contains preserved burrows and moulds of molluscan macrofossils.

Micro Description: Similar to AL2-21, but the bedding/lamination is less distinct and there are more and larger quartz grains. Lamination is highlighted by iron-oxide cementation. Small composite quartz grains, aggregates of muscovite, isotropic heavy minerals and rare detrital actinolite/chlorite/glauconite are dispersed randomly throughout the matrix. The larger quartz grains have small quartz overgrowths in places.

Framework Grains (grainsize, sorting, roundness):

0.1-0.6 mm (av 0.24), moderately sorted, subrounded quartz.

0.15-0.4 mm, moderately sorted, subrounded-rounded, composite quartz grains.

Matrix (grainsize, sorting, roundness):

0.12-0.18 mm, equant, granular, sea-green actinolite/glauconite.

0.1-0.23 mm, elongate needles of muscovite.

Cement:

Amorphous isotropic hematite

Very fine-grained hematitic clay.

Composition (%):		
	Quartz	60 grains 2 - 3 overgrowths
	Feldspar	
	Lithic/Rock Fragments	<0.5 actinolite/glauconite
	Opaques/Accessories	≤1 rutile (euhedral, 0.08-0.15 mm)
	Matrix	1 - 2 muscovite
	Cement	20 hematitic clay
		5 hematite
	Porosity	5 - 10

Sample Number: AL2-25 **Facies:** 12
Section Number: 36 **Area:** Parsons Range South
Stratigraphic distance from base of section: 1.5 m
Location: **latitude** 13° 42.25' **longitude** 135° 11'

Grainsize Name: Fine/medium-grained quartz arenite.

Hand Specimen: Orange, bioturbated, ferruginous, irregularly laminated, slightly clayey, fine-grained sandstone. Contains abundant wood and molluscan macrofossil moulds.

Micro Description: Grain supported fabric of medium/fine-grained quartz with point contacts and slightly undulose extinction. Most grains have a thick coating of iron-oxide (up to 0.1 mm) which also fills in pore spaces in places. Quartz overgrowths are common and overgrowth formation appears to have predated iron staining. Irregularly spaced patches (up to 1 mm wide and 4-5 mm long) are rich in very fine grained clay and contain only a few very fine quartz grains. Small muscovite flakes, rare composite quartz grains, and highly altered lithic grains also occur within the matrix.

Framework Grains (grainsize, sorting, roundness):
0.08-0.38 mm (av 0.23), moderately sorted, subrounded-subangular, quartz and altered lithics.

Matrix (grainsize, sorting, roundness):
0.05-0.2 mm, acicular muscovite.

Cement:
Anisotropic iron-oxide.
Cloudy, brown, very fine-grained clay.

Composition (%):		
	Quartz	55
	Feldspar	
	Lithic/Rock Fragments	<2
	Opaques/Accessories	2 ilmenite (subhedral, 0.18-0.2 mm)
	Matrix	5 muscovite
	Cement	10 - 12 clay
		5 - 8 hematite
	Porositv	10 - 15

Sample Number: AL2-28 **Facies:** 18
Section Number: 39 **Area:** Walker River
Stratigraphic distance from base of section: 4 m
Location: **latitude** 13° 32' **longitude** 135° 26.5'

Grainsize Name: Sandy mudstone.

Hand Specimen: White, very thinly laminated, hard, clayey siltstone with lamination defined by iron-oxide staining. Some layers (up to 3 mm thick) are coarser and contain fine- to fine/medium-grained quartz in a clay matrix.

Micro Description: Major component is a very fine grained kaolinite matrix with dispersed very fine quartz grains, accessory grains, muscovite flakes and fibrous clots of illite. There are several layers (0.9-3 mm, av 2 mm thick) where larger quartz grains and opaque grains are concentrated. This lamination is moderately well defined and encloses poorly sorted quartz grains. Thin laminae are relatively continuous and contain small quartz grains. Thicker laminae are less continuous parallel to bedding, more lense-like perpendicular to bedding, and contain a greater number of larger quartz and highly altered lithic grains. The thicker laminae are cemented locally by iron-oxides.

Framework Grains (grainsize, sorting, roundness):

0.05-0.4 mm (av 0.1), poorly sorted, subangular quartz.
0.1-0.3 mm, moderately sorted, rounded, very highly altered lithic grains.

Matrix (grainsize, sorting, roundness):

0.02-0.06 mm (av 0.04), moderately sorted, subangular quartz.
0.08-0.2 mm, usually single fibres of muscovite.
0.1-0.2 mm, irregular fibrous clots of illite.

Cement:

Dark brown/black, isotropic hematite cementing larger quartz grains.

Composition (%):		
	Quartz	25
	Feldspar	<2
	Lithic/Rock Fragments	
	Opaques/Accessories	2-3 ilmenite (anhedral, 0.08-0.16 mm)
		2 rutile (subhedral, 0.03-0.1 mm)
	Matrix	55 kaolinite
		2-3 illite 1 muscovite
	Cement	2 hematite
	Porosity	5 - 8

Sample Number: AL2-31B **Facies:** 16
Section Number: 44 **Area:** Koolatong River
Stratigraphic distance from base of section: 2 m
Location: **latitude** 13° 01' **longitude** 135° 37.5'

Grainsize Name: Slightly sandy, coarse/medium-grained siltstone.

Hand Specimen: White, hard, clayey siltstone with convolute lamination and/or concretionary lamination parallel to bedding. Difficult to assess degree of bioturbation.

Micro Description: Bulk of sample is a homogeneous matrix of very fine-grained, well sorted quartz with minor muscovite in a very fine-grained clay. Cutting across the matrix are thin, regular, straight and convolute, vein-like structures filled with tightly packed, fine quartz grains with concavo/convex contacts and strongly undulose extinction under XPL. In places the quartz is almost fibrous and appears to have developed as a vein fill with quartz growing perpendicular to the walls of the veins. In some areas the thin veins coalesce to form 5-6 mm thick, 8-10 mm long vugs filled with quartz which is inclusion rich and contains numerous small sericite fragments. The quartz in the 'veins' and 'vugs' appears to have replaced carbonate concretions or calcareous algal lamination. The cores of the 'vugs' contains larger, equant quartz grains which become progressively smaller and more elongate towards the margins.

Framework Grains (grainsize, sorting, roundness):
0.04-0.25 mm (av 0.15), moderately-poorly sorted, subrounded quartz with numerous quartz overgrowths and very low porosity.

Matrix (grainsize, sorting, roundness):
0.003-0.006 mm (av 0.004), well sorted, subrounded quartz.
0.002-0.006 mm (av 0.003), muscovite clots (relicts of feldspar grains).

Cement:
<0.001 mm, clay.

Composition (%):			
	Quartz	15 - 20 grains	3 overgrowths
	Feldspar		
	Lithic/Rock Fragments		
	Opaques/Accessories	1 hematite (rounded, 0.03-0.05 mm)	
	Matrix	60 quartz	
		2 - 3 muscovite	
	Cement	5 clay (kaolinite)	<0.5 hematite
	Porosity	15	

Sample Number: AL3-1 **Facies:** 5
Section Number: 46 **Area:** Yiyintyi Range
Stratigraphic distance from base of section: 4.5 m
Location: **latitude** 15° 26' **longitude** 135° 42.5'

Grainsize Name: Conglomeratic coarse- to very coarse-grained quartz arenite.

Hand Specimen: Pale pink/grey, slightly friable, moderately sorted, very coarse-grained quartz arenite with numerous granule to mid-pebble sized clasts. Clasts are rounded to well rounded and are composed of fine-grained pink quartzite/arkose.

Micro Description: Fabric is a grain supported network of coarse to very coarse single quartz grains with large quartz overgrowths, inclusions and slightly undulose extinction under XPL surrounding randomly oriented pebble-sized clasts. The overgrowths totally surround most of the grains and the overgrowths themselves are corroded and exhibit embayed textures. The voids between these large quartz grains with overgrowths are filled with tightly interlocking fine quartz grains, rare muscovite flakes and are sometimes cemented by iron-oxide. Heavy minerals occasionally form clusters in the pore spaces. The fine quartz grains are themselves incorporated into some of the large quartz overgrowths, indicating at least two stages of quartz overgrowth development. The clast rock type is a slightly ferruginous, moderately-well sorted, subrounded, fine/medium-grained, sedimentary quartzite.

Framework Grains (grainsize, sorting, roundness):

Clasts 3-15 mm, moderately-poorly sorted, rounded fine/medium-grained quartzite.
Coarse Quartz 0.18-1.75 mm (av 0.9), moderately sorted, subrounded quartz.

Matrix (grainsize, sorting, roundness):

Fine Quartz 0.003-0.025 mm (av 0.008), moderately-well sorted, subrounded quartz.
0.002-0.01 mm, mostly single acicular crystals of muscovite.

Cement:

Brown, anisotropic hematite.

Composition (%):		
	Quartz	60 grains 15 clasts
	Lithic/Rock Fragments	
	Opaques/Accessories	2 rutile (anhedral, 0.005-0.008 mm)
		<0.5 ilmenite/hematite (0.1-0.25 mm)
	Matrix	12 - 15 quartz 2 muscovite
	Cement	3 - 4 hematite
	Porosity	5

Sample Number: AL3-3B **Facies:** 6
Section Number: 49 **Area:** Yiyintyi Range
Stratigraphic distance from base of section: 4.5 m
Location: **latitude** 15° 24.5' **longitude** 135° 41.25'

Grainsize Name: Conglomeratic, coarse-/very coarse-grained, iron-cemented, quartz arenite.

Hand Specimen: Components are similar to sample AL3-1, but the framework grains are cemented by dark grey/black, isotropic iron-oxide cement.

Micro Description: Similar to AL3-1, except there is very little matrix (there are no 0.008 mm quartz grains between the coarse quartz grains), only a few accessory grains and rare muscovite; instead coarse quartz grains and the sedimentary clasts are almost totally cemented by iron-oxide.

Framework Grains (grainsize, sorting, roundness):

Clasts 3-13 mm, moderately-poorly sorted, subrounded quartzite clasts.
Coarse quartz 0.18-1.8 mm (av 0.85), moderately sorted, subrounded quartz.

Matrix (grainsize, sorting, roundness):

Cement:

Amorphous, isotropic hematite.

Composition (%):			
	Quartz	55 - 60 grains	15 clasts
	Feldspar		
	Lithic/Rock Fragments		
	Opaques/Accessories	<0.5 rutile (anhedral, 0.08-0.1 mm)	
	Matrix	<<0.5 very rare muscovite	
	Cement	15 - 20 isotropic hematite	
	Porositv	10	

Sample Number: AL3-5 **Facies:** 18
Section Number: 52 **Area:** Kalampirri Creek
Stratigraphic distance from base of section: 7.75 m
Location: **latitude** 15° 36' **longitude** 135° 36.5'

Grainsize Name: Medium/fine-grained (silt) sandy siltstone.

Hand Specimen: Grey/red/green, thinly bedded/laminated, hard, clayey, very fine-grained sandstone. Basal 5-8 cm comprises green laminae (≤4 mm thick) alternating with minor white clay matrix. Next zone is 2-3 cm thick and very similar, except the laminae are red. The upper 5-7 cm is similar to samples AL2-14 and AL2-18 and is pale grey/white, clayey, very fine-grained siltstone with dispersed sand-sized quartz grains in the form of streaks/lenses.

Micro Description: The fabric comprises two major components in three laminated zones; actinolite-rich (green), hematite-rich (red), and clay rich (white). The framework grains, the main component of the green and red laminae, are fine grained single quartz grains. Medium-fine silt-sized quartz grains and rare muscovite fill in the spaces between the larger quartz grains, and comprise the bulk of the clay-rich zone and also occupy the spaces between the laminae in the lower two zones. Laminae in the zones are 0.5-2.5 mm thick and have relatively sharp boundaries, except in the top 5 cm where they become less distinct, less continuous and more lense-like. The colour of the red and green zones is caused by iron oxide cement and scattered actinolite grains respectively. The entire sample has a minor clay component which increases in the upper zone. Quartz overgrowths which predate the iron-oxide cement are apparent on many of the fine sand-size quartz grains.

Framework Grains (grainsize, sorting, roundness):

0.1-0.25 mm (av 0.18), moderately sorted, subrounded quartz with overgrowths.

Matrix (grainsize, sorting, roundness):

0.01-0.04 mm (av 0.02), moderately-well sorted, subrounded-subangular quartz.
0.09-0.15 mm (av 0.12), moderately sorted, subrounded, equant/fibrous actinolite.
0.03-0.1 mm, elongate single crystals of muscovite.

Cement: Hematitic clay and isotropic black hematite.

Composition (%):

Quartz	25 grains 1 - 2 overgrowths
Feldspar	
Lithic/Rock Fragments	≤5 actinolite
Opaques/Accessories	1 rutile (0.05-0.08 mm)
	2-3 hematite/ilmenite
Matrix	45 - 50 quartz 2 - 3 muscovite
Cement	10 - 12 hematitic clay 8 - 10 hematite
Porosity	5 - 8

Sample Number: AL3-6 **Facies:** 13
Section Number: 52 **Area:** Kalampirri Creek
Stratigraphic distance from base of section: 7.5 m
Location: **latitude** 15° 36.75' **longitude** 135° 36.5'

Grainsize Name: Medium/fine-grained quartz arenite (quartzite).

Hand Specimen: White/pale grey/yellow, partially planar laminated, very hard, well sorted, fine-grained quartz arenite with large vertical burrows (*Skolithos*). Sample also contains rare, dispersed, coarse-medium sand-sized quartz grains.

Micro Description: Sample is composed almost entirely of quartz with moderately-well sorted, fine quartz grains with small overgrowths set in a quartz cement. Rare coarse quartz grains, minor muscovite, sphene and opaque heavy minerals are scattered randomly throughout the fabric. The quartz grains have concavo/convex contacts, moderately undulose extinction under XPL and contain, very small, unidentified inclusions.

Framework Grains (grainsize, sorting, roundness):
0.1-0.4 mm (av 0.3), moderately-well sorted, subrounded quartz.
0.6-0.8 mm, moderately-well sorted, subrounded-subangular quartz.

Matrix (grainsize, sorting, roundness):
0.03-0.75 mm (av 0.15), elongate, single grains of muscovite.

Cement:
Quartz in the form of overgrowths.

Composition (%):		
	Quartz	85 - 90
	Feldspar	
	Lithic/Rock Fragments	
	Opaques/Accessories	1 sphene (subhedral, 0.08-0.12 mm)
		1 hematite (anhedral, 0.1-0.3 mm)
		<0.5 rutile (anhedral, 0.03-0.06 mm)
	Matrix	1 muscovite
	Cement	5 - 8 quartz overgrowths
	Porosity	<<1

Sample Number: AL3-9 **Facies:** 14
Section Number: 54 **Area:** Bukalara Plateau
Stratigraphic distance from base of section: 14 m
Location: **latitude** 16° 06.5' **longitude** 136° 09'

Grainsize Name: Medium-grained quartzwacke.

Hand Specimen: White, discontinuously laminated in part, hard, clayey siltstone/very fine-grained sandstone. Contains pockets/streaks of medium-fine quartz grains ± iron-oxide cement. Appears to be heavily bioturbated and contains abundant moulds of a molluscan fossil, forming a coquina in places. Laminae are dipping and are regularly truncated by overlying lamina-sets, thickening of lamina-sets forms hummocky cross-stratification.

Micro Description: Fabric comprises two main framework fractions; 1) medium-grained quartz loosely concentrated into rather ill-defined irregular pockets/streaks up to 4 mm wide and 18 mm long, roughly parallel to bedding. These quartz grains are set in a matrix of very fine clay, minor muscovite and 2) very fine grained quartz. Remainder of sample (besides coarser streaks) consists of very fine-grained quartz set in a clay matrix with dispersed muscovite and very rare, isolated medium quartz grains.

Framework Grains (grainsize, sorting, roundness):

0.2-0.6 mm (av 0.4), moderately sorted, subrounded quartz with undulose extinction, a few inclusions and a slightly corroded texture.

Matrix (grainsize, sorting, roundness):

0.04-0.1 mm (av 0.06), moderately-well sorted, subrounded-subangular quartz.
0.01-0.4 mm (av 0.04), poorly sorted, elongate/radiating aggregates muscovite.

Cement:

Very fine-grained clay (kaolinite).
Rare isotropic hematite rimming larger pore spaces in places.

Composition (%):			
Quartz	30		
Feldspar			
Lithic/Rock Fragments			
Opaques/Accessories	<1 hematite (subhedral <0.13 mm)		
Matrix	15 quartz	5 - 8 muscovite	
Cement	35 clay	2 - 3 hematite	
Porosity	8 - 10		

Sample Number: AL3-12 **Facies:** 12
Section Number: 56 **Area:** Batten Creek
Stratigraphic distance from base of section: 8 m
Location: **latitude** 15° 58' **longitude** 136° 17.5'

Grainsize Name: Fine-grained ferruginous quartz arenite.

Hand Specimen: Dark orange, massive, bioturbated, slightly friable, well sorted, fine-grained, ferruginous sandstone with weak traces of cross-bedding in places.

Micro Description: Framework grains are fine to very fine-grained single quartz with straight to slightly undulose extinction under XPL and rarer altered feldspar grains. Most quartz grains have point contacts or very small grain contacts, quartz overgrowths and a very thin discontinuous coating of iron-oxides (post-dates quartz overgrowths); more rarely several grains are cemented by iron-oxide. The matrix comprises fibrous masses of muscovite, actinolite grains with fibrous/hacksaw terminations, silt-sized quartz and heavy minerals set in a very fine-grained hematitic clay cement.

Framework Grains (grainsize, sorting, roundness):

0.08-0.3 mm (av 0.2), well-moderately sorted, subrounded-rounded quartz.
0.15-0.3 mm (av 0.22), well sorted, highly altered feldspar grains partially replaced by muscovite and clay.

Matrix (grainsize, sorting, roundness):

0.004-0.15 mm (av 0.1), equant, subhedral, green, 'hacksaw' actinolite.
0.05-0.25 mm (av 0.15), fibrous masses of muscovite.

Cement:

Brown, very fine-grained hematitic clay.
Isotropic hematite.

Composition (%):		
	Quartz	55 - 60
	Feldspar	2 - 3
	Lithic/Rock Fragments	3 - 4 actinolite
	Opaques/Accessories	2 hematite/ilmenite (0.06-0.1 mm)
		<1 brookite (squarish, <0.08 mm)
	Matrix	2 - 3 muscovite
	Cement	10 hematitic clay
		5 - 8 isotropic hematite
	Porosity	10 - 12

Sample Number: AL3-13 **Facies:** 21
Section Number: 56 **Area:** Batten Creek
Stratigraphic distance from base of section: 13 m
Location: **latitude** 15° 58' **longitude** 136° 17.5'

Grainsize Name: Sandy mudstone

Hand Specimen: White, massive, bioturbated, clayey siltstone with red/purple, discontinuous, iron-oxide cemented laminae/streaks in places.

Micro Description: Fabric is matrix supported; framework grains are fine-medium sized single and rare composite quartz grains. These grains have slightly undulose extinction under XPL and small quartz overgrowths Matrix is silt-sized quartz, actinolite grains and muscovite set in a very fine-grained clay. Bioturbation/reworking of the sediment has produced irregular patches which are clay-rich, but poor in both matrix and framework sized quartz grains. A few of the fine-medium quartz grains are cemented by opaque iron-oxide, and many are heavily corroded and display strongly etched/embayed textures.

Framework Grains (grainsize, sorting, roundness):

0.13-0.6 mm (av 0.2), poor-moderately sorted, subrounded, corroded quartz with overgrowths.

Matrix (grainsize, sorting, roundness):

0.03-0.09 mm (av 0.06), moderately-poorly sorted, subangular-subrounded quartz.
0.02-1.0 mm (av 0.1), very poorly sorted, elongate muscovite.
0.08-0.13 mm, equant, slightly fibrous, green actinolite.

Cement:

Very fine-grained clay.
Opaque hematite.

Composition (%):		
	Quartz	20 - 25
	Feldspar	
	Lithic/Rock Fragments	1 - 2 actinolite
	Opaques/Accessories	1 - 2 rutile (rounded, <0.09mm)
	Matrix	25 quartz
		5 - 7 muscovite
	Cement	40 clay
		2 - 3 hematite
	Porosity	<5

APPENDIX 5:
GEOCHEMICAL METHODS

5.1 X-RAY FLUORESCENCE (XRF)

Representative samples of most Cretaceous facies were analysed by the XRF method, along with other samples of particular interest with regards to mineralisation, cementation, and alteration products. This method (XRF) is relatively rapid and accurate, and allows easy comparison of the bulk geochemistry of samples of differing habit and grain size, as well as qualitative interpretation of mineral content and paragenesis.

5.1.1 Principle of technique

Upon irradiation with X-rays, elements within a sample (pressed into powder pellets, or melted to form fused discs) are excited to emit a radiation with an element-specific wavelength. The measurement of these wavelengths together with the respective intensities of the lines allows the measurement of numerous elements.

5.1.2 Sample preparation

Hard samples were crushed into gravel-sized chips with a hydraulic jaw crusher. Contamination of samples was prevented by thorough cleaning of the crusher between samples. Soft samples and/or chips were ground to a fine powder in a tungsten carbide mill for 1 to 3 minutes depending on hardness. Quartz gravel was ground to powder several times in the mill and the mill was cleaned with ethanol between milling of samples. Excess chips and/or powders were retained along with the remaining portion of the original samples.

Preparation of pressed powder pellets: approximately 5 g of the powdered sample was mixed with five drops of a PVA binding solution in a pestle and mortar until complete homogenisation occurred. PVA solution was not added to several smectite-rich samples due to problems with swelling of the clays. Each sample was transferred to a steel cylinder and pressed by hand. An inner cylinder was carefully removed and the gap between the sample and the larger cylinder wall was filled with powdered boric acid (H_3BO_3). The pellet was then pressed for approximately one minute to a pressure of about 50,000 kPa.

Preparation of fused discs: after ignition in a programmable furnace (to measure Loss on Ignition), flux (about 1.5 g) is added to each glass vial containing the sample and the

components are mixed thoroughly in a mechanical shaker. The contents of the vial are transferred to a Pt / 5% Au crucible and heated for 5 minutes above a oxy-propane flame at a temperature of approximately 1100°C until fusion is complete. The melt is poured on to a graphite disc and pressed into a glass disc using an aluminium plunger (both disc and plunger are kept at a temperature of approximately 230°C). The fused disc is annealed at 230°C for 30 minutes, cooled to room temperature, and then analysed by XRF.

5.1.3 Equipment

Fortyfive rock samples were analysed for major elements (SiO_2, Al_2O_3, Fe_2O_3Total, MnO, MgO, CaO, Na_2O, K_2O, TiO_2, P_2O_5, SO_3) using a Siemens SRS-1 X-ray Fluorescence instrument situated at the Department of Geology and Geophysics, University of Adelaide. These rock samples were also analysed for trace elements (Cu, Ni, Co, Pb, Zn, Cr, Ba, Sr, Sc, Nd, Nb, V, Zr, Y, La, Ce) using a Philips PW 1480 X-ray spectrometer situated at the Department of Geology and Geophysics, University of Adelaide.

5.2 X-RAY DIFFRACTION (XRD)

A representative suite of samples was analysed to document the mineralogies of typical Cretaceous facies on the shelf. For a subset of these samples, those in which the clay mineral content was of particular interest, the clay-sized component was separated mechanically, prepared on oriented mounts, and additional clay-mineral XRD analyses were performed on these samples. The XRD method was used as a relatively rapid means of identifying minerals in samples, particularly where samples are too fine-grained to identify minerals by optical methods (except for time-consuming and expensive electron microscopy). The XRD method proved reliable in assisting with division of fine-grained Cretaceous samples according to clay mineralogy. XRD was the main analytical technique used on these fine-grained rocks.

5.2.1 Principle of technique

Randomly oriented mineral grains (powder) are irradiated with X-rays, which are reflected by the lattice of the sample. The reflection angle and the peak intensity are mineral-specific, and through the Bragg equation ($n\lambda=2d\sin\theta$), the d-spacings of constituent minerals are obtained. Comparison of the experimental data with published standard tables and computer software mineral databases allows the identification of the minerals within each sample.

5.2.2 Bulk (randomly oriented sample) XRD procedure

Fiftythree samples were analysed using bulk XRD analysis with wet grinding to minimise the damage to the structure of the clays. Method: 2-3 g of sample is placed in a tungsten carbide mill, ethanol is added until the sample is covered, and the sample is mechanically ground for 30

seconds. The resulting liquid is then placed in a beaker and heated overnight in an oven at approximately 90°C. The sample is then *lightly* ground in an agate pestle and mortar and placed in an aluminium holder to be run as a powder pressing. An alternative method was used for three very small samples: a powder smear (with acetone) was made on a glass slide; this method requires only a small amount of sample.

5.2.3 Clay separation (oriented sample) XRD procedure

Twentytwo samples in which the clay mineralogy was of particular interest were prepared as follows: the whole sample was broken into chips with a hammer. 1-2 g of sample was then hand *crushed* (avoiding any grinding action) in an agate pestle and mortar to a fine powder. The crushed sample was placed in a small plastic bottle and 2.5 ml per 10 g of sample of a dispersal solution (500 ml 10% w/v sodium hexametaphosphate + 50 ml 1.0N NaOH, all made up to 2 litre volume with distilled water) was added, and the sample was then covered with distilled water. The contents were shaken manually for 5 minutes and poured into a 500 ml plastic measuring cylinder, made up to 500 ml volume with distilled water, mixed thoroughly and allowed to settle for 35 minutes. The top 5 cm (the <2 micron clay fraction) was pipetted off and placed in a plastic bottle, and 2 ml 5N acetic acid was added.

The solution was then pipetted on to a ceramic suction plate on a suction manifold under a vacuum of 100 kPa and allowed to dry. The process was repeated until a uniform coating was obtained. The clay was saturated with 1M $MgCl_2$ solution and allowed to dry; this saturation was repeated three times. The clay was then washed with distilled water three times with 10 minute intervals between washings. Once dry, the oriented clay sample is analysed by XRD.

After the clay separation XRD analyses of the samples were completed the samples with high observed smectitic-clay content were treated again as follows: one drop of glycerol was applied to the dry ceramic plate and spread evenly with a fine brush (without disturbing the clays) and allowed to dry. Repeated XRD analysis revealed the movement of the smectite peaks due to absorption of glycerol, and enabled detailed identification of the type of smectitic clay present.

5.2.4 Equipment

All samples were analysed by a Philips PW 1050 diffractometer at the Department of Geology and Geophysics, University of Adelaide. The instrument used CoKa radiation.

5.3 ATOMIC ABSORPTION (AA)

This method is the most cumbersome, time-consuming, and potentially inaccurate of the analytical techniques used in this study. However, its one big advantage is that only a tiny amount of sample material is required (samples are prepared as solutions of known volume).

Thus, atomic absorption was used where only a small amount of sample was available *i.e*, for very small samples such as those collected from remaining core of the Numbulwar drillholes.

5.3.1 Principle of technique

Atoms, liberated from a sample by vaporisation, emit light upon heating which interferes with light of a specified (analytical) wavelength emitted from an element-specific lamp. Excited atoms in the sample act as a filter by absorbing the light from the lamp. The decrease in intensity of the analytical wavelength is measured by a photospectrometer, and is proportional to the weight percent of the specific element within the sample.

5.3.2 Sample preparation

0.5-1 g of sample is weighed out into a dry 50 ml teflon beaker. 2 ml of 70% w/w $HClO_4$ and 10 ml (conc) HF are added and the mixture is heated at 180°C until evaporated to dryness. The beaker is removed from the hotplate, 10 ml of 5.0M HCl is added, and the mixture is swirled and then heated for 10 minutes. If residue is still present more acid is added as follows: add 3 ml of 70% w/w nitric acid and reflux for 1 hour. If residue is still present, evaporate to dryness and repeat process (boil at 180°C with 1 ml of 70% w/w $HClO_4$ and 5 ml (conc) HF, then add 10 ml of 5.0M HCl, then add 3 ml of 70% w/w nitric acid and reflux for 1 hour). Contents of the beaker are transferred to 100 ml volumetric flasks and made up to 3/4 volume with distilled water, 10 ml of La/K solution (2.0% w/v La, 2.0% w/v K in 0.5M HCl) is added, and then solutions are made up to exact final (100 ml) volume.

5.3.3 Equipment

Twentyfive samples were analysed by AA using a Varian Techtron AA6 Atomic Absorption Spectrophotometer in the Department of Geology and Geophysics, University of Adelaide.

5.4 INDUCTIVE COUPLED PLASMA SPECTROMETRY (ICP)

5.4.1 Principle of technique and equipment

Atoms from the dissolved sample are excited at high temperatures (>8000°C) in a plasma and emit element specific spectra with intensities depending on the concentrations of the various elements in the sample. The ICP technique suffers little interference compared to XRF and AA analysis, and is more sensitive for trace elements. This method was used for samples showing enrichment of complex ferromanganese- and manganese-oxides in hand specimen; such samples were suspected of being enriched in trace elements which are commonly scavenged by manganese species. Ten samples were analysed under contract by ICP at Classic Laboratories Ltd.

APPENDIX 6:
XRD RESULTS

All constituent minerals are listed in order of decreasing relative abundance from top to bottom
Bulk XRD analyses were performed on all samples.
* denotes samples for which clay separation and additional clay-mount XRD analyses were performed.
# denotes samples for which glycerol was added, and then third-pass XRD analyses were performed.
T = triclinic.

AL1-2	AL1-5	AL1-7 *	AL1-10
Quartz	Kaolinite 1T	Kaolinite 1T	Quartz
Kaolinite 1T	Hematite	Muscovite 3T / Illite T	Kaolinite 1T
Goethite	Goethite		Muscovite 3T / Illite T
	Muscovite 3T / Illite T		

AL1-11	AL1-19	AL2-14	AL2-18 *
Quartz	Quartz	Quartz	Quartz
Kaolinite 1T	Kaolinite 1T	Kaolinite 1T	Kaolinite 1T
Muscovite 3T / Illite T	Hematite	Muscovite 3T / Illite T	Muscovite 3T / Illite T
Goethite	Muscovite 3T / Illite T	Hematite	
Unknown			
Hematite ?			

AL2-28	AL2-31 *	AL3-5 *	AL3-9
Quartz	Quartz	Quartz	Quartz
Kaolinite 1T	Kaolinite 1T	Kaolinite 1T	Kaolinite 1T
Muscovite 3T / Illite T	Muscovite 3T / Illite T	Muscovite 3T / Illite T	Muscovite 3T / Illite T

AL3-11	AL3-20B	AL3-26	AL3-28
Quartz	Quartz	Quartz	Quartz
Kaolinite 1T	Kaolinite 1T	Kaolinite 1T	Kaolinite 1T
Muscovite 3T / Illite T	Muscovite 3T / Illite T	Muscovite 3T / Illite T	Muscovite 3T / Illite T

AL3-31	AL3-41 *	AL3-49	AL3-58
Quartz	Quartz	Quartz	Quartz
Kaolinite 1T	Kaolinite 1T	Kaolinite 1T	Kaolinite 1T
Muscovite 3T / Illite T	Goethite	Muscovite 3T / Illite T	Muscovite 3T / Illite T
Hematite	Muscovite 3T / Illite T		Hematite
	Hematite ?		

AL4-1 *#	AL4-3	AL4-5	AL4-7
Quartz	Quartz	Quartz	Quartz
Montmorillonite	Montmorillonite	Kaolinite 1T	Montmorillonite
Muscovite 3T / Illite T	Nontronite ?	Muscovite 3T / Illite T	Kaolinite 1T
Kaolinite 1T	Kaolinite 1T		Muscovite 3T / Illite T
Orthoclase	Orthoclase		Orthoclase
	Muscovite 3T / Illite T		

AL4-8 *	AL4-10	AL4-12 *#	AL4-13 *
Kaolinite 1T	Quartz	Quartz	Quartz
Quartz	Kaolinite 1T	Montmorillonite	Kaolinite 1T
Muscovite 3T / Illite T	Montmorillonite	Kaolinite 1T	Muscovite 3T / Illite T
	Muscovite 3T / Illite T	Muscovite 3T / Illite T	Hematite
	Orthoclase		

AL4-25 *	AL4-26	AL4-27	AL4-37
Quartz	Quartz	Quartz	Quartz
Kaolinite 1T	Kaolinite 1T	Kaolinite 1T	Kaolinite 1T
Muscovite 3T / Illite T	Hematite	Hematite	Hematite
Hematite	Unknown	Muscovite 3T / Illite T	Muscovite 3T / Illite T
	Muscovite 3T / Illite T	Cryptomelane ?	

AL4-38 *	AL4-43 *	AL4-44	AL4-45
Quartz	Quartz	Quartz	Quartz
Kaolinite 1T	Kaolinite 1T	Kaolinite 1T	Kaolinite 1T
Hematite	Hematite	Muscovite 3T / Illite T	Muscovite 3T / Illite T
Muscovite 3T / Illite T	Muscovite 3T / Illite T	Hematite	

AL4-47 *	AL4-50 *	AL4-51 *	AL4-53 *
Quartz	Kaolinite 1T	Quartz	Quartz
Kaolinite 1T	Quartz	Kaolinite 1T	Kaolinite 1T
Muscovite 3T / Illite T	Muscovite 3T / Illite T	Muscovite 3T / Illite T	Muscovite 3T / Illite T
Unknown ?	Hematite		

AL4-59 *	AL4-61 *	AL4-65 *	AL4-70
Quartz	Quartz	Quartz	Quartz
Kaolinite 1T	Kaolinite 1T	Kaolinite 1T	Kaolinite 1T
Muscovite 3T / Illite T	Unknown	Muscovite 3T / Illite T	Hematite
Unknown	Muscovite 3T / Illite T	Cryptomelane ?	Muscovite 3T / Illite T

AL4-71 *	AL4-75	AL4-76 *
Quartz	Quartz	Quartz
Kaolinite 1T	Kaolinite 1T	Unknown
Goethite	Muscovite 3T / Illite T	Kaolinite 1T
Muscovite 3T / Illite T		Muscovite 3T / Illite T

GE-1 * #	GE-2 * #	GE-3
Quartz	Quartz	Quartz
Montmorillonite	Nontronite	Cryptomelane
Nontronite ?	Kaolinite 1MD	Goethite
Kaolinite 1T	Muscovite 3T / Illite T	Pyrolusite ?
Muscovite 3T / Illite T	Goethite ?	
Goethite ?		

US 21 @ 117 ft	US 38 @ 88.5 ft * #	US 41 @ 93 ft
Quartz	Quartz	Quartz
Nontronite / Montmorill	Nontronite / Montmorill	Nontronite / Montmorill
Kaolinite 1T	Kaolinite 1T	Unknown ?
Muscovite 3T / Illite T	Muscovite 3T / Illite T	Nacrite ?
Orthoclase	Orthoclase	Orthoclase
		Muscovite 3T / Illite T

APPENDIX 7:
XRF & ATOMIC ABSORPTION & ICP RESULTS

7.1 SUMMARY

A selected representative sample suite of Cretaceous facies was analysed by XRF, backed up by AA and ICP analyses. The major and trace element contents of most of these samples do not show particularly unusual or unexpected trends, except for the high iron and manganese contents of some samples compared to global averages. In these mineralised samples trace elements such as Co, Cu, Zn, Ba, and Sr occur in abnormal (high) concentrations, primarily as a result of scavenging and cation swapping by Mn and Fe oxide species (*cf.* Hem, 1972).

These mineralised samples are commonly not restricted to well-defined stratigraphic levels, and the presence of manganese- or iron- oxide mineralisation within the Mullaman Beds does not appear to be particularly useful for detailed stratigraphic correlation, at least not with the reconnaissance level of sampling possible in this study. However, the documentation of broad mineralogical and geochemical trends within facies of the Cretaceous shelf succession in this thesis is important as a background to further research. This work is able to be built upon in the event of more detailed studies being carried out, particularly mineral exploration for manganese-oxide accumulations towards the base of the Cretaceous sequence in the northern region.

Site	2							4	4	5
Sample #	AL1-miscA	AL1-miscB	AL1-1A	AL1-12	AL1-14	AL1-17	AL1-20	AL1-21	AL1-23	AL1-24
SiO2	41.88	33.92	3.87	36.52	2.85	59.09	34.04	16.38	45.14	2.35
AL2O3	2.24	16.01	0.87	5.44	1.65	0.96	5.88	2.85	2.61	2.19
Fe2O3T	2.17	41.63	82.9	53.78	90.9	29.29	49.06	17.44	8.9	3.98
MnO	38	0.07	0.43	0.07	0.07	0.03	0.03	28.12	9.91	70.19
MgO	0.5	0.28	0.28	0.24	0.25	2.55	0.15	2.44	1.41	0.58
CaO	0.59	0.02	0.04	0.04	0.03	0.84	0.02	9.61	14.3	0.38
Na2O	0.32	0.01	0.01	0.01	0.01	0.37	0.02	0.49	0.18	0.3
K2O	2.97	0.08	0.01	0.1	0.01	0.07	0.49	0.13	0.08	4.4
TiO2	0.06	0.63	0	0.24	0.3	0.08	0.32	0.18	0.13	0.07
P2O5	0.35	0.14	0.05	0.13	0.13	0.08	1.18	0.13	0.06	0.97
SO3	0.06	0.02	0.04	0.07	0.03	0.05	0.01	0.58	0.08	0.06
LOI	6.89	6.67	10.77	2.55	2.12	5.42	7.79	18.93	16.4	11.42
Total	96.02	99.47	99.27	99.19	98.36	98.83	98.99	97.27	99.2	96.88
Cu	224	7	3	5	7	10	19	37	5	68
Ni	37	16	<6	10	<6	<6	28	12	10	88
Co	1445	21	10	42	105	154	48	146	167	318
Pb	9	18	<9	9	<9	<9	<9	12	9	51
Zn	611	9	120	17	5	19	115	6	<5	530
Cr	8	343	8	122	273	16	57	46	90	16
Ba	6240	<35	<35	<35	<35	<35	170	8770	400	6060
Sr	367	9	3	11	7	75	15	1517	2014	672

all samples prefixed by 899-
major & minor elements as %
trace elements as ppm

Site	11	15	17		17	17		20	21	23
Sample #	AL1-25	AL1-26	AL1-28	AL1-30	AL1-31	AL1-32	AL1-33	AL1-35	AL1-36	AL1-37
SiO2	3.84	44.14	49.02	85.8	56.51	46.04	51.22	43.32	45.27	15.1
AL2O3	5.33	13.69	4.27	5.83	11.97	14.67	5.2	17.91	4.09	5.91
Fe2O3T	6.22	22.01	23.56	3.57	15.27	13.49	39.65	18.61	0.89	34.42
MnO	61.24	7.53	12.78	0.45	6.81	13.65	0.05	7.44	33.81	28.16
MgO	0.65	0.74	0.78	0.42	0.51	0.49	0.3	0.42	0.31	0.27
CaO	0.4	0.19	0.06	0.02	0.09	0.15	0.02	0.05	0.06	0.05
Na2O	0.3	0.31	0.06	0.02	0.03	0.04	0.01	0.03	0.4	0.08
K2O	3.2	0.69	0.87	0.39	0.55	0.65	0.1	0.15	1.46	1.36
TiO2	0.16	0.46	0.24	0.22	0.58	0.6	0.31	1.09	0.11	0.3
P2O5	0.81	0.16	0.34	0.07	0.07	0.06	0.14	0.08	0.38	0.71
SO3	0.11	0.02	0.02	0.01	0.02	0.02	0.02	0.02	0.02	0.03
LOI	13.19	8.71	7.17	2.67	6.57	9.21	2.29	9.98	7.39	11.6
Total	95.46	98.66	99.18	99.46	98.98	99.06	99.31	99.1	94.19	97.99
Cu	129	17	21	80	35	28	9	24	134	48
Ni	90	24	6	6	37	83	<6	69	20	14
Co	638	147	55	28	133	110	75	242	1297	42
Pb	21	49	<9	<9	18	48	<9	15	12	12
Zn	466	55	<5	8	8	5	5	21	449	133
Cr	<8	94	25	76	84	130	34	115	8	12
Ba	9260	3120	1490	580	3500	3480	<35	2180	28200	6040
Sr	308	158	99	13	88	106	9	60	89	398

all samples prefixed by 899-
major & minor elements as %
trace elements as ppm

Site	42	107	107	107	107					
Sample #	AL2-29A	AL4-X1	AL4-X2	AL4-X3	AL4-X4	AL4-X5	AL4-X6	AL4-X7	AL4-X8	AL4-X9
	*	*	*	*	*	*	*	*	*	*
SiO2	51.4	35.8	33.6	31.8	47.6	38.3	45.7	79.3	35.6	19.9
AL2O3	10.9	3.64	2.88	2.56	2.28	3.88	2.64	10	12.8	15.7
Fe2O3T	23.3	6.3	4.64	4.78	3.86	52.4	45.2	3.68	43.5	55
MnO	2.96	2.22	3.38	3.66	1.62	0.01	<0.01	0.02	<0.01	<0.01
MgO	0.47	9.65	9.6	10.1	7.1	0.17	0.12	0.16	0.15	0.15
CaO	0.05	17.4	17.8	18.3	15.5	0.17	0.1	0.24	0.08	0.15
Na2O	0.12	0.12	0.16	0.18	0.21	0.23	0.13	0.16	0.14	0.07
K2O	1.18	1.08	1.35	1.2	0.76	0.34	0.14	0.43	0.4	0.13
TiO2	0.59	0.14	0.15	0.13	0.09	0.36	0.27	0.43	0.83	0.81
P2O5	0.08	0.07	0.09	0.08	0.19	0.26	0.33	0.16	0.12	0.1
SO3	n.d.	n.d.	n.d.	n.d.	n.d.	n.d.	n.d.	n.d.	n.d.	n.d.
LOI	9.45	21.7	26.7		21.3	4.86	5.9	5.55	7.3	8.95
Total	100.5	98.1	100.3	100.6	100.5	101	100.5	100.1	100.9	100.9
Cu	200	<50	290	<50	<50	60	120	<50	50	<50
Ni	<50	<50	<50	<50	<50	<50	<50	<50	<50	<50
Co	70	<50	<50	<50	<50	<50	80	90	<50	<50
Pb	130	<50	80	120	50	140	50	<50	120	110
Zn	60	60	50	40	50	80	80	50	70	100
Cr	<50	<50	<50	<50	<50	80	<50	<50	<50	160
Ba	1600	50	80	90	40	80	30	90	110	40
Sr	50	30	40	30	20	<20	<20	20	30	<20
As	<50	<50	<50	<50	<50	90	120	<50	60	50
Sn	60	70	<50	70	70	80	<50	<50	<50	<50
Mo	<50	<50	<50	<50	<50	<50	<50	<50	<50	<50
Cd	<20	<20	<20	<20	<20	<20	<20	<20	<20	<20
Ta	<50	<50	<50	<50	<50	<50	<50	<50	<50	<50
Nb	70	<50	<50	<50	<50	130	110	<50	110	150
V	140	<20	<20	<20	<20	1250	850	100	1750	1650
Be	<20	<20	<20	<20	<20	<20	<20	<20	<20	<20
Zr	260	40	80	60	40	120	250	160	170	230
Y	<20	<20	<20	<20	<20	<20	<20	<20	<20	<20
La	<50	<50	<50	<50	<50	<50	<50	<50	<50	<50
Ce	<100	<100	<100	<100	<100	<100	<100	<100	<100	<100

trace elements as ppm
* denotes analysis by ICP

all samples prefixed by 899-
major & minor elements as %

Sample #	AL4-1	AL4-5	AL4-7	AL4-8	AL4-9	AL4-10	AL4-11	AL4-12	AL4-13	AL4-14
SiO2	61.73	67.7	63.36	66.64	65.31	68.62	21.63	64.22	64.48	19.52
AL2O3	18.4	21.83	18.32	23.44	16.97	19.63	17.51	21.13	20.44	15.58
Fe2O3T	4.87	1.82	4.74	0.36	6.59	1.11	52.19	2.66	5.22	55.66
MnO	0.02	0	0.01	0	0.01	0	0.03	0.01	0	0.03
MgO	2.62	0.1	2.29	0.06	1.59	0.84	0.17	1.34	0.18	0.13
CaO	0.29	0.02	0.2	0.03	0.22	0.12	0.21	0.37	0.08	0.07
Na2O	0.2	0	0.3	0	0.1	0.1	0.2	0.2	0	0.1
K2O	2.27	0.22	1.93	0.15	1.07	0.97	0.07	1.12	0.79	0.04
TiO2	0.88	0.33	0.95	0.3	0.77	0.92	0.96	0.94	0.85	0.86
P2O5	0.09	0.02	0.05	0.01	0.07	0.05	0.06	0.02	0.04	0.06
SO3	0.02	-0.02	0.01	-0.01	-0.01	-0.01	0.03	-0.01	-0.01	0.03
LOI	7.56	8.25	7.14	8.86	7.04	7.01	6.78	7.67	7.43	7.52
Total	98.93	100.25	99.25	99.84	99.75	99.36	99.84	99.63	99.54	99.56
Cu	21.4	5	22.3	3.7	14.9	26.8	19.4	23.9	5.6	12.1
Ni	21.8	5.9	39.1	5	17.1	11.6	5.8	17.5	8	11.6
Co	89	0.4	23.3	0.5	7.3	5.1	4.7	3.9	0.5	4.1
Pb	18.8	5.2	10.9	5.8	36.8	11.3	64.4	9.4	18.6	37.1
Zn	79.3	6.9	161.8	4.7	77.9	31.3	36.9	42.2	12.3	26.9
Cr	125	80	132	115	143	79	340	86	152	443
Ba	284	52	267	66	315	198	90	192	192	27
Sr	78.5	8.8	66.8	8.5	110.5	53.6	43.5	53	84.3	0.1
Sc	15.1	4.2	14.1	4.7	13.2	11.1	27.7	16.5	5.8	28.1
Nd	42	2	27	3	19	127	7	17	9	5
Nb	10.1	3.9	10.3	3.4	9.6	11	12.7	11.3	10.9	11.1
V	179.5	44.9	180.2	51.6	161.5	104.4	2229.7	128.9	318	1386.9
Zr	176	85.7	183.4	74.4	189.3	191.5	255.8	170.4	159.7	358.3
Y	23.8	4.5	24.7	3.5	19.4	35.9	7.4	13.8	9.1	8.2
La	40	7	31	5	32	49	35	25	31	19
Ce	85	8	60	5	51	151	49	43	41	24

all samples prefixed by 899-
major & minor elements as %
trace elements as ppm

Sample #	GE-1	GE-2	US 21	US 38	US 41
SiO2	67.88	62.5	65.4	63.7	65.74
AL2O3	16.54	18.92	16.97	16.27	16.73
Fe2O3T	4.22	5.64	3.67	5.18	3.84
MnO	0.21	0.17	0.02	0.02	0.01
MgO	1.97	2.33	2.19	2.8	2.19
CaO	0.13	0.19	0.17	0.55	0.38
Na2O	0.2	0.3	0.1	0.3	0.2
K2O	0.92	1.17	1.63	2.43	2.07
TiO2	0.79	0.96	0.81	0.79	0.8
P2O5	0.02	0.03	0.06	0.11	0.04
SO3	-0.01	-0.01	0.31	0.07	-0.01
LOI	6.77	7.48	8.08	7.8	7.99
Total	99.6	99.66	99.46	99.97	100
Cu	19.4	20.1	*13*	*13*	*9*
Ni	64.5	102.7	*109*	*43*	*10*
Co	17.6	18.4	*25*	*14*	*2*
Pb	5.1	5.4	*19*	*12*	*7*
Zn	74.7	85	*482*	*207*	*69*
Cr	87	137	*138*	*70*	*55*
Ba	126	167	*678*	*447*	*258*
Sr	38.4	48.3	*81*	*83*	*55*
Sc	15.2	18.3			
Nd	68	65			
Nb	7.2	8.9			
V	173.3	270.4			
Zr	142.7	177.5			
Y	61	63.3			
La	37	37			
Ce	60	68			

all samples prefixed by 899-
major & minor elements as %

trace elements as ppm
values in italics indicate results were obtained by AA method